Aus der Poliklinik für Kieferorthopädie
Klinikum / Institut der Ludwig-Maximilians-Universität München

Dissertation
zum Erwerb des Doctor of Philosophy (Ph.D.)
an der Medizinischen Fakultät der
Ludwig-Maximilians-Universität zu München

Establishment of an *in vitro* tensile strain model and application of different stretching parameters to human periodontal ligament cells

vorgelegt von:

Changyun Sun

aus:

Dongying, Shandong, China

Jahr:

2022

Mit Genehmigung der Medizinischen Fakultät der
Ludwig-Maximilians-Universität zu München

First evaluator (1. TAC member):	PD Dr. rer. nat. Uwe Baumert
Second evaluator (2. TAC member):	Prof. Dr. Dr. Matthias Folwaczny
Third evaluator:	Prof. Dr. Bogna Stawarczyk
Fourth evaluator:	PD Dr. Burkhard Summer

Dean: **Prof. Dr. med. Thomas Gudermann**

date of the defense:

20. 07. 2022

Affidavit

Affidavit

Sun, Changyun

Surname, first name

Leipart Str 28. Room 108

Street

81369, München, Germany

Zip code, town, country

I hereby declare, that the submitted thesis entitled:

Establishment of an *in vitro* tensile strain model and application of different stretching parameters to human periodontal ligament cells

is my own work. I have only used the sources indicated and have not made unauthorised use of services of a third party. Where the work of others has been quoted or reproduced, the source is always given.

I further declare that the submitted thesis or parts thereof have not been presented as part of an examination degree to any other university.

Munich, 23.02.2022

place, date

Changyun Sun

Signature doctoral cand

Confirmation of congruency

LMU LUDWIG-MAXIMILIANS-UNIVERSITÄT MÜNCHEN

Promotionsbüro Medizinische Fakultät

MMRS

Confirmation of congruency between printed and electronic version of the doctoral thesis

Sun, Changyun

Surname, first name

Leipart Str 28. Room 108

Street

81369, München, Germany

Zip code, town, country

I hereby declare, that the submitted thesis entitled:

Establishment of an *in vitro* tensile strain model and application of different stretching parameters to human periodontal ligament cells

is congruent with the printed version both in content and format.

Munich, 23.02.2022

place, date

Changyun Sun

Signature doctoral candidate

Table of content

List of abbreviations

ALPL	Alkaline phosphatase: biomineralization associated
BGLAP	Bone gamma-carboxyglutamate protein
DEG	Differentially expressed genes
ELISA	Enzyme-linked immunosorbent assay
GO	GeneOntology
hPDLC	Human periodontal ligament cell
IL10	Interleukin 10
IL1B	Interleukin 1B
IL6	Interleukin 6
IL8	Interleukin 8
OTM	Orthodontic tooth movement
PDLC	Periodontal ligament cell
PGE2	Prostaglandin E2
PTGS2	Prostaglandin-endoperoxide synthase 2
RT-qPCR	Reverse transcription quantitative real-time polymerase chain reaction
RUNX2	Runt-related transcription factor 2
TNF	Tumor necrosis factor α
TNFRSF11	TNF superfamily member 11
TNFRSF11B	Tumor necrosis factor-alpha receptor super-family member 11B

List of publications

Sun C, Janjic Rankovic M, Folwaczny M, Otto S, Wichelhaus A, Baumert U (2021). Effect of Tension on Human Periodontal Ligament Cells: Systematic Review and Network Analysis. Front Bioeng Biotechnol; 9:695053.

Sun C, Janjic Rankovic M, Folwaczny M, Stocker T, Otto S, Wichelhaus A, Baumert U (2022). Effect of Different Parameters of In Vitro Static Tensile Strain on Human Periodontal Ligament Cells Simulating the Tension Side of Orthodontic Tooth Movement. Int J Mol Sci; 23(3):1525.

Contribution to the publications

1.1 Contribution to publication I

Involved in the conceptualization and design of the research, i.e. forming the P.I.C.O. research question and defining the searching formula. Searched in the PubMed database with the predefined searching formula. Screened the included 5,331 studies by title and abstract reading and did first exclusion of unrelated studies. Then did full-text reading for the remaining 183 studies, followed by further exclusion according to the excluding criteria. Involved in defining the criteria of risk of bias and performed assessment for both methodological and reporting quality. Conducted data extraction for the 137 included studies, including both qualitative and quantitative information, i.e. cells used, force applied, gene/metabolites analyzed. Performed analysis for related *in vitro* tensile strain models and frequently used parameters, including magnitudes, durations and frequencies of the tensile strain. Calculated regulation of genes/metabolite in all included studies and summarized corresponding regulation patterns. Identified the 10 most frequently investigated loci and grouped them into 3 categories (osteogenesis, osteoclastogenesis and inflammation), followed by summary of their main regulation tendency. Wrote the original draft and did revision according to suggestions of the co-authors.

1.2 Contribution to publication II

Designed the experiment with the supervisor using relevant information on magnitude and duration of tensile strain from the first publication being related to the experimental set-up used. Designed the primary prototype of the cell stretching apparatus. Tested the apparatus by applying a wide range of tensile strain magnitudes to human periodontal ligament cells (hPDLCs) for up to 3 days, followed by cell viability assessment. Conducted primary cell culture of hPDLCs and applied a wide range of force parameters to the cells, followed by sample preparation, reverse transcription quantitative real-time polymerase chain reaction (RT-qPCR) and Enzyme-linked immunosorbent assay (ELISA). Performed *in silico* assessment for the primers of target genes and reference genes. Assessed the reference genes using samples collected during the experiment. Involved in the data analysis of the qPCR and ELISA results. Prepared the original drafts and revised them according to the suggestions of co-authors and reviewers.

2. Introductory summary

2.1 Summary of the PhD project

The PhD project entitled “Establishment of an *in vitro* tensile strain model and application of different stretching parameters to human periodontal ligament cells” was conducted at the Department of Orthodontics and Dentofacial Orthopedics, University Hospital, Ludwig-Maximilians-Universität München, under the supervision of PD Dr. rer. nat. Uwe Baumert and Prof. Dr. med. dent. Andrea Wichelhaus. During this project, two studies were performed and published to fulfill the requirements for PhD graduation.

Orthodontic tooth movement (OTM) aims to align mal-positioned teeth through application of appropriate external forces (Wichelhaus 2017). In response to external stimuli, bone remodeling is activated resulting in bone resorption on the compression side and bone formation on the tension side (Krishnan and Davidovitch 2015). As the structure between teeth and alveolar bone, the periodontal ligament (PDL) plays an essential role during OTM. The periodontal ligament consists of several type of cells, including but not limited to the fibroblasts (Marchesan et al. 2011) and is essential in transforming mechanical stimuli into biological signals (Krishnan and Davidovitch 2006).

Compression and tension are two essential forces responsible for bone resorption and bone formation correspondingly during OTM. While appropriate therapeutic forces are crucial for bone homeostasis, excessive stimuli will result in tissue destruction and adverse complications (Pavasant and Yongchaitrakul 2011). Therefore, it is of great importance to evaluate the effect of different force magnitudes on human PDL cells (hPDLC). For compression forces, systematic summary and analysis for *in vitro* models have been conducted (Janjic et al. 2018), and related biological regulations have been investigated by several models addressing different force magnitudes (Baumert et al. 2004; Janjic Rankovic et al. 2020; Shi et al. 2019). However, for tensile strain forces, though many studies were published (Yang et al. 2015), there is no systematic and detailed analysis of relevant methodological aspects (apparatus, magnitudes and durations of tensile strain), as well as related biological regulation and pathways. Additionally, most published studies only focused on specific tensile strain magnitudes, leaving a gap in the knowledge related to effect of different tensile strain parameters on hPDLCs under the same experimental condition.

Therefore, this project aimed (1) to perform a systematic review to include all tensile strain related studies, and to make a quantitative summary and analysis for force parameters and related biological regulations; (2) to identify the research gaps in related areas; (3) to establish an *in vitro* static tensile strain model; (4) to investigate the effect of different stretching parameters on hPDLCs, focusing on bone remodelling, mechanosensing and inflammation.

2.2 Summary of the two publications

2.2.1 Publication 1. Effect of Tension on Human Periodontal Ligament Cells: Systematic Review and Network Analysis.

This systematic review was performed to identify all published studies focusing on effect *of in vitro* tensile strain on hPDLCs, to summarize the force parameters and regulations of investigated gene/metabolites, and to identify biological process and pathways that might be affected by tensile strain. In this study, 5,331 publications were identified using a defined search formula. After screening of the title and abstracts and full text reading of relevant literatures, 137 studies were finally included for risk of bias assessment and data extraction (i.e. characteristics of tensile strain and genes/protein/metabolites analyzed) (Sun et al. 2021). Based on the extracted information and summaries listing the investigated genes, network analysis was performed (Sun et al. 2021).

Type of tensile strain and apparatus used: Among the 137 included studies, 103 focused on dynamic and 30 applied static tensile strain (Sun et al. 2021). Both equibiaxial and uniaxial cell stretching were identified, with the former more frequently applied (103/137, 75%). Concerning the apparatuses used, Flexcell Strain Unit® and its revisions were most frequently applied for both dynamic and static equibiaxial tensile strain. The STB-140" system (STREX® Inc., Osaka, Japan), apparatuses with silicone (non Bioflex®-plate) or other elastic membrane were mostly adopted for dynamic uniaxial tensile strain. Static uniaxial tensile strain application was identified in two studies only (Sun et al. 2021).

Magnitudes, durations and frequencies of tensile strain: Dynamic equibiaxial tensile strain was applied with frequencies ranging from 0.005 Hz to 1 Hz, among which 0.1 Hz was most frequently applied (Sun et al. 2021). Tensile strain magnitudes of 10 % and 12 % were more commonly used among a range of 1-24 % (Sun et al. 2021). Force application duration showed a large variation. However, 48h and 72h experimental durations were mostly applied. For dynamic

uniaxial tensile strain application, the most commonly used frequency, magnitudes and duration were 0.5 Hz, 10 % and 12 % magnitudes and 48 h, respectively (Sun et al. 2021). Static tensile strain parameters deviate much in comparison to dynamic tensile strain. Tensile magnitude of 2.5 % and 12 h duration were most frequently used for static equibiaxial cell stretching, while 5 %, 8 % and 10 % magnitudes and 3 h / 12 h experimental durations were commonly used in studies applying static uniaxial cell stretching (Sun et al. 2021).

Selection of force parameters: This review summarized and analyzed the tensile strain related parameters, including magnitudes, durations and frequencies. Selection of magnitudes was mostly either based on *in vivo* studies (Mühlemann 1954; Mühlemann and Zander 1954), or resulted from finite element analysis (Dong-Xu et al. 2011; Natali et al. 2004) as well as related previous publications (Hao et al. 2009; Memmert et al. 2019; Nogueira et al. 2014). Considering the requirement of cell feeding for *in vitro* studies, the maximum duration was limited. For force frequency, selection was mostly based on previous studies or studies investigating tooth contact during sleep (He et al. 2004) or masticatory cycle (Tantilertanant et al. 2019).

Genes, proteins and metabolites investigated: Biological regulations in response to tensile strain application were extracted or calculated, followed by summary of the gene/protein expression patterns. Altogether, 205 genes were identified from all the included studies. The top 10 most frequently investigated genes/proteins/metabolites were Runt-related transcription factor 2 (*RUNX2)*, biomineralization associated alkaline phosphatase (*ALPL*), bone gamma-carboxyglutamate protein (*BGLAP*), interleukin 1B (*IL1B)*, prostaglandin-endoperoxide synthase 2 (*PTGS2)*, tumor necrosis factor-alpha receptor super-family member 11B (*TNFRSF11B)*, TNF superfamily member 11 (*TNFRSF11)*, *COL1A1*, prostaglandin E2 (PGE2) and transcription factor *SP7* (Sun et al. 2021). They were classified into the categories “osteogenesis”, “osteoclastogenesis” and “inflammation”, and further analyzed in relationship to force magnitudes or durations (Sun et al. 2021).

Network analysis: Differentially expressed genes (DEG) were selected from the dynamic and static gene lists, which were extracted from corresponding type of studies (Sun et al. 2021). Using the dynamic and static lists of DEG, corresponding Protein-protein interaction (PPI) networks were generated and analyzed (Sun et al. 2021). Hub genes were identified, and regulation tendency of genes was marked with different colors (Sun et al. 2021). Additionally, both “Biological

Process" of GeneOntology (GO) and GeneAnalytics were applied to identify the involved biological processes and signaling pathways (Sun et al. 2021). All hub genes, enriched GO terms and super signaling pathways identified in this study might provide additional clues for new researching topics.

This systematic review performed a comprehensive data extraction and analysis for both force and biological related information (Sun et al. 2021). The most frequently adopted apparatuses, magnitudes and durations of tensile strain were summarized, followed by comparison and discussion in relationship to clinical situations. Regulation of gene/protein/metabolites was investigated followed by comprehensive network analysis, providing more insights into the biological background of OTM. Some research gaps were identified, including but not limited to the effect of different stretching parameters on hPDLCs, which would be focus for the second part of the PhD project.

2.2.2 Publication 2. Effect of different parameters of *in vitro* static tensile strain on human periodontal ligament cells simulating the tension side of orthodontic tooth movement.

Based on the open questions ("further research need") identified in the systematic review, the second part of PhD study aimed to investigate the effect of different stretching parameters on hPDLCs. For this purpose, an *in vitro* apparatus for static tensile strain was constructed, assessed and finally applied for hPDLCs.

Construction and assessment of the apparatus: As mentioned in the first publication, most apparatuses for tensile strain were based on the deformation of elastic membrane on which cells were attached (Sun et al. 2021). Based on previous publications (Nazet et al. 2020; Toume et al. 2016), a 3D designed apparatus was constructed for applying different cell stretching magnitudes simultaneously. The apparatus contained five parts: a base plate, six 3D-printed caps with pins, a Bioflex® plate, a frame and screws (Sun et al. 2022). Cells were seeded on the elastic membrane of the 6-well Bioflex® plate. Caps with predefined parameter were inserted into the base plate. By fixing the frame and the Bioflex® plate into the baseplate, cells were stretched with specific magnitudes (Sun et al. 2022). Applicability of the apparatus was tested by applying tensile strain of 3%, 10% and 20% to the attached hPDLCs, which covered the most frequently adopted range of magnitudes (Sun et al. 2021). After 1, 2 and 3 days of tensile strain, the specific set-ups

were unloaded. Directly afterwards, cell viability of stretched cells was assessed with live/dead cell staining (Sun et al. 2022). Independent of tensile strain magnitudes and durations, only a small number of dead cells were visible after staining. This confirmed the good applicability of the apparatus for tensile strain experiments.

Study *design*: To investigate the effect of different stretching parameters on hPDLCs regarding bone remodeling, mechanosensing and inflammation, magnitudes of 0%, 3%, 6%, 10%, 15% and 20% were applied for 1, 2 and 3 days (Sun et al. 2022). Supernatants of each well were collected at each end point, followed by ELISA analysis of IL1B, Interleukin 6 (IL6), Interleukin 8 (IL8), Interleukin 10 (IL10), Tumor necrosis factor α (TNF) and PGE2. Cell lysates were collected for further analysis. According to the MIQE guideline (Bustin et al. 2009; Bustin et al. 2010), stability of reference genes should be assessed for each specific study and more than one reference genes was recommended to be used. Therefore, a part of the cell lysates from the study was used to evaluate the stability of a panel of reference genes, followed by analysis with program of RefFinder (Xie et al. 2012). After assessment, the two most stable reference genes (*RPL22* and *POLR2A*) were used for further analysis of target genes (Sun et al. 2022). Regulation of target genes was detected using RT-qPCR, focusing on bone remodeling (*RUNX2*, *SP7*, *ALPL*, *BGLAP* and *TNFRSF11B*), mechanosensing (*FOS*) and inflammation (*IL6* and *PTGS2*) (Sun et al. 2022).

Effect of different parameters of tensile strain on hPDLCs regarding bone remodeling: For genes related to bone remodeling, *TNFRSF11B* was below detection limit (Sun et al. 2022). Duration dependencies were identified for all other related target genes. Gene expression of *RUNX2* and *ALPL* presented a very similar tendency, both showing significant upregulation after 1 day, followed by downregulation after 2 days and returned to corresponding control levels after 3 days of stretching (Sun et al. 2022). For both genes, 3% stretching led to maximum upregulation, while 20% resulted in the minimum expression after 1 day of tensile strain (Sun et al. 2022). Similar as *RUNX2* and *ALPL*, maximum upregulation of *SP7* was also detected after 1 day of cell stretching, with more prominent upregulation for lower magnitudes (6%, 10% and 15%) and less regulation for higher magnitude of 20% (Sun et al. 2022). Regulation of *BGLAP* was not significant after 1 day, while downregulation was identified after 2 days followed by upregulation after 3 days of stretching (Sun et al. 2022). In summary, regulation of these genes was consisted with the timeline of bone remodeling (Rutkovskiy et al. 2016), and it indicated the promoting effect of lower magnitudes and inhibiting effect of higher magnitudes on osteogenesis (Sun et al. 2022).

Effect of different parameters of tensile strain on hPDLCs regarding mechanosensing: After 1 and 2 days of tensile strain, expression of *FOS*, a mechanosensation related gene, was around corresponding control levels (Sun et al. 2022). Upregulation was found after 3 days of cell stretching for magnitudes of 3%, 6% and 15%. However, earlier upregulation of *FOS* was frequently reported in other studies (Kletsas et al. 2002; Papadopoulou et al. 2017; Peverali et al. 2001). Considering the early-responsive characteristic of *FOS*, more earlier detecting time points might be considered in further research (Sun et al. 2022).

Effect of different parameters of tensile strain on hPDLCs regarding inflammation: ELISA results were all below detecting limit for IL1B, IL8, IL10, TNF, while changes in both gene expression and secretion of IL6 and PGE2 were detected (Sun et al. 2022). *IL6* gene was generally upregulated after 1 day, then downregulated after 2 days and returned to the control level after 3 days (Sun et al. 2022). IL6 concentration in the supernatant was upregulated for all durations, with maximum identified after 3 days of cell stretching. Among all magnitudes, 10% of cell stretching resulted in minimal expression for all durations (Sun et al. 2022). *PTGS2* was regulated after 1 day and returned to the control level after 2 and 3 days of tensile strain (Sun et al. 2022). Concentration of PGE2 was upregulated for all durations with maximum found after 1 day of cell stretching (Sun et al. 2022). It showed force magnitude dependence, reaching its maximum at higher magnitudes (15% and 20%) and less prominent expression at lower magnitudes (3%, 6% and 10%). With all these molecules considered, 10% magnitude generally resulted in minimal level of inflammation and might be concluded as an appropriate stretching magnitude (Sun et al. 2022).

In summary, based on the first part of the PhD project (the systematic review), the need for an investigation of wide range of tensile strain magnitudes under the same experimental conditions was identified. Therefore, during the second part of the PhD project, an *in vitro* tensile strain apparatus was constructed, enabling precise verification of cell stretching magnitudes using parameterized 3D printed caps. To enable more precise analysis for the expression of target genes, systematic assessment and selection of reference genes were also performed, followed by investigation of the stretching magnitude and duration dependence of selected target genes. The results of this study provided an overview for bone remodeling/mechanosensing/inflammation related biological regulations in hPDLC exposed to different parameters of static tensile strain, which might also provide some clues for OTM in clinical situations.

3. Publication I

Effect of Tension on Human Periodontal Ligament Cells: Systematic Review and Network Analysis

Changyun Sun, Mila Janjic Rankovic, Matthias Folwaczny, Sven Otto, Andrea Wichelhaus and Uwe Baumert

Front Bioeng Biotechnol. 2021 Aug 27; 9: 695053.

PubMed: https://www.ncbi.nlm.nih.gov/pubmed/34513810

PubMedCentral: https://www.ncbi.nlm.nih.gov/pmc/articles/PMC8429507/

DOI: https://doi.org/10.3389/fbioe.2021.695053

frontiers in Bioengineering and Biotechnology

ORIGINAL RESEARCH
published: 27 August 2021
doi: 10.3389/fbioe.2021.695053

Effect of Tension on Human Periodontal Ligament Cells: Systematic Review and Network Analysis

Changyun Sun[1], *Mila Janjic Rankovic*[1], *Matthias Folwaczny*[2], *Sven Otto*[3], *Andrea Wichelhaus*[1] *and Uwe Baumert*[1]*

[1]Department of Orthodontics and Dentofacial Orthopedics, University Hospital, LMU Munich, Munich, Germany, [2]Department of Conservative Dentistry and Periodontology, University Hospital, LMU Munich, Munich, Germany, [3]Department of Oral and Maxillofacial Plastic Surgery, Martin-Luther-University Halle-Wittenberg, Halle (Saale), Germany

Orthodontic tooth movement is based on the remodeling of tooth-surrounding tissues in response to mechanical stimuli. During this process, human periodontal ligament cells (hPDLCs) play a central role in mechanosensing and mechanotransduction. Various *in vitro* models have been introduced to investigate the effect of tension on hPDLCs. They provide a valuable body of knowledge on how tension influences relevant genes, proteins, and metabolites. However, no systematic review summarizing these findings has been conducted so far. Aim of this systematic review was to identify all related *in vitro* studies reporting tension application on hPDLCs and summarize their findings regarding force parameters, including magnitude, frequency and duration. Expression data of genes, proteins, and metabolites was extracted and summarized. Studies' risk of bias was assessed using tailored risk of bias tools. Signaling pathways were identified by protein-protein interaction (PPI) networks using STRING and GeneAnalytics. According to our results, Flexcell Strain Unit® and other silicone-plate or elastic membrane-based apparatuses were mainly adopted. Frequencies of 0.1 and 0.5 Hz were predominantly applied for dynamic equibiaxial and uniaxial tension, respectively. Magnitudes of 10 and 12% were mostly employed for dynamic tension and 2.5% for static tension. The 10 most commonly investigated genes, proteins and metabolites identified, were mainly involved in osteogenesis, osteoclastogenesis or inflammation. Gene-set enrichment analysis and PPI networks gave deeper insight into the involved signaling pathways. This review represents a brief summary of the massive body of knowledge in this field, and will also provide suggestions for future researches on this topic.

Keywords: periodontal ligament fibroblasts, tension, tissue remodelling, orthodontic tooth movement, mechanical stress

OPEN ACCESS

Edited by:
Georges Limbert, University of Southampton, United Kingdom

Reviewed by:
Vincent Everts, Academic Centre for Dentistry Amsterdam, Netherlands
Klara Janjic, Medical University of Vienna, Austria

***Correspondence:**
Uwe Baumert
uwe.baumert@med.uni-muenchen.de

Specialty section:
This article was submitted to Biomechanics, a section of the journal Frontiers in Bioengineering and Biotechnology

Received: *21 April 2021*
Accepted: *10 August 2021*
Published: *27 August 2021*

Citation:
Sun C, Janjic Rankovic M, Folwaczny M, Otto S, Wichelhaus A and Baumert U (2021) Effect of Tension on Human Periodontal Ligament Cells: Systematic Review and Network Analysis. Front. Bioeng. Biotechnol. 9:695053. doi: 10.3389/fbioe.2021.695053

INTRODUCTION

Orthodontic treatment aims to align malpositioned teeth towards a functional optimal position by application of an appropriate force (Wichelhaus, 2017). This force leads to bone resorption in direction of the movement ("compressive side") and bone formation on the opposite side ("tension side"). Orthodontic tooth movement (OTM) is therefore based on the controlled stimulation of bone remodeling by application of external force ("orthodontic force"). At the cellular level, OTM is based

on remodeling processes in the periodontal ligament (PDL) and the alveolar bone (Cho et al., 2010; Chang et al., 2017). Placed between the teeth and the surrounding alveolar bone, the PDL is a heterogeneous connective tissue, that is composed of several different cell populations including but not limited to fibroblasts, macrophages, stem cells and endothelial cells (Marchesan et al., 2011). In the context of *in vitro* experiments, the term "PDL fibroblast" should be used carefully. Cells described as "PDL fibroblast" are commonly isolated from the middle third of the tooth root. For cell isolation either the "explant" or the "digestion" technique is employed (for further details: see discussion). Yet, both techniques will result in a heterogeneous mixture of different cell types (Marchesan et al., 2011).

The PDL is essential for maintaining the homeostasis and integrity of the tooth supporting tissue (Ren et al., 2015; Wu et al., 2019b) and plays a pivotal role in coping with physiological forces that occur during routine activities, i.e. speaking or mastication and non-physiological external forces (Pavasant and Yongchaitrakul, 2011). Involution and atrophy of PDL is induced by lack of recurring mechanical stimuli (Cohn, 1965), while exposure against excessive forces will impair the subtle balance between osteogenesis and osteoclastogenesis, ultimately leading to the disintegration and loss of the osseous tooth support (Nogueira et al., 2014a). Therapeutic mechanical force applied onto teeth is mediated to the alveolar bone via the PDL thereby inducing bone remodeling and OTM (Vansant et al., 2018). Periodontal ligament cells (PDLCs) play a vital role in the transduction of mechanical force to biological signals, achieving the balance between bone formation and resorption (Kook and Lee, 2012; Li et al., 2019). PDLCs can be activated in response to periodontal ligament injury followed by proliferation, migration and synthesis of new matrix components (Krishnan and Davidovitch, 2006). Potentially, PDLCs can differentiate into cementoblasts or osteoblasts and are involved in the repair and the regeneration of the periodontal tissues (Pavasant and Yongchaitrakul, 2011).

Due to the complex structure of the periodontium and to evaluate inter and intracellular signaling pathways, *in vitro* models have been established to simulate the two major mechanical stimuli occurring during OTM (Yang et al., 2015; Janjic et al., 2018; Vansant et al., 2018): tension and compression. The main working principles of these setups can be summarized as approaches in which tension is applied via substrate deformation, whereas compression is mainly applied via weight, hydrostatic pressure, or centrifugation (Yang et al., 2015). *In vitro* compression models were recently summarized (Janjic et al., 2018) and the underlying molecular signal transduction has been shown by numerous *in vitro* experiments (Baumert et al., 2004; Shi et al., 2019a; Shi et al., 2019b; Janjic Rankovic et al., 2020). Based on these reports various molecular pathways involved in OTM have been identified, including but not limited to genes and proteins which are related to osteogenesis, osteoclastogenesis, inflammation and apoptosis (Yang et al., 2015; Janjic et al., 2018; Vansant et al., 2018). To study the effect of tension on PDLCs, different *in vitro* models have been designed to apply continuous ("static") or intermitted ("dynamic") tension force along one principal axis ("uniaxial") or along all axes in all directions ("equibiaxial") of a cell (definition according to Lee and von Recum, 2015)(**Figure 1**). However, the force parameters in terms of dynamic and static tension used show enormous heterogeneity, depending on the specific objectives of the experiments.

Therefore, this systematic review aimed to summarize the data on different *in vitro* tension models applied to human PDLCs (hPDLCs) as well as the effect of tension on the expression of genes and proteins. Specifically, this systematic review aimed 1) to identify all relevant studies applying tension on hPDLCs e.g. to simulate orthodontic force or other clinically relevant forces; 2) to make an assessment of the methodological and reporting quality of the included studies; 3) to summarize the biological and force parameters, and the commonly adopted methods for detecting biological regulation; and 4) to identify the most frequently investigated genes/proteins and their regulation, as well as the biological processes and pathways that might be affected by tension in hPDLCs.

MATERIALS AND METHODS

This systematic review was conducted following the "Preferred Reporting Items for Systematic Reviews and Meta-Analyses" (PRISMA) guidelines (Moher et al., 2009). The protocol of this systematic review was finalized before data collection. A registration in the PROSPERO database was not possible, since only *in vitro* studies were included.

Eligibility Criteria

Inclusion criteria were defined in accordance with the "P.I.C.O." framework (Schardt et al., 2007):

- P(atient): human periodontal ligament cells (hPDLCs) or human periodontal ligament derived stem cells (hPDLSCs);
- I(ntervention): *in vitro* static and dynamic tension (e.g. to simulate orthodontic force or other clinically relevant forces);
- C(ontrol): human periodontal ligament cells (hPDLCs) or human periodontal ligament derived stem cells (hPDLSCs) not subjected to mechanical force;
- O(utcome): force parameters (i.e. apparatus, force duration, force magnitude, frequency of force exposure) and regulation of gene, protein and/or metabolite expression in response to tension.

The following exclusion criteria were applied:

- *In vivo* studies
- *In vitro* studies not applying tension on hPDLCs or hPDLSCs
- Reviews
- Studies not reporting quantitative data on gene or protein expression
- Application of force other than tension or the specific type of force is undefined
- 3D model
- Co-culture
- Articles not published in English

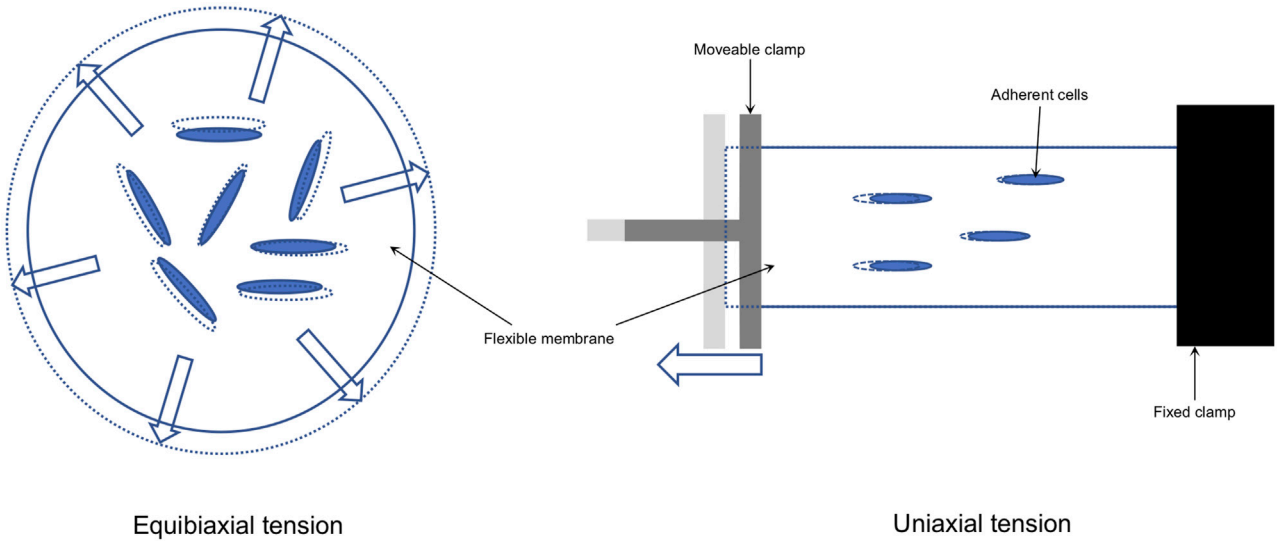

FIGURE 1 | Tension is applied to adherent cells growing on a flexible surface (e.g. a. silicon membrane; solid lines) by elongation (dotted lines) of that surface either with equal forces acting in all directions in the same way (equibiaxial) or equal forces acting in one principle axis (uniaxial).

TABLE 1 | Final PubMed search strategy applied.

Field		Force		Cells
orthodont* OR tooth movement OR periodont*	AND	BioFlex culture plates OR biomechanic* OR mechanical force* OR load* OR stretch* OR tension OR tensile OR dynamic structural remodeling OR equi-biaxial strain OR Flexercell OR four-point bending OR mechanical coupling OR mechanical deformation OR mechano-sensitive OR mechanostimulation OR mechanotransduction OR petri dish OR flexible bottom OR elastic membrane OR silicon* OR strength OR stress OR substrate strain OR Tensile	AND	fibroblast* OR PDL OR hPDLCs OR hPDLFs OR hPDLF OR progenitor cell* OR stem cell* OR human PDL-cells OR human PDL-fibroblasts OR human PDLFs OR human PDLs OR human periodontal ligament OR ligament fibroblast OR periodontal tissue OR Periodontium

Search phrase: (orthodont OR tooth movement OR periodont*) AND (BioFlex culture plates OR biomechanic* OR mechanical force* OR load* OR stretch* OR tension OR tensile OR dynamic structural remodeling OR equi-biaxial strain OR Flexercell OR four-point bending OR mechanical coupling OR mechanical deformation OR mechano-sensitive OR mechanostimulation OR mechanotransduction OR petri dish OR flexible bottom OR elastic membrane OR silicon* OR strength OR stress OR substrate strain OR tensile) AND (fibroblast* OR PDL OR hPDLCs OR hPDLFs OR hPDLF OR progenitor cell* OR stem cell* OR human PDL-cells OR human PDL-fibroblasts OR human PDLFs OR human PDLs OR human periodontal ligament OR ligament fibroblast OR periodontal tissue OR periodontium).*

Search Strategy and Study Selection

The search strategy considered keywords concerning the specific objectives of the studies, the force applied and the cells exposed to experimental force and were summarized in **Table 1**. PubMed search was completed on 31-01-2020 and the results were imported into EndNote® X9.3.1 (Clarivate Analytics, Philadelphia, Pennsylvania, United States).

First, unrelated studies were excluded after reading titles and abstracts according to the eligibility criteria defined. Then, full texts of the remaining studies were acquired. After full text reading, articles not fulfilling the eligibility criteria were excluded (**Supplementary Table S1**), and those in accordance with the inclusion criteria were used for data extraction (**Supplementary Table S2**). Any disagreements or uncertainties during both steps were discussed with two other review authors (U.B. and M.J.R.) until agreement was achieved.

Risk of Bias Assessment (Definition and Table for Assessment)

Risk of bias of the included *in vitro* studies was assessed using the methods described by Vansant et al. (2018) and Samuel et al. (2016). Methodological risk of bias was evaluated using 15 criteria and reporting risk of bias using 10 criteria (**Supplementary Table S3**). Each criterion was scored "low risk of bias" ("+"), "high risk of bias" ("−"), "incomplete or unclear risk of bias" ("?") or "not applicable" ("n.a.") based on the low risk of bias definitions given in **Supplementary Table S3** for both, reporting and methodological quality. Low risk of bias ("LoB") and if necessary high risk of bias ("HoB") of the different criteria were defined according to the information provided in the aforementioned publications, citations therein and the following additional sources: "OHAT Risk of Bias Rating Tool for Human and Animal Studies" and "Biophysical Journal's Guidelines for the Reproducibility in Biophysics Research" (details in **Supplementary Table S3**). To simplify data entry during the assessment, data sheets for both risk of bias assessments were developed (**Supplementary Table S3**).

All included articles were scored by two authors (C.S. and M.J.R.). Any disagreement was discussed internally until consensus was achieved. The results of the risk of bias assessment were recorded and summarized in predefined tables (**Supplementary Tables S4.1, S4.2**).

Data Extraction

After final selection of relevant studies, the following information on experimental design and outcome were extracted and summarized: reference (author, year, journal); cells used (age/gender of donors, tooth type, isolation method, cell culture passages and cell density used in the experiments); force applied ("dynamic"/"static" and "equibiaxial"/"uniaxial" force application; its duration, frequency of exposure, magnitude, and the device used); genes analyzed (official gene symbol if applicable) with reference to force application and the methods applied to measure their expression. "Gene or analyte investigated", "Cells used" and the details on the "Force apparatus" were extracted using the original phrases from the studies and recorded in **Supplementary Table S2**. In addition, gene expression patterns including peak expression and the reported units were recorded; fold changes and ratios were calculated, if applicable.

Information Related to Genes and Proteins

Specificity of primers used in PCR reactions was verified with Primer-BLAST (https://www.ncbi.nlm.nih.gov/tools/primer-blast/). All genes were reported using their official gene symbol according to the HUGO Gene Nomenclature Committee (HGNC; URL: https://www.genenames.org). For protein data, antibody or ELISA specificity was verified using information provided within the studies and the information given by the suppliers. If possible, official gene symbols according to HGNC were applied. If antibody specificity was not sufficient, e.g. no discrimination between isoforms or gene variants, antibody targets were recorded according to the manufacturer given in that publication.

The expression patterns of genes and/or proteins were described using specific terms (**Figure 2**) and numerical data describing specific maxima and minima (stars in **Figure 2**) was collected. Data was directly acquired from the publications itself or extracted from graphs using Engauge Digitizer Software version 10.12 (URL: https://markummitchell.github.io/engauge-digitizer). To allow comparisons between gene or protein expression data from different sources, ratios (experimental condition vs control) or fold changes were calculated if not given by the authors. Gene expression was reported as "fold change" (FC), if its calculation was done either according to Livak and Schmittgen (2001) or similar sources or was clearly described as "$2^{-\Delta\Delta Ct}$" or "$\Delta\Delta Ct$". Gene expression was designated as "ratio", if the control was "defined as 1", otherwise it was described as "relative change" ("rel"). Results reported from more than one donor were listed separately.

Information Related to Force

The frequency of force exposure used in all dynamic tension studies was reported as "Hz" if possible. If frequency was reported in other units, conversion was done according to the information given. Any inconsistencies were resolved by discussion between the authors. Information about the force apparatuses was either directly collected from the publications, by searching the manufacturer information or Google® patent search (URL: https://patents.google.com) if applicable. Equibiaxial and uniaxial tension (**Figure 1**) were distinguished depending on the direction of the force applied in relation to the hPDLCs using information contained in the publications and citation chaining. The information was defined "unclear" or "incomplete", if insufficient information was given that was even not resolved after communication with the manufacturer.

Summary Statistics

A summary of statistics on the force apparatuses was prepared from a unified list based on "apparatus", followed by sorting according to the force type (i.e. "dynamic"/"static" and "equibiaxial"/"uniaxial"). Afterwards, publications using the same type of apparatus were combined into the same category for further analysis. A summary statistic on the different force parameters was compiled from a unified list of publications based on tension type and tension frequency. From each publication reporting dynamic tension application, maximum duration of force exposure and mainly adopted magnitude were summarized

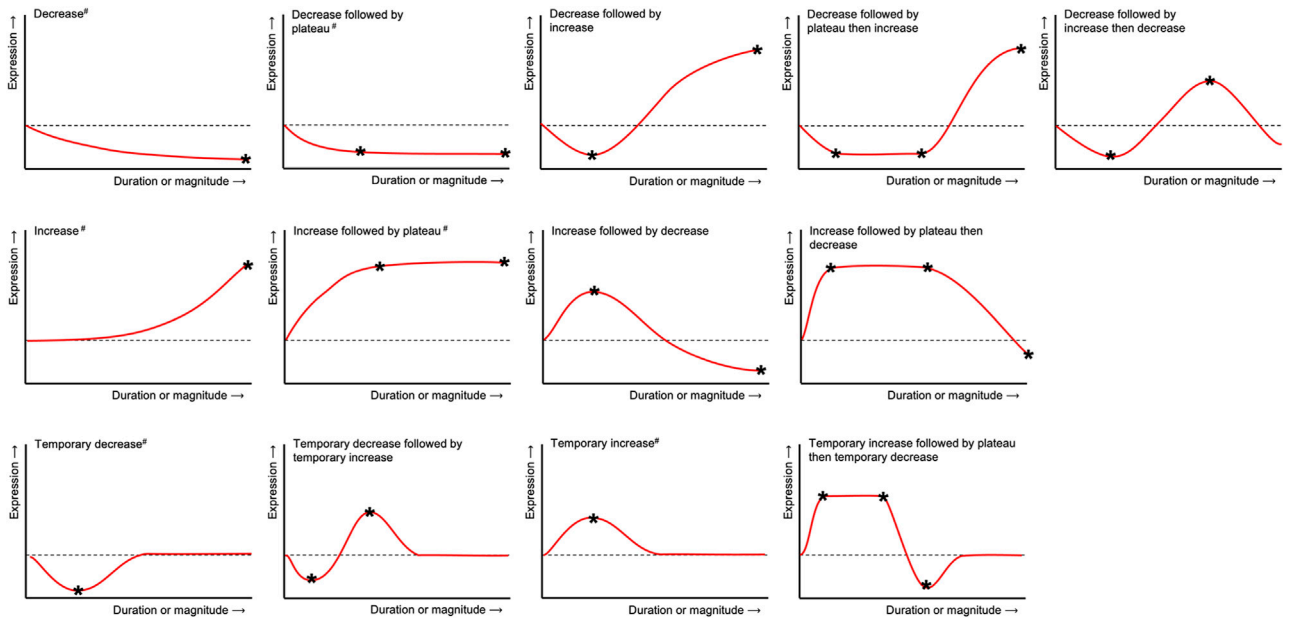

FIGURE 2 | Terms used to describe the general expression patterns in hPDLCs after tension application for each gene, protein or metabolite included herein. Numerical data describing specific maxima and minima (*) was collected and reported in **Supplementary Tables S2, S7**. Expression patterns labeled with a double cross (#) were mapped on the protein-protein interaction networks constructed from gene lists shown in **Figure 5**.

for the same frequency. Studies utilizing static tension were classified first by magnitude followed by maximum force duration. Replicates derived from the same study were removed and all analytes were ranked according to abundance.

Gene-List and Protein-Protein Interaction Network Analysis

Based on the complete lists of examined genes, differential expressed gene (DEG) lists were compiled according to the following criteria: the gene was identified unequivocally and changes in gene expression due to force application were reported using the terms defined in **Figure 2**. Depending on force application, the genes were assigned either to the "dynamic" or to the "static" gene list. Both DEG lists were used to generate protein-protein-interaction (PPI) networks and for gene list enrichment (**Figure 3B**).

To predict potential interactions between the DEGs at the protein level, PPI networks were constructed querying the "Search Tool for the Retrieval of Interacting Genes/Proteins" database (STRING-DB) (v11.0; URL: https://string-db.org) (Szklarczyk et al., 2019) using the *stringApp* plugin version 1.5.1 (Doncheva et al., 2019) with *Cytoscape* version 3.8.0 (Shannon et al., 2003; Su et al., 2014). A minimum required combined score of 0.7 was applied, i.e. only high confidence interactions were included in the predicted networks. Cluster analysis and cluster visualization of both "dynamic" and "static" PPI networks was done applying the "Molecular Complex Detection" (MCODE) algorithm (Bader and Hogue, 2003) as implemented in the *clusterMaker2* app version 1.3.1 (Morris et al., 2011) with default settings and "fluff" activated. Hub genes, i.e. essential genes in a network, were identified with *cytoHubba* version 0.1 (Chin et al., 2014) using default settings. This plugin applies eleven different local and global topological methods to the nodes of a given network. For each node, a total score was calculated based on these eleven measures. A node was considered as a hub node, if its total score was at least twofold higher than the mean total score of all nodes of that particular network. Networks were visualized with *Cytoscape* version 3.8.0.

StringApp was also applied for gene list enrichment using the "GeneOntology/Biological Process" database (Ashburner et al., 2000). The "SuperPaths" database was analyzed online with "GeneAnalytics" (version 4.14 Build 1; URL: https://ga.genecards.org) (Ben-Ari Fuchs et al., 2016). To increase specificity, results from both databases were filtered according to the proportion of query genes in relation to the number of background genes of the specific database entry and a cut-off of ≥0.05 (i.e. 5 %) was applied. In all cases the ten most significant terms or pathways were reported. Individual gene set enrichment was applied to 1) the two complete networks and 2) each identified cluster, using "GeneAnalytics" and *stringApp*.

RESULTS

Study Selection

The whole process of study selection was summarized in the PRISMA flow diagram (**Figure 3A**) (Moher et al., 2009). The applied search strategy identified 5,331 publications. No additional articles were identified through reference chaining or hand-search of specific journals. After removing 11 duplicates, 5,320 studies were left, of which 5,138 publications were excluded after title and abstract reading

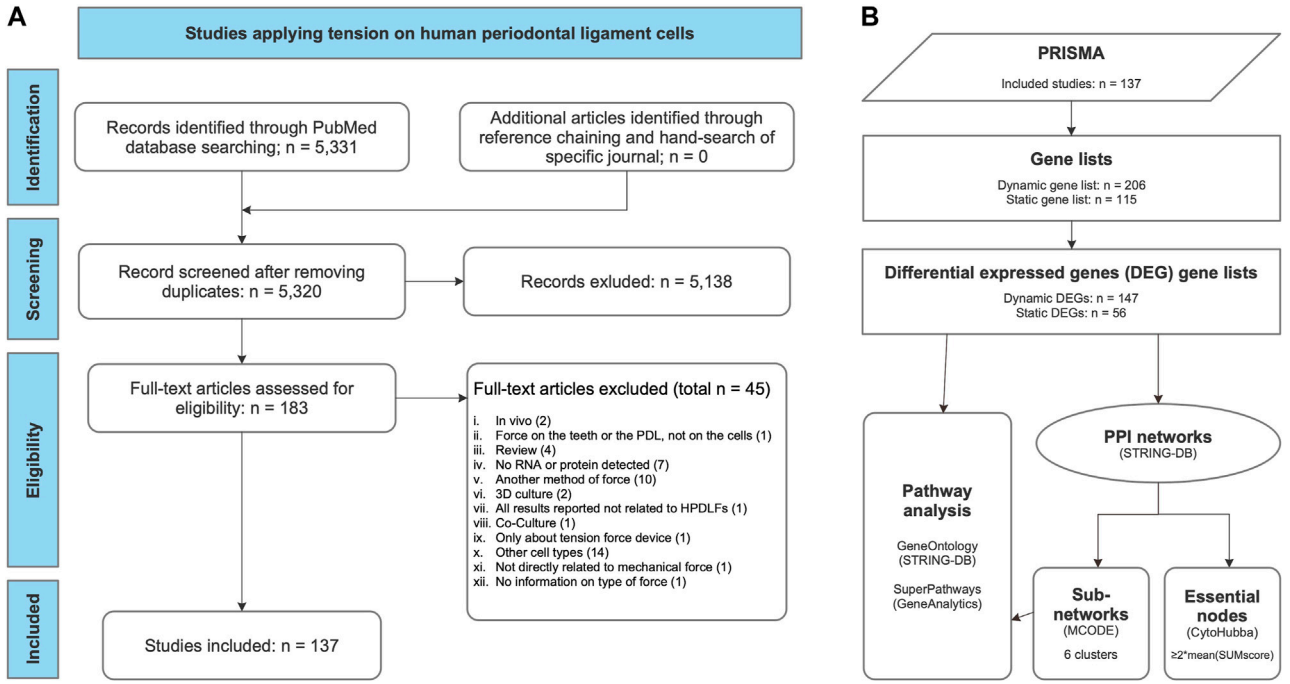

FIGURE 3 | Workflows applied in this systematic review. **(A)** PRISMA flow diagram for the whole process of study selection according to Moher et al. (2009). **(B)** Gene set enrichment and network analysis of gene lists derived from the review process. Gene lists were compiled, listing the examined genes, proteins or metabolites studied either after dynamic or static tension application (**Table 3**, **Supplementary Table S2**). From these, differential expressed gene (DEG) lists were generated according to the specified criteria (**Table 4**). For each of these two DEG lists (dynamic DEG, static DEG) protein-protein interaction (PPI) networks were constructed using STRING-DB (Szklarczyk et al., 2019) (**Figures 5A,B**) and pathway analysis was conducted quering "GeneOntology/Biologcal Process" (Ashburner et al., 2000) and GeneAnalytics' "SuperPath" databases (Ben-Ari Fuchs et al., 2016) (**Supplementary Table S8**). Subnetworks were identified in both PPI networks using MCODE (Bader and Hogue, 2003) (**Table 4**; **Figures 5C,D**) and essential nodes, so called "hub genes", using *cytoHubba* (Chin et al., 2014) (**Table 5**; **Figure 5**).

according to the defined criteria. Afterwards, 182 publications were assessed by full-text reading, of which 45 were excluded according to the exclusion criteria defined previously (**Figure 3A**; **Supplementary Table S1**).

Risk of Bias

Methodological quality was assessed using 15 criteria (**Supplementary Table S3**). The criteria "Randomization", "Blinding of researchers", and "Blinding of outcome assessors" were not applicable to *in vitro* studies. The results of the other risk of bias criteria showed a large variability. "Sample size determination" and "Statistical analysis" were mostly assessed as "high risk of bias" ("HoB"). "Accounting for confounding variables", "Optimal time window used" and "Test organism/system" were found to have a high level of "incomplete or unclear risk of bias". With reference to the remaining criteria, most of the studies were assessed as "low risk of bias" ("LoB") (**Figure 4**; details in **Supplementary Table S4.1**).

The reporting quality of the publications was higher in comparison to the methodological quality, since more studies were classified as "LoB" (**Figure 4**, **Supplementary Table S4.2**). Only the criterion "Justification for model" was found to have a large percent of "Incomplete or unclear risk of bias" (**Figure 4**; details in **Supplementary Table S4.2**).

Tension Characteristics

In 30 out of 137 qualified studies (~22%) static tension was applied, whereas 103 out of 137 included studies (~75%) focused on the effect of dynamic tension (**Supplementary Table S5**). Direct comparison between static and dynamic tension was conducted in three studies (~2%) (Papadopoulou et al., 2017; Wada et al., 2017; Memmert et al., 2020). One study did not clearly define the specific force type applied (**Supplementary Table S5**).

Devices for Tension Application

Regarding the type of apparatus, all included studies were identified as either equibiaxial or uniaxial (**Figure 1**). Various apparatuses were used in these studies either for equibiaxial or uniaxial tension (**Table 2**; Tables S5.1 and S5.2 in **Supplementary Table S5**).

Dynamic equibiaxial tension: Fifty three studies applied dynamic equibiaxial tension using the Flexcell Strain Unit (Flexcell® International Corporation, Burlington, NC, United States) and its revisions (FX-2000, FX-3000, FX-4000, FX-5000) (Banes et al., 1985). This system employs tension to cells seeded on elastic silicone membranes fixed in special 6-well plates (Bioflex® plates; Flexcell® International Corporation) by application of a vacuum below the flexible membrane. In nine studies, Bioflex® plates were used together with individually

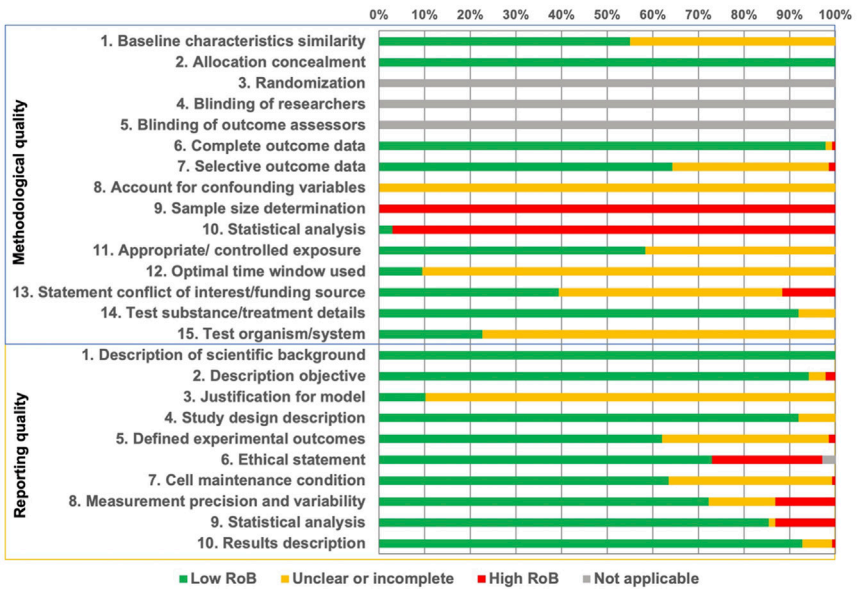

Item	LoB	Unclear	HoB	N. a.
1	75 (55%)	62 (45%)	0 (0%)	0 (0%)
2	137 (100%)	0 (0%)	0 (0%)	0 (0%)
3	0 (0%)	0 (0%)	0 (0%)	137 (100%)
4	0 (0%)	0 (0%)	0 (0%)	137 (100%)
5	0 (0%)	0 (0%)	0 (0%)	137 (100%)
6	134 (98%)	2 (1%)	1 (1%)	0 (0%)
7	88 (64%)	47 (34%)	2 (1%)	0 (0%)
8	0 (0%)	137 (100%)	0 (0%)	0 (0%)
9	0 (0%)	0 (0%)	137 (100%)	0 (0%)
10	4 (3%)	0 (0%)	133 (97%)	0 (0%)
11	80 (58%)	57 (42%)	0 (0%)	0 (0%)
12	13 (9%)	124 (91%)	0 (0%)	0 (0%)
13	54 (39%)	67 (49%)	16 (12%)	0 (0%)
14	126 (92%)	11 (8%)	0 (0%)	0 (0%)
15	31 (23%)	106 (77%)	0 (0%)	0 (0%)
1	137 (100%)	0 (0%)	0 (0%)	0 (0%)
2	129 (94%)	5 (4%)	3 (2%)	0 (0%)
3	14 (10%)	123 (90%)	0 (0%)	0 (0%)
4	126 (92%)	11 (8%)	0 (0%)	0 (0%)
5	85 (62%)	50 (36%)	2 (1%)	0 (0%)
6	100 (73%)	0 (0%)	33(24%)	4 (3%)
7	87 (64%)	49 (36%)	1 (1%)	0 (0%)
8	99 (72%)	20 (15%)	18 (13%)	0 (0%)
9	117 (85%)	2 (1%)	18 (13%)	0 (0%)
10	127 (93%)	9 (7%)	1 (1%)	0 (0%)

FIGURE 4 | Summary of the risk of bias assessments for methodological (upper panel) and reporting quality risk of bias (lower panel). The tabulated data on the right reported frequency and percentage [n(%)] for each item according to its scoring: "LoB" – low risk of bias, "Unclear" – unclear or incomplete, "HoB" – high risk of bias, "N.a." – not applicable.

TABLE 2 | Summary statistics according to tension type and apparatus. Since some publications applied two tension types, the total number given here is larger (n = 140) than the number of studies identified (n = 137).

Tension type (n)	**Tension applied with (*n*)**	**Fraction of Tension type (%)**
Dynamic equibiaxial (72)	Flexcell Strain Unit® and its revisions (53)	73.6
	Bioflex®-plate based apparatus (9)	12.5
	Other silicone (not Bioflex®)-plate based or elastic membrane-based apparatuses (10)	13.9
Dynamic uniaxial (34)	STREX® STB-140 (10)	29.4
	Silicone (not Uniflex®)-plate based and other elastic membrane-based apparatuses (10)	29.4
	Flexcell Strain Unit® and its revisions using Uniflex® plates (8)	23.5
	Four-point bending system (6)	17.6
Static equibiaxial (31)	Flexcell Strain Unit® and its revised version (11)	35.5
	Petriperm® dish (10)	32.2
	Bioflex® based apparatus (7)	22.6
	Lumox® dish (2)	6.5
	Tension incubator (1)	3.2
Static uniaxial (2)	Silicone dishes (1)	50.0
	STREX® system (1)	50.0
Not given (1)	Not given (1)	

constructed devices, including the "CESTRA" (Deschner et al., 2007) and the "Cell Extender" devices (Wada et al., 2017) (**Table 2**; **Supplementary Table S5.1** in **Supplementary Table S5**). Ten studies used different non-Bioflex®-plate based silicone or elastic membrane-based apparatuses including the "Cell Strain Unit (CSU)" (Hao et al., 2009), which was used in eight studies.

Dynamic uniaxial tension: Application of dynamic uniaxial tension using the "STB-140" system (STREX® Inc., Osaka, Japan) was described in ten publications. The Flexcell Strain Unit® in combination with Uniflex® culture plates (Flexcell® International Corporation) was adopted in eight studies. Non Bioflex®-plate based silicone and other elastic membrane-based apparatus were adopted in ten studies. Four-point bending systems were employed in six studies (**Table 2**; **Supplementary Table S5.2** in **Supplementary Table S5**).

Static tension: To apply static equibiaxial tension, the Flexcell Strain Unit and its revisions (FX-3000™, FX-4000™, FX-5000™) were adopted in eleven studies. Apparatuses based on the Petriperm™ dish were used in ten studies, in which the dish was deformed by the weight placed onto a spheroidal template. Bioflex®-based devices were used in seven studies, Lumox® culture dishes were adopted in two and the "*tension incubator*" in one study (**Table 2**; **Supplementary Table S5.3** in **Supplementary Table S5**). Static uniaxial tension was applied

TABLE 3 | Genes, proteins and metabolites analyzed in the included studies. Differential expressed genes (DEGs) used for the subsequent gene list enrichment analysis are given in bold.

Dynamic tension	Static tension
ACE, **ACTA2**, ACTB, ACVR2B, **ACY1**, **ADRB2**, **AGT**, **AGTR1**, AGTR2, AKT1, **ALPP**, **AMDHD2**, ARHGDIA, **ATF1**, **ATF4**, ATP, **BCL2**, **BGLAP**, **BGN**, **BMP2**, **BMP4**, **BMP6**, **BMP7**, **BMPR1A**, BMPR1B, **BMPR2**, CASP1, **CASP3**, CASP3/CASP7, **CASP5**, CASP7, CASP8, CASP9, CCDC88A, **CCL2**, **CCL20**, **CCL3**, **CCL5**, **CCN1**, **CCN2**, CCND1, **CCR5**, **CDC42EP2**, CFL1, **COL12A1**, **COL1A1**, COL1A1/COL1A2, **COL3A1**, **COL4A1**, **COL5A1**, **CREB1**, CSF1, CTNNB1, **CXCL8**, **BHLHE40**, DEFB1, **DEFB103B**, **DEFB4A**, DIAPH1, **DKK1**, **DVL2**, **EGFR**, EIF2AK3, ELN, **FBLN5**, FBN1, FBN2, **FGF2**, FN1, **FOS**, **FST**, **GATA4**, **GDF2**, **GDF5**, **GJA1**, **GLI2**, **GOSR1**, **GRIA3**, **GRIN1**, **GRIN2C**, **GRIN2D**, **GRIN3A**, **GRIN3B**, **GRM2**, **GRM3**, **GRM4**, **GRM5**, **GRM6**, **GSDMD**, Glutamate, **HACD1**, **HIF1A**, **HMOX1**, **HOMER1**, **HSPA5**, **IBSP**, **IER3, IGF1**, **IL10**, **IL11**, **IL12A**, IL18, **IL1B**, **IL1RN**, **IL6**, **IL6R**, **ITGA1**, **ITGA3**, ITGAV, **JUN**, **KLF10**, **LATS1**, LEF1, **LIMD1**, LTBP2, MAPK14, MAPK3/MAPK1, MAPK7, MAPK8, MAPK8/MAPK9/MAPK10, **MCAM**, **MEF2C**, **MGP**, **MMP1**, **MMP14**, **MMP2**, **MMP3**, MMP8, **MSX1**, **MSX2**, **MYH7**, **MYL2**, **MYL7**, **NAMPT**, NFKB1, NFKBIB, **NKX2-5**, **NLRP1**, **NLRP3**, **NOG**, NOS2, NOS3, **NPPA**, **NPPB**, Nitric oxide, **P2RY1**, PARP1, PFN1, PGE_2, **PLAT**, PLAT/PLAU, PLAU, **POSTN**, PTGER1, **PTGER2**, PTGER3, **PTGER4**, **PTGS1**, **PTGS2**, **PYCARD**, **REN**, **RHOA**, **ROCK1**, ROCK1/ROCK2, **RSPO2**, **RUNX2**, **RXFP1**, RXFP2, **SATB2**, SERPINE1, SERPINF1, **SIRT1**, **SLC17A7**, **SMAD7**, **SP7**, SPARC, **SPP1**, **SPRY2**, **SQSTM1**, STMN1, **TAZ**, **TEAD1**, **TEAD2**, **TGFB1**, TGFBI, **TGFBR1**, **TGFBR2**, **TIMP1**, **TIMP2**, **TLR2**, **TLR4**, **TNF**, **TNFRSF11B**, **TNFSF11**, **TNNT2**, **TP53BP2**, **TPM1**, **UNC50**, **VEGFA**, WASL, WNT3A, **WTIP**, **XBP1**, **YAP1**	**ALPP**, **ATG10**, **ATG4C**, **ATG7**, **BAD**, **BCL2**, **BGLAP**, **BID**, cAMP, CCNA1/CCNA2, **CCND1**, CCNE1, CDK2, CDK4, CDKN1A, CDKN1B, **COL1A1**, COL1A1/COL1A2, **CRADD**, **CTSB**, **CTSL**, **DAPK1**, **EFNB2**, **EPHB4**, **FAS**, **FOS**, **GDF15**, HMGB1, **IGF1**, **IGF1R**, **IGF2**, **IGFBP1**, **IGFBP3**, **IGFBP5**, **IL1B**, IL1B/IL1A, **IL6**, **IRS1**, ITGA1, ITGA2, ITGA3, ITGA4, **ITGA5**, ITGA6, ITGAV, **ITGB1**, ITGB3, ITGB4, **JUN**, MAP1LC3A, MAP4, MAPK14, MAPK3/MAPK1, MAPK8, MAPK8/MAPK9/MAPK10, MKI67, **MMP1**, **MMP12**, MMP14, **MMP2**, MMP8, MMP9, MYO1C, **NFKB1**, **NOS2**, **PCNA**, PGE_2, PIK3CG, **PLAT**, PLAT/PLAU, PLAU, **PLXNA1**, PLXNB1, **PLXNC1**, **PTGS2**, PTK2, RAB17, RAB3A, RAB3B, RAB6A, RHOA, RPS15, **RUNX2**, SEMA3A, SEMA3C, **SEMA3D**, SEMA3E, SEMA4A, SEMA4C, SEMA4D, SEMA4F, SEMA5A, **SEMA5B**, SEMA6B, SEMA6C, **SEMA7A**, SERPINE1, **SLC2A1**, **SNCA**, **SPP1**, **SQSTM1**, TCEAL1, **TIMP1**, **TIMP2**, TIMP3, TLN1/TLN2, **TNF**, **TNFRSF11B**, **TNFSF11**, **TP53**, TUBA1B, TUBA1C/TUBA3C/TUBA3D/TUBA4A, **UVRAG**, VIM, YAP1

in two studies (**Table 2**; **Supplementary Table S5.4** in **Supplementary Table S5**): one with the STREX system and the other via a "*silicone dishes based in-house designed device*" with a moving clamp (Papadopoulou et al., 2017).

In summary, dynamic tension was more frequently investigated than static tension, and equibiaxial tension was more commonly adopted than uniaxial tension, both with a ratio ~3:1.

Force Magnitude and Duration in Equibiaxial and Uniaxial Tension

Dynamic equibiaxial tension was applied using frequencies between 0.005–1 Hz, with 0.1 Hz used in the majority of the studies. The maximum magnitude most frequently adopted varied between 1–24% of which 10 and 12% were more commonly applied. The mainly adopted duration of force exposure varied from 1 h to 6 days, using 48 and 72 h in the majority of studies (**Supplementary Table S5.5**).

For *dynamic uniaxial tension* frequencies between 0.005 – 1 Hz were used. The most frequently adopted frequency was 0.5 Hz. The magnitude varied between 0.2 and 33%, with magnitudes of 10 and 12% being most frequently applied. Force duration ranged from 1 h to 7 days and 48 h was the most frequent one (**Supplementary Table S5.6**).

Static equibiaxial tension was applied with force magnitudes varying between 0.28 and 35%, mimicking physiological or pathological mechanical force. The most frequent magnitude was 2.5%. Force duration varied between 0.5 h and 15 days, whereby 12 h was the most commonly used one (**Supplementary Table S5.7**).

For *static uniaxial tension*, magnitudes of 5%, 8 and 10% were applied for a maximum of 12, 3, and 12 h, respectively (**Supplementary Table S5.8**).

Genes, Proteins and Metabolites Analyzed

Relevant data on 205 genes, proteins or metabolites in relation to dynamic tension application to hPDLCs was extracted from 104 publications (**Table 3**). Static tension was applied in 33 publications and expression profiles of 115 different genes, proteins or metabolites related to force application were determined (**Table 3**). Genes or proteins that were not clearly assigned to a specific gene symbol due to ambiguities in the reported PCR primers or antibodies used in western blot or ELISA procedures were also included (e.g. "COL1A1/COL1A2" or "MAPK3/MAPK1").

The most commonly investigated 10 genes or metabolites in these studies were (in descending order): runt-related transcription factor 2 (*RUNX2*), alkaline phosphatase (*ALPP*; also known as ALP), bone gamma-carboxy glutamic acid-containing protein (*BGLAP*; also known as osteocalcin), interleukin 1β (*IL1B*), prostaglandin-endoperoxide synthase 2 (*PTGS2*; also known as *COX2*), tumor necrosis factor-alpha receptor superfamily member 11B (*TNFRSF11B*; also known as osteoprotegerin, OPG), TNF superfamily member 11 (*TNFSF11*; also known as RANKL), collagen Iα1 (*COL1A1*), prostaglandin E_2 (PGE_2) and Osterix (*SP7*; identical with *OSX*) (**Supplementary Table S6**). Their expression profiles and the corresponding force-related information were summarized in **Supplementary Table S7**.

Gene List and Protein-Protein Interaction Network Analysis

Gene list analysis was done as described (**Figure 3B**). The gene list compiled from studies on dynamic forces contained 206 genes, proteins or analytes, of which 147 (~71.4%) were identified as

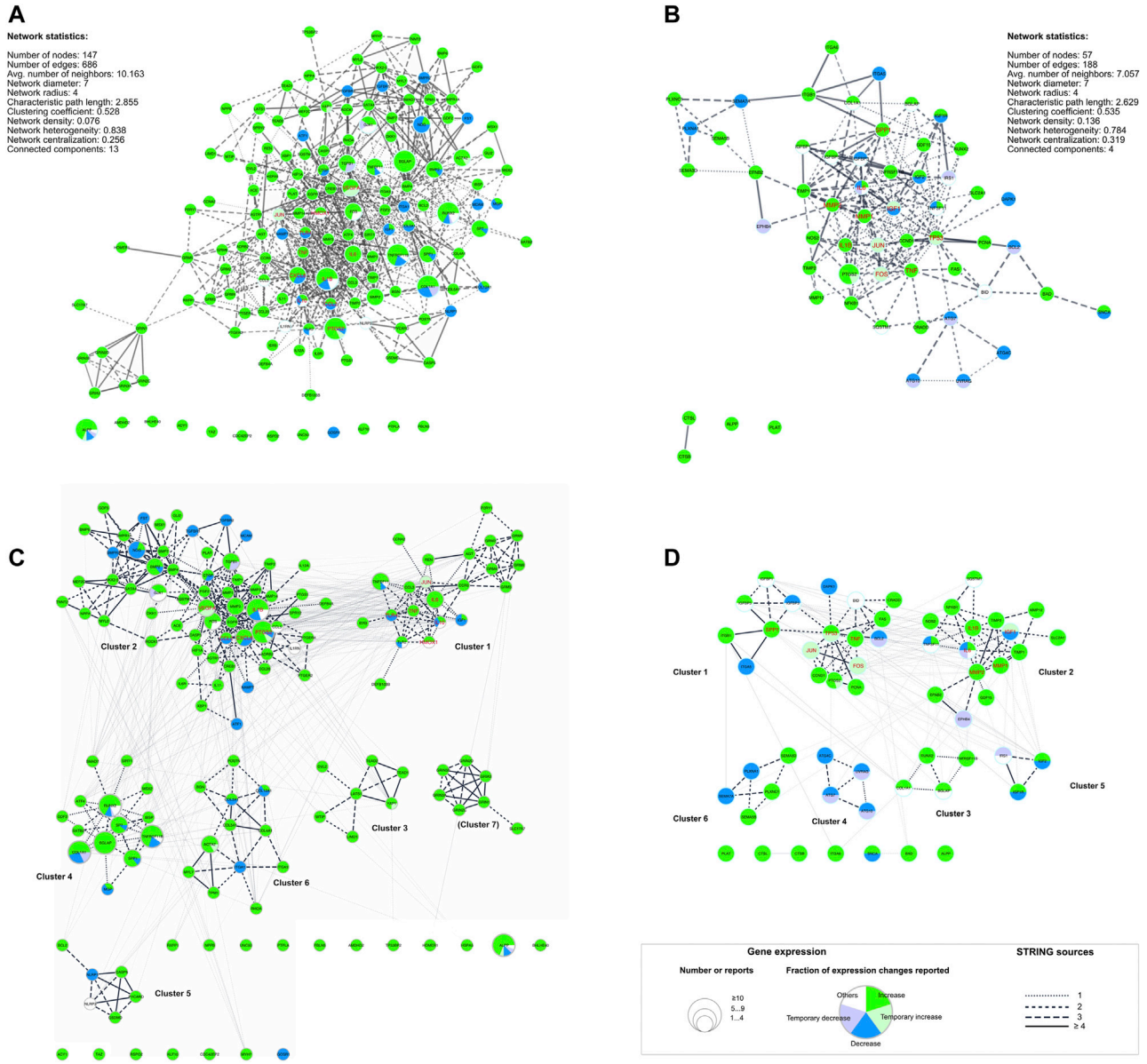

FIGURE 5 | Dynamic **(A, C)** and static **(B, C)** protein-protein-interaction (PPI) networks generated using differential expressed genes (DEG) lists (**Table 4**). **(A, B)** PPI networks including basic network statistics for each were generated using STRING-DB. **(C, D)** show the same networks as in **(A, B)** but herein, the identified subnetworks are emphasized and labeled (**Table 4**, **Supplementary Table S8**). The legend applies to all four networks: The node size corresponds to the number of reports identified for the respective underlying gene. The edges' line style depicts the number of STRING sources for the given connection. Additionally, hub genes identified with *cytoHubba* (Chin et al., 2014) were colored red (**Table 5**). For the complete networks **(A, B)** and each of the subnetworks **(C, D)** pathway analysis was applied (**Supplementary Table S8**).

differential expressed genes (DEG) as defined above. Of 115 entries from the gene list related to studies applying static forces, 56 (~48.7%) were identified as DEGs (**Table 3**).

Protein-protein interaction (PPI) networks were generated using both gene lists with *STRING-DB* as described, and network statistics for both networks were calculated (**Figure 5**). For each gene node shown in **Figure 5** the number of studies (node size) and expression pattern(s) were depicted: most of the genes included in the "dynamic" network showed (**Figure 5A**) an upregulation in gene expression after dynamic tension application. Some genes were downregulated only (e.g. *ATF1*, *BMPR2*, *TGFBR1* and *TGFBR2*) whereas a few genetic loci were reported to be either up- or down regulated (e.g. *ALPP*, *COL1A1*, *CXCL8*, *IL1B*, or *IL10*). In contrast, gene expression of the majority of genes included in the "static" PPI network was either up- or downregulated depending on the particular study (**Figure 5B**). Up- and downregulation was reported for three genes (*IL6*, *IGF*, *TNFSF11*) by different studies.

TABLE 4 | Differential expressed genes (DEGs) from the "dynamic" and "static" gene lists and their affiliation to the "dynamic" and "static" protein-protein interaction networks and one of the MCODE clusters. The corresponding networks and clusters were depicted in **Figure 5**.

Gene list	Genes in network	MCODE clusters		
		Cluster number	Number of genes (n) and genes in cluster	
"Dynamic"	Genes in the "dynamic" PPI network	#1	(22)	*AGT, CCL3, CCNA2, CCR5, DEFB103B, GRM2, GRM3, GRM4, GRM5, GRM6, HMOX1, IER3, IGF1, IL10, IL6, JUN, P2RY1, REN, TLR2, TLR4, TNF, TNFSF11*
	ACE, ACTA2, ADRB2, AGT, AGTR1, ATF1, ATF4, BCL2, BGLAP, BGN, BMP2, BMP4, BMP6, BMP7, BMPR1A, BMPR2, CASP3, CASP5, CCL2, CCL20, CCL3, CCL5, CCNA2, CCR5, COL12A1, COL1A1, COL3A1, COL4A1, COL5A1, CREB1, CTGF, CXCL8, DEFB103B, DEFB4A, DKK1, DVL2, EGFR, FGF2, FOS, FST, GATA4, GDF2, GDF5, GJA1, GLI2, GRIA3, GRIN1, GRIN2C, GRIN2D, GRIN3A, GRIN3B, GRM2, GRM3, GRM4, GRM5, GRM6, GSDMD, HIF1A, HMOX1, HOMER1, HSPA5, IBSP, IER3, IGF1, IL10, IL11, IL12A, IL1B, IL1RN, IL6, IL6R, ITGA1, ITGA3, JUN, LATS1, LIMD1, MCAM, MEF2C, MGP, MMP1, MMP14, MMP2, MMP3, MSX1, MSX2, MYH7, MYL2, MYL7, NAMPT, NKX2-5, NLRP1, NLRP3, NOG, NPPA, NPPB, P2RY1, PLAT, POSTN, PTGER2, PTGER4, PTGS1, PTGS2, PYCARD, REN, RHOA, ROCK1, RUNX2, RXFP1, SATB2, SIRT1, SLC17A7, SMAD7, SP7, SPP1, SPRY2, SQSTM1, TEAD1, TEAD2, TGFB1, TGFBR1, TGFBR2, TIMP1, TIMP2, TLR2, TLR4, TNF, TNFRSF11B, TNFSF11, TNNT2, TP53BP2, TPM1, VEGFA, WTIP, XBP1, YAP1	#2	(61)	*ACE, ADRB2, AGTR1, ATF1, BMP2, BMP4, BMP6, BMP7, BMPR1A, BMPR2, CASP3, CCL2, CCL20, CCL5, CREB1, CTGF, CXCL8, DEFB4A, DKK1, EGFR, FGF2, FOS, FST, GATA4, GDF5, GJA1, GLI2, HIF1A, IL11, IL12A, IL1B, IL1RN, IL6R, MCAM, MEF2C, MMP1, MMP14, MMP2, MMP3, MSX1, MYL2, NAMPT, NKX2-5, NOG, NPPA, PLAT, PTGER2, PTGER4, PTGS1, PTGS2, ROCK1, SPRY2, SQSTM1, TGFB1, TGFBR1, TGFBR2, TIMP1, TIMP2, TNNT2, VEGFA, XBP1*
	Genes outside the "dynamic" PPI network	#3	(7)	*DVL2, LATS1, LIMD1, TEAD1, TEAD2, WTIP, YAP1*
	ACY1, ALPP, AMDHD2, BHLHE40, CDC42EPS, FBLN5, GOSR1, KLF10, PTPLA, RSPO2, TAZ, UNC50	#4	(14)	*ATF4, BGLAP, COL1A1, GDF2, IBSP, MGP, MSX2, RUNX2, SATB2, SIRT1, SMAD7, SP7, SPP1, TNFRSF11B*
		#5	(6)	*BCL2, CASP5, GSDMD, NLRP1, NLRP3, PYCARD*
		#6	(12)	*ACTA2, BGN, COL12A1, COL3A1, COL4A1, COL5A1, ITGA1, ITGA3, MYL7, POSTN, RHOA, TPM1*
		#7	(7)	*GRIA3, GRIN1, GRIN2C, GRIN2D, GRIN3A, GRIN3B, SLC17A7*
"Static"	Genes in the "static" PPI network	#1	(18)	*BCL2, BID, CCND1, CRADD, DAPK1, FAS, FOS, IGFBP1, IGFBP3, IGFBP5, ITGA5, ITGB1, JUN, PCNA, PTGS2, SPP1, TNF, TP53*
	ATG10, ATG4C, ATG7, BAD, BCL2, BGLAP, BID, CCND1, COL1A1, CRADD, DAPK1, EFNB2, EPHB4, FAS, FOS, GDF15, IGF1, IGF1R, IGF2, IGFBP1, IGFBP3, IGFBP5, IL1B, IL6, IRS1, ITGA5, ITGA6, ITGB1, JUN, MMP1, MMP12, MMP2, NFKB1, NOS2, PCNA, PLXNA1, PLXNC1, PTGS2, RUNX2, SEMA3D, SEMA5B, SEMA7A, SLC2A1, SNCA, SPP1, SQSTM1, TIMP1, TIMP2, TNF, TNFRSF11B, TNFSF11, TP53, UVRAG	#2	(16)	*EFNB2, EPHB4, GDF15, IGF1, IL1B, IL6, MMP1, MMP12, MMP2, NFKB1, NOS2, SLC2A1, SQSTM1, TIMP1, TIMP2, TNFSF11*
		#3	(4)	*BGLAP, COL1A1, RUNX2, TNFRSF11B*
		#4	(4)	*ATG10, ATG4C, ATG7, UVRAG*
	Genes outside the "static" PPI network	#5	(3)	*IGF1R, IGF2, IRS1*
	ALPP, CTSB, CTSL, PLAT	#6	(5)	*PLXNA1, PLXNC1, SEMA3D, SEMA5B, SEMA7A*

Interestingly, 12 genes from the "dynamic" DEG list (**Figure 5A**) and 4 genes from the "static" DEG list (**Figure 5B**) were not included in their particular PPI networks (**Table 4**) including *ALPP*, which is one of the 10 most frequently investigated genes or metabolites here.

Biological processes and signaling pathways involved in the regulation of gene expression after dynamic and static tension application on hPDLCs were analyzed querying the "Biological Process" subsection of GeneOntology (GO) and GeneAnalytics' SuperPathway database. The top 10 enriched terms from the "dynamic" and "static" DEG lists were ranked according to $\log_{10}$(FDR) for GO or the SuperPathway's score, respectively. Only GO terms containing at least 5% of the genes from the particular DEG list (ratio ≥0.05) were considered (**Supplementary Table S8**).

Dynamic DEG list. The most significant GO terms describing biological processes were related to "*responses to endogenous stimuli*" (ratio: 0.05/$\log_{10}$(FDR) = 36.16; 0.05/30.14), the action of growth factors (0.09/30.14; 0.09/28.91), ossification (0.15/29.10) or differentiation (0.06/27.36) and motility/movement (0.06/27.80; 0.06/27.77; 0.06/27.54) (**Supplementary Table S8.1**). SuperPathways analysis revealed high scores of the more general ERK (ratio: 0.05/score: 115.97), Akt (0.06/96.02), and PAK (0.06/95.94) signaling pathways (**Supplementary Table S8.2**). Lower scores but higher ratios were attributed to "*Interleukin-4 and 13 signaling*" (0.18/70.16) and the "*Hippo signaling pathway*" (0.14/66.29). Nevertheless, "*Lung Fibrosis*" SuperPathway (0.27/70.05) was also part of the "top 10 list" of enriched terms.

Static DEG list. The most significant GO terms describing biological processes driven by genes from the "static" DEG list were ossification (0.06/10.08), responses to mechanical stimuli (0.05/8.97; 0.10/8.40), regulation by glucocorticoids (0.06/8.91; 0.07/7.99), positive regulation of small molecule metabolic

TABLE 5 | Top hub genes identified in both STRING networks derived from the "dynamic" (*n* = 147) and "static" (*n* = 57) tension DEG lists. Different score measures were calculated by *cytoHubba* (Chin et al., 2014). The total score cut-off was set to ≥ 2*mean total score of each network being 361511.0 for the "dynamic" network and 1209.0 for the "static" network. In both lists the hub genes were sorted in descending order according to the total score. These hub genes were colored red in **Figure 5**.

Gene list	Gene	MCODE cluster #	Local-based methods				Global-based methods							Total score (SUMscore)
			MCC	DMNC	MNC	Degree	EPC	BottleNeck	EcCentricity	Closeness	Radiality	Betweenness	Stress	
Dynamic	*IL6*	1	4949248	0.44127	43	43	55.7020	5	0.22959	84.50000	5.67469	2127.04962	18,402	4970014.6
	CXCL8	2	4946706	0.54262	33	33	54.6030	1	0.22959	76.00000	5.47594	1435.65143	12,426	4960771.5
	IL1B	2	4880486	0.43410	36	36	54.2840	8	0.22959	77.91667	5.48964	1563.68358	12,042	4894310.0
	TNF	1	4859699	0.53877	29	30	53.6020	7	0.22959	74.83333	5.44852	757.28180	5478	4866134.9
	CCL2	2	4704534	0.61776	25	25	52.0030	5	0.22959	71.41667	5.37313	192.83836	1884	4706795.5
	IL10	1	4544888	0.61015	23	23	51.3110	2	0.22959	69.33333	5.31145	221.65300	2056	4547340.4
	VEGFA	2	4450715	0.40116	43	44	55.6160	30	0.22959	85.33333	5.69525	2581.50569	18,952	4472512.8
	HMOX1	1	4357032	0.72691	16	16	47.4180	1	0.22959	65.16667	5.22921	61.59565	766	4358011.4
	JUN	1	4269668	0.63037	25	27	53.6160	3	0.22959	73.58333	5.44167	750.77011	5418	4276025.3
	PTGS2	2	4228086	0.63871	21	21	51.0090	5	0.22959	68.91667	5.32516	421.56904	3358	4232038.7
	TLR4	1	4198470	0.67581	18	18	48.3580	1	0.22959	67.25000	5.29089	124.59022	1334	4200087.4
Static	*IL6*	2	6008	0.44392	22	22	25.7170	7	0.23246	35.08333	5.88293	263.47537	1206	7595.8
	IGF1	2	6088	0.49129	20	20	25.6770	8	0.23246	33.91667	5.82928	174.76358	868	7244.9
	TP53	1	2970	0.32783	21	23	25.2950	21	0.23246	36.16667	5.97233	914.98502	2848	6866.0
	TNF	1	4527	0.46144	17	18	24.7640	8	0.23246	32.83333	5.79352	304.73126	1120	6058.8
	MMP2	2	1598	0.54053	14	16	24.5630	10	0.23246	32.75000	5.86505	581.49581	2310	4593.4
	JUN	1	3792	0.61467	12	12	23.5690	1	0.18596	28.90000	5.52530	22.03107	146	4043.8
	FOS	1	3720	0.69834	10	10	23.1720	1	0.18596	27.90000	5.48954	6.50124	60	3864.9
	IL1B	2	2246	0.48461	16	16	24.8150	1	0.23246	31.41667	5.70412	109.01102	574	3024.7
	MMP1	2	2286	0.60003	12	12	23.9330	1	0.23246	29.58333	5.65047	31.57875	252	2654.6
	SPP1	1	1134	0.49815	13	15	23.9390	4	0.23246	31.75000	5.79352	296.75685	1106	2631.0

Abbreviations: MCC, Maximal Clique Centrality; DMNC, Density of Maximum Neighborhood Component; MNC, Maximum Neighborhood Component; EPC, Edge Percolated Component.

processes (0.07/8.21), and apoptotic signaling pathways (0.09/7.88; 0.19/7.54) (**Supplementary Table S8.3**). SuperPathways related to apoptosis (0.15/76.37) and autophagy (0.07/62.14; 0.03/53.00) but also to ERK signaling (0.02/62.14), cell adhesion/ECM remodeling (0.20/61.73) and interleukin-4 and 13 signaling (0.11/56.77) were significantly enriched (**Supplementary Table S8.4** in **Supplementary Table S8**).

To identify highly connected gene clusters within each network, MCODE clustering was performed. Seven different clusters were identified in the dynamic PPI network (**Figure 5C**; **Table 4**) and six clusters in the static PPI network (**Figure 5D**; **Table 4**). Cluster #7 of the "dynamic" network consisted of seven genes, which were included in this DEG list based on one study only (Fujihara et al., 2010) (**Figure 5C**). This cluster was not further analyzed. All other clusters were re-analyzed concerning GO/Biological Process terms and SuperPathway enrichment (**Supplementary Table S8**). The same ordering and ratio cut-off were applied as above.

Generally, the identified clusters showed a higher ratio of included genes than the whole network (**Supplementary Table S8**) independent of the database used. For example, cluster #1 from the dynamic network was described significantly as "*adenylate cyclase-inhibiting G protein-coupled glutamate receptor signaling pathway*"-related (0.56/8.97). Cluster #3 from the same network was described significantly by the "*ionotropic glutamate receptor signaling pathway*" (0.24/14.10), but also by "*excitatory chemical synaptic transmission*" (0.38/6.97), whereas cluster #4 was dominated by terms related to bone mineralization and remodeling, e.g. "*osteoblast differentiation*" (0.10/12.50) and development (0.22/6.80), or "*regulation of bone resorption*" (0.08/4.09). In general, an increase in specificity (i.e. higher ratio) was also observed for SuperPathways enrichment (**Supplementary Tables S8.2,S8.4** in **Supplementary Table S8**).

Essential nodes (i.e. hub genes) in both networks were identified with *cytoHubba*. Within the network derived from the dynamic DEG list, eleven hub genes were identified (**Table 5**: *IL6*, *CXCL8*, *IL1B*, *TNF*, *CCL2*, *IL10*, *VEGFA*, *HMOX1*, *JUN*, *PTGS2*, *TLR4*; red labeled nodes in **Figures 5A,C**). Altogether, ten hub genes were identified in the network generated from the static DEG list (**Table 5**: *IL6*, *IGF1*, *TP53*, *TNF*, *MMP2*, *JUN*, *FOS*, *IL1B*, *MMP1*, *SPP1*; red labeled nodes in **Figures 5B,D**). In both networks, the hub genes were either located in cluster #1 or #2 of the particular network.

The expression of five of eleven hub genes (*VEGFA*, *JUN*, *TNF*, *IL6*, *HMOX1*) included into the "dynamic" PPI network was upregulated by dynamic tension forces. For the remaining six hub genes both up- and downregulation of gene expression was reported. For eight out of ten hub genes (*SPP1*, *JUN*, *TP53*, *TNF*, *FOS*, *IL1B*, *MMP1* and *MMP2*) upregulated expression was observed after exposure to static tension forces, and for the remaining two genetic loci (*IL6* and *IGF1*) both up- and downregulated expression was reported.

DISCUSSION

This systematic review aimed to identify and analyze studies applying tension forces to human periodontal ligament cells (hPDLCs) and to delineate the impact of different force parameters on the expression of relevant genes. Risk of bias assessment was conducted by application of published criteria using clear definitions. The commonly investigated genes, proteins, and metabolites were summarized and analyzed by gene enrichment and pathway analysis.

Commonly Used Force Apparatuses

To apply tension type of force on hPDLCs *in vitro* three different major groups of apparatuses were identified here: 1) commercially available systems. i.e. the Flexcell® Tension System or the STREX® Cell Stretching System, 2) self-designed apparatuses using commercially available components (e.g. Bioflex® or Uniflex® plates, petriPERM® or Lumox® dishes) as a central part of a stretching device, and 3) solely self-constructed apparatuses. Irrespective of the particular design, cells were grown on a flexible surface undergoing cyclic (or static) equibiaxial or uniaxial stretching in all devices.

According to this review, the Flexcell® Tension System was the most widely adopted apparatus for equibiaxial tension using Bioflex®, and uniaxial tension using Uniflex® cell culture plates. In various reports the mechanical characteristics of these elastic membranes used to apply tension to adherent cells have been studied and limitations of this method have been reported. Specifically, several studies reported a heterogeneous strain distribution within the surface used for cell cultivation and a considerable interference of other types of force (e.g. compression and shear stress) (Gilbert et al., 1994; Vande Geest et al., 2004; Matheson et al., 2006). In the Flexcell® Tension system using Bioflex® plates without a biaxial loading post, equibiaxial strain was mostly focused in the center of the membrane, whereas almost pure uniaxial strain was found at the rigid rim of the well (Gilbert et al., 1994). We consider this setup to be similar to several self-designed apparatuses using Bioflex® plates. As such, we propose, that the heterogeneous strain distribution might also apply to these setups. In contrast, in Flexcell Tension systems using Bioflex® plates with a "*biaxial loading post*" the constant biaxial strain region was located in the membrane area on the post, whereas off-post large radial strain was produced (Vande Geest et al., 2004). Application of uniaxial strain with Flexcell's Uniflex® culture plates using an uniaxial loading post results in almost uniform strain distribution in the membrane area on-post (Matheson et al., 2006). Irregular strain distribution might occur, anyhow, comparing longitudinal and transverse orientation together with a certain amount of compressive strain (Matheson et al., 2006). As a consequence of the heterogenous strain distribution, only some of the cells receive the desired mechanical stimulation (Matsuda et al., 1998) and thus gene expression reflects the average of all cells in the examined area. Irrespective of the not entirely standardized strain parameters, the tension systems identified herein have proven to be efficient models to mimic the *in vivo* mechanical microenvironment to investigate the related biological

reactions on the cellular level. In 2017, the "BioFlex® Cell Seeder" (Flexcell Inc.) was introduced to the market to be used in combination with the BioFlex cell culture plates. Limiting cell growth within a defined area providing uniform strain distribution increases the reproducibility of cell seeding and exposure against mechanical cues. However, none of the included studies reported the application of this device.

The PDL comprises different types of collagen, including type I (about 80%), type III (15%), type V, type VI, and type XII collagen (Berkovitz et al., 2009, pp. 179–180). Most frequently BioFlex plates pre-coated with collagen type I were used, but pronectin coating was also reported (Jacobs et al., 2013). Other silicone-based membranes were used together with coatings of gelatin (Tantilertanant et al., 2019a; b) or collagen type I and/or fibronectin (Konstantonis et al., 2014; Papadopoulou et al., 2019). Further studies did not report any coating, particularly when using PetriPerm or Lumox dishes. Diercke et al. (2011) applied a combination of collagen type-I and fibronectin to coat the PetriPerm dishes. Commonly coatings were applied to increase the biocompatibility of the membrane surface.

Most recently, three-dimensional (3D) cell culture studies have reached increasing significance since they allow for a better simulation of the cells' extracellular matrix (ECM) and *in vivo* microenvironment. Providing structural support and signal transduction to the cells, ECM is involved in various biological processes, including cell migration, proliferation, differentiation and intercellular communication (Dieterle et al., 2021). For simulation matrices made from collagen, polylactic-co-glycolic acid (PLGA) and hydrophilically modified poly-L-lactide (PLLA) are used in cytomechanics (Yang et al., 2015; Janjic et al., 2018). Though 2D coating resembles the *in vivo* situation more than tissue culture plastic alone, differences in porosity, microarchitecture and local rigidity in comparison to 3D substrates effect cell migration (Doyle et al., 2015) and mechanotransduction (Yang et al., 2015).

Interestingly, only two studies reported on the effects of tension force applied to cells within 3D scaffolds (Von den Hoff, 2003; Ku et al., 2009). The first one focused on the assessment of tension force exerted to the substrate by the cells (Von den Hoff, 2003). With only one qualified study (Ku et al., 2009) a comparison between 2D and 3D cell culture setups seemed not conclusive. Yang et al. (2015) emphasized that 3D cell culture techniques are yet not standardized and suggested to establish tissue specific scaffolds along with the identification of appropriate cell densities. The insufficient knowledge on 3D scaffolds might explain its infrequent use to study the effect of tension force on hPDLCs.

Rationale for Force Parameters

Tension type of force was applied either statically or dynamically on hPDLCs. As such, the selection of the relevant model parameters (cell type, type of force and its duration, magnitude and frequency) was mostly based on the purpose of the specific study, being either the simulation of a clinical situation (occlusal forces or OTM), or to investigate the force-related expression of specific genes, group of genes or pathways. Due to the general objectives of the studies analyzed herein, the selection of cell type and type of force seems plausible. The remaining parameters were selected according to: 1) *in vivo* evidence from animal models simulating OTM or measurement of bite force in human subjects (e.g. He et al., 2004; Fujihara et al., 2010; Li et al., 2013; Li et al., 2014; Ren et al., 2015; Tantilertanant et al., 2019a); 2) finite element analysis to study the biomechanical behaviour of the PDL (e.g. Howard et al., 1998; Kletsas et al., 2002; Konstantonis et al., 2014; Chen et al., 2015); 3) *in vitro* studies defining an "optimal" window to study the expression of specific genes or pathways (e.g. Basdra et al., 1996; Hao et al., 2009; Huelter-Hassler et al., 2017; Hülter-Hassler et al., 2017).

Force duration: Continuous exposure to a stretching force is considered as an appropriate surrogate for *in vivo* forces applied by fixed appliances during OTM (Ziegler et al., 2010; Steinberg et al., 2011). As such, time intervals for application were chosen reflecting different stages in OTM or other clinically relevant conditions (Ziegler et al., 2010; Goto et al., 2011; Steinberg et al., 2011). According to our results, the maximum force duration varied between 0.5 h and 15 days. The most commonly used force duration in dynamic tension experiments were either 48 h or 72 h, and static tension was most commonly applied for 12 h. Under experimental *in vitro* conditions the maximum application time is, in fact, limited by the feeding intervals of the cells and the apparatus used. With static tension, cell proliferation should be considered as an influencing factor – especially during long-term force application. Cells undergoing cell division might transiently loose contact to the stretched surface. After reattachment to the already deformed surface they might not be further subjected to stretching force.

Force magnitude: Similar to force duration, force magnitude is a relevant experimental parameter for simulation of both, dynamic and static tension forces. Based on the studies considered herein, force magnitude selection was again mostly related to the objective of the study: 1) expression of a specific gene in response to tension force application allowing to define the dynamic range along with the range of optimum forces (e.g. Long et al., 2002; Agarwal et al., 2003), and 2) to simulate a clinical situation (e.g. Long et al., 2002; Li et al., 2014). In most studies, 10% dynamic tension was applied to mimic the physiologic conditions of occlusal force or OTM (e.g. Fujihara et al., 2010; Li et al., 2014; Ren et al., 2015). This force magnitude was based on *in vivo* studies, which either focused on tissue remodeling and tooth movement after exposure to different levels of orthodontic force (King et al., 1991; Gonzales et al., 2008), or studies on tooth mobility in response to different force levels (Mühlemann, 1954; Mühlemann and Zander, 1954). Several studies (Howard et al., 1998; Kletsas et al., 2002; Konstantonis et al., 2014; Chen et al., 2015) took results from finite element analysis into consideration to select the force magnitude best corresponding with the real clinical situation (Andersen et al., 1991; Natali et al., 2004; Dong-Xu et al., 2011).

Force frequency: To apply dynamic tension different frequencies were adopted. Selection of appropriate force frequencies mostly relied on two different rationales: 1) experience from previous *in vitro* studies either using similar setups or defining appropriate frequency ranges to study the

expression of specific genes (Yamaguchi et al., 1994; Long et al., 2002; Ma et al., 2015; e.g.; Ren et al., 2015; Memmert et al., 2020), and 2) deduction from the real clinical situation, e.g. tooth contact rates during sleep (He et al., 2004) or an average masticatory cycle (Tantilertanant et al., 2019a). In this context various estimates of contact rates were reported so far, e.g. contacts ranging from 17.2 to 104.3 contacts/h (Yamashita et al., 1993), a mean frequency of masticatory cycle of ~70 rpm (Pini et al., 2002), or 1.5–2 Hz (Woda et al., 2006).

According to our review, the most commonly used frequency was 0.1 Hz for dynamic equibiaxial tension and 0.5 Hz for dynamic uniaxial tension. Although the real frequency of tension applied on the PDL cells during OTM yet remains unknown (Long et al., 2002; Padial-Molina et al., 2013; Wang Y. et al., 2019), the clinical and technical evidence summarized in this review will provide clues for design of related experiments.

Most Frequently Investigated Genes, Proteins and Metabolites

To identify the most relevant mechanical responses during OTM, we focused on the top 10 most frequently investigated genes, proteins and metabolites: *RUNX2*, *ALPP, BGLAP*, *IL1B*, *PTG2*, *TNFRSF11B*, *TNFSF11*, *COL1A1*, PGE_2 and *SP7* (**Supplementary Table S6**). According to their functional contribution we grouped these genes into three categories: genes related to osteogenesis (*RUNX2*, *SP7, ALPP*, *BGLAP, COL1A1*), osteoclastogenesis (*TNFRSF11B*, *TNFSF11*), and inflammation (*IL1B*, *PTGS2*, PGE_2).

Osteogenesis

RUNX2 regulation is an integral and central part in the development and remodeling not only of osseous tissue but also of the periodontal ligament (Ziros et al., 2008). PDL cells are capable of differentiation into osteoblasts or cementoblasts in response to mechanical stimulation (Ziros et al., 2002). *RUNX2* upregulation was reported in 19/26 (73%) studies using either RT-qPCR or both RT-qPCR and western blotting. Decrease, temporary changes or other types of regulation were found in the remaining studies (7/16, ~27%). Although several studies revealed partially contradictory results, it was well-supported that *RUNX2* expression increased within the first 12 h of tension application.

Another essential transcription factor in the osteogenic pathway acting downstream of RUNX2 is SP7 (also known as Osterix), which belongs to the zinc finger-containing transcription factor SP family (Tang et al., 2012; Li et al., 2013; Li et al., 2015). Significant gene and/or protein upregulation of *SP7* in response to tension was reported in 9/10 (90%) of the relevant studies, whereas only one study reported downregulation of gene expression and temporary upregulation of the corresponding protein (Li et al., 2013). The authors concluded, that this difference might be due to complex regulation mechanisms and modifications occurring during its transcription and translation (Li et al., 2013).

Alkaline phosphatase (ALPP) also plays a crucial role in the initiation of osteogenic differentiation and bone remodeling (Chen et al., 2014). In all of the 24 relevant studies, *ALPP* gene expression was determined using either semiquantitative or quantitative PCR. ALPP protein was quantified in cell lysates using western blots, ELISA or enzyme activity assays. Significant upregulation in response to tension <12% was reported in 17/24 (71%) of the studies, mostly during the first 12 h of force application.

As the most abundant non-collagenous bone-matrix protein, bone gamma-carboxy glutamic acid-containing protein (BGLAP; osteocalcin) is a late marker of osteoblast differentiation and mineralization (Chen et al., 2014). Significant upregulation of BGLAP in response to tension was reported in 16/18 (89%) of the studies. In contrast, one study reported a slight decrease in *BGLAP* gene expression and it was assumed that an enhanced cell proliferation of young osteoblasts might be responsible (Jacobs et al., 2013). Another study described a transient upregulation of BGLAP following 3 h of exposure against tension force (Qin and Hua, 2016).

The extracellular matrix (ECM) of the periodontal ligament mainly consists of fibrillar collagens, among which type I collagen accounts for ~75% (Kaku and Yamauchi, 2014). The latter is composed of alpha-1 (COL1A1) and alpha-2 (COL1A2) type I collagen chains. COL1A1 is confirmed to be essential for bone remodeling and osteoblastic differentiation in response to tension during OTM (Birkedal-Hansen et al., 1977; Jacobs et al., 2013). Significant upregulation of protein expression was found in 8/13 (62%) of related studies after exposure to ≤12% of tension. Contradicting expression patterns have been reported, which might be due to the heterogeneity of the PDL cells used, digestion of COL1A1 by MMP1 (Nemoto et al., 2010), or the inhibitory effect of IL1β and TNFα on *COL1A1* gene expression (Sun et al., 2017). Although inconsistencies were partially found, upregulation of *COL1A1* in response to tension was confirmed in the majority of the studies considered here.

Osteoclastogenesis

Bone remodeling is primarily regulated by a closely interrelated system of receptors and mediators including TNFSF11 (receptor activator of nuclear factor kappa ligand; RANKL), its cellular receptor, receptor activator of NF-kappaB (RANK), and TNFRSF11B (osteoprotegerin, OPG) ultimately maintaining the balance between osteogenesis and osteoclastogenesis (Krishnan et al., 2015). As a decoy receptor for RANKL, OPG suppresses the binding between RANKL and RANK and thus inhibits osteoclastogenesis and bone resorption (Liao and Hua, 2013).

Upregulation of OPG gene expression and/or protein synthesis was reported in 11/14 (79%) of the included studies. Due to the heterogeneity of force parameters, the correlation between gene expression, force duration and/or force magnitude can only partly be defined. The regulation of RANKL expression showed large variability in comparison to OPG: only 57% (8/14) of the relevant studies reported an upregulation of both gene and protein expression after force application, whereas the remaining studies showed inconsistent expression patterns.

It is commonly accepted, that an increased RANKL/OPG ratio favours osteoclastogenesis, meaning an upregulation of RANKL

in parallel with a downregulation/lower induction of OPG (Boyce and Xing, 2007). The RANKL/OPG ratio was reported in three studies included into this review (Nogueira et al., 2014b; Konstantonis et al., 2014; Jacobs et al., 2015). Two of these studies identified a decreasing RANKL/OPG ratio compatible with a more intensive bone formation after exposure to minor tension forces (≤10%): a temporary decrease of the RANKL/OPG ratio was found by Jacobs et al. (2015) using RT-qPCR, whereas Liao and Hua (2013) reported an increasing OPG/RANKL ratio for both, gene and protein expression. Higher tension forces (20%) were reported to induce an increased RANKL/OPG ratio at both gene and protein levels indicating net bone resorption (Nogueira et al., 2014b).

Inflammation

The response of the PDL to mechanical stress has been characterized as an aseptic transitory inflammatory process, which is regulated by various mediators, including cytokines and chemokines (Lee et al., 2012). Interleukin 1β (IL1B) is an upstream cytokine involved in many inflammatory processes (Lee et al., 2012) and in osteoclast formation, differentiation and activation (Long et al., 2001). Upregulation was reported in 75% (12/16) of the relevant studies depending on the particular duration and magnitude of force application. A reduced expression or inconsistent expression patterns during exposure to forces of various magnitudes and durations were reported in the remaining 4/16 (25%) studies. These differences have been mainly attributed to the particular magnitude of tension: a lower magnitude attenuates the inflammatory response, while a higher one elicits inflammation (Long et al., 2001).

Prostaglandin-endoperoxide synthase 2 (PTGS2; also known as COX2) is known as a key regulator enzyme of the eicosanoid biosynthesis pathway and is thus also involved in prostaglandin E_2 (PGE_2) synthesis (Nogueira et al., 2014b). Amongst others, the activity of PTGS2 and the synthesis of PGE_2 is particularly amplified by pro-inflammatory stimuli including IL1B (Nogueira et al., 2014b). PGE_2 mediates bone resorption under physiological and pathological conditions, and is centrally involved in both, the response of periodontal tissue to mechanical stress and the pathogenesis of periodontitis (Shimizu et al., 1998). Herein, *PTGS2* gene expression and PGE_2 synthesis were reported in 14 and 12 of the included studies, respectively. Of these studies, 9 focused on *PTGS2* and PGE_2, among which 8/9 studies (~89%) found an increasing transcription of the *PTGS2* gene and/or PGE_2 concentration after mechanical stimulation correlating with force duration and force magnitude. The data of the remaining studies revealed mixed expression patterns of *PTGS2* and PGE_2 activity after force exposure, which might be attributable to anti-inflammatory effects of lower tension forces (Long et al., 2002). Taken together *PTGS2* expression and PGE_2 production is induced by the exposure of cell cultures to tensions forces and it is positively correlated to force duration and force magnitude.

Reasons for Heterogeneity of Genes/Proteins/Metabolites Regulation

Considering the list of the most commonly considered genes, inconsistencies between gene and protein expression were found in several reports. The observed non-proportional relationship between gene expression and protein activity can be attributed to the time lag between transcription and translation. This time lag might be prolonged by post-transcriptional processing and degradation of the transcripts, as well as post-translational modifications like phosphorylations (e.g. Li et al., 2013; Ren et al., 2015) or proteolytic cleavage (e.g. Wang et al., 2013; Zhuang et al., 2019). The experimental heterogeneity identified among different studies reporting force-related expression of the same genes can be attributed to: 1) donor-related issues (e.g. age of donor), 2) hPDLC isolation-related issues, 3) cell culture of hPDLCs (e.g. cell culture medium, passage number), 4) reference gene selection in (s)qPCR experiments, and 5) heterogeneity of force parameters. In addition, the pooling of cells from different donors (Stoddart et al., 2012), the seeding density of cells and thus the amount of confluency and the different cell culture media used might have caused heterogeneity of results.

All studies included herein isolated hPDLCs from teeth that have been removed due to orthodontic reasons. When considering all studies the age of donors ranged from 8 to 40 years, but within each study the donors had the same age. This is even more important, since the phenotype of hPDLCs, specifically the proliferation rate, osteogenic potential or *in vitro* life span clearly depends on the age of the donor (Marchesan et al., 2011). Moreover, force-related gene expression has been reported to be significantly dependent on the age of the donor (Mayahara et al., 2007). Accordingly, many studies reported considerable functional inconsistencies between different cell samples most likely caused by the biological heterogeneity among different donors (Monnouchi et al., 2011; Yuda et al., 2015; Papadopoulou et al., 2017; Arima et al., 2019). For experimental simulation of the age, several studies focusing on cellular senescence simply used different passage numbers, supposing a correlation between the passage number and the age. Thus, they designated passage numbers ranging from 3 to 7 as "*young*" and those ranging from 18 to 24 as "*old*" or "*senescent*" (Shimizu et al., 1997; Abiko et al., 1998; Ohzeki et al., 1999; Miura et al., 2000; Konstantonis et al., 2014). Generally, passage numbers of hPDLCs used in the included studies ranged between 2 and 15 (**Supplementary Table S2**). A maximum passage number of 20 was reported in a study using limited dilution cloning (Long et al., 2001). Differences in morphology and biological activity between early and late passages were reported, with the early passages resembling fibroblasts characteristic of original tissue more closely (Marchesan et al., 2011). Therefore, the use of early passage (passage ≤7) of primary culture is recommended to maintain most of the original cell phenotype (Marchesan et al., 2011).

Exclusively all studies analyzed herein applied tension force to human periodontal ligament cells (hPDLCs). These cells were commonly isolated from the middle third of the roots from teeth removed due to mostly orthodontic reasons using two different

cell isolation techniques, i.e. the "explant" (Brunette et al., 1976; Somerman et al., 1988) or the "digestion" technique (Brunette et al., 1976; Seo et al., 2004). Different terms and abbreviations were used to identify these cells, including "hPDLF", hPDL-fibroblasts", "hPDL fibroblasts", "hPDLC", "hPDLCs", "hPDL cells", "hPDLSCs" and "hPDLS cells". In order to identify and include all relevant studies on this topic into this review, the search strategy considered all terms and abbreviations identified. In all cases, PDL tissue derived from premolars or third molars. Both isolation techniques unequivocally result in a heterogeneous mixture of different cell types (Yamaguchi et al., 2002; Marchesan et al., 2011), though the "digestion" technique was shown to result in a cell population enriched with mesenchymal stem cells (Seo et al., 2004). Therefore, hPDLCs should be regarded as a heterogeneous cell population consisting of cells originating from different lineages. Most recently, *in-vitro* cell type verification was increasingly used including several studies on hPDLCs (Marchesan et al., 2011), that were also reported in some of the included studies herein, i.e. flow cytometric analysis of cell surface markers (Wang H. et al., 2019; Wu et al., 2019a), osteogenic potential as reflected by ALP staining and/or Ca^{2+} deposition (Jacobs et al., 2018; Wang H. et al., 2019), cell type specific gene expression pattern (Memmert et al., 2019), and immunohistochemical staining of vimentin and cytokeratin (Sun et al., 2017; Yu et al., 2018; Wang Y. et al., 2019).

Careful reference gene selection is essential to overcome variations in RT-qPCR experiments and to enhance comparability between various studies. In order to reduce the risk of bias in qPCR experiments, the "*Minimum Information for Publication of Quantitative Real-Time PCR Experiments* (MIQE)" guidelines were established, with reference gene selection being one of the most crucial steps in RT-qPCR establishment (Bustin et al., 2009). As such, the MIQE guidelines cover some of the reporting and methodology-related risk of bias criteria considered in the present review, directly or indirectly related to RT-qPCR. According to the present systematic review, *GAPDH* or *ACTB* were the most frequently adopted reference genes for qPCR experiments. The rationale for reference gene selection was only rarely stated. Only recently, MIQE reporting gained more attention (Janjic Rankovic et al., 2020). Several studies evaluated reference gene selection specifically focusing on hPDLCs in different areas of dentistry (Kirschneck et al., 2017; Setiawan et al., 2019; Nazet et al., 2020).

The heterogeneity of force parameters and the limitations of several experimental set-ups as discussed previously might also have considerable impact on the consistency and comparability between studies as included herein. Additionally, optimal force duration, magnitude and frequency mainly depend on the experimental design and the specific objectives of the study.

In Silico Analysis of Gene Lists

To gain additional insights into the biological processes and pathways regulated by dynamic or static tension forces, gene-set enrichment analysis and protein-protein interaction (PPI) network construction were applied. Moreover, the most influential genes and sub-networks were identified in both PPI networks. The gene lists were created from the studies identified in this systematic review. To increase specificity, only those genes showing clear force-dependent expression were included.

Gene-set enrichment analysis: In general, gene-set enrichment analysis is applied to expression data of individual genes obtained by techniques like microarrays, next-generation sequencing or proteomics (Hutchins, 2014; Mooney and Wilmot, 2015). As such, the gene list contains ranking data (e.g. confidence scores, fold changes or similar quantitative information) or is unranked (Hung, 2013; Haw et al., 2020). Both types are then used for over-representation and/or gene-set enrichment analysis to identify relevant signaling and/or regulation pathways. To increase specificity of the gene lists, gene expression data was restricted to the criteria specified in Materials and Method. Additionally, protein expression data was excluded due to the heterogeneity of the methods used for quantification (quantification via western blotting or ELISA vs enzyme activities) and the specificity of some of the antibodies used in the immunoassays. The results of gene enrichment and the pathway analysis showed a close relationship with osteogenesis, osteoclastogenesis and apoptosis. These findings were consistent with the reporting of the relevant studies identified.

The search strategy used herein identified 18 reports applying tension to hPDLCs with subsequent microarray or RNA-seq analysis: 15 studies applied dynamic tension and 3 static tension. All studies reported the most significantly up- and down-regulated genes applying different cut-offs. A re-analysis was not possible, since full (raw) data was publicly not available. Nevertheless, data from these studies was included if qualified reanalysis using (s)qPCR or protein expression was reported additionally.

Protein-Protein Interaction Networks

Complementary to pathway enrichment analysis, protein-protein interaction networks were generated for dynamic and static tension gene sets using the "*Search Tool for the Retrieval of Interacting Genes/Proteins*" database (STRING-DB), which incorporates regularly updated data from different biological pathway and scientific literature databases (Szklarczyk et al., 2019). As such, STRING-DB not only contains data on experimental derived PPI, but also functional annotation from literature and computational predictions. For each individual PPI pair a confidence score is given (range: 0–1), with higher scores are "*meant to express an approximate confidence,* [. . .], *of the association being true, given all the available evidence*" (Szklarczyk et al., 2019; p. D608). Both networks were analyzed regarding subclusters and most-influential nodes (i.e. hub genes) and 7 (dynamic) and 6 (static) subclusters were identified. Subsequent pathway enrichment analysis showed a more specific enrichment of GO/Biological Process terms and GeneAnalytics SuperPathways.

We applied a confidence score cut-off ≥ 0.700, thus only high confidence interactions were included. Interestingly, in both networks several differentially expressed genes were not integrated, including alkaline phosphatase (ALPP), being one of the most frequently analyzed genes/proteins identified herein. With the application of a confidence score cut-off of ≥0.400, thus including medium confidence interactions, ALPP was integrated

into dynamic network due to co-mentioning in PubMed abstracts with bone sialoprotein 2 (IBSP; score: 0.407), osteopontin (SPP1; 0.438), bone morphogenetic protein 2 (BMP2; 0.434), RUNX2 (0.495), and osteocalcin (BGLAP; 0.627). GOSR1, CDC42EP2, UNC50, ACY1, and AMDHD2 were still not integrated. Application of the same threshold to the static network would integrate all nodes including ALPP (ALPP – RUNX2: 0.495; ALPP – BGLAP: 0.627; ALPP – SPP1: 0.438).

Interestingly, cluster #7 of the dynamic network consisted of nodes, that were contributed to the gene list based on one study (Fujihara et al., 2010). This finding demonstrates the limits of the approach applied: both lists of differentially expressed genes were compiled based on publications identified in our search strategy. The more specific an individual study deals with a specific aspect, the more specific it will be described by gene-list enrichment analysis and network cluster analysis. As such, measures were taken, to reduce this impact: 1) the genes included in our gene lists were those only with reports on changes in gene expression due to mechanical stimulation. 2) Additionally, cut-offs were applied to GO, pathway enrichment and PPI network construction, to exclude incorporation of data too general, that means very general biological processes with thousands of genes involved.

Meta-Analysis

Initially, a meta-analysis of the ten most frequently analyzed genes or metabolites was intended to supplement the findings. Unfortunately, due to heterogeneity of the experimental conditions, including force parameters, cell culture, reference gene selection in RT-qPCR experiments and incomplete reporting especially concerning the statistical unit, this was not further considered.

Several identified studies showed that not only gene and protein expression is regulated by tension application, but also post-translational modifications like proteolytic cleavage, activation by GTP-binding, phosphorylations and protein translocation between nucleus and cytoplasm, or cytoplasm and extracellular space. Regulation of second messengers like cAMP (Ngan et al., 1990) and metabolites like glutamate (Fujihara et al., 2010), NOx (Pelaez et al., 2017) and ATP (Tantilertanant et al., 2019a) are also effected by tension application, as well as microRNA and long non-coding RNAs (Chen et al., 2016). Epigenetic effects on gene expression also should be taken into account, since several genes discussed herein like *COL1A1* (Kaku and Yamauchi, 2014) and *RUNX2* (Montecino et al., 2015) are known to be under epigenetic control (Francis et al., 2019).

Summary

In this systematic review we summarized relevant information about tension application on hPDLCs *in vitro* and assessed potential reporting and methodology-associated risk of bias related to this issue. Due to the enormous variety of apparatus in both, dynamic and static tension experiments, it is not possible to universally define optimum force parameters including force magnitude, duration and frequency. However, clinically relevant parameters were identified, that can be used as a reference for *in vitro* studies. Taken together, quantitative and qualitative information on mechanical stimulated gene and protein regulation and a comprehensive network analysis have provided more clear insights into the mechanisms involved in the OTM.

Future studies should focus on the comparison of dynamic and static tension. There is also a need to elucidate the differences between the application of equibiaxial and uniaxial tension in more detail, to develop an optimal *in vitro* model for the simulation of orthodontic force, and to provide more reliable evidence for clinical treatment.

DATA AVAILABILITY STATEMENT

The original contributions presented in the study are included in the article/**Supplementary Material**. Further inquiries can be directed to the corresponding author.

AUTHOR CONTRIBUTIONS

Conceptualization: UB, CS, MJR; Methodology: UB, CS, MJR, SO; Formal analysis and investigation: CS, MJR, UB; Writing-original draft preparation: CS, MJR, UB; Writing-review and editing: CS, MJR, UB, SO, MF, AW; Resources: UB, CS, MJR, AW; Supervision: UB.

FUNDING

CS was supported by a grant from the China Scholarship Council (CSC File No 201809370043).

ACKNOWLEDGMENTS

The authors wish to thank Dipl.-Ing. Thomas Stocker (Biomechanics Laboratory, Department of Orthodontics and Dentofacial Orthopedics, University Hospital, LMU Munich) for helpful discussions during the preparation of the manuscript.

SUPPLEMENTARY MATERIAL

The Supplementary Material for this article can be found online at: https://www.frontiersin.org/articles/10.3389/fbioe.2021.695053/full#supplementary-material

REFERENCES

Abiko, Y., Shimizu, N., Yamaguchi, M., Suzuki, H., and Takiguchi, H. (1998). Effect of Aging on Functional Changes of Periodontal Tissue Cells. *Ann. Periodontol.* 3 (1), 350–369. doi:10.1902/annals.1998.3.1.350

Agarwal, S., Long, P., Al, S., Piesco, N., Shree, A., and Gassner, R. (2003). A central Role for Nuclear factor-κB Pathway in the Antiinflammatory and Proinflammatory Actions of Mechanical Strain. *FASEB J.* 17 (8), 1–15. doi:10.1096/fj.02-0901fje

Andersen, K. L., Pedersen, E. H., and Melsen, B. (1991). Material Parameters and Stress Profiles within the Periodontal Ligament. *Am. J. Orthod. Dentofacial Orthopedics* 99 (5), 427–440. doi:10.1016/s0889-5406(05)81576-8

Arima, M., Hasegawa, D., Yoshida, S., Mitarai, H., Tomokiyo, A., Hamano, S., et al. (2019). R-spondin 2 Promotes Osteoblastic Differentiation of Immature Human Periodontal Ligament Cells through the Wnt/β-Catenin Signaling Pathway. *J. Periodont Res.* 54 (2), 143–153. doi:10.1111/jre.12611

Ashburner, M., Ball, C. A., Blake, J. A., Botstein, D., Butler, H., Cherry, J. M., et al. (2000). Gene Ontology: Tool for the Unification of Biology. *Nat. Genet.* 25 (1), 25–29. doi:10.1038/75556

Bader, G. D., and Hogue, C. W. (2003). An Automated Method for Finding Molecular Complexes in Large Protein Interaction Networks. *BMC Bioinformatics* 4, 2. doi:10.1186/1471-2105-4-2

Banes, A. J., Gilbert, J., Taylor, D., and Monbureau, O. (1985). A New Vacuum-Operated Stress-Providing Instrument that Applies Static or Variable Duration Cyclic Tension or Compression to Cells *In Vitro*. *J. Cell Sci.* 75, 35–42. doi:10.1242/jcs.75.1.35

Basdra, E. K., Kohl, A., and Komposch, G. (1996). Mechanische Dehnung von Desmodontalfibroblasten - eine Untersuchung zur zytoskelettalen Beteiligung. *J. Orofac Orthop/Fortschr Kieferorthop* 57 (1), 24–30. doi:10.1007/BF02189045

Baumert, U., Golan, I., Becker, B., Hrala, B. P., Redlich, M., Roos, H. A., et al. (2004). Pressure Simulation of Orthodontic Force in Osteoblasts: a Pilot Study. *Orthod. Craniofac. Res.* 7 (1), 3–9. doi:10.1046/j.1601-6335.2003.00270.x

Ben-Ari Fuchs, S., Lieder, I., Stelzer, G., Mazor, Y., Buzhor, E., Kaplan, S., et al. (2016). GeneAnalytics: An Integrative Gene Set Analysis Tool for Next Generation Sequencing, RNAseq and Microarray Data. *OMICS: A J. Integr. Biol.* 20 (3), 139–151. doi:10.1089/omi.2015.0168

Berkovitz, B. K. B., Holland, G. R., and Moxham, B. J. (2009). *Oral Anatomy, Histology and Embryology*. 4th Ed. Edinburgh: Mosby.

Birkedal-Hansen, H., Butler, W. T., and Taylor, R. E. (1977). Proteins of the Periodontium. *Calcif. Tissue Res.* 23 (1), 39–44. doi:10.1007/BF02012764

Boyce, B. F., and Xing, L. (2007). Biology of RANK, RANKL, and Osteoprotegerin. *Arthritis Res. Ther.* 9 (Suppl. 1), S1. doi:10.1186/ar2165

Brunette, D. M., Melcher, A. H., and Moe, H. K. (1976). Culture and Origin of Epithelium-like and Fibroblast-like Cells from Porcine Periodontal Ligament Explants and Cell Suspensions. *Arch. Oral Biol.* 21 (7), 393–400. doi:10.1016/0003-9969(76)90001-7

Bustin, S. A., Benes, V., Garson, J. A., Hellemans, J., Huggett, J., Kubista, M., et al. (2009). The MIQE Guidelines: *M*inimum *I*nformation for Publication of Quantitative Real-Time PCR *E*xperiments. *Clin. Chem.* 55 (4), 611–622. doi:10.1373/clinchem.2008.112797

Chang, M., Lin, H., Fu, H., Wang, B., Han, G., and Fan, M. (2017). MicroRNA-195-5p Regulates Osteogenic Differentiation of Periodontal Ligament Cells under Mechanical Loading. *J. Cell. Physiol.* 232 (12), 3762–3774. doi:10.1002/jcp.25856

Chen, N., Sui, B. D., Hu, C. H., Cao, J., Zheng, C. X., Hou, R., et al. (2016). microRNA-21 Contributes to Orthodontic Tooth Movement. *J. Dent. Res.* 95 (12), 1425–1433. doi:10.1177/0022034516657043

Chen, Y.-J., Shie, M.-Y., Hung, C.-J., Wu, B.-C., Liu, S.-L., Huang, T.-H., et al. (2014). Activation of Focal Adhesion Kinase Induces Extracellular Signal-Regulated Kinase-Mediated Osteogenesis in Tensile Force-Subjected Periodontal Ligament Fibroblasts but Not in Osteoblasts. *J. Bone Miner. Metab.* 32 (6), 671–682. doi:10.1007/s00774-013-0549-3

Chen, Y., Mohammed, A., Oubaidin, M., Evans, C. A., Zhou, X., Luan, X., et al. (2015). Cyclic Stretch and Compression Forces Alter microRNA-29 Expression of Human Periodontal Ligament Cells. *Gene* 566 (1), 13–17. doi:10.1016/j.gene.2015.03.055

Chin, C.-H., Chen, S.-H., Wu, H.-H., Ho, C.-W., Ko, M.-T., and Lin, C.-Y. (2014). *cytoHubba*: Identifying Hub Objects and Sub-networks from Complex Interactome. *BMC Syst. Biol.* 8 (Suppl. 4), S11. doi:10.1186/1752-0509-8-S4-S11

Cho, J.-H., Lee, S.-K., Lee, J.-W., and Kim, E.-C. (2010). The Role of Heme Oxygenase-1 in Mechanical Stress- and Lipopolysaccharide-Induced Osteogenic Differentiation in Human Periodontal Ligament Cells. *The Angle Orthodontist* 80 (4), 740–747. doi:10.2319/091509-520.1

Cohn, S. A. (1965). Disuse Atrophy of the Periodontium in Mice. *Arch. Oral Biol.* 10 (6), 909–919. doi:10.1016/0003-9969(65)90084-1

Deschner, J., Rath-Deschner, B., Reimann, S., Bourauel, C., Götz, W., Jepsen, S., et al. (2007). Regulatory Effects of Biophysical Strain on Rat TMJ Discs. *Ann. Anat. - Anatomischer Anzeiger* 189 (4), 326–328. doi:10.1016/j.aanat.2007.02.004

Diercke, K., Kohl, A., Lux, C. J., and Erber, R. (2011). Strain-dependent Up-Regulation of Ephrin-B2 Protein in Periodontal Ligament Fibroblasts Contributes to Osteogenesis during Tooth Movement. *J. Biol. Chem.* 286 (43), 37651–37664. doi:10.1074/jbc.M110.166900

Dieterle, M. P., Husari, A., Steinberg, T., Wang, X., Ramminger, I., and Tomakidi, P. (2021). From the Matrix to the Nucleus and Back: Mechanobiology in the Light of Health, Pathologies, and Regeneration of Oral Periodontal Tissues. *Biomolecules* 11 (6), 824. doi:10.3390/biom11060824

Doncheva, N. T., Morris, J. H., Gorodkin, J., and Jensen, L. J. (2019). Cytoscape StringApp: Network Analysis and Visualization of Proteomics Data. *J. Proteome Res.* 18 (2), 623–632. doi:10.1021/acs.jproteome.8b00702

Dong-Xu, L., Hong-Ning, W., Chun-Ling, W., Hong, L., Ping, S., and Xiao, Y. (2011). Modulus of Elasticity of Human Periodontal Ligament by Optical Measurement and Numerical Simulation. *The Angle Orthodontist* 81 (2), 229–236. doi:10.2319/060710-311.1

Doyle, A. D., Carvajal, N., Jin, A., Matsumoto, K., and Yamada, K. M. (2015). Local 3D Matrix Microenvironment Regulates Cell Migration through Spatiotemporal Dynamics of Contractility-dependent Adhesions. *Nat. Commun.* 6, 8720. doi:10.1038/ncomms9720

Francis, M., Pandya, M., Gopinathan, G., Lyu, H., Ma, W., Foyle, D., et al. (2019). Histone Methylation Mechanisms Modulate the Inflammatory Response of Periodontal Ligament Progenitors. *Stem Cells Develop.* 28 (15), 1015–1025. doi:10.1089/scd.2019.0125

Fujihara, C., Yamada, S., Ozaki, N., Takeshita, N., Kawaki, H., Takano-Yamamoto, T., et al. (2010). Role of Mechanical Stress-Induced Glutamate Signaling-Associated Molecules in Cytodifferentiation of Periodontal Ligament Cells. *J. Biol. Chem.* 285 (36), 28286–28297. doi:10.1074/jbc.M109.097303

Gilbert, J. A., Weinhold, P. S., Banes, A. J., Link, G. W., and Jones, G. L. (1994). Strain Profiles for Circular Cell Culture Plates Containing Flexible Surfaces Employed to Mechanically Deform Cells *In Vitro*. *J. Biomech.* 27 (9), 1169–1177. doi:10.1016/0021-9290(94)90057-4

Gonzales, C., Hotokezaka, H., Yoshimatsu, M., Yozgatian, J. H., Darendeliler, M. A., and Yoshida, N. (2008). Force Magnitude and Duration Effects on Amount of Tooth Movement and Root Resorption in the Rat Molar. *Angle Orthod.* 78 (3), 502–509. doi:10.2319/052007-240.1

Goto, K. T., Kajiya, H., Nemoto, T., Tsutsumi, T., Tsuzuki, T., Sato, H., et al. (2011). Hyperocclusion Stimulates Osteoclastogenesis via CCL2 Expression. *J. Dent. Res.* 90 (6), 793–798. doi:10.1177/0022034511400742

Hao, Y., Xu, C., Sun, S.-y., and Zhang, F.-q. (2009). Cyclic Stretching Force Induces Apoptosis in Human Periodontal Ligament Cells via Caspase-9. *Arch. Oral Biol.* 54 (9), 864–870. doi:10.1016/j.archoralbio.2009.05.012

Haw, R., Loney, F., Ong, E., He, Y., and Wu, G. (2020). Perform Pathway Enrichment Analysis Using ReactomeFIViz. *Methods Mol. Biol.*, 2074, 165–179. doi:10.1007/978-1-4939-9873-9_13

He, Y., Macarak, E. J., Korostoff, J. M., and Howard, P. S. (2004). Compression and Tension: Differential Effects on Matrix Accumulation by Periodontal Ligament Fibroblasts *In Vitro*. *Connect. Tissue Res.* 45 (1), 28–39. doi:10.1080/03008200490278124

Howard, P. S., Kucich, U., Taliwal, R., and Korostoff, J. M. (1998). Mechanical Forces Alter Extracellular Matrix Synthesis by Human Periodontal Ligament Fibroblasts. *J. Periodontal Res.* 33 (8), 500–508. doi:10.1111/j.1600-0765.1998.tb02350.x

Huelter-Hassler, D., Tomakidi, P., Steinberg, T., and Jung, B. A. (2017). Orthodontic Strain Affects the Hippo-Pathway Effector YAP Concomitant

with Proliferation in Human Periodontal Ligament Fibroblasts. *Eur. J. Orthod.* 39 (3), 251–257. doi:10.1093/ejo/cjx012

Hülter-Hassler, D., Wein, M., Schulz, S. D., Proksch, S., Steinberg, T., Jung, B. A., et al. (2017). Biomechanical Strain-Induced Modulation of Proliferation Coincides with an ERK1/2-independent Nuclear YAP Localization. *Exp. Cell Res.* 361 (1), 93–100. doi:10.1016/j.yexcr.2017.10.006

Hung, J.-H. (2013). Gene Set/Pathway Enrichment Analysis. *Methods Mol. Biol.* 939, 201–213. doi:10.1007/978-1-62703-107-3_13

Hutchins, J. R. A. (2014). What's that Gene (Or Protein)? Online Resources for Exploring Functions of Genes, Transcripts, and Proteins. *MBoC* 25 (8), 1187–1201. doi:10.1091/mbc.E13-10-0602

Jacobs, C., Grimm, S., Ziebart, T., Walter, C., and Wehrbein, H. (2013). Osteogenic Differentiation of Periodontal Fibroblasts Is Dependent on the Strength of Mechanical Strain. *Arch. Oral Biol.* 58 (7), 896–904. doi:10.1016/j.archoralbio.2013.01.009

Jacobs, C., Schramm, S., Dirks, I., Walter, C., Pabst, A., Meila, D., et al. (2018). Mechanical Loading Increases Pro-inflammatory Effects of Nitrogen-Containing Bisphosphonate in Human Periodontal Fibroblasts. *Clin. Oral Invest.* 22 (2), 901–907. doi:10.1007/s00784-017-2168-1

Jacobs, C., Walter, C., Ziebart, T., Dirks, I., Schramm, S., Grimm, S., et al. (2015). Mechanical Loading Influences the Effects of Bisphosphonates on Human Periodontal Ligament Fibroblasts. *Clin. Oral Invest.* 19 (3), 699–708. doi:10.1007/s00784-014-1284-4

Janjic, M., Docheva, D., Trickovic Janjic, O., Wichelhaus, A., and Baumert, U. (2018). *In Vitro* Weight-Loaded Cell Models for Understanding Mechanodependent Molecular Pathways Involved in Orthodontic Tooth Movement: A Systematic Review. *Stem Cells Int.* 2018, 1–17. doi:10.1155/2018/3208285

Janjic Rankovic, M., Docheva, D., Wichelhaus, A., and Baumert, U. (2020). Effect of Static Compressive Force on *In Vitro* Cultured PDL Fibroblasts: Monitoring of Viability and Gene Expression over 6 Days. *Clin. Oral Invest.* 24 (7), 2497–2511. doi:10.1007/s00784-019-03113-6

Kaku, M., and Yamauchi, M. (2014). Mechano-regulation of Collagen Biosynthesis in Periodontal Ligament. *J. Prosthodontic Res.* 58 (4), 193–207. doi:10.1016/j.jpor.2014.08.003

King, G. J., Keeling, S. D., McCoy, E. A., and Ward, T. H. (1991). Measuring Dental Drift and Orthodontic Tooth Movement in Response to Various Initial Forces in Adult Rats. *Am. J. Orthod. Dentofacial Orthopedics* 99 (5), 456–465. doi:10.1016/s0889-5406(05)81579-3

Kirschneck, C., Batschkus, S., Proff, P., Köstler, J., Spanier, G., and Schröder, A. (2017). Valid Gene Expression Normalization by RT-qPCR in Studies on hPDL Fibroblasts with Focus on Orthodontic Tooth Movement and Periodontitis. *Sci. Rep.* 7 (1), 14751. doi:10.1038/s41598-017-15281-0

Kletsas, D., Basdra, E. K., and Papavassiliou, A. G. (2002). Effect of Protein Kinase Inhibitors on the Stretch-Elicited C-Fos and C-Jun Up-Regulation in Human PDL Osteoblast-like Cells. *J. Cell. Physiol.* 190 (3), 313–321. doi:10.1002/jcp.10052

Konstantonis, D., Papadopoulou, A., Makou, M., Eliades, T., Basdra, E., and Kletsas, D. (2014). The Role of Cellular Senescence on the Cyclic Stretching-Mediated Activation of MAPK and ALP Expression and Activity in Human Periodontal Ligament Fibroblasts. *Exp. Gerontol.* 57, 175–180. doi:10.1016/j.exger.2014.05.010

Kook, S.-H., and Lee, J.-C. (2012). Tensile Force Inhibits the Proliferation of Human Periodontal Ligament Fibroblasts through Ras-P38 MAPK Up-Regulation. *J. Cell. Physiol.* 227 (3), 1098–1106. doi:10.1002/jcp.22829

Krishnan, V., and Davidovitch, Z. e. (2006). Cellular, Molecular, and Tissue-Level Reactions to Orthodontic Force. *Am. J. Orthod. Dentofacial Orthopedics* 129 (4), 461–469. doi:10.1016/j.ajodo.2005.10.007

Krishnan, V., Viecilli, R. F., and Davidovitch, Z. e. (2015). "Cellular and Molecular Biology behind Orthodontic Tooth Movement," in *Biological Mechanisms of Tooth Movement*. Editors V. Krishnan and Z. Davidovitch. 2nd ed (Chichester, UK: Wiley), 30–50. doi:10.1002/9781118916148.ch3

Ku, S.-J., Chang, Y.-I., Chae, C.-H., Kim, S.-G., Park, Y.-W., Jung, Y.-K., et al. (2009). Static Tensional Forces Increase Osteogenic Gene Expression in Three-Dimensional Periodontal Ligament Cell Culture. *BMB Rep.* 42 (7), 427–432. doi:10.5483/bmbrep.2009.42.7.427

Lee, E. L., and von Recum, H. A. (2015). "Mechanical Conditioning," in *Molecular, Cellular, and Tissue Engineering*. Editors J.D. Bronzino and D.R. Peterson. 4th ed (Boca Raton: CRC Press), 53-51–53-24.

Lee, S.-I., Park, K.-H., Kim, S.-J., Kang, Y.-G., Lee, Y.-M., and Kim, E.-C. (2012). Mechanical Stress-Activated Immune Response Genes via Sirtuin 1 Expression in Human Periodontal Ligament Cells. *Clin. Exp. Immunol.* 168 (1), 113–124. doi:10.1111/j.1365-2249.2011.04549.x

Li, L., Han, M.-x., Li, S., Xu, Y., and Wang, L. (2014). Hypoxia Regulates the Proliferation and Osteogenic Differentiation of Human Periodontal Ligament Cells under Cyclic Tensile Stress via Mitogen-Activated Protein Kinase Pathways. *J. Periodontol.* 85 (3), 498–508. doi:10.1902/jop.2013.130048

Li, L., Han, M., Li, S., Wang, L., and Xu, Y. (2013). Cyclic Tensile Stress during Physiological Occlusal Force Enhances Osteogenic Differentiation of Human Periodontal Ligament Cells via ERK1/2-Elk1 MAPK Pathway. *DNA Cell Biol.* 32 (9), 488–497. doi:10.1089/dna.2013.2070

Li, M., Zhang, C., and Yang, Y. (2019). Effects of Mechanical Forces on Osteogenesis and Osteoclastogenesis in Human Periodontal Ligament Fibroblasts. *Bone Jt. Res.* 8 (1), 19–31. doi:10.1302/2046-3758.81.Bjr-2018-0060.R1

Li, S., Zhang, H., Li, S., Yang, Y., Huo, B., and Zhang, D. (2015). Connexin 43 and ERK Regulate Tension-Induced Signal Transduction in Human Periodontal Ligament Fibroblasts. *J. Orthop. Res.* 33 (7), 1008–1014. doi:10.1002/jor.22830

Liao, C., and Hua, Y. (2013). Effect of Hydrogen Sulphide on the Expression of Osteoprotegerin and Receptor Activator of NF-Kb Ligand in Human Periodontal Ligament Cells Induced by Tension-Force Stimulation. *Arch. Oral Biol.* 58 (12), 1784–1790. doi:10.1016/j.archoralbio.2013.08.004

Livak, K. J., and Schmittgen, T. D. (2001). Analysis of Relative Gene Expression Data Using Real-Time Quantitative PCR and the 2−ΔΔCT Method. *Methods* 25 (4), 402–408. doi:10.1006/meth.2001.1262

Long, P., Hu, J., Piesco, N., Buckley, M., and Agarwal, S. (2001). Low Magnitude of Tensile Strain Inhibits IL-1β-dependent Induction of Pro-inflammatory Cytokines and Induces Synthesis of IL-10 in Human Periodontal Ligament Cells *In Vitro*. *J. Dent. Res.* 80 (5), 1416–1420. doi:10.1177/00220345010800050601

Long, P., Liu, F., Piesco, N. P., Kapur, R., and Agarwal, S. (2002). Signaling by Mechanical Strain Involves Transcriptional Regulation of Proinflammatory Genes in Human Periodontal Ligament Cells *In Vitro*. *Bone* 30 (4), 547–552. doi:10.1016/s8756-3282(02)00673-7

Ma, J., Zhao, D., Wu, Y., Xu, C., and Zhang, F. (2015). Cyclic Stretch Induced Gene Expression of Extracellular Matrix and Adhesion Molecules in Human Periodontal Ligament Cells. *Arch. Oral Biol.* 60 (3), 447–455. doi:10.1016/j.archoralbio.2014.11.019

Marchesan, J. T., Scanlon, C. S., Soehren, S., Matsuo, M., and Kapila, Y. L. (2011). Implications of Cultured Periodontal Ligament Cells for the Clinical and Experimental Setting: a Review. *Arch. Oral Biol.* 56 (10), 933–943. doi:10.1016/j.archoralbio.2011.03.003

Matheson, L., Jackfairbank, N., Maksym, G., Paulsanterre, J., and Labow, R. (2006). Characterization of the Flexcell Uniflex Cyclic Strain Culture System with U937 Macrophage-like Cells. *Biomaterials* 27 (2), 226–233. doi:10.1016/j.biomaterials.2005.05.070

Matsuda, N., Yokoyama, K., Takeshita, S., and Watanabe, M. (1998). Role of Epidermal Growth Factor and its Receptor in Mechanical Stress-Induced Differentiation of Human Periodontal Ligament Cells *In Vitro*. *Arch. Oral Biol.* 43 (12), 987–997. doi:10.1016/s0003-9969(98)00079-x

Mayahara, K., Kobayashi, Y., Takimoto, K., Suzuki, N., Mitsui, N., and Shimizu, N. (2007). Aging Stimulates Cyclooxygenase-2 Expression and Prostaglandin E2production in Human Periodontal Ligament Cells after the Application of Compressive Force. *J. Periodontal Res.* 42 (1), 8–14. doi:10.1111/j.1600-0765.2006.00885.x

Memmert, S., Damanaki, A., Weykopf, B., Rath-Deschner, B., Nokhbehsaim, M., Götz, W., et al. (2019). Autophagy in Periodontal Ligament Fibroblasts under Biomechanical Loading. *Cell Tissue Res* 378 (3), 499–511. doi:10.1007/s00441-019-03063-1

Memmert, S., Nogueira, A. V. B., Damanaki, A., Nokhbehsaim, M., Rath-Deschner, B., Götz, W., et al. (2020). Regulation of the Autophagy-Marker Sequestosome 1 in Periodontal Cells and Tissues by Biomechanical Loading. *J. Orofac. Orthop.* 81 (1), 10–21. doi:10.1007/s00056-019-00197-3

Miura, S., Yamaguchi, M., Shimizu, N., and Abiko, Y. (2000). Mechanical Stress Enhances Expression and Production of Plasminogen Activator in Aging Human Periodontal Ligament Cells. *Mech. Ageing Develop.* 112 (3), 217–231. doi:10.1016/s0047-6374(99)00095-0

Moher, D., Liberati, A., Tetzlaff, J., and Altman, D. G. (2009). Preferred Reporting Items for Systematic Reviews and Meta-Analyses: the PRISMA Statement. *Open Med.* 3 (3), e123–30. doi:10.1371/journal.pmed.1000097

Monnouchi, S., Maeda, H., Fujii, S., Tomokiyo, A., Kono, K., and Akamine, A. (2011). The Roles of Angiotensin II in Stretched Periodontal Ligament Cells. *J. Dent. Res.* 90 (2), 181–185. doi:10.1177/0022034510382118

Montecino, M., Stein, G., Stein, J., Zaidi, K., and Aguilar, R. (2015). Multiple Levels of Epigenetic Control for Bone Biology and Pathology. *Bone* 81, 733–738. doi:10.1016/j.bone.2015.03.013

Mooney, M. A., and Wilmot, B. (2015). Gene Set Analysis: A Step-by-step Guide. *Am. J. Med. Genet.* 168 (7), 517–527. doi:10.1002/ajmg.b.32328

Morris, J. H., Apeltsin, L., Newman, A. M., Baumbach, J., Wittkop, T., Su, G., et al. (2011). *clusterMaker*: a Multi-Algorithm Clustering Plugin for Cytoscape. *BMC Bioinformatics* 12, 436. doi:10.1186/1471-2105-12-436

Mühlemann, H. R. (1954). Tooth Mobility (V): Tooth Mobility Changes through Artificial Trauma. *J. Periodontol.* 25 (3), 202–208. doi:10.1902/jop.1954.25.3.202

Mühlemann, H. R., and Zander, H. A. (1954). Tooth Mobility (III): the Mechanism of Tooth Mobility. *J. Periodontol.* 25 (2), 128–137. doi:10.1902/jop.1954.25.2.128

Natali, A., Pavan, P., and Scarpa, C. (2004). Numerical Analysis of Tooth Mobility: Formulation of a Non-linear Constitutive Law for the Periodontal Ligament. *Dental Mater.* 20 (7), 623–629. doi:10.1016/j.dental.2003.08.003

Nazet, U., Schröder, A., Spanier, G., Wolf, M., Proff, P., and Kirschneck, C. (2020). Simplified Method for Applying Static Isotropic Tensile Strain in Cell Culture Experiments with Identification of Valid RT-qPCR Reference Genes for PDL Fibroblasts. *Eur. J. Orthod.* 42 (4), 359–370. doi:10.1093/ejo/cjz052

Nemoto, T., Kajiya, H., Tsuzuki, T., Takahashi, Y., and Okabe, K. (2010). Differential Induction of Collagens by Mechanical Stress in Human Periodontal Ligament Cells. *Arch. Oral Biol.* 55 (12), 981–987. doi:10.1016/j.archoralbio.2010.08.004

Ngan, P., Saito, S., Saito, M., Lanese, R., Shanfeld, J., and Davidovitch, Z. (1990). The Interactive Effects of Mechanical Stress and Interleukin-1β on Prostaglandin E and Cyclic AMP Production in Human Periodontal Ligament Fibroblasts *In Vitro*: Comparison with Cloned Osteoblastic Cells of Mouse (MC3T3-E1). *Arch. Oral Biol.* 35 (9), 717–725. doi:10.1016/0003-9969(90)90094-Q

Nogueira, A. V. B., Nokhbehsaim, M., Eick, S., Bourauel, C., Jäger, A., Jepsen, S., et al. (2014a). Regulation of Visfatin by Microbial and Biomechanical Signals in PDL Cells. *Clin. Oral Invest.* 18 (1), 171–178. doi:10.1007/s00784-013-0935-1

Nogueira, A. V. B., Nokhbehsaim, M., Eick, S., Bourauel, C., Jäger, A., Jepsen, S., et al. (2014b). Biomechanical Loading Modulates Proinflammatory and Bone Resorptive Mediators in Bacterial-Stimulated PDL Cells. *Mediators Inflamm.* 2014, 1–10. doi:10.1155/2014/425421

Ohzeki, K., Yamaguchi, M., Shimizu, N., and Abiko, Y. (1999). Effect of Cellular Aging on the Induction of Cyclooxygenase-2 by Mechanical Stress in Human Periodontal Ligament Cells. *Mech. Ageing Develop.* 108 (2), 151–163. doi:10.1016/s0047-6374(99)00006-8

Padial-Molina, M., Volk, S. L., Rodriguez, J. C., Marchesan, J. T., Galindo-Moreno, P., and Rios, H. F. (2013). Tumor Necrosis Factor-α andPorphyromonas gingivalisLipopolysaccharides Decrease Periostin in Human Periodontal Ligament Fibroblasts. *J. Periodontol.* 84 (5), 694–703. doi:10.1902/jop.2012.120078

Papadopoulou, A., Iliadi, A., Eliades, T., and Kletsas, D. (2017). Early Responses of Human Periodontal Ligament Fibroblasts to Cyclic and Static Mechanical Stretching. *Eur. J. Orthod.* 39 (3), cjw075–263. doi:10.1093/ejo/cjw075

Papadopoulou, A., Todaro, A., Eliades, T., and Kletsas, D. (2019). Effect of Hyperglycaemic Conditions on the Response of Human Periodontal Ligament Fibroblasts to Mechanical Stretching. *Eur. J. Orthod.* 41 (6), 583–590. doi:10.1093/ejo/cjz051

Pavasant, P., and Yongchaitrakul, T. (2011). Role of Mechanical Stress on the Function of Periodontal Ligament Cells. *Periodontol* 56 (1), 154–165. doi:10.1111/j.1600-0757.2010.00374.x

Pelaez, D., Acosta Torres, Z., Ng, T. K., Choy, K. W., Pang, C. P., and Cheung, H. S. (2017). Cardiomyogenesis of Periodontal Ligament-Derived Stem Cells by Dynamic Tensile Strain. *Cell Tissue Res* 367 (2), 229–241. doi:10.1007/s00441-016-2503-x

Pini, M., Wiskott, H. W. A., Scherrer, S. S., Botsis, J., and Belser, U. C. (2002). Mechanical Characterization of Bovine Periodontal Ligament. *J. Periodontal Res.* 37 (4), 237–244. doi:10.1034/j.1600-0765.2002.00344.x

Qin, J., and Hua, Y. (2016). Effects of Hydrogen Sulfide on the Expression of Alkaline Phosphatase, Osteocalcin and Collagen Type I in Human Periodontal Ligament Cells Induced by Tension Force Stimulation. *Mol. Med. Rep.* 14 (4), 3871–3877. doi:10.3892/mmr.2016.5680

Ren, D., Wei, F., Hu, L., Yang, S., Wang, C., and Yuan, X. (2015). Phosphorylation of Runx2, Induced by Cyclic Mechanical Tension via ERK1/2 Pathway, Contributes to Osteodifferentiation of Human Periodontal Ligament Fibroblasts. *J. Cell. Physiol.* 230 (10), 2426–2436. doi:10.1002/jcp.24972

Samuel, G. O., Hoffmann, S., Wright, R. A., Lalu, M. M., Patlewicz, G., Becker, R. A., et al. (2016). Guidance on Assessing the Methodological and Reporting Quality of Toxicologically Relevant Studies: A Scoping Review. *Environ. Int.* 92–93, 630–646. doi:10.1016/j.envint.2016.03.010

Schardt, C., Adams, M. B., Owens, T., Keitz, S., and Fontelo, P. (2007). Utilization of the PICO Framework to Improve Searching PubMed for Clinical Questions. *BMC Med. Inform. Decis. Mak.* 7, 16. doi:10.1186/1472-6947-7-16

Seo, B.-M., Miura, M., Gronthos, S., Mark Bartold, P., Batouli, S., Brahim, J., et al. (2004). Investigation of Multipotent Postnatal Stem Cells from Human Periodontal Ligament. *The Lancet* 364 (9429), 149–155. doi:10.1016/S0140-6736(04)16627-0

Setiawan, M., Jäger, A., and Konermann, A. (2019). The Stability of Different Housekeeping Genes in Human Periodontal Ligament Cells under Inflammatory Conditions. *Ann. Anat. - Anatomischer Anzeiger* 224, 81–87. doi:10.1016/j.aanat.2019.04.001

Shannon, P., Markiel, A., Ozier, O., Baliga, N. S., Wang, J. T., Ramage, D., et al. (2003). Cytoscape: a Software Environment for Integrated Models of Biomolecular Interaction Networks. *Genome Res.* 13 (11), 2498–2504. doi:10.1101/gr.1239303

Shi, J., Baumert, U., Folwaczny, M., and Wichelhaus, A. (2019a). Influence of Static Forces on the Expression of Selected Parameters of Inflammation in Periodontal Ligament Cells and Alveolar Bone Cells in a Co-culture *In Vitro* Model. *Clin. Oral Invest.* 23 (6), 2617–2628. doi:10.1007/s00784-018-2697-2

Shi, J., Folwaczny, M., Wichelhaus, A., and Baumert, U. (2019b). Differences in RUNX 2 and P2 RX 7 Gene Expression between Mono- and Coculture of Human Periodontal Ligament Cells and Human Osteoblasts under Compressive Force Application. *Orthod. Craniofac. Res.* 22, 168–176. doi:10.1111/ocr.12307

Shimizu, N., Goseki, T., Yamaguchi, M., Iwasawa, T., Takiguchi, H., and Abiko, Y. (1997). *In Vitro* Cellular Aging Stimulates Interleukin-1β Production in Stretched Human Periodontal-Ligament-Derived Cells. *J. Dent. Res.* 76 (7), 1367–1375. doi:10.1177/00220345970760070601

Shimizu, N., Ozawa, Y., Yamaguchi, M., Goseki, T., Ohzeki, K., and Abiko, Y. (1998). Induction of COX-2 Expression by Mechanical Tension Force in Human Periodontal Ligament Cells. *J. Periodontol.* 69 (6), 670–677. doi:10.1902/jop.1998.69.6.670

Somerman, M. J., Archer, S. Y., Imm, G. R., and Foster, R. A. (1988). A Comparative Study of Human Periodontal Ligament Cells and Gingival Fibroblasts *In Vitro*. *J. Dent. Res.* 67 (1), 66–70. doi:10.1177/00220345880670011301

Steinberg, T., Ziegler, N., Alonso, A., Kohl, A., Müssig, E., Proksch, S., et al. (2011). Strain Response in Fibroblasts Indicates a Possible Role of the Ca2+-dependent Nuclear Transcription Factor NM1 in RNA Synthesis. *Cell Calcium* 49 (4), 259–271. doi:10.1016/j.ceca.2011.03.001

Stoddart, M., Richards, R. G., Richards, R., and Alini, M. (2012). *In Vitro* experiments with Primary Mammalian Cells: to Pool or Not to Pool? *eCM* 24, i–ii. doi:10.22203/ecm.v024a00

Su, G., Morris, J. H., Demchak, B., and Bader, G. D. (2014). Biological Network Exploration with Cytoscape 3. *Curr. Protoc. Bioinformatics* 47, 8 13 11–24. doi:10.1002/0471250953.bi0813s47

Sun, C., Liu, F., Cen, S., Chen, L., Wang, Y., Sun, H., et al. (2017). Tensile Strength Suppresses the Osteogenesis of Periodontal Ligament Cells in Inflammatory

Microenvironments. *Mol. Med. Rep.* 16 (1), 666–672. doi:10.3892/mmr.2017.6644

Szklarczyk, D., Gable, A. L., Lyon, D., Junge, A., Wyder, S., Huerta-Cepas, J., et al. (2019). STRING V11: Protein-Protein Association Networks with Increased Coverage, Supporting Functional Discovery in Genome-wide Experimental Datasets. *Nucleic Acids Res.* 47 (D1), D607–D613. doi:10.1093/nar/gky1131

Tang, N., Zhao, Z., Zhang, L., Yu, Q., Li, J., Xu, Z., et al. (2012). Up-regulated Osteogenic Transcription Factors during Early Response of Human Periodontal Ligament Stem Cells to Cyclic Tensile Strain. *Arch. Med. Sci.* 3 (3), 422–430. doi:10.5114/aoms.2012.28810

Tantilertanant, Y., Niyompanich, J., Everts, V., Supaphol, P., Pavasant, P., and Sanchavanakit, N. (2019a). Cyclic Tensile Force Stimulates BMP9 Synthesis and *In Vitro* Mineralization by Human Periodontal Ligament Cells. *J. Cell. Physiol.* 234 (4), 4528–4539. doi:10.1002/jcp.27257

Tantilertanant, Y., Niyompanich, J., Everts, V., Supaphol, P., Pavasant, P., and Sanchavanakit, N. (2019b). Cyclic Tensile Force-Upregulated IL6 Increases MMP3 Expression by Human Periodontal Ligament Cells. *Arch. Oral Biol.* 107, 104495. doi:10.1016/j.archoralbio.2019.104495

Vande Geest, J. P., Di Martino, E. S., and Vorp, D. A. (2004). An Analysis of the Complete Strain Field within FlexercellTM Membranes. *J. Biomech.* 37 (12), 1923–1928. doi:10.1016/j.jbiomech.2004.02.022

Vansant, L., Cadenas De Llano-Pérula, M., Verdonck, A., and Willems, G. (2018). Expression of Biological Mediators during Orthodontic Tooth Movement: A Systematic Review. *Arch. Oral Biol.* 95, 170–186. doi:10.1016/j.archoralbio.2018.08.003

Von den Hoff, J. W. (2003). Effects of Mechanical Tension on Matrix Degradation by Human Periodontal Ligament Cells Cultured in Collagen Gels. *J. Periodontal Res.* 38 (5), 449–457. doi:10.1034/j.1600-0765.2003.00404.x

Wada, S., Kanzaki, H., Narimiya, T., and Nakamura, Y. (2017). Novel Device for Application of Continuous Mechanical Tensile Strain to Mammalian Cells. *Biol. Open* 6 (4), 518–524. doi:10.1242/bio.023671

Wang, H., Feng, C., Jin, Y., Tan, W., and Wei, F. (2019a). Identification and Characterization of Circular RNAs Involved in Mechanical Force-induced Periodontal Ligament Stem Cells. *J. Cell. Physiol.* 234 (7), 10166–10177. doi:10.1002/jcp.27686

Wang, L., Pan, J., Wang, T., Song, M., and Chen, W. (2013). Pathological Cyclic Strain-Induced Apoptosis in Human Periodontal Ligament Cells through the RhoGDIα/Caspase-3/PARP Pathway. *PLoS One* 8 (10), e75973. doi:10.1371/journal.pone.0075973

Wang, Y., Hu, B., Hu, R., Tong, X., Zhang, M., Xu, C., et al. (2019b). TAZ Contributes to Osteogenic Differentiation of Periodontal Ligament Cells under Tensile Stress. *J. Periodont Res.* 55, 152–160. doi:10.1111/jre.12698

Wichelhaus, A. (2017). *Orthodontic Therapy - Fundamental Treatment Concepts*. New York: Georg Thieme.

Woda, A., Mishellany, A., and Peyron, M.-A. (2006). The Regulation of Masticatory Function and Food Bolus Formation. *J. Oral Rehabil.* 33 (11), 840–849. doi:10.1111/j.1365-2842.2006.01626.x

Wu, Y., Ou, Y., Liao, C., Liang, S., and Wang, Y. (2019). High-throughput Sequencing Analysis of the Expression Profile of microRNAs and Target Genes in Mechanical Force-Induced Osteoblastic/cementoblastic Differentiation of Human Periodontal Ligament Cells. *Am. J. Transl. Res.* 11 (6), 3398–3411.

Wu, Y., Zhuang, J., Zhao, D., and Xu, C. (2019). Interaction between Caspase-3 and Caspase-5 in the Stretch-induced Programmed Cell Death in the Human Periodontal Ligament Cells. *J. Cell. Physiol.* 234 (8), 13571–13581. doi:10.1002/jcp.28035

Yamaguchi, M., Shimizu, N., Goseki, T., Shibata, Y., Takiguchi, H., Iwasawa, T., et al. (1994). Effect of Different Magnitudes of Tension Force on Prostaglandin E2 Production by Human Periodontal Ligament Cells. *Arch. Oral Biol.* 39 (10), 877–884. doi:10.1016/0003-9969(94)90019-1

Yamaguchi, N., Chiba, M., and Mitani, H. (2002). The Induction of C-Fos mRNA Expression by Mechanical Stress in Human Periodontal Ligament Cells. *Arch. Oral Biol.* 47 (6), 465–471. doi:10.1016/s0003-9969(02)00022-5

Yamashita, S., Ai, M., and Mizutani, H. (1993). A New Method for Measuring Nocturnal Tooth Contacts. *J. Oral Rehabil.* 20 (5), 525–532. doi:10.1111/j.1365-2842.1993.tb01639.x

Yang, L., Yang, Y., Wang, S., Li, Y., and Zhao, Z. (2015). *In Vitro* mechanical Loading Models for Periodontal Ligament Cells: from Two-Dimensional to Three-Dimensional Models. *Arch. Oral Biol.* 60 (3), 416–424. doi:10.1016/j.archoralbio.2014.11.012

Yu, W., Hu, B., Shi, X., Cao, Z., Ren, M., He, Z., et al. (2018). Nicotine Inhibits Osteogenic Differentiation of Human Periodontal Ligament Cells under Cyclic Tensile Stress through Canonical Wnt Pathway and α7 Nicotinic Acetylcholine Receptor. *J. Periodont Res.* 53 (4), 555–564. doi:10.1111/jre.12545

Yuda, A., Maeda, H., Fujii, S., Monnouchi, S., Yamamoto, N., Wada, N., et al. (2015). Effect of CTGF/CCN2 on Osteo/cementoblastic and Fibroblastic Differentiation of a Human Periodontal Ligament Stem/progenitor Cell Line. *J. Cell. Physiol* 230 (1), 150–159. doi:10.1002/jcp.24693

Zhuang, J., Wang, Y., Qu, F., Wu, Y., Zhao, D., and Xu, C. (2019). Gasdermin-d Played a Critical Role in the Cyclic Stretch-Induced Inflammatory Reaction in Human Periodontal Ligament Cells. *Inflammation* 42 (2), 548–558. doi:10.1007/s10753-018-0912-6

Ziegler, N., Alonso, A., Steinberg, T., Woodnutt, D., Kohl, A., Müssig, E., et al. (2010). Mechano-transduction in Periodontal Ligament Cells Identifies Activated States of MAP-Kinases P42/44 and P38-Stress Kinase as a Mechanism for MMP-13 Expression. *BMC Cell Biol* 11, 10. doi:10.1186/1471-2121-11-10

Ziros, P. G., Basdra, E. K., and Papavassiliou, A. G. (2008). Runx2: of Bone and Stretch. *Int. J. Biochem. Cell Biol.* 40 (9), 1659–1663. doi:10.1016/j.biocel.2007.05.024

Ziros, P. G., Gil, A.-P. R., Georgakopoulos, T., Habeos, I., Kletsas, D., Basdra, E. K., et al. (2002). The Bone-specific Transcriptional Regulator Cbfa1 Is a Target of Mechanical Signals in Osteoblastic Cells. *J. Biol. Chem.* 277 (26), 23934–23941. doi:10.1074/jbc.M109881200

Conflict of Interest: The authors declare that the research was conducted in the absence of any commercial or financial relationships that could be construed as a potential conflict of interest.

Publisher's Note: All claims expressed in this article are solely those of the authors and do not necessarily represent those of their affiliated organizations, or those of the publisher, the editors and the reviewers. Any product that may be evaluated in this article, or claim that may be made by its manufacturer, is not guaranteed or endorsed by the publisher.

GLOSSARY

ALP Alkaline phosphatase

BGLAP Bone gamma-carboxy glutamic acid-containing protein

BMPs Bone morphogenetic proteins

COL I Collagen type I

DEG Differential expressed gene

ECM Extracellular matrix

FC Fold change

FGFs Fibroblast growth factors

GO GeneOntology

HoB High risk of bias

hPDLFs Human periodontal ligament fibroblasts

IL6 Interleukin 6

IL8 Interleukin 8

KEGG Kyoto Encyclopedia of Genes and Genomes

LoB Low risk of bias

MAPK Mitogen-activated protein kinase

MCODE Molecular Complex Detection

MIQE Minimum Information for Publication of Quantitative Real-Time PCR Experiments

n. a. Not applicable

OPG Osteoprotegerin

OTM Orthodontic tooth movement

PCR Polymerase chain reaction

PDL Periodontal ligament

PDLFs Periodontal ligament fibroblasts

PDLSCs Periodontal ligament stem cells

PGE_2 Prostaglandin E_2

PPI Protein-protein interaction

PRISMA Preferred Reporting Items for Systematic Reviews and Meta-Analyses

qPCR Quantitative polymerase chain reaction

RANK Receptor activator of NF-kappa B

RANKL Receptor activator of the nuclear factor kappa ligand

RT-qPCR Reverse transcriptase quantitative polymerase chain reaction

RT-sqPCR Reverse transcriptase semi-quantitative polymerase chain reaction

RUNX2 Runt-related transcription factor 2 (identical with CBFA1)

STRING-DB "Search Tool for the Retrieval of Interacting Genes/Proteins" database

TNFRSF11B Tumor necrosis factor-alpha receptor superfamily member 11B

TNFSF11 TNF superfamily member 11

WB Western blotting

Supplement 1: Reason for Exclusion

After full text reading, articles not fulfilling the eligibility criteria were excluded. In line with the quantitative report given in the PRISMA workflow (Figure 3A) the reasoning is reported here with references.

Table S1: Reasons for exclusion after full text reading

Total number of excluded publications: n = 45

Reason for exclusion (N)	**Study**
i. In vivo loading (2)	Anastasi et al. (2008); Xu et al. (2017)
ii. Force application *in vitro* on extracted teeth only (1)	Atkinson and Ralph (1977)
iii. Review (4)	Pavasant and Yongchaitrakul (2011); Yamaguchi and Kasai (2005); Yang et al. (2015); Li et al. (2019a)
iv. No quantitative information on gene or protein expression (7)	Basdra (1997); Norton et al. (1995); Norton et al. (1990); Pender and McCulloch (1991); Kletsas et al. (1998); Zhong et al. (2008); Wan et al. (2019)
v. Another type of force applied (10)	Wongkhantee et al. (2008); Wolf et al. (2013), Saminathan et al. (2015); Marciniak et al. (2019); Liu et al. (2017); Kaku et al. (2016); Huang et al. (2013); Feng et al. (2017); Berendsen et al. (2009); Li et al. (2019b)
vi. 3D model (2)	Von den Hoff (2003), (Ku et al., 2009)
vii. Results not related to hPDL (1)	Rosselli-Murai et al. (2013)
viii. No information on force type (1)	Wang et al. (2016)
ix. Co-culture (1)	Xu et al. (2014)
x. Only the apparatus (1)	Andersen and Norton (1991)
xi. Other cell types or not of human origin (14)	Duarte et al. (1999); Bellows et al. (1982); Chen et al. (2013); Glogauer et al. (1995); Zhao et al. (2008); Takimoto et al. (2015); Pavlin and Gluhak-Heinrich (2001); Loesberg et al. (2005); Lew et al. (1999); Gadhari et al. (2013); Fu et al. (2016); Duncan et al. (1984); Andrade et al. (2009); Carano and Siciliani (1996)
xii. Not directly related to mechanical force (conditioned medium) (1)	Wang et al. (2019)

References

Anastasi, G., Cordasco, G., Matarese, G., Rizzo, G., Nucera, R., Mazza, M., et al. (2008). An immunohistochemical, histological, and electron-microscopic study of the human periodontal ligament during orthodontic treatment. *Int. J. Mol. Med.* 21(5), 545-554.

Andersen, K.L., and Norton, L.A. (1991). A device for the application of known simulated orthodontic forces to human cells in vitro. *J. Biomech.* 24(7), 649-654.

Andrade, I., Jr., Taddei, S.R., Garlet, G.P., Garlet, T.P., Teixeira, A.L., Silva, T.A., et al. (2009). CCR5 down-regulates osteoclast function in orthodontic tooth movement. *J. Dent. Res.* 88(11), 1037-1041. doi: 10.1177/0022034509346230.

Atkinson, H.F., and Ralph, W.J. (1977). In vitro strength of the human periodontal ligament. *J. Dent. Res.* 56(1), 48-52. doi: 10.1177/00220345770560011001.

Basdra, E.K. (1997). Biological reactions to orthodontic tooth movement. *J. Orofac. Orthop.* 58(1), 2-15.

Bellows, C.G., Melcher, A.H., and Aubin, J.E. (1982). Association between tension and orientation of periodontal ligament fibroblasts and exogenous collagen fibres in collagen gels in vitro. *J. Cell Sci.* 58, 125-138.

Berendsen, A.D., Smit, T.H., Walboomers, X.F., Everts, V., Jansen, J.A., and Bronckers, A.L. (2009). Three-dimensional loading model for periodontal ligament regeneration in vitro. *Tissue engineering. Part C, Methods* 15(4), 561-570. doi: 10.1089/ten.TEC.2008.0336.

Carano, A., and Siciliani, G. (1996). Effects of continuous and intermittent forces on human fibroblasts in vitro. *Eur. J. Orthod.* 18(1), 19-26.

Chen, Y.J., Jeng, J.H., Chang, H.H., Huang, M.Y., Tsai, F.F., and Yao, C.C. (2013). Differential regulation of collagen, lysyl oxidase and MMP-2 in human periodontal ligament cells by low- and high-level mechanical stretching. *J. Periodontal Res.* 48(4), 466-474. doi: 10.1111/jre.12028.

Duarte, W.R., Mikuni-Takagaki, Y., Kawase, T., Limura, T., Oida, S., Ohya, K., et al. (1999). Effects of mechanical stress on the mRNA expression of S100A4 and cytoskeletal components by periodontal ligament cells. *Journal of medical and dental sciences* 46(3), 117-122.

Duncan, G.W., Yen, E.H., Pritchard, E.T., and Suga, D.M. (1984). Collagen and prostaglandin synthesis in force-stressed periodontal ligament in vitro. *J. Dent. Res.* 63(5), 665-669. doi: 10.1177/00220345840630051201.

Feng, L., Zhang, Y., Kou, X., Yang, R., Liu, D., Wang, X., et al. (2017). Cadherin-11 modulates cell morphology and collagen synthesis in periodontal ligament cells under mechanical stress. *Angle Orthod.* 87(2), 193-199. doi: 10.2319/020716-107.1.

Fu, H.D., Wang, B.K., Wan, Z.Q., Lin, H., Chang, M.L., and Han, G.L. (2016). Wnt5a mediated canonical Wnt signaling pathway activation in orthodontic tooth movement: possible role in the tension force-induced bone formation. *Journal of molecular histology* 47(5), 455-466. doi: 10.1007/s10735-016-9687-y.

Gadhari, N., Charnley, M., Marelli, M., Brugger, J., and Chiquet, M. (2013). Cell shape-dependent early responses of fibroblasts to cyclic strain. *Biochim. Biophys. Acta* 1833(12), 3415-3425. doi: 10.1016/j.bbamcr.2013.10.012.

Glogauer, M., Ferrier, J., and McCulloch, C.A. (1995). Magnetic fields applied to collagen-coated ferric oxide beads induce stretch-activated Ca2+ flux in fibroblasts. *The American journal of physiology* 269(5 Pt 1), C1093-1104. doi: 10.1152/ajpcell.1995.269.5.C1093.

Huang, T.H., Liu, S.L., Chen, C.L., Shie, M.Y., and Kao, C.T. (2013). Low-level laser effects on simulated orthodontic tension side periodontal ligament cells. *Photomedicine and laser surgery* 31(2), 72-77. doi: 10.1089/pho.2012.3359.

Kaku, M., Rosales Rocabado, J.M., Kitami, M., Ida, T., Akiba, Y., Yamauchi, M., et al. (2016). Mechanical Loading Stimulates Expression of Collagen Cross-Linking Associated Enzymes in Periodontal Ligament. *J. Cell. Physiol.* 231(4), 926-933. doi: 10.1002/jcp.25184.

Kletsas, D., Basdra, E.K., and Papavassiliou, A.G. (1998). Mechanical stress induces DNA synthesis in PDL fibroblasts by a mechanism unrelated to autocrine growth factor action. *FEBS letters* 430(3), 358-362.

Ku, S.J., Chang, Y.I., Chae, C.H., Kim, S.G., Park, Y.W., Jung, Y.K., et al. (2009). Static tensional forces increase osteogenic gene expression in three-dimensional periodontal ligament cell culture. *BMB Rep.* 42(7), 427-432. doi: 10.5483/bmbrep.2009.42.7.427.

Lew, A.M., Glogauer, M., and McUlloch, C.A. (1999). Specific inhibition of skeletal alpha-actin gene transcription by applied mechanical forces through integrins and actin. *The Biochemical journal* 341 (Pt 3), 647-653.

Li, M., Zhang, C., and Yang, Y. (2019a). Effects of mechanical forces on osteogenesis and osteoclastogenesis in human periodontal ligament fibroblasts: A systematic review of in vitro studies. *Bone Joint Res* 8(1), 19-31. doi: 10.1302/2046-3758.81.Bjr-2018-0060.R1.

Li, Q., Han, G., Liu, D., and Zhou, Y. (2019b). Force-induced decline of TEA domain family member 1 contributes to osteoclastogenesis via regulation of Osteoprotegerin. *Arch. Oral Biol.* 100, 23-32. doi: 10.1016/j.archoralbio.2019.01.020.

Liu, F., Wen, F., He, D., Liu, D., Yang, R., Wang, X., et al. (2017). Force-Induced H2S by PDLSCs Modifies Osteoclastic Activity during Tooth Movement. *J. Dent. Res.* 96(6), 694-702. doi: 10.1177/0022034517690388.

Loesberg, W.A., Walboomers, X.F., van Loon, J.J., and Jansen, J.A. (2005). The effect of combined cyclic mechanical stretching and microgrooved surface topography on the behavior of fibroblasts. *Journal of biomedical materials research. Part A* 75(3), 723-732. doi: 10.1002/jbm.a.30480.

Marciniak, J., Lossdorfer, S., Kirschneck, C., Deschner, J., Jager, A., and Wolf, M. (2019). Heat shock protein 70 dampens the inflammatory response of human PDL cells to mechanical loading in vitro. *J. Periodontal Res.* doi: 10.1111/jre.12648.

Norton, L.A., Andersen, K.L., Arenholt-Bindslev, D., Andersen, L., and Melsen, B. (1995). A methodical study of shape changes in human oral cells perturbed by a simulated orthodontic strain in vitro. *Arch. Oral Biol.* 40(9), 863-872.

Norton, L.A., Andersen, K.L., Melsen, B., Bindslev, D.A., and Celis, J.E. (1990). Buccal mucosa fibroblasts and periodontal ligament cells perturbed by tensile stimuli in vitro. *Scandinavian journal of dental research* 98(1), 36-46.

Pavasant, P., and Yongchaitrakul, T. (2011). Role of mechanical stress on the function of periodontal ligament cells. *Periodontol. 2000* 56(1), 154-165. doi: 10.1111/j.1600-0757.2010.00374.x.

Pavlin, D., and Gluhak-Heinrich, J. (2001). Effect of mechanical loading on periodontal cells. *Critical reviews in oral biology and medicine : an official publication of the American Association of Oral Biologists* 12(5), 414-424.

Pender, N., and McCulloch, C.A. (1991). Quantitation of actin polymerization in two human fibroblast sub-types responding to mechanical stretching. *J. Cell Sci.* 100 (Pt 1), 187-193.

Rosselli-Murai, L.K., Almeida, L.O., Zagni, C., Galindo-Moreno, P., Padial-Molina, M., Volk, S.L., et al. (2013). Periostin responds to mechanical stress and tension by activating the MTOR signaling pathway. *PloS One* 8(12), e83580. doi: 10.1371/journal.pone.0083580.

Saminathan, A., Sriram, G., Vinoth, J.K., Cao, T., and Meikle, M.C. (2015). Engineering the periodontal ligament in hyaluronan-gelatin-type I collagen constructs: upregulation of apoptosis and alterations in gene expression by cyclic compressive strain. *Tissue engineering. Part A* 21(3-4), 518-529. doi: 10.1089/ten.TEA.2014.0221.

Takimoto, A., Kawatsu, M., Yoshimoto, Y., Kawamoto, T., Seiryu, M., Takano-Yamamoto, T., et al. (2015). Scleraxis and osterix antagonistically regulate tensile force-responsive remodeling of the periodontal ligament and alveolar bone. *Development (Cambridge, England)* 142(4), 787-796. doi: 10.1242/dev.116228.

Von den Hoff, J.W. (2003). Effects of mechanical tension on matrix degradation by human periodontal ligament cells cultured in collagen gels. *J. Periodontal Res.* 38(5), 449-457.

Wan, W., He, C., Du, C., Wang, Y., Wu, S., Wang, T., et al. (2019). Effect of ILK on small-molecule metabolism of human periodontal ligament fibroblasts with mechanical stretching. *J. Periodontal Res.* doi: 10.1111/jre.12706.

Wang, T., Li, G., Chen, J., Lin, Z., Qin, H., and Ji, J. (2016). Three-dimensional stress In vitro promotes the proliferation and differentiation of periodontal ligament stem cells implanted by bioactive glass. *Cellular and molecular biology (Noisy-le-Grand, France)* 62(10), 62-67.

Wang, Z., Maruyama, K., Sakisaka, Y., Suzuki, S., Tada, H., Suto, M., et al. (2019). Cyclic Stretch Force Induces Periodontal Ligament Cells to Secrete Exosomes That Suppress IL-1beta Production Through the Inhibition of the NF-kappaB Signaling Pathway in Macrophages. *Frontiers in immunology* 10, 1310. doi: 10.3389/fimmu.2019.01310.

Wolf, M., Lossdorfer, S., Craveiro, R., Gotz, W., and Jager, A. (2013). Regulation of macrophage migration and activity by high-mobility group box 1 protein released from periodontal ligament cells during orthodontically induced periodontal repair: an in vitro and in vivo experimental study. *J. Orofac. Orthop.* 74(5), 420-434. doi: 10.1007/s00056-013-0167-7.

Wongkhantee, S., Yongchaitrakul, T., and Pavasant, P. (2008). Mechanical stress induces osteopontin via ATP/P2Y1 in periodontal cells. *J. Dent. Res.* 87(6), 564-568. doi: 10.1177/154405910808700601.

Xu, H., Han, X., Meng, Y., Gao, L., Guo, Y., Jing, Y., et al. (2014). Favorable effect of myofibroblasts on collagen synthesis and osteocalcin production in the periodontal ligament. *Am. J. Orthod. Dentofacial Orthop.* 145(4), 469-479. doi: 10.1016/j.ajodo.2013.12.019.

Xu, Y., Shen, J., Muhammed, F.K., Zheng, B., Zhang, Y., and Liu, Y. (2017). Effect of orthodontic force on the expression of PI3K, Akt, and P70S6 K in the human periodontal ligament during orthodontic loading. *Cell Biochem. Funct.* 35(7), 372-377. doi: 10.1002/cbf.3284.

Yamaguchi, M., and Kasai, K. (2005). Inflammation in periodontal tissues in response to mechanical forces. *Arch. Immunol. Ther. Exp. (Warsz.)* 53(5), 388-398.

Yang, L., Yang, Y., Wang, S., Li, Y., and Zhao, Z. (2015). In vitro mechanical loading models for periodontal ligament cells: from two-dimensional to three-dimensional models. *Arch. Oral Biol.* 60(3), 416-424. doi: 10.1016/j.archoralbio.2014.11.012.

Zhao, Z., Fan, Y., Bai, D., Wang, J., and Li, Y. (2008). The adaptive response of periodontal ligament to orthodontic force loading - a combined biomechanical and biological study. *Clinical biomechanics (Bristol, Avon)* 23 Suppl 1, S59-66. doi: 10.1016/j.clinbiomech.2007.10.016.

Zhong, W., Xu, C., Zhang, F., Jiang, X., Zhang, X., and Ye, D. (2008). Cyclic stretching force-induced early apoptosis in human periodontal ligament cells. *Oral diseases* 14(3), 270-276. doi: 10.1111/j.1601-0825.2007.01375.x.

Supplement 2: Extracted data from included studies

Tabulated were the study citation and extracted information on the cells use (age/gender of donors, tooth type, isolation method, passages and cell density used in the experiments), force-related information ("dynamic"/"static" and "equibiaxial"/"uniaxial"; its duration, frequency of exposure, magnitude, and the device used), and the genes, proteins and/or metaoblites analyzed includng the official gene symbol, methods applied to measure their expression and data on the expression pattern (Figure 2) and the peak expression data.

Reference	Gene/ Analyte[a]	Official gene symbol / abbreviation[b]	Cell (age/gender of donors, tooth type, isolation method, passages used, cell density)[a,c]	Force type (stat./ dyn.)[a]	Force duration and frequency[d]	Force magnitude[a]	Force apparatus[a]	Force type: equibiaxial or uniaxial[e]	Gene expression: Increase, decrease, no change (method w/ reference gene); Methods: qPCR, sqPCR, Northern blot[f]	Gene expression: When it reaches peak and peak's magnitude (fold change; times or ratio; unclear = ?)[f]	Protein expression: Increase, decrease, no change (method w/ reference); Methods: ELISA, WB, RIA, EMSA, IF[f]	Protein expression: When it reaches peak and peak's magnitude (times or ratio; unclear = ?)[f]
Abiko et al. (1998)	COX1	*PTGS1*	HPDLF (18/n.g., 19/n.g., 23/n.g., PM, exp, P5-6, P18-20, 5×10³)	dynamic	**0.1Hz** (6cyc/min) for 1d, 3d, 5d	18%	Flexercell Strain Unit + Flexcell Corp. plate + vacuum (Yamaguchi et al, 1997)	equibiaxial	no change (sqPCR, GAPDH)	only day 3 reported (no quantitative information is given)	n.g.	n.g.
Abiko et al. (1998)	COX2	*PTGS2*	HPDLF (18/n.g., 19/n.g., 23/n.g., PM, exp, P5-6, P18-20, 5×10³)	dynamic	**0.1Hz** (6cyc/min) for 1d, 3d, 5d	18%	Flexercell Strain Unit + Flexcell Corp. plate + vacuum (Yamaguchi et al, 1997)	equibiaxial	increase (sqPCR, GAPDH)	only day 3 reported (no quantitative information is given)	n.g.	n.g.
Abiko et al. (1998)	ICE	*CASP1*	HPDLF (18/n.g., 19/n.g., 23/n.g., PM, exp, P5-6, P18-20, 5×10³)	dynamic	**0.1Hz** (6cyc/min) for 1d, 3d, 5d	18%	Flexercell Strain Unit + Flexcell Corp. plate + vacuum (Yamaguchi et al, 1997)	equibiaxial	no change (sqPCR, GAPDH)	only day 3 reported (no quantitative information is given)	n.g.	n.g.
Abiko et al. (1998)	IL-1β	*IL1B*	HPDLF (18/n.g., 19/n.g., 23/n.g., PM, exp, P5-6, P18-20, 5×10³)	dynamic	**0.1Hz** (6cyc/min) for 1d, 3d, 5d	18%	Flexercell Strain Unit + Flexcell Corp. plate + vacuum (Yamaguchi et al, 1997)	equibiaxial	n.g.	n.g.	"young cells" (P5-6): increase followed by plateau (ELISA) "old cells" (P18-20): increase (ELISA)	"young cells" @ 3d…5d: 40.15 (ng/10⁶ cellls) / 2.1 (ratio-calc) "old cells" @ 5d: 58.10 (ng/10⁶ cellls) / 2.8 (ratio-calc)
Abiko et al. (1998)	PA	*PLAT; PLAU*	HPDLF (18/n.g., 19/n.g., 23/n.g., PM, exp, P5-6, P18-20, 5×10³)	dynamic	**0.1Hz** (6cyc/min) for 1d, 3d, 5d	18%	Flexercell Strain Unit + Flexcell Corp. plate + vacuum (Yamaguchi et al, 1997)	equibiaxial	n.g.	n.g.	"young cells" (P5-6): increase (ELISA) "old cells" (P18-20): increase (ELISA)	"young cells" @ 5d: 7.90 (ng/10⁶ cellls) / 2.1 (ratio-calc) "old cells" @ 5d: 11.75 (ng/10⁶ cellls) / 3.1 (ratio-calc)
Abiko et al. (1998)	PAI-1	*SERPINE1*	HPDLF (18/n.g., 19/n.g., 23/n.g., PM, exp, P5-6, P18-20, 5×10³)	dynamic	**0.1Hz** (6cyc/min) for 1d, 3d, 5d	18%	Flexercell Strain Unit + Flexcell Corp. plate + vacuum (Yamaguchi et al, 1997)	equibiaxial	no change (sqPCR, GAPDH)	only day 3 reported (no quantitative information is given)	n.g.	n.g.
Abiko et al. (1998)	PGE_2	PGE_2	HPDLF (18/n.g., 19/n.g., 23/n.g., PM, exp, P5-6, P18-20, 5×10³)	dynamic	**0.1Hz** (6cyc/min) for 1d, 3d, 5d	18%	Flexercell Strain Unit + Flexcell Corp. plate + vacuum (Yamaguchi et al, 1997)	equibiaxial	n.a.	n.a.	"young cells" (P5-6): increase (ELISA) "old cells" (P18-20): increase (ELISA)	"young cells" @ 5d: 8.20 (ng/10⁶ cellls) / 14.9 (ratio-calc) "old cells" @ 5d: 12.25 (ng/10⁶ cellls) / 18 (ratio-calc)
Abiko et al. (1998)	tPA	*PLAT*	HPDLF (18/n.g., 19/n.g., 23/n.g., PM, exp, P5-6, P18-20, 5×10³)	dynamic	**0.1Hz** (6cyc/min) for 1d, 3d, 5d	18%	Flexercell Strain Unit + Flexcell Corp. plate + vacuum (Yamaguchi et al, 1997)	equibiaxial	increase (sqPCR, GAPDH)	only day 3 reported (no quantitative information is given)	n.g.	n.g.
Abiko et al. (1998)	uPA	*PLAU*	HPDLF (18/n.g., 19/n.g., 23/n.g., PM, exp, P5-6, P18-20, 5×10³)	dynamic	**0.1Hz** (6cyc/min) for 1d, 3d, 5d	18%	Flexercell Strain Unit + Flexcell Corp. plate + vacuum (Yamaguchi et al, 1997)	equibiaxial	no change (sqPCR, GAPDH)	only day 3 reported (no quantitative information is given)	n.g.	n.g.
Agarwal et al. (2003)	COX2	*PTGS2*	HPDLF (18/F, 18/F, 22/M, M, exp, P6-12, 80% confluence)	dynamic	0.005Hz for 4h	3%, 6%, 8%	Flexercell Strain Unit + collagen type I-coated Bioflex II, six-well plates + vacuum	equibiaxial	increase (sqPCR; GAPDH)	6%: 7.6 (rel)† / 2.2 (ratio-calc)	n.g.	n.g.
Agarwal et al. (2003)	COX2	*PTGS2*	HPDLF (18/F, 18/F, 22/M, M, exp, P6-12, 80% confluence)	dynamic	0.005Hz for 4h, 24h, 48h	15%	Flexercell Strain Unit + collagen type I-coated Bioflex II, six-well plates + vacuum	equibiaxial	increase (sqPCR; GAPDH)	48h: 116.8 (rel)† / 31.8 (ratio-calc)	n.g.	n.g.
Agarwal et al. (2003)	I-κBβ	*NFKBIB*	HPDLF (18/F, 18/F, 22/M, M, exp, P6-12, 80% confluence)	dynamic	0.005Hz for 30min	6%	Flexercell Strain Unit + collagen type I-coated Bioflex II, six-well plates + vacuum	equibiaxial	n.g.	n.g.	n.g.	n.g.
Agarwal et al. (2003)	I-κBβ	*NFKBIB*	HPDLF (18/F, 18/F, 22/M, M, exp, P6-12, 80% confluence)	dynamic	0.005Hz for 30min	15%	Flexercell Strain Unit + collagen type I-coated Bioflex II, six-well plates + vacuum	equibiaxial	n.g.	n.g.	n.g.	n.g.
Agarwal et al. (2003)	NF-kB	*NFKB1*	HPDLF (18/F, 18/F, 22/M, M, exp, P6-12, 80% confluence)	dynamic	0.005Hz for 30min, 60min, 90min, 120min	6%	Flexercell Strain Unit + collagen type I-coated Bioflex II, six-well plates + vacuum	equibiaxial	n.g.	n.g.	n.g.	n.g.
Agarwal et al. (2003)	NF-kB	*NFKB1*	HPDLF (18/F, 18/F, 22/M, M, exp, P6-12, 80% confluence)	dynamic	0.005Hz for 30min, 60min, 120min	15%	Flexercell Strain Unit + collagen type I-coated Bioflex II, six-well plates + vacuum	equibiaxial	n.g.	n.g.	n.g.	n.g.
Agarwal et al. (2003)	PGE_2	PGE_2	HPDLF (18/F, 18/F, 22/M, M, exp, P6-12, 80% confluence)	dynamic	0.005Hz for 24h	1%, 2%, 3%, 4%, 5%, 6%, 7%, 8%, 10%, 12.5%, 15%, 18%	Flexercell Strain Unit + collagen type I-coated Bioflex II, six-well plates + vacuum	equibiaxial	n.a.	n.a.	1%, 2%, 3%, 4%, 5%, 6%, 7%, 8%: no expression (RIA) 10%, 12.5%, 15%, 18%: increase (RIA)	18%: 135 (ng/10⁶ cells)* / control n.g.
Agarwal et al. (2003)	PGE_2	PGE_2	HPDLF (18/F, 18/F, 22/M, M, exp, P6-12, 80% confluence)	dynamic	0.005Hz for 12h, 24h, 48h	15%	Flexercell Strain Unit + collagen type I-coated Bioflex II, six-well plates + vacuum	equibiaxial	n.a.	n.a.	increase followed by plateau (RIA)	24h…48h: 75.1† (?) / 15.6 (ratio-calc)
Arima et al. (2019)	DKK1	*DKK1*	HPDLC (3 donors: 22/F, 23/M, 25/F, M, exp, P4-P6, Subconfluence)	dynamic	0.5Hz for 24h	10%	STREX STB-140 + culture chambers (STREX Co., Osaka, Japan) coated with type-I collagen (Cell matrix I-P, Nitta Gelatin Inc., Osaka, Japan) + motor	uniaxial	donor 3D: increase (qPCR, β-actin) donor 3S: increase (qPCR, β-actin) donor 3U: increase (qPCR, β-actin)	donor 3D: 11.7 (FC)* donor 3S: 1.7 (FC)* donor 3U: 1.6 (FC)*	n.g.	n.g.
Arima et al. (2019)	RSPO2	*RSPO2*	HPDLC (3 donors: 22/F, 23/M, 25/F, M, exp, P4-P6, Subconfluence)	dynamic	0.5Hz for 24h	10%	STREX STB-140 + culture chambers (STREX Co., Osaka, Japan) coated with type-I collagen (Cell matrix I-P, Nitta Gelatin Inc., Osaka, Japan) + motor	uniaxial	donor 3D: increase (qPCR, β-actin) donor 3S: increase (qPCR, β-actin) donor 3U: increase (qPCR, β-actin)	donor 3D: 5.2 (FC)* donor 3S: 2 (FC)* donor 3U: 1.6 (FC)*	n.g.	n.g.

[a] Entry given as reported in the study.
[b] All official gene symbols come from the HUGO Gene Nomenclature Committee (HGNC; URL: https://www.genenames.org) after checking specificity of primers with Primer-BLAST.
[c] Gender/Sex of donors: "M" – male, "F" – female; Tooth type: "PM" – premolar, "M" – molar; Cell density: given in cells/well if not otherwise mentioned.
[d] Frequencies labeled bold orange were converted to hertz (Hz) according to its definition using the information reported in the study (in brackets)
[e] Force type deduced from the description of the force apparatus given by the authors.
[f] Gene and protein expression: 1. conclusion of change (increase, decrease…) was given according to the defined criteria in Figure 2; 2. different markers to describe the amount of change; † Information derived from figures using Engauge Digitizer; *Folds calculated by measuring the graphs, without using the Engauge Digitizer; No makers: Information derived from figures by description in the articles

Reference	Gene/ Analyte[a]	Official gene symbol / abbreviation[b]	Cell (age/gender of donors, tooth type, isolation method, passages used, cell density)[a,c]	Force type (stat./ dyn.)[a]	Force duration and frequency[d]	Force magnitude[a]	Force apparatus[a]	Force type: equibiaxial or uniaxial[e]	Gene expression: Increase, decrease, no change (method w/ reference gene); Methods: qPCR, sqPCR, Northern blot[f]	Gene expression: When it reaches peak and peak's magnitude (fold change; times or ratio; unclear = ?)[f]	Protein expression: Increase, decrease, no change (method w/ reference); Methods: ELISA, WB, RIA, EMSA, IF[f]	Protein expression: When it reaches peak and peak's magnitude (times or ratio; unclear = ?)[f]
Basdra et al. (1995)	Rab17	*RAB17*	HPDL-fibroblasts outgrowth (n.g./n.g., M, exp, P n.g., 4×10^5)	static	1h	2.5%	Petriperm dish + brass spheroidal convex template + brass weight	equibiaxial	n.g.	n.g.	increase (WB)	no quantitative information is given
Basdra et al. (1995)	rab3a	*RAB3A*	HPDL-fibroblasts outgrowth (n.g./n.g., M, exp, P n.g., 4×10^5)	static	1h	2.5%	Petriperm dish + brass spheroidal convex template + brass weight	equibiaxial	n.g.	n.g.	increase (WB)	no quantitative information is given
Basdra et al. (1995)	rab3b	*RAB3B*	HPDL-fibroblasts outgrowth (n.g./n.g., M, exp, P n.g., 4×10^5)	static	1h	2.5%	Petriperm dish + brass spheroidal convex template + brass weight	equibiaxial	n.g.	n.g.	increase (WB)	no quantitative information is given
Basdra et al. (1995)	rab6	*RAB6A*	HPDL-fibroblasts outgrowth (n.g./n.g., M, exp, P n.g., 4×10^5)	static	1h	2.5%	Petriperm dish + brass spheroidal convex template + brass weight	equibiaxial	n.g.	n.g.	increase (WB)	no quantitative information is given
Basdra et al. (1995)	rhoA	*RHOA*	HPDL-fibroblasts outgrowth (n.g./n.g., M, exp, P n.g., 4×10^5)	static	1h	2.5%	Petriperm dish + brass spheroidal convex template + brass weight	equibiaxial	n.g.	n.g.	decrease (WB)	no quantitative information is given
Basdra et al. (1996)	Vimentin	*VIM*	HPDL-fibroblasts outgrowth (n.g./n.g., M, exp, P n.g., 3×10^5)	static	12h	2.5%	Petriperm dish + spheroidal copper template + weight	equibiaxial	n.g.	n.g.	no change (WB)	no quantitative information is given
Basdra et al. (1996)	α-tubulin	*TUBA1C; TUBA3C; TUBA3D; TUBA4A*	HPDL-fibroblasts outgrowth (n.g./n.g., M, exp, P n.g., 3×10^5)	static	12h	2.5%	Petriperm dish + spheroidal copper template + weight	equibiaxial	n.g.	n.g.	no change (WB)	no quantitative information is given
Basdra et al. (1996)	β-tubulin	*TUBA1B*	HPDL-fibroblasts outgrowth (n.g./n.g., M, exp, P n.g., 3×10^5)	static	12h	2.5%	Petriperm dish + spheroidal copper template + weight	equibiaxial	n.g.	n.g.	no change (WB)	no quantitative information is given
Bolcato-Bellemin et al. (2000)	integrin α1	*ITGA1*	HPDL fibroblasts (n.g./F, M, exp, P4, 4×10^5)	static	12h	20kPa	Flexercell Strain Unit + Bioflex Culture Plate + vacuum (Carvalho et al 1996)	equibiaxial	no change (sqPCR, β-actin)	no change	n.g.	n.g.
Bolcato-Bellemin et al. (2000)	integrin α2	*ITGA2*	HPDL fibroblasts (n.g./F, M, exp, P4, 4×10^5)	static	12h	20kPa	Flexercell Strain Unit + Bioflex Culture Plate + vacuum (Carvalho et al 1996)	equibiaxial	no change (sqPCR, β-actin)	no change	n.g.	n.g.
Bolcato-Bellemin et al. (2000)	Integrin α3	*ITGA3*	HPDL fibroblasts (n.g./F, M, exp, P4, 4×10^5)	static	12h	20kPa	Flexercell Strain Unit + Bioflex Culture Plate + vacuum (Carvalho et al 1996)	equibiaxial	no change (sqPCR, β-actin)	no change	n.g.	n.g.
Bolcato-Bellemin et al. (2000)	Integrin α4	*ITGA4*	HPDL fibroblasts (n.g./F, M, exp, P4, 4×10^5)	static	12h	20kPa	Flexercell Strain Unit + Bioflex Culture Plate + vacuum (Carvalho et al 1996)	equibiaxial	no change (sqPCR, β-actin)	no change	n.g.	n.g.
Bolcato-Bellemin et al. (2000)	Integrin α5	*ITGA5*	HPDL fibroblasts (n.g./F, M, exp, P4, 4×10^5)	static	12h	20kPa	Flexercell Strain Unit + Bioflex Culture Plate + vacuum (Carvalho et al 1996)	equibiaxial	decrease (sqPCR, β-actin)	0.283 (rel) / 0.5 (ratio-calc)	n.g.	n.g.
Bolcato-Bellemin et al. (2000)	Integrin α6	*ITGA6*	HPDL fibroblasts (n.g./F, M, exp, P4, 4×10^5)	static	12h	20kPa	Flexercell Strain Unit + Bioflex Culture Plate + vacuum (Carvalho et al 1996)	equibiaxial	increase (sqPCR, β-actin)	0.247 (rel) / 2.2 (ratio-calc)	n.g.	n.g.
Bolcato-Bellemin et al. (2000)	Integrin αv	*ITGAV*	HPDL fibroblasts (n.g./F, M, exp, P4, 4×10^5)	static	12h	20kPa	Flexercell Strain Unit + Bioflex Culture Plate + vacuum (Carvalho et al 1996)	equibiaxial	no change (sqPCR, β-actin)	no change	n.g.	n.g.
Bolcato-Bellemin et al. (2000)	Integrin β1	*ITGB1*	HPDL fibroblasts (n.g./F, M, exp, P4, 4×10^5)	static	12h	20kPa	Flexercell Strain Unit + Bioflex Culture Plate + vacuum (Carvalho et al 1996)	equibiaxial	increase (sqPCR, β-actin)	0.360 (rel) / 3.3 (ratio-calc)	n.g.	n.g.
Bolcato-Bellemin et al. (2000)	Integrin β3	*ITGB3*	HPDL fibroblasts (n.g./F, M, exp, P4, 4×10^5)	static	12h	20kPa	Flexercell Strain Unit + Bioflex Culture Plate + vacuum (Carvalho et al 1996)	equibiaxial	no change (sqPCR, β-actin)	no change	n.g.	n.g.
Bolcato-Bellemin et al. (2000)	Integrin β4	*ITGB4*	HPDL fibroblasts (n.g./F, M, exp, P4, 4×10^5)	static	12h	20kPa	Flexercell Strain Unit + Bioflex Culture Plate + vacuum (Carvalho et al 1996)	equibiaxial	no change (sqPCR, β-actin)	no change	n.g.	n.g.
Bolcato-Bellemin et al. (2000)	MMP-1	*MMP1*	HPDL fibroblasts (n.g./F, M, exp, P4, 4×10^5)	static	12h	20kPa	Flexercell Strain Unit + Bioflex Culture Plate + vacuum (Carvalho et al 1996)	equibiaxial	increase (sqPCR, β-actin)	0.250 (rel) / 5 (ratio-calc)	n.g.	n.g.
Bolcato-Bellemin et al. (2000)	MMP-2	*MMP2*	HPDL fibroblasts (n.g./F, M, exp, P4, 4×10^5)	static	12h	20kPa	Flexercell Strain Unit + Bioflex Culture Plate + vacuum (Carvalho et al 1996)	equibiaxial	increase (sqPCR, β-actin)	0.210 (rel) / 2.1 (ratio-calc)	n.g.	n.g.
Bolcato-Bellemin et al. (2000)	MMP-9	*MMP9*	HPDL fibroblasts (n.g./F, M, exp, P4, 4×10^5)	static	12h	20kPa	Flexercell Strain Unit + Bioflex Culture Plate + vacuum (Carvalho et al 1996)	equibiaxial	no expression (sqPCR, β-actin)	no expression	n.g.	n.g.
Bolcato-Bellemin et al. (2000)	MT1-MMP	*MMP14*	HPDL fibroblasts (n.g./F, M, exp, P4, 4×10^5)	static	12h	20kPa	Flexercell Strain Unit + Bioflex Culture Plate + vacuum (Carvalho et al 1996)	equibiaxial	no change (sqPCR, β-actin)	no change	n.g.	n.g.
Bolcato-Bellemin et al. (2000)	TIMP-1	*TIMP1*	HPDL fibroblasts (n.g./F, M, exp, P4, 4×10^5)	static	12h	20kPa	Flexercell Strain Unit + Bioflex Culture Plate + vacuum (Carvalho et al 1996)	equibiaxial	increase (sqPCR, β-actin)	0.075 (rel) / 1.5 (ratio-calc)	n.g.	n.g.
Bolcato-Bellemin et al. (2000)	TIMP-2	*TIMP2*	HPDL fibroblasts (n.g./F, M, exp, P4, 4×10^5)	static	12h	20kPa	Flexercell Strain Unit + Bioflex Culture Plate + vacuum (Carvalho et al 1996)	equibiaxial	increase (sqPCR, β-actin)	0.291 (rel) / 5 (ratio-calc)	n.g.	n.g.
Bolcato-Bellemin et al. (2000)	TIMP-3	*TIMP3*	HPDL fibroblasts (n.g./F, M, exp, P4, 4×10^5)	static	12h	20kPa	Flexercell Strain Unit + Bioflex Culture Plate + vacuum (Carvalho et al 1996)	equibiaxial	no change (sqPCR, β-actin)	no change	n.g.	n.g.
Chang et al. (2015)	ALP	*ALPP*	HPDLCs (n.g./n.g., PM, exp, P3, 1.0×10^6)	dynamic	**0.1Hz** (6cyc/min: 5s on and 5s off) for 6h, 12h, 24h, 48h, 72h	12%	Flexercell FX-4000 Strain Unit + 6-well BioFlex plates coated with type I collagen + vacuum	equibiaxial	increase (qPCR, GAPDH)	72h: 5.3 (ratio)*	n.g.	n.g.
Chang et al. (2015)	ARRAY	ARRAY	HPDLCs (n.g./n.g., PM, exp, P3, 1.0×10^6)	dynamic	**0.1Hz** (6cyc/min: 5s on and 5s off) for 6h, 12h, 24h, 48h, 72h	12%	Flexercell FX-4000 Strain Unit + 6-well BioFlex plates coated with type I collagen + vacuum	equibiaxial	mRNA: Agilent Whole Genome Oligo Microarrays (Agilent, Santa Clara, CA) miRNA: Exiqon miRNA Array (Exiqon, Vedbaek, Denmark)		n.g.	n.g.
Chang et al. (2015)	CREB1	*CREB1*	HPDLCs (n.g./n.g., PM, exp, P3, 1.0×10^6)	dynamic	**0.1Hz** (6cyc/min: 5s on and 5 s off) for 72h	12%	Flexercell FX-4000 Strain Unit + 6-well BioFlex plates coated with type I collagen + vacuum	equibiaxial	increase (qPCR, GAPDH)	72h: 1.8 (ratio)*	n.g.	n.g.
Chang et al. (2015)	FGF2	*FGF2*	HPDLCs (n.g./n.g., PM, exp, P3, 1.0×10^6)	dynamic	**0.1Hz** (6cyc/min: 5s on and 5s off) for 72h	12%	Flexercell FX-4000 Strain Unit + 6-well BioFlex plates coated with type I collagen + vacuum	equibiaxial	increase (qPCR, GAPDH)	72h: 2.2 (ratio)*	n.g.	n.g.

[a] Entry given as reported in the study.
[b] All official gene symbols come from the HUGO Gene Nomenclature Committee (HGNC; URL: https://www.genenames.org) after checking specificity of primers with Primer-BLAST.
[c] Gender/Sex of donors: "M" – male, "F" – female; Tooth type: "PM" – premolar, "M" – molar; Cell density: given in cells/well if not otherwise mentioned.
[d] Frequencies labeled bold orange were converted to hertz (Hz) according to its definition using the information reported in the study (in brackets)
[e] Force type deduced from the description of the force apparatus given by the authors.
[f] Gene and protein expression: 1. conclusion of change (increase, decrease…) was given according to the defined criteria in Figure 2; 2. different markers to describe the amount of change; † Information derived from figures using Engauge Digitizer; *Folds calculated by measuring the graphs, without using the Engauge Digitizer; No makers: Information derived from figures by description in the articles

Reference	Gene/ Analyte[a]	Official gene symbol / abbreviation[b]	Cell (age/gender of donors, tooth type, isolation method, passages used, cell density)[a,c]	Force type (stat./ dyn.)[a]	Force duration and frequency[d]	Force magnitude[a]	Force apparatus[a]	Force type: equibiaxial or uniaxial[e]	Gene expression: Increase, decrease, no change (method w/ reference gene); Methods: qPCR, sqPCR, Northern blot[f]	Gene expression: When it reaches peak and peak's magnitude (fold change; times or ratio; unclear = ?)[f]	Protein expression: Increase, decrease, no change (method w/ reference); Methods: ELISA, WB, RIA, EMSA, IF[f]	Protein expression: When it reaches peak and peak's magnitude (times or ratio; unclear = ?)[f]
Chang et al. (2015)	miR-424-5p miR-1297 miR-3607-5p miR-145-5p miR-4328 miR-224-5p miR-195-5p	*MIR424* *MIR1297* *miR-3607-5p* *MIR145* *MIR4328* *MIR224* *MIR195*	HPDLCs (n.g./n.g., PM, exp, P3, 1.0×10^6)	dynamic	**0.1Hz** (6cyc/min: 5s on and 5s off) for 72h	12%	Flexercell FX-4000 Strain Unit + 6-well BioFlex plates coated with type I collagen + vacuum	equibiaxial	decrease (qPCR, U6 SnRNA) decrease (qPCR, U6 SnRNA) decrease (qPCR, U6 SnRNA) decrease (qPCR, U6 SnRNA) decrease (qPCR, U6 SnRNA) decrease (qPCR, U6 SnRNA) decrease (qPCR, U6 SnRNA)	miR-424-5p: 0.4 (ratio)* miR-1297: 0.6 (ratio)* miR-3607-5p: 0.2 (ratio)* miR-145-5p: 0.3 (ratio)* miR-4328: 0.8 (ratio)* miR-224-5p: 0.4 (ratio)* miR-195-5p: 0.6 (ratio)*	n.g.	n.g.
Chang et al. (2015)	OCN	*BGLAP*	HPDLCs (n.g./n.g., PM, exp, P3, 1.0×10^6)	dynamic	**0.1Hz** (6cyc/min: 5s on and 5s off) for 6h, 12h, 24h, 48h, 72h	12%	Flexercell FX-4000 Strain Unit + 6-well BioFlex plates coated with type I collagen + vacuum	equibiaxial	increase (qPCR, GAPDH)	72h: 2 (ratio)*	n.g.	n.g.
Chang et al. (2017)	ALP	*ALPP*	HPDLCs (14-20/n.g., PM, dig, P<5, 80% confluence)	dynamic	0.1Hz for 24h, 48h, 72h	12%	Custom-made strain device Tension Plus System (Chang et al 2015; Wescott et al 2007) + flexible-bottomed culture plates (Flexcell)	equibiaxial	n.g.	n.g.	increase (PNPP)	72h: 0.8 (U/mg)* / 2.7 (ratio-calc)
Chang et al. (2017)	BMPR1A	*BMPR1A*	HPDLCs (14-20/n.g., PM, dig, P<5, 80% confluence)	dynamic	0.1Hz for 72h	12%	Custom-made strain device Tension Plus System (Chang et al 2015; Wescott et al 2007) + flexible-bottomed culture plates (Flexcell)	equibiaxial	n.g.	n.g.	increase (WB, β-actin)	72h: 3.3 (ratio)*
Chang et al. (2017)	FGF2	*FGF2*	HPDLCs (14-20/n.g., PM, dig, P<5, 80% confluence)	dynamic	0.1Hz for 72h	12%	Custom-made strain device Tension Plus System (Chang et al 2015; Wescott et al 2007) + flexible-bottomed culture plates (Flexcell)	equibiaxial	n.g.	n.g.	increase (WB, β-actin)	72h: 3.1 (ratio)*
Chang et al. (2017)	miR-195-5p	*MIR195*	HPDLCs (14-20/n.g., PM, dig, P<5, 80% confluence)	dynamic	0.1Hz for 24h, 48h, 72h	12%	Custom-made strain device Tension Plus System (Chang et al 2015; Wescott et al 2007) + flexible-bottomed culture plates (Flexcell)	equibiaxial	decrease (qPCR, U6 snRNA)	24h: 0.5 (FC)*	n.g.	n.g.
Chang et al. (2017)	OCN	*BGLAP*	HPDLCs (14-20/n.g., PM, dig, P<5, 80% confluence)	dynamic	0.1Hz for 72h	12%	Custom-made strain device Tension Plus System (Chang et al 2015; Wescott et al 2007) + flexible-bottomed culture plates (Flexcell)	equibiaxial	n.g.	n.g.	increase (WB, β-actin)	72h: 1.8 (ratio)*
Chang et al. (2017)	OPN	*SPP1*	HPDLCs (14-20/n.g., PM, dig, P<5, 80% confluence)	dynamic	0.1Hz for 72h	12%	Custom-made strain device Tension Plus System (Chang et al 2015; Wescott et al 2007) + flexible-bottomed culture plates (Flexcell)	equibiaxial	n.g.	n.g.	increase (WB, β-actin)	72h: 2.4 (ratio)*
Chang et al. (2017)	OSX	*SP7*	HPDLCs (14-20/n.g., PM, dig, P<5, 80% confluence)	dynamic	0.1Hz for 72h	12%	Custom-made strain device Tension Plus System (Chang et al 2015; Wescott et al 2007) + flexible-bottomed culture plates (Flexcell)	equibiaxial	n.g.	n.g.	increase (WB, β-actin)	72h: 26 (ratio)*
Chang et al. (2017)	Runx2	*RUNX2*	HPDLCs (14-20/n.g., PM, dig, P<5, 80% confluence)	dynamic	0.1Hz for 24h, 48h, 72h	12%	Custom-made strain device Tension Plus System (Chang et al 2015; Wescott et al 2007) + flexible-bottomed culture plates (Flexcell)	equibiaxial	increase (qPCR, GAPDH)	72h: 3 (FC)*	n.g.	n.g.
Chang et al. (2017)	WNT3A	*WNT3A*	HPDLCs (14-20/n.g., PM, dig, P<5, 80% confluence)	dynamic	0.1Hz for 72h	12%	Custom-made strain device Tension Plus System (Chang et al 2015; Wescott et al 2007) + flexible-bottomed culture plates (Flexcell)	equibiaxial	n.g.	n.g.	increase (WB, β-actin)	72h: 51 (ratio)*
Chen et al. (2014)	ALP	*ALPP*	HPDLs (n.g./n.g., M, dig, P3-9, 10^4 cells/mL)	static	sqPCR for 1d, 3d, 7d, 15d ELISA for 3d, 7d, 15d	-100 kPa (1Pa=1/100,000kg/cm², equal to a negative force of 101g/mm²)	"a tension incubator" (TI, Model 3618P; LabLine Instrument, Thermolyne Co., IL, USA) + 24-well plate + vacuum	equibiaxial	increase (?, actin)	7d: 0.5 (?)* / 2.1 (ratio-calc)	increase (ELISA)	15d: 0.2 (μM/μg DNA)* / 1.2 (ratio-calc)
Chen et al. (2014)	Collagen-1	*COL1A1; COL1A2*	HPDLs (n.g./n.g., M, dig, P3-9, 10^4 cells/mL)	static	1d, 3d, 7d, 15d	-100 kPa (1Pa=1/100,000kg/cm², equal to a negative force of 101g/mm²)	"a tension incubator" (TI, Model 3618P; LabLine Instrument, Thermolyne Co., IL, USA) + 24-well plate + vacuum	equibiaxial	no change (?, actin)		n.g.	n.g.
Chen et al. (2014)	ERK/p-ERK	MAPK3; MAPK1	HPDLs (n.g./n.g., M, dig, P3-9, 10^4 cells/mL)	static	3h, 6h, 12h, 24h	-100 kPa (1Pa=1/100,000kg/cm², equal to a negative force of 101g/mm²)	"a tension incubator" (TI, Model 3618P; LabLine Instrument, Thermolyne Co., IL, USA) + 24-well plate + vacuum	equibiaxial	n.g.	n.g.	p-ERK/ERK: increase (WB)	p-ERK/ERK: 24h: 0.6 (ratio)* / 2 (ratio-calc)
Chen et al. (2014)	FAK/p-FAK	PTK2	HPDLs (n.g./n.g., M, dig, P3-9, 10^4 cells/mL)	static	3h, 6h, 12h, 24h	-100 kPa (1Pa=1/100,000kg/cm², equal to a negative force of 101g/mm²)	"a tension incubator" (TI, Model 3618P; LabLine Instrument, Thermolyne Co., IL, USA) + 24-well plate + vacuum	equibiaxial	n.g.	n.g.	p-FAK/FAK: increase (WB)	p-FAK/FAK: 24h: 0.7 (ratio)* / 1.3 (ratio-calc)
Chen et al. (2014)	IL-1	*IL1B; IL1A*	HPDLs (n.g./n.g., M, dig, P3-9, 10^4 cells/mL)	static	1d, 3d, 7d, 15d	-100 kPa (1Pa=1/100,000kg/cm², equal to a negative force of 101g/mm²)	"a tension incubator" (TI, Model 3618P; LabLine Instrument, Thermolyne Co., IL, USA) + 24-well plate + vacuum	equibiaxial	increase (?, actin)	7d: 1.2 (?)* / 2.8 (ratio-calc)	n.g.	n.g.
Chen et al. (2014)	iNOS	*NOS2*	HPDLs (n.g./n.g., M, dig, P3-9, 10^4 cells/mL)	static	1d, 3d, 7d, 15d	-100 kPa (1Pa=1/100,000kg/cm², equal to a negative force of 101g/mm²)	"a tension incubator" (TI, Model 3618P; LabLine Instrument, Thermolyne Co., IL, USA) + 24-well plate + vacuum	equibiaxial	increase (?, actin)	7d: 1.2 (?)* / 2.4 (ratio-calc)	n.g.	n.g.
Chen et al. (2014)	OC	BGLAP	HPDLs (n.g./n.g., M, dig, P3-9, 10^4 cells/mL)	static	sqPCR for 1d, 3d, 7d, 15d ELISA for 7d, 15d	-100 kPa (1Pa=1/100,000kg/cm², equal to a negative force of 101g/mm²)	"a tension incubator" (TI, Model 3618P; LabLine Instrument, Thermolyne Co., IL, USA) + 24-well plate + vacuum	equibiaxial	increase (?, actin)	15d: 0.3 (?)* / 2.8 (ratio-calc)	increase (ELISA)	15d: 31.4 (pg/ml/cell)* / 1.3 (ratio-calc)

[a] Entry given as reported in the study.
[b] All official gene symbols come from the HUGO Gene Nomenclature Committee (HGNC; URL: https://www.genenames.org) after checking specificity of primers with Primer-BLAST.
[c] Gender/Sex of donors: "M" – male, "F" – female; Tooth type: "PM" – premolar, "M" – molar; Cell density: given in cells/well if not otherwise mentioned.
[d] Frequencies labeled bold orange were converted to hertz (Hz) according to its definition using the information reported in the study (in brackets)
[e] Force type deduced from the description of the force apparatus given by the authors.
[f] Gene and protein expression: 1. conclusion of change (increase, decrease…) was given according to the defined criteria in Figure 2; 2. different markers to describe the amount of change; † Information derived from figures using Engauge Digitizer; *Folds calculated by measuring the graphs, without using the Engauge Digitizer; No makers: Information derived from figures by description in the articles

Reference	Gene/ Analyte[a]	Official gene symbol / abbreviation[b]	Cell (age/gender of donors, tooth type, isolation method, passages used, cell density)[a,c]	Force type (stat./ dyn.)[a]	Force duration and frequency[d]	Force magnitude[a]	Force apparatus[a]	Force type: equibiaxial or uniaxial[e]	Gene expression: Increase, decrease, no change (method w/ reference gene); Methods: qPCR, sqPCR, Northern blot[f]	Gene expression: When it reaches peak and peak's magnitude (fold change; times or ratio; unclear = ?)[f]	Protein expression: Increase, decrease, no change (method w/ reference); Methods: ELISA, WB, RIA, EMSA, IF[f]	Protein expression: When it reaches peak and peak's magnitude (times or ratio; unclear = ?)[f]
Chen et al. (2014)	TNFα	*TNF*	HPDLs (n.g./n.g., M, dig, P3-9, 10^4 cells/mL)	static	1d, 3d, 7d, 15d	-100 kPa (1Pa=1/100,000kg/cm², equal to a negative force of 101g/mm²)	"a tension incubator" (TI, Model 3618P; LabLine Instrument, Thermolyne Co., IL, USA) + 24-well plate + vacuum	equibiaxial	increase (?, actin)	7d: 0.6 (?)* / 2.6 (ratio-calc)	n.g.	n.g.
Chen et al. (2015)	ARRAY	ARRAY	HPDLCs (18-25/n.g., M, exp, P3-5, 2×10^5)	dynamic	**0.1Hz** (6cyc/min) for 24h	12%	Flexcell FX-4000 strain unit + six-well flexible-bottomed uniflex-plates + vacuum	uniaxial	miRCURY LNA microRNA Array 7th generation (Exiqon A/S, Vedbaek, Denmark)		n.g.	n.g.
Chen et al. (2015)	COL1A1	*COL1A1*	HPDLCs (18-25/n.g., M, exp, P3-5, 2×10^5)	dynamic	**0.1Hz** (6cyc/min) for 24h	12%	Flexcell FX-4000 strain unit + six-well flexible-bottomed uniflex-plates + vacuum	uniaxial	increase (qPCR, β actin)	1.2 (FC)*	n.g.	n.g.
Chen et al. (2015)	COL3A1	*COL3A1*	HPDLCs (18-25/n.g., M, exp, P3-5, 2×10^5)	dynamic	**0.1Hz** (6cyc/min) for 24h	12%	Flexcell FX-4000 strain unit + six-well flexible-bottomed uniflex-plates + vacuum	uniaxial	increase (qPCR, β actin)	1.4 (FC)*	n.g.	n.g.
Chen et al. (2015)	COL5A1	*COL5A1*	HPDLCs (18-25/n.g., M, exp, P3-5, 2×10^5)	dynamic	**0.1Hz** (6cyc/min) for 24h	12%	Flexcell FX-4000 strain unit + six-well flexible-bottomed uniflex-plates + vacuum	uniaxial	increase (qPCR, β actin)	1.5 (FC)*	n.g.	n.g.
Chen et al. (2015)	miR-29a miR-29b miR-29c	*MIR29A* *MIR29B1* *MIR29C*	HPDLCs (18-25/n.g., M, exp, P3-5, 2×10^5)	dynamic	**0.1Hz** (6cyc/min) for 24h	12%	Flexcell FX-4000 strain unit + six-well flexible-bottomed uniflex-plates + vacuum	uniaxial	miR-29a: decrease (qPCR, U6snNA) miR-29b: decrease (qPCR, U6snNA) miR-29c: decrease (qPCR, U6snNA)	miR-29a: 0.6 (FC)* miR-29b: 0.5 (FC)* miR-29c: 0.6 (FC)*	n.g.	n.g.
Chen et al. (2015)	POSTN	*POSTN*	HPDLCs (18-25/n.g., M, exp, P3-5, 2×10^5)	dynamic	**0.1Hz** (6cyc/min) for 24h	12%	Flexcell FX-4000 strain unit + six-well flexible-bottomed uniflex-plates + vacuum	uniaxial	no change (qPCR, β actin)		n.g.	n.g.
Chiba and Mitani (2004)	ALP	*ALPP*	Human PDL cells (n.g./n.g., n.g., exp, P4-6, n.g.)	dynamic	**0.5Hz** (30cyc/min: 1s stretch and 1s relaxation) for 2d, 5d	15%	Flexercell strain unit + Bioflex plates + vacuum	equibiaxial	n.g.	n.g.	decrease (ALP activity, colorimetric assay)	5d: 0.8 (ratio)*
Cho et al. (2010)	BMP-2	*BMP2*	Human immortalized PDLCs (n.g./n.g., n.g., gene transfection, n.g., 3×10^5)	dynamic	**0.2Hz** (12cyc/min: stretch for 2.5s, 2.5s of relaxation) for 3h, 6h, 12h, 24h, 48h	12%	Flexercell FX-4000 Strain Unit + six-well, 35-mm flexible-bottomed Uniflex culture plates with a centrally located rectangular portion (15.25mm × 24.18mm) coated with type I collagen + vacuum	uniaxial	increase (sqPCR, GAPDH)	48h: 6.2 (ratio)†	n.g.	n.g.
Cho et al. (2010)	BMP-2	*BMP2*	Human immortalized PDLCs (n.g./n.g., n.g., gene transfection, n.g., 3×10^5)	dynamic	**0.2Hz** (12cyc/min: stretch for 2.5s, 2.5s of relaxation) for 48h	3%, 6%, 12%, 15%	Flexercell FX-4000 Strain Unit + six-well, 35-mm flexible-bottomed Uniflex culture plates with a centrally located rectangular portion (15.25mm × 24.18mm) coated with type I collagen + vacuum	uniaxial	increase (sqPCR, GAPDH)	15%: 2 (ratio)*	n.g.	n.g.
Cho et al. (2010)	BMP-7	*BMP7*	Human immortalized PDLCs (n.g./n.g., n.g., gene transfection, n.g., 3×10^5)	dynamic	**0.2Hz** (12cyc/min: stretch for 2.5s, 2.5s of relaxation) for 3h, 6h, 12h, 24h, 48h	12%	Flexercell FX-4000 Strain Unit + six-well, 35-mm flexible-bottomed Uniflex culture plates with a centrally located rectangular portion (15.25mm × 24.18mm) coated with type I collagen + vacuum	uniaxial	increase (sqPCR, GAPDH)	48h: 3.5 (ratio)†	n.g.	n.g.
Cho et al. (2010)	BMP-7	*BMP7*	Human immortalized PDLCs (n.g./n.g., n.g., gene transfection, n.g., 3×10^5)	dynamic	**0.2Hz** (12cyc/min: stretch for 2.5s, 2.5s of relaxation) for 48h	3%, 6%, 12%, 15%	Flexercell FX-4000 Strain Unit + six-well, 35-mm flexible-bottomed Uniflex culture plates with a centrally located rectangular portion (15.25mm × 24.18mm) coated with type I collagen + vacuum	uniaxial	increase (sqPCR, GAPDH)	15%: 7.1 (ratio)†	n.g.	n.g.
Cho et al. (2010)	HO-1	*HMOX1*	Human immortalized PDLCs (n.g./n.g., n.g., gene transfection, n.g., 3×10^5)	dynamic	**0.2Hz** (12cyc/min: stretch for 2.5s, 2.5s of relaxation) for 3h, 6h, 12h, 24h, 48h	12%	Flexercell FX-4000 Strain Unit + six-well, 35-mm flexible-bottomed Uniflex culture plates with a centrally located rectangular portion (15.25mm × 24.18mm) coated with type I collagen + vacuum	uniaxial	increase (sqPCR, GAPDH)	24h: 2.4 (ratio)†	increase (WB, β-actin)	48h: 2.3 (ratio)†
Cho et al. (2010)	HO-1	*HMOX1*	Human immortalized PDLCs (n.g./n.g., n.g., gene transfection, n.g., 3×10^5)	dynamic	**0.2Hz** (12cyc/min: stretch for 2.5s, 2.5s of relaxation) for 48h	3%, 6%, 12%, 15%	Flexercell FX-4000 Strain Unit + six-well, 35-mm flexible-bottomed Uniflex culture plates with a centrally located rectangular portion (15.25mm × 24.18mm) coated with type I collagen + vacuum	uniaxial	increase followed by decrease (sqPCR, GAPDH)	12%: 3.7 (ratio)† 15%: 0.6 (ratio)†	increase (WB, β-actin)	12%: 4.6 (ratio)†
Cho et al. (2010)	Noggin	*NOG*	Human immortalized PDLCs (n.g./n.g., n.g., gene transfection, n.g., 3×10^5)	dynamic	**0.2Hz** (12cyc/min: stretch for 2.5s, 2.5s of relaxation) for 48h	3%, 6%, 12%, 15%	Flexercell FX-4000 Strain Unit + six-well, 35-mm flexible-bottomed Uniflex culture plates with a centrally located rectangular portion (15.25mm × 24.18mm) coated with type I collagen + vacuum	uniaxial	decrease followed by plateau (sqPCR, GAPDH)	12h…24h: 0.3 (ratio)†	n.g.	n.g.

[a] Entry given as reported in the study.
[b] All official gene symbols come from the HUGO Gene Nomenclature Committee (HGNC; URL: https://www.genenames.org) after checking specificity of primers with Primer-BLAST.
[c] Gender/Sex of donors: "M" – male, "F" – female; Tooth type: "PM" – premolar, "M" – molar; Cell density: given in cells/well if not otherwise mentioned.
[d] Frequencies labeled bold orange were converted to hertz (Hz) according to its definition using the information reported in the study (in brackets)
[e] Force type deduced from the description of the force apparatus given by the authors.
[f] Gene and protein expression: 1. conclusion of change (increase, decrease…) was given according to the defined criteria in Figure 2; 2. different markers to describe the amount of change; † Information derived from figures using Engauge Digitizer; *Folds calculated by measuring the graphs, without using the Engauge Digitizer; No makers: Information derived from figures by description in the articles

Reference	Gene/ Analyte[a]	Official gene symbol / abbreviation[b]	Cell (age/gender of donors, tooth type, isolation method, passages used, cell density)[a,c]	Force type (stat./ dyn.)[a]	Force duration and frequency[d]	Force magnitude[a]	Force apparatus[a]	Force type: equibiaxial or uniaxial[e]	Gene expression: Increase, decrease, no change (method w/ reference gene); Methods: qPCR, sqPCR, Northern blot[f]	Gene expression: When it reaches peak and peak's magnitude (fold change; times or ratio; unclear = ?)[f]	Protein expression: Increase, decrease, no change (method w/ reference); Methods: ELISA, WB, RIA, EMSA, IF[f]	Protein expression: When it reaches peak and peak's magnitude (times or ratio; unclear = ?)[f]
Cho et al. (2010)	Noggin	*NOG*	Human immortalized PDLCs (n.g./n.g., n.g., gene transfection, n.g., 3×10^5)	dynamic	**0.2Hz** (12cyc/min: stretch for 2.5s, 2.5s of relaxation) for 3h, 6h, 12h, 24h, 48h	12%	Flexercell FX-4000 Strain Unit + six-well, 35-mm flexible-bottomed Uniflex culture plates with a centrally located rectangular portion (15.25mm × 24.18mm) coated with type I collagen + vacuum	uniaxial	decrease (sqPCR, GAPDH)	15%: 0.2 (ratio)†	n.g.	n.g.
Cho et al. (2010)	Runx2	*RUNX2*	Human immortalized PDLCs (n.g./n.g., n.g., gene transfection, n.g., 3×10^5)	dynamic	**0.2Hz** (12cyc/min: stretch for 2.5s, 2.5s of relaxation) for 0h, 3h, 6h, 12h, 24h, 48h	12%	Flexercell FX-4000 Strain Unit + six-well, 35-mm flexible-bottomed Uniflex culture plates with a centrally located rectangular portion (15.25mm × 24.18mm) coated with type I collagen + vacuum	uniaxial	decrease followed by plateau then increase (sqPCR, GAPDH)	3h…6h: 0.5 (ratio)† 48h: 3 (ratio)†	n.g.	n.g.
Cho et al. (2010)	Runx2	*RUNX2*	Human immortalized PDLCs (n.g./n.g., n.g., gene transfection, n.g., 3×10^5)	dynamic	**0.2Hz** (12cyc/min: stretch for 2.5s, 2.5s of relaxation) for 48h	3%, 6%, 12%, 15%	Flexercell FX-4000 Strain Unit + six-well, 35-mm flexible-bottomed Uniflex culture plates with a centrally located rectangular portion (15.25mm × 24.18mm) coated with type I collagen + vacuum	uniaxial	decrease followed by increase (sqPCR, GAPDH)	12%: 0.8 (ratio)† 15%: 1.5 (ratio)†	n.g.	n.g.
Deschner et al. (2012)	ARRAY	ARRAY	hPDL cells (n.g./n.g., n.g., exp, P4, 5×10^4)	dynamic	0.05Hz for 24h	3%	CESTRA cell strain device + BioFlex plates (silicone membranes) coated with collagen type I + stepping motor (Nokhbehsaim, 2010)	equibiaxial	PCR array (RT² PCR array)		n.g.	n.g.
Diercke et al. (2011)	Eph-B4	*EPHB4*	hPDL cells (12-20/n.g., PM, exp, P3-6, 80% confluence)	static	1h, 4h, 24h, 48h, 72h	2.5%	flexible bottomed dishes (Greiner Bio-One) coated with collagen type-I and fibronectin (Hasegawa,1985) Petriperm dish placed + template with a convex surface + weight	equibiaxial	temporary decrease (qPCR, GAPDH)	4h: 0.6 (FC)* 48h: 0.7 (FC)*	n.g.	n.g.
Diercke et al. (2011)	Ephrin-B2	*EFNB2*	hPDL cells (12-20/n.g., PM, exp, P3-6, 80% confluence)	static	1h, 4h, 24h, 48h, 72h	2.5%	flexible bottomed dishes (Greiner Bio-One) coated with collagen type-I and fibronectin (Hasegawa,1985) Petriperm dish placed + template with a convex surface + weight	equibiaxial	increase (qPCR, GAPDH)	24h: 1.9 (FC)*	n.g.	n.g.
Diercke et al. (2011)	FAK / p-FAK(Tyr^{576})	*PTK2*	hPDL cells (12-20/n.g., PM, exp, P3-6, 80% confluence)	static	5min, 15min, 30min, 60min, 4h, 24h, 48h, 72h	2.5%	flexible bottomed dishes (Greiner Bio-One) coated with collagen type-I and fibronectin (Hasegawa,1985) Petriperm dish placed + template with a convex surface + weight	equibiaxial	n.g.	n.g.	t-FAK: no change (WB, β-actin) p-FAK: increase (WB,β-actin)	t-FAK: no quantitative information is given p-FAK @ 72h: 1.6 (ratio)*
Doi et al. (2003)	RGD-CAP	*TGFBI*	hPDL cells (n.g./n.g., PM, exp, P4-5, 5×10^4)	dynamic	**0.5Hz** (30cyc/min) for 24h, 48h	7.2 kPa, 15.4 kPa	Flexercell strain unit + Flexercell plate dish + vacuum	equibiaxial	7.2 kPa: no change (qPCR, GAPDH) 15.4 kPa: increase (qPCR, GAPDH)	15.4 kPa @ 48h:1.7 (ratio)*	n.g.	n.g.
Fujihara et al. (2010)	ALP	*ALPP*	hPDL cells (n.g./n.g., PM, exp, P n.g., 1.5×10^4)	dynamic	0.5Hz (30cyc/min) for 48h	10% (110%)	Scholertec NS-350 (Scholertec) + 10cm² silicon membrane chambers (Scholertec, Osaka, Japan)	uniaxial	increase (qPCR, HPRT)	0.12 (rel)* / 3 (ratio-calc)	n.g.	n.g.
Fujihara et al. (2010)	ARRAY	ARRAY	hPDL cells (n.g./n.g., PM, exp, P n.g., 1.5×10^4)	dynamic	0.5Hz (30cyc/min) for 48h	10% (110%)	Scholertec NS-350 (Scholertec) + 10cm² silicon membrane chambers (Scholertec, Osaka, Japan)	uniaxial	Oligo-DNA Chip Analysis: AceGene Human Oligo Chip 30K (Hitachi Software Eng. Co., Ibaraki, Japan)			
Fujihara et al. (2010)	c-FOS	*FOS*	hPDL cells (n.g./n.g., PM, exp, P n.g., 1.5×10^4)	dynamic	0.5Hz (30cyc/min) for 48h	10% (110%)	Scholertec NS-350 (Scholertec) + 10cm² silicon membrane chambers (Scholertec, Osaka, Japan)	uniaxial	increase (qPCR, HPRT)	2.6 (rel)* / 2.9 (ratio-calc)	n.g.	n.g.
Fujihara et al. (2010)	CREB/p-CREB	*CREB1*	hPDL cells (n.g./n.g., PM, exp, P n.g., 1.5×10^4)	dynamic	0.5Hz (30cyc/min) for 24h, 48h	10% (110%)	Scholertec NS-350 (Scholertec) + 10cm² silicon membrane chambers (Scholertec, Osaka, Japan)	uniaxial	n.g.	n.g.	p-CREB/CREB increase (WB, CREB)	48h: 1.5 (p-CREB/CREB)* / 1.5 (ratio stretch/control)*
Fujihara et al. (2010)	Glutamate	Glutamate	hPDL cells (n.g./n.g., PM, exp, P n.g., 1.5×10^4)	dynamic	0.5Hz (30cyc/min) for 12h, 24h, 48h	10% (110%)	Scholertec NS-350 (Scholertec) + 10cm² silicon membrane chambers (Scholertec, Osaka, Japan)	uniaxial	n.a.	n.a.	increase (ELISA)	48h: 114.6 (nmol/µg)† / 3.5 (ratio-calc)
Fujihara et al. (2010)	GRIA3	*GRIA3*	hPDL cells (n.g./n.g., PM, exp, P n.g., 1.5×10^4)	dynamic	0.5Hz (30cyc/min) for 24h	10% (110%)	Scholertec NS-350 (Scholertec) + 10cm² silicon membrane chambers (Scholertec, Osaka, Japan)	uniaxial	increase (sqPCR, HPRT)	0.9 (rel)† / 1.4 (ratio-calc)	n.g.	n.g.
Fujihara et al. (2010)	GRIN1	*GRIN1*	hPDL cells (n.g./n.g., PM, exp, P n.g., 1.5×10^4)	dynamic	0.5Hz (30cyc/min) for 24h	10% (110%)	Scholertec NS-350 (Scholertec) + 10cm² silicon membrane chambers (Scholertec, Osaka, Japan)	uniaxial	increase (sqPCR, HPRT)	0.6 (rel)†/ control n.g.	n.g.	n.g.
Fujihara et al. (2010)	GRIN2C	*GRIN2C*	hPDL cells (n.g./n.g., PM, exp, P n.g., 1.5×10^4)	dynamic	0.5Hz (30cyc/min) for 24h	10% (110%)	Scholertec NS-350 (Scholertec) + 10cm² silicon membrane chambers (Scholertec, Osaka, Japan)	uniaxial	increase (sqPCR, HPRT)	2.1 (rel)† / 2.2 (ratio-calc)	n.g.	n.g.
Fujihara et al. (2010)	GRIN2D	*GRIN2D*	hPDL cells (n.g./n.g., PM, exp, P n.g., 1.5×10^4)	dynamic	0.5Hz (30cyc/min) for 24h	10% (110%)	Scholertec NS-350 (Scholertec) + 10cm² silicon membrane chambers (Scholertec, Osaka, Japan)	uniaxial	increase (sqPCR, HPRT)	7.6 (rel)† / 1.2 (ratio-calc)	n.g.	n.g.
Fujihara et al. (2010)	GRIN3A	*GRIN3A*	hPDL cells (n.g./n.g., PM, exp, P n.g., 1.5×10^4)	dynamic	0.5Hz (30cyc/min) for 24h, 48h	10% (110%)	Scholertec NS-350 (Scholertec) + 10cm² silicon membrane chambers (Scholertec, Osaka, Japan)	uniaxial	increase (qPCR, HPRT)	48h: 3 (ratio)*	n.g.	n.g.
Fujihara et al. (2010)	GRIN3A	*GRIN3A*	hPDL cells (n.g./n.g., PM, exp, P n.g., 1.5×10^4)	dynamic	0.5Hz (30cyc/min) for 48h	10% (110%)	Scholertec NS-350 (Scholertec) + 10cm² silicon membrane chambers (Scholertec, Osaka, Japan)	uniaxial	increase (qPCR, HPRT)	0.3 (rel)* / 3.8 (ratio-calc)	n.g.	n.g.

[a] Entry given as reported in the study.
[b] All official gene symbols come from the HUGO Gene Nomenclature Committee (HGNC; URL: https://www.genenames.org) after checking specificity of primers with Primer-BLAST.
[c] Gender/Sex of donors: "M" – male, "F" – female; Tooth type: "PM" – premolar, "M" – molar; Cell density: given in cells/well if not otherwise mentioned.
[d] Frequencies labeled bold orange were converted to hertz (Hz) according to its definition using the information reported in the study (in brackets)
[e] Force type deduced from the description of the force apparatus given by the authors.
[f] Gene and protein expression: 1. conclusion of change (increase, decrease…) was given according to the defined criteria in Figure 2; 2. different markers to describe the amount of change; † Information derived from figures using Engauge Digitizer; *Folds calculated by measuring the graphs, without using the Engauge Digitizer; No makers: Information derived from figures by description in the articles

Reference	Gene/ Analyte[a]	Official gene symbol / abbreviation[b]	Cell (age/gender of donors, tooth type, isolation method, passages used, cell density)[a,c]	Force type (stat./ dyn.)[a]	Force duration and frequency[d]	Force magnitude[a]	Force apparatus[a]	Force type: equibiaxial or uniaxial[e]	Gene expression: Increase, decrease, no change (method w/ reference gene); Methods: qPCR, sqPCR, Northern blot[f]	Gene expression: When it reaches peak and peak's magnitude (fold change; times or ratio; unclear = ?)[f]	Protein expression: Increase, decrease, no change (method w/ reference); Methods: ELISA, WB, RIA, EMSA, IF[f]	Protein expression: When it reaches peak and peak's magnitude (times or ratio; unclear = ?)[f]
Fujihara et al. (2010)	GRIN3B	*GRIN3B*	hPDL cells (n.g./n.g., PM, exp, P n.g., 1.5×10^4)	dynamic	0.5Hz (30cyc/min) for 24h	10% (110%)	Scholertec NS-350 (Scholertec) + $10cm^2$ silicon membrane chambers (Scholertec, Osaka, Japan)	uniaxial	increase (sqPCR, HPRT)	0.6 (rel)† / control n.g.	n.g.	n.g.
Fujihara et al. (2010)	HOMER1	*HOMER1*	hPDL cells (n.g./n.g., PM, exp, P n.g., 1.5×10^4)	dynamic	0.5Hz (30cyc/min) for 24h, 48h	10% (110%)	Scholertec NS-350 (Scholertec) + $10cm^2$ silicon membrane chambers (Scholertec, Osaka, Japan)	uniaxial	increase (qPCR, HPRT)	48h: 3.3 (ratio)*	n.g.	n.g.
Fujihara et al. (2010)	HOMER1	*HOMER1*	hPDL cells (n.g./n.g., PM, exp, P n.g., 1.5×10^4)	dynamic	0.5Hz (30cyc/min) for 48h	10% (110%)	Scholertec NS-350 (Scholertec) + $10cm^2$ silicon membrane chambers (Scholertec, Osaka, Japan)	uniaxial	increase (qPCR, HPRT)	0.8 (rel)* / 2 (ratio-calc)	n.g.	n.g.
Fujihara et al. (2010)	mGluR2	*GRM2*	hPDL cells (n.g./n.g., PM, exp, P n.g., 1.5×10^4)	dynamic	0.5Hz (30cyc/min) for 24h	10% (110%)	Scholertec NS-350 (Scholertec) + $10cm^2$ silicon membrane chambers (Scholertec, Osaka, Japan)	uniaxial	increase (sqPCR, HPRT)	2.3 (rel)† / control n.g.	n.g.	n.g.
Fujihara et al. (2010)	mGluR3	*GRM3*	hPDL cells (n.g./n.g., PM, exp, P n.g., 1.5×10^4)	dynamic	0.5Hz (30cyc/min) for 24h	10% (110%)	Scholertec NS-350 (Scholertec) + $10cm^2$ silicon membrane chambers (Scholertec, Osaka, Japan)	uniaxial	increase (sqPCR, HPRT)	4.4 (rel)† / control n.g.	n.g.	n.g.
Fujihara et al. (2010)	mGluR4	*GRM4*	hPDL cells (n.g./n.g., PM, exp, P n.g., 1.5×10^4)	dynamic	0.5Hz (30cyc/min) for 24h	10% (110%)	Scholertec NS-350 (Scholertec) + $10cm^2$ silicon membrane chambers (Scholertec, Osaka, Japan)	uniaxial	increase (sqPCR, HPRT)	4.3 (rel)†/ 2.5 (ratio-calc)	n.g.	n.g.
Fujihara et al. (2010)	mGluR5	*GRM5*	hPDL cells (n.g./n.g., PM, exp, P n.g., 1.5×10^4)	dynamic	0.5Hz (30cyc/min) for 24h	10% (110%)	Scholertec NS-350 (Scholertec) + $10cm^2$ silicon membrane chambers (Scholertec, Osaka, Japan)	uniaxial	increase (sqPCR, HPRT)	1.3 (rel)† / control n.g.	n.g.	n.g.
Fujihara et al. (2010)	mGluR6	*GRM6*	hPDL cells (n.g./n.g., PM, exp, P n.g., 1.5×10^4)	dynamic	0.5Hz (30cyc/min) for 24h	10% (110%)	Scholertec NS-350 (Scholertec) + $10cm^2$ silicon membrane chambers (Scholertec, Osaka, Japan)	uniaxial	increase (sqPCR, HPRT)	2.8 (rel)† / control n.g.	n.g.	n.g.
Fujihara et al. (2010)	RUNX2	*RUNX2*	hPDL cells (n.g./n.g., PM, exp, P n.g., 1.5×10^4)	dynamic	0.5Hz (30cyc/min) for 48h	10% (110%)	Scholertec NS-350 (Scholertec) + $10cm^2$ silicon membrane chambers (Scholertec, Osaka, Japan)	uniaxial	increase (qPCR, HPRT)	0.7 (rel)* / 1.6 (ratio-calc)	n.g.	n.g.
Fujihara et al. (2010)	VGLUT1	*SLC17A7*	hPDL cells (n.g./n.g., PM, exp, P n.g., 1.5×10^4)	dynamic	0.5Hz (30cyc/min) for 24h	10% (110%)	Scholertec NS-350 (Scholertec) + $10cm^2$ silicon membrane chambers (Scholertec, Osaka, Japan)	uniaxial	increase (sqPCR, HPRT)	2.1 (rel)† / control n.g.	n.g.	n.g.
Goto et al. (2011)	ARRAY	ARRAY	hPDLCs (n.g./n.g., M., dig, P4-8, 5 x 10^5 cells/cm^2)	dynamic	**0.017Hz (1/60Hz)** (conditions: 60s/returns; resting time: 29s) for 48h	5% (105%)	STB-140 (Strex Co) + silicon chamber	uniaxial	GeneChip Human Genome U133 plus 2.0 arrays (Agilent Technologies, Santa Clara, CA, USA)	too many	n.a.	n.a.
Goto et al. (2011)	CCL2	*CCL2*	hPDLCs (n.g./n.g., M., dig, P4-8, 5 x 10^5 cells/cm^2)	dynamic	**0.017Hz (1/60Hz)** (conditions: 60s/returns; resting time: 29s) sqPCR for 1d, 2d, 3d, 5d, 7d; qPCR for 1d,3d,5d, 7d; ELISA for 1d, 2d, 3d, 5d; WB for 1d, 2d, 3d, 5d, 7d	5% (105%)	STB-140 (Strex Co) + silicon chamber	uniaxial	increase (sqPCR, β-actin) decrease followed by increase (qPCR, β-actin)	sqPCR: no quantitative information is given qPCR lowest @ 1d: 0.3 (ratio)† qPCR highest @ 7d: 27.3 (ratio)†	increase followed by plateau (ELISA)	3d...5d: 3.3 (ng/ml)* / ratio can not be calculated
Goto et al. (2011)	CCL3	*CCL3*	hPDLCs (n.g./n.g., M., dig, P4-8, 5 x 10^5 cells/cm^2)	dynamic	**0.017Hz (1/60Hz)** (conditions: 60s/returns; resting time: 29s) sqPCR for 1d, 2d, 3d, 5d, 7d; qPCR for 1d, 3d, 5d, 7d; WB for 1d, 2d, 3d, 5d, 7d	5% (105%)	STB-140 (Strex Co) + silicon chamber	uniaxial	temporary increase (sqPCR, β-actin) increase (qPCR, β-actin)	sqPCR: no quantitative information is given qPCR: 7d: 16.2 (ratio)†	increase (WB, β-actin)	no quantitative information is given
Goto et al. (2011)	CCL5	*CCL5*	hPDLCs (n.g./n.g., M., dig, P4-8, 5 x 10^5 cells/cm^2)	dynamic	**0.017Hz (1/60Hz)** (conditions: 60s/returns; resting time: 29s) sqPCR for 1d, 2d, 3d, 5d, 7d; qPCR for 1d, 3d, 5d, 7d; WB for 1d, 2d, 3d, 5d, 7d	5% (105%)	STB-140 (Strex Co) + silicon chamber	uniaxial	temporary increase (sqPCR, β-actin) decrease followed by increase (qPCR, β-actin)	sqPCR: no quantitative information is given qPCR lowest @ 3d: 0.8 (ratio)† qPCR highest @ 7d: 7.0 (ratio)†	increase (WB, β-actin)	no quantitative information is given

[a] Entry given as reported in the study.
[b] All official gene symbols come from the HUGO Gene Nomenclature Committee (HGNC; URL: https://www.genenames.org) after checking specificity of primers with Primer-BLAST.
[c] Gender/Sex of donors: "M" – male, "F" – female; Tooth type: "PM" – premolar, "M" – molar; Cell density: given in cells/well if not otherwise mentioned.
[d] Frequencies labeled bold orange were converted to hertz (Hz) according to its definition using the information reported in the study (in brackets)
[e] Force type deduced from the description of the force apparatus given by the authors.
[f] Gene and protein expression: 1. conclusion of change (increase, decrease…) was given according to the defined criteria in Figure 2; 2. different markers to describe the amount of change; † Information derived from figures using Engauge Digitizer; *Folds calculated by measuring the graphs, without using the Engauge Digitizer; No makers: Information derived from figures by description in the articles

Reference	Gene/ Analyte[a]	Official gene symbol / abbreviation[b]	Cell (age/gender of donors, tooth type, isolation method, passages used, cell density)[a,c]	Force type (stat./ dyn.)[a]	Force duration and frequency[d]	Force magnitude[a]	Force apparatus[a]	Force type: equibiaxial or uniaxial[e]	Gene expression: Increase, decrease, no change (method w/ reference gene); Methods: qPCR, sqPCR, Northern blot[f]	Gene expression: When it reaches peak and peak's magnitude (fold change; times or ratio; unclear = ?)[f]	Protein expression: Increase, decrease, no change (method w/ reference); Methods: ELISA, WB, RIA, EMSA, IF[f]	Protein expression: When it reaches peak and peak's magnitude (times or ratio; unclear = ?)[f]
Hao et al. (2009)	Caspase-3	*CASP3*	hPDL cells (13/F, 15/M, PM, exp, P 3-5, n.g.)	dynamic	**0.1Hz** (6cyc/min: Spherical cap ascended from the initial point to the highest point for 1s, kept at the highest point for 4s, descended to the initial point for 1s, and then kept at the initial point for 4s) for 6h, 12h, 24h, 48h	1%, 10%, 20%	"Cell Strain Unit (CSU)" + elastic silicon rubber membrane + spherical cap (step motor)	equibiaxial	n.g.	n.g.	1%: increase (Caspase-3 colorimetric assay) 10%: increase (Caspase-3 colorimetric assay) 20%: increase (Caspase-3 colorimetric assay)	1% @ 24h: 2.6 (ratio)* 10% @ 24h: 3 (ratio)* 20% @ 24h: 3.8 (ratio)*
He et al. (2004)	COL1A1	*COL1A1*	hPDL cells (n.g./n.g., M, dig, P3-12, 10^5 cells/cm^2)	dynamic	**0.5Hz** (30cyc/min) for 24h	10%	plastic culture cylinder + elastic silicone membrane + movable plate	equibiaxial	increase (qPCR, GAPDH)	5.695 (rel) / 4.4 (ratio-calc)	increase (ELISA)	4.1 (pg/cell)* / 3.5 (ratio-calc)
He et al. (2004)	Fibronectin	FN1	hPDL cells (n.g./n.g., M, dig, P3-12, 10^5 cells/cm^2)	dynamic	**0.5Hz** (30cyc/min) for 24h	10%	plastic culture cylinder + elastic silicone membrane + movable plate	equibiaxial	n.g.	n.g.	increase (ELISA)	10.5 (pg/cell)* / 1.4 (ratio-calc)
He et al. (2004)	MMP2	MMP2	hPDL cells (n.g./n.g., M, dig, P3-12, 10^5 cells/cm^2)	dynamic	**0.5Hz** (30cyc/min) for 24h	10%	plastic culture cylinder + elastic silicone membrane + movable plate	equibiaxial	increase (Northern, GAPDH)	0.241 (rel) / 1.4 (ratio-calc)	decrease (zymography)	7.6 (rel) / 0.9 (ratio-calc)
He et al. (2004)	TIMP2	TIMP2	hPDL cells (n.g./n.g., M, dig, P3-12, 10^5 cells/cm^2)	dynamic	**0.5Hz** (30cyc/min) for 24h	10%	plastic culture cylinder + elastic silicone membrane + movable plate	equibiaxial	increase (Northern, GAPDH)	0.118 (rel) / 1.6 (ratio-calc)	n.g.	n.g.
He et al. (2019)	RhoA	*RHOA*	hPDLCs ($) (n.g./n.g., n.g., n.g., P n.g., 80-90 confluence)	dynamic	0.5Hz for 3h	n. g.	a uniaxial four-point bending system (developed at Sichuan University, patents CN2534576 and CN1425905)	uniaxial	increase (qPCR, β-actin)	40.2 (rel)† / 28.9 (ratio-calc)	n.g.	n.g.
He et al. (2019)	ROCK	*ROCK1*	hPDLCs ($) (n.g./n.g., n.g., n.g., P n.g., 80-90 confluence)	dynamic	0.5Hz for 3h	n. g.	a uniaxial four-point bending system (developed at Sichuan University, patents CN2534576 and CN1425905)	uniaxial	increase (qPCR, β-actin)	10.7 (rel)† / 10.8 (ratio-calc)	n.g.	n.g.
He et al. (2019)	RUNX2	*RUNX2*	hPDLCs ($) (n.g./n.g., n.g., n.g., P n.g., 80-90 confluence)	dynamic	0.5Hz for 3h	n. g.	a uniaxial four-point bending system (developed at Sichuan University, patents CN2534576 and CN1425905)	uniaxial	increase (qPCR, β-actin)	10.1 (rel)† / 10.6 (ratio-calc)	n.g.	n.g.
He et al. (2019)	TGF-β1	*TGFB1*	hPDLCs ($) (n.g./n.g., n.g., n.g., P n.g., 80-90 confluence)	dynamic	0.5Hz for 3h	n. g.	a uniaxial four-point bending system (developed at Sichuan University, patents CN2534576 and CN1425905)	uniaxial	increase (qPCR, β-actin)	12.7 (rel)† / 12.8 (ratio-calc)	n.g.	n.g.
He et al. (2019)	YAP	*YAP1*	hPDLCs ($) (n.g./n.g., n.g., n.g., P n.g., 80-90 confluence)	dynamic	0.5Hz for 1h, 3h, 6h, 12h, 18h	**0.2%** (2000μstrain)	a uniaxial four-point bending system (developed at Sichuan University, patents CN2534576 and CN1425905)	uniaxial	temporary increase (qPCR, β-actin)	3h: 10.3 (FC)†	n.g.	n.g.
He et al. (2019)	YAP	*YAP1*	hPDLCs ($) (n.g./n.g., n.g., n.g., P n.g., 80-90 confluence)	dynamic	0.5Hz for 3h	**0.4%** (4000μstrain)	a uniaxial four-point bending system (developed at Sichuan University, patents CN2534576 and CN1425905)	uniaxial	increase (qPCR, β-actin)	16.3 (FC)†	n.g.	n.g.
He et al. (2019)	YAP	*YAP1*	hPDLCs ($) (n.g./n.g., n.g., n.g., P n.g., 80-90 confluence)	dynamic	0.5Hz for 3h	n. g.	a uniaxial four-point bending system (developed at Sichuan University, patents CN2534576 and CN1425905)	uniaxial	increase (qPCR, β-actin)	9.1 (rel)† / 8.8 (ratio-calc)	whole protein: increase (GAPDH) nucleo-protein: increase (GAPDH)	no quantitative information is given
He et al. (2019)	α-SMA	*ACTA2*	hPDLCs ($) (n.g./n.g., n.g., n.g., P n.g., 80-90 confluence)	dynamic	0.5Hz for 1h, 3h, 6h, 12h, 18h	**0.2%** (2000μstrain)	a uniaxial four-point bending system (developed at Sichuan University, patents CN2534576 and CN1425905)	uniaxial	temporary increase (qPCR, β-actin)	6h: 13.4 (FC)†	n.g.	n.g.
He et al. (2019)	α-SMA	*ACTA2*	hPDLCs ($) (n.g./n.g., n.g., n.g., P n.g., 80-90 confluence)	dynamic	0.5Hz for 3h	**0.4%** (4000μstrain)	a uniaxial four-point bending system (developed at Sichuan University, patents CN2534576 and CN1425905)	uniaxial	increase (qPCR, β-actin)	12.6 (FC)†	n.g.	n.g.
He et al. (2019)	α-SMA	*ACTA2*	hPDLCs ($) (n.g./n.g., n.g., n.g., P n.g., 80-90 confluence)	dynamic	0.5Hz for 3h	n. g.	a uniaxial four-point bending system (developed at Sichuan University, patents CN2534576 and CN1425905)	uniaxial	increase (qPCR, β-actin)	21.5 (rel)† / 21.8 (ratio-calc)	whole protein: increase (GAPDH)	no quantitative information is given
Howard et al. (1998)	Fibronectin	FN1	hPDL cells (n.g./n.g., PM, dig, P3-8, Confluent)	dynamic	**0.5Hz** (30times/min) for 24h	5%, 10%	circularly clamped compliant membrane + spherical cap + vacuum	equibiaxial	n.g.	n.g.	increase (ELISA)	5%: 11.6 (pg/cell)* / 2.9 (ratio-calc) 10%: 3.7 (pg/cell)* / 5.1 (ratio-calc)
Howard et al. (1998)	Tropoelastin	*ELN*	hPDL cells (n.g./n.g., PM, dig, P3-8, Confluent)	dynamic	**0.5Hz** (30times/min) for 24h	5%, 10%	circularly clamped compliant membrane + spherical cap + vacuum	equibiaxial	n.g.	n.g.	5% (ELISA): decrease 10% (ELISA): decrease	5%: 0.02 (pg/cell)* / 0.4 (ratio-calc) 10%: 0.006 (pg/cell)* / 0.4 (ratio-calc)
Howard et al. (1998)	Type I Collagen	*COL1A1; COL1A2*	hPDL cells (n.g./n.g., PM, dig, P3-8, Confluent)	dynamic	**0.5Hz** (30times/min) for 24h	5%, 10%	circularly clamped compliant membrane + spherical cap + vacuum	equibiaxial	n.g.	n.g.	5% (ELISA): increase 10% (ELISA): no change	5%: 0.3 (pg/cell)* / 1.7 (ratio-calc)
Huelter-Hassler et al. (2017)	ERK1/2 / p-ERK1/2($T^{202,204}$)	MAPK3; MAPK1	hPDL cells (14/M, M, dig, P5-8, 1×10^4 cells/cm^2,)	static	equiaxial strain for 15min, 1h, 6h, 24h	2.5%	Flexercell Strain Unit FX5000-T + silicone bottomed six-well plates coated with collagen type I (Flexcell Int. Corp.) + vacuum	equibiaxial	n.g.	n.g.	ERK1/2 (WB): decrease followed by increase p-ERK1/2 (WB): decrease	ERK1/2: lowest @15min: 0.5 (ratio)* ERK1/2: highest @ 24h: 1.5 (ratio)* p-ERK1/2: 1h: 0.4 (ratio)*

[a] Entry given as reported in the study.
[b] All official gene symbols come from the HUGO Gene Nomenclature Committee (HGNC; URL: https://www.genenames.org) after checking specificity of primers with Primer-BLAST.
[c] Gender/Sex of donors: "M" – male, "F" – female; Tooth type: "PM" – premolar, "M" – molar; Cell density: given in cells/well if not otherwise mentioned.
[d] Frequencies labeled bold orange were converted to hertz (Hz) according to its definition using the information reported in the study (in brackets)
[e] Force type deduced from the description of the force apparatus given by the authors.
[f] Gene and protein expression: 1. conclusion of change (increase, decrease…) was given according to the defined criteria in Figure 2; 2. different markers to describe the amount of change; † Information derived from figures using Engauge Digitizer; *Folds calculated by measuring the graphs, without using the Engauge Digitizer; No makers: Information derived from figures by description in the articles

Reference	Gene/ Analyte[a]	Official gene symbol / abbreviation[b]	Cell (age/gender of donors, tooth type, isolation method, passages used, cell density)[a,c]	Force type (stat./ dyn.)[a]	Force duration and frequency[d]	Force magnitude[a]	Force apparatus[a]	Force type: equibiaxial or uniaxial[e]	Gene expression: Increase, decrease, no change (method w/ reference gene); Methods: qPCR, sqPCR, Northern blot[f]	Gene expression: When it reaches peak and peak's magnitude (fold change; times or ratio; unclear = ?)[f]	Protein expression: Increase, decrease, no change (method w/ reference); Methods: ELISA, WB, RIA, EMSA, IF[f]	Protein expression: When it reaches peak and peak's magnitude (times or ratio; unclear = ?)[f]
Huelter-Hassler et al. (2017)	KI-67	*MKI67*	hPDL cells (14/M, M, dig, P5-8, 1×10^4 cells/cm^2,)	static	equiaxial strain for 15min, 1h, 6h, 24h	2.5%	Flexercell Strain Unit FX5000-T + silicone bottomed six-well plates coated with collagen type I (Flexcell Int. Corp.) + vacuum	equibiaxial	n.g.	n.g.	Increase followed by decrease (WB)	highest @ 15min: 1.8 (ratio)* lowest @ 24h: 0.3 (ratio)*
Huelter-Hassler et al. (2017)	YAP	*YAP1*	hPDL cells (14/M, M, dig, P5-8, 1×10^4 cells/cm^2,)	static	equiaxial strain for 15min, 1h, 6h, 24h	2.5%	Flexercell Strain Unit FX5000-T + silicone bottomed six-well plates coated with collagen type I (Flexcell Int. Corp.) + vacuum	equibiaxial	n.g.	n.g.	cytoplasmic YAP (WB): no change nuclear YAP (WB): increase followed by decrease	nuclear YAP: highest @ 1h: 1.3 (ratio)* nucelar YAP: lowest @ 24h: 0.6 (ratio)*
Hülter-Hassler et al. (2017)	ERK1/2 / p-ERK1/2($T^{202,204}$)	MAPK3; MAPK1	hPDL cells (14/M, M, dig, P5-8, 1×10^4 cells/cm^2,)	static	equiaxial mechanical strain for 15min, 1h, 6h, 24h	2.5%	Flexercell Strain Unit FX5000-T + silicone bottomed six-well plates coated with collagen type I (Flexcell Int. Corp.) + vacuum	equibiaxial	n.g.	n.g.	ERK1/2 (WB): decrease followed by increase p-ERK1/2 (WB): decrease	ERK1/2: lowest @ 15min: 0.6 (ratio)* ERK1/2: highest @ 24h: 1.5 (ratio)* p-ERK1/2 (WB): 1h: 0.4 (ratio)*
Hülter-Hassler et al. (2017)	FAK / p-FAK(Y^{397})	*PTK2*	hPDL cells (14/M, M, dig, P5-8, 1×10^4 cells/cm^2,)	static	equiaxial mechanical strain for 15min, 1h, 6h, 24h	2.5%	Flexercell Strain Unit FX5000-T + silicone bottomed six-well plates coated with collagen type I (Flexcell Int. Corp.) + vacuum	equibiaxial	n.g.	n.g.	FAK increase followed by decrease (WB) p-FAK increase followed by decrease (WB):	FAK: highest @ 1h: 1.7 (ratio)* FAK: lowest @ 24h: 0.8 (ratio)* p-FAK: highest @ 1h: 1.4 (ratio)* p-FAK: lowest @ 24h: 0.7 (ratio)*
Hülter-Hassler et al. (2017)	KI-67	*MKI67*	hPDL cells (14/M, M, dig, P5-8, 1×10^4 cells/cm^2,)	static	equiaxial mechanical strain for 15min, 1h, 6h, 24h	2.5%	Flexercell Strain Unit FX5000-T + silicone bottomed six-well plates coated with collagen type I (Flexcell Int. Corp.) + vacuum	equibiaxial	n.g.	n.g.	increase followed by decrease (WB)	highest @ 15min: 1.8 (ratio)* lowest @ 24h: 0.3 (ratio)*
Hülter-Hassler et al. (2017)	YAP	*YAP1*	hPDL cells (14/M, M, dig, P5-8, 1×10^4 cells/cm^2,)	static	equiaxial mechanical strain for 15min, 1h, 6h, 24h	2.5%	Flexercell Strain Unit FX5000-T + silicone bottomed six-well plates coated with collagen type I (Flexcell Int. Corp.) + vacuum	equibiaxial	n.g.	n.g.	cytoplasmic extract (WB): no change nuclear extract (WB): increase followed by decrease	YAP (nuclear extract): highest @ 1h: 1.3 ratio)* YAP (nuclear extract): lowest @ 24h: 0.6 (ratio)*
Jacobs et al. (2013)	ALP	*ALPP*	hPDL cells ($) (n.g./n.g., n.g, method n.g., P4-6, subconfluency)	static	12h	1% (0.7cN/mm^2), 5% (3cN/mm^2), 10% (5.2cN/mm^2)	Flexercell Strain Unit FX 3000 + BioFlex® Plates coated with pronectin + vacuum	equibiaxial	increase (qPCR, actin + GAPDH)	5%: 2.7 (FC)*	n.g.	n.g.
Jacobs et al. (2013)	Collagen type-I (COL-1)	*COL1A1*	hPDL cells ($) (n.g./n.g., n.g, method n.g., P4-6, subconfluency)	static	12h	1% (0.7cN/mm^2), 5% (3cN/mm^2), 10% (5.2cN/mm^2)	Flexercell Strain Unit FX 3000 + BioFlex® Plates coated with pronectin + vacuum	equibiaxial	decrease followed by increase then decrease (qPCR, actin + GAPDH)	1%: 0.8 (FC)† 5%: 1.1 (FC)† 10%: 0.7 (FC)†	n.g.	n.g.
Jacobs et al. (2013)	Cyclin D1	*CCND1*	hPDL cells ($) (n.g./n.g., n.g, method n.g., P4-6, subconfluency)	static	12h	1% (0.7cN/mm^2), 5% (3cN/mm^2), 10% (5.2cN/mm^2)	Flexercell Strain Unit FX 3000 + BioFlex® Plates coated with pronectin + vacuum	equibiaxial	increase (qPCR, actin + GAPDH)	10%: 8.3 (FC)*	n.g.	n.g.
Jacobs et al. (2013)	OCN	*BGLAP*	hPDL cells ($) (n.g./n.g., n.g, method n.g., P4-6, subconfluency)	static	12h	1% (0.7cN/mm^2), 5% (3cN/mm^2), 10% (5.2cN/mm^2)	Flexercell Strain Unit FX 3000 + BioFlex® Plates coated with pronectin + vacuum	equibiaxial	increase followed by decrease (qPCR, actin + GAPDH)	highest @ 1%: 1.3 (FC)* lowest @ 5%: 0.6 (FC)*	n.g.	n.g.
Jacobs et al. (2013)	OPG	*TNFRSF11B*	hPDL cells ($) (n.g./n.g., n.g, method n.g., P4-6, subconfluency)	static	12h	1% (0.7cN/mm^2), 5% (3cN/mm^2), 10% (5.2cN/mm^2)	Flexercell Strain Unit FX 3000 + BioFlex® Plates coated with pronectin + vacuum	equibiaxial	increase (qPCR, actin + GAPDH)	5%: 2.7 (FC)*	increase (ELISA)	10%: 44.6 (ng/10^5 cells)* / control no OPG detectable
Jacobs et al. (2013)	RANKL	*TNFSF11*	hPDL cells ($) (n.g./n.g., n.g, method n.g., P4-6, subconfluency)	static	12h	1% (0.7cN/mm^2), 5% (3cN/mm^2), 10% (5.2cN/mm^2)	Flexercell Strain Unit FX 3000 + BioFlex® Plates coated with pronectin + vacuum	equibiaxial	increase followed by decrease (qPCR, actin + GAPDH)	highest @1%: 1.6 (FC)* lowest @ 5%: 0.7 (FC)*	n.g.	n.g.
Jacobs et al. (2014)	COX-2	*PTGS2*	hPDL cells ($) (n.g./n.g., n.g, method n.g., P4-6, subconfluency)	static	12h	1% (0.7cN/mm^2), 5% (3cN/mm^2), 10% (5.2cN/mm^2)	Flexercell Strain Unit FX 3000 + Bioflex® Plates + vacuum	equibiaxial	increase (qPCR, actin + GAPDH)	10%: 31.4 (FC)	n.g.	n.g.
Jacobs et al. (2014)	IL-6	*IL6*	hPDL cells ($) (n.g./n.g., n.g, method n.g., P4-6, subconfluency)	static	12h	1% (0.7cN/mm2), 5% (3 cN/mm^2), 10% (5.2 cN/mm^2)	Flexercell Strain Unit FX 3000 + Bioflex® Plates + vacuum	equibiaxial	decrease followed by increase (qRT-PCR, actin + GAPDH)	lowest @ 1%: 0.5 (FC)* highest @ 10%: 1.6 (FC)*	decrease followed by increase (ELISA)	lowest @ 1%: 5.6 (pg/ml)* / 0.6 (ratio-calc) highest @ 10%: 13.8 (pg/ml)* / 1.5 (ratio-calc)
Jacobs et al. (2014)	MMP-8	*MMP8*	hPDL cells ($) (n.g./n.g., n.g, method n.g., P4-6, subconfluency)	static	12h	1% (0.7 cN/mm^2), 5% (3 cN/mm^2), 10% (5.2 cN/mm^2)	Flexercell Strain Unit FX 3000 + Bioflex® Plates + vacuum	equibiaxial	n.g.	n.g.	MMP8: increase (ELISA) TIMP1/MMP8: increase followed by decrease (ELISA)	MMP8 @10%: 38.8 (pg/ml) / 12.1 (ratio-calc) TIMP1/MMP8 highest @ 5%: 17.2 (rel×1000) / 2 (ratio-calc ×1000) TIMP1/MMP8 lowest @ 10%: 2 (rel×1000)* / 0.2 (ratio-calc ×1000)
Jacobs et al. (2014)	PGE_2	PGE_2	hPDL cells ($) (n.g./n.g., n.g, method n.g., P4-6, subconfluency)	static	12h	1% (0.7cN/mm^2), 5% (3cN/mm^2), 10% (5.2cN/mm^2)	Flexercell Strain Unit FX 3000 + Bioflex® Plates + vacuum	equibiaxial	n.a.	n.a.	increase (ELISA)	10%: 47.9 (pg/ml), ration can not be calculated
Jacobs et al. (2014)	TIMP-1	*TIMP1*	hPDL cells ($) (n.g./n.g., n.g, method n.g., P4-6, subconfluency)	static	12h	1% (0.7cN/mm^2), 5% (3cN/mm^2), 10% (5.2cN/mm^2)	Flexercell Strain Unit FX 3000 + Bioflex® Plates + vacuum	equibiaxial	n.g.	n.g.	TIMP1: increase (ELISA) TIMP1/MMP8: increase followed by decrease (ELISA)	TIMP1 @10%: 71.2 (qng/ml) / 4.5 (ratio-calc) TIMP1/MMP8 highest @ 5%: 17.2 (rel×1000) / 2 (ratio-calc ×1000) TIMP1/MMP8 lowest @ 10%: 2 (rel×1000)* / 0.2 (ratio-calc ×1000)
Jacobs et al. (2015)	OPG	*TNFRSF11B*	hPDL cells ($) (n.g./n.g., n.g, method n.g., P4-6, subconfluency)	static	12h	5% (3cN/mm^2), 10% (5.2cN/mm^2)	Flexercell Strain Unit FX 3000 + Bioflex® Plates + vacuum	equibiaxial	OPG: increase (qPCR, actin + GAPDH) RANKL/OPG: temporary decrease	OPG @ 5%: 2.9 (FC)* RANKL/OPG @ 5%: 0.2 (ratio)*	increase (ELISA)	5%: 13.7 (ng/ml)* / 3.1 (ratio-calc)
Jacobs et al. (2015)	RANKL	*TNFSF11*	hPDL cells ($) (n.g./n.g., n.g, method n.g., P4-6, subconfluency)	static	12h	5% (3cN/mm^2), 10% (5.2cN/mm^2)	Flexercell Strain Unit FX 3000 + Bioflex® Plates + vacuum	equibiaxial	RANKL: decrease followed by increase (qPCR, actin + GAPDH) RANKL/OPG: temporary decrease	RANKL lowest @ 5%: 0.6 (FC)* RANKL highest @ 10%: 2.4 (FC)* RANKL/OPG @ 5%: 0.2 (ratio)*	n.g.	n.g.
Jacobs et al. (2018)	COX-2	*PTGS2*	hPDL cells ($) (n.g./n.g., n.g, method n.g., P4-6, subconfluency)	static	12h	3% (2cN/mm^2)	Flexercell Strain Unit FX 3000 + Bioflex® Plates + vacuum	equibiaxial	increase (qPCR; actin + GAPDH)	3.8 (FC)†	n.g.	n.g.
Jacobs et al. (2018)	MMP-8	*MMP8*	hPDL cells ($) (n.g./n.g., n.g, method n.g., P4-6, subconfluency)	static	12h	3% (2cN/mm^2)	Flexercell Strain Unit FX 3000 + Bioflex® Plates + vacuum	equibiaxial	n.g.	n.g.	increase (ELISA)	17.7 (pg/ml)* / 1.5 (ratio-calc)

[a] Entry given as reported in the study.
[b] All official gene symbols come from the HUGO Gene Nomenclature Committee (HGNC; URL: https://www.genenames.org) after checking specificity of primers with Primer-BLAST.
[c] Gender/Sex of donors: "M" – male, "F" – female; Tooth type: "PM" – premolar, "M" – molar; Cell density: given in cells/well if not otherwise mentioned.
[d] Frequencies labeled bold orange were converted to hertz (Hz) according to its definition using the information reported in the study (in brackets)
[e] Force type deduced from the description of the force apparatus given by the authors.
[f] Gene and protein expression: 1. conclusion of change (increase, decrease…) was given according to the defined criteria in Figure 2; 2. different markers to describe the amount of change; † Information derived from figures using Engauge Digitizer; *Folds calculated by measuring the graphs, without using the Engauge Digitizer; No makers: Information derived from figures by description in the articles

Reference	Gene/ Analyte[a]	Official gene symbol / abbreviation[b]	Cell (age/gender of donors, tooth type, isolation method, passages used, cell density)[a,c]	Force type (stat./ dyn.)[a]	Force duration and frequency[d]	Force magnitude[a]	Force apparatus[a]	Force type: equibiaxial or uniaxial[e]	Gene expression: Increase, decrease, no change (method w/ reference gene); Methods: qPCR, sqPCR, Northern blot[f]	Gene expression: When it reaches peak and peak's magnitude (fold change; times or ratio; unclear = ?)[f]	Protein expression: Increase, decrease, no change (method w/ reference); Methods: ELISA, WB, RIA, EMSA, IF[f]	Protein expression: When it reaches peak and peak's magnitude (times or ratio; unclear = ?)[f]
Jacobs et al. (2018)	PGE_2	PGE_2	hPDL cells ($) (n.g./n.g., n.g, method n.g., P4-6, subconfluency)	static	12h	3% (2cN/mm²)	Flexercell Strain Unit FX 3000 + Bioflex® Plates + vacuum	equibiaxial	n.a.	n.a.	no change (ELISA)	
Jacobs et al. (2018)	TIMP-1	*TIMP1*	hPDL cells ($) (n.g./n.g., n.g, method n.g., P4-6, subconfluency)	static	12h	3% (2cN/mm²)	Flexercell Strain Unit FX 3000 + Bioflex® Plates + vacuum	equibiaxial	n.g.	n.g.	increase (ELISA)	1947 (pg/ml)* / 1.3 (ratio-calc)
Jiang and Hua (2016)	ALP	*ALPP*	hPDL cells (12-18/n.g., PM, exp, P n.g., n.g.)	dynamic	0.1Hz (5s stretch and 5s relaxation) for 6h, 12h, 24h, 48h	5%	Flexcell FX-5000 Tension System + flexible-bottomed six-well plates coated with type I collagen (Sigma) + vacuum	equibiaxial	increase (sqPCR, GAPDH)	24h: 2.7 (FC)*	increase (WB, GAPDH)	24h: no quantitative information is given
Jiang and Hua (2016)	OCN	*BGLAP*	hPDL cells (12-18/n.g., PM, exp, P n.g., n.g.)	dynamic	0.1Hz (5s stretch and 5s relaxation) for 6h, 12h, 24h, 48h	5%	Flexcell FX-5000 Tension System + flexible-bottomed six-well plates coated with type I collagen (Sigma) + vacuum	equibiaxial	increase (sqPCR, GAPDH)	24h: 3 (FC)*	increase (WB, GAPDH)	24h: no quantitative information is given
Jiang and Hua (2016)	RUNX2	*RUNX2*	hPDL cells (12-18/n.g., PM, exp, P n.g., n.g.)	dynamic	0.1Hz (5s stretch and 5s relaxation) for 6h, 12h, 24h, 48h	5%	Flexcell FX-5000 Tension System + flexible-bottomed six-well plates coated with type I collagen (Sigma) + vacuum	equibiaxial	increase (sqPCR, GAPDH)	24h: 2.9 (FC)*	increase (WB, GAPDH)	24h: no quantitative information is given
Kaku et al. (2019)	CSF1	*CSF1*	hPDLCs (n.g./n.g., n.g., exp, P4-6, 1×10^5)	dynamic	0.5Hz (30 cyc/min) for 48h	12%	Flexcell FX-2000 + silicon membrane + vaccum	equibiaxial	n.g.	n.g.	increase (ELISA)	301.9 (pg/ml)† / 3.1 (ratio-calc)
Kaku et al. (2019)	IL-1B	*IL1B*	hPDLCs (n.g./n.g., n.g., exp, P4-6, 1×10^5)	dynamic	0.5Hz (30 cyc/min) for 48h	12%	Flexcell FX-2000 + silicon membrane + vaccum	equibiaxial	n.g.	n.g.	increase (ELISA)	12.1 (pg/ml)† / 1.6 (ratio-calc)
Kaku et al. (2019)	RANKL	*TNFSF11*	hPDLCs (n.g./n.g., n.g., exp, P4-6, 1×10^5)	dynamic	0.5Hz (30 cyc/min) for 48h	12%	Flexcell FX-2000 + silicon membrane + vaccum	equibiaxial	n.g.	n.g.	increase (ELISA)	27.8 (pg/ml)† / 3.3 (ratio-calc)
Kaku et al. (2019)	TNFα	*TNF*	hPDLCs (n.g./n.g., n.g., exp, P4-6, 1×10^5)	dynamic	0.5Hz (30 cyc/min) for 48h	12%	Flexcell FX-2000 + silicon membrane + vaccum	equibiaxial	n.g.	n.g.	increase (ELISA)	4.7 (pg/ml)† / 4.8 (ratio-calc)
Kanzaki et al. (2006)	OPG	*TNFRSF11B*	hPDL cells (n.g./n.g., n.g., exp, P4-8, n.g.)	dynamic	0.5Hz (1s stretch/1s relaxation) sqPCR for 48h; ELISA for 72h	15%	Flexercell Strain-Unit + type I collagen-coated silicone membrane + vacuum	equibiaxial	increase (sqPCR, β-actin)	1.7 (ratio)*	increase (ELISA)	277.1 (pmol/L)* / 1.3 (ratio-calc)
Kanzaki et al. (2006)	RANKL	*TNFSF11*	hPDL cells (n.g./n.g., n.g., exp, P4-8, n.g.)	dynamic	0.5Hz (1s stretch/1s relaxation) for 48h	15%	Flexercell Strain-Unit + type I collagen-coated silicone membrane + vacuum	equibiaxial	increase (sqPCR, β-actin)	12.9 (ratio)*	n.g.	n.g.
Kanzaki et al. (2006)	TGF-β	*TGFB1*	hPDL cells (n.g./n.g., n.g., exp, P4-8, n.g.)	dynamic	0.5Hz (1s stretch/1s relaxation) sqPCR for 48h; ELISA for 6h, 24h, 48h, 72h	15%	Flexercell Strain-Unit + type I collagen-coated silicone membrane + vacuum	equibiaxial	increase (sqPCR, β-actin)	1.5 (ratio)*	increase (ELISA)	72h: 2 (ng/ml)* / 1.1 (ratio-calc)
Kanzaki et al. (2019)	ARRAY	ARRAY	immortalized hPDLCs (n.g./n.g., n.g., gene transfection, n.g., n.g.)	dynamic	0.5Hz (1s stretch/1s relaxation) for 24h	15%	Flexercell Strain-Unit + type I collagen-coated silicone membrane + vacuum (Kanzaki et al 2006)	equibiaxial	SurePrint G3 Human miRNA microarray 8 × 60 K miRBase 16.0 (Agilent Technologies)	too many	n.a.	n.a.
Kanzaki et al. (2019)	OPG	*TNFRSF11B*	immortalized hPDLCs (n.g./n.g., n.g., gene transfection, n.g., n.g.)	dynamic	0.5Hz (1s stretch/1s relaxation) for 24h	15%	Flexercell Strain-Unit + type I collagen-coated silicone membrane + vacuum (Kanzaki et al 2006)	equibiaxial	increase (qPCR, RPS18)	2.2 (FC)*	increase (WB, n.g.) increase (ELISA)	WB: 1.8 (ratio)* ELISA: 16.3 (ng/ml)* / 1.3 (ratio-calc)
Kanzaki et al. (2019)	RANKL	*TNFSF11*	immortalized hPDLCs (n.g./n.g., n.g., gene transfection, n.g., n.g.)	dynamic	0.5Hz (1s stretch/1s relaxation) for 24h	15%	Flexercell Strain-Unit + type I collagen-coated silicone membrane + vacuum (Kanzaki et al 2006)	equibiaxial	increase (qPCR, RPS18)	9.9 (FC)*	n.g.	n.g.
Kikuiri et al. (2000)	ecNOS	*NOS3*	hPDL cells (14-17/n.g., PM, dig, P5-10, 4×10^5)	dynamic	0.1Hz (elongation for 5s, relaxation for 5s) sqPCR for 3h,12h; WB for 3h, 6h	18%	Flexercell Strain Unit (Shimizu 1994) + flexible silicon rubber bottoms + vacuum	equibiaxial	ecNOS (sqPCR, GAPDH), expressed in both control and experimental groups	no quantitative information is given	control groups (WB): no expression experimental group (WB): strong expression	no quantitative information is given
Kikuiri et al. (2000)	iNOS	*NOS2*	hPDL cells (14-17/n.g., PM, dig, P5-10, 4×10^5)	dynamic	0.1Hz (elongation for 5s, relaxation for 5s) for 12h	18%	Flexercell Strain Unit (Shimizu 1994) + flexible silicon rubber bottoms + vacuum	equibiaxial	no expression (sqPCR, GAPDH)		no expression (WB)	

[a] Entry given as reported in the study.
[b] All official gene symbols come from the HUGO Gene Nomenclature Committee (HGNC; URL: https://www.genenames.org) after checking specificity of primers with Primer-BLAST.
[c] Gender/Sex of donors: "M" – male, "F" – female; Tooth type: "PM" – premolar, "M" – molar; Cell density: given in cells/well if not otherwise mentioned.
[d] Frequencies labeled bold orange were converted to hertz (Hz) according to its definition using the information reported in the study (in brackets)
[e] Force type deduced from the description of the force apparatus given by the authors.
[f] Gene and protein expression: 1. conclusion of change (increase, decrease…) was given according to the defined criteria in Figure 2; 2. different markers to describe the amount of change; † Information derived from figures using Engauge Digitizer; *Folds calculated by measuring the graphs, without using the Engauge Digitizer; No makers: Information derived from figures by description in the articles

Reference	Gene/ Analyte[a]	Official gene symbol / abbreviation[b]	Cell (age/gender of donors, tooth type, isolation method, passages used, cell density)[a,c]	Force type (stat./ dyn.)[a]	Force duration and frequency[d]	Force magnitude[a]	Force apparatus[a]	Force type: equibiaxial or uniaxial[e]	Gene expression: Increase, decrease, no change (method w/ reference gene); Methods: qPCR, sqPCR, Northern blot[f]	Gene expression: When it reaches peak and peak's magnitude (fold change; times or ratio; unclear = ?)[f]	Protein expression: Increase, decrease, no change (method w/ reference); Methods: ELISA, WB, RIA, EMSA, IF[f]	Protein expression: When it reaches peak and peak's magnitude (times or ratio; unclear = ?)[f]
Kim et al. (2007)	Osteocalcin	*BGLAP*	hPDL cells (n.g./n.g., n.g., exp, P5-10, 5×10^4)	dynamic	**0.1Hz** (6 cyc/min: strain for 5s followed by a 5s relaxation) for 6d	9%	Flexcell strain unit FX-2000 + 35-mm Flexercell plate dish + vacuum	equibiaxial	increase (sqPCR, GAPDH)	75 (rel)* / 1.7 (ratio-calc)	n.g.	n.g.
Kim et al. (2007)	UNCL	*UNC50*	hPDL cells (n.g./n.g., n.g., exp, P5-10, 5×10^4)	dynamic	**0.1Hz** (6 cyc/min: strain for 5s followed by a 5s relaxation) for 6d	9%	Flexcell strain unit FX-2000 + 35-mm Flexercell plate dish + vacuum	equibiaxial	increase (sqPCR, GAPDH)	117 (rel)* / 1.3 (ratio-calc)	n.g.	n.g.
Kletsas et al. (2002)	c-Fos	*FOS*	hPDL cells (n.g./n.g., n.g., exp, P3-4, 90% confluency)	static	0.5h, 1h, 3h, 6h, 12h, 24h	2.5%	Petriperm dish + plexiglass template with a convex surface + weight	equibiaxial	n.g.	n.g.	increase (WB)	3h: 225% (rel)* / 2.3 (ratio-calc)
Kletsas et al. (2002)	c-Jun	*JUN*	hPDL cells (n.g./n.g., n.g., exp, P3-4, 90% confluency)	static	0.5h, 1h, 3h, 6h, 12h, 24h	2.5%	Petriperm dish + plexiglass template with a convex surface + weight	equibiaxial	n.g.	n.g.	increase (WB)	1h: 186% (rel)* / 1.9 (ratio-calc)
Konstantonis et al. (2014)	ALP	*ALPP*	hPDL cells (n.g./n.g., n.g., exp, P3-6 & P20-24, n.g.)	dynamic	1Hz for 12h	8%	six station stretching apparatus + optically transparent silicone dishes pre-coated with fibronectin + moving clamp (Neidlinger-Wilke et al 2001)	uniaxial	"young cells" (P3-6): increase (qPCR, GAPDH) "senescent cells" (P20-24): increase (qPCR, GAPDH)	"young cells":150% (rel)* / 1.5 (ratio-calc) "senescent cells": 50% (rel)* / 1.5 (ratio-calc)	"young cells": ALP activity increase (colorimetric assay) "senescent cells": ALP activity increase (colorimetric assay)	"young cells":150% (rel)* / 1.5 (ratio-calc) "senescent cells": 95% (rel)* / 1.6 (ratio-calc)
Konstantonis et al. (2014)	c-fos	*FOS*	hPDL cells (n.g./n.g., n.g., exp, P3-6 & P20-24, n.g.)	dynamic	1Hz for 0.5h, 1h, 1.5h, 2h, 2.5h, 3h	8%	six station stretching apparatus + optically transparent silicone dishes pre-coated with fibronectin + moving clamp (Neidlinger-Wilke et al 2001)	uniaxial	"young cells" (P3-6): increase followed by decrease (qPCR, GAPDH) "senescent cells" (P20-24): increase followed by decrease (qPCR, GAPDH)	"young cells" highest @ 0.5h: 1300% (rel)* / 1.3 (ratio-calc) "young cells" lowest @ 3h: 50% (rel)* / 0.5 (ratio-calc) "senescent cells" highest @ 1h: 740% (rel)* / 7.4 (ratio-calc) "senescent cells" lowest @ 3h: 50% (rel)* / 0.5 (ratio-calc)	n.g.	n.g.
Konstantonis et al. (2014)	ERK / p-ERK	MAPK3; MAPK1	hPDL cells (n.g./n.g., n.g., exp, P3-6 & P20-24, n.g.)	dynamic	1Hz for 15min, 30min, 60min, 180min	8%	six station stretching apparatus + optically transparent silicone dishes pre-coated with fibronectin + moving clamp (Neidlinger-Wilke et al 2001)	uniaxial	n.g.	n.g.	"young cells" (P3-6): not reported p-ERK in "senescent cells" (P20-24) (WB, actin): temporary increase ERK in "senescent cells" (WB, actin): no change	no quantitative information is given
Konstantonis et al. (2014)	JNK / p-JNK	*MAPK8*	hPDL cells (n.g./n.g., n.g., exp, P3-6 & P20-24, n.g.)	dynamic	1Hz for 15min, 30min, 60min, 180min	8%	six station stretching apparatus + optically transparent silicone dishes pre-coated with fibronectin + moving clamp (Neidlinger-Wilke et al 2001)	uniaxial	n.g.	n.g.	"young cells" (P3-6): not reported p-JNK in "senescent cells" (P20-24) (WB, actin): temporary increase JNK in "senescent cells" (WB, actin): no change	no quantitative information is given
Konstantonis et al. (2014)	p38-MAPK / p-p38-MAPK	*MAPK14*	hPDL cells (n.g./n.g., n.g., exp, P3-6 & P20-24, n.g.)	dynamic	1Hz for 15min, 30min, 60min, 180min	8%	six station stretching apparatus + optically transparent silicone dishes pre-coated with fibronectin + moving clamp (Neidlinger-Wilke et al 2001)	uniaxial	n.g.	n.g.	"young cells" (P3-6): not reported p-p38 in "senescent cells" (P20-24) (WB, actin): temporary increase p38 in "senescent cells" (WB, actin): no change	no quantitative information is given
Kook and Lee (2012)	CDK2	*CDK2*	hPLF (20-30/M, PM, dig, P4-7, 80% confluency)	static	1h	1.5%	FX-4000 Tension Plus System + flexible bottomed six-well plates coated with COL I + vacuum	equibiaxial	n.g.	n.g.	decrease (WB, α-tubulin)	1 (?) * / 0.4 (ratio-calc)
Kook and Lee (2012)	CDK4	*CDK4*	hPLF (20-30/M, PM, dig, P4-7, 80% confluency)	static	1h	1.5%	FX-4000 Tension Plus System + flexible bottomed six-well plates coated with COL I + vacuum	equibiaxial	n.g.	n.g.	decrease (WB, α-tubulin)	1 (?) * / 0.3 (ratio-calc)
Kook and Lee (2012)	CyclinA	*CCNA1; CCNA2*	hPLF (20-30/M, PM, dig, P4-7, 80% confluency)	static	1h	1.5%	FX-4000 Tension Plus System + flexible bottomed six-well plates coated with COL I + vacuum	equibiaxial	n.g.	n.g.	decrease (WB, α-tubulin)	no quantitative information is given
Kook and Lee (2012)	CyclinD1	*CCND1*	hPLF (20-30/M, PM, dig, P4-7, 80% confluency)	static	1h	1.5%	FX-4000 Tension Plus System + flexible bottomed six-well plates coated with COL I + vacuum	equibiaxial	n.g.	n.g.	decrease (WB, α-tubulin)	1 (?) * / 0.4 (ratio-calc)
Kook and Lee (2012)	CyclinE	*CCNE1*	hPLF (20-30/M, PM, dig, P4-7, 80% confluency)	static	1h	1.5%	FX-4000 Tension Plus System + flexible bottomed six-well plates coated with COL I + vacuum	equibiaxial	n.g.	n.g.	decrease (WB, α-tubulin)	1 (?) * / 0.3 (ratio-calc)
Kook and Lee (2012)	ERK / p-ERK	MAPK3; MAPK1	hPLF (20-30/M, PM, dig, P4-7, 80% confluency)	static	1h	1.5%	FX-4000 Tension Plus System + flexible bottomed six-well plates coated with COL I + vacuum	equibiaxial	n.g.	n.g.	p-ERK: increase (ELISA)	0.5 (ng/ml)* / 3 (ratio-calc)
Kook and Lee (2012)	ERK / p-ERK	MAPK3; MAPK1	hPLF (20-30/M, PM, dig, P4-7, 80% confluency)	static	1h	1.5%, 3%, 5%, 10%	FX-4000 Tension Plus System + flexible bottomed six-well plates coated with COL I + vacuum	equibiaxial	n.g.	n.g.	p-ERK: temporary increase (WB, ERK)	p-ERK @ 1.5%: no quantitative information is given
Kook and Lee (2012)	JNK / p-JNK	*MAPK8*	hPLF (20-30/M, PM, dig, P4-7, 80% confluency)	static	1h	1.5%, 3%, 5%, 10%	FX-4000 Tension Plus System + flexible bottomed six-well plates coated with COL I + vacuum	equibiaxial	n.g.	n.g.	p-JNK: temporary increase (WB, JNK)	p-JNK @ 1.5%: no quantitative information given
Kook and Lee (2012)	JNK / p-JNK	*MAPK8*	hPLF (20-30/M, PM, dig, P4-7, 80% confluency)	static	1h	1.5%	FX-4000 Tension Plus System + flexible bottomed six-well plates coated with COL I + vacuum	equibiaxial	n.g.	n.g.	p-JNK: increase (WB, JNK)	1.8 (OD at 450nm) * / 7 (ratio-calc)
Kook and Lee (2012)	P21	*CDKN1A*	hPLF (20-30/M, PM, dig, P4-7, 80% confluency)	static	1h	1.5%, 3%, 5%, 10%	FX-4000 Tension Plus System + flexible bottomed six-well plates coated with COL I + vacuum	equibiaxial	n.g.	n.g.	increase (WB, α-tubulin)	3%: 3.6 (ratio)†
Kook and Lee (2012)	p21 / p-p21	*TCEAL1*	hPLF (20-30/M, PM, dig, P4-7, 80% confluency)	static	1h	1.5%	FX-4000 Tension Plus System + flexible bottomed six-well plates coated with COL I + vacuum	equibiaxial	n.g.	n.g.	p-p21: increase (WB, α-tubulin)	p-p21: 3.2 (FC) * / 3.2 (ratio)*

[a] Entry given as reported in the study.
[b] All official gene symbols come from the HUGO Gene Nomenclature Committee (HGNC; URL: https://www.genenames.org) after checking specificity of primers with Primer-BLAST.
[c] Gender/Sex of donors: "M" – male, "F" – female; Tooth type: "PM" – premolar, "M" – molar; Cell density: given in cells/well if not otherwise mentioned.
[d] Frequencies labeled bold orange were converted to hertz (Hz) according to its definition using the information reported in the study (in brackets)
[e] Force type deduced from the description of the force apparatus given by the authors.
[f] Gene and protein expression: 1. conclusion of change (increase, decrease…) was given according to the defined criteria in Figure 2; 2. different markers to describe the amount of change; † Information derived from figures using Engauge Digitizer; *Folds calculated by measuring the graphs, without using the Engauge Digitizer; No makers: Information derived from figures by description in the articles

Reference	Gene/ Analyte[a]	Official gene symbol / abbreviation[b]	Cell (age/gender of donors, tooth type, isolation method, passages used, cell density)[a,c]	Force type (stat./ dyn.)[a]	Force duration and frequency[d]	Force magnitude[a]	Force apparatus[a]	Force type: equibiaxial or uniaxial[e]	Gene expression: Increase, decrease, no change (method w/ reference gene); Methods: qPCR, sqPCR, Northern blot[f]	Gene expression: When it reaches peak and peak's magnitude (fold change; times or ratio; unclear = ?)[f]	Protein expression: Increase, decrease, no change (method w/ reference); Methods: ELISA, WB, RIA, EMSA, IF[f]	Protein expression: When it reaches peak and peak's magnitude (times or ratio; unclear = ?)[f]
Kook and Lee (2012)	P27	*CDKN1B*	hPLF (20-30/M, PM, dig, P4-7, 80% confluency)	static	1h	1.5%, 3%, 5%, 10%	FX-4000 Tension Plus System + flexible bottomed six-well plates coated with COL I + vacuum	equibiaxial	n.g.	n.g.	increase (WB, α-tubulin)	10%: 1.6 (ratio)†
Kook and Lee (2012)	p38-MAPK / p-p38-MAPK	*MAPK14*	hPLF (20-30/M, PM, dig, P4-7, 80% confluency)	static	1h	1.5%, 3%, 5%, 10%	FX-4000 Tension Plus System + flexible bottomed six-well plates coated with COL I + vacuum	equibiaxial	n.g.	n.g.	p-p38: temporary increase (WB, p38)	p-p38 @ 1.5%: no quantitative information is given
Kook and Lee (2012)	p38-MAPK / p-p38-MAPK	*MAPK14*	hPLF (20-30/M, PM, dig, P4-7, 80% confluency)	static	1h	1.5%	FX-4000 Tension Plus System + flexible bottomed six-well plates coated with COL I + vacuum	equibiaxial	n.g.	n.g.	p-p38: increase (ELISA)	4.2 (ng/ml)* / 6.8 (ratio-calc)
Kook and Lee (2012)	PCNA	*PCNA*	hPLF (20-30/M, PM, dig, P4-7, 80% confluency)	static	1h	1.5%	FX-4000 Tension Plus System + flexible bottomed six-well plates coated with COL I + vacuum	equibiaxial	n.g.	n.g.	decrease (WB, α-tubulin)	no quantitative information is given
Lee et al. (2012)	CCL-20	*CCL20*	hPDLF-hTERT (n.g./n.g., PM, dig, P n.g., 70% confluent)	dynamic	**0.2Hz** (12cyc/min: stretch for 2.5s followed by 2.5s of relaxation) for 3h, 6h, 12h, 24h, 48h	12%	Flexercell FX-4000 Strain Unit + 35-mm flexible-bottomed Uniflex culture plates with a centrally located rectangular portion (15.25 mm×24.18 mm) coated with type I collagen + vacuum	uniaxial	increase (sqPCR, GAPDH)	48h: 4.4 (ratio)†	n.g.	n.g.
Lee et al. (2012)	CCL-20	*CCL20*	hPDLF-hTERT (n.g./n.g., PM, dig, P n.g., 70% confluent)	dynamic	**0.2Hz** (12cyc/min: stretch for 2.5s followed by 2.5s of relaxation) for 24h	3%, 6%, 12%,15%	Flexercell FX-4000 Strain Unit + 35-mm flexible-bottomed Uniflex culture plates with a centrally located rectangular portion (15.25 mm×24.18 mm) coated with type I collagen + vacuum	uniaxial	increase (sqPCR, GAPDH)	12%: 4.0 (ratio)†	n.g.	n.g.
Lee et al. (2012)	hBD-1	*DEFB1*	hPDLF-hTERT (n.g./n.g., PM, dig, P n.g., 70% confluent)	dynamic	**0.2Hz** (12cyc/min: stretch for 2.5s followed by 2.5s of relaxation) for 3h, 6h, 12h, 24h, 48h	12%	Flexercell FX-4000 Strain Unit + 35-mm flexible-bottomed Uniflex culture plates with a centrally located rectangular portion (15.25 mm×24.18 mm) coated with type I collagen + vacuum	uniaxial	no change		n.g.	n.g.
Lee et al. (2012)	hBD-1	*DEFB1*	hPDLF-hTERT (n.g./n.g., PM, dig, P n.g., 70% confluent)	dynamic	**0.2Hz** (12cyc/min: stretch for 2.5s followed by 2.5s of relaxation) for 24h	3%, 6%, 12%, 15%	Flexercell FX-4000 Strain Unit + 35-mm flexible-bottomed Uniflex culture plates with a centrally located rectangular portion (15.25 mm×24.18 mm) coated with type I collagen + vacuum	uniaxial	no change		n.g.	n.g.
Lee et al. (2012)	hBD-2	*DEFB4A*	hPDLF-hTERT (n.g./n.g., PM, dig, P n.g., 70% confluent)	dynamic	**0.2Hz** (12cyc/min: stretch for 2.5s followed by 2.5s of relaxation) for 3h, 6h, 12h, 24h, 48h	12%	Flexercell FX-4000 Strain Unit + 35-mm flexible-bottomed Uniflex culture plates with a centrally located rectangular portion (15.25 mm×24.18 mm) coated with type I collagen + vacuum	uniaxial	increase (sqPCR, GAPDH)	12h…24h:.5.6 (ratio)†	n.g.	n.g.
Lee et al. (2012)	hBD-2	*DEFB4A*	hPDLF-hTERT (n.g./n.g., PM, dig, P n.g., 70% confluent)	dynamic	**0.2Hz** (12cyc/min: stretch for 2.5s followed by 2.5s of relaxation) for 24h	3%, 6%, 12%, 15%	Flexercell FX-4000 Strain Unit + 35-mm flexible-bottomed Uniflex culture plates with a centrally located rectangular portion (15.25 mm×24.18 mm) coated with type I collagen + vacuum	uniaxial	increase (sqPCR, GAPDH)	15%: 5.9 (ratio)†	n.g.	n.g.
Lee et al. (2012)	hBD-3	*DEFB103B*	hPDLF-hTERT (n.g./n.g., PM, dig, P n.g., 70% confluent)	dynamic	**0.2Hz** (12cyc/min: stretch for 2.5s followed by 2.5s of relaxation) for 3h, 6h, 12h, 24h, 48h	12%	Flexercell FX-4000 Strain Unit + 35-mm flexible-bottomed Uniflex culture plates with a centrally located rectangular portion (15.25 mm×24.18 mm) coated with type I collagen + vacuum	uniaxial	increase (sqPCR, GAPDH)	48h: 3 (ratio)†	n.g.	n.g.
Lee et al. (2012)	hBD-3	*DEFB103B*	hPDLF-hTERT (n.g./n.g., PM, dig, P n.g., 70% confluent)	dynamic	**0.2Hz** (12cyc/min: stretch for 2.5s followed by 2.5s of relaxation) for 24h	3%, 6%, 12%, 15%	Flexercell FX-4000 Strain Unit + 35-mm flexible-bottomed Uniflex culture plates with a centrally located rectangular portion (15.25 mm×24.18 mm) coated with type I collagen + vacuum	uniaxial	increase (sqPCR, GAPDH)	15%: 2.8 (ratio)†	n.g.	n.g.

[a] Entry given as reported in the study.
[b] All official gene symbols come from the HUGO Gene Nomenclature Committee (HGNC; URL: https://www.genenames.org) after checking specificity of primers with Primer-BLAST.
[c] Gender/Sex of donors: "M" – male, "F" – female; Tooth type: "PM" – premolar, "M" – molar; Cell density: given in cells/well if not otherwise mentioned.
[d] Frequencies labeled bold orange were converted to hertz (Hz) according to its definition using the information reported in the study (in brackets)
[e] Force type deduced from the description of the force apparatus given by the authors.
[f] Gene and protein expression: 1. conclusion of change (increase, decrease…) was given according to the defined criteria in Figure 2; 2. different markers to describe the amount of change; † Information derived from figures using Engauge Digitizer; *Folds calculated by measuring the graphs, without using the Engauge Digitizer; No makers: Information derived from figures by description in the articles

Reference	Gene/ Analyte[a]	Official gene symbol / abbreviation[b]	Cell (age/gender of donors, tooth type, isolation method, passages used, cell density)[a,c]	Force type (stat./ dyn.)[a]	Force duration and frequency[d]	Force magnitude[a]	Force apparatus[a]	Force type: equibiaxial or uniaxial[e]	Gene expression: Increase, decrease, no change (method w/ reference gene); Methods: qPCR, sqPCR, Northern blot[f]	Gene expression: When it reaches peak and peak's magnitude (fold change; times or ratio; unclear = ?)[f]	Protein expression: Increase, decrease, no change (method w/ reference); Methods: ELISA, WB, RIA, EMSA, IF[f]	Protein expression: When it reaches peak and peak's magnitude (times or ratio; unclear = ?)[f]
Lee et al. (2012)	IL-1β	*IL1B*	hPDLF-hTERT (n.g./n.g., PM, dig, P n.g., 70% confluent)	dynamic	**0.2Hz** (12cyc/min: stretch for 2.5s followed by 2.5s of relaxation) for 3h, 6h, 12h, 24h, 48h	12%	Flexercell FX-4000 Strain Unit + 35-mm flexible-bottomed Uniflex culture plates with a centrally located rectangular portion (15.25 mm×24.18 mm) coated with type I collagen + vacuum	uniaxial	increase (sqPCR, GAPDH)	48h: 3 (ratio)†	n.g.	n.g.
Lee et al. (2012)	IL-1β	*IL1B*	hPDLF-hTERT (n.g./n.g., PM, dig, P n.g., 70% confluent)	dynamic	**0.2Hz** (12cyc/min: stretch for 2.5s followed by 2.5s of relaxation) for 24h	3%, 6%, 12%, 15%	Flexercell FX-4000 Strain Unit + 35-mm flexible-bottomed Uniflex culture plates with a centrally located rectangular portion (15.25 mm×24.18 mm) coated with type I collagen + vacuum	uniaxial	increase (sqPCR, GAPDH)	15%: 3.3 (ratio)†	n.g.	n.g.
Lee et al. (2012)	IL-8	*CXCL8*	hPDLF-hTERT (n.g./n.g., PM, dig, P n.g., 70% confluent)	dynamic	**0.2Hz** (12cyc/min: stretch for 2.5s followed by 2.5s of relaxation) for 3h, 6h, 12h, 24h, 48h	12%	Flexercell FX-4000 Strain Unit + 35-mm flexible-bottomed Uniflex culture plates with a centrally located rectangular portion (15.25 mm×24.18 mm) coated with type I collagen + vacuum	uniaxial	increase (sqPCR, GAPDH)	48h: 2.6 (ratio)†	n.g.	n.g.
Lee et al. (2012)	IL-8	*CXCL8*	hPDLF-hTERT (n.g./n.g., PM, dig, P n.g., 70% confluent)	dynamic	**0.2Hz** (12cyc/min: stretch for 2.5s followed by 2.5s of relaxation) for 24h	3%, 6%, 12%,15%	Flexercell FX-4000 Strain Unit + 35-mm flexible-bottomed Uniflex culture plates with a centrally located rectangular portion (15.25 mm×24.18 mm) coated with type I collagen + vacuum	uniaxial	increase (sqPCR, GAPDH)	15%: 2.3 (ratio)†	n.g.	n.g.
Lee et al. (2012)	SIRT1	*SIRT1*	hPDLF-hTERT (n.g./n.g., PM, dig, P n.g., 70% confluent)	dynamic	**0.2Hz** (12cyc/min: stretch for 2.5s followed by 2.5s of relaxation) for 3h, 6h, 12h, 24h, 48h	12%	Flexercell FX-4000 Strain Unit + 35-mm flexible-bottomed Uniflex culture plates with a centrally located rectangular portion (15.25 mm×24.18 mm) coated with type I collagen + vacuum	uniaxial	increase (sqPCR, GADPDH)	24h: 3.4 (ratio)†	increase (WB, β-actin)	24h: 3.4 (ratio)†
Lee et al. (2012)	SIRT1	*SIRT1*	hPDLF-hTERT (n.g./n.g., PM, dig, P n.g., 70% confluent)	dynamic	**0.2Hz** (12cyc/min: stretch for 2.5s followed by 2.5s of relaxation) for 24h	3%, 6%, 12%, 15%	Flexercell FX-4000 Strain Unit + 35-mm flexible-bottomed Uniflex culture plates with a centrally located rectangular portion (15.25 mm×24.18 mm) coated with type I collagen + vacuum	uniaxial	increase (sqPCR, GAPDH)	12%: 3.2 (ratio)†	increase (WB, β-actin)	12%: 3.3 (ratio)†
Lee et al. (2012)	TLR-2	*TLR2*	hPDLF-hTERT (n.g./n.g., PM, dig, P n.g., 70% confluent)	dynamic	**0.2Hz** (12cyc/min: stretch for 2.5s followed by 2.5s of relaxation) for 3h, 6h, 12h, 24h, 48h	12%	Flexercell FX-4000 Strain Unit + 35-mm flexible-bottomed Uniflex culture plates with a centrally located rectangular portion (15.25 mm×24.18 mm) coated with type I collagen + vacuum	uniaxial	increase (sqPCR, GAPDH)	24h: 6.5 (ratio)†	n.g.	n.g.
Lee et al. (2012)	TLR-2	*TLR2*	hPDLF-hTERT (n.g./n.g., PM, dig, P n.g., 70% confluent)	dynamic	**0.2Hz** (12cyc/min: stretch for 2.5s followed by 2.5s of relaxation) for 24h	3%, 6%, 12%, 15%	Flexercell FX-4000 Strain Unit + 35-mm flexible-bottomed Uniflex culture plates with a centrally located rectangular portion (15.25 mm×24.18 mm) coated with type I collagen + vacuum	uniaxial	increase (sqPCR, GAPDH)	12%: 6.3 (ratio)†	n.g.	n.g.
Lee et al. (2012)	TLR-4	*TLR4*	hPDLF-hTERT (n.g./n.g., PM, dig, P n.g., 70% confluent)	dynamic	**0.2Hz** (12cyc/min: stretch for 2.5s followed by 2.5s of relaxation)for 3h, 6h, 12h, 24h, 48h	12%	Flexercell FX-4000 Strain Unit + 35-mm flexible-bottomed Uniflex culture plates with a centrally located rectangular portion (15.25 mm×24.18 mm) coated with type I collagen + vacuum	uniaxial	increase (sqPCR, GAPDH)	24h: 4.6 (ratio)†	n.g.	n.g.
Lee et al. (2012)	TLR-4	*TLR4*	hPDLF-hTERT (n.g./n.g., PM, dig, P n.g., 70% confluent)	dynamic	**0.2Hz** (12cyc/min: stretch for 2.5s followed by 2.5s of relaxation) for 24h	3%, 6%, 12%, 15%	Flexercell FX-4000 Strain Unit + 35-mm flexible-bottomed Uniflex culture plates with a centrally located rectangular portion (15.25 mm×24.18 mm) coated with type I collagen + vacuum	uniaxial	increase (sqPCR, GAPDH)	12%: 4.6 (ratio)†	n.g.	n.g.

[a] Entry given as reported in the study.
[b] All official gene symbols come from the HUGO Gene Nomenclature Committee (HGNC; URL: https://www.genenames.org) after checking specificity of primers with Primer-BLAST.
[c] Gender/Sex of donors: "M" – male, "F" – female; Tooth type: "PM" – premolar, "M" – molar; Cell density: given in cells/well if not otherwise mentioned.
[d] Frequencies labeled bold orange were converted to hertz (Hz) according to its definition using the information reported in the study (in brackets)
[e] Force type deduced from the description of the force apparatus given by the authors.
[f] Gene and protein expression: 1. conclusion of change (increase, decrease…) was given according to the defined criteria in Figure 2; 2. different markers to describe the amount of change; † Information derived from figures using Engauge Digitizer; *Folds calculated by measuring the graphs, without using the Engauge Digitizer; No makers: Information derived from figures by description in the articles

Reference	Gene/ Analyte[a]	Official gene symbol / abbreviation[b]	Cell (age/gender of donors, tooth type, isolation method, passages used, cell density)[a,c]	Force type (stat./ dyn.)[a]	Force duration and frequency[d]	Force magnitude[a]	Force apparatus[a]	Force type: equibiaxial or uniaxial[e]	Gene expression: Increase, decrease, no change (method w/ reference gene); Methods: qPCR, sqPCR, Northern blot[f]	Gene expression: When it reaches peak and peak's magnitude (fold change; times or ratio; unclear = ?)[f]	Protein expression: Increase, decrease, no change (method w/ reference); Methods: ELISA, WB, RIA, EMSA, IF[f]	Protein expression: When it reaches peak and peak's magnitude (times or ratio; unclear = ?)[f]
Lee et al. (2012)	TNF-α	*TNF*	hPDLF-hTERT (n.g./n.g., PM, dig, P n.g., 70% confluent)	dynamic	**0.2Hz** (12cyc/min: stretch for 2.5s followed by 2.5s of relaxation) for 3h, 6h, 12h, 24h, 48h	12%	Flexercell FX-4000 Strain Unit + 35-mm flexible-bottomed Uniflex culture plates with a centrally located rectangular portion (15.25 mm×24.18 mm) coated with type I collagen + vacuum	uniaxial	increase (sqPCR, GAPDH)	48h: 4.7 (ratio)†	n.g.	n.g.
Lee et al. (2012)	TNF-α	*TNF*	hPDLF-hTERT (n.g./n.g., PM, dig, P n.g., 70% confluent)	dynamic	**0.2Hz** (12cyc/min: stretch for 2.5s followed by 2.5s of relaxation) for 24h	3%, 6%, 12%, 15%	Flexercell FX-4000 Strain Unit + 35-mm flexible-bottomed Uniflex culture plates with a centrally located rectangular portion (15.25 mm×24.18 mm) coated with type I collagen + vacuum	uniaxial	increase (sqPCR, GAPDH)	15%: 4.1 (ratio)†	n.g.	n.g.
Lee et al. (2015)	ALP	*ALPP*	hPDL cells (n.g./n.g., n.g., n.g., P n.g., 3×10^5)	dynamic	**0.1Hz** (6cyc/min) for 48h	12%	Flexcell FX-5000 Tension Unit + BioFlex Culture Plate + vacuum	equibiaxial	increase (qPCR, β-actin)	3.8 (ratio)*	n.g.	n.g.
Lee et al. (2015)	CCL3	*CCL3*	hPDL cells (n.g./n.g., n.g., n.g., P n.g., 3×10^5)	dynamic	**0.1Hz** (6cyc/min) for 2h, 4h, 8h, 24h, 48h	12%	Flexcell FX-5000 Tension Unit + BioFlex Culture Plate + vacuum	equibiaxial	increase (qPCR, β-actin)	48h: 2.8 (ratio)†	n.g.	n.g.
Lee et al. (2015)	CCL5	*CCL5*	hPDL cells (n.g./n.g., n.g., n.g., P n.g., 3×10^5)	dynamic	**0.1Hz** (6cyc/min) for 2h, 4h, 8h, 24h, 48h	12%	Flexcell FX-5000 Tension Unit + BioFlex Culture Plate + vacuum	equibiaxial	increase (qPCR, β-actin)	48h: 7.9 (ratio)†	n.g.	n.g.
Lee et al. (2015)	CCR5	*CCR5*	hPDL cells (n.g./n.g., n.g., n.g., P n.g., 3×10^5)	dynamic	**0.1Hz** (6cyc/min) qPCR for 2h, 4h, 8h, 24h, 48h; WB for 1d, 2d, 3d, 4d	12%	Flexcell FX-5000 Tension Unit + BioFlex Culture Plate + vacuum	equibiaxial	increase (qPCR, β-actin)	48h: 11.3 (ratio)†	temporary increase (WB, β-actin)	no quantitative information is given
Lee et al. (2015)	Colα1 (collagen α1)	*COL1A1*	hPDL cells (n.g./n.g., n.g., n.g., P n.g., 3×10^5)	dynamic	**0.1Hz** (6cyc/min) for 48h	12%	Flexcell FX-5000 Tension Unit + BioFlex Culture Plate + vacuum	equibiaxial	increase (qPCR, β-actin)	4.1 (ratio)*	n.g.	n.g.
Lee et al. (2015)	IL-12	*IL12A*	hPDL cells (n.g./n.g., n.g., n.g., P n.g., 3×10^5)	dynamic	**0.1Hz** (6cyc/min) for 48h	12%	Flexcell FX-5000 Tension Unit + BioFlex Culture Plate + vacuum	equibiaxial	increase (qPCR, β-actin)	8.4 (ratio)*	n.g.	n.g.
Lee et al. (2015)	OCN	*BGLAP*	hPDL cells (n.g./n.g., n.g., n.g., P n.g., 3×10^5)	dynamic	**0.1Hz** (6cyc/min) for 48h	12%	Flexcell FX-5000 Tension Unit + BioFlex Culture Plate + vacuum	equibiaxial	increase (qPCR, β-actin)	4.2 (FC?)† / 4.7 (ratio-calc)	n.g.	n.g.
Lee et al. (2015)	OPG	*TNFRSF11B*	hPDL cells (n.g./n.g., n.g., n.g., P n.g., 3×10^5)	dynamic	**0.1Hz** (6cyc/min) for 48h	12%	Flexcell FX-5000 Tension Unit + BioFlex Culture Plate + vacuum	equibiaxial	increase (qPCR, β-actin)	7.7 (ratio)*	n.g.	n.g.
Lee et al. (2015)	Periostin	*POSTN*	hPDL cells (n.g./n.g., n.g., n.g., P n.g., 3×10^5)	dynamic	**0.1Hz** (6cyc/min) for 48h	12%	Flexcell FX-5000 Tension Unit + BioFlex Culture Plate + vacuum	equibiaxial	increase (qPCR, β-actin)	8.8 (ratio)*	n.g.	n.g.
Lee et al. (2015)	RANKL	*TNFSF11*	hPDL cells (n.g./n.g., n.g., n.g., P n.g., 3×10^5)	dynamic	**0.1Hz** (6cyc/min) for 48h	12%	Flexcell FX-5000 Tension Unit + BioFlex Culture Plate + vacuum	equibiaxial	increase (qPCR, β-actin)	1.9 (rel)* / 1.2 (ratio-calc)	n.g.	n.g.
Lee et al. (2015)	Runx2	*RUNX2*	hPDL cells (n.g./n.g., n.g., n.g., P n.g., 3×10^5)	dynamic	**0.1Hz** (6cyc/min) for 48h	12%	Flexcell FX-5000 Tension Unit + BioFlex Culture Plate + vacuum	equibiaxial	increase (qPCR, β-actin)	3.8 (ratio)*	n.g.	n.g.
Li et al. (2013)	ERK1/2 / p-ERK1/2	MAPK3; MAPK1	hPDL cells (12-20/n.g., PM, exp, P3-6, 80% confluence)	dynamic	0.5Hz (30cyc/min) for 12h, 24h, 48h	10%	Flexcell FX-5000 Tension Unit + flexible-bottomed BioFlex Culture Plates coated with type I collagen + vacuum	equibiaxial	n.g.	n.g.	p-ERK1/2: increase (WB, ERK)	p-ERK1/2 @ 24h: 3.2 (rel)† / 13.7 (ratio-calc)
Li et al. (2013)	ERK5 / p-ERK5	*MAPK7*	hPDL cells (12-20/n.g., PM, exp, P3-6, 80% confluence)	dynamic	0.5Hz (30cyc/min) for 12h, 24h, 48h	10%	Flexcell FX-5000 Tension Unit + flexible-bottomed BioFlex Culture Plates coated with type I collagen + vacuum	equibiaxial	n.g.	n.g.	p-ERK5: no change (WB, ERK5)	
Li et al. (2013)	JNK / p-JNK	*MAPK8*	hPDL cells (12-20/n.g., PM, exp, P3-6, 80% confluence)	dynamic	0.5Hz (30cyc/min) for 12h, 24h, 48h	10%	Flexcell FX-5000 Tension Unit + flexible-bottomed BioFlex Culture Plates coated with type I collagen + vacuum	equibiaxial	n.g.	n.g.	p-JNK: no change (WB, JNK)	
Li et al. (2013)	P38 / p-P38	*MAPK14*	hPDL cells (12-20/n.g., PM, exp, P3-6, 80% confluence)	dynamic	0.5Hz (30cyc/min) for 12h, 24h, 48h	10%	Flexcell FX-5000 Tension Unit + flexible-bottomed BioFlex Culture Plates coated with type I collagen + vacuum	equibiaxial	n.g.	n.g.	p-P38: no change (WB, P38)	
Li et al. (2013)	RUNX2	*RUNX2*	hPDL cells (12-20/n.g., PM, exp, P3-6, 80% confluence)	dynamic	0.5Hz (30cyc/min) for 12h, 24h, 48h	10%	Flexcell FX-5000 Tension Unit + flexible-bottomed BioFlex Culture Plates coated with type I collagen + vacuum	equibiaxial	increase followed by decrease (qPCR, GAPDH)	highest @ 24h: 3.2 (FC)* lowest @ 48h: 0.2 (FC)*	increase followed by decrease (WB, GAPDH)	hightest @ 24h: 0.8 (rel)* / 2.0 (ratio-calc) lowest @ 48h: 0.1 (rel)* / 0.4 (ratio-calc)

[a] Entry given as reported in the study.
[b] All official gene symbols come from the HUGO Gene Nomenclature Committee (HGNC; URL: https://www.genenames.org) after checking specificity of primers with Primer-BLAST.
[c] Gender/Sex of donors: "M" – male, "F" – female; Tooth type: "PM" – premolar, "M" – molar; Cell density: given in cells/well if not otherwise mentioned.
[d] Frequencies labeled bold orange were converted to hertz (Hz) according to its definition using the information reported in the study (in brackets)
[e] Force type deduced from the description of the force apparatus given by the authors.
[f] Gene and protein expression: 1. conclusion of change (increase, decrease…) was given according to the defined criteria in Figure 2; 2. different markers to describe the amount of change; † Information derived from figures using Engauge Digitizer; *Folds calculated by measuring the graphs, without using the Engauge Digitizer; No makers: Information derived from figures by description in the articles

Reference	Gene/ Analyte[a]	Official gene symbol / abbreviation[b]	Cell (age/gender of donors, tooth type, isolation method, passages used, cell density)[a,c]	Force type (stat./ dyn.)[a]	Force duration and frequency[d]	Force magnitude[a]	Force apparatus[a]	Force type: equibiaxial or uniaxial[e]	Gene expression: Increase, decrease, no change (method w/ reference gene); Methods: qPCR, sqPCR, Northern blot[f]	Gene expression: When it reaches peak and peak's magnitude (fold change; times or ratio; unclear = ?)[f]	Protein expression: Increase, decrease, no change (method w/ reference); Methods: ELISA, WB, RIA, EMSA, IF[f]	Protein expression: When it reaches peak and peak's magnitude (times or ratio; unclear = ?)[f]
Li et al. (2013)	SP7	*SP7*	hPDL cells (12-20/n.g., PM, exp, P3-6, 80% confluence)	dynamic	0.5Hz (30cyc/min) for 12h, 24h, 48h	10%	Flexcell FX-5000 Tension Unit + flexible-bottomed BioFlex Culture Plates coated with type I collagen + vacuum	equibiaxial	decrease (qPCR, GAPDH)	48h: 0.1 (FC)*	temporary increase (WB, GAPDH)	24h: 0.5 (rel)* / 1.3 (ratio-calc)
Li et al. (2013)	SPP1	*SPP1*	hPDL cells (12-20/n.g., PM, exp, P3-6, 80% confluence)	dynamic	0.5Hz (30cyc/min) for 12h, 24h, 48h	10%	Flexcell FX-5000 Tension Unit + flexible-bottomed BioFlex Culture Plates coated with type I collagen + vacuum	equibiaxial	increase (qPCR, GAPDH)	24h: 3.4 (FC)*	temporary increase (WB, GAPDH)	24h: 0.3 (rel)* / 2.8 (ratio-calc)
Li et al. (2014)	ERK1/2 / p-ERK1/2	MAPK3; MAPK1	hPDL cells (12-16/F, 12-16/M, PM, exp, P3-6, 80% confluence)	dynamic	0.5Hz (30cyc/min) for 24h	10%	Flexcell FX-5000 Tension Unit + six-well culture plates coated with type I collagen + vacuum	equibiaxial	n.g.	n.g.	p-ERK1/2: increase (WB, ERK)	p-ERK1/2: 0.5 (rel)* / 8.0 (ratio-calc)
Li et al. (2014)	HIF-1α	*HIF1A*	hPDL cells (12-16/F, 12-16/M, PM, exp, P3-6, 80% confluence)	dynamic	0.5Hz (30cyc/min) for 0h, 12h, 24h, 48h	10%	Flexcell FX-5000 Tension Unit + six-well culture plates coated with type I collagen + vacuum	equibiaxial	increase (qPCR, GAPDH)	24h: 2.4 (ratio)*	increase (WB, GAPDH)	24h: 1.1 (rel)* / 1.9 (ratio-calc)
Li et al. (2014)	JNK / p-JNK	*MAPK8*	hPDL cells (12-16/F, 12-16/M, PM, exp, P3-6, 80% confluence)	dynamic	0.5Hz (30cyc/min) for 24h	10%	Flexcell FX-5000 Tension Unit + six-well culture plates coated with type I collagen + vacuum	equibiaxial	n.g.	n.g.	p-JNK: increase (WB, JNK)	p-JNK: 0.6 (rel)* / 1.1 (ratio-calc)
Li et al. (2014)	P38 / p-P38	*MAPK14*	hPDL cells (12-16/F, 12-16/M, PM, exp, P3-6, 80% confluence)	dynamic	0.5Hz (30cyc/min) for 24h	10%	Flexcell FX-5000 Tension Unit + six-well culture plates coated with type I collagen + vacuum	equibiaxial	n.g.	n.g.	increase (WB, p38)	0.8 (rel)* / 1.4 (ratio-calc)
Li et al. (2014)	RUNX2	*RUNX2*	hPDL cells (12-16/F, 12-16/M, PM, exp, P3-6, 80% confluence)	dynamic	0.5Hz (30cyc/min) for 24h	10%	Flexcell FX-5000 Tension Unit + six-well culture plates coated with type I collagen + vacuum	equibiaxial	increase (qPCR, GAPDH)	3.3 (rel)* / 6.6 (ratio-calc)*	increase (WB, GAPDH)	0.1 (rel)* / 2.7 (ratio-calc)
Li et al. (2014)	SP7	*SP7*	hPDL cells (12-16/F, 12-16/M, PM, exp, P3-6, 80% confluence)	dynamic	0.5Hz (30cyc/min) for 24h	10%	Flexcell FX-5000 Tension Unit + six-well culture plates coated with type I collagen + vacuum	equibiaxial	increase (qPCR, GAPDH)	2.7 (rel)* / 5.7 (ratio)*	increase (WB, GAPDH)	0.05 (rel)* / 1.3 (ratio-calc)
Li et al. (2014)	SPP1	*SPP1*	hPDL cells (12-16/F, 12-16/M, PM, exp, P3-6, 80% confluence)	dynamic	0.5Hz (30cyc/min) for 24h	10%	Flexcell FX-5000 Tension Unit + six-well culture plates coated with type I collagen + vacuum	equibiaxial	increase (qPCR, GAPDH)	2.4 (rel)* / 4.8 (ratio)*	increase (WB, GAPDH)	0.02 (rel)* / 1.5 (ratio-calc)
Li et al. (2015)	Cx43	*GJA1*	hPDL cells ($) (n.g./n.g., n.g., n.g., P3-6, 75%-85% confluence)	dynamic	**0.005Hz** (3min/cyc) for 0.5h, 1h, 2h, 4h, 8h, 12h, 24h	5%	"custom-made tensile device + elastic membranes were made of polydimethyl-siloxane (PDMS) gel +motor"	uniaxial	increase (qPCR, GAPDH)	24h: 6.3 (ratio)*	increase (WB, GAPDH)	24h: 0.8 (rel)* / 2.1 (ratio-calc)
Li et al. (2015)	OPG	*TNFRSF11B*	hPDL cells ($) (n.g./n.g., n.g., n.g., P3-6, 75%-85% confluence)	dynamic	**0.005Hz** (3min/cyc) for 0.5h, 1h, 2h, 4h, 8h, 12h, 24h	5%	"custom-made tensile device + elastic membranes were made of polydimethyl-siloxane (PDMS) gel +motor"	uniaxial	increase (qPCR, GAPDH)	12h: 4.0 (ratio)*	increase (WB, GAPDH)	8h: 0.9 (rel)* / 4.4 (ratio-calc)
Li et al. (2015)	Osterix	*SP7*	hPDL cells ($) (n.g./n.g., n.g., n.g., P3-6, 75%-85% confluence)	dynamic	**0.005Hz** (3min/cyc) for 0.5h, 1h, 2h, 4h, 8h, 12h, 24h	5%	"custom-made tensile device + elastic membranes were made of polydimethyl-siloxane (PDMS) gel +motor"	uniaxial	increase (qPCR, GAPDH)	24h: 14.0 (ratio)*	increase followed by plateau (WB, GAPDH)	12h…24h: 1.6 (rel)* / 4.2 (ratio-calc)
Li et al. (2015)	RANKL	*TNFSF11*	hPDL cells ($) (n.g./n.g., n.g., n.g., P3-6, 75%-85% confluence)	dynamic	**0.005Hz** (3min/cyc) for 0.5h, 1h, 2h, 4h, 8h, 12h, 24h	5%	"custom-made tensile device + elastic membranes were made of polydimethyl-siloxane (PDMS) gel +motor"	uniaxial	increase (qPCR, GAPDH)	1h: 3.9 (ratio)*	increase (WB, GAPDH)	4h: 1.3 (rel)* / 3.3 (ratio-calc)
Li et al. (2015)	RUNX2	*RUNX2*	hPDL cells ($) (n.g./n.g., n.g., n.g., P3-6, 75%-85% confluence)	dynamic	**0.005Hz** (3min/cyc) for 0.5h, 1h, 2h, 4h, 8h, 12h, 24h	5%	"custom-made tensile device + elastic membranes were made of polydimethyl-siloxane (PDMS) gel +motor"	uniaxial	increase (qPCR, GAPDH)	24h: 12.0 (ratio)*	increase followed by plateau (WB, GAPDH)	12h…24h: 2 (rel)* / 1.4 (ratio-calc)
Liao and Hua (2013)	CSE	*SLC2A1*	hPDL cells (13-18/n.g., PM, dig, P3-8, Confluence)	static	30min, 60min, 90min, 120min	1.5%	Flexcell FX-5000 Tension System + flexible-bottomed six-well plates + vacuum	equibiaxial	increase (qPCR, GAPDH)	60min: 3.7 (ratio)*	n.g.	n.g.
Liao and Hua (2013)	OPG	*TNFRSF11B*	hPDL cells (13-18/n.g., PM, dig, P3-8, Confluence)	static	60min	1.5%	Flexcell FX-5000 Tension System + flexible-bottomed six-well plates + vacuum	equibiaxial	*OPG:* increase (qPCR, GAPDH) *OPG/RANKL*: increase (qPCR, GAPDH)	1.4 (ratio)* 1.2 (ratio)*	OPG: increase (ELISA) OPG/RANKL: increase (ELISA)	2127.7 (ng/mL)* / 1.2 (ratio-calc) 1.2 (rel)* / 1.7 (ratio-calc)
Liao and Hua (2013)	RANKL	*TNFSF11*	hPDL cells (13-18/n.g., PM, dig, P3-8, Confluence)	static	60min	1.5%	Flexcell FX-5000 Tension System + flexible-bottomed six-well plates + vacuum	equibiaxial	*RANKL:* increase (qPCR, GAPDH) *OPG/RANKL*: increase (qPCR, GAPDH)	1.2 (ratio)* 1.2 (ratio)*	RANKL: decrease (ELISA) OPG/RANKL: increase (ELISA)	1787.2 (ng/mL)* / 0.7 (ratio-calc) 1.2 (rel)* / 1.7 (ratio-calc)
Liu et al. (2012)	BGN	*BGN*	hPDL cells (12-15/n.g., PM, exp, P3-4, Confluent)	dynamic	**0.1Hz** (6cyc/min) for 24h	12%	Flexcell FX 3000 + six-well, flexible-bottomed plates + vacuum (Li et al 2010; Tang et al 2006)	equibiaxial	increase (qPCR, GAPDH)	1.9 (rel)* / 4.6 (ratio-calc)	n.g.	n.g.
Liu et al. (2012)	Col12A1	*COL12A1*	hPDL cells (12-15/n.g., PM, exp, P3-4, Confluent)	dynamic	**0.1Hz** (6cyc/min) for 24h	12%	Flexcell FX 3000 + six-well, flexible-bottomed plates + vacuum (Li et al 2010; Tang et al 2006)	equibiaxial	Increase (qPCR, GAPDH)	1.4 (rel)* / 3.9 (ratio-calc)	n.g.	n.g.

[a] Entry given as reported in the study.
[b] All official gene symbols come from the HUGO Gene Nomenclature Committee (HGNC; URL: https://www.genenames.org) after checking specificity of primers with Primer-BLAST.
[c] Gender/Sex of donors: "M" – male, "F" – female; Tooth type: "PM" – premolar, "M" – molar; Cell density: given in cells/well if not otherwise mentioned.
[d] Frequencies labeled bold orange were converted to hertz (Hz) according to its definition using the information reported in the study (in brackets)
[e] Force type deduced from the description of the force apparatus given by the authors.
[f] Gene and protein expression: 1. conclusion of change (increase, decrease…) was given according to the defined criteria in Figure 2; 2. different markers to describe the amount of change; † Information derived from figures using Engauge Digitizer; *Folds calculated by measuring the graphs, without using the Engauge Digitizer; No makers: Information derived from figures by description in the articles

Reference	Gene/ Analyte[a]	Official gene symbol / abbreviation[b]	Cell (age/gender of donors, tooth type, isolation method, passages used, cell density)[a,c]	Force type (stat./ dyn.)[a]	Force duration and frequency[d]	Force magnitude[a]	Force apparatus[a]	Force type: equibiaxial or uniaxial[e]	Gene expression: Increase, decrease, no change (method w/ reference gene); Methods: qPCR, sqPCR, Northern blot[f]	Gene expression: When it reaches peak and peak's magnitude (fold change; times or ratio; unclear = ?)[f]	Protein expression: Increase, decrease, no change (method w/ reference); Methods: ELISA, WB, RIA, EMSA, IF[f]	Protein expression: When it reaches peak and peak's magnitude (times or ratio; unclear = ?)[f]
Liu et al. (2012)	EGFR	*EGFR*	hPDL cells (12-15/n.g., PM, exp, P3-4, Confluent)	dynamic	**0.1Hz** (6cyc/min) for 24h	12%	Flexcell FX 3000 + six-well, flexible-bottomed plates + vacuum (Li et al 2010; Tang et al 2006)	equibiaxial	increase (qPCR, GAPDH)	1.8 (rel)* / 4.9 (ratio-calc)	n.g.	n.g.
Liu et al. (2012)	IGF-1	*IGF1*	hPDL cells (12-15/n.g., PM, exp, P3-4, Confluent)	dynamic	**0.1Hz** (6cyc/min) for 24h	12%	Flexcell FX 3000 + six-well, flexible-bottomed plates + vacuum (Li et al 2010; Tang et al 2006)	equibiaxial	increase (qPCR, GAPDH)	1.2 (rel)* / 6.0 (ratio-calc)	n.g.	n.g.
Liu et al. (2012)	ITGA1	*ITGA1*	hPDL cells (12-15/n.g., PM, exp, P3-4, Confluent)	dynamic	**0.1Hz** (6cyc/min) for 24h	12%	Flexcell FX 3000 + six-well, flexible-bottomed plates + vacuum (Li et al 2010; Tang et al 2006)	equibiaxial	decrease (qPCR, GAPDH)	0.6 (rel)* / 0.4 (ratio-calc)	n.g.	n.g.
Liu et al. (2012)	ITGA3	*ITGA3*	hPDL cells (12-15/n.g., PM, exp, P3-4, Confluent)	dynamic	**0.1Hz** (6cyc/min) for 24h	12%	Flexcell FX 3000 + six-well, flexible-bottomed plates + vacuum (Li et al 2010; Tang et al 2006)	equibiaxial	Increase (qPCR, GAPDH)	0.7 (rel)* / 3.3 (ratio-calc)	n.g.	n.g.
Liu et al. (2012)	MMP-2	*MMP2*	hPDL cells (12-15/n.g., PM, exp, P3-4, Confluent)	dynamic	**0.1Hz** (6cyc/min) for 24h	12%	Flexcell FX 3000 + six-well, flexible-bottomed plates + vacuum (Li et al 2010; Tang et al 2006)	equibiaxial	Increase (qPCR, GAPDH)	2.0 (rel)* / 3.6 (ratio-calc)	n.g.	n.g.
Liu et al. (2012)	MSX1	*MSX1*	hPDL cells (12-15/n.g., PM, exp, P3-4, Confluent)	dynamic	**0.1Hz** (6cyc/min) for 24h	12%	Flexcell FX 3000 + six-well, flexible-bottomed plates + vacuum (Li et al 2010; Tang et al 2006)	equibiaxial	increase (qPCR, GAPDH)	0.8 (rel)* / 4.7 (ratio-calc)	n.g.	n.g.
Liu et al. (2012)	SMAD7	*SMAD7*	hPDL cells (12-15/n.g., PM, exp, P3-4, Confluent)	dynamic	**0.1Hz** (6cyc/min) for 24h	12%	Flexcell FX 3000 + six-well, flexible-bottomed plates + vacuum (Li et al 2010; Tang et al 2006)	equibiaxial	increase (qPCR, GAPDH)	0.4 (rel)* / 2.1 (ratio-calc)	n.g.	n.g.
Liu et al. (2012)	TGFβR1	*TGFBR1*	hPDL cells (12-15/n.g., PM, exp, P3-4, Confluent)	dynamic	**0.1Hz** (6cyc/min) for 24h	12%	Flexcell FX 3000 + six-well, flexible-bottomed plates + vacuum (Li et al 2010; Tang et al 2006)	equibiaxial	decrease (qPCR, GAPDH)	0.4 (rel)* / 0.5 (ratio-calc)	n.g.	n.g.
Liu et al. (2017)	ALP	*ALPP*	hPDLSCs cells (37.9±7.2/n.g., PM and M, dig, P3, 95% confluence) from healthy (HPDLSCs) and patients w/ periodontitis (PPDLSCs: 38.9 ± 7.9/n.g., n.g., dig, P3, 95% confluence)	dynamic	0.1Hz for 12h	6%, 8%, 10%, 12%, 14%	Flexcell FX-4000T + 6-well Bioflex plates + vacuum	equibiaxial	HPDLSCs: increase (qPCR, β-actin)	HPDLSCs @ 12%: 1.6 (ratio)*	n.g.	n.g.
Liu et al. (2017)	C-fos	*FOS*	hPDLSCs cells (37.9±7.2/n.g., PM and M, dig, P3, 95% confluence) from healthy (HPDLSCs) and patients w/ periodontitis (PPDLSCs: 38.9 ± 7.9/n.g., n.g., dig, P3, 95% confluence)	dynamic	0.1Hz for 12h	6%, 8%, 10%, 12%, 14%	Flexcell FX-4000T + 6-well Bioflex plates + vacuum	equibiaxial	HPDLSCs: increase (qPCR, β-actin)	HPDLSCs @ 14%: 1.7 (ratio)*	n.g.	n.g.
Liu et al. (2017)	IL-1β	*IL1B*	hPDLSCs cells (37.9±7.2/n.g., PM and M, dig, P3, 95% confluence) from healthy (HPDLSCs) and patients w/ periodontitis (PPDLSCs: 38.9 ± 7.9/n.g., n.g., dig, P3, 95% confluence)	dynamic	0.1Hz for 12h	6%, 8%, 10%, 12%, 14%	Flexcell FX-4000T + 6-well Bioflex plates + vacuum	equibiaxial	n.g.	n.g.	HPDLSCs: increase followed by plateau (ELISA)	HPDLSCs @ 6%...14%: 3.2 (pg/10^6 cells)* / 1.5 (ratio)*
Liu et al. (2017)	IL-6	*IL6*	hPDLSCs cells (37.9±7.2/n.g., PM and M, dig, P3, 95% confluence) from healthy (HPDLSCs) and patients w/ periodontitis (PPDLSCs: 38.9 ± 7.9/n.g., n.g., dig, P3, 95% confluence)	dynamic	0.1Hz for 12h	6%, 8%, 10%, 12%, 14%	Flexcell FX-4000T + 6-well Bioflex plates + vacuum	equibiaxial	n.g.	n.g.	HPDLSCs: increase (ELISA)	HPDLSCs @ 14%: 585.7 (pg/10^6 cells)* / 11.7 (ratio)*
Liu et al. (2017)	IL-8	*CXCL8*	hPDLSCs cells (37.9±7.2/n.g., PM and M, dig, P3, 95% confluence) from healthy (HPDLSCs) and patients w/ periodontitis (PPDLSCs: 38.9 ± 7.9/n.g., n.g., dig, P3, 95% confluence)	dynamic	0.1Hz for 12h	6%, 8%, 10%, 12%, 14%	Flexcell FX-4000T + 6-well Bioflex plates + vacuum	equibiaxial	n.g.	n.g.	HPDLSCs: increase (ELISA)	HPDLSCs @ 14%: 466.7 (pg/10^6 cells)* / 128.2 (ratio)*
Liu et al. (2017)	OPG	*TNFRSF11B*	hPDLSCs cells (37.9±7.2/n.g., PM and M, dig, P3, 95% confluence) from healthy (HPDLSCs) and patients w/ periodontitis (PPDLSCs: 38.9 ± 7.9/n.g., n.g., dig, P3, 95% confluence)	dynamic	0.1Hz for 12h	6%, 8%, 10%, 12%, 14%	Flexcell FX-4000T + 6-well Bioflex plates + vacuum	equibiaxial	HPDLSCs: increase (qPCR, β-actin)	HPDLSCs @ 12%: 1.6 (ratio)*	n.g.	n.g.
Liu et al. (2017)	RANKL	*TNFSF11*	hPDLSCs cells (37.9±7.2/n.g., PM and M, dig, P3, 95% confluence) from healthy (HPDLSCs) and patients w/ periodontitis (PPDLSCs: 38.9 ± 7.9/n.g., n.g., dig, P3, 95% confluence)	dynamic	0.1Hz for 12h	6%, 8%, 10%, 12%, 14%	Flexcell FX-4000T + 6-well Bioflex plates + vacuum	equibiaxial	HPDLSCs: increase (qPCR, β-actin)	HPDLSCs @ 14%: 1.8 (ratio)*	n.g.	n.g.
Liu et al. (2017)	RUNX2	*RUNX2*	hPDLSCs cells (37.9±7.2/n.g., PM and M, dig, P3, 95% confluence) from healthy (HPDLSCs) and patients w/ periodontitis (PPDLSCs: 38.9 ± 7.9/n.g., n.g., dig, P3, 95% confluence)	dynamic	0.1Hz for 12h	6%, 8%, 10%, 12%, 14%	Flexcell FX-4000T + 6-well Bioflex plates + vacuum	equibiaxial	HPDLSCs: increase (qPCR, β-actin)	HPDLSCs @ 12%: 3.7 (ratio)*	n.g.	n.g.

[a] Entry given as reported in the study.
[b] All official gene symbols come from the HUGO Gene Nomenclature Committee (HGNC; URL: https://www.genenames.org) after checking specificity of primers with Primer-BLAST.
[c] Gender/Sex of donors: "M" – male, "F" – female; Tooth type: "PM" – premolar, "M" – molar; Cell density: given in cells/well if not otherwise mentioned.
[d] Frequencies labeled bold orange were converted to hertz (Hz) according to its definition using the information reported in the study (in brackets)
[e] Force type deduced from the description of the force apparatus given by the authors.
[f] Gene and protein expression: 1. conclusion of change (increase, decrease…) was given according to the defined criteria in Figure 2; 2. different markers to describe the amount of change; † Information derived from figures using Engauge Digitizer; *Folds calculated by measuring the graphs, without using the Engauge Digitizer; No makers: Information derived from figures by description in the articles

Reference	Gene/ Analyte[a]	Official gene symbol / abbreviation[b]	Cell (age/gender of donors, tooth type, isolation method, passages used, cell density)[a,c]	Force type (stat./ dyn.)[a]	Force duration and frequency[d]	Force magnitude[a]	Force apparatus[a]	Force type: equibiaxial or uniaxial[e]	Gene expression: Increase, decrease, no change (method w/ reference gene); Methods: qPCR, sqPCR, Northern blot[f]	Gene expression: When it reaches peak and peak's magnitude (fold change; times or ratio; unclear = ?)[f]	Protein expression: Increase, decrease, no change (method w/ reference); Methods: ELISA, WB, RIA, EMSA, IF[f]	Protein expression: When it reaches peak and peak's magnitude (times or ratio; unclear = ?)[f]
Liu et al. (2017)	TNF-α	*TNF*	hPDLSCs cells (37.9±7.2/n.g., PM and M, dig, P3, 95% confluence) from healthy (HPDLSCs) and patients w/ periodontitis (PPDLSCs: 38.9 ± 7.9/n.g., n.g., dig, P3, 95% confluence)	dynamic	0.1Hz for 12h	6%, 8%, 10%, 12%, 14%	Flexcell FX-4000T + 6-well Bioflex plates + vacuum	equibiaxial	n.g.	n.g.	HPDLSCs: increase followed by plateau (ELISA)	HPDLSCs @ 6%...14%: 18.6 (pg/10^6 cells)* / 1.2 (ratio)*
Long et al. (2001)	IL-10	*IL10*	hPDL cells ($) (18/F, 16/F, 22/M, 16/M, M, n.g., P6-20, 5×10^5)	dynamic	0.005Hz sqPCR for 4h, 24h, 48h; ELISA for 24h, 48h	6%	Flexercell unit + pronectin-coated six-well Flexercell plates + vacuum (Gassner et al 1999)	equibiaxial	increase (sqPCR, GAPDH)	24h: 781.3 (rel)* / not detectable in the control	increase (ELISA)	48h: 62.2 (pg/ml)* / control not detectable
Long et al. (2001)	IL-1β	*IL1B*	hPDL cells ($) (18/F, 16/F, 22/M, 16/M, M, n.g., P6-20, 5×10^5)	dynamic	0.005Hz for 24h	sqPCR: 3%, 6%, 10%, 15%; ELISA: 6%, 10%, 15%	Flexercell unit + pronectin-coated six-well Flexercell plates + vacuum (Gassner et al 1999)	equibiaxial	decrease followed by plateau then increase (sqPCR, GAPDH)	lowest @ 6%…10%: 11.4 (rel) / 0.1 (ratio-calc) highest @15%: 152.3 (rel) / 1.5 (ratio-calc)	increase (ELISA)	15%: 85.7 (pg/ml)* / control n.g
Long et al. (2001)	IL-1β	*IL1B*	hPDL cells ($) (18/F, 16/F, 22/M, 16/M, M, n.g., P6-20, 5×10^5)	dynamic	0.005Hz sqPCR for 4h, 24h, 48h; ELISA for 24h, 48h	6%	Flexercell unit + pronectin-coated six-well Flexercell plates + vacuum (Gassner et al 1999)	equibiaxial	no expression (sqPCR, GAPDH)	no quantitative information is given	no expression (ELISA)	no quantitative information is given
Long et al. (2001)	IL-6	*IL6*	hPDL cells ($) (18/F, 16/F, 22/M, 16/M, M, n.g., P6-20, 5×10^5)	dynamic	0.005Hz sqPCR for 4h, 24h, 48h; ELISA for 24h, 48h	6%	Flexercell unit + pronectin-coated six-well Flexercell plates + vacuum (Gassner et al 1999)	equibiaxial	no expression (sqPCR, GAPDH)	no quantitative information is given	no expression (ELISA)	no quantitative information is given
Long et al. (2001)	IL-8	*CXCL8*	hPDL cells ($) (18/F, 16/F, 22/M, 16/M, M, n.g., P6-20, 5×10^5)	dynamic	0.005Hz sqPCR for 4h, 24h, 48h; ELISA for 24h, 48h	6%	Flexercell unit + pronectin-coated six-well Flexercell plates + vacuum (Gassner et al 1999)	equibiaxial	no expression (sqPCR, GAPDH)	no quantitative information is given	no expression (ELISA)	no quantitative information is given
Long et al. (2001)	TNF-α	*TNF*	hPDL cells ($) (18/F, 16/F, 22/M, 16/M, M, n.g., P6-20, 5×10^5)	dynamic	0.005Hz sqPCR for 4h, 24h, 48h; ELISA for 24h, 48h	6%	Flexercell unit + pronectin-coated six-well Flexercell plates + vacuum (Gassner et al 1999)	equibiaxial	no expression (sqPCR, GAPDH)	no quantitative information is given	n.g.	n.g.
Long et al. (2002)	COX-2	*PTGS2*	hPDL cells (18/F, 16/F, 18/M, 16/M, M, exp, P3-6, Confluent)	dynamic	0.005Hz for 4h, 24h, 48h	6%	Flexercell unit + collagen type 1-coated Bioflex II plates + vacuum	equibiaxial	decrease (sqPCR, GAPDH)	no quantitative information is given	n.g.	n.g.
Long et al. (2002)	iNOS	*NOS2*	hPDL cells (18/F, 16/F, 18/M, 16/M, M, exp, P3-6, Confluent)	dynamic	0.005Hz for 4h, 24h, 48h	6%	Flexercell unit + collagen type 1-coated Bioflex II plates + vacuum	equibiaxial	no change (sqPCR, GAPDH)	no quantitative information is given	n.g.	n.g.
Long et al. (2002)	MMP-1	*MMP1*	hPDL cells (18/F, 16/F, 18/M, 16/M, M, exp, P3-6, Confluent)	dynamic	0.005Hz for 4h, 24h, 48h	6%	Flexercell unit + collagen type 1-coated Bioflex II plates + vacuum	equibiaxial	no change (sqPCR, GAPDH)	no quantitative information is given	no expression (WB)	
Long et al. (2002)	MMP-3	*MMP3*	hPDL cells (18/F, 16/F, 18/M, 16/M, M, exp, P3-6, Confluent)	dynamic	0.005Hz for 4h, 24h, 48h	6%	Flexercell unit + collagen type 1-coated Bioflex II plates + vacuum	equibiaxial	no change (sqPCR, GAPDH)	no quantitative information is given	no expression (WB)	
Long et al. (2002)	PGE_2	PGE_2	hPDL cells (18/F, 16/F, 18/M, 16/M, M, exp, P3-6, Confluent)	dynamic	0.005Hz for 24h	1.8%, 3%, 6%, 10%, 12.5%	Flexercell unit + collagen type 1-coated Bioflex II plates + vacuum	equibiaxial	n.a.	n.a.	1.8%, 3%, 6%: no expression (RIA) 10%, 12.5%: increase (RIA)	12.5%: 102.8 (ng /10^6 cells) / control: no PGE_2 detectable
Long et al. (2002)	TIMP-II	*TIMP2*	hPDL cells (18/F, 16/F, 18/M, 16/M, M, exp, P3-6, Confluent)	dynamic	0.005Hz sqPCR for 4h, 24h; WB for 24h, 48h	6%	Flexercell unit + collagen type 1-coated Bioflex II plates + vacuum	equibiaxial	no change (sqPCR, GAPDH)	no quantitative information is given	no change (WB)	
Ma et al. (2015)	ARRAY	ARRAY	hPDL cells (11/F, PM, exp, P4-6, confluence)	dynamic	**0.1Hz** (6cyc/min: 5s stretch followed by 5s relaxation) for 6h, 24h	10%	Cell Strain Unit (CSU + flexible-bottomed culture dish made of elastic silicon rubber (Q7-4750, Dow Corning Co., Midland, MI, USA) + spherical cap	equibiaxial	Human Extracellular Matrix & Adhesion Molecules RT2 Profiler PCR Array (PAHS-013, SABiosciences)			
Ma et al. (2015)	Integrin α 5	*ITGAV*	hPDL cells (11/F, PM, exp, P4-6, confluence)	dynamic	**0.1Hz** (6cyc/min: 5s stretch followed by 5s relaxation) for 6h, 24h	10%	Cell Strain Unit (CSU + flexible-bottomed culture dish made of elastic silicon rubber (Q7-4750, Dow Corning Co., Midland, MI, USA) + spherical cap	equibiaxial	n.g.	n.g.	increase (WB, GAPDH)	24h: 1.1 (rel)* / 1.3 (ratio-calc)
Matsuda et al. (1998a)	ERK1/2 / p-ERK(Tyr204)	MAPK3; MAPK1	hPDL cells (n.g./n.g., n.g., exp, P3-5, confluence)	dynamic	**0.1Hz** (6cyc/min: strain for 5s and then 5s relaxation) for 15min, 30min, 60min	9%	Flexercell Strain Unit Model FX-2000 (Banes et al 1985) + flexible substratum (25 mm dia., Flex I culture plate) + vacuum	equibiaxial	n.g.	n.g.	no change (WB)	no quantitative information is given
Matsuda et al. (1998a)	JNK / p-JNK(Thr183/Tyr185)	*MAPK8*	hPDL cells (n.g./n.g., n.g., exp, P3-5, confluence)	dynamic	**0.1Hz** (6cyc/min: strain for 5s and then 5s relaxation) for 15min, 30min, 60min	9%	Flexercell Strain Unit Model FX-2000 (Banes et al 1985) + flexible substratum (25 mm dia., Flex I culture plate) + vacuum	equibiaxial	n.g.	n.g.	increase (WB)	no quantitative information is given

[a] Entry given as reported in the study.
[b] All official gene symbols come from the HUGO Gene Nomenclature Committee (HGNC; URL: https://www.genenames.org) after checking specificity of primers with Primer-BLAST.
[c] Gender/Sex of donors: "M" – male, "F" – female; Tooth type: "PM" – premolar, "M" – molar; Cell density: given in cells/well if not otherwise mentioned.
[d] Frequencies labeled bold orange were converted to hertz (Hz) according to its definition using the information reported in the study (in brackets)
[e] Force type deduced from the description of the force apparatus given by the authors.
[f] Gene and protein expression: 1. conclusion of change (increase, decrease…) was given according to the defined criteria in Figure 2; 2. different markers to describe the amount of change; † Information derived from figures using Engauge Digitizer; *Folds calculated by measuring the graphs, without using the Engauge Digitizer; No makers: Information derived from figures by description in the articles

Reference	Gene/ Analyte[a]	Official gene symbol / abbreviation[b]	Cell (age/gender of donors, tooth type, isolation method, passages used, cell density)[a,c]	Force type (stat./ dyn.)[a]	Force duration and frequency[d]	Force magnitude[a]	Force apparatus[a]	Force type: equibiaxial or uniaxial[e]	Gene expression: Increase, decrease, no change (method w/ reference gene); Methods: qPCR, sqPCR, Northern blot[f]	Gene expression: When it reaches peak and peak's magnitude (fold change; times or ratio; unclear = ?)[f]	Protein expression: Increase, decrease, no change (method w/ reference); Methods: ELISA, WB, RIA, EMSA, IF[f]	Protein expression: When it reaches peak and peak's magnitude (times or ratio; unclear = ?)[f]
Matsuda et al. (1998a)	p38 / p-p38(Thr180/Tyr182)	*MAPK14*	hPDL cells (n.g./n.g., n.g., exp, P3-5, confluence)	dynamic	**0.1Hz** (6cyc/min: strain for 5s and then 5s relaxation) for 15min, 30min, 60min	9%	Flexercell Strain Unit Model FX-2000 (Banes et al 1985) + flexible substratum (25 mm dia., Flex I culture plate) + vacuum	equibiaxial	n.g.	n.g.	no change (WB)	no quantitative information is given
Matsuda et al. (1998b)	ALP	*ALPP*	hPDL cells (n.g./n.g., M, exp, P3-7, n.g.)	dynamic	**0.1Hz** (6cyc/min: strain for 5s followed by 5s relaxation) for 2d, 4d, 6d	9%,18%	Flexercell Strain Unit Model FX-2000 (Banes et al 1985) + flexible substratum (25 mm dia., Flex I culture plate) + vacuum	equibiaxial	n.g.	n.g.	9%: increase (ALP activity) 18%: increase (ALP activity)	9% @ 6d: 257.7 (U/mg protein)* / 1.4 (ratio-calc) 18% @ 4…6d: 230.8 (U/mg protein)* / 1.3 (ratio-calc)
Matsuda et al. (1998b)	EGF-R	*EGFR*	hPDL cells (n.g./n.g., M, exp, P3-7, n.g.)	dynamic	**0.1Hz** (6cyc/min: strain for 5s followed by 5s relaxation) for 4d	9%	Flexercell Strain Unit Model FX-2000 (Banes et al 1985) + flexible substratum (25 mm dia., Flex I culture plate) + vacuum	equibiaxial	n.g.	n.g.	decrease (WB)	0.4 (ratio)
Memmert et al. (2019)	ARRAY	ARRAY	hPDLCs (11-19/n.g., n.g., exp, P3-5, 80% confluence)	static	24h	3%, 20%	CESTRA cell strain device + BioFlex-II-culture plates + stepping motor (Deschner et al. 2012)	equibiaxial	PrimePCR™ Assay (Autophagy (SAB Target List) H96, Bio-Rad Laboratories, Munich, Germany)		n.g.	n.g.
Memmert et al. (2019)	ATG10	*ATG10*	hPDLCs (11-19/n.g., n.g., exp, P3-5, 80% confluence)	static	4h, 24h	3%, 20%	CESTRA cell strain device + BioFlex-II-culture plates + stepping motor (Deschner et al. 2012)	equibiaxial	3%: temporary decrease (qPCR, GAPDH) 20%: decrease (qPCR, GAPDH)	3% @ 4h: 0.9 (FC)† 20% @ 24h: 0.3 (FC)†	n.g.	n.g.
Memmert et al. (2019)	ATG4C	*ATG4C*	hPDLCs (11-19/n.g., n.g., exp, P3-5, 80% confluence)	static	4h, 24h	3%, 20%	CESTRA cell strain device + BioFlex-II-culture plates + stepping motor (Deschner et al. 2012)	equibiaxial	3%: no change (qPCR, GAPDH) 20%: decrease (qPCR, GAPDH)	20% @ 24h: 0.4 (FC)†	n.g.	n.g.
Memmert et al. (2019)	ATG7	*ATG7*	hPDLCs (11-19/n.g., n.g., exp, P3-5, 80% confluence)	static	4h, 24h	3%, 20%	CESTRA cell strain device + BioFlex-II-culture plates + stepping motor (Deschner et al. 2012)	equibiaxial	3%: temporary decrease (qPCR, GAPDH) 20%: decrease (qPCR, GAPDH)	3% @ 4h: 0.8 (FC)† 20% @ 24h: 0.4 (FC)†	n.g.	n.g.
Memmert et al. (2019)	BCL2	*BCL2*	hPDLCs (11-19/n.g., n.g., exp, P3-5, 80% confluence)	static	4h, 24h	3%, 20%	CESTRA cell strain device + BioFlex-II-culture plates + stepping motor (Deschner et al. 2012)	equibiaxial	3%: temporary decrease (qPCR, GAPDH) 20%: decrease (qPCR, GAPDH)	3% @ 4h: 0.7 (FC)† 20% @ 24h: 0.7 (FC)†	n.g.	n.g.
Memmert et al. (2019)	BID	*BID*	hPDLCs (11-19/n.g., n.g., exp, P3-5, 80% confluence)	static	4h, 24h	3%, 20%	CESTRA cell strain device + BioFlex-II-culture plates + stepping motor (Deschner et al. 2012)	equibiaxial	3%: decrease followed by increase (qPCR, GAPDH) 20%: no change (qPCR, GAPDH)	3% lowest @ 4h: 0.9 (FC)† 3% highest @ 24h: 1.9 (FC)†	n.g.	n.g.
Memmert et al. (2019)	DAPK1	*DAPK1*	hPDLCs (11-19/n.g., n.g., exp, P3-5, 80% confluence)	static	4h, 24h	3%, 20%	CESTRA cell strain device + BioFlex-II-culture plates + stepping motor (Deschner et al. 2012)	equibiaxial	3%: decrease (qPCR, GAPDH) 20%: decrease (qPCR, GAPDH)	3% @ 24h: 0.7 (FC)† 20% @ 24h: 0.3 (FC)†	n.g.	n.g.
Memmert et al. (2019)	LC3-I	*Map1lc3a*	hPDLCs (11-19/n.g., n.g., exp, P3-5, 80% confluence)	static	4h	20%	CESTRA cell strain device + BioFlex-II-culture plates + stepping motor (Deschner et al. 2012)	equibiaxial	n.g.	n.g.	increase (WB, GAPDH)	no quantitative information is given
Memmert et al. (2019)	LC3-II	*Map1lc3a*	hPDLCs (11-19/n.g., n.g., exp, P3-5, 80% confluence)	static	4h	20%	CESTRA cell strain device + BioFlex-II-culture plates + stepping motor (Deschner et al. 2012)	equibiaxial	n.g.	n.g.	increase (WB, GAPDH)	1.4 (ratio)†
Memmert et al. (2019)	PIK3CG	*PIK3CG*	hPDLCs (11-19/n.g., n.g., exp, P3-5, 80% confluence)	static	4h, 24h	3%, 20%	CESTRA cell strain device + BioFlex-II-culture plates + stepping motor (Deschner et al. 2012)	equibiaxial	3%: no change (qPCR, GAPDH) 20%: no change (qPCR, GAPDH)		n.g.	n.g.
Memmert et al. (2019)	SNCA	*SNCA*	hPDLCs (11-19/n.g., n.g., exp, P3-5, 80% confluence)	static	4h, 24h	3%, 20%	CESTRA cell strain device + BioFlex-II-culture plates + stepping motor (Deschner et al. 2012)	equibiaxial	3%: increase (qPCR, GAPDH) 20%: decrease (qPCR, GAPDH)	3% @ 24h: 1.2 (FC)† 20% @ 24h: 0.3 (FC)†	n.g.	n.g.
Memmert et al. (2019)	TP53	*TP53*	hPDLCs (11-19/n.g., n.g., exp, P3-5, 80% confluence)	static	4h, 24h	3%, 20%	CESTRA cell strain device + BioFlex-II-culture plates + stepping motor (Deschner et al. 2012)	equibiaxial	3%: increase (qPCR, GAPDH) 20%: temporary increase (qPCR, GAPDH)	3% @ 4h: 2.1 (FC)† 20% @ 4h: 4.2 (FC)†	n.g.	n.g.
Memmert et al. (2019)	UVRAG	*UVRAG*	hPDLCs (11-19/n.g., n.g., exp, P3-5, 80% confluence)	static	4h, 24h	3%, 20%	CESTRA cell strain device + BioFlex-II-culture plates + stepping motor (Deschner et al. 2012)	equibiaxial	3%: temporary decrease (qPCR, GAPDH) 20%: decrease (qPCR, GAPDH)	3% @ 4h: 0.7(FC)† 20% @ 24h: 0.5 (FC)†	n.g.	n.g.
Memmert et al. (2020)	ARRAY	ARRAY	hPDLFs (11-19/n.g., n.g., exp, P3-5, 80% confluency)	dynamic	0.1Hz for 24h	3%	CESTRA cell strain device + 6-well BioFlex plates coated with collagen type I + stepping motor	equibiaxial	PrimePCR assay (Autophagy [SAB Target List] H96,Bio-Rad Laboratories, Munich, Germany)		n.g.	n.g.
Memmert et al. (2020)	SQSTM1	*SQSTM1*	hPDLFs (11-19/n.g., n.g., exp, P3-5, 80% confluency)	static	qPCR for 8h, 16h, 24h; WB for 1h	3%	CESTRA cell strain device + 6-well BioFlex plates coated with collagen type I + stepping motor	equibiaxial	increase (qPCR, GAPDH)	16h: 1.5 (FC)†	no change (WB, GAPDH)	
Memmert et al. (2020)	SQSTM1	*SQSTM1*	hPDLFs (11-19/n.g., n.g., exp, P3-5, 80% confluency)	static	qPCR for 8h, 16h, 24h; WB for 1h	20%	CESTRA cell strain device + 6-well BioFlex plates coated with collagen type I + stepping motor	equibiaxial	decrease followed by increase (qPCR, GAPDH)	lowest @ 8h: 0.6 (FC)† highest @ 16h: 1.8 (FC)†	increase (WB, GAPDH)	1.7 (ratio)†
Memmert et al. (2020)	SQSTM1	*SQSTM1*	hPDLFs (11-19/n.g., n.g., exp, P3-5, 80% confluency)	dynamic	0.1Hz qPCR for 8h, 16h, 24h; WB for 1h	3%	CESTRA cell strain device + 6-well BioFlex plates coated with collagen type I + stepping motor	equibiaxial	increase (qPCR, GAPDH)	24h: 3.2 (FC)†	increase (WB, GAPDH)	3.2 (ratio)†
Meng et al. (2010)	α-SMA	*ACTA2*	hPDL cells (12-17/n.g., n.g., exp, P3-4, 80% confluence)	dynamic	0.5 Hz for 1h, 3h, 6h, 12h	**0.4%** (4000μstrain)	"a uniaxial four point bending system" (Yu 2009; Sichuan University, patents CN2534576 and CN1425905) consists of a digital control part, an actuator, and cell culture plates)	uniaxial	increase (sqPCR, GAPDH)	12h: 8.4 (ratio)*	increase (WB, GAPDH)	12h: 2 (rel)* / 9.8 (ratio-calc)

[a] Entry given as reported in the study.
[b] All official gene symbols come from the HUGO Gene Nomenclature Committee (HGNC; URL: https://www.genenames.org) after checking specificity of primers with Primer-BLAST.
[c] Gender/Sex of donors: "M" – male, "F" – female; Tooth type: "PM" – premolar, "M" – molar; Cell density: given in cells/well if not otherwise mentioned.
[d] Frequencies labeled bold orange were converted to hertz (Hz) according to its definition using the information reported in the study (in brackets)
[e] Force type deduced from the description of the force apparatus given by the authors.
[f] Gene and protein expression: 1. conclusion of change (increase, decrease…) was given according to the defined criteria in Figure 2; 2. different markers to describe the amount of change; † Information derived from figures using Engauge Digitizer; *Folds calculated by measuring the graphs, without using the Engauge Digitizer; No makers: Information derived from figures by description in the articles

Reference	Gene/ Analyte[a]	Official gene symbol / abbreviation[b]	Cell (age/gender of donors, tooth type, isolation method, passages used, cell density)[a,c]	Force type (stat./ dyn.)[a]	Force duration and frequency[d]	Force magnitude[a]	Force apparatus[a]	Force type: equibiaxial or uniaxial[e]	Gene expression: Increase, decrease, no change (method w/ reference gene); Methods: qPCR, sqPCR, Northern blot[f]	Gene expression: When it reaches peak and peak's magnitude (fold change; times or ratio; unclear = ?)[f]	Protein expression: Increase, decrease, no change (method w/ reference); Methods: ELISA, WB, RIA, EMSA, IF[f]	Protein expression: When it reaches peak and peak's magnitude (times or ratio; unclear = ?)[f]
Miura et al. (2000)	PA	*PLAT; PLAU*	hPDL cells (12/M, 10/M, 11/F, exp, PM, P5-7 and P19-22, confluent)	dynamic	**0.1Hz** (6cyc/min: 5s elongation and 5s relaxation) for 5d	9%, 18%	Flexercell strain unit + culture plates coated with type I collagen (Flexcell)	equibiaxial	n.g.	n.g.	9%: increase (PA activity, chromogenic substrate assay) 15%: increase (PA activity, chromogenic substrate assay)	"young cells" (P5-7) @ 9%: 5.9 (mU/10^{5}cells)* / 1.6 (ratio-calc) "old cells" (P19-22) @ 9%: 8.2 (mU/10^{5}cells)* / 2.2 (ratio-calc) "young cells" (P5-7) @ 15%: 8 (mU/10^{5}cells)* / 2.2 (ratio-calc) "old cells" (P19-22) @ 15%:10.9 (mU/10^{5}cells)* / 2.9 (ratio-calc)
Miura et al. (2000)	PA	*PLAT; PLAU*	hPDL cells (12/M, 10/M, 11/F, exp, PM, P5-7 and P19-22, confluent)	dynamic	**0.1Hz** (6cyc/min: 5s elongation and 5s relaxation) for 1d, 3d, 5d	18%	Flexercell strain unit + culture plates coated with type I collagen (Flexcell)	equibiaxial	n.g.	n.g.	"young cells" (P5-7): increase (PA activity, chromogenic substrate assay) "old cells" (P19-22): increase (PA activity, chromogenic substrate assay)	"young cells" @ 5d: 7.8 (mU/10^{5}cells)* / 2.1 (ratio-calc) "old cells" @ 5d: 11.8 (mU/10^{5}cells)* / 3 (ratio-calc)
Miura et al. (2000)	PA	*PLAT; PLAU*	hPDL cells (12/M, 10/M, 11/F, exp, PM, P5-7 and P19-22, confluent)	dynamic	**0.1Hz** (6cyc/min: 5s elongation and 5s relaxation) for duration n.g.	18%	Flexercell strain unit + culture plates coated with type I collagen (Flexcell)	equibiaxial	n.g.	n.g.	"young cells" (P5-7): increase (PA activity, chromogenic substrate assay) "old cells" (P19-22): increase (PA activity, chromogenic substrate assay)	Donor 1, "young cells" : 7.9 (mU/10^{5}cells)† / 2.2 (ratio-calc) Donor 1, "old cells" : 11.5 (mU/10^{5}cells)† / 3.1 (ratio-calc) Donor 1, "young cells" : 2.5 (U/mg protein)† / 1.8 (ratio-calc) Donor 1, "old cells" : 3.0 (U/mg protein)† / 2.2 (ratio-calc) Donor 2, "young cells": 7.6 (mU/10^{5}cells)† / 2.3 (ratio-calc) Donor 2, "old cells" : 12.3 (mU/10^{5}cells)† / 3.4 (ratio-calc) Donor 2, "young cells" : 2.4 (U/mg protein)† / 1.6 (ratio-calc) Donor 2, "old cells" : 2.9 (U/mg protein)† / 2.1 (ratio-calc) Donor 3, "young cells" : 7.2 (mU/10^{5}cells)† / 2.4 (ratio-calc) Donor 3, "old cells" : 12.6 (mU/10^{5}cells)† / 3.9 (ratio-calc) Donor 3, "young cells" : 2.5 (U/mg protein)† / 1.6 (ratio-calc) Donor 3, "old cells" : 2.9 (U/mg protein)† / 2.1 (ratio-calc)
Miura et al. (2000)	PAI-1	*SERPINE1*	hPDL cells (12/M, 10/M, 11/F, exp, PM, P5-7 and P19-22, confluent)	dynamic	**0.1Hz** (6cyc/min: 5s elongation and 5s relaxation) for duration n.g.	18%	Flexercell strain unit + culture plates coated with type I collagen (Flexcell)	equibiaxial	"young cells" (P5-7): no change (sqPCR, GAPDH) "old cells" (P19-22): no change (sqPCR, GAPDH)	no quantitative information is given	n.g.	n.g.
Miura et al. (2000)	tPA	*PLAT*	hPDL cells (12/M, 10/M, 11/F, exp, PM, P5-7 and P19-22, confluent)	dynamic	**0.1Hz** (6cyc/min: 5s elongation and 5s relaxation) for duration n.g.	18%	Flexercell strain unit + culture plates coated with type I collagen (Flexcell)	equibiaxial	"young cells" (P5-7): increase (sqPCR, GAPDH) "old cells" (P19-22): increase (sqPCR, GAPDH)	no quantitative information is given	"young cells": increase (WB) "old cells": increase (WB)	no quantitative information is given
Miura et al. (2000)	uPA	*PLAU*	hPDL cells (12/M, 10/M, 11/F, exp, PM, P5-7 and P19-22, confluent)	dynamic	**0.1Hz** (6cyc/min: 5s elongation and 5s relaxation) for duration n.g.	18%	Flexercell strain unit + culture plates coated with type I collagen (Flexcell)	equibiaxial	"young cells" (P5-7): no expression (sqPCR, GAPDH) "old cells" (P19-22): no expression (sqPCR, GAPDH)	no quantitative information is given	"young cells": no expression (WB) "old cells": no expression (WB)	no quantitative information is given
Molina et al. (2001)	Focal Adhesion Kinase 1 (p125^{FAK}) / p-FAK	*PTK2*	hPDL cells (12-14/n.g., PM, exp, P3-6, confluence)	static	15min, 30min, 45min, 1h, 24h, 48h, 72h	2.5%	Petriperm dishes stretched by being placed on top of a spheroidal convex template (Saito et al1991) + weight	equibiaxial	n.g.	n.g.	p-FAK: increase followed by plateau then decrease (WB, FAK total)	p-FAK: highest @ 45…60min: 7.1% (rel)* / 2.3 (ratio-calc) p-FAK: lowest @ 72min: 2% (rel)* / 0.6 (ratio-calc)
Monnouchi et al. (2011)	ACE	*ACE*	hPDL cells (30/F, 39/F, 26/m, M, dig, P5-6, Sub-confluence)	dynamic	**1Hz** (0.5s stretch and 0.5s relaxation per cycle) for 1h	8%, 12%	STB-140 (STREX Co) + culture chambers coated with type I collagen (Cell matrix I-P; Nitta Gelatin Inc., Osaka, Japan)	uniaxial	increase (sqPCR, GAPDH)	8%: 6.1 (FC)*	n.g.	n.g.
Monnouchi et al. (2011)	AGT	*AGT*	hPDL cells (30/F, 39/F, 26/m, M, dig, P5-6, Sub-confluence)	dynamic	**1Hz** (0.5s stretch and 0.5s relaxation per cycle) for 1h	8%	STB-140 (STREX Co) + culture chambers coated with type I collagen (Cell matrix I-P; Nitta Gelatin Inc., Osaka, Japan)	uniaxial	increase (qPCR, β-actin)	HPLF-2E: 1.8 (FC)* HPLF-2D: 2.3 (FC)* HPLF-3M: 1.6 (FC)*	n.g.	n.g.
Monnouchi et al. (2011)	ALP	*ALPP*	hPDL cells (30/F, 39/F, 26/m, M, dig, P5-6, Sub-confluence)	dynamic	**1Hz** (0.5s stretch and 0.5s relaxation per cycle) for 1h	8%	STB-140 (STREX Co) + culture chambers coated with type I collagen (Cell matrix I-P; Nitta Gelatin Inc., Osaka, Japan)	uniaxial	increase (qPCR, β-actin)	HPLF-2E: 2.3 (FC)* HPLF-2D: 2.1 (FC)* HPLF-3M: 2.9 (FC)*	n.g.	n.g.
Monnouchi et al. (2011)	AT1	*AGTR1*	hPDL cells (30/F, 39/F, 26/m, M, dig, P5-6, Sub-confluence)	dynamic	**1Hz** (0.5s stretch and 0.5s relaxation per cycle) for 1h	8%	STB-140 (STREX Co) + culture chambers coated with type I collagen (Cell matrix I-P; Nitta Gelatin Inc., Osaka, Japan)	uniaxial	increase (sqPCR, GAPDH)	HPLF-2E: no quantitative information is given HPLF-2D: no quantitative information is given	increase (WB, β-actin)	HPLF-3M: no quantitative information is given

[a] Entry given as reported in the study.
[b] All official gene symbols come from the HUGO Gene Nomenclature Committee (HGNC; URL: https://www.genenames.org) after checking specificity of primers with Primer-BLAST.
[c] Gender/Sex of donors: "M" – male, "F" – female; Tooth type: "PM" – premolar, "M" – molar; Cell density: given in cells/well if not otherwise mentioned.
[d] Frequencies labeled bold orange were converted to hertz (Hz) according to its definition using the information reported in the study (in brackets)
[e] Force type deduced from the description of the force apparatus given by the authors.
[f] Gene and protein expression: 1. conclusion of change (increase, decrease…) was given according to the defined criteria in Figure 2; 2. different markers to describe the amount of change; † Information derived from figures using Engauge Digitizer; *Folds calculated by measuring the graphs, without using the Engauge Digitizer; No makers: Information derived from figures by description in the articles

Reference	Gene/ Analyte[a]	Official gene symbol / abbreviation[b]	Cell (age/gender of donors, tooth type, isolation method, passages used, cell density)[a,c]	Force type (stat./ dyn.)[a]	Force duration and frequency[d]	Force magnitude[a]	Force apparatus[a]	Force type: equibiaxial or uniaxial[e]	Gene expression: Increase, decrease, no change (method w/ reference gene); Methods: qPCR, sqPCR, Northern blot[f]	Gene expression: When it reaches peak and peak's magnitude (fold change; times or ratio; unclear = ?)[f]	Protein expression: Increase, decrease, no change (method w/ reference); Methods: ELISA, WB, RIA, EMSA, IF[f]	Protein expression: When it reaches peak and peak's magnitude (times or ratio; unclear = ?)[f]
Monnouchi et al. (2011)	AT2	*AGTR2*	hPDL cells (30/F, 39/F, 26/m, M, dig, P5-6, Sub-confluence)	dynamic	**1Hz** (0.5s stretch and 0.5s relaxation per cycle) for 1h	8%	STB-140 (STREX Co) + culture chambers coated with type I collagen (Cell matrix I-P; Nitta Gelatin Inc., Osaka, Japan)	uniaxial	no change (sqPCR, GAPDH)	HPLF-2E: no quantitative information is given HPLF-2D: no quantitative information is given	no change (WB, β-actin)	HPLF-3M: no quantitative information is given
Monnouchi et al. (2011)	OPG	*TNFRSF11B*	hPDL cells (30/F, 39/F, 26/m, M, dig, P5-6, Sub-confluence)	dynamic	**1Hz** (0.5s stretch and 0.5s relaxation per cycle) for 1h	8%, 12%	STB-140 (STREX Co) + culture chambers coated with type I collagen (Cell matrix I-P; Nitta Gelatin Inc., Osaka, Japan)	uniaxial	increase (sqPCR, GAPDH)	HPDLF-2E: 12%: 2.2 (FC)*	n.g.	n.g.
Monnouchi et al. (2011)	RANKL	*TNFSF11*	hPDL cells (30/F, 39/F, 26/m, M, dig, P5-6, Sub-confluence)	dynamic	**1Hz** (0.5s stretch and 0.5s relaxation per cycle) for 1h	8%, 12%	STB-140 (STREX Co) + culture chambers coated with type I collagen (Cell matrix I-P; Nitta Gelatin Inc., Osaka, Japan)	uniaxial	decrease followed by inccrease (sqPCR, GAPDH)	HPDLF-2E: lowest @ 8%: 0.5 (FC)* HPDLF-2E: highest @ 12%: 1.3 (FC)*	n.g.	n.g.
Monnouchi et al. (2011)	Renin	*REN*	hPDL cells (30/F, 39/F, 26/m, M, dig, P5-6, Sub-confluence)	dynamic	**1Hz** (0.5s stretch and 0.5s relaxation per cycle) for 1h	8%, 12%	STB-140 (STREX Co) + culture chambers coated with type I collagen (Cell matrix I-P; Nitta Gelatin Inc., Osaka, Japan)	uniaxial	increase (sqPCR, GAPDH)	8%: 2.4 (FC)*	n.g.	n.g.
Monnouchi et al. (2011)	TGF-β1	*TGFB1*	hPDL cells (30/F, 39/F, 26/m, M, dig, P5-6, Sub-confluence)	dynamic	**1Hz** (0.5s stretch and 0.5s relaxation per cycle) for 1h	8%	STB-140 (STREX Co) + culture chambers coated with type I collagen (Cell matrix I-P; Nitta Gelatin Inc., Osaka, Japan)	uniaxial	increase (qPCR, β-actin)	HPLF-2E: 2.6 (FC)* HPLF-2D: 1.7 (FC)* HPLF-3M: 2.1 (FC)*	n.g.	n.g.
Monnouchi et al. (2015)	IL-11	*IL11*	hPDL cells (30/F, 39/F, 26/M, M, exp, P5-7, 2×10^4/cm^2)	dynamic	**1Hz** (0.5s stretch and 0.5s relaxation per cycle) for 1h	8%	STB-140 (STREX Co) + culture chambers coated with type I collagen (Cell matrix I-P; Nitta Gelatin Inc., Osaka, Japan) (Monnouchi 2011)	uniaxial	increase (qPCR, β-actin)	HPDLC-2D: 2.6 (FC)* HPDLC-2E: 5.5 (FC)* HPDLC-3M: 3.5 (FC)*	increase (ELISA)	HPDLC-2D: 124.0 (pg/ml)* / 4 (ratio-calc) HPDLC-2E: 88.0 (pg/ml)* / 2.8 (ratio-calc) HPDLC-3M: 217.0 (pg/ml)* / 2.3 (ratio-calc)
Nakashima et al. (2009)	Fibulin-5	*FBLN5*	hPDL cells (n.g./n.g., M, exp, P6, Confluent)	dynamic	**0.01Hz** (1/60Hz) for 7d	5%	STB-140 STREX cell stretch system (Strex Co) + elastic silicone chamber	uniaxial	increase (Northern blot, β-actin)	1.5 (ratio)	increase (WB, β-actin)	1.9 (ratio)
Narimiya et al. (2017)	MMP-12	*MMP12*	Human immortalized PDLCs (n.g./n.g., n.g., gene transfection, n.g., 4×10^5)	static	qPCR for 6h, 12h, 24h; ELISA for 24h WB for 24h	15%	Cell Extender version3 (MOLCURE, Tokyo, Japan) + Bioflex® plates (Flexcell) + actuator (Wada 2017)	equibiaxial	increase (qPCR, GAPDH)	24h: 10.5 (FC)*	increase (ELISA) increase (WB)	ELISA: 420 (pg/ml)* / 1.5 (ratio-calc) WB: no quantitative information given
Narimiya et al. (2017)	TIMP-1	*TIMP1*	Human immortalized PDLCs (n.g./n.g., n.g., gene transfection, n.g., 4×10^5)	static	24h	15%	Cell Extender version3 (MOLCURE, Tokyo, Japan) + Bioflex® plates (Flexcell) + actuator (Wada 2017)	equibiaxial	no change (qPCR, GAPDH)		n.g.	n.g.
Narimiya et al. (2017)	TIMP-2	*TIMP2*	Human immortalized PDLCs (n.g./n.g., n.g., gene transfection, n.g., 4×10^5)	static	24h	15%	Cell Extender version3 (MOLCURE, Tokyo, Japan) + Bioflex® plates (Flexcell) + actuator (Wada 2017)	equibiaxial	no change (qPCR, GAPDH)		n.g.	n.g.
Narimiya et al. (2017)	TIMP-3	*TIMP3*	Human immortalized PDLCs (n.g./n.g., n.g., gene transfection, n.g., 4×10^5)	static	24h	15%	Cell Extender version3 (MOLCURE, Tokyo, Japan) + Bioflex® plates (Flexcell) + actuator (Wada 2017)	equibiaxial	no change (qPCR, GAPDH)		n.g.	n.g.
Nazet et al. (2020)	ALP	*ALPP*	hPDLF (17-27/F, 17-27/M, M, n.g., P3-6, 7×10^4)	static	24h, 48h, 72h	35%	six-well bioflex membrane plates coated with collagen I + custom-made spherical cap silicone stamps	equibiaxial	n.g.	n.g.	increase followed by platform (ELISA)	48h...72h: 1.4 (ratio)†
Nazet et al. (2020)	ALP	*ALPP*	hPDLF (17-27/F, 17-27/M, M, n.g., P3-6, 7×10^4)	static	48h	7%, 10%, 16%. 35%	six-well bioflex membrane plates coated with collagen I + custom-made spherical cap silicone stamps	equibiaxial	n.g.	n.g.	increase (ELISA)	16%: 1.5 (ratio)†
Nazet et al. (2020)	COX-2	*PTGS2*	hPDLF (17-27/F, 17-27/M, M, n.g., P3-6, 7×10^4)	static	24h, 48h, 72h	35%	six-well bioflex membrane plates coated with collagen I + custom-made spherical cap silicone stamps	equibiaxial	temporary increase (qPCR, TBP/PPIB)	48h: 2.2 (FC)†	n.g.	n.g.
Nazet et al. (2020)	COX-2	*PTGS2*	hPDLF (17-27/F, 17-27/M, M, n.g., P3-6, 7×10^4)	static	48h	7%, 10%, 16%. 35%	six-well bioflex membrane plates coated with collagen I + custom-made spherical cap silicone stamps	equibiaxial	increase (qPCR, TBP/PPIB)	35%: 2.5 (FC)†	n.g.	n.g.
Nazet et al. (2020)	IL-6	*IL6*	hPDLF (17-27/F, 17-27/M, M, n.g., P3-6, 7×10^4)	static	24h, 48h, 72h	35%	six-well bioflex membrane plates coated with collagen I + custom-made spherical cap silicone stamps	equibiaxial	temporary decrease (qPCR, TBP/PPIB)	48h: 0.6 (FC)†	n.g.	n.g.
Nazet et al. (2020)	IL-6	*IL6*	hPDLF (17-27/F, 17-27/M, M, n.g., P3-6, 7×10^4)	static	48h	7%, 10%, 16%. 35%	six-well bioflex membrane plates coated with collagen I + custom-made spherical cap silicone stamps	equibiaxial	decrease (qPCR, TBP/PPIB)	35%: 0.7 (FC)†	n.g.	n.g.
Nemoto et al. (2010)	ARRAY	ARRAY	hPDL cells (20/n.g., 40/n.g., M, dig, P4-8, 5×10^5 cells/cm^2)	dynamic	**0.017Hz (1/60Hz)** (conditions: 60s/returns; resting time: 29s) short time for 1h, 3h, 12h, 24h, 48h; long time for 1d, 3d, 5d, 7d	**5%** (Stretch length: 1.6mm, stretch ratio: 105%)	STB-140 (Strex Co) + 50 cm^2 silicon chambers coated with 50 mg/ml COL1 + stepping motor	uniaxial	Gene Chip Human Genome U133 plus (Agilent)	too many	n.g.	n.g.

[a] Entry given as reported in the study.
[b] All official gene symbols come from the HUGO Gene Nomenclature Committee (HGNC; URL: https://www.genenames.org) after checking specificity of primers with Primer-BLAST.
[c] Gender/Sex of donors: "M" – male, "F" – female; Tooth type: "PM" – premolar, "M" – molar; Cell density: given in cells/well if not otherwise mentioned.
[d] Frequencies labeled bold orange were converted to hertz (Hz) according to its definition using the information reported in the study (in brackets)
[e] Force type deduced from the description of the force apparatus given by the authors.
[f] Gene and protein expression: 1. conclusion of change (increase, decrease…) was given according to the defined criteria in Figure 2; 2. different markers to describe the amount of change; † Information derived from figures using Engauge Digitizer; *Folds calculated by measuring the graphs, without using the Engauge Digitizer; No makers: Information derived from figures by description in the articles

Reference	Gene/ Analyte[a]	Official gene symbol / abbreviation[b]	Cell (age/gender of donors, tooth type, isolation method, passages used, cell density)[a,c]	Force type (stat./ dyn.)[a]	Force duration and frequency[d]	Force magnitude[a]	Force apparatus[a]	Force type: equibiaxial or uniaxial[e]	Gene expression: Increase, decrease, no change (method w/ reference gene); Methods: qPCR, sqPCR, Northern blot[f]	Gene expression: When it reaches peak and peak's magnitude (fold change; times or ratio; unclear = ?)[f]	Protein expression: Increase, decrease, no change (method w/ reference); Methods: ELISA, WB, RIA, EMSA, IF[f]	Protein expression: When it reaches peak and peak's magnitude (times or ratio; unclear = ?)[f]
Nemoto et al. (2010)	COLIVα1	*COL4A1*	hPDL cells (20/n.g., 40/n.g., M, dig, P4-8, 5×10^5 cells/cm^2)	dynamic	**0.017Hz (1/60Hz)** (Conditions: 60s/returns; resting time: 29s) short time for 1h, 3h, 12h, 24h, 48h; long time for 1d, 3d, 5d, 7d	**5%** (Stretch length: 1.6mm, stretch ratio: 105%)	STB-140 (Strex Co) + 50 cm^2 silicon chambers coated with 50 mg/ml COL1 + stepping motor	uniaxial	short time: increase followed by plateau (qPCR, GAPDH) long time: increase (qPCR, GAPDH)	short time @ 1h…48h: 0.3 (rel)* / 1.7 (ratio-calc) long time @ 7d: 0.5 (rel)* / 5.4 (ratio-calc)	n.g.	n.g.
Nemoto et al. (2010)	COLIα1	*COL1A1*	hPDL cells (20/n.g., 40/n.g., M, dig, P4-8, 5×10^5 cells/cm^2)	dynamic	**0.017Hz (1/60Hz)** (Conditions: 60s/returns; resting time: 29s) short time for 1h, 3h, 12h, 24h, 48h; long time for 1d, 3d, 5d, 7d	**5%** (Stretch length: 1.6mm, stretch ratio: 105%)	STB-140 (Strex Co) + 50 cm^2 silicon chambers coated with 50 mg/ml COL1 + stepping motor	uniaxial	short time: decrease (qPCR, GAPDH) long time: decrease (qPCR, GAPDH)	short time @ 24h: 0.3 (rel)* / 0.3 (ratio-calc) long time @ 3d: 0.2 (rel)* / 0.3 (ratio-calc)	n.g.	n.g.
Nemoto et al. (2010)	COLXIIα1	*COL12A1*	hPDL cells (20/n.g., 40/n.g., M, dig, P4-8, 5×10^5 cells/cm^2)	dynamic	**0.017Hz (1/60Hz)** (conditions: 60s/returns; resting time: 29s) short time for 1h, 3h, 12h, 24h, 48h; long time for 1d, 3d, 5d, 7d	**5%** (Stretch length: 1.6mm, stretch ratio: 105%)	STB-140 (Strex Co) + 50 cm^2 silicon chambers coated with 50 mg/ml COL1 + stepping motor	uniaxial	short time: decrease (qPCR, GAPDH) long time: decrease (qPCR, GAPDH)	short time @ 12h: 0.1 (rel)* / 0.3 (ratio-calc) long time @ 1d: 0.2 (rel)* / 0.4 (ratio-calc)	n.g.	n.g.
Ngan et al. (1990)	cAMP	cAMP	hPDL cells (n.g./n.g., PM, dig, P4-6, 4×10^5 cells/cm^2)	static	5min, 15min, 30min, 60min	n.g.	Petriperm dishes + spheroidal convex template + weight	equibiaxial	n.a.	n.a.	increase (cAMP assay)	60min: 0.8 (pmol/10^4 PDL cells)* / 1.1 (ratio-calc)
Ngan et al. (1990)	PGE_2	PGE_2	hPDL cells (n.g./n.g., PM, dig, P4-6, 4×10^5 cells/cm^2)	static	5min, 15min, 30min, 60min	0.28%, 0.95%, 1.09%, 1.72%	Petriperm dishes + spheroidal convex template + weight	equibiaxial	n.a.	n.a.	0.28%: increase (RIA) 0.95%: temporary decrease (RIA) 1.09%: increase (RIA) 1.72%: increase (RIA)	0.28% @ 120min: 109 (pg/10^4 PDL cells)* / 1.1 (ratio-calc) 0.95% @ 15min: 98 (pg/10^4 PDL cells)* / 0.9 (ratio-calc) 1.09% @ 120min: 111 (pg/10^4 PDL cells)* / 1.1 (ratio-calc) 1.72% @ 30min: 101 (pg/10^4 PDL cells)* / 1.7 (ratio-calc)
Nogueira et al. (2014a)	TLR2	*TLR2*	hPDL cells (n.g./n.g., n.g., n.g., P3-5, 80% confluence)	dynamic	0.05Hz for 1d, 3d	3%, 20%	strain device (CESTRA) + six-well BioFlex® collagen-coated culture plates + stepping motor (Nokhbehsaim 2012; further reference to Rath-Deschner 2009)	equibiaxial	3%: increase followed by decrease (qPCR, GAPDH) 20%: decrease (qPCR, GAPDH)	3% highest @ 1d: 1.1 (FC)* 3% lowest @ 3d: 0.88 (FC) 20% @ 3d: 0.31 (FC)	n.g.	n.g.
Nogueira et al. (2014a)	TLR4	*TLR4*	hPDL cells (n.g./n.g., n.g., n.g., P3-5, 80% confluence)	dynamic	0.05Hz for 1d, 3d	3%, 20%	strain device (CESTRA) + six-well BioFlex® collagen-coated culture plates + stepping motor (Nokhbehsaim 2012; further reference to Rath-Deschner 2009)	equibiaxial	3%: decrease (qPCR, GAPDH) 20%: decrease (qPCR, GAPDH)	3% @ 3d: 0.88 (FC) 20% @ 3d: 0.48 (FC)	n.g.	n.g.
Nogueira et al. (2014a)	Visfatin	*NAMPT*	hPDL cells (n.g./n.g., n.g., n.g., P3-5, 80% confluence)	dynamic	0.05Hz for 1d, 3d	3%, 20%	strain device (CESTRA) + six-well BioFlex® collagen-coated culture plates + stepping motor (Nokhbehsaim 2012; further reference to Rath-Deschner 2009)	equibiaxial	1d: decrease followed by plateau (qPCR, GAPDH) 3d: decrease (qPCR, GAPDH)	3...20% @ 1d: 0.7 (FC)† 20% @ 3d: 0.6 (FC)†	n.g.	n.g.
Nogueira et al. (2014b)	COX2	*PTGS2*	hPDL cells (n.g./n.g., n.g., n.g., P3-5, 80% confluence)	dynamic	0.05Hz for 36h	3%, 20%	strain device (CESTRA) + six-well BioFlex® collagen-coated culture plates + stepping motor	equibiaxial	n.g.	n.g.	increase (ELISA)	20%: 210 (pg/mL)* / 1.8 (ratio-calc)
Nogueira et al. (2014b)	OPG	*TNFRSF11B*	hPDL cells (n.g./n.g., n.g., n.g., P3-5, 80% confluence)	dynamic	0.05Hz for 1d, 3d	20%	strain device (CESTRA) + six-well BioFlex® collagen-coated culture plates + stepping motor	equibiaxial	OPG: decrease followed by plateau (qPCR, GAPDH) *RANKL/OPG: increase*	OPG @ 1d…3d: 0.2 (FC)* *RANKL/OPG @ 1d: 4.5 (ratio)**	OPG: decrease (ELISA) *RANKL/OPG: increase*	OPG @ 1d: 0.6 (ratio)* *RANKL/OPG @ 3d: 1.4 (ratio)**
Nogueira et al. (2014b)	PGE_2	PGE_2	hPDL cells (n.g./n.g., n.g., n.g., P3-5, 80% confluence)	dynamic	0.05Hz for 1d, 3d	3%, 20%	strain device (CESTRA) + six-well BioFlex® collagen-coated culture plates + stepping motor	equibiaxial	n.a.	n.a.	1d: increase (ELISA) 3d: increase followed by plateau (ELISA)	20% @ 1d: 28.3 (ratio)† 3…20% @ 3d: 4.3 (ratio)†
Nogueira et al. (2014b)	RANKL	TNFSF11	hPDL cells (n.g./n.g., n.g., n.g., P3-5, 80% confluence)	dynamic	0.05Hz for 1d, 3d	20%	strain device (CESTRA) + six-well BioFlex® collagen-coated culture plates + stepping motor	equibiaxial	RANKL: decrease (qPCR, GAPDH) *RANKL/OPG: increase*	RANKL @ 3d: 0.3 (FC)* *RANKL/OPG @ 1d: 4.5 (ratio)**	RANKL: decrease (ELISA) *RANKL/OPG: increase*	RANKL @ 1d: 0.6 (ratio)* *RANKL/OPG @ 3d: 1.4 (ratio)**
Nokhbehsaim et al. (2010)	ALP	*ALPP*	hPDL cells (n.g./n.g., n.g., n.g., P3-5, n.g.)	dynamic	0.05Hz for 1d, 6d	3%, 20%	strain device (CESTRA) + six-well BioFlex® collagen-coated culture plates + stepping motor	equibiaxial	3%: increase followed by decrease (qPCR, GAPDH) 20%: decrease (qPCR, GAPDH)	3% highest @1d: 1.13 (FC) 3% lowest @ 6d: 0.59 (FC) 20% @ 6d: 0.34 (FC)	n.g.	n.g.
Nokhbehsaim et al. (2010)	COL1	*COL1A1; COL1A2*	hPDL cells (n.g./n.g., n.g., n.g., P3-5, n.g.)	dynamic	0.05Hz for 1d, 6d	3%, 20%	strain device (CESTRA) + six-well BioFlex® collagen-coated culture plates + stepping motor	equibiaxial	3%: decrease (qPCR, GAPDH) 20% decrease (qPCR, GAPDH)	3% @ 1d: 0.25 (FC) 20% @ 6d: 0.30 (FC)	n.g.	n.g.
Nokhbehsaim et al. (2010)	COX2	PTGS2	hPDL cells (n.g./n.g., n.g., n.g., P3-5, n.g.)	dynamic	0.05Hz for 1d, 6d	3%, 20%	strain device (CESTRA) + six-well BioFlex® collagen-coated culture plates + stepping motor	equibiaxial	3% temporary increase (qPCR, GAPDH) 20% increase (qPCR, GAPDH)	3% @ 1d: 1.29 (FC) 20% @ 6d: 3.32 (FC)	n.g.	n.g.
Nokhbehsaim et al. (2010)	IGF1	*IGF1*	hPDL cells (n.g./n.g., n.g., n.g., P3-5, n.g.)	dynamic	0.05Hz for 1d, 6d	3%, 20%	strain device (CESTRA) + six-well BioFlex® collagen-coated culture plates + stepping motor	equibiaxial	3%: decrease followed by plateau (qPCR, GAPDH) 20%: decrease (qPCR, GAPDH)	3% @ 1d...6d: 0.57 (FC) 20% @ 1d: 0.25 (FC)	n.g.	n.g.

[a] Entry given as reported in the study.
[b] All official gene symbols come from the HUGO Gene Nomenclature Committee (HGNC; URL: https://www.genenames.org) after checking specificity of primers with Primer-BLAST.
[c] Gender/Sex of donors: "M" – male, "F" – female; Tooth type: "PM" – premolar, "M" – molar; Cell density: given in cells/well if not otherwise mentioned.
[d] Frequencies labeled bold orange were converted to hertz (Hz) according to its definition using the information reported in the study (in brackets)
[e] Force type deduced from the description of the force apparatus given by the authors.
[f] Gene and protein expression: 1. conclusion of change (increase, decrease…) was given according to the defined criteria in Figure 2; 2. different markers to describe the amount of change; † Information derived from figures using Engauge Digitizer; *Folds calculated by measuring the graphs, without using the Engauge Digitizer; No makers: Information derived from figures by description in the articles

Reference	Gene/ Analyte[a]	Official gene symbol / abbreviation[b]	Cell (age/gender of donors, tooth type, isolation method, passages used, cell density)[a,c]	Force type (stat./ dyn.)[a]	Force duration and frequency[d]	Force magnitude[a]	Force apparatus[a]	Force type: equibiaxial or uniaxial[e]	Gene expression: Increase, decrease, no change (method w/ reference gene); Methods: qPCR, sqPCR, Northern blot[f]	Gene expression: When it reaches peak and peak's magnitude (fold change; times or ratio; unclear = ?)[f]	Protein expression: Increase, decrease, no change (method w/ reference); Methods: ELISA, WB, RIA, EMSA, IF[f]	Protein expression: When it reaches peak and peak's magnitude (times or ratio; unclear = ?)[f]
Nokhbehsaim et al. (2010)	IL-1B	*IL1B*	hPDL cells (n.g./n.g., n.g., n.g., P3-5, n.g.)	dynamic	0.05Hz for 1d, 6d	3%, 20%	strain device (CESTRA) + six-well BioFlex® collagen-coated culture plates + stepping motor	equibiaxial	3%: increase (qPCR, GAPDH) 20%: increase (qPCR, GAPDH)	3% @ 1d: 12.41 (FC) 20% @ 6d: 36.16 (FC)	n.g.	n.g.
Nokhbehsaim et al. (2010)	IL-8	*CXCL8*	hPDL cells (n.g./n.g., n.g., n.g., P3-5, n.g.)	dynamic	0.05Hz qPCR for 1d, 6d; ELISA for 1d	3%, 20%	strain device (CESTRA) + six-well BioFlex® collagen-coated culture plates + stepping motor	equibiaxial	3%: increase (qPCR, GAPDH) 20%: increase (qPCR, GAPDH)	3% @ 6d: 17.48 (FC) 20% @ 6d: 7.54 (FC)	3%: increase (ELISA) 20%: increase (ELISA)	3%: 394.16 (pg/10^5 cells) / 11.6 (ratio-calc) 20%: 109.47 (pg/10^5 cells) / 3.2 (ratio-calc)
Nokhbehsaim et al. (2010)	RUNX2	*RUNX2*	hPDL cells (n.g./n.g., n.g., n.g., P3-5, n.g.)	dynamic	0.05Hz for 1d, 6d	3%, 20%	strain device (CESTRA) + six-well BioFlex® collagen-coated culture plates + stepping motor	equibiaxial	3%: decrease (qPCR, GAPDH) 20%: decrease (qPCR, GAPDH)	3% @ 1d: 0.24 (FC) 20% @ 1d: 0.27 (FC)	n.g.	n.g.
Nokhbehsaim et al. (2010)	TGFB1	*TGFB1*	hPDL cells (n.g./n.g., n.g., n.g., P3-5, n.g.)	dynamic	0.05Hz for 1d, 6d	3%, 20%	strain device (CESTRA) + six-well BioFlex® collagen-coated culture plates + stepping motor	equibiaxial	3%: temporary decrease (qPCR, GAPDH) 20%: increase (qPCR, GAPDH)	3% @ 1d: 0.58 (FC) 20% @ 6d: 1.38 (FC)	n.g.	n.g.
Nokhbehsaim et al. (2010)	VEGF	*VEGFA*	hPDL cells (n.g./n.g., n.g., n.g., P3-5, n.g.)	dynamic	0.05Hz for 1d, 6d	3%, 20%	strain device (CESTRA) + six-well BioFlex® collagen-coated culture plates + stepping motor	equibiaxial	3%: temporary decrease (qPCR, GAPDH) 20%: increase (qPCR, GAPDH)	3% @ 1d: 0.70 (FC) 20% @ 6d: 2.51 (FC)	3%: decrease (ELISA) 20%: increase (ELISA)	3%: 431.81 (pg/10^5 cells) / 0.1 (ratio-calc) 20%: 4669.43 (pg/10^5 cells) / 1.4 (ratio-calc)
Nokhbehsaim et al. (2011a)	BMPR1A	*BMPR1A*	hPDL cells (8-17/F, 8-14/M, n.g., n.g., P3-5, 80% confluence)	dynamic	0.05Hz for 6d	3%	strain device (CESTRA) + six-well BioFlex® collagen-coated culture plates + stepping motor (Rath-Deschner 2009)	equibiaxial	increase (qPCR, GAPDH)	1.2 (FC)*	n.g.	n.g.
Nokhbehsaim et al. (2011a)	BMPR1B	*BMPR1B*	hPDL cells (8-17/F, 8-14/M, n.g., n.g., P3-5, 80% confluence)	dynamic	0.05Hz for 6d	3%	strain device (CESTRA) + six-well BioFlex® collagen-coated culture plates + stepping motor (Rath-Deschner 2009)	equibiaxial	no change (qPCR, GAPDH)		n.g.	n.g.
Nokhbehsaim et al. (2011a)	BMPR2	*BMPR2*	hPDL cells (8-17/F, 8-14/M, n.g., n.g., P3-5, 80% confluence)	dynamic	0.05Hz for 6d	3%	strain device (CESTRA) + six-well BioFlex® collagen-coated culture plates + stepping motor (Rath-Deschner 2009)	equibiaxial	decrease (qPCR, GAPDH)	0.8 (FC)*	n.g.	n.g.
Nokhbehsaim et al. (2011a)	Collagen I (COL1)	*COL1A1; COL1A2*	hPDL cells (8-17/F, 8-14/M, n.g., n.g., P3-5, 80% confluence)	dynamic	0.05Hz for 1d, 6d	3%	strain device (CESTRA) + six-well BioFlex® collagen-coated culture plates + stepping motor (Rath-Deschner 2009)	equibiaxial	decrease (qPCR, GAPDH)	1d: 0.3 (FC)*	n.g.	n.g.
Nokhbehsaim et al. (2011a)	RUNX2	*RUNX2*	hPDL cells (8-17/F, 8-14/M, n.g., n.g., P3-5, 80% confluence)	dynamic	0.05Hz for 1d, 6d	3%	strain device (CESTRA) + six-well BioFlex® collagen-coated culture plates + stepping motor	equibiaxial	decrease (qPCR, GAPDH)	1d: 0.2 (FC)*	n.g.	n.g.
Nokhbehsaim et al. (2011a)	TGF-β1	*TGFB1*	hPDL cells (8-17/F, 8-14/M, n.g., n.g., P3-5, 80% confluence)	dynamic	0.05Hz for 1d, 6d	3%	strain device (CESTRA) + six-well BioFlex® collagen-coated culture plates + stepping motor	equibiaxial	temporary decrease (qPCR, GAPDH)	1d: 0.6 (FC)*	n.g.	n.g.
Nokhbehsaim et al. (2011a)	TGF-βR1	*TGFBR1*	hPDL cells (8-17/F, 8-14/M, n.g., n.g., P3-5, 80% confluence)	dynamic	0.05Hz for 6d	3%	strain device (CESTRA) + six-well BioFlex® collagen-coated culture plates + stepping motor	equibiaxial	no change (qPCR, GAPDH)		n.g.	n.g.
Nokhbehsaim et al. (2011a)	TGF-βR2	*TGFBR2*	hPDL cells (8-17/F, 8-14/M, n.g., n.g., P3-5, 80% confluence)	dynamic	0.05Hz for 6d	3%	strain device (CESTRA) + six-well BioFlex® collagen-coated culture plates + stepping motor	equibiaxial	decrease (qPCR, GAPDH)	0.8 (FC)*	n.g.	n.g.
Nokhbehsaim et al. (2011a)	VEGF	*VEGFA*	hPDL cells (8-17/F, 8-14/M, n.g., n.g., P3-5, 80% confluence)	dynamic	0.05Hz for 1d, 6d	3%	strain device (CESTRA) + six-well BioFlex® collagen-coated culture plates + stepping motor	equibiaxial	temporary decrease (qPCR, GAPDH)	1d: 0.7 (FC)*	n.g.	n.g.
Nokhbehsaim et al. (2011b)	BMP-2	*BMP2*	hPDL cells (n.g./n.g., n.g., n.g., P3-5, 80% confluen)	dynamic	0.05Hz for 1d, 6d	3%, 20%	strain device (CESTRA) + six-well BioFlex® collagen-coated culture plates + stepping motor (Rath-Deschner 2009)	equibiaxial	3%: decrease (qPCR, GAPDH) 20%: increase (qPCR, GAPDH)	3% @ 6d: 0.59 (FC) 20% @ 1d: 2.6 (FC)	n.g.	n.g.
Nokhbehsaim et al. (2011b)	Follistatin	*FST*	hPDL cells (n.g./n.g., n.g., n.g., P3-5, 80% confluen)	dynamic	0.05Hz for 1d, 6d	3%, 20%	strain device (CESTRA) + six-well BioFlex® collagen-coated culture plates + stepping motor (Rath-Deschner 2009)	equibiaxial	3%: decrease (qPCR, GAPDH) 20%: decrease (qPCR, GAPDH)	3% @ 1d: 0.5 (FC)* 20% @ 6d: 0.6 (FC)*	n.g.	n.g.
Nokhbehsaim et al. (2011b)	MGP	*MGP*	hPDL cells (n.g./n.g., n.g., n.g., P3-5, 80% confluen)	dynamic	0.05Hz for 1d, 6d	3%, 20%	strain device (CESTRA) + six-well BioFlex® collagen-coated culture plates + stepping motor (Rath-Deschner 2009)	equibiaxial	3%: decrease (qPCR, GAPDH) 20%: decrease (qPCR, GAPDH)	3% @ 6d: 0.4 (FC)* 20% @ 6d: 0.3 (FC)*	n.g.	n.g.
Nokhbehsaim et al. (2011b)	Noggin	*NOG*	hPDL cells (n.g./n.g., n.g., n.g., P3-5, 80% confluen)	dynamic	0.05Hz for 1d, 6d	3%, 20%	strain device (CESTRA) + six-well BioFlex® collagen-coated culture plates + stepping motor (Rath-Deschner 2009)	equibiaxial	3%: decrease followed by plateau (qPCR, GAPDH) 20%: decrease followed by plateau (qPCR, GAPDH)	3% @ 1d...6d: 0.5 (FC)* 20% @ 1d...6d: 0.6 (FC)*	n.g.	n.g.
Nokhbehsaim et al. (2012)	COX2	*PTGS2*	hPDL cells (n.g./n.g., n.g., n.g., P3-5, n.g.)	dynamic	0.05Hz for 1d, 6d	3%, 20%	strain device (CESTRA) + six-well BioFlex® collagen-coated culture plates + stepping motor (Rath-Deschner 2009)	equibiaxial	3%: no change (qPCR, GAPDH) 20%: increase (qPCR, GAPDH)	20% @ 6d: 1.5 (FC)*	n.g.	n.g.
Nokhbehsaim et al. (2012)	IL10	*IL10*	hPDL cells (n.g./n.g., n.g., n.g., P3-5, n.g.)	dynamic	0.05Hz for 1d, 6d	3%, 20%	strain device (CESTRA) + six-well BioFlex® collagen-coated culture plates + stepping motor (Rath-Deschner 2009)	equibiaxial	3%: decrease followed by increase (qPCR, GAPDH) 20%: decrease (qPCR, GAPDH)	3% lowest @ 1d: 0.5 (FC)* 3% highest @ 6d: 1.6 (FC)* 20% @ 1d: 0.7 (FC)*	n.g.	n.g.
Nokhbehsaim et al. (2012)	IL1RN	*IL1RN*	hPDL cells (n.g./n.g., n.g., n.g., P3-5, n.g.)	dynamic	0.05Hz for 1d, 6d	3%, 20%	strain device (CESTRA) + six-well BioFlex® collagen-coated culture plates + stepping motor (Rath-Deschner 2009)	equibiaxial	3%: decrease followed by increase (qPCR, GAPDH) 20%: decrease followed by increase (qPCR, GAPDH)	3% lowest @ 1d: 0.7 (FC)* 3% highest @ 6d: 2.2 (FC)* 20% lowest @ 1d: 0.5 (FC)* 20% highest @ 6d: 2 (FC)*	n.g.	n.g.
Nokhbehsaim et al. (2012)	IL-1β	*IL1B*	hPDL cells (n.g./n.g., n.g., n.g., P3-5, n.g.)	dynamic	0.05Hz for 1d, 6d	3%, 20%	strain device (CESTRA) + six-well BioFlex® collagen-coated culture plates + stepping motor (Rath-Deschner 2009)	equibiaxial	3%: decrease (qPCR, GAPDH) 20%: decrease (qPCR, GAPDH)	3% @ 6d: 0.08 (FC)* 20% @ 6d: 0.5 (FC)*	n.g.	n.g.
Nokhbehsaim et al. (2012)	IL-6	*IL6*	hPDL cells (n.g./n.g., n.g., n.g., P3-5, n.g.)	dynamic	0.05Hz for qPCR 1d, 6d; ELISA for 1d, 2d	3%, 20%	strain device (CESTRA) + six-well BioFlex® collagen-coated culture plates + stepping motor (Rath-Deschner 2009)	equibiaxial	3%: increase (qPCR, GAPDH) 20%: increase (qPCR, GAPDH)	3% @ 1d: 2 (FC)* 20% @ 6d: 3.6 (FC)*	3%: decrease (ELISA) 20%: decrease followed by increase (ELISA)	3% @ 2d: 1.1 (pg/10^4 cells)†/ 0.04 (ratio-calc) 20% lowest @ 1d: 32.4 (pg/10^4 cells)† / 0.8 (ratio-calc) 20% highest @ 2d: 63.0 (pg/10^4 cells)† / 2.3 (ratio-calc)
Nokhbehsaim et al. (2012)	IL-8	*CXCL8*	hPDL cells (n.g./n.g., n.g., n.g., P3-5, n.g.)	dynamic	0.05Hz for 1d, 6d	3%, 20%	strain device (CESTRA) + six-well BioFlex® collagen-coated culture plates + stepping motor (Rath-Deschner 2009)	equibiaxial	3%: decrease (qPCR, GAPDH) 20%: decrease (qPCR, GAPDH)	3% @ 6d: 0.08 (FC)* 20% @ 1d: 0.8 (FC)*	n.g.	n.g.

[a] Entry given as reported in the study.
[b] All official gene symbols come from the HUGO Gene Nomenclature Committee (HGNC; URL: https://www.genenames.org) after checking specificity of primers with Primer-BLAST.
[c] Gender/Sex of donors: "M" – male, "F" – female; Tooth type: "PM" – premolar, "M" – molar; Cell density: given in cells/well if not otherwise mentioned.
[d] Frequencies labeled bold orange were converted to hertz (Hz) according to its definition using the information reported in the study (in brackets)
[e] Force type deduced from the description of the force apparatus given by the authors.
[f] Gene and protein expression: 1. conclusion of change (increase, decrease…) was given according to the defined criteria in Figure 2; 2. different markers to describe the amount of change; † Information derived from figures using Engauge Digitizer; *Folds calculated by measuring the graphs, without using the Engauge Digitizer; No makers: Information derived from figures by description in the articles

Reference	Gene/ Analyte[a]	Official gene symbol / abbreviation[b]	Cell (age/gender of donors, tooth type, isolation method, passages used, cell density)[a,c]	Force type (stat./ dyn.)[a]	Force duration and frequency[d]	Force magnitude[a]	Force apparatus[a]	Force type: equibiaxial or uniaxial[e]	Gene expression: Increase, decrease, no change (method w/ reference gene); Methods: qPCR, sqPCR, Northern blot[f]	Gene expression: When it reaches peak and peak's magnitude (fold change; times or ratio; unclear = ?)[f]	Protein expression: Increase, decrease, no change (method w/ reference); Methods: ELISA, WB, RIA, EMSA, IF[f]	Protein expression: When it reaches peak and peak's magnitude (times or ratio; unclear = ?)[f]
Ohzeki et al. (1999)	COX-1	*PTGS1*	hPDL cells (12/M, 10/M, 11/F , PM, exp, P5-7 and P19-22, Confluent)	dynamic	**0.1Hz** (6cyc/min: 5s elongation and 5s relaxation) for unclear	unclear	Flexercell strain unit (Shimizu et al 1994) + flexible-bottom culture plates coated with type I collagen (Flexcell) + vacuum	equibiaxial	increase (sqPCR, GAPDH)	no quantitative information is given	n.g.	n.g.
Ohzeki et al. (1999)	COX-2	*PTGS2*	hPDL cells (12/M, 10/M, 11/F , PM, exp, P5-7 and P19-22, Confluent)	dynamic	**0.1Hz** (6cyc/min: 5s elongation and 5s relaxation) for unclear	unclear	Flexercell strain unit (Shimizu et al 1994) + flexible-bottom culture plates coated with type I collagen (Flexcell) + vacuum	equibiaxial	increase (sqPCR, GAPDH)	no quantitative information is given	n.g.	n.g.
Ohzeki et al. (1999)	PGE_2	PGE_2	hPDL cells (12/M, 10/M, 11/F , PM, exp, P5-7 and P19-22, Confluent)	dynamic	**0.1Hz** (6cyc/min: 5s elongation and 5s relaxation) for 5d	9%, 18%	Flexercell strain unit (Shimizu et al 1994) + flexible-bottom culture plates coated with type I collagen (Flexcell) + vacuum	equibiaxial	n.a.	n.a.	"young cells" (P5-7): increase (RIA) "aged cells" (P19-22): increase (RIA)	"young cells" @ 18%: 5.9 (ng/10^6 cells) / 5.6 (ratio-calc) "aged cells" @ 18%: 11.6 (ng/10^6 cells) / 9.4 (ratio-calc)
Ohzeki et al. (1999)	PGE_2	PGE_2	hPDL cells (12/M, 10/M, 11/F , PM, exp, P5-7 and P19-22, Confluent)	dynamic	**0.1Hz** (6cyc/min: 5s elongation and 5s relaxation) for 1d, 3d, 5d	18%	Flexercell strain unit (Shimizu et al 1994) + flexible-bottom culture plates coated with type I collagen (Flexcell) + vacuum	equibiaxial	n.a.	n.a.	"young cells" (P5-7): increase (RIA) "aged cells" (P19-22): increase (RIA)	"young cells" @ 5d: 5.9 (ng/10^6 cells) / 11.2 (ratio-calc) "aged cells" @ 5d: 12.1 (ng/10^6 cells) / 17.3 (ratio-calc)
Ohzeki et al. (1999)	PGE_2	PGE_2	hPDL cells (12/M, 10/M, 11/F , PM, exp, P5-7 and P19-22, Confluent)	dynamic	**0.1Hz** (6cyc/min: 5s elongation and 5s relaxation) for 5d	18%	Flexercell strain unit (Shimizu et al 1994) + flexible-bottom culture plates coated with type I collagen (Flexcell) + vacuum	equibiaxial	n.a.	n.a.	increase (RIA)	"young cells" (P5-7) (donor 1): 8.3 (ng/10^6 cells) / 13.2 (ratio-calc) "aged cells" (P19-22) (donor 1): 12.0 (ng/10^6 cells) / 24 (ratio-calc) "young cells" (P5-7) (donor 1): 2.5 (ug/mg protein) / 8.1 (ratio-calc) "aged cells" (P19-22) (donor 1): 2.9 (ug/mg protein) / 11.6 (ratio-calc) "young cells" (P5-7) (donor 2): 9.3 (ng/10^6 cells) / 18.6 (ratio-calc) "aged cells" (P19-22) (donor 2): 14.0 (ng/10^6 cells) / 18.7 (ratio-calc) "young cells" (P5-7) (donor 2): 2.6 (ug/mg protein) / 8.4 (ratio-calc) "aged cells" (P19-22) (donor 2): 3.2 (ug/mg protein) / 12.8 (ratio-calc) "young cells" (P5-7) (donor 3): 9.3 (ng/10^6 cells) / 14.8 (ratio-calc) "aged cells" (P19-22) (donor 3): 12.0 (ng/10^6 cells) / 19.0 (ratio-calc) "young cells" (P5-7) (donor 3): 2.5 (ug/mg protein) / 8.2 (ratio-calc) "aged cells" (P19-22) (donor 3): 3.0 (ug/mg protein) / 10.7 (ratio-calc)
Ozawa et al. (1997)	PA	*PLAT; PLAU*	hPDL cells (n.g./n.g., n.g., exp, P n.g., Confluent)	dynamic	**0.1Hz** (6cyc/min: 5s elongation and 5s relaxation) sqPCR for 3d; Photometry for 1d, 3d, 5d	18%	Flexercell strain unit (Banes et al 1985) + flexible-bottom culture plates coated with type I collagen (Flexcell) + vacuum	equibiaxial	n.a.	n.a.	increase (PA activity; photometric)	5d: 8.1 (mU/10^5 cells) / 1.9 (ratio-calc)
Ozawa et al. (1997)	PAI-1	*SERPINE1*	hPDL cells (n.g./n.g., n.g., exp, P n.g., Confluent)	dynamic	**0.1Hz** (6cyc/min: 5s elongation and 5s relaxation) sqPCR for 3d; ELISA for 1d, 3d, 5d	18%	Flexercell strain unit (Banes et al 1985) + flexible-bottom culture plates coated with type I collagen (Flexcell) + vacuum	equibiaxial	no change (sqPCR, GAPDH)	no quantitative information is given	no change (ELISA)	
Ozawa et al. (1997)	tPA	*PLAT*	hPDL cells (n.g./n.g., n.g., exp, P n.g., Confluent)	dynamic	**0.1Hz** (6cyc/min: 5s elongation and 5s relaxation) sqPCR for 3d; Photometry for 1d, 3d, 5d	18%	Flexercell strain unit (Banes et al 1985) + flexible-bottom culture plates coated with type I collagen (Flexcell) + vacuum	equibiaxial	increase (sqPCR, GAPDH)	no quantitative information is given	n.g.	n.g.
Padial-Molina et al. (2013)	POSTN	*POSTN*	hPDL cells (35/F, 29/M, PM, n.g., P4-7, 2.5×10^5)	dynamic	**0.1Hz** (6cyc/min) for 24h, 4d, 7d	14%	Flexcell FX-5000 Tension System + BioFlex Culture Plates coated with Collagen I + vacuum	equibiaxial	no change (sqPCR, GAPDH)		no change (WB)	

[a] Entry given as reported in the study.
[b] All official gene symbols come from the HUGO Gene Nomenclature Committee (HGNC; URL: https://www.genenames.org) after checking specificity of primers with Primer-BLAST.
[c] Gender/Sex of donors: "M" – male, "F" – female; Tooth type: "PM" – premolar, "M" – molar; Cell density: given in cells/well if not otherwise mentioned.
[d] Frequencies labeled bold orange were converted to hertz (Hz) according to its definition using the information reported in the study (in brackets)
[e] Force type deduced from the description of the force apparatus given by the authors.
[f] Gene and protein expression: 1. conclusion of change (increase, decrease…) was given according to the defined criteria in Figure 2; 2. different markers to describe the amount of change; † Information derived from figures using Engauge Digitizer; *Folds calculated by measuring the graphs, without using the Engauge Digitizer; No makers: Information derived from figures by description in the articles

Reference	Gene/ Analyte[a]	Official gene symbol / abbreviation[b]	Cell (age/gender of donors, tooth type, isolation method, passages used, cell density)[a,c]	Force type (stat./ dyn.)[a]	Force duration and frequency[d]	Force magnitude[a]	Force apparatus[a]	Force type: equibiaxial or uniaxial[e]	Gene expression: Increase, decrease, no change (method w/ reference gene); Methods: qPCR, sqPCR, Northern blot[f]	Gene expression: When it reaches peak and peak's magnitude (fold change; times or ratio; unclear = ?)[f]	Protein expression: Increase, decrease, no change (method w/ reference); Methods: ELISA, WB, RIA, EMSA, IF[f]	Protein expression: When it reaches peak and peak's magnitude (times or ratio; unclear = ?)[f]
Padial-Molina et al. (2013)	βIGH3	*TGFBI*	hPDL cells (35/F, 29/M, PM, n.g., P4-7, 2.5×10^5)	dynamic	**0.1Hz** (6cyc/min) for 24h, 4d, 7d	14%	Flexcell FX-5000 Tension System + BioFlex Culture Plates coated with Collagen I + vacuum	equibiaxial	no change (sqPCR, GAPDH)		no change (WB)	
Pan et al. (2014)	Cofilin/p-Cofilin	*CFL1*	hPDL cells (n.g./n.g., n.g., dig, P4-8, 95% confluence)	dynamic	0.1Hz for 6h, 24h	10%	Flexercell Tension Plus system FX-5000T + collagen I-coated 6-well Bioflex plates + vacuum	equibiaxial	n.g.	n.g.	cofilin: no change (WB, β-actin) p-cofilin: increase (WB, β-actin)	p-cofilin: 24h: 2.5 (ratio)*
Pan et al. (2014)	RhoA / GTP-RhoA	*RHOA*	hPDL cells (n.g./n.g., n.g., dig, P4-8, 95% confluence)	dynamic	0.1Hz for 6h, 24h	10%	Flexercell Tension Plus system FX-5000T + collagen I-coated 6-well Bioflex plates + vacuum	equibiaxial	n.g.	n.g.	RhoA: no change (WB, β-actin) GTP-RhoA: increase (WB, β-actin)	GTP-RhoA: 24h: 1.7 (ratio)*
Pan et al. (2014)	Rho-GDIα	*ARHGDIA*	hPDL cells (n.g./n.g., n.g., dig, P4-8, 95% confluence)	dynamic	0.1Hz for 6h, 24h	10%	Flexercell Tension Plus system FX-5000T + collagen I-coated 6-well Bioflex plates + vacuum	equibiaxial	n.g.	n.g.	decrease (WB, β-actin)	24h: 0.5 (ratio)*
Pan et al. (2014)	ROCK	*ROCK1; ROCK2*	hPDL cells (n.g./n.g., n.g., dig, P4-8, 95% confluence)	dynamic	0.1Hz for 6h, 24h	10%	Flexercell Tension Plus system FX-5000T + collagen I-coated 6-well Bioflex plates + vacuum	equibiaxial	n.g.	n.g.	increase (WB, β-actin)	ROCK: 24h: 2.4 (ratio)*
Papadopoulou et al. (2017)	c-fos	*FOS*	hPDL cells (3 donors: 9-20/n.g., n.g., exp, P3-6, n.g.)	static	15min, 30min, 60min, 180min	8%	in-house designed device prepared by Controla (Advanced Technology Equipment, Athens, Greece) + silicone dishes + moving clamp	uniaxial	temporary increase (qPCR, GAPDH)	donor A @ 30min: 4.0 ((FC)† donor B @ 30min: 6.7 (FC)† donor C @ 1h: 4.2 (FC)†	n.g.	n.g.
Papadopoulou et al. (2017)	c-fos	*FOS*	hPDL cells (3 donors: 9-20/n.g., n.g., exp, P3-6, n.g.)	dynamic	1Hz for 15min, 30min, 60min, 180min	8%	six station stretching appratus + optically transparent silicone dishes pre-coated with fibronectin + moving clamp (Konstantonis et al 2014; further reference to Neidlinger-Wilke et al 2001)	uniaxial	temporary increase (qPCR, GAPDH)	donor A @ 1h: 8.3 ((FC)† donor B @ 1h: 10.6 (FC)† donor C @ 1h: 10.9 (FC)†	n.g.	n.g.
Papadopoulou et al. (2017)	c-jun	*JUN*	hPDL cells (3 donors: 9-20/n.g., n.g., exp, P3-6, n.g.)	static	15min, 30min, 60min, 180min	8%	in-house designed device prepared by Controla (Advanced Technology Equipment, Athens, Greece). + silicone dishes + moving clamp	uniaxial	temporary increase (qPCR, GAPDH)	donor A @ 1h: 1.6 (FC)† donor B @ 1h: 1.7 (FC)† donor C @ 1h: 1.7 (FC)†	n.g.	n.g.
Papadopoulou et al. (2017)	c-jun	*JUN*	hPDL cells (3 donors: 9-20/n.g., n.g., exp, P3-6, n.g.)	dynamic	1Hz for 15min, 30min, 60min, 180min	8%	six station stretching appratus + optically transparent silicone dishes pre-coated with fibronectin + moving clamp (Konstantonis et al 2014; further reference to Neidlinger-Wilke et al 2001)	uniaxial	temporary increase (qPCR, GAPDH)	donor A @ 1h: 2.3 (FC)† donor B @ 1h: 1.7 (FC)† donor C @ 1h: 4.2 (FC)†	n.g.	n.g.
Papadopoulou et al. (2017)	ERK (pan ERK) / p-ERK1/2	MAPK3; MAPK1	hPDL cells (3 donors: 9-20/n.g., n.g., exp, P3-6, n.g.)	static	15min, 30min, 60min, 180min	8%	in-house designed device prepared by Controla (Advanced Technology Equipment, Athens, Greece). + silicone dishes + moving clamp	uniaxial	n.g.	n.g.	ERK1/2: no change (WB, actin) p-ERK1/2: temporary increase (WB, actin)	ERK1/2: no quantitative information is given p-ERK1/2: no quantitative information is given
Papadopoulou et al. (2017)	ERK (pan ERK) / p-ERK1/2	MAPK3; MAPK1	hPDL cells (3 donors: 9-20/n.g., n.g., exp, P3-6, n.g.)	dynamic	1Hz for 15min, 30min, 60min, 180min	8%	six station stretching appratus + optically transparent silicone dishes pre-coated with fibronectin + moving clamp (Konstantonis et al 2014; further reference to Neidlinger-Wilke et al 2001)	uniaxial	n.g.	n.g.	ERK: no change (WB, actin) p-ERK1/2: temporary increase (WB, actin)	ERK: no quantitative information is given p-ERK1/2: no quantitative information is given
Papadopoulou et al. (2017)	JNKs / p-JNKs	*MAPK8; MAPK9; MAPK10*	hPDL cells (3 donors: 9-20/n.g., n.g., exp, P3-6, n.g.)	static	15min, 30min, 60min, 180min	8%	in-house designed device prepared by Controla (Advanced Technology Equipment, Athens, Greece) + silicone dishes + moving clamp	uniaxial	n.g.	n.g.	JNKs: no change (WB, actin) p-JNKs: temporary increase (WB, actin)	JNKs: no quantitative information is given p-JNKs: no quantitative information is given
Papadopoulou et al. (2017)	JNKs / p-JNKs	*MAPK8; MAPK9; MAPK10*	hPDL cells (3 donors: 9-20/n.g., n.g., exp, P3-6, n.g.)	dynamic	1Hz for 15min, 30min, 60min, 180min	8%	six station stretching appratus + optically transparent silicone dishes pre-coated with fibronectin + moving clamp (Konstantonis et al 2014; further reference to Neidlinger-Wilke et al 2001)	uniaxial	n.g.	n.g.	JNKs: no change (WB, actin) p-JNKs: temporary increase (WB, actin)	JNKs: no quantitative information is given p-JNKs: no quantitative information is given
Papadopoulou et al. (2017)	p38 MAPK / p-p38(Thr180/ Tyr182)	*MAPK14*	hPDL cells (3 donors: 9-20/n.g., n.g., exp, P3-6, n.g.)	static	15min, 30min, 60min, 180min	8%	in-house designed device prepared by Controla (Advanced Technology Equipment, Athens, Greece). + silicone dishes + moving clamp	uniaxial	n.g.	n.g.	p-p38: temporary increase (WB, actin) p38: no change (WB, actin)	p-p38: no quantitative information is given p38: no quantitative information is given
Papadopoulou et al. (2017)	p38 MAPK / p-p38(Thr180/ Tyr182)	*MAPK14*	hPDL cells (3 donors: 9-20/n.g., n.g., exp, P3-6, n.g.)	dynamic	1Hz for 15min, 30min, 60min, 180min	8%	six station stretching appratus + optically transparent silicone dishes pre-coated with fibronectin + moving clamp (Konstantonis et al 2014; further reference to Neidlinger-Wilke et al 2001)	uniaxial	n.g.	n.g.	p-p38: temporary increase (WB, actin) p38: no change (WB, actin)	p-p38: no quantitative information is given p38: no quantitative information is given
Papadopoulou et al. (2019)	ALP	*ALPP*	hPDLF (n.g./n.g., n.g., exp, P n.g., n.g.)	dynamic	1Hz for 18h	8%	six station stretching apparatus + optically transparent silicone dishes pre-coated with fibronectin + moving clamp (Neidlinger-Wilke et al 2001)	uniaxial	increase (qPCR, GAPDH)	2.3 (FC)†	n.g.	n.g.
Papadopoulou et al. (2019)	c-fos	*FOS*	hPDLF (n.g./n.g., n.g., exp, P n.g., n.g.)	dynamic	1Hz for 0.5h	8%	six station stretching apparatus + optically transparent silicone dishes pre-coated with fibronectin + moving clamp (Neidlinger-Wilke et al 2001)	uniaxial	increase (qPCR, GAPDH)	4.2 (FC)†	n.g.	n.g.
Papadopoulou et al. (2019)	JNK / p-JNK(Thr183/Tyr185)	*MAPK8*	hPDLF (n.g./n.g., n.g., exp, P n.g., n.g.)	dynamic	1Hz for 0.33h (20min)	8%	six station stretching apparatus + optically transparent silicone dishes pre-coated with fibronectin + moving clamp (Neidlinger-Wilke et al 2001)	uniaxial	n.g.	n.g.	JNK: no change (WB, GAPDH) p-JNK(Thr183/Tyr185): increase (WB, GAPDH)	no quantitative information is given
Papadopoulou et al. (2019)	OPN	*SPP1*	hPDLF (n.g./n.g., n.g., exp, P n.g., n.g.)	dynamic	1Hz for 18h	8%	six station stretching apparatus + optically transparent silicone dishes pre-coated with fibronectin + moving clamp (Neidlinger-Wilke et al 2001)	uniaxial	increase (qPCR, GAPDH)	1.6 (FC)†	n.g.	n.g.

[a] Entry given as reported in the study.
[b] All official gene symbols come from the HUGO Gene Nomenclature Committee (HGNC; URL: https://www.genenames.org) after checking specificity of primers with Primer-BLAST.
[c] Gender/Sex of donors: "M" – male, "F" – female; Tooth type: "PM" – premolar, "M" – molar; Cell density: given in cells/well if not otherwise mentioned.
[d] Frequencies labeled bold orange were converted to hertz (Hz) according to its definition using the information reported in the study (in brackets)
[e] Force type deduced from the description of the force apparatus given by the authors.
[f] Gene and protein expression: 1. conclusion of change (increase, decrease…) was given according to the defined criteria in Figure 2; 2. different markers to describe the amount of change; † Information derived from figures using Engauge Digitizer; *Folds calculated by measuring the graphs, without using the Engauge Digitizer; No makers: Information derived from figures by description in the articles

Reference	Gene/ Analyte[a]	Official gene symbol / abbreviation[b]	Cell (age/gender of donors, tooth type, isolation method, passages used, cell density)[a,c]	Force type (stat./ dyn.)[a]	Force duration and frequency[d]	Force magnitude[a]	Force apparatus[a]	Force type: equibiaxial or uniaxial[e]	Gene expression: Increase, decrease, no change (method w/ reference gene); Methods: qPCR, sqPCR, Northern blot[f]	Gene expression: When it reaches peak and peak's magnitude (fold change; times or ratio; unclear = ?)[f]	Protein expression: Increase, decrease, no change (method w/ reference); Methods: ELISA, WB, RIA, EMSA, IF[f]	Protein expression: When it reaches peak and peak's magnitude (times or ratio; unclear = ?)[f]
Papadopoulou et al. (2019)	p38 / p-p38(Thr180/Tyr182)	*MAPK14*	hPDLF (n.g./n.g., n.g., exp, P n.g., n.g.)	dynamic	1Hz for 0.33h (20min)	8%	six station stretching apparatus + optically transparent silicone dishes pre-coated with fibronectin + moving clamp (Neidlinger-Wilke et al 2001)	uniaxial	n.g.	n.g.	p38: no change (WB, GAPDH) p38(Thr180/Tyr182): increase (WB, GAPDH)	no quantitative information is given
Papadopoulou et al. (2019)	pan ERK / p-ERK1/2(Thr202/Tyr204)	*MAPK3;* *MAPK1*	hPDLF (n.g./n.g., n.g., exp, P n.g., n.g.)	dynamic	1Hz for 0.33h (20min)	8%	six station stretching apparatus + optically transparent silicone dishes pre-coated with fibronectin + moving clamp (Neidlinger-Wilke et al 2001)	uniaxial	n.g.	n.g.	pan ERK: no change (WB, GAPDH) p-ERK1/2(Thr202/Tyr204): increase (WB, GAPDH)	no quantitative information is given
Pelaez et al. (2017)	ARRAY	ARRAY	hPDLSC cells (n.g./n.g., M, dig, P2-3, 85–90 % confluent)	dynamic	0.5Hz for 2h	5%	"custom-built bioreactor system" + chambers + linear actuator	uniaxial	SurePrint G3 Human v.16 miRNA Array Kit (8x60K, Release 16.0, Agilent)			
Pelaez et al. (2017)	Cx43	*GJA1*	hPDLSC cells (n.g./n.g., M, dig, P2-3, 85–90 % confluent)	dynamic	0.5Hz for 2h	5%	"custom-built bioreactor system" + chambers + linear actuator	uniaxial	increase (qPCR, GAPDH)	2.0 (rel)* / 2.0 (ratio-calc)	n.g.	n.g.
Pelaez et al. (2017)	GATA4	*GATA4*	hPDLSC cells (n.g./n.g., M, dig, P2-3, 85–90 % confluent)	dynamic	0.5Hz for 2h	5%	"custom-built bioreactor system" + chambers + linear actuator	uniaxial	increase (qPCR, GAPDH)	1.9 (rel)* / 3.3 (ratio-calc)	n.g.	n.g.
Pelaez et al. (2017)	MEF2C	*MEF2C*	hPDLSC cells (n.g./n.g., M, dig, P2-3, 85–90 % confluent)	dynamic	0.5Hz for 2h	5%	"custom-built bioreactor system" + chambers + linear actuator	uniaxial	increase (qPCR, GAPDH)	3.6 (rel)* / 20.0 (ratio-calc)	n.g.	n.g.
Pelaez et al. (2017)	MYH7	*MYH7*	hPDLSC cells (n.g./n.g., M, dig, P2-3, 85–90 % confluent)	dynamic	0.5Hz for 2h	5%	"custom-built bioreactor system" + chambers + linear actuator	uniaxial	increase (qPCR, GAPDH)	15.7 (rel)* / 16.5 (ratio-calc)	n.g.	n.g.
Pelaez et al. (2017)	MYL2	*MYL2*	hPDLSC cells (n.g./n.g., M, dig, P2-3, 85–90 % confluent)	dynamic	0.5Hz for 2h	5%	"custom-built bioreactor system" + chambers + linear actuator	uniaxial	increase (qPCR, GAPDH)	1.9 (rel)* / 2.0 (ratio-calc)	n.g.	n.g.
Pelaez et al. (2017)	MYL7	*MYL7*	hPDLSC cells (n.g./n.g., M, dig, P2-3, 85–90 % confluent)	dynamic	0.5Hz for 2h	5%	"custom-built bioreactor system" + chambers + linear actuator	uniaxial	increase (qPCR, GAPDH)	16.2 (rel)* / 17.1 (ratio-calc)	n.g.	n.g.
Pelaez et al. (2017)	Nitric oxide	Nitric oxide	hPDLSC cells (n.g./n.g., M, dig, P2-3, 85–90 % confluent)	dynamic	0.5Hz for 2h	5%	"custom-built bioreactor system" + chambers + linear actuator	uniaxial	n.a.	n.a.	increase (photometric)	20 min: 1.048 (relative NO levels)* / 1.07 (ratio-calc)
Pelaez et al. (2017)	Nkx2.5	*NKX2-5*	hPDLSC cells (n.g./n.g., M, dig, P2-3, 85–90 % confluent)	dynamic	0.5Hz for 2h	5%	"custom-built bioreactor system" + chambers + linear actuator	uniaxial	increase (qPCR, GAPDH)	5.1 (rel)* / 2 (ratio-calc)	n.g.	n.g.
Pelaez et al. (2017)	NPPA	*NPPA*	hPDLSC cells (n.g./n.g., M, dig, P2-3, 85–90 % confluent)	dynamic	0.5Hz for 2h	5%	"custom-built bioreactor system" + chambers + linear actuator	uniaxial	increase (qPCR, GAPDH)	3.6 (rel)* / 1.9 (ratio-calc)	n.g.	n.g.
Pelaez et al. (2017)	NPPB	*NPPB*	hPDLSC cells (n.g./n.g., M, dig, P2-3, 85–90 % confluent)	dynamic	0.5Hz for 2h	5%	"custom-built bioreactor system" + chambers + linear actuator	uniaxial	increase (qPCR, GAPDH)	1.2 (rel)* / 2.4 (ratio-calc)	n.g.	n.g.
Pelaez et al. (2017)	TNNT2	*TNNT2*	hPDLSC cells (n.g./n.g., M, dig, P2-3, 85–90 % confluent)	dynamic	0.5Hz for 2h	5%	"custom-built bioreactor system" + chambers + linear actuator	uniaxial	increase (qPCR, GAPDH)	2.1 (rel)* / 1.3 (ratio-calc)	n.g.	n.g.
Pelaez et al. (2017)	TPM1	*TPM1*	hPDLSC cells (n.g./n.g., M, dig, P2-3, 85–90 % confluent)	dynamic	0.5Hz for 2h	5%	"custom-built bioreactor system" + chambers + linear actuator	uniaxial	increase (qPCR, GAPDH)	2.5 (rel)* / 6.8 (ratio-calc)	n.g.	n.g.
Peverali et al. (2001)	AP-1	not clear	hPDL fibroblasts (n.g./n.g., n.g., exp, P3-6, 80% confluency)	static	15min, 30min	2.5%	Petriperm dish + template with a convex surface + weight	equibiaxial	n.g.	n.g.	increase (EMSA)	no quantitative information is given
Peverali et al. (2001)	C-FOS	*FOS*	hPDL fibroblasts (n.g./n.g., n.g., exp, P3-6, 80% confluency)	static	15min, 30min	2.5%	Petriperm dish + template with a convex surface + weight	equibiaxial	n.g.	n.g.	increase (in-gel kinase assay)	no quantitative information is given
Peverali et al. (2001)	C-JUN	*JUN*	hPDL fibroblasts (n.g./n.g., n.g., exp, P3-6, 80% confluency)	static	7min, 15min, 30min	2.5%	Petriperm dish + template with a convex surface + weight	equibiaxial	n.g.	n.g.	increase (in-gel kinase assay)	no quantitative information is given
Pinkerton et al. (2008)	ARRAY	ARRAY	hPDL cells (n.g./n.g., PM, exp, P4, 3×10^5)	dynamic	**0.01Hz** (Strain for 6s every 90s) for 6h, 12h, 24h	12%	Flexercell FX-4000 Strain Unit + 6-well, 35 mm flexible-bottomed Uniflex culture plates with a centrally located, rectangular type I collagen-coated culture strip (15.25 mm×24.18 mm) + vacuum	uniaxial	RT² Profiler PCR Array System (Superarray Bioscience Corp.) testing the expression of 79 genes encoding common cytokines	ARRAY	n.g.	n.g.
Qin and Hua (2016)	ALP	*ALPP*	hPDL cells (12-14/n.g., PM, n.g., P3-8, 1×10^6 cells/ml)	dynamic	0.5Hz (2s) for 1h, 3h, 6h	5%	n.g.	n.g.	not reported with reference to force (qPCR, GAPDH)		temporary decrease (WB, GAPDH)	1h: 0.03 (rel)* / 0.2 (ratio-calc)
Qin and Hua (2016)	Col-1	*COL1A1*	hPDL cells (12-14/n.g., PM, n.g., P3-8, 1×10^6 cells/ml)	dynamic	0.5Hz (2s) for 1h, 3h, 6h	5%	n.g.	n.g.	not reported with reference to force (qPCR, GAPDH)		increase (WB, GAPDH)	3h: 0.16 (rel)* / 3.2 (ratio-calc)
Qin and Hua (2016)	OCN	*BGLAP*	hPDL cells (12-14/n.g., PM, n.g., P3-8, 1×10^6 cells/ml)	dynamic	0.5Hz (2s) for 1h, 3h, 6h	5%	n.g.	n.g.	not reported with reference to force (qPCR, GAPDH)		temporary decrease followed by temporary increase (WB, GAPDH)	lowest @ 1h: 0.09 (rel)* / 0.7 (ratio-calc) highest @ 3h: 0.2 (rel)* / 1.5 (ratio-calc)
Rath-Deschner et al. (2009)	IGF1	*IGF1*	hPDL cells (n.g./n.g., n.g., exp, P3-5, 80% confluency)	static	qPCR for 4h, 24h; WB for 24h	3%, 20%	loading platform with cylindrical posts + collagen type I-coated BioFlex plates (Flexcells) + screws (Deschner et al 2007)	equibiaxial	3%: temporary increase (qPCR, GAPDH) 20%: decrease followed by plateau (qPCR, GAPDH)	3% @ 4h: 171.69% (rel) / 1.7 (ratio-calc) 20% @ 4h...24h: 54.42% (rel) / 0.5 (ratio-calc)	3%: increase (WB, β-actin) 20%: no change (WB, β-actin)	no quantitative information is given
Rath-Deschner et al. (2009)	IGF1R	*IGF1R*	hPDL cells (n.g./n.g., n.g., exp, P3-5, 80% confluency)	static	4h, 24h	3%, 20%	loading platform with cylindrical posts + collagen type I-coated BioFlex plates (Flexcells) + screws (Deschner et al 2007)	equibiaxial	3%: increase followed by plateau (qPCR, GAPDH) 20%: decrease (qPCR, GAPDH)	3% @ 4h: 115.72% (rel) / 1.2 (ratio-calc) 20% @ 24h: 82.97% (rel) / 0.8 (ratio-calc)	n.g.	n.g.
Rath-Deschner et al. (2009)	IGF2	*IGF2*	hPDL cells (n.g./n.g., n.g., exp, P3-5, 80% confluency)	static	4h, 24h	3%, 20%	loading platform with cylindrical posts + collagen type I-coated BioFlex plates (Flexcells) + screws (Deschner et al 2007)	equibiaxial	3%: increase followed by plateau (qPCR, GAPDH) 20%: decrease followed by plateau (qPCR, GAPDH)	3% @ 4h: 112.49% (rel) / 1.1 (ratio-calc) 20% @ 4h...24h: 82.97% (rel) / 0.8 (ratio-calc)	n.g.	n.g.
Rath-Deschner et al. (2009)	IGFBP1	*IGFBP1*	hPDL cells (n.g./n.g., n.g., exp, P3-5, 80% confluency)	static	qPCR for 4h, 24h; WB for 24h	3%, 20%	loading platform with cylindrical posts + collagen type I-coated BioFlex plates (Flexcells) + screws (Deschner et al 2007)	equibiaxial	3%: decrease followed by increase (qPCR, GAPDH) 20%: increase (qPCR, GAPDH)	3% lowest @ 4h: 65.99% (rel) / 0.7 (ratio-calc) 3% highest @ 24h: 144.50% (rel) / 1.4 (ratio-calc) 20% @ 24h: 291.49% (rel) / 2.9 (ratio-calc)	3%: no change (WB, β-actin) 20%: increase (WB, β-actin)	no quantitative information is given

[a] Entry given as reported in the study.
[b] All official gene symbols come from the HUGO Gene Nomenclature Committee (HGNC; URL: https://www.genenames.org) after checking specificity of primers with Primer-BLAST.
[c] Gender/Sex of donors: "M" – male, "F" – female; Tooth type: "PM" – premolar, "M" – molar; Cell density: given in cells/well if not otherwise mentioned.
[d] Frequencies labeled bold orange were converted to hertz (Hz) according to its definition using the information reported in the study (in brackets)
[e] Force type deduced from the description of the force apparatus given by the authors.
[f] Gene and protein expression: 1. conclusion of change (increase, decrease…) was given according to the defined criteria in Figure 2; 2. different markers to describe the amount of change; † Information derived from figures using Engauge Digitizer; *Folds calculated by measuring the graphs, without using the Engauge Digitizer; No makers: Information derived from figures by description in the articles

Reference	Gene/ Analyte[a]	Official gene symbol / abbreviation[b]	Cell (age/gender of donors, tooth type, isolation method, passages used, cell density)[a,c]	Force type (stat./ dyn.)[a]	Force duration and frequency[d]	Force magnitude[a]	Force apparatus[a]	Force type: equibiaxial or uniaxial[e]	Gene expression: Increase, decrease, no change (method w/ reference gene); Methods: qPCR, sqPCR, Northern blot[f]	Gene expression: When it reaches peak and peak's magnitude (fold change; times or ratio; unclear = ?)[f]	Protein expression: Increase, decrease, no change (method w/ reference); Methods: ELISA, WB, RIA, EMSA, IF[f]	Protein expression: When it reaches peak and peak's magnitude (times or ratio; unclear = ?)[f]
Rath-Deschner et al. (2009)	IGFBP3	*IGFBP3*	hPDL cells (n.g./n.g., n.g., exp, P3-5, 80% confluency)	static	qPCR for 4h, 24h; WB for 24h	3%, 20%	loading platform with cylindrical posts + collagen type I-coated BioFlexs plates (Flexcells) + screws (Deschner et al 2007)	equibiaxial	3%: decrease (qPCR, GAPDH) 20%: increase followed by decrease (qPCR, GAPDH)	3% @ 24h: 84.33% (rel) / 0.8 (ratio-calc) 20% @ highest at 4h:158.27% (rel) / 1.6 (ratio-calc) 20% lowest at 24h:75.80% (rel) / 0.8 (ratio-calc)	3%: no change (WB, β-actin) 20%: increase (WB, β-actin)	no quantitative information is given
Rath-Deschner et al. (2009)	IGFBP5	*IGFBP5*	hPDL cells (n.g./n.g., n.g., exp, P3-5, 80% confluency)	static	qPCR for 4h, 24h; WB for 24h	3%, 20%	loading platform with cylindrical posts + collagen type I-coated BioFlexs plates (Flexcells) + screws (Deschner et al 2007)	equibiaxial	3%: increase (qPCR, GAPDH) 20%: increase followed by decrease (qPCR, GAPDH)	3% @ 4h: 136.06% (rel) / 1.4 (ratio-calc) 20% @ highest at 4h:127.34% (rel) / 1.3 (ratio-calc) 20% @ lowest at 24h: 69.00% (rel) / 0.7 (ratio-calc)	3%: increase (WB, β-actin) 20%: no change (WB, β-actin)	no quantitative information is given
Rath-Deschner et al. (2009)	IRS1	*IRS1*	hPDL cells (n.g./n.g., n.g., exp, P3-5, 80% confluency)	static	4h, 24h	3%, 20%	loading platform with cylindrical posts + collagen type I-coated BioFlexs plates (Flexcells) + screws (Deschner et al 2007)	equibiaxial	3%: temporary decrease (qPCR, GAPDH) 20%: increase followed by decrease (qPCR, GAPDH)	3% @ 4h: 82.46% (rel) / 0.8 (ratio-calc) 20% highest at 4h: 112.39% (rel) / 1.1 (ratio-calc) 20% lowest at 24h: 86.49% (rel) / 0.9 (ratio-calc)	n.g.	n.g.
Rath-Deschner et al. (2009)	PCNA	*PCNA*	hPDL cells (n.g./n.g., n.g., exp, P3-5, 80% confluency)	static	4h, 24h, 48h	3%, 20%	loading platform with cylindrical posts + collagen type I-coated BioFlexs plates (Flexcells) + screws (Deschner et al 2007)	equibiaxial	3%: increase (qPCR, GAPDH) 20%: increase (qPCR, GAPDH)	3% @ 48h: 114.97% (rel) / 1.1 (ratio-calc) 20% @ 48h: 146.32% (rel) / 1.5 (ratio-calc)	n.g.	n.g.
Ren et al. (2015)	ATF4	*ATF4*	hPDL cells (12-18, PM, exp, P4-6, 80% confluency)	dynamic	0.5Hz for 1h, 3h, 6h, 12h, 18h, 24h	10%	Flexercell FX-4000 Strain Unit + six-well 35mm silicone membrane culture plates coated with type I collagen + vacuum	equibiaxial	increase (qPCR, GAPDH)	1h: 1.7 (FC)*	n.g.	n.g.
Ren et al. (2015)	BSP	*IBSP*	hPDL cells (12-18, PM, exp, P4-6, 80% confluency)	dynamic	0.5Hz for 1h, 3h, 6h, 12h, 18h, 24h	10%	Flexercell FX-4000 Strain Unit + six-well 35mm silicone membrane culture plates coated with type I collagen + vacuum	equibiaxial	increase (qPCR, GAPDH)	24h: 3.2 (FC)*	n.g.	n.g.
Ren et al. (2015)	ERK1/2 / p-ERK1/2	MAPK3; MAPK1	hPDL cells (12-18, PM, exp, P4-6, 80% confluency)	dynamic	0.5Hz for 1h, 3h, 6h, 12h, 18h, 24h	10%	Flexercell FX-4000 Strain Unit + six-well 35mm silicone membrane culture plates coated with type I collagen + vacuum	equibiaxial	n.g.	n.g.	ERK1/2: no change (WB, GAPDH) p-ERK1/2: increase (WB, GAPDH)	ERK1/2: no quantitative information is given p-ERK1/2: 3h: 0.7 (rel)* / 6.2 (ratio-calc)
Ren et al. (2015)	OCN	*BGLAP*	hPDL cells (12-18, PM, exp, P4-6, 80% confluency)	dynamic	0.5Hz for 1h, 3h, 6h, 12h, 18h, 24h	10%	Flexercell FX-4000 Strain Unit + six-well 35mm silicone membrane culture plates coated with type I collagen + vacuum	equibiaxial	increase followed by plateau (qPCR, GAPDH)	18…24h: 1.5 (FC)*	n.g.	n.g.
Ren et al. (2015)	RUNX2 / p-RUNX2	*RUNX2*	hPDL cells (12-18, PM, exp, P4-6, 80% confluency)	dynamic	0.5Hz for 1h, 3h, 6h, 12h, 18h, 24h	10%	Flexercell FX-4000 Strain Unit + six-well 35mm silicone membrane culture plates coated with type I collagen + vacuum	equibiaxial	RUNX2: increase (qPCR, GAPDH)	RUNX2 @ 3h: 2.9 (FC)*	RUNX2: temporary increase followed by plateau then temporary decrease (WB, GAPDH) p-RUNX2: increase followed by plateau (WB, GAPDH)	RUNX2: highest @ 3h…6h: 0.7 (rel)† / 1.9 (ratio-calc) RUNX2: lowest @12h: 0.2 (rel)† / 0.6 (ratio-calc) p-RUNX2 @ 3h…6h: 0.4 (rel)* / 9.5 (ratio-calc)
Ren et al. (2015)	SP7	*SP7*	hPDL cells (12-18, PM, exp, P4-6, 80% confluency)	dynamic	0.5Hz for 1h, 3h, 6h, 12h, 18h, 24h	10%	Flexercell FX-4000 Strain Unit + six-well 35mm silicone membrane culture plates coated with type I collagen + vacuum	equibiaxial	increase (qPCR, GAPDH)	12h: 4.3 (FC)*	n.g.	n.g.
Ritter et al. (2007)	ARRAY	ARRAY	hPDL cells (12-14/n.g., PM, exp, P3-6, near-confluence)	static	6h	2.5%	Petriperm dish + template made of brass + weight (Saito et al 1991)	equibiaxial	apoptosis and NFκ-B pathway GEArray Q Series kit (SuperArray, Bethesda, Md.)	ARRAY		
Ritter et al. (2007)	BAD	*BAD*	hPDL cells (12-14/n.g., PM, exp, P3-6, near-confluence)	static	6h	2.5%	Petriperm dish + template made of brass + weight (Saito et al 1991)	equibiaxial	increase (qPCR, β-actin)	5.2 (FC)	n.g.	n.g.
Ritter et al. (2007)	CRADD	*CRADD*	hPDL cells (12-14/n.g., PM, exp, P3-6, near-confluence)	static	6h	2.5%	Petriperm dish + template made of brass + weight (Saito et al. 1991)	equibiaxial	increase (qPCR, β-actin)	2.1 (FC)	n.g.	n.g.
Ritter et al. (2007)	FAS	*FAS*	hPDL cells (12-14/n.g., PM, exp, P3-6, near-confluence)	static	6h	2.5%	Petriperm dish + template made of brass + weight (Saito et al. 1991)	equibiaxial	increase (qPCR, β-actin)	2.0 (FC)	n.g.	n.g.
Ritter et al. (2007)	IL1β	*IL1B*	hPDL cells (12-14/n.g., PM, exp, P3-6, near-confluence)	static	6h	2.5%	Petriperm dish + template made of brass + weight (Saito et al. 1991)	equibiaxial	increase (qPCR, β-actin)	5.8 (FC)	n.g.	n.g.
Ritter et al. (2007)	NFkB	*NFKB1*	hPDL cells (12-14/n.g., PM, exp, P3-6, near-confluence)	static	6h	2.5%	Petriperm dish + template made of brass + weight (Saito et al. 1991)	equibiaxial	increase (qPCR, β-actin)	1.7 (FC)	n.g.	n.g.
Saminathan et al. (2012)	ARRAY	ARRAY	hPDL cells (n.g./n.g., n.g., exp, P3-4, confluence)	dynamic	**0.01Hz (1/95Hz)** (square waveform: 5s (0.2Hz) every 90s) for 6h, 12h, 24h	12%	Flexercell FX-4000 strain unit + six-well, 35 mm flexible-bottomed UniFlex® Series culture plates containing a centrally located rectangular strip (15.25×24.18 mm) coated with type I collagen + vacuum	uniaxial	extracellular matrix and adhesion molecules using the RT² Profiler PCR Array System (SABiosciences)	ARRAY	n.g.	n.g.
Saminathan et al. (2012)	Caspases 3/7 (combined assay)	*CASP3; CASP7*	hPDL cells (n.g./n.g., n.g., exp, P3-4, confluence)	dynamic	**0.01Hz (1/95Hz)** (square waveform: 5s (0.2Hz) every 90s) for 6h, 12h, 24h	12%	Flexercell FX-4000 strain unit + six-well, 35 mm flexible-bottomed UniFlex® Series culture plates containing a centrally located rectangular strip (15.25×24.18 mm) coated with type I collagen + vacuum	uniaxial	n.g.	n.g.	decrease (Caspase-Glo 3/7 Assay)	6h: 100.87 ($RLU \times 10^3$) / 0.9 (ratio-calc)
Shen et al. (2014)	ALP	*ALPP*	hPDLSC cells (12-24/n.g., PM, dig, P4-6, 100% confluence)	dynamic	0.1Hz for 6h, 12h, 24h	12%	Flexcell FX-4000T Tension Plus System + 6-well, flexible-bottomed culture plate coated with type I collagen (Sigma)+ vacuum	equibiaxial	increase (qPCR, β-actin)	24h: 13.8 (rel)* / 2.5 (ratio-calc)	increase (WB, GAPDH)	24h: 347.2 (rel)* / 1.5 (ratio-calc)
Shen et al. (2014)	CD146	*MCAM*	hPDLSC cells (12-24/n.g., PM, dig, P4-6, 100% confluence)	dynamic	0.1Hz for 6h, 12h, 24h	12%	Flexcell FX-4000T Tension Plus System + 6-well, flexible-bottomed culture plate coated with type I collagen (Sigma)+ vacuum	equibiaxial	decrease (qPCR, β-actin)	24h: 1.2 (rel)* / 0.4 (ratio-calc)	decrease (WB, GAPDH)	24h: 158.5 (rel) * / 0.8 (ratio-calc)

[a] Entry given as reported in the study.
[b] All official gene symbols come from the HUGO Gene Nomenclature Committee (HGNC; URL: https://www.genenames.org) after checking specificity of primers with Primer-BLAST.
[c] Gender/Sex of donors: "M" – male, "F" – female; Tooth type: "PM" – premolar, "M" – molar; Cell density: given in cells/well if not otherwise mentioned.
[d] Frequencies labeled bold orange were converted to hertz (Hz) according to its definition using the information reported in the study (in brackets)
[e] Force type deduced from the description of the force apparatus given by the authors.
[f] Gene and protein expression: 1. conclusion of change (increase, decrease…) was given according to the defined criteria in Figure 2; 2. different markers to describe the amount of change; † Information derived from figures using Engauge Digitizer; *Folds calculated by measuring the graphs, without using the Engauge Digitizer; No makers: Information derived from figures by description in the articles

Reference	Gene/ Analyte[a]	Official gene symbol / abbreviation[b]	Cell (age/gender of donors, tooth type, isolation method, passages used, cell density)[a,c]	Force type (stat./ dyn.)[a]	Force duration and frequency[d]	Force magnitude[a]	Force apparatus[a]	Force type: equibiaxial or uniaxial[e]	Gene expression: Increase, decrease, no change (method w/ reference gene); Methods: qPCR, sqPCR, Northern blot[f]	Gene expression: When it reaches peak and peak's magnitude (fold change; times or ratio; unclear = ?)[f]	Protein expression: Increase, decrease, no change (method w/ reference); Methods: ELISA, WB, RIA, EMSA, IF[f]	Protein expression: When it reaches peak and peak's magnitude (times or ratio; unclear = ?)[f]
Shen et al. (2014)	OCN	*BGLAP*	hPDLSC cells (12-24/n.g., PM, dig, P4-6, 100% confluence)	dynamic	0.1Hz for 6h, 12h, 24h	12%	Flexcell FX-4000T Tension Plus System + 6-well, flexible-bottomed culture plate coated with type I collagen (Sigma)+ vacuum	equibiaxial	increase (qPCR, β-actin)	24h: 10.5 (rel)* / 2.6 (ratio-calc)	increase (WB, GAPDH)	24h: 279.2 (rel) * / 1.5 (ratio-calc)
Shen et al. (2014)	Runx2	*RUNX2*	hPDLSC cells (12-24/n.g., PM, dig, P4-6, 100% confluence)	dynamic	0.1Hz for 6h, 12h, 24h	12%	Flexcell FX-4000T Tension Plus System + 6-well, flexible-bottomed culture plate coated with type I collagen (Sigma)+ vacuum	equibiaxial	increase (qPCR, β-actin)	24h: 13.5 (rel)* / 3.4 (ratio-calc)	increase (WB, GAPDH)	24h: 415.1 (rel)* / 1.3 (ratio-calc)
Shimizu et al. (1994)	IL-1β	*IL1B*	hPDL cells (12/M, PM, exp, P4, confluent)	dynamic	**0.1Hz** (6cyc/min) for 1d, 3d, 5d	9%, 18%	Flexercell Strain Unit + flexible bottomed culture plates (Flexcell Corp) + vacuum	equibiaxial	n.g.	n.g.	9%: increase followed by plateau (RIA) 18%: increase followed by plateau (RIA)	9% @ 3d…5d: 27.9 (fmol/10^5 cells)* / 1.2 (ratio-calc) 18% @ 3d…5d: 42.3 (fmol/10^5 cells)* / 1.8 (ratio-calc)
Shimizu et al. (1995)	IL-1β	*IL1B*	hPDL cells (12/M, PM, exp, P4, confluent)	dynamic	**0.1Hz** (6cyc/min) for 1d, 3d, 5d	18%	Flexercell Strain Unit + flexible bottomed culture plates (Flexcell Corp) + vacuum	equibiaxial	n.g.	n.g.	increase followed by plateau (radioactivity)	3d...5d: 54.1 (fmol/10^5 cells)* / 2.1 (ratio-calc)
Shimizu et al. (1995)	PGE_2	PGE_2	hPDL cells (12/M, PM, exp, P4, confluent)	dynamic	**0.1Hz** (6cyc/min) for 1d, 3d, 5d	18%	Flexercell Strain Unit + flexible bottomed culture plates (Flexcell Corp) + vacuum	equibiaxial	n.a.	n.a.	increase (RIA)	5d: 7.9 (ng/10^6 cells)* / 19.8 (ratio-calc)
Shimizu et al. (1997)	ICE	*CASP1*	hPDL cells (18/F, 19/F, 23/F, PM, exp, P5-6 and P18-20, n.g.)	dynamic	**0.1Hz** (6cyc/min) for 3d	9%, 18%	Flexcell strain unit + flexible-bottomed culture plates + vacuum (Shimizu 1994; further reference to Banes 1985)	equibiaxial	"young cells" (P5-6): no change (sqPCR, GAPDH) "old cells" (P18-20): no change (sqPCR, GAPDH)	no quantitative information is given	n.g.	n.g.
Shimizu et al. (1997)	IL-1β	*IL1B*	hPDL cells (18/F, 19/F, 23/F, PM, exp, P5-6 and P18-20, n.g.)	dynamic	**0.1Hz** (6cyc/min) RIA for 1d, 3d, 5d sqPCR for 3d	18%	Flexcell strain unit + flexible-bottomed culture plates + vacuum (Shimizu 1994; further reference to Banes 1985)	equibiaxial	"young cells" (P5-6): increase (sqPCR, GAPDH) "old cells" (P18-20): increase (sqPCR, GAPDH)	no quantitative information is given	"young cells": increase followed by plateau (RIA) "old cells" increase (RIA)	"young cells" @ 3d…5d: 40 (fmol/10^5 cells)* / 2.1 (ratio-calc) "old cells" @ 5d: 60 (fmol/10^5 cells)* / 3 (ratio-calc)
Shimizu et al. (1997)	IL-1β	*IL1B*	hPDL cells (18/F, 19/F, 23/F, PM, exp, P5-6 and P18-20, n.g.)	dynamic	**0.1Hz** (6cyc/min) for 5d	9%, 18%	Flexcell strain unit + flexible-bottomed culture plates + vacuum (Shimizu 1994; further reference to Banes 1985)	equibiaxial	n.g.	n.g.	"young cells" (P5-6): increase (RIA) "old cells" (P18-20): increase (RIA)	"young cells" @ 18%: 41.6 (fmol/10^5 cells)* / 2.1 (ratio-calc) "old cells" @ 18%: 61.3 (fmol/10^5 cells)* / 3.1 (ratio-calc)
Shimizu et al. (1997)	IL-1β	*IL1B*	hPDL cells (18/F, 19/F, 23/F, PM, exp, P5-6 and P18-20, n.g.)	dynamic	**0.1Hz** (6cyc/min) for 5d	n.g.	Flexcell strain unit + flexible-bottomed culture plates + vacuum (Shimizu 1994; further reference to Banes 1985)	equibiaxial	n.g.	n.g.	Donor 1, "young cells" (P5-6): increase (RIA) Donor 1, "old cells" (P18-20): increase (RIA) Donor 2, "young cells" (P5-6): increase (RIA) Donor 2, "old cells" (P18-20): increase (RIA) Donor 3, "young cells" (P5-6): increase (RIA) Donor 3, "old cells" (P18-20): increase (RIA)	Donor 1, "young cells": 39.8 (fmol/10^5 cells)† / 2.1 (ratio-calc) Donor 1, "old cells" 60.2 (fmol/10^5 cells)† / 3.0 (ratio-calc) Donor 2, "young cells": 35.0 (fmol/10^5 cells)† / 2.4 (ratio-calc) Donor 2, "old cells": 51.7 (fmol/10^5 cells)† / 3.3 (ratio-calc) Donor 3, "young cells": 39.3 (fmol/10^5 cells)† / 2.2 (ratio-calc) Donor 3, "old cells": 55.3 (fmol/10^5 cells)† / 3.2 (ratio-calc)
Shimizu et al. (1998)	COX-1	*PTGS1*	hPDL cells (12/M, PM, exp, P5, confluent)	dynamic	**0.1Hz** (6cyc/min) for 3d	18%	vacuum unit from Flexcell Corporation	equibiaxial	no change (sqPCR, GAPDH)	no quantitative information is given	n.g.	n.g.
Shimizu et al. (1998)	COX-2	*PTGS2*	hPDL cells (12/M, PM, exp, P5, confluent)	dynamic	**0.1Hz** (6cyc/min) for 6h, 24h, 3d, 5d	18%	Flexcell strain unit + flexible-bottomed culture plates + vacuum (Shimizu 1994; further reference to Banes 1985)	equibiaxial	increase (sqPCR, GAPDH)	no quantitative information is given	n.g.	n.g.
Shimizu et al. (1998)	PGE_2	PGE_2	hPDL cells (12/M, PM, exp, P5, confluent)	dynamic	**0.1Hz** (6cyc/min) for 1d, 2d, 3d, 4d, 5d	18%	vacuum unit from Flexcell Corporation	equibiaxial	n.a.	n.a.	increase (RIA)	5d: 9.1(ng/10^6 cells) / 10.1 (ratio-calc)
Spencer and Lallier (2009)	OPG	*TNFRSF11B*	hPDL cells (16-35/n.g., n.g., n.g., P8-15, n.g.)	static	12h	10%	Petriperm dish + two pieces of acrylic + screws	equibiaxial	increase (sqPCR, S15rRNA)	2.3 (ratio)*	n.g.	n.g.
Spencer and Lallier (2009)	Plexin A1	*PLXNA1*	hPDL cells (16-35/n.g., n.g., n.g., P8-15, n.g.)	static	12h	10%	Petriperm dish + two pieces of acrylic + screws	equibiaxial	decrease (sqPCR, S15rRNA)	0.3 (ratio)*	n.g.	n.g.
Spencer and Lallier (2009)	Plexin B1	*PLXNB1*	hPDL cells (16-35/n.g., n.g., n.g., P8-15, n.g.)	static	12h	10%	Petriperm dish + two pieces of acrylic + screws	equibiaxial	no change (sqPCR, S15rRNA)		n.g.	n.g.
Spencer and Lallier (2009)	Plexin C1	*PLXNC1*	hPDL cells (16-35/n.g., n.g., n.g., P8-15, n.g.)	static	12h	10%	Petriperm dish + two pieces of acrylic + screws	equibiaxial	increase (sqPCR, S15rRNA)	3.5 (ratio)*	n.g.	n.g.
Spencer and Lallier (2009)	RANKL	*TNFSF11*	hPDL cells (16-35/n.g., n.g., n.g., P8-15, n.g.)	static	12h	10%	Petriperm dish + two pieces of acrylic + screws	equibiaxial	decrease (sqPCR, S15rRNA)	0.2 (ratio)*	n.g.	n.g.
Spencer and Lallier (2009)	rRNA S15	*RPS15*	hPDL cells (16-35/n.g., n.g., n.g., P8-15, n.g.)	static	12h	10%	Petriperm dish + two pieces of acrylic + screws	equibiaxial	no change (sqPCR, S15rRNA)		n.g.	n.g.
Spencer and Lallier (2009)	Sem3A	*SEMA3A*	hPDL cells (16-35/n.g., n.g., n.g., P8-15, n.g.)	static	12h	10%	Petriperm dish + two pieces of acrylic + screws	equibiaxial	no change (sqPCR, S15rRNA)		n.g.	n.g.
Spencer and Lallier (2009)	Sem3C	*SEMA3C*	hPDL cells (16-35/n.g., n.g., n.g., P8-15, n.g.)	static	12h	10%	Petriperm dish + two pieces of acrylic + screws	equibiaxial	no change (sqPCR, S15rRNA)		n.g.	n.g.
Spencer and Lallier (2009)	Sem3D	*SEMA3D*	hPDL cells (16-35/n.g., n.g., n.g., P8-15, n.g.)	static	12h	10%	Petriperm dish + two pieces of acrylic + screws	equibiaxial	increase (sqPCR, S15rRNA)	22 (ratio)*	n.g.	n.g.
Spencer and Lallier (2009)	Sem3E	*SEMA3E*	hPDL cells (16-35/n.g., n.g., n.g., P8-15, n.g.)	static	12h	10%	Petriperm dish + two pieces of acrylic + screws	equibiaxial	no change (sqPCR, S15rRNA)		n.g.	n.g.
Spencer and Lallier (2009)	Sem4A	*SEMA4A*	hPDL cells (16-35/n.g., n.g., n.g., P8-15, n.g.)	static	12h	10%	Petriperm dish + two pieces of acrylic + screws	equibiaxial	no change (sqPCR, S15rRNA)		n.g.	n.g.

[a] Entry given as reported in the study.
[b] All official gene symbols come from the HUGO Gene Nomenclature Committee (HGNC; URL: https://www.genenames.org) after checking specificity of primers with Primer-BLAST.
[c] Gender/Sex of donors: "M" – male, "F" – female; Tooth type: "PM" – premolar, "M" – molar; Cell density: given in cells/well if not otherwise mentioned.
[d] Frequencies labeled bold orange were converted to hertz (Hz) according to its definition using the information reported in the study (in brackets)
[e] Force type deduced from the description of the force apparatus given by the authors.
[f] Gene and protein expression: 1. conclusion of change (increase, decrease…) was given according to the defined criteria in Figure 2; 2. different markers to describe the amount of change; † Information derived from figures using Engauge Digitizer; *Folds calculated by measuring the graphs, without using the Engauge Digitizer; No makers: Information derived from figures by description in the articles

Reference	Gene/ Analyte[a]	Official gene symbol / abbreviation[b]	Cell (age/gender of donors, tooth type, isolation method, passages used, cell density)[a,c]	Force type (stat./ dyn.)[a]	Force duration and frequency[d]	Force magnitude[a]	Force apparatus[a]	Force type: equibiaxial or uniaxial[e]	Gene expression: Increase, decrease, no change (method w/ reference gene); Methods: qPCR, sqPCR, Northern blot[f]	Gene expression: When it reaches peak and peak's magnitude (fold change; times or ratio; unclear = ?)[f]	Protein expression: Increase, decrease, no change (method w/ reference); Methods: ELISA, WB, RIA, EMSA, IF[f]	Protein expression: When it reaches peak and peak's magnitude (times or ratio; unclear = ?)[f]
Spencer and Lallier (2009)	Sem4C	*SEMA4C*	hPDL cells (16-35/n.g., n.g., n.g., P8-15, n.g.)	static	12h	10%	Petriperm dish + two pieces of acrylic + screws	equibiaxial	no change (sqPCR, S15rRNA)		n.g.	n.g.
Spencer and Lallier (2009)	Sem4D	*SEMA4D*	hPDL cells (16-35/n.g., n.g., n.g., P8-15, n.g.)	static	12h	10%	Petriperm dish + two pieces of acrylic + screws	equibiaxial	no change (sqPCR, S15rRNA)		n.g.	n.g.
Spencer and Lallier (2009)	Sem4F	*SEMA4F*	hPDL cells (16-35/n.g., n.g., n.g., P8-15, n.g.)	static	12h	10%	Petriperm dish + two pieces of acrylic + screws	equibiaxial	no change (sqPCR, S15rRNA)		n.g.	n.g.
Spencer and Lallier (2009)	Sem5A	*SEMA5A*	hPDL cells (16-35/n.g., n.g., n.g., P8-15, n.g.)	static	12h	10%	Petriperm dish + two pieces of acrylic + screws	equibiaxial	no change (sqPCR, S15rRNA)		n.g.	n.g.
Spencer and Lallier (2009)	Sem5B	*SEMA5B*	hPDL cells (16-35/n.g., n.g., n.g., P8-15, n.g.)	static	12h	10%	Petriperm dish + two pieces of acrylic + screws	equibiaxial	increase (sqPCR, S15rRNA)	8 (ratio)*	n.g.	n.g.
Spencer and Lallier (2009)	Sem6B	*SEMA6B*	hPDL cells (16-35/n.g., n.g., n.g., P8-15, n.g.)	static	12h	10%	Petriperm dish + two pieces of acrylic + screws	equibiaxial	no change (sqPCR, S15rRNA)		n.g.	n.g.
Spencer and Lallier (2009)	Sem6C	*SEMA6C*	hPDL cells (16-35/n.g., n.g., n.g., P8-15, n.g.)	static	12h	10%	Petriperm dish + two pieces of acrylic + screws	equibiaxial	no change (sqPCR, S15rRNA)		n.g.	n.g.
Spencer and Lallier (2009)	Sem7A	*SEMA7A*	hPDL cells (16-35/n.g., n.g., n.g., P8-15, n.g.)	static	12h	10%	Petriperm dish + two pieces of acrylic + screws	equibiaxial	decrease (sqPCR, S15rRNA)	0.07 (ratio)*	n.g.	n.g.
Spencer and Lallier (2009)	B1 integrin	*ITGB1*	hPDL cells (16-35/n.g., n.g., n.g., P8-15, n.g.)	static	12h	10%	Petriperm dish + two pieces of acrylic + screws	equibiaxial	no change (sqPCR, S15rRNA)		n.g.	n.g.
Steinberg et al. (2011)	MAP4	*MAP4*	hPDL cells (14/n.g., PM, exp, P6-10, 75-85% confluence)	static	6h, 12h, 18h, 24h	2.5%	Lumox culture dishes (Greiner Bio-One) + template with convex surface + weight (Hasegawa et al 1985)	equibiaxial	n.g.	n.g.	temporary decrease (WB)	6h: 36% (% of control) / 0.4 (ratio-calc)
Steinberg et al. (2011)	Myo IC, cytoplasmic	*MYO1C*	hPDL cells (14/n.g., PM, exp, P6-10, 75-85% confluence)	static	6h, 12h, 18h, 24h	2.5%	Lumox culture dishes (Greiner Bio-One) + template with convex surface + weight (Hasegawa et al 1985)	equibiaxial	n.g.	n.g.	increase (WB)	18h: 257% (% of control) / 2.6 (ratio-calc)
Steinberg et al. (2011)	NM1	*MYO1C*	hPDL cells (14/n.g., PM, exp, P6-10, 75-85% confluence)	static	6h, 12h, 18h, 24h	2.5%	Lumox culture dishes (Greiner Bio-One) + template with convex surface + weight (Hasegawa et al 1985)	equibiaxial	n.g.	n.g.	decrease (WB)	18h: 42% (% of control) / 0.4 (ratio-calc)
Steinberg et al. (2011)	PROTEOMICS	PROTEOMICS	hPDL cells (14/n.g., PM, exp, P6-10, 75-85% confluence)	static	3h, 6h, 12h	2.5%	Lumox culture dishes (Greiner Bio-One) + template with convex surface + weight (Hasegawa et al 1985)	equibiaxial	n.a.	n.a.	1D-SDS-PAGE of subcellular protein fractions; LC-ESI-MS/MS; MASCOT search	
Steinberg et al. (2011)	Talin	*TLN1; TLN2*	hPDL cells (14/n.g., PM, exp, P6-10, 75-85% confluence)	static	6h, 12h, 18h, 24h	2.5%	Lumox culture dishes (Greiner Bio-One) + template with convex surface + weight (Hasegawa et al 1985)	equibiaxial	n.g.	n.g.	temporary decrease (WB)	6h: 53% (% of control) / 0.5 (ratio-calc)
Sun et al. (2016)	COL1	*COL1A1*	hPDL cells (18/M, 20/M, 20/F, 24/F, PM and M, dig, P3-5, confluency)	dynamic	0.5Hz for 4h per day for 1d, 5d	12%	FX-5000T Flexcell Tension Plus unit + Bioflex Flexcell + vacuum	uniaxial	temporary decrease (qPCR, GAPDH)	1d: 0.7 (ratio)*	decrease (WB, GAPDH)	1d: 0.6 (ratio)*
Sun et al. (2016)	IL-1β	*IL1B*	hPDL cells (18/M, 20/M, 20/F, 24/F, PM and M, dig, P3-5, confluency)	dynamic	0.5Hz for 4h per day for 1d, 5d	12%	FX-5000T Flexcell Tension Plus unit + Bioflex Flexcell + vacuum	uniaxial	n.g.	n.g.	increase (ELISA)	5d: 53 (pg/ml)* / control not detectable
Sun et al. (2016)	RUNX2	*RUNX2*	hPDL cells (18/M, 20/M, 20/F, 24/F, PM and M, dig, P3-5, confluency)	dynamic	0.5Hz for 4h per day for 1d, 5d	12%	FX-5000T Flexcell Tension Plus unit + Bioflex Flexcell + vacuum	uniaxial	increase followed by decrease (qPCR, GAPDH)	highest @ 1d: 2.0 (ratio)* lowest @ 5d: 0.9 (ratio)*	increase followed by decrease (WB, GAPDH)	highest @ 1d: 1.5 (ratio)* lowest @ 5d: 0.8 (ratio)*
Sun et al. (2016)	TNF-α	*TNF*	hPDL cells (18/M, 20/M, 20/F, 24/F, PM and M, dig, P3-5, confluency)	dynamic	0.5Hz for 4h per day for 1d, 5d	12%	FX-5000T Flexcell Tension Plus unit + Bioflex Flexcell + vacuum	uniaxial	n.g.	n.g.	increase (ELISA)	5d: 41 (pg/ml)* / control not detectable
Sun et al. (2017)	COL1	*COL1A1*	hPDL cells (18-28/n.g., n.g., dig, P3-5, 70-80% confluence)	dynamic	0.5Hz for 12h, 24h, 48h	12%	FX-5000T™ Flexercell Tension Plus™ + COL-I-coated silicone Bioflex® culture plates + vacuum	uniaxial	decrease (qPCR, GAPDH)	24h: 0.5 (ratio)*	decrease (WB,GAPDH)	24h: 0.4 (ratio)*
Sun et al. (2017)	IL-1β	*IL1B*	hPDL cells (18-28/n.g., n.g., dig, P3-5, 70-80% confluence)	dynamic	0.5Hz for 12h, 24h, 48h	12%	FX-5000T™ Flexercell Tension Plus™ + COL-I-coated silicone Bioflex® culture plates + vacuum	uniaxial	n.g.	n.g.	increase (ELISA)	48h: 89.76 (pg/ml) / 89.8 (ratio-calc)
Sun et al. (2017)	RUNX2	*RUNX2*	hPDL cells (18-28/n.g., n.g., dig, P3-5, 70-80% confluence)	dynamic	0.5Hz for 12h, 24h, 48h	12%	FX-5000T™ Flexercell Tension Plus™ + COL-I-coated silicone Bioflex® culture plates + vacuum	uniaxial	temporary decrease (qPCR, GAPDH)	12h: 0.5 (ratio)	temporary decrease (WB,GAPDH)	12h: 0.8 (ratio)*
Sun et al. (2017)	TNF-α	*TNF*	hPDL cells (18-28/n.g., n.g., dig, P3-5, 70-80% confluence)	dynamic	0.5Hz for 12h, 24h, 48h	12%	FX-5000T™ Flexercell Tension Plus™ + COL-I-coated silicone Bioflex® culture plates + vacuum	uniaxial	n.g.	n.g.	increase (ELISA)	48h: 77.52 (pg/ml) / 77.5 (ratio-calc)
Suzuki et al. (2014)	BMP-2	*BMP2*	hPDL cells (19-29/n.g., M, n.g., P3-10, confluent)	dynamic	**0.017Hz** (1/60Hz) for 6h	3%, 5%, 10%	STB-140 STREX cell stretch system (Strex Co) + silicone resin chamber (size 32×32 mm, STB-CH-10.0, Strex Co.) + motor	uniaxial	increase (qPCR, GAPDH)	10%: 5.3 (ratio)*	n.g.	n.g.
Suzuki et al. (2014)	BMP-2	*BMP2*	hPDL cells (19-29/n.g., M, n.g., P3-10, confluent)	dynamic	**0.017Hz** (1/60Hz) for 6h, 12h, 24h	5%	STB-140 STREX cell stretch system (Strex Co) + silicone resin chamber (size 32×32 mm, STB-CH-10.0, Strex Co.) + motor	uniaxial	increase (qPCR, GAPDH)	6h: 5 (ratio)*	n.g.	n.g.
Suzuki et al. (2014)	BMP-4	*BMP4*	hPDL cells (19-29/n.g., M, n.g., P3-10, confluent)	dynamic	**0.017Hz** (1/60Hz) for 6h	5%	STB-140 STREX cell stretch system (Strex Co) + silicone resin chamber (size 32×32 mm, STB-CH-10.0, Strex Co.) + motor	uniaxial	increase (qPCR, GAPDH)	1.3 (ratio)*	n.g.	n.g.
Suzuki et al. (2014)	COX-2	*PTGS2*	hPDL cells (19-29/n.g., M, n.g., P3-10, confluent)	dynamic	**0.017Hz** (1/60Hz) for 6h	5%	STB-140 STREX cell stretch system (Strex Co) + silicone resin chamber (size 32×32 mm, STB-CH-10.0, Strex Co.) + motor	uniaxial	increase (qPCR, GAPDH)	6h: 66.3 (rel)* / 25.2 (ratio-calc)	n.g.	n.g.
Suzuki et al. (2014)	EP1	*PTGER1*	hPDL cells (19-29/n.g., M, n.g., P3-10, confluent)	dynamic	**0.017Hz** (1/60Hz) for 6h	5%	STB-140 STREX cell stretch system (Strex Co) + silicone resin chamber (size 32×32 mm, STB-CH-10.0, Strex Co.) + motor	uniaxial	not detectable (sqPCR, GAPDH)		n.g.	n.g.

[a] Entry given as reported in the study.
[b] All official gene symbols come from the HUGO Gene Nomenclature Committee (HGNC; URL: https://www.genenames.org) after checking specificity of primers with Primer-BLAST.
[c] Gender/Sex of donors: "M" – male, "F" – female; Tooth type: "PM" – premolar, "M" – molar; Cell density: given in cells/well if not otherwise mentioned.
[d] Frequencies labeled bold orange were converted to hertz (Hz) according to its definition using the information reported in the study (in brackets)
[e] Force type deduced from the description of the force apparatus given by the authors.
[f] Gene and protein expression: 1. conclusion of change (increase, decrease…) was given according to the defined criteria in Figure 2; 2. different markers to describe the amount of change; † Information derived from figures using Engauge Digitizer; *Folds calculated by measuring the graphs, without using the Engauge Digitizer; No makers: Information derived from figures by description in the articles

Reference	Gene/ Analyte[a]	Official gene symbol / abbreviation[b]	Cell (age/gender of donors, tooth type, isolation method, passages used, cell density)[a,c]	Force type (stat./ dyn.)[a]	Force duration and frequency[d]	Force magnitude[a]	Force apparatus[a]	Force type: equibiaxial or uniaxial[e]	Gene expression: Increase, decrease, no change (method w/ reference gene); Methods: qPCR, sqPCR, Northern blot[f]	Gene expression: When it reaches peak and peak's magnitude (fold change; times or ratio; unclear = ?)[f]	Protein expression: Increase, decrease, no change (method w/ reference); Methods: ELISA, WB, RIA, EMSA, IF[f]	Protein expression: When it reaches peak and peak's magnitude (times or ratio; unclear = ?)[f]
Suzuki et al. (2014)	EP2	*PTGER2*	hPDL cells (19-29/n.g., M, n.g., P3-10, confluent)	dynamic	**0.017Hz** (1/60Hz) for 6h	5%	STB-140 STREX cell stretch system (Strex Co) + silicone resin chamber (size 32×32 mm, STB-CH-10.0, Strex Co.) + motor	uniaxial	increase (sqPCR, GAPDH)	1.6 (ratio)*	n.g.	n.g.
Suzuki et al. (2014)	EP3	*PTGER3*	hPDL cells (19-29/n.g., M, n.g., P3-10, confluent)	dynamic	**0.017Hz** (1/60Hz) for 6h	5%	STB-140 STREX cell stretch system (Strex Co) + silicone resin chamber (size 32×32 mm, STB-CH-10.0, Strex Co.) + motor	uniaxial	no change (sqPCR, GAPDH)		n.g.	n.g.
Suzuki et al. (2014)	EP4	*PTGER4*	hPDL cells (19-29/n.g., M, n.g., P3-10, confluent)	dynamic	**0.017Hz** (1/60Hz) for 6h	5%	STB-140 STREX cell stretch system (Strex Co) + silicone resin chamber (size 32×32 mm, STB-CH-10.0, Strex Co.) + motor	uniaxial	increase (sqPCR, GAPDH)	3.6 (ratio)*	n.g.	n.g.
Suzuki et al. (2014)	ERK1/2 / p-ERK1/2	MAPK3; MAPK1	hPDL cells (19-29/n.g., M, n.g., P3-10, confluent)	dynamic	**0.017Hz** (1/60Hz) for 15min, 45min	5%	STB-140 STREX cell stretch system (Strex Co) + silicone resin chamber (size 32×32 mm, STB-CH-10.0, Strex Co.) + motor	uniaxial	n.g.	n.g.	ERK1/2: no change (WB) p-ERK1/2: increase (WB)	ERK1/2: no quantitative information is given p-ERK1/2 @ 45min: 6.3 (rel)* / 3.9 (ratio-calc)
Suzuki et al. (2014)	IGF-1	*IGF1*	hPDL cells (19-29/n.g., M, n.g., P3-10, confluent)	dynamic	**0.017Hz** (1/60Hz) for 6h	5%	STB-140 STREX cell stretch system (Strex Co) + silicone resin chamber (size 32×32 mm, STB-CH-10.0, Strex Co.) + motor	uniaxial	decrease (qPCR, GAPDH)	0.4 (ratio)*	n.g.	n.g.
Suzuki et al. (2014)	JNK / p-JNK	*MAPK8*	hPDL cells (19-29/n.g., M, n.g., P3-10, confluent)	dynamic	**0.017Hz** (1/60Hz) for 15min, 45min	5%	STB-140 STREX cell stretch system (Strex Co) + silicone resin chamber (size 32×32 mm, STB-CH-10.0, Strex Co.) + motor	uniaxial	n.g.	n.g.	JNK: no change (WB) p-JNK: increase (WB)	JNK: no quantitative information is given p-JNK @ 45min: 32 (rel)* / 10 (ratio-calc)
Suzuki et al. (2014)	p38 / p-p38	*MAPK14*	hPDL cells (19-29/n.g., M, n.g., P3-10, confluent)	dynamic	**0.017Hz** (1/60Hz) for 15min, 45min	5%	STB-140 STREX cell stretch system (Strex Co) + silicone resin chamber (size 32×32 mm, STB-CH-10.0, Strex Co.) + motor	uniaxial	n.g.	n.g.	p38: no change (WB) p-p38: increase (WB)	p38: no quantitative information is given p-p38 @ 45min: 4 (rel)* / 1.9 (ratio-calc)
Suzuki et al. (2014)	PGE_2	PGE_2	hPDL cells (19-29/n.g., M, n.g., P3-10, confluent)	dynamic	**0.017Hz** (1/60Hz) for 6h	5%	STB-140 STREX cell stretch system (Strex Co) + silicone resin chamber (size 32×32 mm, STB-CH-10.0, Strex Co.) + motor	uniaxial	n.a.	n.a.	increase followed by plateau (ELISA)	1h…6h: 229.9 (pg/ml)* / 2.9 (ratio-calc)
Symmank et al. (2019)	GDF15	*GDF15*	hPDLFs (n.g./n.g., n.g., n.g., P4-6, confluence)	static	3h, 6h, 12h	5%	Flexcell FX-3000™ Tension System + pronectin-coated Biofex plates + vacuum	equibiaxial	increase (qPCR, GAPDH and ACTB)	3h: 2.9 (FC)†	increase (ELISA)	12h: 615.5 (pg/ml)† / 4.4 (ratio-calc)
Takano et al. (2009)	COL1	*COL1A1*	hPDL cells (14-16/n.g., PM, exp, P6-9, confluent)	static	12h	5%, 10%	STREX system + STREX-chamber ST-CH-10 (STREX Co.) + manual device (STB-10; STREX Co.)	uniaxial	increase (qPCR, β-actin)	10%: 1.9 (ratio)*	increase (ELISA)	10%: 2.4 (ug/ml)* / 1.7 (ratio-calc)
Takano et al. (2009)	MMP-1	*MMP1*	hPDL cells (14-16/n.g., PM, exp, P6-9, confluent)	static	12h	5%, 10%	STREX system + STREX-chamber ST-CH-10 (STREX Co.) + manual device (STB-10; STREX Co.)	uniaxial	increase (qPCR, β-actin)	10%: 1.6 (rel)* / 2 (ratio-calc)	increase (ELISA)	10%: 3.8 (ug/ml)* / 1.6 (ratio-calc)
Tang et al. (2012)	Osx	*SP7*	hPDLSCs (12-18/n.g., PM, dig, CD146 enrichment, P2, $1×10^5$ cells/cm^2)	dynamic	0.5Hz for 3h, 6h, 12h, 24h	**0.3%** (3000μstrain)	four-point bending strain unit (SXG4201, University of Electronic Science and Technology of China, China) + force-loading plates made from bottom part of the 75 cm^2 cell culture flasks (with canted neck (No.353135, BD Falcon) + actuator (Li et al 2009, Wang et al 2010; further reference to Liu 2006)	uniaxial	increase (qPCR, GAPDH)	24h: 15.4 (rel)* / 8.6 (ratio-calc)	increase (WB, GAPDH)	24h: 1.2 (rel)* / 1.4 (ratio-calc)
Tang et al. (2012)	Runx2	*RUNX2*	hPDLSCs (12-18/n.g., PM, dig, CD146 enrichment, P2, $1×10^5$ cells/cm^2)	dynamic	0.5Hz for 3h, 6h, 12h, 24h	**0.3%** (3000μstrain)	four-point bending strain unit (SXG4201, University of Electronic Science and Technology of China, China) + force-loading plates made from bottom part of the 75 cm^2 cell culture flasks (with canted neck (No.353135, BD Falcon) + actuator (Li et al 2009, Wang et al 2010; further reference to Liu 2006)	uniaxial	increase (qPCR, GAPDH)	24h: 9.6 (rel)* / 7.4 (ratio-calc)	increase followed by plateau (WB, GAPDH)?	12h…24h: 1.1 (rel)* / 1.4 (ratio-calc)
Tang et al. (2012)	Satb2	*SATB2*	hPDLSCs (12-18/n.g., PM, dig, CD146 enrichment, P2, $1×10^5$ cells/cm^2)	dynamic	0.5Hz for 3h, 6h, 12h, 24h	**0.3%** (3000μstrain)	four-point bending strain unit (SXG4201, University of Electronic Science and Technology of China, China) + force-loading plates made from bottom part of the 75 cm^2 cell culture flasks (with canted neck (No.353135, BD Falcon) + actuator (Li et al 2009, Wang et al 2010; further reference to Liu 2006)	uniaxial	increase follwed by plateau (qPCR, GAPDH)	6h…24h: 4.5 (rel)* / 4.1 (ratio-calc)	increase followed by plateau (WB, GAPDH)	6h…24h: 1.2 (rel)* / 1.3 (ratio-calc)
Tantilertanant et al. (2019a)	IL6	*IL6*	hPDLCs (n.g./n.g., n.g., 3 donors, exp, P3-8, $2x10^5$)	dynamic	**1Hz** (frequency of 60 rpm) for 2h, 6h	10%	uniaxial stretch apparatus developed at the Faculty of Dentistry, Chulalongkorn University + gelatin-coated silicone membranes (2.5×2cm^2; Silastic T-4, Dow Corning, GmbH, Germany)	equibiaxial	donor 1: increase (qPCR, GAPDH) donor 2: increase (qPCR, GAPDH) donor 3: increase (qPCR, GAPDH)	donor 1: 6h: 9.4 (FC)† donor 2: 6h: 10.5 (FC)† donor 3: 6h: 9.9 (FC)†	n.a.	n.a.
Tantilertanant et al. (2019a)	IL6R	*IL6R*	hPDLCs (n.g./n.g., n.g., 3 donors, exp, P3-8, $2x10^5$)	dynamic	**1Hz** (frequency of 60 rpm) for 2h	10%	uniaxial stretch apparatus developed at the Faculty of Dentistry, Chulalongkorn University + gelatin-coated silicone membranes (2.5×2cm^2; Silastic T-4, Dow Corning, GmbH, Germany)	equibiaxial	increase (qPCR, GAPDH)	3.2 (FC)†	n.g.	n.g.
Tantilertanant et al. (2019a)	MMP1	*MMP1*	hPDLCs (n.g./n.g., n.g., 3 donors, exp, P3-8, $2x10^5$)	dynamic	**1Hz** (frequency of 60 rpm) for 6h	10%	uniaxial stretch apparatus developed at the Faculty of Dentistry, Chulalongkorn University + gelatin-coated silicone membranes (2.5×2cm^2; Silastic T-4, Dow Corning, GmbH, Germany)	equibiaxial	increase (qPCR, GAPDH)	6h: 1.5 (FC)†	n.g.	n.g.
Tantilertanant et al. (2019a)	MMP14	*MMP14*	hPDLCs (n.g./n.g., n.g., 3 donors, exp, P3-8, $2x10^5$)	dynamic	**1Hz** (frequency of 60 rpm) for 6h	10%	uniaxial stretch apparatus developed at the Faculty of Dentistry, Chulalongkorn University + gelatin-coated silicone membranes (2.5×2cm^2; Silastic T-4, Dow Corning, GmbH, Germany)	equibiaxial	6h: increase (qPCR, GAPDH)	6h: 1.4 (FC)†	n.g.	n.g.

[a] Entry given as reported in the study.
[b] All official gene symbols come from the HUGO Gene Nomenclature Committee (HGNC; URL: https://www.genenames.org) after checking specificity of primers with Primer-BLAST.
[c] Gender/Sex of donors: "M" – male, "F" – female; Tooth type: "PM" – premolar, "M" – molar; Cell density: given in cells/well if not otherwise mentioned.
[d] Frequencies labeled bold orange were converted to hertz (Hz) according to its definition using the information reported in the study (in brackets)
[e] Force type deduced from the description of the force apparatus given by the authors.
[f] Gene and protein expression: 1. conclusion of change (increase, decrease…) was given according to the defined criteria in Figure 2; 2. different markers to describe the amount of change; † Information derived from figures using Engauge Digitizer; *Folds calculated by measuring the graphs, without using the Engauge Digitizer; No makers: Information derived from figures by description in the articles

Reference	Gene/ Analyte[a]	Official gene symbol / abbreviation[b]	Cell (age/gender of donors, tooth type, isolation method, passages used, cell density)[a,c]	Force type (stat./ dyn.)[a]	Force duration and frequency[d]	Force magnitude[a]	Force apparatus[a]	Force type: equibiaxial or uniaxial[e]	Gene expression: Increase, decrease, no change (method w/ reference gene); Methods: qPCR, sqPCR, Northern blot[f]	Gene expression: When it reaches peak and peak's magnitude (fold change; times or ratio; unclear = ?)[f]	Protein expression: Increase, decrease, no change (method w/ reference); Methods: ELISA, WB, RIA, EMSA, IF[f]	Protein expression: When it reaches peak and peak's magnitude (times or ratio; unclear = ?)[f]
Tantilertanant et al. (2019a)	MMP2	*MMP2*	hPDLCs (n.g./n.g., n.g., 3 donors, exp, P3-8, 2x10^5)	dynamic	**1Hz** (frequency of 60 rpm) for 6h	10%	uniaxial stretch apparatus developed at the Faculty of Dentistry, Chulalongkorn University + gelatin-coated silicone membranes (2.5×2cm^2; Silastic T-4, Dow Corning, GmbH, Germany)	equibiaxial	increase (qPCR, GAPDH)	6h: 1.4 (FC)†	n.g.	n.g.
Tantilertanant et al. (2019a)	MMP3	*MMP3*	hPDLCs (n.g./n.g., n.g., 3 donors, exp, P3-8, 2x10^5)	dynamic	**1Hz** (frequency of 60 rpm) for 6h	10%	uniaxial stretch apparatus developed at the Faculty of Dentistry, Chulalongkorn University + gelatin-coated silicone membranes (2.5×2cm^2; Silastic T-4, Dow Corning, GmbH, Germany)	equibiaxial	increase (qPCR, GAPDH)	6h: 1.5 (FC)†		
Tantilertanant et al. (2019a)	MMP8	*MMP8*	hPDLCs (n.g./n.g., n.g., 3 donors, exp, P3-8, 2x10^5)	dynamic	**1Hz** (frequency of 60 rpm) for 6h	10%	uniaxial stretch apparatus developed at the Faculty of Dentistry, Chulalongkorn University + gelatin-coated silicone membranes (2.5×2cm^2; Silastic T-4, Dow Corning, GmbH, Germany)	equibiaxial	no change (qPCR, GAPDH)		n.g.	n.g.
Tantilertanant et al. (2019a)	TIMP1	*TIMP1*	hPDLCs (n.g./n.g., n.g., 3 donors, exp, P3-8, 2x10^5)	dynamic	**1Hz** (frequency of 60 rpm) for 6h	10%	uniaxial stretch apparatus developed at the Faculty of Dentistry, Chulalongkorn University + gelatin-coated silicone membranes (2.5×2cm^2; Silastic T-4, Dow Corning, GmbH, Germany)	equibiaxial	no change (qPCR, GAPDH)		n.g.	n.g.
Tantilertanant et al. (2019a)	TIMP2	*TIMP2*	hPDLCs (n.g./n.g., n.g., 3 donors, exp, P3-8, 2x10^5)	dynamic	**1Hz** (frequency of 60 rpm) for 6h	10%	uniaxial stretch apparatus developed at the Faculty of Dentistry, Chulalongkorn University + gelatin-coated silicone membranes (2.5×2cm^2; Silastic T-4, Dow Corning, GmbH, Germany)	equibiaxial	no change (qPCR, GAPDH)		n.g.	n.g.
Tantilertanant et al. (2019b)	ATP	ATP	hPDL cells (n.g./n.g., M, exp, P3-4, 2×10^5)	dynamic	**1Hz** (frequency of 60 rpm) for 10min, 20min, 30min, 60min, 120min	10%	uniaxial stretch apparatus developed at the Faculty of Dentistry, Chulalongkorn University + gelatin-coated silicone membranes (2.5×2cm^2; Silastic T-4, Dow Corning, GmbH, Germany)	uniaxial	n.a.	n.a.	increase (Luminescence)	10min: 4.7 (ratio)
Tantilertanant et al. (2019b)	BMP2	*BMP2*	hPDL cells (n.g./n.g., M, exp, P3-4, 2×10^5)	dynamic	**1Hz** (frequency of 60 rpm) for 2h, 6h	10%	uniaxial stretch apparatus developed at the Faculty of Dentistry, Chulalongkorn University + gelatin-coated silicone membranes (2.5×2cm^2; Silastic T-4, Dow Corning, GmbH, Germany)	uniaxial	increase (sqPCR, GAPDH)	6h: 7.2 (FC)*	n.g.	n.g.
Tantilertanant et al. (2019b)	BMP6	*BMP6*	hPDL cells (n.g./n.g., M, exp, P3-4, 2×10^5)	dynamic	**1Hz** (frequency of 60 rpm) for 2h, 6h	10%	uniaxial stretch apparatus developed at the Faculty of Dentistry, Chulalongkorn University + gelatin-coated silicone membranes (2.5×2cm^2; Silastic T-4, Dow Corning, GmbH, Germany)	uniaxial	increase (sqPCR, GAPDH)	6h: 7.2 (FC)*	n.g.	n.g.
Tantilertanant et al. (2019b)	BMP9	*GDF2*	hPDL cells (n.g./n.g., M, exp, P3-4, 2×10^5)	dynamic	**1Hz** (frequency of 60 rpm) sqPCR: for 2h, 6h; ELISA: for 48h	10%	uniaxial stretch apparatus developed at the Faculty of Dentistry, Chulalongkorn University + gelatin-coated silicone membranes (2.5×2cm^2; Silastic T-4, Dow Corning, GmbH, Germany)	uniaxial	increase (sqPCR, GAPDH)	6h: 6.5 (FC)*	conditioned medium: increase (ELISA) cell lysate: increase (ELISA)	conditioned medium: 282.9 (pg)† / 11.0 (ratio-calc) cell lysate increase: 16.24 (pg)† / 3.7 (ratio-calc)
Tantilertanant et al. (2019b)	Noggin	*NOG*	hPDL cells (n.g./n.g., M, exp, P3-4, 2×10^5)	dynamic	**1Hz** (frequency of 60 rpm) for 2h, 6h	10%	uniaxial stretch apparatus developed at the Faculty of Dentistry, Chulalongkorn University + gelatin-coated silicone membranes (2.5×2cm^2; Silastic T-4, Dow Corning, GmbH, Germany)	uniaxial	increase (sqPCR, GAPDH)	6h: 2.4 (FC)*	n.g.	n.g.
Tantilertanant et al. (2019b)	$P2Y_1$	*P2RY1*	hPDL cells (n.g./n.g., M, exp, P3-4, 2×10^5)	dynamic	**1Hz** (frequency of 60 rpm) for 2h, 6h	10%	uniaxial stretch apparatus developed at the Faculty of Dentistry, Chulalongkorn University + gelatin-coated silicone membranes (2.5×2cm^2; Silastic T-4, Dow Corning, GmbH, Germany)	uniaxial	increase (sqPCR, GAPDH)	6h: 3.5 (FC)*	n.g.	n.g.
Tsuji et al. (2004)	MMP-1	*MMP1*	hPDL cells (n.g./n.g., PM, exp, P n.g., 1×10^5)	dynamic	**0.17Hz (1/6Hz)** (10cyc/min) for 48h	20%	Flexercell Strain Unit + culture plates coated with type I collagen (Flex I) + vacuum	equibiaxial	no change (sqPCR, GAPDH)		n.g.	n.g.
Tsuji et al. (2004)	MMP-2	*MMP2*	hPDL cells (n.g./n.g., PM, exp, P n.g., 1×10^5)	dynamic	**0.17Hz (1/6Hz)** (10cyc/min) for 48h	20%	Flexercell Strain Unit + culture plates coated with type I collagen (Flex I) + vacuum	equibiaxial	increase (sqPCR, GAPDH)	0.8 (rel)* / 1.6 (ratio-calc)	n.g.	n.g.
Tsuji et al. (2004)	OPG	*TNFRSF11B*	hPDL cells (n.g./n.g., PM, exp, P n.g., 1×10^5)	dynamic	**0.17Hz (1/6Hz)** (10cyc/min) sqPCR for 12h, 24h, 48h, 72h, 120h; qPCR for 48h	20%	Flexercell Strain Unit + culture plates coated with type I collagen (Flex I) + vacuum	equibiaxial	increase (sqPCR, GAPDH) increase (qPCR, β-actin)	sqPCR @ 48h: 2.2 (ratio)* qPCR @ 48h: 34.8 (rel)* / 6.4 (ratio-calc)	n.g.	n.g.
Tsuji et al. (2004)	OPG	*TNFRSF11B*	hPDL cells (n.g./n.g., PM, exp, P n.g., 1×10^5)	dynamic	**0.17Hz (1/6Hz)** (10cyc/min) for 48h	sqPCR for 5%, 20%, 25%; ELISA for 20%	Flexercell Strain Unit + culture plates coated with type I collagen (Flex I) + vacuum	equibiaxial	increase (sqPCR, GAPDH)	20%: 1.5 (rel)*/ 2.2 (ratio-calc)	increase (ELISA)	20%: 339 (pM) / 3.0 (ratio-calc)

[a] Entry given as reported in the study.
[b] All official gene symbols come from the HUGO Gene Nomenclature Committee (HGNC; URL: https://www.genenames.org) after checking specificity of primers with Primer-BLAST.
[c] Gender/Sex of donors: "M" – male, "F" – female; Tooth type: "PM" – premolar, "M" – molar; Cell density: given in cells/well if not otherwise mentioned.
[d] Frequencies labeled bold orange were converted to hertz (Hz) according to its definition using the information reported in the study (in brackets)
[e] Force type deduced from the description of the force apparatus given by the authors.
[f] Gene and protein expression: 1. conclusion of change (increase, decrease…) was given according to the defined criteria in Figure 2; 2. different markers to describe the amount of change; † Information derived from figures using Engauge Digitizer; *Folds calculated by measuring the graphs, without using the Engauge Digitizer; No makers: Information derived from figures by description in the articles

Reference	Gene/ Analyte[a]	Official gene symbol / abbreviation[b]	Cell (age/gender of donors, tooth type, isolation method, passages used, cell density)[a,c]	Force type (stat./ dyn.)[a]	Force duration and frequency[d]	Force magnitude[a]	Force apparatus[a]	Force type: equibiaxial or uniaxial[e]	Gene expression: Increase, decrease, no change (method w/ reference gene); Methods: qPCR, sqPCR, Northern blot[f]	Gene expression: When it reaches peak and peak's magnitude (fold change; times or ratio; unclear = ?)[f]	Protein expression: Increase, decrease, no change (method w/ reference); Methods: ELISA, WB, RIA, EMSA, IF[f]	Protein expression: When it reaches peak and peak's magnitude (times or ratio; unclear = ?)[f]
Tsuji et al. (2004)	RANKL	*TNFSF11*	hPDL cells (n.g./n.g., PM, exp, P n.g., 1×10^5)	dynamic	**0.17Hz (1/6Hz)** (10cyc/min) for 48h	20%	Flexercell Strain Unit + culture plates coated with type I collagen (Flex I) + vacuum	equibiaxial	no change (sqPCR, GAPDH)		n.g.	n.g.
Tsuji et al. (2004)	TIMP-1	*TIMP1*	hPDL cells (n.g./n.g., PM, exp, P n.g., 1×10^5)	dynamic	**0.17Hz (1/6Hz)** (10cyc/min) for 48h	20%	Flexercell Strain Unit + culture plates coated with type I collagen (Flex I) + vacuum	equibiaxial	increase (sqPCR, GAPDH)	0.9 (rel)* / 2.3 (ratio-calc)	n.g.	n.g.
Tsuji et al. (2004)	TIMP-2	*TIMP2*	hPDL cells (n.g./n.g., PM, exp, P n.g., 1×10^5)	dynamic	**0.17Hz (1/6Hz)** (10cyc/min) for 48h	20%	Flexercell Strain Unit + culture plates coated with type I collagen (Flex I) + vacuum	equibiaxial	increase (sqPCR, GAPDH)	1.1 (rel)* / 1.8 (ratio-calc)	n.g.	n.g.
Tsuruga et al. (2009)	Fibrillin-1	*FBN1*	hPDL cells (n.g./n.g., M, exp, P3-6, confluent)	dynamic	**0.017Hz** (1/60Hz)) for 7d	5%	STB-140 STREX cell stretch system (Strex Co) + silicone chamber precoated with type I collagen + motor	uniaxial	no change (Northern blot, β-actin)	no quantitative information is given	increase (WB, β-actin)	increase of 27% (rel) / 1.3 (ratio-calc)
Tsuruga et al. (2009)	Fibrillin-2	*FBN2*	hPDL cells (n.g./n.g., M, exp, P3-6, confluent)	dynamic	**0.017Hz** (1/60Hz) for 7d	5%	STB-140 STREX cell stretch system (Strex Co) + silicone chamber precoated with type I collagen + motor	uniaxial	no change (Northern blot, β-actin)	no quantitative information is given	increase (WB, β-actin)	increase of 23% (rel) / 1.2 (ratio-calc)
Tsuruga et al. (2009)	MMP-2	*MMP2*	hPDL cells (n.g./n.g., M, exp, P3-6, confluent)	dynamic	**0.017Hz** (1/60Hz) for 7d	5%	STB-140 STREX cell stretch system (Strex Co) + silicone chamber precoated with type I collagen + motor	uniaxial	n.g.	n.g.	increase (WB, β-actin)	2.5 (ratio)
Tsuruga et al. (2012)	Fibulin-5	*FBLN5*	hPDL cells (n.g./n.g., PM, exp, P3-6, confluent)	dynamic	**0.017Hz** (1/60Hz) for 7d	5%	STB-140 STREX cell stretch system (Strex Co) + silicone chamber precoated with type I collagen + motor	uniaxial	n.g.	n.g.	FBLN5: no change (WB, β-actin) LTBP-2/Fibulin-5: decrease	FBLN5: no quantitative information reported; LTBP-2/Fibulin-5: 41% (% of control) / 0.4 (ratio-calc)
Tsuruga et al. (2012)	LTBP-2	*LTBP2*	hPDL cells (n.g./n.g., PM, exp, P3-6, confluent)	dynamic	**0.017Hz** (1/60Hz) for 7d	5%	STB-140 STREX cell stretch system (Strex Co) + silicone chamber precoated with type I collagen + motor	uniaxial	no change (Norhtern blot, β-actin)		cell lysates: decrease (WB, β-actin) cell surface and extracellular proteins (WB, β-actin): biotinylated decrease; nonbiotinylated no change medium: increase (WB, β-actin) LTBP-2/Fibulin-5: decrease	cell lysates: 0.29 (ratio) cell surface and extracellular proteins: biotinylated and nonbiotinylated: no quantity is given medium: no quantity is given 41% (rel) / 0.4 (ratio-calc)
Wada et al. (2017)	COX-2	*PTGS2*	immortalized human PDLCs via gene transfection (n.g./n.g., n.g., dig, P n.g., 4.0×10^5)	static	6h, 12h, 24h	15%	Cell Extender (ver. 3, Molcure, Tokyo, Japan) + Bioflex® plates (Flexcell®) + moving screw	equibiaxial	increase (qPCR, GAPDH)	12h: 3.8 (FC)*	n.g.	n.g.
Wada et al. (2017)	IL-1β	*IL1B*	immortalized human PDLCs via gene transfection (n.g./n.g., n.g., dig, P n.g., 4.0×10^5)	static	6h, 12h, 24h	15%	Cell Extender (ver. 3, Molcure, Tokyo, Japan) + Bioflex® plates (Flexcell®) + moving screw	equibiaxial	increase (qPCR, GAPDH)	24h: 5.2 (FC)*	n.g.	n.g.
Wada et al. (2017)	IL-6	*IL6*	immortalized human PDLCs via gene transfection (n.g./n.g., n.g., dig, P n.g., 4.0×10^5)	static	6h, 12h, 24h	15%	Cell Extender (ver. 3, Molcure, Tokyo, Japan) + Bioflex® plates (Flexcell®) + moving screw	equibiaxial	increase (qPCR, GAPDH)	6h: 21 (FC)*	n.g.	n.g.
Wada et al. (2017)	IL-6	*IL6*	immortalized human PDLCs via gene transfection (n.g./n.g., n.g., dig, P n.g., 4.0×10^5)	dynamic	0.5Hz for n.g.	15%	Cell Extender (ver. 3, Molcure, Tokyo, Japan) + Bioflex® plates (Flexcell®) + moving screw	equibiaxial	increase (qPCR, GAPDH)	duration n.g.: 72.6 (FC)*	n.g.	n.g.
Wada et al. (2017)	Osteopontin	*SPP1*	immortalized human PDLCs via gene transfection (n.g./n.g., n.g., dig, P n.g., 4.0×10^5)	static	6h, 12h, 24h	15%	Cell Extender (ver. 3, Molcure, Tokyo, Japan) + Bioflex® plates (Flexcell®) + moving screw	equibiaxial	increase (qPCR, GAPDH)	6h: 27 (FC)*	increase (WB, β-actin)	2.2 (ratio)*
Wada et al. (2017)	Runx2	*RUNX2*	immortalized human PDLCs via gene transfection (n.g./n.g., n.g., dig, P n.g., 4.0×10^5)	static	6h, 12h, 24h	15%	Cell Extender (ver. 3, Molcure, Tokyo, Japan) + Bioflex® plates (Flexcell®) + moving screw	equibiaxial	increase (qPCR, GAPDH)	24h: 1.7 (FC)*	n.g.	n.g.
Wada et al. (2017)	TNF-α	*TNF*	immortalized human PDLCs via gene transfection (n.g./n.g., n.g., dig, P n.g., 4.0×10^5)	static	6h, 12h, 24h	15%	Cell Extender (ver. 3, Molcure, Tokyo, Japan) + Bioflex® plates (Flexcell®) + moving screw	equibiaxial	increase (qPCR, GAPDH)	12h: 5.4 (FC)*	n.g.	n.g.
Wang et al. (2011)	ARRAY	ARRAY	hPDL cells (12-16/n.g., PM, dig, P4, 1×10^5 cells/ml)	dynamic	0.5Hz for 2h	0.5% (5000μstrain)	four-point bending system + force-loading plates made out of the bottoms of 250 ml cell culture flasks (Falcon) 8×4 cm^2 in size and 1.15 mm thick	uniaxial	CapitalBio human whole-genome oligonucleotide chip 35k (CapitalBio Co, Beijing, China) spotted with 35,000 genes		n.a.	n.a.
Wang et al. (2011)	BHLHB2	*DEC1*	hPDL cells (12-16/n.g., PM, dig, P4, 1×10^5 cells/ml)	dynamic	0.5Hz for 2h	0.5% (5000μstrain)	four-point bending system + force-loading plates made out of the bottoms of 250 ml cell culture flasks (Falcon) 8×4 cm^2 in size and 1.15 mm thick	uniaxial	increase (qPCR, GAPDH)	4.4 (FC)*	n.g.	n.g.
Wang et al. (2011)	CCL2	*CCL2*	hPDL cells (12-16/n.g., PM, dig, P4, 1×10^5 cells/ml)	dynamic	0.5Hz for 2h	0.5% (5000μstrain)	four-point bending system + force-loading plates made out of the bottoms of 250 ml cell culture flasks (Falcon) 8×4 cm^2 in size and 1.15 mm thick	uniaxial	increase (qPCR, GAPDH)	3.9 (FC)*	n.g.	n.g.
Wang et al. (2011)	CDC42EP2	*CDC42EP2*	hPDL cells (12-16/n.g., PM, dig, P4, 1×10^5 cells/ml)	dynamic	0.5Hz for 2h	0.5% (5000μstrain)	four-point bending system + force-loading plates made out of the bottoms of 250 ml cell culture flasks (Falcon) 8×4 cm^2 in size and 1.15 mm thick	uniaxial	increase (qPCR, GAPDH)	4.9 (FC)*	n.g.	n.g.
Wang et al. (2011)	COX-2	*PTGS2*	hPDL cells (12-16/n.g., PM, dig, P4, 1×10^5 cells/ml)	dynamic	0.5Hz for 2h	0.5% (5000μstrain)	four-point bending system + force-loading plates made out of the bottoms of 250 ml cell culture flasks (Falcon) 8×4 cm^2 in size and 1.15 mm thick	uniaxial	increase (qPCR, GAPDH)	6.4 (FC)*	n.g.	n.g.
Wang et al. (2011)	IER3	*IER3*	hPDL cells (12-16/n.g., PM, dig, P4, 1×10^5 cells/ml)	dynamic	0.5Hz for 2h	0.5% (5000μstrain)	four-point bending system + force-loading plates made out of the bottoms of 250 ml cell culture flasks (Falcon) 8×4 cm^2 in size and 1.15 mm thick	uniaxial	increase (qPCR, GAPDH)	4.2 (FC)*	n.g.	n.g.

[a] Entry given as reported in the study.
[b] All official gene symbols come from the HUGO Gene Nomenclature Committee (HGNC; URL: https://www.genenames.org) after checking specificity of primers with Primer-BLAST.
[c] Gender/Sex of donors: "M" – male, "F" – female; Tooth type: "PM" – premolar, "M" – molar; Cell density: given in cells/well if not otherwise mentioned.
[d] Frequencies labeled bold orange were converted to hertz (Hz) according to its definition using the information reported in the study (in brackets)
[e] Force type deduced from the description of the force apparatus given by the authors.
[f] Gene and protein expression: 1. conclusion of change (increase, decrease…) was given according to the defined criteria in Figure 2; 2. different markers to describe the amount of change; † Information derived from figures using Engauge Digitizer; *Folds calculated by measuring the graphs, without using the Engauge Digitizer; No makers: Information derived from figures by description in the articles

Reference	Gene/ Analyte[a]	Official gene symbol / abbreviation[b]	Cell (age/gender of donors, tooth type, isolation method, passages used, cell density)[a,c]	Force type (stat./ dyn.)[a]	Force duration and frequency[d]	Force magnitude[a]	Force apparatus[a]	Force type: equibiaxial or uniaxial[e]	Gene expression: Increase, decrease, no change (method w/ reference gene); Methods: qPCR, sqPCR, Northern blot[f]	Gene expression: When it reaches peak and peak's magnitude (fold change; times or ratio; unclear = ?)[f]	Protein expression: Increase, decrease, no change (method w/ reference); Methods: ELISA, WB, RIA, EMSA, IF[f]	Protein expression: When it reaches peak and peak's magnitude (times or ratio; unclear = ?)[f]
Wang et al. (2011)	KLF10	*KLF10*	hPDL cells (12-16/n.g., PM, dig, P4, 1×10^5 cells/ml)	dynamic	0.5Hz for 2h	0.5% (5000µstrain)	four-point bending system + force-loading plates made out of the bottoms of 250 ml cell culture flasks (Falcon) 8×4 cm^2 in size and 1.15 mm thick	uniaxial	increase (qPCR, GAPDH)	6.2 (FC)*	n.g.	n.g.
Wang et al. (2011)	SPRY2	*SPRY2*	hPDL cells (12-16/n.g., PM, dig, P4, 1×10^5 cells/ml)	dynamic	0.5Hz for 2h	0.5% (5000µstrain)	four-point bending system + force-loading plates made out of the bottoms of 250 ml cell culture flasks (Falcon) 8×4 cm^2 in size and 1.15 mm thick	uniaxial	increase (qPCR, GAPDH)	4.1 (FC)*	n.g.	n.g.
Wang et al. (2013)	Caspase-3, Pro- / Caspase-3, cleaved	*CASP3*	hPDL cells (n.g./n.g., PM, dig, P4-8, 95% confluency)	dynamic	0.1Hz for 6h, 24h	20%	Flexcell Tension Plus system FX-5000T + collagen I-coated six-well Bioflex plates (Flexcel) + vacuum	equibiaxial	n.g.	n.g.	Pro-Caspase 3: no change (WB, β-actin) Cleaved caspase-3: increase (WB, β-actin)	Pro-Caspase-3: no quantitative information is given Cleaved caspase-3: 24h: 2.1 (ratio)*
Wang et al. (2013)	PARP	*PARP1*	hPDL cells (n.g./n.g., PM, dig, P4-8, 95% confluency)	dynamic	0.1Hz for 6h, 24h	20%	Flexcell Tension Plus system FX-5000T + collagen I-coated six-well Bioflex plates (Flexcel) + vacuum	equibiaxial	n.g.	n.g.	116kD PARP: no change (WB, β-actin) 85kD PARP: increase (WB, β-actin)	116kD PARP: no quantitative information is given 85kD PARP: 24h: 2.2 (ratio)*
Wang et al. (2013)	RhoGDIα	*ARHGDIA*	hPDL cells (n.g./n.g., PM, dig, P4-8, 95% confluency)	dynamic	0.1Hz for 6h, 24h	20%	Flexcell Tension Plus system FX-5000T + collagen I-coated six-well Bioflex plates (Flexcel) + vacuum	equibiaxial	n.g.	n.g.	decrease (WB, β-actin)	24h: 0.4 (ratio)*
Wang et al. (2018)	Actin (f-actin)	*ACTB*	hPDL cells (n.g./n.g., n.g., n.g., P n.g., 1×10^5 cells/cm^2)	dynamic	0.5Hz for 2h, 6h	**0.4%** (4000µstrain)	four-point bending strength device (west China college of Stomatology, Sichuan University, number of national patents of RP China: CN2534576 and CN1425905) (Hu 2015)	uniaxial	n.g.	n.g.	increase (WB, β-actin)	6h: 1.2 (rel)* / 1.7 (ratio-calc)
Wang et al. (2018)	Akt	*AKT1*	hPDL cells (n.g./n.g., n.g., n.g., P n.g., 1×10^5 cells/cm^2)	dynamic	0.5Hz for 2h, 6h	**0.4%** (4000µstrain)	four-point bending strength device (west China college of Stomatology, Sichuan University, number of national patents of RP China: CN2534576 and CN1425905) (Hu 2015)	uniaxial	n.g.	n.g.	increase followed by plateau (WB, β-actin)	2h...6h: 1.2 (rel)* / 2 (ratio-calc)
Wang et al. (2018)	Girdin	*CCDC88A*	hPDL cells (n.g./n.g., n.g., n.g., P n.g., 1×10^5 cells/cm^2)	dynamic	0.5Hz for 2h, 6h	**0.4%** (4000µstrain)	four-point bending strength device (west China college of Stomatology, Sichuan University, number of national patents of RP China: CN2534576 and CN1425905) (Hu 2015)	uniaxial	n.g.	n.g.	increase (WB, β-actin)	6h: 2.7 (rel)* / 1.7 (ratio-calc)
Wang et al. (2019a)	circRNA3154 circRNA5034 circRNA3133 circRNA5045 circRNA1818 circRNA1358	circRNA3154 circRNA5034 circRNA3133 circRNA5045 circRNA1818 circRNA1358	hPDLSC (14-16/n.g., PM, dig and limited dilution, P3, 5×10^5)	dynamic	1.0Hz for 12h	10%	Flexcell FX-5000 + Flexcell amino silicone-bottom plates were coated with a 0.6 g/L collagen I solution (Sigma-Aldrich) + vacuum	equibiaxial	increase (qPCR, GAPDH) increase (qPCR, GAPDH) increase (qPCR, GAPDH) increase (qPCR, GAPDH) decrease (qPCR, GAPDH) decrease (qPCR, GAPDH)	3.7 (FC)* 2.7 (FC)* 4.5 (FC)* 7.0 (FC)* 0.3 (FC)* 0.3 (FC)*	n.a.	n.a.
Wang et al. (2019a)	OCN	*BGLAP*	hPDLSC (14-16/n.g., PM, dig and limited dilution, P3, 5×10^5)	dynamic	1.0Hz for 12h	10%	Flexcell FX-5000 + Flexcell amino silicone-bottom plates were coated with a 0.6 g/L collagen I solution (Sigma-Aldrich) + vacuum	equibiaxial	increase (qPCR, GAPDH)	5.8 (FC)*	n.g.	n.g.
Wang et al. (2019a)	RNA-Seq	RNA-SEQ	hPDLSC (14-16/n.g., PM, dig and limited dilution, P3, 5×10^5)	dynamic	1.0Hz for 12h	10%	Flexcell FX-5000 + Flexcell amino silicone-bottom plates were coated with a 0.6 g/L collagen I solution (Sigma-Aldrich) + vacuum	equibiaxial	Illumina Hiseq. 4000 with focus on circRNA species	n.a.	n.a.	n.a.
Wang et al. (2019a)	RUNX2	*RUNX2*	hPDLSC (14-16/n.g., PM, dig and limited dilution, P3, 5×10^5)	dynamic	1.0Hz for 12h	10%	Flexcell FX-5000 + Flexcell amino silicone-bottom plates were coated with a 0.6 g/L collagen I solution (Sigma-Aldrich) + vacuum	equibiaxial	increase (qPCR, GAPDH)	2.5 (FC)*	n.g.	n.g.
Wang et al. (2019a)	SP7	*SP7*	hPDLSC (14-16/n.g., PM, dig and limited dilution, P3, 5×10^5)	dynamic	1.0Hz for 12h	10%	Flexcell FX-5000 + Flexcell amino silicone-bottom plates were coated with a 0.6 g/L collagen I solution (Sigma-Aldrich) + vacuum	equibiaxial	increase (qPCR, GAPDH)	4.5 (FC)*	n.g.	n.g.
Wang et al. (2019b)	Cbfα1	*RUNX2*	hPDLCs (18-30/n.g., M, dig, P2-5, confluence)	dynamic	**0.1Hz** (6cyc/min, 5s on and 5s off) qPCR for 12h, 24h, 48h; WB for 24h, 48h	12%	Flexcell FX-5000TM + Bioflex plates + vaccum	equibiaxial	increase (qPCR, β-actin)	48h: 1.3 (FC)†	increase (WB, GAPDH)	48h: no quantitative information is given
Wang et al. (2019b)	COL-1	*COL1A1*	hPDLCs (18-30/n.g., M, dig, P2-5, confluence)	dynamic	**0.1Hz** (6cyc/min, 5s on and 5s off) qPCR for 12h, 24h, 48h; WB for 24h, 48h	12%	Flexcell FX-5000TM + Bioflex plates + vaccum	equibiaxial	increase (qPCR, β-actin)	48h: 1.6 (FC)†	increase (WB, GAPDH)	48h: no quantitative information is given
Wang et al. (2019b)	OCN	*BGLAP*	hPDLCs (18-30/n.g., M, dig, P2-5, confluence)	dynamic	**0.1Hz** (6cyc/min, 5s on and 5s off) qPCR for 12h, 24h, 48h; WB for 24h, 48h	12%	Flexcell FX-5000TM + Bioflex plates + vaccum	equibiaxial	increase (qPCR, β-actin)	48h: 1.3 (FC)†	increase (WB, GAPDH)	24h: no quantitative information is given

[a] Entry given as reported in the study.
[b] All official gene symbols come from the HUGO Gene Nomenclature Committee (HGNC; URL: https://www.genenames.org) after checking specificity of primers with Primer-BLAST.
[c] Gender/Sex of donors: "M" – male, "F" – female; Tooth type: "PM" – premolar, "M" – molar; Cell density: given in cells/well if not otherwise mentioned.
[d] Frequencies labeled bold orange were converted to hertz (Hz) according to its definition using the information reported in the study (in brackets)
[e] Force type deduced from the description of the force apparatus given by the authors.
[f] Gene and protein expression: 1. conclusion of change (increase, decrease…) was given according to the defined criteria in Figure 2; 2. different markers to describe the amount of change; † Information derived from figures using Engauge Digitizer; *Folds calculated by measuring the graphs, without using the Engauge Digitizer; No makers: Information derived from figures by description in the articles

Reference	Gene/ Analyte[a]	Official gene symbol / abbreviation[b]	Cell (age/gender of donors, tooth type, isolation method, passages used, cell density)[a,c]	Force type (stat./ dyn.)[a]	Force duration and frequency[d]	Force magnitude[a]	Force apparatus[a]	Force type: equibiaxial or uniaxial[e]	Gene expression: Increase, decrease, no change (method w/ reference gene); Methods: qPCR, sqPCR, Northern blot[f]	Gene expression: When it reaches peak and peak's magnitude (fold change; times or ratio; unclear = ?)[f]	Protein expression: Increase, decrease, no change (method w/ reference); Methods: ELISA, WB, RIA, EMSA, IF[f]	Protein expression: When it reaches peak and peak's magnitude (times or ratio; unclear = ?)[f]
Wang et al. (2019b)	OSX	*SP7*	hPDLCs (18-30/n.g., M, dig, P2-5, confluence)	dynamic	**0.1Hz** (6cyc/min, 5s on and 5s off) qPCR for 12h, 24h, 48h; WB for 24h, 48h	12%	Flexcell FX-5000TM + Bioflex plates + vaccum	equibiaxial	increase followed by plateau (qPCR, β-actin)	24h...48h: 1.5 (FC)†	increase (WB, GAPDH)	48h: no quantitative information is given
Wang et al. (2019b)	TAZ	*TAZ*	hPDLCs (18-30/n.g., M, dig, P2-5, confluence)	dynamic	**0.1Hz** (6cyc/min, 5s on and 5s off) qPCR for 12h, 24h, 48h; WB for 24h, 48h	12%	Flexcell FX-5000TM + Bioflex plates + vaccum	equibiaxial	increase (qPCR, β-actin)	48h: (FC)†	increase (WB, GAPDH)	48h: no quantitative information is given
Wei et al. (2014)	ARRAY	ARRAY	hPDLSCs cells (12-16/ n.g., PM, dig, P2-3, 80% confluence)	dynamic	1.0Hz for 12h	10%	Flexcell FX-5000 Tension system + Flexcell Amino silicone bottomed plates coated with 0.6mg/mL collagen I solution (Sigma Aldrich) + vacuum	equibiaxial	Paraflo™ miRNA Microarray Assay			
Wei et al. (2014)	BSP	*IBSP*	hPDLSCs cells (12-16/ n.g., PM, dig, P2-3, 80% confluence)	dynamic	1.0Hz for 12h	10%	Flexcell FX-5000 Tension system + Flexcell Amino silicone bottomed plates coated with 0.6mg/mL collagen I solution (Sigma Aldrich) + vacuum	equibiaxial	increase (qPCR, GAPDH)	2.8 (ratio)*	increase (WB, β-actin)	no quantitative information is given
Wei et al. (2014)	OCN	*BGLAP*	hPDLSCs cells (12-16/ n.g., PM, dig, P2-3, 80% confluence)	dynamic	1.0Hz for 12h	10%	Flexcell FX-5000 Tension system + Flexcell Amino silicone bottomed plates coated with 0.6mg/mL collagen I solution (Sigma Aldrich) + vacuum	equibiaxial	increase (qPCR, GAPDH)	2.1 (ratio)*	increase (WB, β-actin)	no quantitative information is given
Wei et al. (2014)	Runx2	*RUNX2*	hPDLSCs cells (12-16/ n.g., PM, dig, P2-3, 80% confluence)	dynamic	1.0Hz for 12h	10%	Flexcell FX-5000 Tension system + Flexcell Amino silicone bottomed plates coated with 0.6mg/mL collagen I solution (Sigma Aldrich) + vacuum	equibiaxial	increase (qPCR, GAPDH)	1.8 (ratio)*	increase (WB, β-actin)	no quantitative information is given
Wei et al. (2015)	ACVR2B	*ACVR2B*	hPDLSCs cells (10-14/n.g., n.g., dig, P3, 80% confluence)	dynamic	1.0 Hz for 6h, 12h, 24h, 48h	10%	Flexcell FX-5000 Tension system + Flexcell Amino silicone bottomed plates coated with 0.6mg/mL collagen I solution (Sigma Aldrich) + vacuum	equibiaxial	n.g.	n.g.	decrease (WB, β-actin)	24h: 0.6 (rel)* / 0.7 (ratio-calc)
Wei et al. (2015)	ALP	*ALPP*	hPDLSCs cells (10-14/n.g., n.g., dig, P3, 80% confluence)	dynamic	1.0Hz for 6h, 12h, 24h, 48h	10%	Flexcell FX-5000 Tension system + Flexcell Amino silicone bottomed plates coated with 0.6mg/mL collagen I solution (Sigma Aldrich) + vacuum	equibiaxial	n.g.	n.g.	increase (ALP activity)	48h: 0.6 [Sigma unit/(min * mg protein)]* / 11.0 (ratio-calc)
Wei et al. (2015)	OCN	*BGLAP*	hPDLSCs cells (10-14/n.g., n.g., dig, P3, 80% confluence)	dynamic	1.0Hz for 6h, 12h, 24h, 48h	10%	Flexcell FX-5000 Tension system + Flexcell Amino silicone bottomed plates coated with 0.6mg/mL collagen I solution (Sigma Aldrich) + vacuum	equibiaxial	increase (qPCR, GAPDH)	24h: 3.5 (FC)*	n.g.	n.g.
Wei et al. (2015)	Runx2	*RUNX2*	hPDLSCs cells (10-14/n.g., n.g., dig, P3, 80% confluence)	dynamic	1.0Hz for 6h, 12h, 24h, 48h	10%	Flexcell FX-5000 Tension system + Flexcell Amino silicone bottomed plates coated with 0.6mg/mL collagen I solution (Sigma Aldrich) + vacuum	equibiaxial	increase (qPCR, GAPDH)	48h: 1.8 (FC)*	n.g.	n.g.
Wescott et al. (2007)	ARRAY	ARRAY	hPDL fibroblasts (n.g./n.g., PM, exp, P4, 3×10^5)	dynamic	**0.01Hz (1/96Hz)** (intermittent deformation of 12% for 6s every 90s) for 6h, 12h, 24h	12%	Flexercell FX-4000 Strain Unit + six-well, 35-mm flexible-bottomed Uniflex culture plates + vacuum	uniaxial	Osteogenic RT^2 Profiler PCR Array (Superarray Bioscience Corp.)	too many	n.g.	n.g.
Wolf et al. (2014)	HMGB1	*HMGB1*	hPDL cells (12-14/n.g., PM, n.g., P n.g., confluence)	static	8h	20%	loading platform with cylindrical posts + collagen type I-coated BioFlex plates (Flexcells Int.) + screws (Deschner et al., 2007, Rath-Deschner et al 2009)	equibiaxial	n.g.	n.g.	increase (ELISA)	1.4 (ratio)*
Wu et al. (2015)	mDia1	*DIAPH1*	hPDL cells (n.g./n.g., PM, n.g., P3-6, 95% confluence)	dynamic	0.1Hz for 6h, 24h	10%	Flexercell Tension Plus system FX-5000T + six-well Bioflex plates + vacuum	equibiaxial	n.g.	n.g.	increase followed with platform (WB, GAPDH)	6h...24h: 1.1 (ratio)*
Wu et al. (2015)	Profilin-1	*PFN1*	hPDL cells (n.g./n.g., PM, n.g., P3-6, 95% confluence)	dynamic	0.1Hz for 6h, 24h	10%	Flexercell Tension Plus system FX-5000T + six-well Bioflex plates + vacuum	equibiaxial	n.g.	n.g.	increase (WB, GAPDH)	24h: 2.4 (ratio)*
Wu et al. (2015)	RhoA-GTP	*RHOA*	hPDL cells (n.g./n.g., PM, n.g., P3-6, 95% confluence)	dynamic	0.1Hz for 6h, 24h	10%	Flexercell Tension Plus system FX-5000T + six-well Bioflex plates + vacuum	equibiaxial	n.g.	n.g.	increase (WB, GAPDH)	24h: 4.9 (ratio)*
Wu et al. (2015)	Rho-GDIα	*ARHGDIA*	hPDL cells (n.g./n.g., PM, n.g., P3-6, 95% confluence)	dynamic	0.1Hz for 6h, 24h	10%	Flexercell Tension Plus system FX-5000T + six-well Bioflex plates + vacuum	equibiaxial	n.g.	n.g.	decrease (WB, GAPDH)	24h: 0.5 (ratio)*
Wu et al. (2016)	Caspase 7, Pro- / Caspase 7, cleaved	*CASP7*	hPDL cells (11-13/n.g., PM, exp, P4-6, 70-80% confluence)	dynamic	**0.1Hz** (6cyc/min: 5s stretch and 5s relaxation) for 6h, 24h	20%	Cell Strain Unit (CSU) + elastic silicon rubber membrane + spherical cap (step motor) (Hao et al 2009)	equibiaxial	n.g.	n.g.	Pro-caspase 7: increase (WB, GAPDH) Cleaved caspase 7: increase (WB, GAPDH)	Pro-Caspase 3 @ 24h: 0.3 (rel)† / 21.1 (ratio-calc) Cleaved caspase 7 @ 24h: 0.6 (rel)† / 6.3 (ratio-calc)
Wu et al. (2016)	Caspase 8, cleaved (18kDa)	*CASP8*	hPDL cells (11-13/n.g., PM, exp, P4-6, 70-80% confluence)	dynamic	**0.1Hz** (6cyc/min: 5s stretch and 5s relaxation) for 6h, 24h	20%	Cell Strain Unit (CSU) + elastic silicon rubber membrane + spherical cap (step motor) (Hao et al 2009)	equibiaxial	n.g.	n.g.	increase (WB, GAPDH)	24h: 0.2 (rel)† / 4.9 (ratio-calc)

[a] Entry given as reported in the study.
[b] All official gene symbols come from the HUGO Gene Nomenclature Committee (HGNC; URL: https://www.genenames.org) after checking specificity of primers with Primer-BLAST.
[c] Gender/Sex of donors: "M" – male, "F" – female; Tooth type: "PM" – premolar, "M" – molar; Cell density: given in cells/well if not otherwise mentioned.
[d] Frequencies labeled bold orange were converted to hertz (Hz) according to its definition using the information reported in the study (in brackets)
[e] Force type deduced from the description of the force apparatus given by the authors.
[f] Gene and protein expression: 1. conclusion of change (increase, decrease…) was given according to the defined criteria in Figure 2; 2. different markers to describe the amount of change; † Information derived from figures using Engauge Digitizer; *Folds calculated by measuring the graphs, without using the Engauge Digitizer; No makers: Information derived from figures by description in the articles

Reference	Gene/ Analyte[a]	Official gene symbol / abbreviation[b]	Cell (age/gender of donors, tooth type, isolation method, passages used, cell density)[a,c]	Force type (stat./ dyn.)[a]	Force duration and frequency[d]	Force magnitude[a]	Force apparatus[a]	Force type: equibiaxial or uniaxial[e]	Gene expression: Increase, decrease, no change (method w/ reference gene); Methods: qPCR, sqPCR, Northern blot[f]	Gene expression: When it reaches peak and peak's magnitude (fold change; times or ratio; unclear = ?)[f]	Protein expression: Increase, decrease, no change (method w/ reference); Methods: ELISA, WB, RIA, EMSA, IF[f]	Protein expression: When it reaches peak and peak's magnitude (times or ratio; unclear = ?)[f]
Wu et al. (2016)	Caspase 8, cleaved (43/45kDa)	*CASP8*	hPDL cells (11-13/n.g., PM, exp, P4-6, 70-80% confluence)	dynamic	**0.1Hz** (6cyc/min: 5s stretch and 5s relaxation) for 6h, 24h	20%	Cell Strain Unit (CSU) + elastic silicon rubber membrane + spherical cap (step motor) (Hao et al 2009)	equibiaxial	n.g.	n.g.	increase (WB, GAPDH)	24h: 0.5 (rel)† / 8.3 (ratio-calc)
Wu et al. (2016)	Caspase 8, Pro-	*CASP8*	hPDL cells (11-13/n.g., PM, exp, P4-6, 70-80% confluence)	dynamic	**0.1Hz** (6cyc/min: 5s stretch and 5s relaxation) for 6h, 24h	20%	Cell Strain Unit (CSU) + elastic silicon rubber membrane + spherical cap (step motor) (Hao et al 2009)	equibiaxial	n.g.	n.g.	increase (WB, GAPDH)	24h: 0.6 (rel)† / 8.4 (ratio-calc)
Wu et al. (2016)	Caspase 9, Pro- / Caspase 9, cleaved	*CASP9*	hPDL cells (11-13/n.g., PM, exp, P4-6, 70-80% confluence)	dynamic	**0.1Hz** (6cyc/min: 5s stretch and 5s relaxation) for 6h, 24h	20%	Cell Strain Unit (CSU) + elastic silicon rubber membrane + spherical cap (step motor) (Hao et al 2009)	equibiaxial	n.g.	n.g.	Pro-caspase 9: increase (WB, GAPDH) Cleaved caspase 9: increase (WB, GAPDH)	Pro-caspase 9 @ 24h: 0.8 (rel)† 31.8 (ratio-calc) Cleaved caspase 9 @ 24h: 0.7 (rel)† / 7.7 (ratio-calc)
Wu et al. (2016)	Caspase-3, cleaved	*CASP3*	hPDL cells (11-13/n.g., PM, exp, P4-6, 70-80% confluence)	dynamic	**0.1Hz** (6cyc/min: 5s stretch and 5s relaxation) for 6h, 24h	20%	Cell Strain Unit (CSU) + elastic silicon rubber membrane + spherical cap (step motor) (Hao et al 2009)	equibiaxial	n.g.	n.g.	increase (WB, GAPDH)	24h: 0.1 (rel)* / 1.7 (ratio-calc)
Wu et al. (2017)	ARRAY	ARRAY	hPDL cells (11/F, 12/F, 13/F, PM, exp, P4, confluence)	dynamic	**0.1Hz** (6cyc/min: 5s stretch and 5s relaxation) qPCR for 24h; WB for 6h, 24h	1%, 10%, 20%	Cell Strain Unit (CSU) + elastic silicon rubber membrane + spherical cap (step motor) (Hao et al 2009)	equibiaxial	Human Cytoskeleton Regulators RT^2 ProfilerTM PCR Array (PAHS-088, SABiosciences, Frederick, MD)	ARRAY	n.a.	n.a.
Wu et al. (2017)	CDC42EP2	*CDC42EP2*	hPDL cells (11/F, 12/F, 13/F, PM, exp, P4, confluence)	dynamic	**0.1Hz** (6cyc/min: 5s stretch and 5s relaxation) qPCR for 24h; WB for 6h, 24h	1%, 10%, 20%	Cell Strain Unit (CSU) + elastic silicon rubber membrane + spherical cap (step motor) (Hao et al 2009)	equibiaxial	n.a.	n.a.	decrease (WB, GAPDH)	no quantitative information is given
Wu et al. (2017)	STMN1	*STMN1*	hPDL cells (11/F, 12/F, 13/F, PM, exp, P4, confluence)	dynamic	**0.1Hz** (6cyc/min: 5s stretch and 5s relaxation) qPCR for 24h; WB for 6h, 24h	1%, 10%, 20%	Cell Strain Unit (CSU) + elastic silicon rubber membrane + spherical cap (step motor) (Hao et al 2009)	equibiaxial	n.a.	n.a.	decrease (WB, GAPDH)	no quantitative information is given
Wu et al. (2017)	WASL	*WASL*	hPDL cells (11/F, 12/F, 13/F, PM, exp, P4, confluence)	dynamic	**0.1Hz** (6cyc/min: 5s stretch and 5s relaxation) for 24h	1%, 10%, 20%	Cell Strain Unit (CSU) + elastic silicon rubber membrane + spherical cap (step motor) (Hao et al 2009)	equibiaxial	n.a.	n.a.	increase (WB, GAPDH)	no quantitative information is given
Wu et al. (2019a)	BSP	*IBSP*	hPDLCs (14-25/n.g., M, exp, P3-6, 70-80% confluence)	dynamic	0.1Hz for 24h	10%	Flexcell FX-5000TM + six-well Bioflex plates coated with type I collagen + vaccum	equibiaxial	increase (qPCR, GAPDH)	1.6 (FC)†	n.g.	n.g.
Wu et al. (2019a)	CAP	*HACD1*	hPDLCs (14-25/n.g., M, exp, P3-6, 70-80% confluence)	dynamic	0.1Hz for 24h	10%	Flexcell FX-5000TM + six-well Bioflex plates coated with type I collagen + vaccum	equibiaxial	increase (qPCR, GAPDH)	2.4 (FC)†	n.g.	n.g.
Wu et al. (2019a)	CEMP1	*AMDHD2*	hPDLCs (14-25/n.g., M, exp, P3-6, 70-80% confluence)	dynamic	0.1Hz for 24h	10%	Flexcell FX-5000TM + six-well Bioflex plates coated with type I collagen + vaccum	equibiaxial	increase (qPCR, GAPDH)	2.0 (FC)†	increase (WB, GAPDH)	no quantitative information is given
Wu et al. (2019a)	CTGF	*CCN2*	hPDLCs (14-25/n.g., M, exp, P3-6, 70-80% confluence)	dynamic	0.1Hz for 24h	10%	Flexcell FX-5000TM + six-well Bioflex plates coated with type I collagen + vaccum	equibiaxial	decrease (qPCR, GAPDH)	0.8 (FC)†	n.g.	n.g.
Wu et al. (2019a)	DVL2	*DVL2*	hPDLCs (14-25/n.g., M, exp, P3-6, 70-80% confluence)	dynamic	0.1Hz for 24h	10%	Flexcell FX-5000TM + six-well Bioflex plates coated with type I collagen + vaccum	equibiaxial	increase (qPCR, GAPDH)	3.1 (FC)†	n.g.	n.g.
Wu et al. (2019a)	GDF5	*GDF5*	hPDLCs (14-25/n.g., M, exp, P3-6, 70-80% confluence)	dynamic	0.1Hz for 24h	10%	Flexcell FX-5000TM + six-well Bioflex plates coated with type I collagen + vaccum	equibiaxial	increase (qPCR, GAPDH)	4.7 (FC)†	n.g.	n.g.
Wu et al. (2019a)	GLI2	*GLI2*	hPDLCs (14-25/n.g., M, exp, P3-6, 70-80% confluence)	dynamic	0.1Hz for 24h	10%	Flexcell FX-5000TM + six-well Bioflex plates coated with type I collagen + vaccum	equibiaxial	increase (qPCR, GAPDH)	1.6 (FC)†	n.g.	n.g.
Wu et al. (2019a)	LATS1	*LATS1*	hPDLCs (14-25/n.g., M, exp, P3-6, 70-80% confluence)	dynamic	0.1Hz for 24h	10%	Flexcell FX-5000TM + six-well Bioflex plates coated with type I collagen + vaccum	equibiaxial	increase (qPCR, GAPDH)	1.5 (FC)†	n.g.	n.g.
Wu et al. (2019a)	LIMD1	*LIMD1*	hPDLCs (14-25/n.g., M, exp, P3-6, 70-80% confluence)	dynamic	0.1Hz for 24h	10%	Flexcell FX-5000TM + six-well Bioflex plates coated with type I collagen + vaccum	equibiaxial	increase (qPCR, GAPDH)	2.9 (FC)†	n.g.	n.g.
Wu et al. (2019a)	MSX2	*MSX2*	hPDLCs (14-25/n.g., M, exp, P3-6, 70-80% confluence)	dynamic	0.1Hz for 24h	10%	Flexcell FX-5000TM + six-well Bioflex plates coated with type I collagen + vaccum	equibiaxial	increase (qPCR, GAPDH)	1.5 (FC)†	n.g.	n.g.
Wu et al. (2019a)	OCN	*BGLAP*	hPDLCs (14-25/n.g., M, exp, P3-6, 70-80% confluence)	dynamic	0.1Hz for 24h	10%	Flexcell FX-5000TM + six-well Bioflex plates coated with type I collagen + vaccum	equibiaxial	increase (qPCR, GAPDH)	2.1 (FC)†	n.g.	n.g.

[a] Entry given as reported in the study.
[b] All official gene symbols come from the HUGO Gene Nomenclature Committee (HGNC; URL: https://www.genenames.org) after checking specificity of primers with Primer-BLAST.
[c] Gender/Sex of donors: "M" – male, "F" – female; Tooth type: "PM" – premolar, "M" – molar; Cell density: given in cells/well if not otherwise mentioned.
[d] Frequencies labeled bold orange were converted to hertz (Hz) according to its definition using the information reported in the study (in brackets)
[e] Force type deduced from the description of the force apparatus given by the authors.
[f] Gene and protein expression: 1. conclusion of change (increase, decrease…) was given according to the defined criteria in Figure 2; 2. different markers to describe the amount of change; † Information derived from figures using Engauge Digitizer; *Folds calculated by measuring the graphs, without using the Engauge Digitizer; No makers: Information derived from figures by description in the articles

Reference	Gene/ Analyte[a]	Official gene symbol / abbreviation[b]	Cell (age/gender of donors, tooth type, isolation method, passages used, cell density)[a,c]	Force type (stat./ dyn.)[a]	Force duration and frequency[d]	Force magnitude[a]	Force apparatus[a]	Force type: equibiaxial or uniaxial[e]	Gene expression: Increase, decrease, no change (method w/ reference gene); Methods: qPCR, sqPCR, Northern blot[f]	Gene expression: When it reaches peak and peak's magnitude (fold change; times or ratio; unclear = ?)[f]	Protein expression: Increase, decrease, no change (method w/ reference); Methods: ELISA, WB, RIA, EMSA, IF[f]	Protein expression: When it reaches peak and peak's magnitude (times or ratio; unclear = ?)[f]
Wu et al. (2019a)	RUNX2	*RUNX2*	hPDLCs (14-25/n.g., M, exp, P3-6, 70-80% confluence)	dynamic	0.1Hz for 24h	10%	Flexcell FX-5000TM + six-well Bioflex plates coated with type I collagen + vaccum	equibiaxial	increase (qPCR, GAPDH)	1.6 (FC)†	increase (WB, GAPDH)	no quantitative information is given
Wu et al. (2019a)	SATB2	*SATB2*	hPDLCs (14-25/n.g., M, exp, P3-6, 70-80% confluence)	dynamic	0.1Hz for 24h	10%	Flexcell FX-5000TM + six-well Bioflex plates coated with type I collagen + vaccum	equibiaxial	increase (qPCR, GAPDH)	1.7 (FC)†	n.g.	n.g.
Wu et al. (2019a)	SPP1	*SPP1*	hPDLCs (14-25/n.g., M, exp, P3-6, 70-80% confluence)	dynamic	0.1Hz for 24h	10%	Flexcell FX-5000TM + six-well Bioflex plates coated with type I collagen + vaccum	equibiaxial	increase (qPCR, GAPDH)	2.3 (FC)†	increase (WB, GAPDH)	no quantitative information is given
Wu et al. (2019a)	TEAD1	*TEAD1*	hPDLCs (14-25/n.g., M, exp, P3-6, 70-80% confluence)	dynamic	0.1Hz for 24h	10%	Flexcell FX-5000TM + six-well Bioflex plates coated with type I collagen + vaccum	equibiaxial	increase (qPCR,GAPDH)	1.3 (FC)†	n.g.	n.g.
Wu et al. (2019a)	TEAD2	*TEAD2*	hPDLCs (14-25/n.g., M, exp, P3-6, 70-80% confluence)	dynamic	0.1Hz for 24h	10%	Flexcell FX-5000TM + six-well Bioflex plates coated with type I collagen + vaccum	equibiaxial	increase (qPCR, GAPDH)	2.2 (FC)†	n.g.	n.g.
Wu et al. (2019a)	WTIP	*WTIP*	hPDLCs (14-25/n.g., M, exp, P3-6, 70-80% confluence)	dynamic	0.1Hz for 24h	10%	Flexcell FX-5000TM + six-well Bioflex plates coated with type I collagen + vaccum	equibiaxial	increase (qPCR, GAPDH)	1.8 (FC)†	n.g.	n.g.
Wu et al. (2019a)	WWTR1	*TAZ*	hPDLCs (14-25/n.g., M, exp, P3-6, 70-80% confluence)	dynamic	0.1Hz for 24h	10%	Flexcell FX-5000TM + six-well Bioflex plates coated with type I collagen + vaccum	equibiaxial	increase (qPCR, GAPDH)	3.7 (FC)†	n.g.	n.g.
Wu et al. (2019a)	YAP1	*YAP1*	hPDLCs (14-25/n.g., M, exp, P3-6, 70-80% confluence)	dynamic	0.1Hz for 24h	10%	Flexcell FX-5000TM + six-well Bioflex plates coated with type I collagen + vaccum	equibiaxial	increase (qPCR, GAPDH)	2.2 (FC)†	n.g.	n.g.
Wu et al. (2019b)	Caspase 3, Pro- / Caspase 3, cleaved	*CASP3*	hPDLFs (11-13/n.g., PM, exp, P4-6, confluence)	dynamic	**0.1Hz** (6cyc/min: 5s stretch and 5s relaxation) for 6h, 24h	20%	Cell Strain Unit (CSU) + elastic silicon rubber membrane + spherical cap (step motor) (Hao et al 2009)	equibiaxial	n.g.	n.g.	Pro-caspase-3 (35 kDa): increase (WB, GAPDH) Cleaved caspase-3 (ca. 17 kDa): increase (WB, GAPDH) Cleaved caspase-3: increase (colorimetric assay)	Pro-caspase-3: 12h: 0.6 (rel)* / 1.2 (ratio-calc) Cleaved caspase-3: WB @ 24h: 0.1 (rel)* / 3.3 (ratio-calc) Cleaved caspase-3: colorimetric assay @ 24h: 1.5 (ratio)*
Wu et al. (2019b)	Caspase 5, Pro- / Caspase 5, cleaved	*CASP5*	hPDLFs (11-13/n.g., PM, exp, P4-6, confluence)	dynamic	**0.1Hz** (6cyc/min: 5s stretch and 5s relaxation) for 6h, 24h	20%	Cell Strain Unit (CSU) + elastic silicon rubber membrane + spherical cap (step motor) (Hao et al 2009)	equibiaxial	n.g.	n.g.	Pro-caspase-5 (45 kDa): decrease (WB, GAPDH) Cleaved caspase-5 (20 kDa): increase (WB, GAPDH) Cleaved caspase-5: increase followed by plateau (colorimetric assay)	Pro-caspase-5: 24h: 0.2 (rel)† / 0.6 (ratio-calc) Cleaved caspase-5: WB @ 24h: 0.2 (rel)† / 15.0 (ratio-calc) Cleaved caspase-5: colorimetric assay @ 6h…24h: 1.7 (ratio)*
Xu et al. (2011)	ARRAY	ARRAY	hPDL cells (12/F, PM, exp, P4, confluence)	dynamic	**0.1Hz** (6cyc/min) for 6h, 24h	20%	Cell Strain Unit (CSU) + elastic silicon rubber membrane + spherical cap (step motor) (Hao et al 2009)	equibiaxial	Human Apoptosis RT² Profiler PCR Array (PAHS-012; Superarray) with *B2M*, *GAPDH* and *ACTB* as reference genes	too many	n.g.	n.g.
Xu et al. (2012)	Cx43	*GJA1*	hPDL cells (12/F, 15/M, PM, exp, P4-6, confluence)	dynamic	**0.1Hz** (6cyc/min) for 0.5h, 1h, 24h	1%, 10%, 20%	Cell Strain Unit (CSU) + elastic silicon rubber membrane + spherical cap (step motor) (Hao et al 2009)	equibiaxial	1% strain: temporary decrease followed by temporary increase (qPCR, β-actin) 10% strain: temporary decrease (qPCR, β-actin) 20% strain: decrease followed by plateau then increase (qPCR, β-actin)	1% strain lowest @ 0.5h: 0.2 (rel)† / 0.2 (ratio-calc) 1% strain highest @ 1h: 2.1 (rel)† / 1.9 (ratio-calc) 10% strain lowest@ 0.5h: 0.2 (rel)† / 0.2 (ratio-calc) 20% strain lowest @ 0.5h…1h: 0.4 (rel)† / 0.4 (ratio-calc) 20% strain highest @ 24h: 1.8 (rel)† / 2 (ratio-calc)	n.g.	n.g.
Xu et al. (2015)	α-SMA	*ACTA2*	hPDL cells (n.g./n.g., PM, exp, P3-5, 80% confluence)	dynamic	0.5Hz qPCR for 6h; ELISA for 0h, 1h, 3h, 6h, 12h	**0.2%** (2000μstrain), **0.4%** (4000μstrain)	a uniaxial four-point bending system (developed at Sichuan University, patents CN2534576 and CN1425905)	uniaxial	2000μstrain: increase (qPCR, GAPDH) 4000μstrain: increase (qPCR, GAPDH)	2000 μstrain: 1.2 (ratio)* 4000 μstrain: 2.6 (ratio)*	2000 μstrain: increase (ELISA) 4000 μstrain: increase (ELISA)	2000 μstrain @ 12h: 348.5 (pg/ml)* / 1.4 (ratio-calc) 4000 μstrain @ 12h: 393.9 (pg/ml)* / 1.6 (ratio-calc)
Xu et al. (2017)	Periostin	*POSTN*	hPDL cells (n.g./n.g., PM and M, exp, P3, n.g.)	dynamic	0.5Hz for 0h, 12h, 24h, 48h	10%	Flexcell FX-5000 Tension system + Flexcell Amino silicone bottomed plates coated with 0.6mg/mL collagen I solution (Sigma Aldrich) + vacuum (Wei et al 2014)	equibiaxial	increase (qPCR, GAPDH)	48h: 3.3 (FC)*	increase (WB, α-tubulin)	48h: 3.6 (ratio)*
Xu et al. (2017)	TGF-β	*TGFB1*	hPDL cells (n.g./n.g., PM and M, exp, P3, n.g.)	dynamic	0.5Hz for 0h, 12h, 24h, 48h	10%	Flexcell FX-5000 Tension system + Flexcell Amino silicone bottomed plates coated with 0.6mg/mL collagen I solution (Sigma Aldrich) + vacuum (Wei et al 2014)	equibiaxial	increase (qPCR, GAPDH)	48h: 3.5 (FC)*	increase (WB, α-tubulin)	no quantitative information is given
Yamaguchi and Shimizu (1994)	ALP	*ALPP*	hPDL fibroblasts (12/M, 10/M, 11/F, 3 donors, PM, exp, donor#1 P4, donor#2 P6, donor#3 P4, confluent)	dynamic	**0.1Hz** (6cyc/min: 5s elongation and 5s relaxation) for 3d	24%	Flexercell strain unit + flexible-bottom culture plates coated with type I collagen (Flexcell) + vacuum (Banes et al 1985)	equibiaxial	n.g.	n.g.	donor 1: decrease (ALP activity) donor 2: decrease (ALP activity) donor 3: decrease (ALP activity)	donor 1: 10.3 (mU/10^5 cells) / 0.6 (ratio-calc) donor 2: 10.0 (mU/10^5 cells) / 0.6 (ratio-calc) donor 3: 10.6 (mU/10^5 cells) / 0.6 (ratio-calc)
Yamaguchi et al. (1994)	PGE_2	PGE_2	hPDL fibroblasts (12/M, 19/F, 11/M, PM, exp, P4, $1×10^5$)	dynamic	**0.1Hz** (6cyc/min: 5s on and 5s off) for 1d, 3d, 5d	18%	Flexercell strain unit + flexible-bottom culture plates coated with type I collagen (Flexcell) + vacuum (Banes et al 1985)	equibiaxial	n.a.	n.a.	increase (RIA)	5d: 8.9 (ng/10^6 cells)* / 17.8 (ratio-calc)
Yamaguchi et al. (1994)	PGE_2	PGE_2	hPDL fibroblasts (12/M, 19/F, 11/M, PM, exp, P4, $1×10^5$)	dynamic	**0.1Hz** (6cyc/min: 5s on and 5s off) for 5d	9%, 12%, 15%, 18%, 21%, 24%	Flexercell strain unit + flexible-bottom culture plates coated with type I collagen (Flexcell) + vacuum (Banes et al 1985)	equibiaxial	n.a.	n.a.	increase (RIA)	24%: 14 (ng/10^6 cells)* / 28 (ratio-calc)

[a] Entry given as reported in the study.
[b] All official gene symbols come from the HUGO Gene Nomenclature Committee (HGNC; URL: https://www.genenames.org) after checking specificity of primers with Primer-BLAST.
[c] Gender/Sex of donors: "M" – male, "F" – female; Tooth type: "PM" – premolar, "M" – molar; Cell density: given in cells/well if not otherwise mentioned.
[d] Frequencies labeled bold orange were converted to hertz (Hz) according to its definition using the information reported in the study (in brackets)
[e] Force type deduced from the description of the force apparatus given by the authors.
[f] Gene and protein expression: 1. conclusion of change (increase, decrease…) was given according to the defined criteria in Figure 2; 2. different markers to describe the amount of change; † Information derived from figures using Engauge Digitizer; *Folds calculated by measuring the graphs, without using the Engauge Digitizer; No makers: Information derived from figures by description in the articles

Reference	Gene/ Analyte[a]	Official gene symbol / abbreviation[b]	Cell (age/gender of donors, tooth type, isolation method, passages used, cell density)[a,c]	Force type (stat./ dyn.)[a]	Force duration and frequency[d]	Force magnitude[a]	Force apparatus[a]	Force type: equibiaxial or uniaxial[e]	Gene expression: Increase, decrease, no change (method w/ reference gene); Methods: qPCR, sqPCR, Northern blot[f]	Gene expression: When it reaches peak and peak's magnitude (fold change; times or ratio; unclear = ?)[f]	Protein expression: Increase, decrease, no change (method w/ reference); Methods: ELISA, WB, RIA, EMSA, IF[f]	Protein expression: When it reaches peak and peak's magnitude (times or ratio; unclear = ?)[f]
Yamaguchi et al. (1996)	ALP	*ALPP*	hPDL fibroblasts (12/M, PM, exp, P n.g., 1×10^5)	dynamic	**0.1Hz** (6cyc/min: 5s on and 5s off) for 1d, 3d, 5d	24%	Flexercell strain unit + flexible-bottom culture plates coated with type I collagen (Flexcell) + vacuum (Banes et al 1990)	equibiaxial	n.g.	n.g.	decrease followed by plateau (ALP activity)	3d…5d: 10.7 (mU/10^5 cells)* / 0.6 (ratio-calc)
Yamaguchi et al. (1996)	ALP	*ALPP*	hPDL fibroblasts (12/M, PM, exp, P n.g., 1×10^5)	dynamic	**0.1Hz** (6cyc/min: 5s on and 5s off) ALP activity for 5d; sqPCR for 3d	ALP activity for 9%, 12%, 15%, 18%, 21%, 24%; sqPCR for 12%, 24%	Flexercell strain unit + flexible-bottom culture plates coated with type I collagen (Flexcell) + vacuum (Banes et al 1990)	equibiaxial	decrease (Northern blot, β-actin)	no quantitative information is given	decrease (ALP activity)	24%: 9.4 (mU/10^5 cells)* / 0.5 (ratio-calc)
Yamaguchi et al. (1997)	PAI-1	*SERPINE1*	hPDL fibroblasts (12/M, 10/M, 11/F, exp, 3 donors, P unclear, confluent)	static	5d	18%	Flexercell strain unit + flexible-bottom culture plates coated with type I collagen (Flexcell) + vacuum (Banes et al 1985)	equibiaxial	no change (sqPCR, GAPDH)	no quantitative information is given	n.g.	n.g.
Yamaguchi et al. (1997)	Plasminogen activator	*PLAT; PLAU*	hPDL fibroblasts (12/M, 10/M, 11/F, exp, 3 donors, P unclear, confluent)	static	1d, 3d, 5d	18%	Flexercell strain unit + flexible-bottom culture plates coated with type I collagen (Flexcell) + vacuum (Banes et al 1985)	equibiaxial	n.g.	n.g.	increase (PA activity, photometric)	5d: 7.5 (mU/10^5 cells)* / 2.2 (ratio-calc)
Yamaguchi et al. (1997)	Plasminogen activator	*PLAT; PLAU*	hPDL fibroblasts (12/M, 10/M, 11/F, exp, 3 donors, P unclear, confluent)	static	5d	9%, 18%	Flexercell strain unit + flexible-bottom culture plates coated with type I collagen (Flexcell) + vacuum (Banes et al 1985)	equibiaxial	n.g.	n.g.	increase (PA activity, photometric)	18%: 7.9 (mU/10^5 cells)* / 2.2 (ratio-calc)
Yamaguchi et al. (1997)	tPA	*PLAT*	hPDL fibroblasts (12/M, 10/M, 11/F, exp, 3 donors, P unclear, confluent)	static	5d	18%	Flexercell strain unit + flexible-bottom culture plates coated with type I collagen (Flexcell) + vacuum (Banes et al 1985)	equibiaxial	increase (sqPCR, GAPDH)	no quantitative information is given	increase (WB)	no quantitative information is given
Yamaguchi et al. (1997)	uPA	*PLAU*	hPDL fibroblasts (12/M, 10/M, 11/F, exp, 3 donors, P unclear, confluent)	static	5d	18%	Flexercell strain unit + flexible-bottom culture plates coated with type I collagen (Flexcell) + vacuum (Banes et al 1985)	equibiaxial	not detectable (sqPCR, GAPDH)	no quantitative information is given	not detectable (WB)	no quantitative information is given
Yamaguchi et al. (2002)	ALP	*ALPP*	hPDL fibroblasts (n.g./n.g., PM, n.g., P8, confluent)	dynamic	**0.5Hz** (30cyc/min: 1s on and 1s off) for 30min, 90min, 6h	15%	a strain unit (Flexercell) + type I collagen-coated, silicon membrane) culture plates (Flex I; Flexercell) + vacuum	equibiaxial	temporary decrease (sqPCR, GAPDH)	90min: 0.8 (ratio)*	n.g.	n.g.
Yamaguchi et al. (2002)	c-fos	*FOS*	hPDL fibroblasts (n.g./n.g., PM, n.g., P8, confluent)	dynamic	**0.5Hz** (30cyc/min: 1s on and 1s off) for 30min, 90min, 6h	15%	a strain unit (Flexercell) + type I collagen-coated, silicon membrane) culture plates (Flex I; Flexercell) + vacuum	equibiaxial	increase (sqPCR, GAPDH)	30min: 55.8 (ratio)*	n.g.	n.g.
Yamaguchi et al. (2002)	COL-I	*COL1A1*	hPDL fibroblasts (n.g./n.g., PM, n.g., P8, confluent)	dynamic	**0.5Hz** (30cyc/min: 1s on and 1s off) for 30min, 90min, 6h	15%	a strain unit (Flexercell) + type I collagen-coated, silicon membrane) culture plates (Flex I; Flexercell) + vacuum	equibiaxial	temporary increase (sqPCR, GAPDH)	30min: 1.2 (ratio)*	n.g.	n.g.
Yamaguchi et al. (2002)	COL-III	*COL3A1*	hPDL fibroblasts (n.g./n.g., PM, n.g., P8, confluent)	dynamic	**0.5Hz** (30cyc/min: 1s on and 1s off) for 30min, 90min, 6h	15%	a strain unit (Flexercell) + type I collagen-coated, silicon membrane) culture plates (Flex I; Flexercell) + vacuum	equibiaxial	decrease (sqPCR, GAPDH)	6h: 0.6 (ratio)*	n.g.	n.g.
Yamaguchi et al. (2002)	MGP	*MGP*	hPDL fibroblasts (n.g./n.g., PM, n.g., P8, confluent)	dynamic	**0.5Hz** (30cyc/min: 1s on and 1s off) for 30min, 90min, 6h	15%	a strain unit (Flexercell) + type I collagen-coated, silicon membrane) culture plates (Flex I; Flexercell) + vacuum	equibiaxial	increase (sqPCR, GAPDH)	6h: 1.5 (ratio)*	n.g.	n.g.
Yamaguchi et al. (2002)	ON	*SPARC*	hPDL fibroblasts (n.g./n.g., PM, n.g., P8, confluent)	dynamic	**0.5Hz** (30cyc/min: 1s on and 1s off) for 30min, 90min, 6h	15%	a strain unit (Flexercell) + type I collagen-coated, silicon membrane) culture plates (Flex I; Flexercell) + vacuum	equibiaxial	no change (sqPCR, GAPDH)		n.g.	n.g.
Yamaguchi et al. (2002)	OPN	*SPP1*	hPDL fibroblasts (n.g./n.g., PM, n.g., P8, confluent)	dynamic	**0.5Hz** (30cyc/min: 1s on and 1s off) for 30min, 90min, 6h	15%	a strain unit (Flexercell) + type I collagen-coated, silicon membrane) culture plates (Flex I; Flexercell) + vacuum	equibiaxial	decrease (sqPCR, GAPDH)	6h: 0.7 (ratio)*	n.g.	n.g.
Yamaguchi et al. (2004)	Cathepsin B	*CTSB*	hPDL fibroblasts (15-18/F and 15-18/F, PM, exp, P n.g., 4×10^6)	static	12h	0.28%, 0.95%, 1.72%, 2.50%	Petriperm dish + spheroidal convex template + weight	equibiaxial	n.g.	n.g.	increase (ELISA)	2.5%: 15 (ng/g of cellular protein)* / 2.4 (ratio-calc)
Yamaguchi et al. (2004)	Cathepsin B	*CTSB*	hPDL fibroblasts (15-18/F and 15-18/F, PM, exp, P n.g., 4×10^6)	static	sqPCR for 12h; ELISA for 3h, 6h, 9h, 12h, 24h	2.50%	Petriperm dish + spheroidal convex template + weight	equibiaxial	increase (sqPCR, GAPDH)	no quantitative information is given	increase (ELISA)	12h: 15 (ng/g of cellular protein)* / 1.6 (ratio-calc)
Yamaguchi et al. (2004)	Cathepsin L	*CTSL*	hPDL fibroblasts (15-18/F and 15-18/F, PM, exp, P n.g., 4×10^6)	static	12h	0.28%, 0.95%, 1.72%, 2.50%	Petriperm dish + spheroidal convex template + weight	equibiaxial	n.g.	n.g.	increase (ELISA)	2.5%: 22 (ng/g of cellular protein)* / 3.1 (ratio-calc)
Yamaguchi et al. (2004)	Cathepsin L	*CTSL*	hPDL fibroblasts (15-18/F and 15-18/F, PM, exp, P n.g., 4×10^6)	static	3h, 6h, 9h, 12h, 24h	2.50%	Petriperm dish + spheroidal convex template + weight	equibiaxial	increase (sqPCR, GAPDH)	no quantitative information is given	increase (ELISA)	12h: 20.8 (ng/g of cellular protein)* / 2.7 (ratio-calc)

[a] Entry given as reported in the study.
[b] All official gene symbols come from the HUGO Gene Nomenclature Committee (HGNC; URL: https://www.genenames.org) after checking specificity of primers with Primer-BLAST.
[c] Gender/Sex of donors: "M" – male, "F" – female; Tooth type: "PM" – premolar, "M" – molar; Cell density: given in cells/well if not otherwise mentioned.
[d] Frequencies labeled bold orange were converted to hertz (Hz) according to its definition using the information reported in the study (in brackets)
[e] Force type deduced from the description of the force apparatus given by the authors.
[f] Gene and protein expression: 1. conclusion of change (increase, decrease…) was given according to the defined criteria in Figure 2; 2. different markers to describe the amount of change; † Information derived from figures using Engauge Digitizer; *Folds calculated by measuring the graphs, without using the Engauge Digitizer; No makers: Information derived from figures by description in the articles

Reference	Gene/ Analyte[a]	Official gene symbol / abbreviation[b]	Cell (age/gender of donors, tooth type, isolation method, passages used, cell density)[a,c]	Force type (stat./ dyn.)[a]	Force duration and frequency[d]	Force magnitude[a]	Force apparatus[a]	Force type: equibiaxial or uniaxial[e]	Gene expression: Increase, decrease, no change (method w/ reference gene); Methods: qPCR, sqPCR, Northern blot[f]	Gene expression: When it reaches peak and peak's magnitude (fold change; times or ratio; unclear = ?)[f]	Protein expression: Increase, decrease, no change (method w/ reference); Methods: ELISA, WB, RIA, EMSA, IF[f]	Protein expression: When it reaches peak and peak's magnitude (times or ratio; unclear = ?)[f]
Yamashiro et al. (2007)	ACY1	*ACY1*	hPDL fibroblasts (21/F, 24/F, 17/F, 22/M, n.g., n.g., P5-9, 2×10^5)	dynamic	**0.1Hz** (6cyc/min) for 0.5h, 1h, 2h, 16h	18%	Flexercell Strain Unit + flexible-bottomed culture plates (FLEX II) + vacuum (Myokai et al 2003; Banes et al 1990)	equibiaxial	increase (qPCR, β-actin)	duration n.g.: 2.7 (ratio)*	n.g.	n.g.
Yamashiro et al. (2007)	ADRB2	*ADRB2*	hPDL fibroblasts (21/F, 24/F, 17/F, 22/M, n.g., n.g., P5-9, 2×10^5)	dynamic	**0.1Hz** (6cyc/min) for 0.5h, 1h, 2h, 16h	18%	Flexercell Strain Unit + flexible-bottomed culture plates (FLEX II) + vacuum (Myokai et al 2003; Banes et al 1990)	equibiaxial	increase (qPCR, β-actin)	duration n.g.: 1.6 (ratio)*	n.g.	n.g.
Yamashiro et al. (2007)	ARRAY	ARRAY	hPDL fibroblasts (21/F, 24/F, 17/F, 22/M, n.g., n.g., P5-9, 2×10^5)	dynamic	**0.1Hz** (6cyc/min) for 0.5h, 1h, 2h, 16h	18%	Flexercell Strain Unit + flexible-bottomed culture plates (FLEX II) + vacuum (Myokai et al 2003; Banes et al 1990)	equibiaxial	Human Genome Focus GeneChip probe array #900377 (Affymetrix)		n.a.	n.a.
Yamashiro et al. (2007)	ATF1	*ATF1*	hPDL fibroblasts (21/F, 24/F, 17/F, 22/M, n.g., n.g., P5-9, 2×10^5)	dynamic	**0.1Hz** (6cyc/min) for 0.5h, 1h, 2h, 16h	18%	Flexercell Strain Unit + flexible-bottomed culture plates (FLEX II) + vacuum (Myokai et al 2003; Banes et al 1990)	equibiaxial	decrease (qPCR, β-actin)	duration n.g.: 0.6 (ratio)*	n.g.	n.g.
Yamashiro et al. (2007)	BCL2	*BCL2*	hPDL fibroblasts (21/F, 24/F, 17/F, 22/M, n.g., n.g., P5-9, 2×10^5)	dynamic	**0.1Hz** (6cyc/min) for 0.5h, 1h, 2h, 16h	18%	Flexercell Strain Unit + flexible-bottomed culture plates (FLEX II) + vacuum (Myokai et al 2003; Banes et al 1990)	equibiaxial	increase (qPCR, β-actin)	duration n.g.: 1.3 (ratio)*	n.g.	n.g.
Yamashiro et al. (2007)	CASP3	*CASP3*	hPDL fibroblasts (21/F, 24/F, 17/F, 22/M, n.g., n.g., P5-9, 2×10^5)	dynamic	**0.1Hz** (6cyc/min) for 0.5h, 1h, 2h, 16h	18%	Flexercell Strain Unit + flexible-bottomed culture plates (FLEX II) + vacuum (Myokai et al 2003; Banes et al 1990)	equibiaxial	increase (qPCR, β-actin)	duration n.g.: 1.2 (ratio)*	n.g.	n.g.
Yamashiro et al. (2007)	FOS	*FOS*	hPDL fibroblasts (21/F, 24/F, 17/F, 22/M, n.g., n.g., P5-9, 2×10^5)	dynamic	**0.1Hz** (6cyc/min) for 0.5h, 1h, 2h, 16h	18%	Flexercell Strain Unit + flexible-bottomed culture plates (FLEX II) + vacuum (Myokai et al 2003; Banes et al 1990)	equibiaxial	increase (qPCR, β-actin)	duration n.g.: 2.0 (ratio)*	n.g.	n.g.
Yamashiro et al. (2007)	GOSR1	*GOSR1*	hPDL fibroblasts (21/F, 24/F, 17/F, 22/M, n.g., n.g., P5-9, 2×10^5)	dynamic	**0.1Hz** (6cyc/min) for 0.5h, 1h, 2h, 16h	18%	Flexercell Strain Unit + flexible-bottomed culture plates (FLEX II) + vacuum (Myokai et al 2003; Banes et al 1990)	equibiaxial	decrease (qPCR, β-actin)	duration n.g.: 0.4 (ratio)*	n.g.	n.g.
Yamashiro et al. (2007)	TP53BP2	*TP53BP2*	hPDL fibroblasts (21/F, 24/F, 17/F, 22/M, n.g., n.g., P5-9, 2×10^5)	dynamic	**0.1Hz** (6cyc/min) for 0.5h, 1h, 2h, 16h	18%	Flexercell Strain Unit + flexible-bottomed culture plates (FLEX II) + vacuum (Myokai et al 2003; Banes et al 1990)	equibiaxial	increase (qPCR, β-actin)	duration n.g.: 1.4 (ratio)*	n.g.	n.g.
Yang et al. (2006)	ALP	*ALPP*	hPDLCs (10-13/n.g., PM, exp, P4-8, confluent)	dynamic	**0.05Hz** (cycle of 3/min) for 2h, 4h, 6h, 12h, 24h	310-320 grams force	"A new model to apply intermittent mechanical stress on cells" (Zhang 1999)	uniaxial	n.g.	n.g.	increase (biochemistry test)	4h: 3 (unit/10^4 cellls)* / 4.3 (ratio-calc)
Yang et al. (2006)	OCN	*BGLAP*	hPDLCs (10-13/n.g., PM, exp, P4-8, confluent)	dynamic	**0.05Hz** (cycle of 3/min) for 2h, 4h, 6h, 12h, 24h	310-320 grams force	"A new model to apply intermittent mechanical stress on cells" (Zhang 1999)	uniaxial	n.g.	n.g.	increase (RIA)	12h: 1.6 (ng/10^4 cellls)* / 8 (ratio-calc)
Yang et al. (2006)	OPG	*TNFRSF11B*	hPDLCs (10-13/n.g., PM, exp, P4-8, confluent)	dynamic	**0.05Hz** (cycle of 3/min) for 2h, 4h, 6h, 12h, 24h	310-320 grams force	"A new model to apply intermittent mechanical stress on cells" (Zhang 1999)	uniaxial	decrease (in-situ hybridization staining)	4h: 0.3 (optical density)* / 0.5 (ratio-calc)	decrease (ELISA)	24h: 38.9 (10^{-15} mol)* / 0.9 (ratio-calc)
Yang et al. (2010)	ALP	*ALPP*	hPDLCs (10-13/n.g., PM, dig, P4-6, 80% confluent)	dynamic	**0.005Hz** (cycle of 3 minutes) for 0.5h,1h, 2h, 4h, 6h, 12h, 24h	12%	"A new model to apply intermittent mechanical stress on cells" (Yang et al 2006; further reference to Zhang 1999)	uniaxial	temporary increase (sqPCR, β-actin)	4h: 0.8 (rel)* / t_0 = 0	n.g.	n.g.
Yang et al. (2010)	CBFA1	*RUNX2*	hPDLCs (10-13/n.g., PM, dig, P4-6, 80% confluent)	dynamic	**0.005Hz** (cycle of 3 minutes) for 0.5h,1h, 2h, 4h, 6h, 12h, 24h	12%	"A new model to apply intermittent mechanical stress on cells" (Yang et al 2006; further reference to Zhang 1999)	uniaxial	increase followed by decrease (sqPCR, β-actin)	highest @ 1h: 2.0 (optical density)* / 3.3 (ratio-calc relative to t_0) lowest @ 12h: 0.3 (optical density)* / 0.5 (ratio-calc relative to t_0)	n.g.	n.g.
Yang et al. (2010)	OPG	*TNFRSF11B*	hPDLCs (10-13/n.g., PM, dig, P4-6, 80% confluent)	dynamic	**0.005Hz** (cycle of 3 minutes) for 0.5h,1h, 2h, 4h, 6h, 12h, 24h	12%	"A new model to apply intermittent mechanical stress on cells" (Yang et al 2006; further reference to Zhang 1999)	uniaxial	increase followed by decrease (sqPCR, β-actin)	highest @ 2h: 1.5 (rel)* / 1.4 (ratio-calc relative to t_0) lowest @ 6h: 0.3 (rel)* / 0.3 (ratio-calc relative to t_0)	n.g.	n.g.
Yang et al. (2010)	OPN	*SPP1*	hPDLCs (10-13/n.g., PM, dig, P4-6, 80% confluent)	dynamic	**0.005Hz** (cycle of 3 minutes) for 0.5h,1h, 2h, 4h, 6h, 12h, 24h	12%	"A new model to apply intermittent mechanical stress on cells" (Yang et al 2006; further reference to Zhang 1999)	uniaxial	increase (sqPCR, β-actin)	0.5h: 1.8 (rel)* / t_0 = 0	n.g.	n.g.

[a] Entry given as reported in the study.
[b] All official gene symbols come from the HUGO Gene Nomenclature Committee (HGNC; URL: https://www.genenames.org) after checking specificity of primers with Primer-BLAST.
[c] Gender/Sex of donors: "M" – male, "F" – female; Tooth type: "PM" – premolar, "M" – molar; Cell density: given in cells/well if not otherwise mentioned.
[d] Frequencies labeled bold orange were converted to hertz (Hz) according to its definition using the information reported in the study (in brackets)
[e] Force type deduced from the description of the force apparatus given by the authors.
[f] Gene and protein expression: 1. conclusion of change (increase, decrease…) was given according to the defined criteria in Figure 2; 2. different markers to describe the amount of change; † Information derived from figures using Engauge Digitizer; *Folds calculated by measuring the graphs, without using the Engauge Digitizer; No makers: Information derived from figures by description in the articles

Reference	Gene/ Analyte[a]	Official gene symbol / abbreviation[b]	Cell (age/gender of donors, tooth type, isolation method, passages used, cell density)[a,c]	Force type (stat./ dyn.)[a]	Force duration and frequency[d]	Force magnitude[a]	Force apparatus[a]	Force type: equibiaxial or uniaxial[e]	Gene expression: Increase, decrease, no change (method w/ reference gene); Methods: qPCR, sqPCR, Northern blot[f]	Gene expression: When it reaches peak and peak's magnitude (fold change; times or ratio; unclear = ?)[f]	Protein expression: Increase, decrease, no change (method w/ reference); Methods: ELISA, WB, RIA, EMSA, IF[f]	Protein expression: When it reaches peak and peak's magnitude (times or ratio; unclear = ?)[f]
Yang et al. (2010)	RANKL	*TNFSF11*	hPDLCs (10-13/n.g., PM, dig, P4-6, 80% confluent)	dynamic	**0.005Hz** (cycle of 3 minutes) for 0.5h,1h, 2h, 4h, 6h, 12h, 24h	12%	"A new model to apply intermittent mechanical stress on cells" (Yang et al 2006; further reference to Zhang 1999)	uniaxial	increase (sqPCR, β-actin)	24h: 0.7 (optical density)† / 14.0 (ratio-calc relative to t_0)	n.g.	n.g.
Yang et al. (2015)	IL-6	*IL6*	hPDLCs (n.g./n.g., PM, n.g., P4-6, 3×10^5)	dynamic	**0.1Hz** (6cyc/min) for 2h,4h, 8h, 24h, 48h	12%	Flexcell FX-5000™ Tension Unit + BioFlex culture plate + vacuum	equibiaxial	increase (qPCR, β-actin)	48h: 20.0 (ratio)	n.g.	n.g.
Yang et al. (2015)	MMP-1	*MMP1*	hPDLCs (n.g./n.g., PM, n.g., P4-6, 3×10^5)	dynamic	**0.1Hz** (6cyc/min) for 2h,4h, 8h, 24h, 48h	12%	Flexcell FX-5000™ Tension Unit + BioFlex culture plate + vacuum	equibiaxial	increase (qPCR, β-actin)	48h: 4.0 (ratio)*	n.g.	n.g.
Yang et al. (2015)	MMP-2	*MMP2*	hPDLCs (n.g./n.g., PM, n.g., P4-6, 3×10^5)	dynamic	**0.1Hz** (6cyc/min) for 2h,4h, 8h, 24h, 48h	12%	Flexcell FX-5000™ Tension Unit + BioFlex culture plate + vacuum	equibiaxial	increase (qPCR, β-actin)	48h: 8.0 (ratio)	n.g.	n.g.
Yang et al. (2015)	Rxfp1	*RXFP1*	hPDLCs (n.g./n.g., PM, n.g., P4-6, 3×10^5)	dynamic	**0.1Hz** (6cyc/min) for 2h, 4h, 8h, 24h	12%	Flexcell FX-5000™ Tension Unit + BioFlex culture plate + vacuum	equibiaxial	increase (sqPCR, β-actin) increase (qPCR, β-actin)	sqPCR: no quantitative information is given qPCR @ 24h: 8.5 (ratio)*	n.g.	n.g.
Yang et al. (2015)	Rxfp2	*RXFP2*	hPDLCs (n.g./n.g., PM, n.g., P4-6, 3×10^5)	dynamic	**0.1Hz** (6cyc/min) for 2h,4h, 8h, 24h	12%	Flexcell FX-5000™ Tension Unit + BioFlex culture plate + vacuum	equibiaxial	no change (sqPCR, β-actin) qPCR is not given	no quantitative information is given	n.g.	n.g.
Yang et al. (2015)	VEGF	*VEGFA*	hPDLCs (n.g./n.g., PM, n.g., P4-6, 3×10^5)	dynamic	**0.1Hz** (6cyc/min) for 2h,4h, 8h, 24h, 48h	12%	Flexcell FX-5000™ Tension Unit + BioFlex culture plate + vacuum	equibiaxial	increase (qPCR, β-actin)	48h: 20.9 (ratio)	n.g.	n.g.
Yang et al. (2016)	ATF4	*ATF4*	hPDLCs (12-16/n.g., PM, exp, P3-4, 80% confluences)	dynamic	0.5Hz (30cyc/min) for 1h, 3h, 6h, 12h, 24h	10%	Flexcell® FX-5000™ Tension System + "six-well culture plates with 35-mm silicone membrane coated on the bottom" + vacuum	equibiaxial	increase (qPCR,GAPDH)	24h: 1.9 (FC)*	increase (WB, GAPDH)	1h: 2.2 (ratio)*
Yang et al. (2016)	Bip	*HSPA5*	hPDLCs (12-16/n.g., PM, exp, P3-4, 80% confluences)	dynamic	0.5Hz (30cyc/min) for 1h, 3h, 6h, 12h, 24h	10%	Flexcell® FX-5000™ Tension System + "six-well culture plates with 35-mm silicone membrane coated on the bottom" + vacuum	equibiaxial	increase (qPCR,GAPDH)	24h: 2.5 (FC)*	n.g.	n.g.
Yang et al. (2016)	BSP	*IBSP*	hPDLCs (12-16/n.g., PM, exp, P3-4, 80% confluences)	dynamic	0.5Hz (30cyc/min) for 1h, 3h, 6h, 12h, 24h	10%	Flexcell® FX-5000™ Tension System + "six-well culture plates with 35-mm silicone membrane coated on the bottom" + vacuum	equibiaxial	increase (qPCR,GAPDH)	24h: 2.0 (FC)*	n.g.	n.g.
Yang et al. (2016)	eIF2α / p-eIF2α	*EIF2AK3*	hPDLCs (12-16/n.g., PM, exp, P3-4, 80% confluences)	dynamic	0.5Hz (30cyc/min) for 1h, 3h, 6h, 12h, 24h	10%	Flexcell® FX-5000™ Tension System + "six-well culture plates with 35-mm silicone membrane coated on the bottom" + vacuum	equibiaxial	n.g.	n.g.	eIF2α: no change (WB, GAPDH) p-eIF2α: increase (WB, GAPDH)	eIF2α: no quantitative information is given p-eIF2α @ 6h: 0.6 (rel)* / 15 (ratio-calc)
Yang et al. (2016)	OCN	*BGLAP*	hPDLCs (12-16/n.g., PM, exp, P3-4, 80% confluences)	dynamic	0.5Hz (30cyc/min) for 1h, 3h, 6h, 12h, 24h	10%	Flexcell® FX-5000™ Tension System + "six-well culture plates with 35-mm silicone membrane coated on the bottom" + vacuum	equibiaxial	increase (qPCR,GAPDH)	24h: 3.2 (FC)*	n.g.	n.g.
Yang et al. (2016)	PERK	*EIF2AK3*	hPDLCs (12-16/n.g., PM, exp, P3-4, 80% confluences)	dynamic	0.5Hz (30cyc/min) for 1h, 3h, 6h, 12h, 24h	10%	Flexcell® FX-5000™ Tension System + "six-well culture plates with 35-mm silicone membrane coated on the bottom" + vacuum	equibiaxial	n.g.	n.g.	increase (WB, GAPDH)	6h: 0.7 (rel)* / 2.3 (ratio-calc)
Yang et al. (2016)	Xbp1	*XBP1*	hPDLCs (12-16/n.g., PM, exp, P3-4, 80% confluences)	dynamic	0.5Hz (30cyc/min) for 1h, 3h, 6h, 12h, 24h	10%	Flexcell® FX-5000™ Tension System + "six-well culture plates with 35-mm silicone membrane coated on the bottom" + vacuum	equibiaxial	increase (qPCR,GAPDH)	24h: 3.2 (FC)*	n.g.	n.g.
Yang et al. (2018)	ALP	*ALPP*	hPDLCs (12-24/n.g., PM, dig, P3-8, 80% confluence)	dynamic	0.1Hz (5s stress and 5s rest) for 24h	10%	Flexercell FX-4000 Strain Unit + silicon membranes of wells coated with type I collagen (BioFlex) + vacuum (Chang et al 2015)	equibiaxial	increase (qPCR, GAPDH)	1.8 (FC)*	n.g.	n.g.
Yang et al. (2018)	COL1	*COL1A1*	hPDLCs (12-24/n.g., PM, dig, P3-8, 80% confluence)	dynamic	0.1Hz (5s stress and 5s rest) for 24h	10%	Flexercell FX-4000 Strain Unit + silicon membranes of wells coated with type I collagen (BioFlex) + vacuum (Chang et al 2015)	equibiaxial	increase (qPCR, GAPDH)	1.7 (FC)*	n.g.	n.g.
Yang et al. (2018)	CTGF	*CCN2*	hPDLCs (12-24/n.g., PM, dig, P3-8, 80% confluence)	dynamic	0.1Hz (5s stress and 5s rest) for 24h	10%	Flexercell FX-4000 Strain Unit + silicon membranes of wells coated with type I collagen (BioFlex) + vacuum (Chang et al 2015)	equibiaxial	increase (qPCR, GAPDH)	3.0 (FC)	n.g.	n.g.
Yang et al. (2018)	CYR61	*CCN1*	hPDLCs (12-24/n.g., PM, dig, P3-8, 80% confluence)	dynamic	0.1Hz (5s stress and 5s rest) for 24h	10%	Flexercell FX-4000 Strain Unit + silicon membranes of wells coated with type I collagen (BioFlex) + vacuum (Chang et al 2015)	equibiaxial	increase (qPCR, GAPDH)	1.5 (FC)	n.g.	n.g.

[a] Entry given as reported in the study.
[b] All official gene symbols come from the HUGO Gene Nomenclature Committee (HGNC; URL: https://www.genenames.org) after checking specificity of primers with Primer-BLAST.
[c] Gender/Sex of donors: "M" – male, "F" – female; Tooth type: "PM" – premolar, "M" – molar; Cell density: given in cells/well if not otherwise mentioned.
[d] Frequencies labeled bold orange were converted to hertz (Hz) according to its definition using the information reported in the study (in brackets)
[e] Force type deduced from the description of the force apparatus given by the authors.
[f] Gene and protein expression: 1. conclusion of change (increase, decrease…) was given according to the defined criteria in Figure 2; 2. different markers to describe the amount of change; † Information derived from figures using Engauge Digitizer; *Folds calculated by measuring the graphs, without using the Engauge Digitizer; No makers: Information derived from figures by description in the articles

Reference	Gene/ Analyte[a]	Official gene symbol / abbreviation[b]	Cell (age/gender of donors, tooth type, isolation method, passages used, cell density)[a,c]	Force type (stat./ dyn.)[a]	Force duration and frequency[d]	Force magnitude[a]	Force apparatus[a]	Force type: equibiaxial or uniaxial[e]	Gene expression: Increase, decrease, no change (method w/ reference gene); Methods: qPCR, sqPCR, Northern blot[f]	Gene expression: When it reaches peak and peak's magnitude (fold change; times or ratio; unclear = ?)[f]	Protein expression: Increase, decrease, no change (method w/ reference); Methods: ELISA, WB, RIA, EMSA, IF[f]	Protein expression: When it reaches peak and peak's magnitude (times or ratio; unclear = ?)[f]
Yang et al. (2018)	OCN	*BGLAP*	hPDLCs (12-24/n.g., PM, dig, P3-8, 80% confluence)	dynamic	0.1Hz (5s stress and 5s rest) qPCR for 24 h; WB for 72h	10%	Flexercell FX-4000 Strain Unit + silicon membranes of wells coated with type I collagen (BioFlex) + vacuum (Chang et al 2015)	equibiaxial	increase (qPCR, GAPDH)	2.0 (FC)*	increase (WB, GAPDH)	1.8 (ratio)*
Yang et al. (2018)	OPN	*SPP1*	hPDLCs (12-24/n.g., PM, dig, P3-8, 80% confluence)	dynamic	0.1Hz (5s stress and 5s rest) qPCR for 24 h WB for 72h	10%	Flexercell FX-4000 Strain Unit + silicon membranes of wells coated with type I collagen (BioFlex) + vacuum (Chang et al 2015)	equibiaxial	increase (qPCR, GAPDH)	3.3 (FC)*	increase (WB, GAPDH)	2.4 (ratio)*
Yang et al. (2018)	OSX	*SP7*	hPDLCs (12-24/n.g., PM, dig, P3-8, 80% confluence)	dynamic	0.1Hz (5s stress and 5s rest) for 24h	10%	Flexercell FX-4000 Strain Unit + silicon membranes of wells coated with type I collagen (BioFlex) + vacuum (Chang et al 2015)	equibiaxial	increase (qPCR, GAPDH)	1.7 (FC)*	n.g.	n.g.
Yang et al. (2018)	RUNX2	*RUNX2*	hPDLCs (12-24/n.g., PM, dig, P3-8, 80% confluence)	dynamic	0.1Hz (5s stress and 5s rest) for 24h	10%	Flexercell FX-4000 Strain Unit + silicon membranes of wells coated with type I collagen (BioFlex) + vacuum (Chang et al 2015)	equibiaxial	increase (qPCR, GAPDH)	1.8 (FC)*	n.g.	n.g.
Yang et al. (2018)	YAP	*YAP1*	hPDLCs (12-24/n.g., PM, dig, P3-8, 80% confluence)	dynamic	0.1Hz (5s stress and 5s rest) for 72h	10%	Flexercell FX-4000 Strain Unit + silicon membranes of wells coated with type I collagen (BioFlex) + vacuum (Chang et al 2015)	equibiaxial	n.g.	n.g.	nucleus YAP: increase (WB, GAPDH) cytoplasm YAP: decrease (WB, GAPDH)	nucleus YAP: 11.9 (ratio)* cytoplasm YAP: no quantitative information is given
Yoshino et al. (2003)	PEDF	*SERPINF1*	hPDL fibroblasts (n.g./n.g., M, exp, P4-6, confluency)	dynamic	**0.2Hz** (12cyc/min: stretch for 2.5s followed by 2.5s of relaxation) sqPCR duration n.g.; WB for 24h	14%	Flexercell Strain Unit + type I collagen (35-mm 6-well) + vacuum	equibiaxial	no change (sqPCR, GAPDH)	no quantitative information is given	decrease (WB, GAPDH)	0.4 (rel)* / 0.7 (ratio-calc)
Yoshino et al. (2003)	VEGF	*VEGFA*	hPDL fibroblasts (n.g./n.g., M, exp, P4-6, confluency)	dynamic	**0.2Hz** (12cyc/min: stretch for 2.5s followed by 2.5s of relaxation) for 24h	7%, 14%, 21%	Flexercell Strain Unit + type I collagen (35-mm 6-well) + vacuum	equibiaxial	n.g.	n.g.	increase (ELISA)	14%: 1.4 (ng/2×10^5 cellls)* / 2.3 (ratio-calc)
Yoshino et al. (2003)	VEGF	*VEGFA*	hPDL fibroblasts (n.g./n.g., M, exp, P4-6, confluency)	dynamic	**0.2Hz** (12cyc/min: stretch for 2.5s followed by 2.5s of relaxation) sqPCR duration n.g.; ELISA for 12h, 24h, 36h, 48h	14%	Flexercell Strain Unit + type I collagen (35-mm 6-well) + vacuum	equibiaxial	increase (sqPCR, GAPDH)	no quantitative information is given	increase (ELISA)	48h: 3.1 (ng/2×10^5 cellls)* / 2.8 (ratio-calc)
Yu et al. (2018)	COL1	*COL1A1*	hPDLCs (18-30/n.g., M, dig, P3-5, 3×10^5)	dynamic	0.5Hz (30cyc/min) for 24h, 48h, 72h	12%	Flexcell 5000 Tension System + 6-well, flexible-bottomed culture plates (Flexcell) which were coated with type I collagen + vacuum	equibiaxial	increase (qPCR, ACTB)	48h: 1.3 (FC)*	increase (WB, β-actin)	no quantitative information is given
Yu et al. (2018)	Cyclin D1	*CCND1*	hPDLCs (18-30/n.g., M, dig, P3-5, 3×10^5)	dynamic	0.5Hz (30cyc/min) for 24h, 48h, 72h	12%	Flexcell 5000 Tension System + 6-well, flexible-bottomed culture plates (Flexcell) which were coated with type I collagen + vacuum	equibiaxial	n.g.	n.g.	decrease (WB, β-actin)	no quantitative information is given
Yu et al. (2018)	LEF1	*LEF1*	hPDLCs (18-30/n.g., M, dig, P3-5, 3×10^5)	dynamic	0.5Hz (30cyc/min) for 24h, 48h, 72h	12%	Flexcell 5000 Tension System + 6-well, flexible-bottomed culture plates (Flexcell) which were coated with type I collagen + vacuum	equibiaxial	n.g.	n.g.	decrease (WB, β-actin)	no quantitative information is given
Yu et al. (2018)	RUNX2	*RUNX2*	hPDLCs (18-30/n.g., M, dig, P3-5, 3×10^5)	dynamic	0.5Hz (30cyc/min) for 24h, 48h, 72h	12%	Flexcell 5000 Tension System + 6-well, flexible-bottomed culture plates (Flexcell) which were coated with type I collagen + vacuum	equibiaxial	increase (qPCR, ACTB)	48h: 3.4 (FC)*	increase (WB, β-actin)	no quantitative information is given
Yu et al. (2018)	SP7	*SP7*	hPDLCs (18-30/n.g., M, dig, P3-5, 3×10^5)	dynamic	0.5Hz (30cyc/min) for 24h, 48h, 72h	12%	Flexcell 5000 Tension System + 6-well, flexible-bottomed culture plates (Flexcell) which were coated with type I collagen + vacuum	equibiaxial	increase (qPCR, ACTB)	72h: 3.3 (FC)*	increase (WB, β-actin)	no quantitative information is given
Yu et al. (2018)	β-Catenin / β-Catenin, active	*CTNNB1*	hPDLCs (18-30/n.g., M, dig, P3-5, 3×10^5)	dynamic	0.5Hz (30cyc/min) for 24h, 48h, 72h	12%	Flexcell 5000 Tension System + 6-well, flexible-bottomed culture plates (Flexcell) which were coated with type I collagen + vacuum	equibiaxial	n.g.	n.g.	β-catenin: no change (WB, β-actin) active β-catenin: decrease (WB, β-actin)	β-catenin: no quantitative information is given active β-catenin: no quantitative information is given

[a] Entry given as reported in the study.
[b] All official gene symbols come from the HUGO Gene Nomenclature Committee (HGNC; URL: https://www.genenames.org) after checking specificity of primers with Primer-BLAST.
[c] Gender/Sex of donors: "M" – male, "F" – female; Tooth type: "PM" – premolar, "M" – molar; Cell density: given in cells/well if not otherwise mentioned.
[d] Frequencies labeled bold orange were converted to hertz (Hz) according to its definition using the information reported in the study (in brackets)
[e] Force type deduced from the description of the force apparatus given by the authors.
[f] Gene and protein expression: 1. conclusion of change (increase, decrease…) was given according to the defined criteria in Figure 2; 2. different markers to describe the amount of change; † Information derived from figures using Engauge Digitizer; *Folds calculated by measuring the graphs, without using the Engauge Digitizer; No makers: Information derived from figures by description in the articles

Reference	Gene/ Analyte[a]	Official gene symbol / abbreviation[b]	Cell (age/gender of donors, tooth type, isolation method, passages used, cell density)[a,c]	Force type (stat./ dyn.)[a]	Force duration and frequency[d]	Force magnitude[a]	Force apparatus[a]	Force type: equibiaxial or uniaxial[e]	Gene expression: Increase, decrease, no change (method w/ reference gene); Methods: qPCR, sqPCR, Northern blot[f]	Gene expression: When it reaches peak and peak's magnitude (fold change; times or ratio; unclear = ?)[f]	Protein expression: Increase, decrease, no change (method w/ reference); Methods: ELISA, WB, RIA, EMSA, IF[f]	Protein expression: When it reaches peak and peak's magnitude (times or ratio; unclear = ?)[f]
Yuda et al. (2015)	CTGF/CCN2	*CCN2*	hPDLCs (23/M. 25/F, 21/F, PM, 3 donors, n.g., P n.g., subconfluence)	dynamic	**1Hz** (60cyc/min: 0.5s stretch and 0.5s relaxation per cycle) qPCR for 1h; ELISA for 3h	8%	STB-140 (STREX, Osaka, Japan) + flexiblebottomed culture chambers coated with type I collagen (Cellmatrix I-P, Nitta Gelatin Inc, Osaka, Japan) + motor	uniaxial	donor 1: increase (qPCR, GAPDH) donor 2: increase (qPCR, GAPDH) donor 3: increase (qPCR, GAPDH)	donor 1: 2 (FC)* donor 2: 2.4 (FC)* donor 3: 1.3 (FC)*	donor 1: Increase (ELISA) donor 2: Increase (ELISA) donor 3: Increase (ELISA)	donor 1: 91.2 (pg/mg)* / 1.9 (ratio-calc) donor 2: 82.4 (pg/mg)* / 1.6 (ratio-calc) donor 3: 57.4 (pg/mg)* / 1.6 (ratio-calc)
Zhao et al. (2016)	ASC	*PYCARD*	hPDLCs (11-13/n.g., PM, exp, P4-6, confluence)	dynamic	**0.1Hz** (6cyc/min: 5s stretch and 5s relaxation) for 6h, 24h	20%	Flexcell Tension Plus system FX-5000T + six-well Bioflex plates + vacuum	equibiaxial	decrease (qPCR, GAPDH)	6h: 1.2 (ratio)*	increase followed by decrease (WB, GAPDH)	highest @ 6h: 0.8 (rel)* / 1.3 (ratio-calc) lowest @ 24h: 0.3 (rel)* / 0.5 (ratio-calc)
Zhao et al. (2016)	Caspase 1	*CASP1*	hPDLCs (11-13/n.g., PM, exp, P4-6, confluence)	dynamic	**0.1Hz** (6 cyc/min: 5s stretch and 5s relaxation) for 6h, 24h	20%	Flexcell Tension Plus system FX-5000T + six-well Bioflex plates + vacuum	equibiaxial	increase followed by decrease (qPCR, GAPDH)	highest @ 6h: 1.2 (ratio)* lowest @ 24h: 0.6 (ratio)*	Pro-caspase-1 (50 kDa): temporary increase (WB, GAPDH) Caspase-1 (20 kDa): increase (WB, GAPDH) Caspase-1-activity: increase (caspase colorimetric assay kit)	Pro-caspase-1 @ 6h: 5.2 (ratio)* Caspase-1@ 6h: 6.7 (ratio)* Caspase-1 activity @ 6h: 1.5 (ratio)*
Zhao et al. (2016)	Caspase 5	*CASP5*	hPDLCs (11-13/n.g., PM, exp, P4-6, confluence)	dynamic	**0.1Hz** (6 cyc/min: 5s stretch and 5s relaxation) for 6h, 24h	20%	Flexcell Tension Plus system FX-5000T + six-well Bioflex plates + vacuum	equibiaxial	increase (qPCR, GAPDH)	6h: 10 (ratio)*	Pro-caspase-5 (48 kDa): increase (WB, GAPDH) Caspase-5 (20 kDa): increase (WB, GAPDH) Caspase-5-activity: increase (caspase colorimetric assay kit)	Pro-caspase-5 @ 6h: 2.8 (ratio)* Caspase-5 @ 6h: 2.5 (ratio)* Caspase-5-activity @ 6h: 1.6 (ratio)*
Zhao et al. (2016)	IL-1β	*IL1B*	hPDLCs (11-13/n.g., PM, exp, P4-6, confluence)	dynamic	**0.1Hz** (6 cyc/min: 5s stretch and 5s relaxation) qPCR and WB for 0h, 6h, 24h; ELISA for 1h, 2h, 4h, 6h, 12h, 24h	20%	Flexcell Tension Plus system FX-5000T + six-well Bioflex plates + vacuum	equibiaxial	increase followed by decrease (qPCR, GAPDH)	highest @ 6h: 1.4 (ratio)* lowest @ 24h: 0.6 (ratio)*	Pro-IL-1β (31 kDa): increase (WB, GAPDH) IL-1β (17 kDa): increase (WB, GAPDH) IL-1β in the culture medium: temporary increase (ELISA)	Pro-IL-1β @ 6h: 1.7 (ratio)* IL-1β @6h: 1.8 (ratio)* IL-1β in the culture medium @ 6h: 5.5 (ratio)*
Zhao et al. (2016)	NLRP1	*NLRP1*	hPDLCs (11-13/n.g., PM, exp, P4-6, confluence)	dynamic	**0.1Hz** (6cyc/min: 5s stretch and 5s relaxation) for 6h, 24h	20%	Flexcell Tension Plus system FX-5000T + six-well Bioflex plates + vacuum	equibiaxial	decrease (qPCR, GAPDH)	24h: 0.4 (ratio)*	increase (WB, GAPDH)	6h: 2.1 (ratio)*
Zhao et al. (2016)	NLRP3	*NLRP3*	hPDLCs (11-13/n.g., PM, exp, P4-6, confluence)	dynamic	**0.1Hz** (6cyc/min: 5s stretch and 5s relaxation) for 6h, 24h	20%	Flexcell Tension Plus system FX-5000T + six-well Bioflex plates + vacuum	equibiaxial	increase followed by decrease (qPCR, GAPDH)	highest @ 6h: 5.3 (ratio)* lowest @ 24h: 0.5 (ratio)*	increase (WB, GAPDH)	24h: 8.3 (ratio)*
Zhao et al. (2017)	Caspase-5, Pro- / Caspase-5	*CASP5*	hPDLCs (11-13/n.g., PM, exp, P4-6, confluence)	dynamic	**0.1Hz** (6 cyc/min: 5s stretch followed by 5s relaxation) for 6h, 24h	10%, 20%	Cell Strain Unit (CSU) + elastic silicon rubber membrane + spherical cap (step motor) (Hao et al 2009)	equibiaxial	Caspase 5 @ 10%: increase (qPCR, β-actin) Caspase 5 @ 20%: increase (qPCR, β-actin)	Caspase 5 @ 10% + 24h: 11.2 (FC)* Caspase 5 @ 20% + 24h: 15.2 (FC)*	Caspase 5: 10%: increase (WB, GAPDH) Caspase 5: 20%: increase (WB, GAPDH) Pro-caspase 5: 10%: increase (WB, GAPDH) Pro-caspase 5: 20%: increase (WB, GAPDH)	Caspase 5 @ 10% + 24h: 0.4 (rel)† / 36.2 (ratio-calc) Caspase 5 @ 20% + 24h: 0.8 (rel)† / 69.1 (ratio-calc) Pro-caspase 5 @ 10% + 24h: 0.5 (rel)† / 7.9 (ratio-calc) Pro-caspase 5 @ 20% + 24h: 0.7 (rel)† / 12.2 (ratio-calc)
Zhuang et al. (2019)	GSDMD	*GSDMD*	hPDLCs (11-16/n.g., PM, exp, P4-6, 80-90% confluence)	dynamic	**0.1Hz** (6cyc/min: 5s stretch and 5s relaxation) for 6h, 24h	20%	Flexcell Tension Plus system FX-5000T + six-well BioFlex plates + vacuum	equibiaxial	increase (qPCR, GAPDH)	24h: 6.6 (ratio)*	GSDMD (53 kDa): no change (WB, GAPDH) GSDMD (31 kDa): increase (WB, GAPDH)	GSDMD (31 kDa) @ 6h: 0.7 (rel)* / 1.8 (ratio-calc)
Zhuang et al. (2019)	IL-18	*IL18*	hPDLCs (11-16/n.g., PM, exp, P4-6, 80-90% confluence)	dynamic	**0.1Hz** (6cyc/min: 5s stretch and 5s relaxation) WB for 6h, 24h; ELISA for 1h, 2h, 4h, 6h, 12h, 24h	20%	Flexcell Tension Plus system FX-5000T + six-well BioFlex plates + vacuum	equibiaxial	n.g.	n.g.	increase followed by decrease (WB, GAPDH) IL-18 in culture medium: increase (ELISA)	highest @ 6h: 0.7 (rel)* / 1.4 (ratio-calc) lowest @ 24h: 0.3 (rel)* / 0.6 (ratio-calc) IL-18 in culture medium 6h: 6.6 (ratio)*
Zhuang et al. (2019)	IL-1β	*IL1B*	hPDLCs (11-16/n.g., PM, exp, P4-6, 80-90% confluence)	dynamic	**0.1Hz** (6cyc/min: 5s stretch and 5s relaxation) WB for 6h, 24h; ELISA for 1h, 2h, 4h, 6h, 12h, 24h	20%	Flexcell Tension Plus system FX-5000T + six-well BioFlex plates + vacuum	equibiaxial	n.g.	n.g.	Pro-IL-1β (31 kDa): increase followed by decrease (WB, GAPDH) Mature-IL-1β (17 kDa): decrease (WB, GAPDH) IL-1β in culture medium: increase (ELISA)	Pro-IL-1β highest @ 6h: 0.8 (rel)* / 1.1 (ratio-calc) Pro-IL-1β lowest @24h: 0.6 (rel)* / 0.9 (ratio-calc) Mature-IL-1β @ 24h: 0.3 (rel)* / 0.6 (ratio-calc) IL-1β in culture medium 6h: 10.4 ((ratio)*
Ziegler et al. (2010)	ARRAY	ARRAY	hPDLFs (12-14/n.g., PM, exp, P8-12, near-confluence)	static	0.5h, 3h, 6h	2.5%	Lumox dish + template with convex surface + weight (Hasegawa et al 1985)	equibiaxial	RT^2-Profiler qPCR-Array (SA Biosciences) not further specified	too many!	n.a.	n.a.
Ziegler et al. (2010)	FAK / p-FAK	*PTK2*	hPDLFs (12-14/n.g., PM, exp, P8-12, near-confluence)	static	0.25h, 0.5h, 1h, 3h, 6h	2.5%	Lumox dish + template with convex surface + weight (Hasegawa et al 1985)	equibiaxial	n.g.	n.g.	FAK: increase (WB, β-actin) p-FAK: increase (WB, β-actin)	FAK @ 6h: 42.8 (rel)* / 1.3 (ratio-calc) p-FAK: 0.25h: 35.9 (rel)* / 1.1 (ratio-calc)
Ziegler et al. (2010)	Intergrin β3	*ITGB3*	hPDLFs (12-14/n.g., PM, exp, P8-12, near-confluence)	static	0.25h, 0.5h, 1h, 3h, 6h	2.5%	Lumox dish + template with convex surface + weight (Hasegawa et al 1985)	equibiaxial	n.g.	n.g.	increase (WB, β-actin)	6h: 44 (rel)* / 1.3 (ratio)*

[a] Entry given as reported in the study.
[b] All official gene symbols come from the HUGO Gene Nomenclature Committee (HGNC; URL: https://www.genenames.org) after checking specificity of primers with Primer-BLAST.
[c] Gender/Sex of donors: "M" – male, "F" – female; Tooth type: "PM" – premolar, "M" – molar; Cell density: given in cells/well if not otherwise mentioned.
[d] Frequencies labeled bold orange were converted to hertz (Hz) according to its definition using the information reported in the study (in brackets)
[e] Force type deduced from the description of the force apparatus given by the authors.
[f] Gene and protein expression: 1. conclusion of change (increase, decrease…) was given according to the defined criteria in Figure 2; 2. different markers to describe the amount of change; † Information derived from figures using Engauge Digitizer; *Folds calculated by measuring the graphs, without using the Engauge Digitizer; No makers: Information derived from figures by description in the articles

Reference	Gene/ Analyte[a]	Official gene symbol / abbreviation[b]	Cell (age/gender of donors, tooth type, isolation method, passages used, cell density)[a,c]	Force type (stat./ dyn.)[a]	Force duration and frequency[d]	Force magnitude[a]	Force apparatus[a]	Force type: equibiaxial or uniaxial[e]	Gene expression: Increase, decrease, no change (method w/ reference gene); Methods: qPCR, sqPCR, Northern blot[f]	Gene expression: When it reaches peak and peak's magnitude (fold change; times or ratio; unclear = ?)[f]	Protein expression: Increase, decrease, no change (method w/ reference); Methods: ELISA, WB, RIA, EMSA, IF[f]	Protein expression: When it reaches peak and peak's magnitude (times or ratio; unclear = ?)[f]
Ziegler et al. (2010)	p38-MAP-kinase / p-p38-MAP-kinase(Thr180/ Tyr182)	*MAPK14*	hPDLFs (12-14/n.g., PM, exp, P8-12, near-confluence)	static	0.25h, 0.5h, 1h, 3h, 6h	2.5%	Lumox dish + template with convex surface + weight (Hasegawa et al 1985)	equibiaxial	n.g.	n.g.	p38: decrease followed by increase (WB, β-actin) p-p38: increase (WB, β-actin)	p38 lowest @ 0.5h: 29.6 (rel)* / 0.9 (ratio-calc) p38 highest @ 6h: 43.9 (rel)* / 1.3 (ratio-calc) p-p38 @ 6h: 36.1 (rel)* / 1.1 (ratio-calc)
Ziegler et al. (2010)	p44/42-MAP-kinase / p-p44/42-MAP-kinase(Thr202/ Tyr204)	MAPK3; MAPK1	hPDLFs (12-14/n.g., PM, exp, P8-12, near-confluence)	static	0.25h, 0.5h, 1h, 3h, 6h	2.5%	Lumox dish + template with convex surface + weight (Hasegawa et al 1985)	equibiaxial	n.g.	n.g.	p44/42: increase followed by decrease (WB, β-actin) p-p44/42: decrease followed by increase (WB, β-actin)	p44/42: highest @ 0.5h: 55.6 (rel)* / 1.1 (ratio-calc) p44/42: lowest @ 3h: 45 (rel)* / 0.9 (ratio-calc) p-p44/42: highest @ 6h: 37.8 (rel)* / 1.1 (ratio-calc) p-p44/42: lowest @ 1h: 31.7 (rel)* / 0.9 (ratio-calc)

References

Abiko, Y., Shimizu, N., Yamaguchi, M., Suzuki, H., and Takiguchi, H. (1998). Effect of aging on functional changes of periodontal tissue cells. *Ann. Periodontol.* 3(1), 350-369. doi: 10.1902/annals.1998.3.1.350.

Agarwal, S., Long, P., Seyedain, A., Piesco, N., Shree, A., and Gassner, R. (2003). A central role for the nuclear factor-κB pathway in anti-inflammatory and proinflammatory actions of mechanical strain. *FASEB J.* 17(8), 899-901. doi: 10.1096/fj.02-0901fje.

Arima, M., Hasegawa, D., Yoshida, S., Mitarai, H., Tomokiyo, A., Hamano, S., et al. (2019). R-spondin 2 promotes osteoblastic differentiation of immature human periodontal ligament cells through the Wnt/beta-catenin signaling pathway. *J. Periodontal Res.* 54(2), 143-153. doi: 10.1111/jre.12611.

Basdra, E.K., Kohl, A., and Komposch, G. (1996). Mechanical stretching of periodontal ligament fibroblasts--a study on cytoskeletal involvement. *J. Orofac. Orthop.* 57(1), 24-30. doi: 10.1007/BF02189045.

Basdra, E.K., Papavassiliou, A.G., and Huber, L.A. (1995). Rab and rho GTPases are involved in specific response of periodontal ligament fibroblasts to mechanical stretching. *Biochim. Biophys. Acta* 1268(2), 209-213. doi: 10.1016/0167-4889(95)00090-f.

Bolcato-Bellemin, A.L., Elkaim, R., Abehsera, A., Fausser, J.L., Haikel, Y., and Tenenbaum, H. (2000). Expression of mRNAs encoding for alpha and beta integrin subunits, MMPs, and TIMPs in stretched human periodontal ligament and gingival fibroblasts. *J. Dent. Res.* 79(9), 1712-1716. doi: 10.1177/00220345000790091201.

Chang, M., Lin, H., Fu, H., Wang, B., Han, G., and Fan, M. (2017). MicroRNA-195-5p regulates osteogenic differentiation of periodontal ligament cells under mechanical loading. *J. Cell. Physiol.* 232(12), 3762-3774. doi: 10.1002/jcp.25856.

Chang, M., Lin, H., Luo, M., Wang, J., and Han, G. (2015). Integrated miRNA and mRNA expression profiling of tension force-induced bone formation in periodontal ligament cells. *In Vitro Cell. Dev. Biol. Anim.* 51(8), 797-807. doi: 10.1007/s11626-015-9892-0.

Chen, Y., Mohammed, A., Oubaidin, M., Evans, C.A., Zhou, X., Luan, X., et al. (2015). Cyclic stretch and compression forces alter microRNA-29 expression of human periodontal ligament cells. *Gene* 566(1), 13-17. doi: 10.1016/j.gene.2015.03.055.

Chen, Y.J., Shie, M.Y., Hung, C.J., Wu, B.C., Liu, S.L., Huang, T.H., et al. (2014). Activation of focal adhesion kinase induces extracellular signal-regulated kinase-mediated osteogenesis in tensile force-subjected periodontal ligament fibroblasts but not in osteoblasts. *J. Bone Miner. Metab.* 32(6), 671-682. doi: 10.1007/s00774-013-0549-3.

Chiba, M., and Mitani, H. (2004). Cytoskeletal changes and the system of regulation of alkaline phosphatase activity in human periodontal ligament cells induced by mechanical stress. *Cell Biochem. Funct.* 22(4), 249-256. doi: 10.1002/cbf.1097.

Cho, J.H., Lee, S.K., Lee, J.W., and Kim, E.C. (2010). The role of heme oxygenase-1 in mechanical stress- and lipopolysaccharide-induced osteogenic differentiation in human periodontal ligament cells. *Angle Orthod.* 80(4), 552-559. doi: 10.2319/091509-520.1.

Deschner, B., Rath, B., Jager, A., Deschner, J., Denecke, B., Memmert, S., et al. (2012). Gene analysis of signal transduction factors and transcription factors in periodontal ligament cells following application of dynamic strain. *J. Orofac. Orthop.* 73(6), 486-495, 497. doi: 10.1007/s00056-012-0104-1.

Diercke, K., Kohl, A., Lux, C.J., and Erber, R. (2011). Strain-dependent up-regulation of ephrin-B2 protein in periodontal ligament fibroblasts contributes to osteogenesis during tooth movement. *J. Biol. Chem.* 286(43), 37651-37664. doi: 10.1074/jbc.M110.166900.

Doi, T., Ohno, S., Tanimoto, K., Honda, K., Tanaka, N., Ohno-Nakahara, M., et al. (2003). Mechanical stimuli enhances the expression of RGD-CAP/betaig-h3 in the periodontal ligament. *Arch. Oral Biol.* 48(8), 573-579. doi: 10.1016/s0003-9969(03)00103-1.

Fujihara, C., Yamada, S., Ozaki, N., Takeshita, N., Kawaki, H., Takano-Yamamoto, T., et al. (2010). Role of mechanical stress-induced glutamate signaling-associated molecules in cytodifferentiation of periodontal ligament cells. *J. Biol. Chem.* 285(36), 28286-28297. doi: 10.1074/jbc.M109.097303.

Goto, K.T., Kajiya, H., Nemoto, T., Tsutsumi, T., Tsuzuki, T., Sato, H., et al. (2011). Hyperocclusion stimulates osteoclastogenesis via CCL2 expression. *J. Dent. Res.* 90(6), 793-798. doi: 10.1177/0022034511400742.

Hao, Y., Xu, C., Sun, S.Y., and Zhang, F.Q. (2009). Cyclic stretching force induces apoptosis in human periodontal ligament cells via caspase-9. *Arch. Oral Biol.* 54(9), 864-870. doi: 10.1016/j.archoralbio.2009.05.012.

He, Y., Macarak, E.J., Korostoff, J.M., and Howard, P.S. (2004). Compression and tension: differential effects on matrix accumulation by periodontal ligament fibroblasts in vitro. *Connect Tissue Res.* 45(1), 28-39. doi: 10.1080/03008200490278124.

He, Y., Xu, H., Xiang, Z., Yu, H., Xu, L., Guo, Y., et al. (2019). YAP regulates periodontal ligament cell differentiation into myofibroblast interacted with RhoA/ROCK pathway. *J. Cell. Physiol.* 234(4), 5086-5096. doi: 10.1002/jcp.27312.

Howard, P.S., Kucich, U., Taliwal, R., and Korostoff, J.M. (1998). Mechanical forces alter extracellular matrix synthesis by human periodontal ligament fibroblasts. *J. Periodontal Res.* 33(8), 500-508. doi: 10.1111/j.1600-0765.1998.tb02350.x.

Huelter-Hassler, D., Tomakidi, P., Steinberg, T., and Jung, B.A. (2017). Orthodontic strain affects the Hippo-pathway effector YAP concomitant with proliferation in human periodontal ligament fibroblasts. *Eur. J. Orthod.* 39(3), 251-257. doi: 10.1093/ejo/cjx012.

Hülter-Hassler, D., Wein, M., Schulz, S.D., Proksch, S., Steinberg, T., Jung, B.A., et al. (2017). Biomechanical strain-induced modulation of proliferation coincides with an ERK1/2-independent nuclear YAP localization. *Exp. Cell Res.* 361(1), 93-100. doi: 10.1016/j.yexcr.2017.10.006.

Jacobs, C., Grimm, S., Ziebart, T., Walter, C., and Wehrbein, H. (2013). Osteogenic differentiation of periodontal fibroblasts is dependent on the strength of mechanical strain. *Arch. Oral Biol.* 58(7), 896-904. doi: 10.1016/j.archoralbio.2013.01.009.

Jacobs, C., Schramm, S., Dirks, I., Walter, C., Pabst, A., Meila, D., et al. (2018). Mechanical loading increases pro-inflammatory effects of nitrogen-containing bisphosphonate in human periodontal fibroblasts. *Clin. Oral Investig.* 22(2), 901-907. doi: 10.1007/s00784-017-2168-1.

Jacobs, C., Walter, C., Ziebart, T., Dirks, I., Schramm, S., Grimm, S., et al. (2015). Mechanical loading influences the effects of bisphosphonates on human periodontal ligament fibroblasts. *Clin. Oral Investig.* 19(3), 699-708. doi: 10.1007/s00784-014-1284-4.

Jacobs, C., Walter, C., Ziebart, T., Grimm, S., Meila, D., Krieger, E., et al. (2014). Induction of IL-6 and MMP-8 in human periodontal fibroblasts by static tensile strain. *Clin. Oral Investig.* 18(3), 901-908. doi: 10.1007/s00784-013-1032-1.

Jiang, Z., and Hua, Y. (2016). Hydrogen sulfide promotes osteogenic differentiation of human periodontal ligament cells via p38-MAPK signaling pathway under proper tension stimulation. *Arch. Oral Biol.* 72, 8-13. doi: 10.1016/j.archoralbio.2016.08.008.

Kaku, M., Yamamoto, T., Yashima, Y., Izumino, J., Kagawa, H., Ikeda, K., et al. (2019). Acetaminophen reduces apical root resorption during orthodontic tooth movement in rats. *Arch. Oral Biol.* 102, 83-92. doi: 10.1016/j.archoralbio.2019.04.002.

Kanzaki, H., Chiba, M., Sato, A., Miyagawa, A., Arai, K., Nukatsuka, S., et al. (2006). Cyclical tensile force on periodontal ligament cells inhibits osteoclastogenesis through OPG induction. *J. Dent. Res.* 85(5), 457-462. doi: 10.1177/154405910608500512.

Kanzaki, H., Wada, S., Yamaguchi, Y., Katsumata, Y., Itohiya, K., Fukaya, S., et al. (2019). Compression and tension variably alter Osteoprotegerin expression via miR-3198 in periodontal ligament cells. *BMC Mol. Cell Biol.* 20(1), 6. doi: 10.1186/s12860-019-0187-2.

Kikuiri, T., Hasegawa, T., Yoshimura, Y., Shirakawa, T., and Oguchi, H. (2000). Cyclic tension force activates nitric oxide production in cultured human periodontal ligament cells. *J. Periodontol.* 71(4), 533-539. doi: 10.1902/jop.2000.71.4.533.

Kim, H.J., Choi, Y.S., Jeong, M.J., Kim, B.O., Lim, S.H., Kim, D.K., et al. (2007). Expression of UNCL during development of periodontal tissue and response of periodontal ligament fibroblasts to mechanical stress in vivo and in vitro. *Cell Tissue Res.* 327(1), 25-31. doi: 10.1007/s00441-006-0304-3.

Kletsas, D., Basdra, E.K., and Papavassiliou, A.G. (2002). Effect of protein kinase inhibitors on the stretch-elicited c-Fos and c-Jun up-regulation in human PDL osteoblast-like cells. *J. Cell. Physiol.* 190(3), 313-321. doi: 10.1002/jcp.10052.

Konstantonis, D., Papadopoulou, A., Makou, M., Eliades, T., Basdra, E., and Kletsas, D. (2014). The role of cellular senescence on the cyclic stretching-mediated activation of MAPK and ALP expression and activity in human periodontal ligament fibroblasts. *Exp. Gerontol.* 57, 175-180. doi: 10.1016/j.exger.2014.05.010.

Kook, S.H., and Lee, J.C. (2012). Tensile force inhibits the proliferation of human periodontal ligament fibroblasts through Ras-p38 MAPK up-regulation. *J. Cell. Physiol.* 227(3), 1098-1106. doi: 10.1002/jcp.22829.

Lee, S.I., Park, K.H., Kim, S.J., Kang, Y.G., Lee, Y.M., and Kim, E.C. (2012). Mechanical stress-activated immune response genes via Sirtuin 1 expression in human periodontal ligament cells. *Clin. Exp. Immunol.* 168(1), 113-124. doi: 10.1111/j.1365-2249.2011.04549.x.

Lee, S.Y., Yoo, H.I., and Kim, S.H. (2015). CCR5-CCL Axis in PDL during Orthodontic Biophysical Force Application. *J. Dent. Res.* 94(12), 1715-1723. doi: 10.1177/0022034515603926.

Li, L., Han, M., Li, S., Wang, L., and Xu, Y. (2013). Cyclic tensile stress during physiological occlusal force enhances osteogenic differentiation of human periodontal ligament cells via ERK1/2-Elk1 MAPK pathway. *DNA Cell Biol.* 32(9), 488-497. doi: 10.1089/dna.2013.2070.

Li, L., Han, M.X., Li, S., Xu, Y., and Wang, L. (2014). Hypoxia regulates the proliferation and osteogenic differentiation of human periodontal ligament cells under cyclic tensile stress via mitogen-activated protein kinase pathways. *J. Periodontol.* 85(3), 498-508. doi: 10.1902/jop.2013.130048.

Li, S., Zhang, H., Li, S., Yang, Y., Huo, B., and Zhang, D. (2015). Connexin 43 and ERK regulate tension-induced signal transduction in human periodontal ligament fibroblasts. *J. Orthop. Res.* 33(7), 1008-1014. doi: 10.1002/jor.22830.

Liao, C., and Hua, Y. (2013). Effect of hydrogen sulphide on the expression of osteoprotegerin and receptor activator of NF-kappaB ligand in human periodontal ligament cells induced by tension-force stimulation. *Arch. Oral Biol.* 58(12), 1784-1790. doi: 10.1016/j.archoralbio.2013.08.004.

Liu, J., Li, Q., Liu, S., Gao, J., Qin, W., Song, Y., et al. (2017). Periodontal Ligament Stem Cells in the Periodontitis Microenvironment Are Sensitive to Static Mechanical Strain. *Stem Cells Int.* 2017, 1380851. doi: 10.1155/2017/1380851.

Liu, M., Dai, J., Lin, Y., Yang, L., Dong, H., Li, Y., et al. (2012). Effect of the cyclic stretch on the expression of osteogenesis genes in human periodontal ligament cells. *Gene* 491(2), 187-193. doi: 10.1016/j.gene.2011.09.031.

Long, P., Hu, J., Piesco, N., Buckley, M., and Agarwal, S. (2001). Low magnitude of tensile strain inhibits IL-1beta-dependent induction of pro-inflammatory cytokines and induces synthesis of IL-10 in human periodontal ligament cells in vitro. *J. Dent. Res.* 80(5), 1416-1420. doi: 10.1177/00220345010800050601.

Long, P., Liu, F., Piesco, N.P., Kapur, R., and Agarwal, S. (2002). Signaling by mechanical strain involves transcriptional regulation of proinflammatory genes in human periodontal ligament cells in vitro. *Bone* 30(4), 547-552. doi: 10.1016/s8756-3282(02)00673-7.

Ma, J., Zhao, D., Wu, Y., Xu, C., and Zhang, F. (2015). Cyclic stretch induced gene expression of extracellular matrix and adhesion molecules in human periodontal ligament cells. *Arch. Oral Biol.* 60(3), 447-455. doi: 10.1016/j.archoralbio.2014.11.019.

Matsuda, N., Morita, N., Matsuda, K., and Watanabe, M. (1998a). Proliferation and differentiation of human osteoblastic cells associated with differential activation of MAP kinases in response to epidermal growth factor, hypoxia, and mechanical stress in vitro. *Biochem. Biophys. Res. Commun.* 249(2), 350-354. doi: 10.1006/bbrc.1998.9151.

[a] Entry given as reported in the study.
[b] All official gene symbols come from the HUGO Gene Nomenclature Committee (HGNC; URL: https://www.genenames.org) after checking specificity of primers with Primer-BLAST.
[c] Gender/Sex of donors: "M" – male, "F" – female; Tooth type: "PM" – premolar, "M" – molar; Cell density: given in cells/well if not otherwise mentioned.
[d] Frequencies labeled bold orange were converted to hertz (Hz) according to its definition using the information reported in the study (in brackets)
[e] Force type deduced from the description of the force apparatus given by the authors.
[f] Gene and protein expression: 1. conclusion of change (increase, decrease…) was given according to the defined criteria in Figure 2; 2. different markers to describe the amount of change; † Information derived from figures using Engauge Digitizer; *Folds calculated by measuring the graphs, without using the Engauge Digitizer; No makers: Information derived from figures by description in the articles

Matsuda, N., Yokoyama, K., Takeshita, S., and Watanabe, M. (1998b). Role of epidermal growth factor and its receptor in mechanical stress-induced differentiation of human periodontal ligament cells in vitro. *Arch. Oral Biol.* 43(12), 987-997. doi: 10.1016/s0003-9969(98)00079-x.

Memmert, S., Damanaki, A., Weykopf, B., Rath-Deschner, B., Nokhbehsaim, M., Gotz, W., et al. (2019). Autophagy in periodontal ligament fibroblasts under biomechanical loading. *Cell Tissue Res.* doi: 10.1007/s00441-019-03063-1.

Memmert, S., Nogueira, A.V.B., Damanaki, A., Nokhbehsaim, M., Rath-Deschner, B., Götz, W., et al. (2020). Regulation of the autophagy-marker Sequestosome 1 in periodontal cells and tissues by biomechanical loading. *J. Orofac. Orthop.* 81(1), 10-21. doi: 10.1007/s00056-019-00197-3.

Meng, Y., Han, X., Huang, L., Bai, D., Yu, H., He, Y., et al. (2010). Orthodontic mechanical tension effects on the myofibroblast expression of alpha-smooth muscle actin. *Angle Orthod.* 80(5), 912-918. doi: 10.2319/101609-578.1.

Miura, S., Yamaguchi, M., Shimizu, N., and Abiko, Y. (2000). Mechanical stress enhances expression and production of plasminogen activator in aging human periodontal ligament cells. *Mech. Ageing Dev.* 112(3), 217-231. doi: 10.1016/s0047-6374(99)00095-0.

Molina, T., Kabsch, K., Alonso, A., Kohl, A., Komposch, G., and Tomakidi, P. (2001). Topographic changes of focal adhesion components and modulation of p125FAK activation in stretched human periodontal ligament fibroblasts. *J. Dent. Res.* 80(11), 1984-1989. doi: 10.1177/00220345010800110701.

Monnouchi, S., Maeda, H., Fujii, S., Tomokiyo, A., Kono, K., and Akamine, A. (2011). The roles of angiotensin II in stretched periodontal ligament cells. *J. Dent. Res.* 90(2), 181-185. doi: 10.1177/0022034510382118.

Monnouchi, S., Maeda, H., Yuda, A., Hamano, S., Wada, N., Tomokiyo, A., et al. (2015). Mechanical induction of interleukin-11 regulates osteoblastic/cementoblastic differentiation of human periodontal ligament stem/progenitor cells. *J. Periodontal Res.* 50(2), 231-239. doi: 10.1111/jre.12200.

Nakashima, K., Tsuruga, E., Hisanaga, Y., Ishikawa, H., and Sawa, Y. (2009). Stretching stimulates fibulin-5 expression and controls microfibril bundles in human periodontal ligament cells. *J. Periodontal Res.* 44(5), 622-627. doi: 10.1111/j.1600-0765.2008.01170.x.

Narimiya, T., Wada, S., Kanzaki, H., Ishikawa, M., Tsuge, A., Yamaguchi, Y., et al. (2017). Orthodontic tensile strain induces angiogenesis via type IV collagen degradation by matrix metalloproteinase-12. *J. Periodontal Res.* 52(5), 842-852. doi: 10.1111/jre.12453.

Nazet, U., Schröder, A., Spanier, G., Wolf, M., Proff, P., and Kirschneck, C. (2020). Simplified method for applying static isotropic tensile strain in cell culture experiments with identification of valid RT-qPCR reference genes for PDL fibroblasts. *Eur. J. Orthod.* 42(4), 359-370. doi: 10.1093/ejo/cjz052.

Nemoto, T., Kajiya, H., Tsuzuki, T., Takahashi, Y., and Okabe, K. (2010). Differential induction of collagens by mechanical stress in human periodontal ligament cells. *Arch. Oral Biol.* 55(12), 981-987. doi: 10.1016/j.archoralbio.2010.08.004.

Ngan, P., Saito, S., Saito, M., Lanese, R., Shanfeld, J., and Davidovitch, Z. (1990). The interactive effects of mechanical stress and interleukin-1 beta on prostaglandin E and cyclic AMP production in human periodontal ligament fibroblasts in vitro: comparison with cloned osteoblastic cells of mouse (MC3T3-E1). *Arch. Oral Biol.* 35(9), 717-725. doi: 10.1016/0003-9969(90)90094-Q.

Nogueira, A.V., Nokhbehsaim, M., Eick, S., Bourauel, C., Jäger, A., Jepsen, S., et al. (2014a). Regulation of visfatin by microbial and biomechanical signals in PDL cells. *Clin. Oral Investig.* 18(1), 171-178. doi: 10.1007/s00784-013-0935-1.

Nogueira, A.V., Nokhbehsaim, M., Eick, S., Bourauel, C., Jäger, A., Jepsen, S., et al. (2014b). Biomechanical loading modulates proinflammatory and bone resorptive mediators in bacterial-stimulated PDL cells. *Mediators Inflamm.* 2014, 425421. doi: 10.1155/2014/425421.

Nokhbehsaim, M., Deschner, B., Bourauel, C., Reimann, S., Winter, J., Rath, B., et al. (2011a). Interactions of enamel matrix derivative and biomechanical loading in periodontal regenerative healing. *J. Periodontol.* 82(12), 1725-1734. doi: 10.1902/jop.2011.100678.

Nokhbehsaim, M., Deschner, B., Winter, J., Bourauel, C., Jäger, A., Jepsen, S., et al. (2012). Anti-inflammatory effects of EMD in the presence of biomechanical loading and interleukin-1β in vitro. *Clin. Oral Investig.* 16(1), 275-283. doi: 10.1007/s00784-010-0505-8.

Nokhbehsaim, M., Deschner, B., Winter, J., Bourauel, C., Rath, B., Jager, A., et al. (2011b). Interactions of regenerative, inflammatory and biomechanical signals on bone morphogenetic protein-2 in periodontal ligament cells. *J. Periodontal Res.* 46(3), 374-381. doi: 10.1111/j.1600-0765.2011.01357.x.

Nokhbehsaim, M., Deschner, B., Winter, J., Reimann, S., Bourauel, C., Jepsen, S., et al. (2010). Contribution of orthodontic load to inflammation-mediated periodontal destruction. *J. Orofac. Orthop.* 71(6), 390-402. doi: 10.1007/s00056-010-1031-7.

Ohzeki, K., Yamaguchi, M., Shimizu, N., and Abiko, Y. (1999). Effect of cellular aging on the induction of cyclooxygenase-2 by mechanical stress in human periodontal ligament cells. *Mech. Ageing Dev.* 108(2), 151-163. doi: 10.1016/s0047-6374(99)00006-8.

Ozawa, Y., Shimizu, N., and Abiko, Y. (1997). Low-energy diode laser irradiation reduced plasminogen activator activity in human periodontal ligament cells. *Lasers Surg. Med.* 21(5), 456-463. doi: 10.1002/(sici)1096-9101(1997)21:5<456::aid-lsm7>3.0.co;2-p.

Padial-Molina, M., Volk, S.L., Rodriguez, J.C., Marchesan, J.T., Galindo-Moreno, P., and Rios, H.F. (2013). Tumor necrosis factor-alpha and Porphyromonas gingivalis lipopolysaccharides decrease periostin in human periodontal ligament fibroblasts. *J. Periodontol.* 84(5), 694-703. doi: 10.1902/jop.2012.120078.

Pan, J., Wang, T., Wang, L., Chen, W., and Song, M. (2014). Cyclic strain-induced cytoskeletal rearrangement of human periodontal ligament cells via the Rho signaling pathway. *PloS One* 9(3), e91580. doi: 10.1371/journal.pone.0091580.

Papadopoulou, A., Iliadi, A., Eliades, T., and Kletsas, D. (2017). Early responses of human periodontal ligament fibroblasts to cyclic and static mechanical stretching. *Eur. J. Orthod.* 39(3), 258-263. doi: 10.1093/ejo/cjw075.

Papadopoulou, A., Todaro, A., Eliades, T., and Kletsas, D. (2019). Effect of hyperglycaemic conditions on the response of human periodontal ligament fibroblasts to mechanical stretching. *Eur. J. Orthod.* doi: 10.1093/ejo/cjz051.

Pelaez, D., Acosta Torres, Z., Ng, T.K., Choy, K.W., Pang, C.P., and Cheung, H.S. (2017). Cardiomyogenesis of periodontal ligament-derived stem cells by dynamic tensile strain. *Cell Tissue Res.* 367(2), 229-241. doi: 10.1007/s00441-016-2503-x.

Peverali, F.A., Basdra, E.K., and Papavassiliou, A.G. (2001). Stretch-mediated activation of selective MAPK subtypes and potentiation of AP-1 binding in human osteoblastic cells. *Mol. Med.* 7(1), 68-78.

Pinkerton, M.N., Wescott, D.C., Gaffey, B.J., Beggs, K.T., Milne, T.J., and Meikle, M.C. (2008). Cultured human periodontal ligament cells constitutively express multiple osteotropic cytokines and growth factors, several of which are responsive to mechanical deformation. *J. Periodontal Res.* 43(3), 343-351. doi: 10.1111/j.1600-0765.2007.01040.x.

Qin, J., and Hua, Y. (2016). Effects of hydrogen sulfide on the expression of alkaline phosphatase, osteocalcin and collagen type I in human periodontal ligament cells induced by tension force stimulation. *Mol. Med. Rep.* 14(4), 3871-3877. doi: 10.3892/mmr.2016.5680.

Rath-Deschner, B., Deschner, J., Reimann, S., Jager, A., and Gotz, W. (2009). Regulatory effects of biomechanical strain on the insulin-like growth factor system in human periodontal cells. *J. Biomech.* 42(15), 2584-2589. doi: 10.1016/j.jbiomech.2009.07.013.

Ren, D., Wei, F., Hu, L., Yang, S., Wang, C., and Yuan, X. (2015). Phosphorylation of Runx2, induced by cyclic mechanical tension via ERK1/2 pathway, contributes to osteodifferentiation of human periodontal ligament fibroblasts. *J. Cell. Physiol.* 230(10), 2426-2436. doi: 10.1002/jcp.24972.

Ritter, N., Mussig, E., Steinberg, T., Kohl, A., Komposch, G., and Tomakidi, P. (2007). Elevated expression of genes assigned to NF-kappaB and apoptotic pathways in human periodontal ligament fibroblasts following mechanical stretch. *Cell Tissue Res.* 328(3), 537-548. doi: 10.1007/s00441-007-0382-x.

Saminathan, A., Vinoth, K.J., Wescott, D.C., Pinkerton, M.N., Milne, T.J., Cao, T., et al. (2012). The effect of cyclic mechanical strain on the expression of adhesion-related genes by periodontal ligament cells in two-dimensional culture. *J. Periodontal Res.* 47(2), 212-221. doi: 10.1111/j.1600-0765.2011.01423.x.

Shen, T., Qiu, L., Chang, H., Yang, Y., Jian, C., Xiong, J., et al. (2014). Cyclic tension promotes osteogenic differentiation in human periodontal ligament stem cells. *Int. J. Clin. Exp. Pathol.* 7(11), 7872-7880.

Shimizu, N., Goseki, T., Yamaguchi, M., Iwasawa, T., Takiguchi, H., and Abiko, Y. (1997). In vitro cellular aging stimulates interleukin-1 beta production in stretched human periodontal-ligament-derived cells. *J. Dent. Res.* 76(7), 1367-1375. doi: 10.1177/00220345970760070601.

Shimizu, N., Ozawa, Y., Yamaguchi, M., Goseki, T., Ohzeki, K., and Abiko, Y. (1998). Induction of COX-2 expression by mechanical tension force in human periodontal ligament cells. *J. Periodontol.* 69(6), 670-677. doi: 10.1902/jop.1998.69.6.670.

Shimizu, N., Yamaguchi, M., Goseki, T., Ozawa, Y., Saito, K., Takiguchi, H., et al. (1994). Cyclic-tension force stimulates interleukin-1 beta production by human periodontal ligament cells. *J. Periodontal Res.* 29(5), 328-333. doi: 10.1111/j.1600-0765.1994.tb01230.x.

Shimizu, N., Yamaguchi, M., Goseki, T., Shibata, Y., Takiguchi, H., Iwasawa, T., et al. (1995). Inhibition of prostaglandin E2 and interleukin 1-beta production by low-power laser irradiation in stretched human periodontal ligament cells. *J. Dent. Res.* 74(7), 1382-1388. doi: 10.1177/00220345950740071001.

Spencer, A.Y., and Lallier, T.E. (2009). Mechanical tension alters semaphorin expression in the periodontium. *J. Periodontol.* 80(10), 1665-1673. doi: 10.1902/jop.2009.090212.

Steinberg, T., Ziegler, N., Alonso, A., Kohl, A., Mussig, E., Proksch, S., et al. (2011). Strain response in fibroblasts indicates a possible role of the Ca(2+)-dependent nuclear transcription factor NM1 in RNA synthesis. *Cell Calcium* 49(4), 259-271. doi: 10.1016/j.ceca.2011.03.001.

Sun, C., Chen, L., Shi, X., Cao, Z., Hu, B., Yu, W., et al. (2016). Combined effects of proinflammatory cytokines and intermittent cyclic mechanical strain in inhibiting osteogenicity in human periodontal ligament cells. *Cell Biol. Int.* 40(9), 999-1007. doi: 10.1002/cbin.10641.

Sun, C., Liu, F., Cen, S., Chen, L., Wang, Y., Sun, H., et al. (2017). Tensile strength suppresses the osteogenesis of periodontal ligament cells in inflammatory microenvironments. *Mol. Med. Rep.* 16(1), 666-672. doi: 10.3892/mmr.2017.6644.

Suzuki, R., Nemoto, E., and Shimauchi, H. (2014). Cyclic tensile force up-regulates BMP-2 expression through MAP kinase and COX-2/PGE2 signaling pathways in human periodontal ligament cells. *Exp. Cell Res.* 323(1), 232-241. doi: 10.1016/j.yexcr.2014.02.013.

Symmank, J., Zimmermann, S., Goldschmitt, J., Schiegnitz, E., Wolf, M., Wehrbein, H., et al. (2019). Mechanically-induced GDF15 Secretion by Periodontal Ligament Fibroblasts Regulates Osteogenic Transcription. *Sci. Rep.* 9(1), 11516. doi: 10.1038/s41598-019-47639-x.

Takano, M., Yamaguchi, M., Nakajima, R., Fujita, S., Kojima, T., and Kasai, K. (2009). Effects of relaxin on collagen type I released by stretched human periodontal ligament cells. *Orthod. Craniofac. Res.* 12(4), 282-288. doi: 10.1111/j.1601-6343.2009.01463.x.

Tang, N., Zhao, Z., Zhang, L., Yu, Q., Li, J., Xu, Z., et al. (2012). Up-regulated osteogenic transcription factors during early response of human periodontal ligament stem cells to cyclic tensile strain. *Arch. Med. Sci.* 8(3), 422-430. doi: 10.5114/aoms.2012.28810.

Tantilertanant, Y., Niyompanich, J., Everts, V., Supaphol, P., Pavasant, P., and Sanchavanakit, N. (2019a). Cyclic tensile force-upregulated IL6 increases MMP3 expression by human periodontal ligament cells. *Arch. Oral Biol.* 107, 104495. doi: 10.1016/j.archoralbio.2019.104495.

Tantilertanant, Y., Niyompanich, J., Everts, V., Supaphol, P., Pavasant, P., and Sanchavanakit, N. (2019b). Cyclic tensile force stimulates BMP9 synthesis and in vitro mineralization by human periodontal ligament cells. *J. Cell. Physiol.* 234(4), 4528-4539. doi: 10.1002/jcp.27257.

Tsuji, K., Uno, K., Zhang, G.X., and Tamura, M. (2004). Periodontal ligament cells under intermittent tensile stress regulate mRNA expression of osteoprotegerin and tissue inhibitor of matrix metalloprotease-1 and -2. *J. Bone Miner. Metab.* 22(2), 94-103. doi: 10.1007/s00774-003-0456-0.

Tsuruga, E., Nakashima, K., Ishikawa, H., Yajima, T., and Sawa, Y. (2009). Stretching modulates oxytalan fibers in human periodontal ligament cells. *J. Periodontal Res.* 44(2), 170-174. doi: 10.1111/j.1600-0765.2008.01099.x.

Tsuruga, E., Oka, K., Hatakeyama, Y., Isokawa, K., and Sawa, Y. (2012). Latent transforming growth factor-beta binding protein 2 negatively regulates coalescence of oxytalan fibers induced by stretching stress. *Connect Tissue Res.* 53(6), 521-527. doi: 10.3109/03008207.2012.702816.

Wada, S., Kanzaki, H., Narimiya, T., and Nakamura, Y. (2017). Novel device for application of continuous mechanical tensile strain to mammalian cells. *Biol. Open* 6(4), 518-524. doi: 10.1242/bio.023671.

Wang, H., Feng, C., Jin, Y., Tan, W., and Wei, F. (2019a). Identification and characterization of circular RNAs involved in mechanical force-induced periodontal ligament stem cells. *J. Cell. Physiol.* 234(7), 10166-10177. doi: 10.1002/jcp.27686.

Wang, L., Pan, J., Wang, T., Song, M., and Chen, W. (2013). Pathological cyclic strain-induced apoptosis in human periodontal ligament cells through the RhoGDIalpha/caspase-3/PARP pathway. *PloS One* 8(10), e75973. doi: 10.1371/journal.pone.0075973.

Wang, Y., Hu, B., Hu, R., Tong, X., Zhang, M., Xu, C., et al. (2019b). TAZ contributes to osteogenic differentiation of periodontal ligament cells under tensile stress. *J. Periodontal Res.* doi: 10.1111/jre.12698.

Wang, Y., Li, Y., Fan, X., Zhang, Y., Wu, J., and Zhao, Z. (2011). Early proliferation alteration and differential gene expression in human periodontal ligament cells subjected to cyclic tensile stress. *Arch. Oral Biol.* 56(2), 177-186. doi: 10.1016/j.archoralbio.2010.09.009.

Wang, Y.F., Zuo, Z.H., Luo, P., Pang, F.S., and Hu, J.T. (2018). The effect of cyclic tensile force on the actin cytoskeleton organization and morphology of human periodontal ligament cells. *Biochem. Biophys. Res. Commun.* 506(4), 950-955. doi: 10.1016/j.bbrc.2018.10.163.

Wei, F., Liu, D., Feng, C., Zhang, F., Yang, S., Hu, Y., et al. (2015). microRNA-21 mediates stretch-induced osteogenic differentiation in human periodontal ligament stem cells. *Stem Cells Dev.* 24(3), 312-319. doi: 10.1089/scd.2014.0191.

Wei, F.L., Wang, J.H., Ding, G., Yang, S.Y., Li, Y., Hu, Y.J., et al. (2014). Mechanical force-induced specific MicroRNA expression in human periodontal ligament stem cells. *Cells Tissues Organs* 199(5-6), 353-363. doi: 10.1159/000369613.

Wescott, D.C., Pinkerton, M.N., Gaffey, B.J., Beggs, K.T., Milne, T.J., and Meikle, M.C. (2007). Osteogenic gene expression by human periodontal ligament cells under cyclic tension. *J. Dent. Res.* 86(12), 1212-1216. doi: 10.1177/154405910708601214.

Wolf, M., Lossdorfer, S., Kupper, K., and Jager, A. (2014). Regulation of high mobility group box protein 1 expression following mechanical loading by orthodontic forces in vitro and in vivo. *Eur. J. Orthod.* 36(6), 624-631. doi: 10.1093/ejo/cjt037.

Wu, J., Song, M., Li, T., Zhu, Z., and Pan, J. (2015). The Rho-mDia1 signaling pathway is required for cyclic strain-

[a] Entry given as reported in the study.
[b] All official gene symbols come from the HUGO Gene Nomenclature Committee (HGNC; URL: https://www.genenames.org) after checking specificity of primers with Primer-BLAST.
[c] Gender/Sex of donors: "M" – male, "F" – female; Tooth type: "PM" – premolar, "M" – molar; Cell density: given in cells/well if not otherwise mentioned.
[d] Frequencies labeled bold orange were converted to hertz (Hz) according to its definition using the information reported in the study (in brackets)
[e] Force type deduced from the description of the force apparatus given by the authors.
[f] Gene and protein expression: 1. conclusion of change (increase, decrease…) was given according to the defined criteria in Figure 2; 2. different markers to describe the amount of change; † Information derived from figures using Engauge Digitizer; *Folds calculated by measuring the graphs, without using the Engauge Digitizer; No makers: Information derived from figures by description in the articles

induced cytoskeletal rearrangement of human periodontal ligament cells. *Exp. Cell Res.* 337(1)**,** 28-36. doi: 10.1016/j.yexcr.2015.07.016.

Wu, Y., Ou, Y., Liao, C., Liang, S., and Wang, Y. (2019a). High-throughput sequencing analysis of the expression profile of microRNAs and target genes in mechanical force-induced osteoblastic/cementoblastic differentiation of human periodontal ligament cells. *Am. J. Transl. Res.* 11(6)**,** 3398-3411.

Wu, Y., Zhao, D., Zhuang, J., Zhang, F., and Xu, C. (2016). Caspase-8 and Caspase-9 Functioned Differently at Different Stages of the Cyclic Stretch-Induced Apoptosis in Human Periodontal Ligament Cells. *PloS One* 11(12)**,** e0168268. doi: 10.1371/journal.pone.0168268.

Wu, Y., Zhuang, J., Zhao, D., and Xu, C. (2019b). Interaction between caspase-3 and caspase-5 in the stretch-induced programmed cell death in the human periodontal ligament cells. *J. Cell. Physiol.* 234(8)**,** 13571-13581. doi: 10.1002/jcp.28035.

Wu, Y., Zhuang, J., Zhao, D., Zhang, F., Ma, J., and Xu, C. (2017). Cyclic stretch-induced the cytoskeleton rearrangement and gene expression of cytoskeletal regulators in human periodontal ligament cells. *Acta Odontol. Scand.* 75(7)**,** 507-516. doi: 10.1080/00016357.2017.1347823.

Xu, C., Fan, Z., Shan, W., Hao, Y., Ma, J., Huang, Q., et al. (2012). Cyclic stretch influenced expression of membrane connexin 43 in human periodontal ligament cell. *Arch. Oral Biol.* 57(12)**,** 1602-1608. doi: 10.1016/j.archoralbio.2012.07.002.

Xu, C., Hao, Y., Wei, B., Ma, J., Li, J., Huang, Q., et al. (2011). Apoptotic gene expression by human periodontal ligament cells following cyclic stretch. *J. Periodontal Res.* 46(6)**,** 742-748. doi: 10.1111/j.1600-0765.2011.01397.x.

Xu, H., Bai, D., Ruest, L.B., Feng, J.Q., Guo, Y.W., Tian, Y., et al. (2015). Expression analysis of alpha-smooth muscle actin and tenascin-C in the periodontal ligament under orthodontic loading or in vitro culture. *Int. J. Oral Sci.* 7(4)**,** 232-241. doi: 10.1038/ijos.2015.26.

Xu, H.Y., Nie, E.M., Deng, G., Lai, L.Z., Sun, F.Y., Tian, H., et al. (2017). Periostin is essential for periodontal ligament remodeling during orthodontic treatment. *Mol. Med. Rep.* 15(4)**,** 1800-1806. doi: 10.3892/mmr.2017.6200.

Yamaguchi, M., Ozawa, Y., Nogimura, A., Aihara, N., Kojima, T., Hirayama, Y., et al. (2004). Cathepsins B and L increased during response of periodontal ligament cells to mechanical stress in vitro. *Connect Tissue Res.* 45(3)**,** 181-189. doi: 10.1080/03008200490514149.

Yamaguchi, M., and Shimizu, N. (1994). Identification of factors mediating the decrease of alkaline phosphatase activity caused by tension-force in periodontal ligament cells. *Gen. Pharmacol.* 25(6)**,** 1229-1235. doi: 10.1016/0306-3623(94)90142-2.

Yamaguchi, M., Shimizu, N., Goseki, T., Shibata, Y., Takiguchi, H., Iwasawa, T., et al. (1994). Effect of different magnitudes of tension force on prostaglandin E2 production by human periodontal ligament cells. *Arch. Oral Biol.* 39(10)**,** 877-884. doi: 10.1016/0003-9969(94)90019-1.

Yamaguchi, M., Shimizu, N., Ozawa, Y., Saito, K., Miura, S., Takiguchi, H., et al. (1997). Effect of tension-force on plasminogen activator activity from human periodontal ligament cells. *J. Periodontal Res.* 32(3)**,** 308-314. doi: 10.1111/j.1600-0765.1997.tb00539.x.

Yamaguchi, M., Shimizu, N., Shibata, Y., and Abiko, Y. (1996). Effects of different magnitudes of tension-force on alkaline phosphatase activity in periodontal ligament cells. *J. Dent. Res.* 75(3)**,** 889-894. doi: 10.1177/00220345960750030501.

Yamaguchi, N., Chiba, M., and Mitani, H. (2002). The induction of c-fos mRNA expression by mechanical stress in human periodontal ligament cells. *Arch. Oral Biol.* 47(6)**,** 465-471. doi: 10.1016/s0003-9969(02)00022-5.

Yamashiro, K., Myokai, F., Hiratsuka, K., Yamamoto, T., Senoo, K., Arai, H., et al. (2007). Oligonucleotide array analysis of cyclic tension-responsive genes in human periodontal ligament fibroblasts. *Int. J. Biochem. Cell Biol.* 39(5)**,** 910-921. doi: 10.1016/j.biocel.2007.01.015.

Yang, S.Y., Kim, J.W., Lee, S.Y., Kang, J.H., Ulziisaikhan, U., Yoo, H.I., et al. (2015). Upregulation of relaxin receptors in the PDL by biophysical force. *Clin. Oral Investig.* 19(3)**,** 657-665. doi: 10.1007/s00784-014-1276-4.

Yang, S.Y., Wei, F.L., Hu, L.H., and Wang, C.L. (2016). PERK-eIF2alpha-ATF4 pathway mediated by endoplasmic reticulum stress response is involved in osteodifferentiation of human periodontal ligament cells under cyclic mechanical force. *Cell. Signal.* 28(8)**,** 880-886. doi: 10.1016/j.cellsig.2016.04.003.

Yang, Y., Wang, B.K., Chang, M.L., Wan, Z.Q., and Han, G.L. (2018). Cyclic Stretch Enhances Osteogenic Differentiation of Human Periodontal Ligament Cells via YAP Activation. *Biomed Res. Int.* 2018**,** 2174824. doi: 10.1155/2018/2174824.

Yang, Y., Yang, Y., Li, X., Cui, L., Fu, M., Rabie, A.B., et al. (2010). Functional analysis of core binding factor a1 and its relationship with related genes expressed by human periodontal ligament cells exposed to mechanical stress. *Eur. J. Orthod.* 32(6)**,** 698-705. doi: 10.1093/ejo/cjq010.

Yang, Y.Q., Li, X.T., Rabie, A.B., Fu, M.K., and Zhang, D. (2006). Human periodontal ligament cells express osteoblastic phenotypes under intermittent force loading in vitro. *Front. Biosci.* 11**,** 776-781. doi: 10.2741/1835.

Yoshino, H., Morita, I., Murota, S.I., and Ishikawa, I. (2003). Mechanical stress induces production of angiogenic regulators in cultured human gingival and periodontal ligament fibroblasts. *J. Periodontal Res.* 38(4)**,** 405-410. doi: 10.1034/j.1600-0765.2003.00660.x.

Yu, W., Hu, B., Shi, X., Cao, Z., Ren, M., He, Z., et al. (2018). Nicotine inhibits osteogenic differentiation of human periodontal ligament cells under cyclic tensile stress through canonical Wnt pathway and alpha7 nicotinic acetylcholine receptor. *J. Periodontal Res.* 53(4)**,** 555-564. doi: 10.1111/jre.12545.

Yuda, A., Maeda, H., Fujii, S., Monnouchi, S., Yamamoto, N., Wada, N., et al. (2015). Effect of CTGF/CCN2 on osteo/cementoblastic and fibroblastic differentiation of a human periodontal ligament stem/progenitor cell line. *J. Cell. Physiol.* 230(1)**,** 150-159. doi: 10.1002/jcp.24693.

Zhao, D., Wu, Y., Xu, C., and Zhang, F. (2017). Cyclic-stretch induces apoptosis in human periodontal ligament cells by activation of caspase-5. *Arch. Oral Biol.* 73**,** 129-135. doi: 10.1016/j.archoralbio.2016.10.009.

Zhao, D., Wu, Y., Zhuang, J., Xu, C., and Zhang, F. (2016). Activation of NLRP1 and NLRP3 inflammasomes contributed to cyclic stretch-induced pyroptosis and release of IL-1beta in human periodontal ligament cells. *Oncotarget* 7(42)**,** 68292-68302. doi: 10.18632/oncotarget.11944.

Zhuang, J., Wang, Y., Qu, F., Wu, Y., Zhao, D., and Xu, C. (2019). Gasdermin-d Played a Critical Role in the Cyclic Stretch-Induced Inflammatory Reaction in Human Periodontal Ligament Cells. *Inflammation* 42(2)**,** 548-558. doi: 10.1007/s10753-018-0912-6.

Ziegler, N., Alonso, A., Steinberg, T., Woodnutt, D., Kohl, A., Mussig, E., et al. (2010). Mechano-transduction in periodontal ligament cells identifies activated states of MAP-kinases p42/44 and p38-stress kinase as a mechanism for MMP-13 expression. *BMC Cell Biol.* 11**,** 10. doi: 10.1186/1471-2121-11-10.

[a] Entry given as reported in the study.
[b] All official gene symbols come from the HUGO Gene Nomenclature Committee (HGNC; URL: https://www.genenames.org) after checking specificity of primers with Primer-BLAST.
[c] Gender/Sex of donors: "M" – male, "F" – female; Tooth type: "PM" – premolar, "M" – molar; Cell density: given in cells/well if not otherwise mentioned.
[d] Frequencies labeled bold orange were converted to hertz (Hz) according to its definition using the information reported in the study (in brackets)
[e] Force type deduced from the description of the force apparatus given by the authors.
[f] Gene and protein expression: 1. conclusion of change (increase, decrease…) was given according to the defined criteria in Figure 2; 2. different markers to describe the amount of change; † Information derived from figures using Engauge Digitizer; *Folds calculated by measuring the graphs, without using the Engauge Digitizer; No makers: Information derived from figures by description in the articles

Supplement 3: Criteria for Risk of Bias assessment

Included are the criteria (and their definitions) to assess the reporting quality of *in vitro* studies ("Reporting Risk of Bias") and the methodlogical quality of *in vitro* studies ("Methodological Risk of Bias") and the data sheets that were applied for the actual assessment.

Content

Criteria for Risk of Bias

Reporting quality of *in vitro* studies

This table was compiled from different sources. The main structure derived from supplementary Table S4 published by Vasant et al (2018), that is based on Samuel et al. (2016).

Criterion #	Variable/Sub variable	Where should it be found?	Definition for "low risk of bias" (LoB)
1	Description of scientific background	→ Introduction	LoB: Scientific background is described.
2	Description objective	Research question – What I'm interested in? Hypotheses to be tested. → In the last paragraph of the introduction and/or the Abstract	LoB: All objectives (primary and secondary) clearly reported. ("Aim of the study was…", "We hypnotized …", etc.)
3	Justification for model	→ Abstract, Introduction and M&M	LoB: Reason for choosing cell type(s) and the type of force, its magnitude and its duration are given. Optional: Reasons for choosing analytes and assays used.
4	Study design description	→ Abstract; last paragraph of the Introduction; M&M	LoB: The materials and methods are described in a way, that the experimental procedures can be replicated if the samples are given.
5	Defined experimental outcomes	→ Experimental procedures outlined in M&M and outcomes presented in results correspond	LoB: Results as presented in the Results section and the experimental procedures outlined in M&M correspond.
6	Ethical statement	→ M&M: Cell culture	LoB: Ethical statement is provided. n.a.: not applicable for commercial vendors of primary cells (e.g. Lonza, Promocell, etc.) or cell lines from official sources (RIKEN, ATCC, ECACC, etc.)
7	Cell maintenance condition	→ M&M: Cell culture	LoB: Minimum required are source of cells (primary cells and cell lines), their isolation method (primary cells), culture conditions (both), passage used (primary cells) and seeding density (both), confluency level (both).
8	Description of measurement precision and variability	"*Statistics should be fully reported in the manuscript/article, including the statistical test used, exact value of N and the definitions. value of N and the definitions of center and dispersion and the precision measures (e.g., mean, median, SD, SEM, confidence intervals).*" (Biophysical Journal's Guidelines for the Reproducibility of Biophysics Research) → M&M: Statistics; Results	LoB: Measurement precision and variability are described.
9	Statistical analysis		LoB: All statistical procedures for data analysis are provided; all statistical results derive from statistical procedures described in M&M.
10	Results description	→ Results	LoB: All results outlined in "Objective" and generated by experimental procedures described M&M are given.

Abbreviations:

LoB	Low risk of bias
M&M	Materials and Methods

Levels:

"+"	Low risk of bias (LoB)
"-"	High risk of bias (HoB)
"?"	Incomplete/unclear risk of bias
n. a.	Not applicable

Methodological quality of *in vitro* studies

This table was compiled from different sources. The main structure derived from supplementary Table S3 published by Vansant et al. (2018) that is based on Samuel et al. (2016). Additionally, table 1 ("Glossary key terms") and further definitions listed in table 2, both from Samuel et al. (2016), were used to prepare the following table.

Criterion #	Variable/Sub variable	Definition of variable or sub variable	Definition for "low risk of bias" (LoB)
	Selection bias	Samuel et al (2016): "*Selection bias: Systematic differences in the comparison groups."* OHAT RoBT, p. 5: "*Selection bias refers to systematic differences between baseline characteristics of the groups that are compared (Higgins and Green 2011)."*	
1*	Selection bias / Baseline characteristics similarity/appropriate control group selection	OHAT RoBT, p. 9: "*Comparison group appropriateness refers to having similar baseline characteristics of factors related to the outcome measures of interest between groups aside from the exposures (and outcomes for case- control studies).*"	LoB: *Control and treated groups are similar at the start of the study (e.g. cell type, passage, cell density [cells/well], confluency).* => Appropriate/controlled exposure
2	Selection bias / Allocation concealment	OHAT RoBT, p. 7: "*Allocation concealment prior to assigning the exposure level or treatment group (along with randomization in question #1) helps to assure that treatment is not given selectively based on potential differences in human subjects or non-human experimental animals."* Samuel et al (2016): "*A process that it used to prevent selection bias. The person allocating subjects to experimental arms is unaware of which arm the subjects are being allocated* ***until the moment of assignment****. This prevents researchers from (unconsciously or otherwise) influencing the allocation of subjects.*"	LoB: The experimental subjects (i.e. cell culture plates) are all prepared at the same time without allocating them to specific experimental arms (no definition in advance of the experiment). Directly before an experiment, plates are randomly chosen and allocated to the experimental arms.
3	Selection bias / Randomization	OHAT RoBT, p. 5: "*Randomization of exposure or sequence generation (along with allocation concealment in question #2) helps to assure that treatment is not given selectively based on potential differences in human subjects or non-human experimental animals (e.g., randomization by animal body weight avoids potential selection bias introduced by assigning all of the smallest animals to the high-dose exposure group).*"	n. a.
4	Performance bias / Blinding of researchers	OHAT RoBT, p. 15: "*Performance bias refers to systematic differences in the care provided to human participants or experimental animals by study groups. Examples include contamination of the control group with the exposure or intervention, unbalanced provision of additional interventions or co-interventions, difference in co-interventions, inadequate blinding of providers and participants in human studies (Viswanathan et al. 2012), and inadequate blinding of research personnel to the animal's study group (Sena et al. 2007).*" OHAT RoBT, p. 16: "*Blinding requires that research personnel do not know which administered dose or exposure level the human subject or animal is being given (i.e., study group). Human studies also require blinding of the human subjects when possible.*"	n. a.
5	Detection bias / Blinding of outcome assessors	Samuel et al (2016): "*Detection bias: Systematic differences in the outcome assessment between groups."* OHAT RoBT, p. 22: *"Detection bias refers to systematic differences between experimental and control groups with regards to how outcomes and exposures are assessed (Higgins and Green 2011) and also considers validity and reliability of methods used to assess outcomes and exposures (Viswanathan et al. 2012)."* OHAT RoBT, p. 25: *"Detection bias can be minimized by using valid and reliable methods to assess the outcome applied consistently across groups (i.e., under the same method and time-frame). Objectivity of the outcome assessment and the need for blinding are two sides of the same issue. Blinding requires that outcome assessors do not know the study group or exposure level of the human subject or animal when the outcome was assessed."*	n. a.

Criterion #	Variable/Sub variable	Definition of variable or sub variable	Definition for "low risk of bias" (LoB)
6	Attrition bias / Complete outcome data	Samuel et al (2016): "*Systematic differences in excluding study units between groups*" OHAT RoBT, p. 19: *"Attrition or exclusion bias: systematic differences in the loss or exclusion from analyses of participants or animals.* […] *Incomplete outcome data includes loss due to attrition (nonresponse, dropout, or loss of follow-up) or exclusion from analyses."*	LoB: Accounting for all included study units. HoB: Reports on incomplete outcome data including loss due to attrition or exclusion from analyses.
7	Reporting bias / Selective outcome data	Samuel et al (2016): "*Reporting bias: Systematic omission of results in the study documentation/ publication*." And: "*Selective outcome reporting: The reporting of only selected results, not all results*." OHAT RoBT, p. 30: *"Selective reporting bias refers to selective inclusion of outcomes in the publication of the study on the basis of the results (Hutton and Williamson 2000, Higgins and Green 2011).* […] *Selective reporting is present if pre-specified outcomes are not reported or incompletely reported.* […] *Selective reporting bias can be assessed by comparing the "methods" and "results" section of the paper, and by considering outcomes measured in the context of knowledge in the field."*	LoB: The outcome data from all experiments as given in M&M is reported and accounted for. All results given in the Results section must derive from materials and methods reported in M&M. All uninterpretable or intermediate test results and withdrawals are explained including lost samples; e.g. ELISA measurements below detection limit.
8	Confounding bias / Account for confounding variables	Samuel et al (2016): "*Systematic differences in factors potentially influencing the results between groups. […] Is very context depending. In an animal study of endocrine disruption, bedding material potentially containing phytoestrogens should be the same for all groups."* OHAT RoBT, p. 11: "*Confounding variables or confounders include any factor that is: 1) associated with the exposure, 2) an independent risk factor for a given outcome, and 3) unequally distributed between study groups (Gerstman 2013). The potential confounder cannot be an intermediate effect on the causal pathway between exposure and the outcome (Gerstman 2013, Sterne et al. 2014). Appropriate methods to account for these differences would include multivariable analysis, stratification, matching of cases and controls, or other approaches."* see also OHAT RoBT, p. 32! OHAT RoBT, p. 13: Low risk of bias can be assumed, if "*There is direct evidence that appropriate adjustments or explicit considerations were made for primary covariates and confounders in the final analyses through the use of statistical models to reduce research-specific bias including standardization, matching, adjustment in multivariate model, stratification, propensity scoring, or other methods that were appropriately justified."*	LoB: Confounding variables were identified/named in connection with: • exposure (e.g. uneven force distribution), • test procedures (e.g. vehicle controls), • cell culture (e.g. age and gender of donors, and passage numbers of primary cells used for experiment). Appropriate adjustments or explicit considerations were made in the final analyses using statistical methods or other methods that were appropriately justified and discussed or discussed only in an appropriate section in the Discussion part.
9	Appropriate statistical methods / Sample size determination	Samuel et al (2016): "*Appropriateness of statistical methods of experimental design and data analysis has to be demonstrated/justified*." OHAT RoBT, p. 31: "*One of the common statistical issues identified has been reporting of statistical tests that require normally distributed data (e.g., t-test or ANOVA) without reporting that the homogeneity of variance was tested or confirmed. It is recommended that experts with some knowledge of statistical methods used in the literature participate in drafting the risk-of-bias criteria for identifying inappropriate statistical methods when a review protocol is developed. Even with early expert consultation and planning, statistical methods questions may arise when the actual studies are assessed. Additional consultation and modifications to the statistical methods risk-of-bias criteria may be necessary. When changes are made, they should be documented along with the date on which modifications were made and the logic for the changes*."	LoB: Sample size calculation is given.
10	Appropriate statistical methods / Statistical analysis		LoB: Appropriate statistical analysis and their justification are given. • Why was that specific test chosen? • Preliminaries for statistical procedures are tested – e.g. normal distribution – and the tests were chosen accordingly.

Criterion #	Variable/Sub variable	Definition of variable or sub variable	Definition for "low risk of bias" (LoB)
11*	Appropriate/controlled exposure (incl. characterization)	Samuel et al (2016): "*It needs to be ensured that all subjects are treated/exposed in the same way, e.g., by controlling the food consumption per animal in a feeding study.*" OHAT RoBT, p. 22-23: "*Detection bias refers to systematic differences between experimental and control groups with regards to how outcomes and exposures are assessed (Higgins and Green 2011) and also considers validity and reliability of methods used to assess outcomes and exposures (Viswanathan et al. 2012).* […] *For controlled exposure studies (i.e., experimental human or animal studies), the use of reliable methods to measure exposure depends primarily on ensuring the purity and stability of the treatment compound."*	LoB: All data on the exposure characteristics are reported for both experimental and control groups. In cell culture: • same cell type, • cultivated identically, • same seeding density or same confluency, • same passage numbers.
12*	Optimal time window used	Samuel et al (2016): "*This refers to the age and status (e.g., pregnancy or disease status) of the animals. In a developmental toxicity study, for example, the exposure should take place during the most appropriate gestation days. In cell culture experiments, the cells should be exposed at their optimal developmental state, e.g., at confluency, or within certain cell passage numbers, for which the stability of the karyotype is guaranteed."* OHAT RoBT, p. 2: "*Was the exposure in the appropriate biological window to affect the outcome? This is considered under indirectness. Was the outcome assessed at an adequate amount of time after the exposure for the development of the outcome? This is considered under indirectness. Does the timing of exposure or outcome assessment impact the consistency of results? If the appropriate biological window is unclear for an outcome of interest, differences in timing of exposure or outcome assessment could be used to stratify results when considering unexplained inconsistency.* […] *Does the duration of the experiment lasts long enough to cause the biological response?"*	LoB: In cell culture experiments, the same cell type is used for experimental and control(s) condition, cultivated identically, seeded at the same densities/confluency and same passage number. For force application, force type, force duration and force magnitude are proved to be of biological relevance. Proved e.g. by presenting a dose-response curve or by reference to previous publications where a dose-response curve or similar was published.
13	Statement conflict of interest/funding source	Samuel et al (2016): "*Conflicts or funding by bodies with vested interests may result in (un-)conscious biases during the entire study, from planning to publication.*"	LoB: Statement conflict of interest and funding source are given.
14*	Test substance/treatment details	Samuel et al (2016): "*The test substance identity should be known, including possibly interfering impurities. Treatment details should be known, in order to assess issues such as optimal time window used.*"	LoB: All chemicals, kits or tools/apparatuses used are named with their manufacture, purity and their specificity (e.g. order/article number) and preparation for experimental application is given (e.g. dilution and diluent, etc.); PCR primers sequence, etc.
15	Test organism/system	Samuel et al (2016): "*The animal type/strain or the cell system needs to be stated, e.g. using different cell batches may introduce bias.*"	LoB: Primary cells isolated from donors of the same age range and sex. In cell culture experiments, the same cell type is used for experimental and control(s) condition, cultivated identically, seeded at the same densities/confluency and same passage number.

Abbreviations:

LoB	Low risk of bias
HoB	High risk of bias
M&M	Materials and Methods

Levels:

"+"	Low risk of bias (LoB)
"-"	High risk of bias (HoB)
"?"	Incomplete/unclear risk of bias
n. a.	Not applicable

References

Vansant et al (2018). Expression of biological mediators during orthodontic tooth movement: A systematic review. Arch Oral Biol 95:170-186.

Samuel et al (2016). Guidance on assessing the methodological and reporting quality of toxicologically relevant studies: A scoping review. Environment International 92-93: 630-646.

OHAT RoBT – OHAT Risk of Bias Rating Tool for Human and Animal Studies (January 2015). URL : https://ntp.niehs.nih.gov/ntp/ohat/pubs/riskofbiastool_508.pdf (assessed: 2019-02-11); National Toxicology Program (2015). Handbook for Conducting a Literature-Based Health Assessment Using OHAT Approach for Systematic Review and Evidence Integration. URL: https://ntp.niehs.nih.gov/ntp/ohat/pubs/handbookjan2015_508.pdf (assessed: 2019-02-11)

On mechanistic studies: National Research Council (2014). Review of EPA's Integrated Risk Information System (IRIS) process. Washington, DC: The National Academies Press. URL: https://doi.org/10.17226/18764 ; https://nap.edu/18764 (assessed: 2019-02-11)

Biophysical Journal's Guidelines for the Reproducibility of Biophysics Research (April 2017) (URL: http://www.cell.com/pb/assets/raw/journals/society/biophysj/PDFs/reproducibility-guidelines.pdf) as referenced from National Institutes of Health's Principles and Guidelines for Reporting Preclinical Research (http://www.nih.gov/about/reporting-preclinical-research.htm) (assessed: 2019-02-11)

Data sheets for „Risk of Bias“ Assessment

Reporting quality of *in vitro* studies

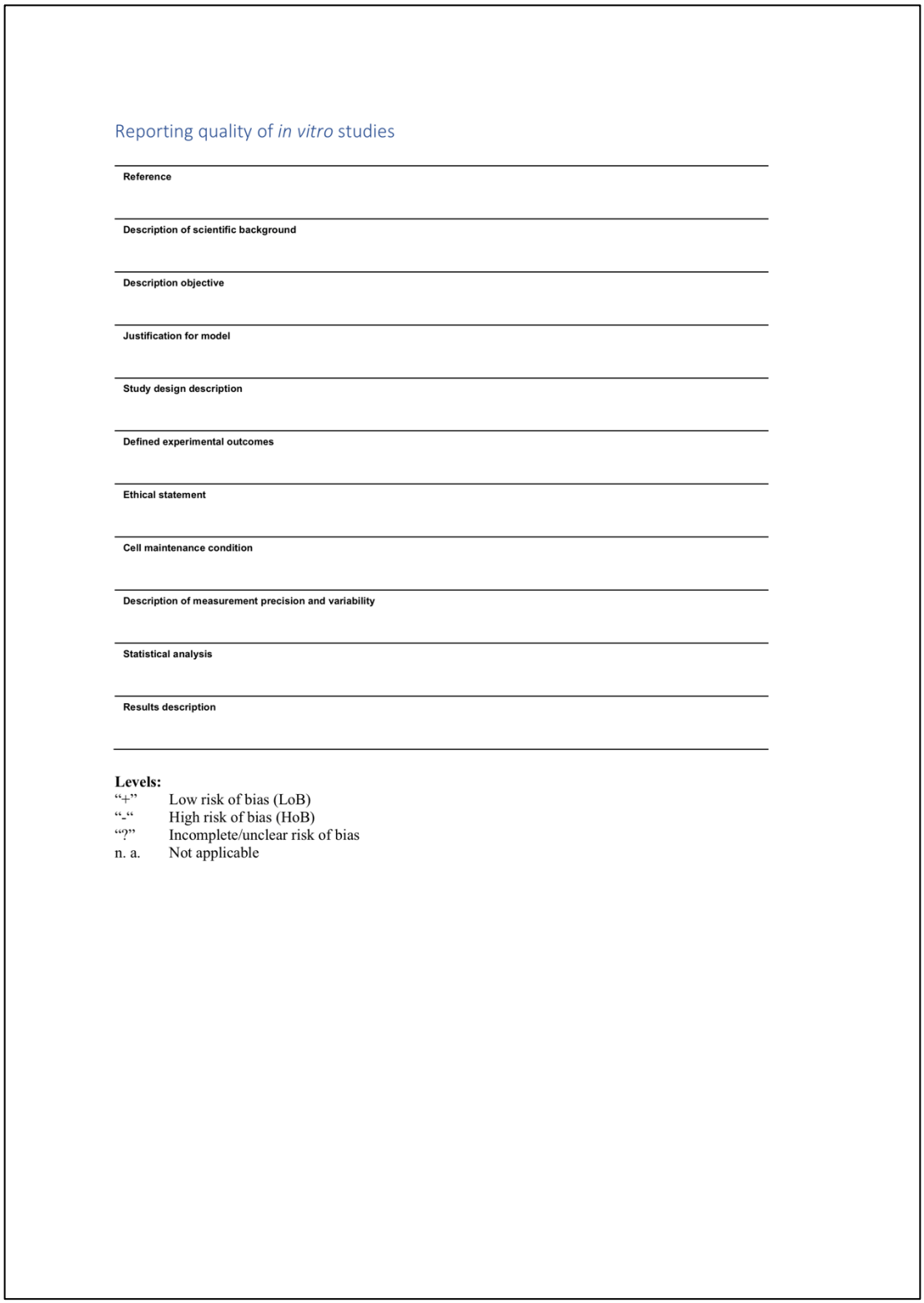

Reporting quality of *in vitro* studies

Reference
Description of scientific background
Description objective
Justification for model
Study design description
Defined experimental outcomes
Ethical statement
Cell maintenance condition
Description of measurement precision and variability
Statistical analysis
Results description

Levels:

“+”	Low risk of bias (LoB)
“-“	High risk of bias (HoB)
“?”	Incomplete/unclear risk of bias
n. a.	Not applicable

Methodological quality of *in vitro* studies

Methodological quality of *in vitro* studies

Reference
Selection bias
Selection bias / Baseline characteristics similarity/appropriate control group selection
Selection bias / Allocation concealment
Selection bias / Randomization
Performance bias / Blinding of researchers
Detection bias / Blinding of outcome assessors
Attrition bias / Complete outcome data
Reporting bias / Selective outcome data
Confounding bias / Account for confounding variables
Appropriate statistical methods / Sample size determination
Appropriate statistical methods / Statistical analysis
Appropriate/controlled exposure (incl. characterization)
Optimal time window used
Statement conflict of interest/funding source
Test substance/treatment details
Test organism/system

Levels:

"+"	Low risk of bias (LoB)
"-"	High risk of bias (HoB)
"?"	Incomplete/unclear risk of bias
n. a.	Not applicable

Supplement 4.1 Risk of bias assessment for the methodological quality of the included *in vitro* studies

Reference	Selection bias			Performance bias	Detection bias	Attrition bias	Reporting bias	Confounding bias	Appropriate statistical methods		Appropriate/ controlled exposure (incl. characterization)	Optimal time window used	Statement conflict of interest/fund-ing source	Test substance/treat-ment details	Test organism/system
	Baseline characteristics similarity / appropriate control group selection	Allocation concealment	Randomi-zation	Blinding of researchers	Blinding of outcome assessors	Complete outcome data	Selective outcome data	Account for confounding variables	Sample size determination	Statistical analysis					
Abiko et al. (1998)	+	+	n. a.	n. a.	n. a.	+	+	?	-	-	+	?	?	+	?
Agarwal et al. (2003)	+	+	n. a.	n. a.	n. a.	+	+	?	-	-	+	?	-	+	+
Arima et al. (2019)	?	+	n. a.	n. a.	n. a.	+	+	?	-	-	?	?	?	+	?
Basdra et al. (1995)	?	+	n. a.	n. a.	n. a.	+	+	?	-	-	?	?	-	+	?
Basdra et al. (1996)	?	+	n. a.	n. a.	n. a.	+	+	?	-	-	?	?	-	+	?
Bolcato-Bellemin et al. (2000)	+	+	n. a.	n. a.	n. a.	+	+	?	-	-	?	?	?	+	?
Chang et al. (2015)	?	+	n. a.	n. a.	n. a.	+	+	?	-	-	+	?	?	+	?
Chang et al. (2017)	+	+	n. a.	n. a.	n. a.	+	+	?	-	-	+	?	-	+	+
Chen et al. (2014)	+	+	n. a.	n. a.	n. a.	-	-	?	-	-	+	?	+	?	?
Chen et al. (2015)	+	+	n. a.	n. a.	n. a.	+	+	?	-	-	+	?	+	+	?
Chiba and Mitani (2004)	+	+	n. a.	n. a.	n. a.	+	?	?	-	-	?	?	?	?	?
Cho et al. (2010)	?	+	n. a.	n. a.	n. a.	+	+	?	-	-	?	?	-	+	?
Deschner et al. (2012)	+	+	n. a.	n. a.	n. a.	+	+	?	-	-	+	?	+	+	?
Diercke et al. (2011)	?	+	n. a.	n. a.	n. a.	+	+	?	-	-	+	?	-	+	?
Doi et al. (2003)	?	+	n. a.	n. a.	n. a.	+	+	?	-	-	?	?	?	+	?
Fujihara et al. (2010)	+	+	n. a.	n. a.	n. a.	+	+	?	-	-	?	?	-	+	?
Goto et al. (2011)	?	+	n. a.	n. a.	n. a.	+	?	?	-	-	?	?	+	?	?
Hao et al. (2009)	+	+	n. a.	n. a.	n. a.	+	+	?	-	-	+	?	+	+	+
He et al. (2004)	+	+	n. a.	n. a.	n. a.	+	+	?	-	-	+	?	?	+	?
He et al. (2019)	?	+	n. a.	n. a.	n. a.	+	+	?	-	-	?	+	+	+	+
Howard et al. (1998)	+	+	n. a.	n. a.	n. a.	+	+	?	-	-	+	?	?	+	?
Huelter-Hassler et al. (2017)	+	+	n. a.	n. a.	n. a.	+	+	?	-	-	+	?	+	+	+
Hülter-Hassler et al. (2017)	+	+	n. a.	n. a.	n. a.	+	+	?	-	-	+	?	+	+	?
Jacobs et al. (2013)	?	+	n. a.	n. a.	n. a.	+	+	?	-	-	+	?	+	+	+
Jacobs et al. (2014)	?	+	n. a.	n. a.	n. a.	+	+	?	-	-	+	?	?	+	+
Jacobs et al. (2015)	?	+	n. a.	n. a.	n. a.	+	+	?	-	-	+	?	?	+	+
Jacobs et al. (2018)	?	+	n. a.	n. a.	n. a.	+	?	?	-	-	?	?	+	+	?
Jiang and Hua (2016)	+	+	n. a.	n. a.	n. a.	+	+	?	-	-	?	?	+	+	+
Kaku et al. (2019)	+	+	n. a.	n. a.	n. a.	+	+	?	-	-	+	?	+	+	?
Kanzaki et al. (2006)	?	+	n. a.	n. a.	n. a.	+	?	?	-	-	?	?	?	+	?
Kanzaki et al. (2019)	?	+	n. a.	n. a.	n. a.	+	?	?	-	-	?	?	+	+	?
Kikuiri et al. (2000)	+	+	n. a.	n. a.	n. a.	+	+	?	-	-	+	?	?	+	?
Kim et al. (2007)	?	+	n. a.	n. a.	n. a.	+	?	?	-	-	?	?	-	+	?
Kletsas et al. (2002)	+	+	n. a.	n. a.	n. a.	+	?	?	-	-	+	?	-	+	?
Konstantonis et al. (2014)	?	+	n. a.	n. a.	n. a.	+	?	?	-	-	?	?	+	?	?
Kook and Lee (2012)	+	+	n. a.	n. a.	n. a.	+	+	?	-	-	+	+	?	?	?
Lee et al. (2012)	?	+	n. a.	n. a.	n. a.	+	?	?	-	-	?	?	+	+	?
Lee et al. (2015)	?	+	n. a.	n. a.	n. a.	+	?	?	-	-	?	?	?	+	?
Li et al. (2013)	+	+	n. a.	n. a.	n. a.	+	+	?	-	-	+	?	+	+	?
Li et al. (2014)	+	+	n. a.	n. a.	n. a.	+	+	?	-	-	+	?	+	+	+
Li et al. (2015)	?	+	n. a.	n. a.	n. a.	+	+	?	-	-	?	?	?	+	?

Supplement 4.1 Risk of bias assessment for the methodological quality of the included *in vitro* studies

Reference	Selection bias			Performance bias	Detection bias	Attrition bias	Reporting bias	Confounding bias	Appropriate statistical methods		Appropriate/ controlled exposure (incl. characterization)	Optimal time window used	Statement conflict of interest/fund-ing source	Test substance/treat-ment details	Test organism/system
	Baseline characteristics similarity / appropriate control group selection	Allocation concealment	Randomi-zation	Blinding of researchers	Blinding of outcome assessors	Complete outcome data	Selective outcome data	Account for confounding variables	Sample size determination	Statistical analysis					
Liao and Hua (2013)	+	+	n. a.	n. a.	n. a.	+	+	?	-	-	+	?	+	+	?
Liu et al. (2012)	+	+	n. a.	n. a.	n. a.	+	+	?	-	-	+	?	?	+	?
Liu et al. (2017)	+	+	n. a.	n. a.	n. a.	+	+	?	-	-	+	?	+	+	?
Long et al. (2001)	+	+	n. a.	n. a.	n. a.	+	+	?	-	-	+	?	?	+	+
Long et al. (2002)	+	+	n. a.	n. a.	n. a.	+	+	?	-	-	+	?	?	+	?
Ma et al. (2015)	+	+	n. a.	n. a.	n. a.	+	+	?	-	-	+	?	+	+	+
Matsuda et al. (1998a)	?	+	n. a.	n. a.	n. a.	+	+	?	-	-	?	?	?	+	+
Matsuda et al. (1998b)	?	+	n. a.	n. a.	n. a.	+	+	?	-	-	?	?	?	+	+
Memmert et al. (2019)	?	+	n. a.	n. a.	n. a.	+	+	?	-	-	+	?	+	+	?
Memmert et al. (2020)	+	+	n. a.	n. a.	n. a.	+	+	?	-	-	+	?	+	?	?
Meng et al. (2010)	+	+	n. a.	n. a.	n. a.	+	+	?	-	-	+	?	?	+	+
Miura et al. (2000)	?	+	n. a.	n. a.	n. a.	+	?	?	-	-	?	?	?	?	?
Molina et al. (2001)	?	+	n. a.	n. a.	n. a.	+	+	?	-	-	?	?	?	+	?
Monnouchi et al. (2011)	?	+	n. a.	n. a.	n. a.	+	+	?	-	-	?	?	+	+	?
Monnouchi et al. (2015)	+	+	n. a.	n. a.	n. a.	+	+	?	-	-	+	?	?	+	+
Nakashima et al. (2009)	?	+	n. a.	n. a.	n. a.	+	?	?	-	-	?	?	?	+	+
Narimiya et al. (2017)	?	+	n. a.	n. a.	n. a.	+	?	?	-	-	?	?	?	+	?
Nazet et al. (2020)	?	+	n. a.	n. a.	n. a.	+	+	?	-	+	+	+	+	+	?
Nemoto et al. (2010)	?	+	n. a.	n. a.	n. a.	+	?	?	-	-	?	?	+	+	?
Ngan et al. (1990)	?	+	n. a.	n. a.	n. a.	+	?	?	-	-	?	+	-	+	?
Nogueira et al. (2014a)	?	+	n. a.	n. a.	n. a.	+	?	?	-	-	?	?	+	+	?
Nogueira et al. (2014b)	?	+	n. a.	n. a.	n. a.	+	?	?	-	-	?	?	+	+	?
Nokhbehsaim et al. (2010)	?	+	n. a.	n. a.	n. a.	+	?	?	-	-	?	?	?	?	?
Nokhbehsaim et al. (2011a)	?	+	n. a.	n. a.	n. a.	+	?	?	-	-	?	?	+	+	?
Nokhbehsaim et al. (2011b)	?	+	n. a.	n. a.	n. a.	+	?	?	-	-	?	?	?	+	?
Nokhbehsaim et al. (2012)	?	+	n. a.	n. a.	n. a.	+	+	?	-	-	?	?	+	+	?
Ohzeki et al. (1999)	?	+	n. a.	n. a.	n. a.	+	?	?	-	+	?	?	?	+	?
Ozawa et al. (1997)	?	+	n. a.	n. a.	n. a.	+	?	?	-	-	?	+	?	+	?
Padial-Molina et al. (2013)	+	+	n. a.	n. a.	n. a.	+	+	?	-	-	+	+	+	+	?
Pan et al. (2014)	+	+	n. a.	n. a.	n. a.	+	+	?	-	-	+	?	?	+	?
Papadopoulou et al. (2017)	?	+	n. a.	n. a.	n. a.	+	?	?	-	-	?	?	?	?	?
Papadopoulou et al. (2019)	?	+	n. a.	n. a.	n. a.	+	+	?	-	-	?	?	+	?	?
Pelaez et al. (2017)	+	+	n. a.	n. a.	n. a.	+	+	?	-	+	+	?	?	+	?
Peverali et al. (2001)	+	+	n. a.	n. a.	n. a.	+	+	?	-	-	+	?	-	+	?
Pinkerton et al. (2008)	+	+	n. a.	n. a.	n. a.	+	+	?	-	-	+	?	?	+	?
Qin and Hua (2016)	?	+	n. a.	n. a.	n. a.	?	?	?	-	-	?	?	?	?	?
Rath-Deschner et al. (2009)	+	+	n. a.	n. a.	n. a.	+	+	?	-	-	+	+	+	?	?
Ren et al. (2015)	+	+	n. a.	n. a.	n. a.	+	+	?	-	-	+	?	-	+	?
Ritter et al. (2007)	+	+	n. a.	n. a.	n. a.	+	+	?	-	-	+	?	-	+	?
Saminathan et al. (2012)	?	+	n. a.	n. a.	n. a.	+	?	?	-	-	+	?	?	+	?
Shen et al. (2014)	+	+	n. a.	n. a.	n. a.	+	+	?	-	-	+	?	+	+	?

Supplement 4.1 Risk of bias assessment for the methodological quality of the included *in vitro* studies

Reference	Selection bias			Performance bias	Detection bias	Attrition bias	Reporting bias	Confounding bias	Appropriate statistical methods		Appropriate/ controlled exposure (incl. characterization)	Optimal time window used	Statement conflict of interest/fund-ing source	Test substance/treat-ment details	Test organism/system
	Baseline characteristics similarity / appropriate control group selection	Allocation concealment	Randomi-zation	Blinding of researchers	Blinding of outcome assessors	Complete outcome data	Selective outcome data	Account for confounding variables	Sample size determination	Statistical analysis					
Shimizu et al. (1994)	?	+	n. a.	n. a.	n. a.	+	?	?	-	-	?	?	?	+	?
Shimizu et al. (1995)	?	+	n. a.	n. a.	n. a.	+	?	?	-	-	+	+	?	+	?
Shimizu et al. (1997)	?	+	n. a.	n. a.	n. a.	+	?	?	-	-	?	?	?	+	?
Shimizu et al. (1998)	?	+	n. a.	n. a.	n. a.	+	?	?	-	-	+	?	?	+	?
Spencer and Lallier (2009)	?	+	n. a.	n. a.	n. a.	+	?	?	-	-	?	?	+	+	?
Steinberg et al. (2011)	+	+	n. a.	n. a.	n. a.	+	+	?	-	-	+	?	?	+	?
Sun et al. (2016)	+	+	n. a.	n. a.	n. a.	+	+	?	-	-	+	?	+	+	+
Sun et al. (2017)	+	+	n. a.	n. a.	n. a.	+	+	?	-	-	+	?	?	+	+
Suzuki et al. (2014)	+	+	n. a.	n. a.	n. a.	+	+	?	-	-	+	?	+	+	+
Symmank et al. (2019)	?	+	n. a.	n. a.	n. a.	+	+	?	-	-	?	?	?	+	?
Takano et al. (2009)	+	+	n. a.	n. a.	n. a.	+	?	?	-	-	+	?	?	+	+
Tang et al. (2012)	+	+	n. a.	n. a.	n. a.	+	+	?	-	-	+	?	?	+	?
Tantilertanant et al. (2019a)	+	+	n. a.	n. a.	n. a.	+	+	?	-	-	+	?	+	+	?
Tantilertanant et al. (2019b)	+	+	n. a.	n. a.	n. a.	+	+	?	-	-	+	?	+	+	?
Tsuji et al. (2004)	?	+	n. a.	n. a.	n. a.	+	?	?	-	-	?	?	?	+	?
Tsuruga et al. (2009)	?	+	n. a.	n. a.	n. a.	+	?	?	-	-	?	?	?	+	?
Tsuruga et al. (2012)	?	+	n. a.	n. a.	n. a.	+	?	?	-	-	?	?	+	+	?
Wada et al. (2017)	?	+	n. a.	n. a.	n. a.	+	?	?	-	-	?	?	+	+	?
Wang et al. (2011)	+	+	n. a.	n. a.	n. a.	+	+	?	-	-	+	?	+	+	+
Wang et al. (2013)	+	+	n. a.	n. a.	n. a.	+	+	?	-	-	+	?	?	+	?
Wang et al. (2018)	?	+	n. a.	n. a.	n. a.	+	+	?	-	-	?	?	?	+	?
Wang et al. (2019a)	+	+	n. a.	n. a.	n. a.	+	+	?	-	-	+	?	+	+	?
Wang et al. (2019b)	+	+	n. a.	n. a.	n. a.	+	+	?	-	-	+	?	+	+	?
Wei et al. (2014)	+	+	n. a.	n. a.	n. a.	+	+	?	-	-	+	?	+	+	?
Wei et al. (2015)	+	+	n. a.	n. a.	n. a.	+	+	?	-	+	+	?	+	+	?
Wescott et al. (2007)	+	+	n. a.	n. a.	n. a.	+	+	?	-	-	+	?	?	+	?
Wolf et al. (2014)	+	+	n. a.	n. a.	n. a.	+	?	?	-	-	?	?	?	+	?
Wu et al. (2015)	+	+	n. a.	n. a.	n. a.	+	+	?	-	-	+	?	?	+	?
Wu et al. (2016)	+	+	n. a.	n. a.	n. a.	+	+	?	-	-	+	?	-	+	?
Wu et al. (2017)	+	+	n. a.	n. a.	n. a.	+	+	?	-	-	+	+	+	+	+
Wu et al. (2019a)	+	+	n. a.	n. a.	n. a.	+	+	?	-	-	+	?	+	+	?
Wu et al. (2019b)	+	+	n. a.	n. a.	n. a.	+	+	?	-	-	+	+	+	+	+
Xu et al. (2011)	+	+	n. a.	n. a.	n. a.	+	+	?	-	-	+	?	?	+	+
Xu et al. (2012)	+	+	n. a.	n. a.	n. a.	+	+	?	-	-	+	?	+	+	+
Xu et al. (2015)	?	+	n. a.	n. a.	n. a.	+	?	?	-	-	?	?	?	+	?
Xu et al. (2017)	+	+	n. a.	n. a.	n. a.	+	+	?	-	-	+	?	?	+	+
Yamaguchi and Shimizu (1994)	?	+	n. a.	n. a.	n. a.	+	?	?	-	-	?	?	-	+	?
Yamaguchi et al. (1994)	?	+	n. a.	n. a.	n. a.	+	?	?	-	-	?	+	?	+	?
Yamaguchi et al. (1996)	?	+	n. a.	n. a.	n. a.	+	?	?	-	-	?	?	?	+	?
Yamaguchi et al. (1997)	?	+	n. a.	n. a.	n. a.	+	?	?	-	-	?	?	?	+	?
Yamaguchi et al. (2002)	+	+	n. a.	n. a.	n. a.	+	+	?	-	-	+	?	?	+	?

Supplement 4.1 Risk of bias assessment for the methodological quality of the included *in vitro* studies

Reference	Selection bias			Performance bias	Detection bias	Attrition bias	Reporting bias	Confounding bias	Appropriate statistical methods		Appropriate/ controlled exposure (incl. characterization)	Optimal time window used	Statement conflict of interest/fund-ing source	Test substance/treat-ment details	Test organism/system
	Baseline characteristics similarity / appropriate control group selection	Allocation concealment	Randomi-zation	Blinding of researchers	Blinding of outcome assessors	Complete outcome data	Selective outcome data	Account for confounding variables	Sample size determination	Statistical analysis					
Yamaguchi et al. (2004)	?	+	n. a.	n. a.	n. a.	+	?	?	-	-	?	?	-	+	?
Yamashiro et al. (2007)	+	+	n. a.	n. a.	n. a.	+	-	?	-	-	+	?	?	+	+
Yang et al. (2006)	?	+	n. a.	n. a.	n. a.	+	?	?	-	-	?	?	?	+	?
Yang et al. (2010)	+	+	n. a.	n. a.	n. a.	+	+	?	-	-	+	?	?	+	?
Yang et al. (2015)	+	+	n. a.	n. a.	n. a.	+	+	?	-	-	+	?	+	+	?
Yang et al. (2016)	+	+	n. a.	n. a.	n. a.	+	?	?	-	-	+	?	?	+	?
Yang et al. (2018)	+	+	n. a.	n. a.	n. a.	+	+	?	-	-	+	?	+	+	+
Yoshino et al. (2003)	+	+	n. a.	n. a.	n. a.	?	?	?	-	-	+	?	?	+	?
Yu et al. (2018)	+	+	n. a.	n. a.	n. a.	+	?	?	-	-	+	?	?	+	?
Yuda et al. (2015)	?	+	n. a.	n. a.	n. a.	+	?	?	-	-	?	?	?	+	?
Zhao et al. (2016)	+	+	n. a.	n. a.	n. a.	+	+	?	-	-	+	?	+	+	+
Zhao et al. (2017)	+	+	n. a.	n. a.	n. a.	+	+	?	-	-	+	+	+	?	+
Zhuang et al. (2019)	+	+	n. a.	n. a.	n. a.	+	+	?	-	-	+	+	+	+	?
Ziegler et al. (2010)	+	+	n. a.	n. a.	n. a.	+	+	?	-	-	+	?	?	+	?

Summary	Selection bias			Perfor-mance bias	Detection bias	Attrition bias	Reporting bias	Confounding bias	Appropriate statistical methods		Appropriate/ controlled exposure (incl. characterization)	Optimal time window used	Statement conflict of interest/funding source	Test substance/ treatment details	Test organism/ system
	Baseline characteristics similarity / appropriate control group selection	Allocation concealment	Randomi-zation	Blinding of researchers	Blinding of outcome assessors	Complete outcome data	Selective outcome data	Account for confounding variables	Sample size determination	Statistical analysis					
Low risk of bias ("+")	75 (55%)	137 (100%)	0 (n.a.)	0 (n.a.)	0 (n.a.)	134 (98%)	88 (64%)	0 (0%)	0 (0%)	4 (3%)	80 (58%)	13 (9%)	54 (39%)	126 (92%)	31 (23%)
Number of "?"	62 (45%)	0 (0%)	0 (n.a.)	0 (n.a.)	0 (n.a.)	2 (1%)	47 (34%)	137 (100%)	0 (0%)	0 (0%)	57 (42%)	124 (91%)	67 (49%)	11 (8%)	106 (77%)
Number of "-"	0 (0%)	0 (0%)	0 (n.a.)	0 (n.a.)	0 (n.a.)	1 (1%)	2 (1%)	0 (0%)	137 (100%)	133 (97%)	0 (0%)	00 (0%)	16 (12%)	0 (0%)	0 (0%)
Sum	**137**	**137**	**0**	**0**	**0**	**137**	**137**	**137**	**137**	**137**	**137**	**137**	**137**	**137**	**137**

Supplement 4.1 Risk of bias assessment for the methodological quality of the included *in vitro* studies

References

Abiko, Y., Shimizu, N., Yamaguchi, M., Suzuki, H., and Takiguchi, H. (1998). Effect of aging on functional changes of periodontal tissue cells. *Ann. Periodontol.* 3(1), 350-369. doi: 10.1902/annals.1998.3.1.350.

Agarwal, S., Long, P., Seyedain, A., Piesco, N., Shree, A., and Gassner, R. (2003). A central role for the nuclear factor-κB pathway in anti-inflammatory and proinflammatory actions of mechanical strain. *FASEB J.* 17(8), 899-901. doi: 10.1096/fj.02-0901fje.

Arima, M., Hasegawa, D., Yoshida, S., Mitarai, H., Tomokiyo, A., Hamano, S., et al. (2019). R-spondin 2 promotes osteoblastic differentiation of immature human periodontal ligament cells through the Wnt/beta-catenin signaling pathway. *J. Periodontal Res.* 54(2), 143-153. doi: 10.1111/jre.12611.

Basdra, E.K., Kohl, A., and Komposch, G. (1996). Mechanical stretching of periodontal ligament fibroblasts--a study on cytoskeletal involvement. *J. Orofac. Orthop.* 57(1), 24-30. doi: 10.1007/BF02189045.

Basdra, E.K., Papavassiliou, A.G., and Huber, L.A. (1995). Rab and rho GTPases are involved in specific response of periodontal ligament fibroblasts to mechanical stretching. *Biochim. Biophys. Acta* 1268(2), 209-213. doi: 10.1016/0167-4889(95)00090-f.

Bolcato-Bellemin, A.L., Elkaim, R., Abehsera, A., Fausser, J.L., Haikel, Y., and Tenenbaum, H. (2000). Expression of mRNAs encoding for alpha and beta integrin subunits, MMPs, and TIMPs in stretched human periodontal ligament and gingival fibroblasts. *J. Dent. Res.* 79(9), 1712-1716. doi: 10.1177/00220345000790091201.

Chang, M., Lin, H., Fu, H., Wang, B., Han, G., and Fan, M. (2017). MicroRNA-195-5p regulates osteogenic differentiation of periodontal ligament cells under mechanical loading. *J. Cell. Physiol.* 232(12), 3762-3774. doi: 10.1002/jcp.25856.

Chang, M., Lin, H., Luo, M., Wang, J., and Han, G. (2015). Integrated miRNA and mRNA expression profiling of tension force-induced bone formation in periodontal ligament cells. *In Vitro Cell. Dev. Biol. Anim.* 51(8), 797-807. doi: 10.1007/s11626-015-9892-0.

Chen, Y., Mohammed, A., Oubaidin, M., Evans, C.A., Zhou, X., Luan, X., et al. (2015). Cyclic stretch and compression forces alter microRNA-29 expression of human periodontal ligament cells. *Gene* 566(1), 13-17. doi: 10.1016/j.gene.2015.03.055.

Chen, Y.J., Shie, M.Y., Hung, C.J., Wu, B.C., Liu, S.L., Huang, T.H., et al. (2014). Activation of focal adhesion kinase induces extracellular signal-regulated kinase-mediated osteogenesis in tensile force-subjected periodontal ligament fibroblasts but not in osteoblasts. *J. Bone Miner. Metab.* 32(6), 671-682. doi: 10.1007/s00774-013-0549-3.

Chiba, M., and Mitani, H. (2004). Cytoskeletal changes and the system of regulation of alkaline phosphatase activity in human periodontal ligament cells induced by mechanical stress. *Cell Biochem. Funct.* 22(4), 249-256. doi: 10.1002/cbf.1097.

Cho, J.H., Lee, S.K., Lee, J.W., and Kim, E.C. (2010). The role of heme oxygenase-1 in mechanical stress- and lipopolysaccharide-induced osteogenic differentiation in human periodontal ligament cells. *Angle Orthod.* 80(4), 552-559. doi: 10.2319/091509-520.1.

Deschner, B., Rath, B., Jager, A., Deschner, J., Denecke, B., Memmert, S., et al. (2012). Gene analysis of signal transduction factors and transcription factors in periodontal ligament cells following application of dynamic strain. *J. Orofac. Orthop.* 73(6), 486-495, 497. doi: 10.1007/s00056-012-0104-1.

Diercke, K., Kohl, A., Lux, C.J., and Erber, R. (2011). Strain-dependent up-regulation of ephrin-B2 protein in periodontal ligament fibroblasts contributes to osteogenesis during tooth movement. *J. Biol. Chem.* 286(43), 37651-37664. doi: 10.1074/jbc.M110.166900.

Doi, T., Ohno, S., Tanimoto, K., Honda, K., Tanaka, N., Ohno-Nakahara, M., et al. (2003). Mechanical stimuli enhances the expression of RGD-CAP/betaig-h3 in the periodontal ligament. *Arch. Oral Biol.* 48(8), 573-579. doi: 10.1016/s0003-9969(03)00103-1.

Fujihara, C., Yamada, S., Ozaki, N., Takeshita, N., Kawaki, H., Takano-Yamamoto, T., et al. (2010). Role of mechanical stress-induced glutamate signaling-associated molecules in cytodifferentiation of periodontal ligament cells. *J. Biol. Chem.* 285(36), 28286-28297. doi: 10.1074/jbc.M109.097303.

Goto, K.T., Kajiya, H., Nemoto, T., Tsutsumi, T., Tsuzuki, T., Sato, H., et al. (2011). Hyperocclusion stimulates osteoclastogenesis via CCL2 expression. *J. Dent. Res.* 90(6), 793-798. doi: 10.1177/0022034511400742.

Hao, Y., Xu, C., Sun, S.Y., and Zhang, F.Q. (2009). Cyclic stretching force induces apoptosis in human periodontal ligament cells via caspase-9. *Arch. Oral Biol.* 54(9), 864-870. doi: 10.1016/j.archoralbio.2009.05.012.

He, Y., Macarak, E.J., Korostoff, J.M., and Howard, P.S. (2004). Compression and tension: differential effects on matrix accumulation by periodontal ligament fibroblasts in vitro. *Connect Tissue Res.* 45(1), 28-39. doi: 10.1080/03008200490278124.

He, Y., Xu, H., Xiang, Z., Yu, H., Xu, L., Guo, Y., et al. (2019). YAP regulates periodontal ligament cell differentiation into myofibroblast interacted with RhoA/ROCK pathway. *J. Cell. Physiol.* 234(4), 5086-5096. doi: 10.1002/jcp.27312.

Howard, P.S., Kucich, U., Taliwal, R., and Korostoff, J.M. (1998). Mechanical forces alter extracellular matrix synthesis by human periodontal ligament fibroblasts. *J. Periodontal Res.* 33(8), 500-508. doi: 10.1111/j.1600-0765.1998.tb02350.x.

Huelter-Hassler, D., Tomakidi, P., Steinberg, T., and Jung, B.A. (2017). Orthodontic strain affects the Hippo-pathway effector YAP concomitant with proliferation in human periodontal ligament fibroblasts. *Eur. J. Orthod.* 39(3), 251-257. doi: 10.1093/ejo/cjx012.

Hülter-Hassler, D., Wein, M., Schulz, S.D., Proksch, S., Steinberg, T., Jung, B.A., et al. (2017). Biomechanical strain-induced modulation of proliferation coincides with an ERK1/2-independent nuclear YAP localization. *Exp. Cell Res.* 361(1), 93-100. doi: 10.1016/j.yexcr.2017.10.006.

Jacobs, C., Grimm, S., Ziebart, T., Walter, C., and Wehrbein, H. (2013). Osteogenic differentiation of periodontal fibroblasts is dependent on the strength of mechanical strain. *Arch. Oral Biol.* 58(7), 896-904. doi: 10.1016/j.archoralbio.2013.01.009.

Jacobs, C., Schramm, S., Dirks, I., Walter, C., Pabst, A., Meila, D., et al. (2018). Mechanical loading increases pro-inflammatory effects of nitrogen-containing bisphosphonate in human periodontal fibroblasts. *Clin. Oral Investig.* 22(2), 901-907. doi: 10.1007/s00784-017-2168-1.

Jacobs, C., Walter, C., Ziebart, T., Dirks, I., Schramm, S., Grimm, S., et al. (2015). Mechanical loading influences the effects of bisphosphonates on human periodontal ligament fibroblasts. *Clin. Oral Investig.* 19(3), 699-708. doi: 10.1007/s00784-014-1284-4.

Supplement 4.1 Risk of bias assessment for the methodological quality of the included *in vitro* studies

Jacobs, C., Walter, C., Ziebart, T., Grimm, S., Meila, D., Krieger, E., et al. (2014). Induction of IL-6 and MMP-8 in human periodontal fibroblasts by static tensile strain. *Clin. Oral Investig.* 18(3), 901-908. doi: 10.1007/s00784-013-1032-1.

Jiang, Z., and Hua, Y. (2016). Hydrogen sulfide promotes osteogenic differentiation of human periodontal ligament cells via p38-MAPK signaling pathway under proper tension stimulation. *Arch. Oral Biol.* 72, 8-13. doi: 10.1016/j.archoralbio.2016.08.008.

Kaku, M., Yamamoto, T., Yashima, Y., Izumino, J., Kagawa, H., Ikeda, K., et al. (2019). Acetaminophen reduces apical root resorption during orthodontic tooth movement in rats. *Arch. Oral Biol.* 102, 83-92. doi: 10.1016/j.archoralbio.2019.04.002.

Kanzaki, H., Chiba, M., Sato, A., Miyagawa, A., Arai, K., Nukatsuka, S., et al. (2006). Cyclical tensile force on periodontal ligament cells inhibits osteoclastogenesis through OPG induction. *J. Dent. Res.* 85(5), 457-462. doi: 10.1177/154405910608500512.

Kanzaki, H., Wada, S., Yamaguchi, Y., Katsumata, Y., Itohiya, K., Fukaya, S., et al. (2019). Compression and tension variably alter Osteoprotegerin expression via miR-3198 in periodontal ligament cells. *BMC Mol. Cell Biol.* 20(1), 6. doi: 10.1186/s12860-019-0187-2.

Kikuiri, T., Hasegawa, T., Yoshimura, Y., Shirakawa, T., and Oguchi, H. (2000). Cyclic tension force activates nitric oxide production in cultured human periodontal ligament cells. *J. Periodontol.* 71(4), 533-539. doi: 10.1902/jop.2000.71.4.533.

Kim, H.J., Choi, Y.S., Jeong, M.J., Kim, B.O., Lim, S.H., Kim, D.K., et al. (2007). Expression of UNCL during development of periodontal tissue and response of periodontal ligament fibroblasts to mechanical stress in vivo and in vitro. *Cell Tissue Res.* 327(1), 25-31. doi: 10.1007/s00441-006-0304-3.

Kletsas, D., Basdra, E.K., and Papavassiliou, A.G. (2002). Effect of protein kinase inhibitors on the stretch-elicited c-Fos and c-Jun up-regulation in human PDL osteoblast-like cells. *J. Cell. Physiol.* 190(3), 313-321. doi: 10.1002/jcp.10052.

Konstantonis, D., Papadopoulou, A., Makou, M., Eliades, T., Basdra, E., and Kletsas, D. (2014). The role of cellular senescence on the cyclic stretching-mediated activation of MAPK and ALP expression and activity in human periodontal ligament fibroblasts. *Exp. Gerontol.* 57, 175-180. doi: 10.1016/j.exger.2014.05.010.

Kook, S.H., and Lee, J.C. (2012). Tensile force inhibits the proliferation of human periodontal ligament fibroblasts through Ras-p38 MAPK up-regulation. *J. Cell. Physiol.* 227(3), 1098-1106. doi: 10.1002/jcp.22829.

Lee, S.I., Park, K.H., Kim, S.J., Kang, Y.G., Lee, Y.M., and Kim, E.C. (2012). Mechanical stress-activated immune response genes via Sirtuin 1 expression in human periodontal ligament cells. *Clin. Exp. Immunol.* 168(1), 113-124. doi: 10.1111/j.1365-2249.2011.04549.x.

Lee, S.Y., Yoo, H.I., and Kim, S.H. (2015). CCR5-CCL Axis in PDL during Orthodontic Biophysical Force Application. *J. Dent. Res.* 94(12), 1715-1723. doi: 10.1177/0022034515603926.

Li, L., Han, M., Li, S., Wang, L., and Xu, Y. (2013). Cyclic tensile stress during physiological occlusal force enhances osteogenic differentiation of human periodontal ligament cells via ERK1/2-Elk1 MAPK pathway. *DNA Cell Biol.* 32(9), 488-497. doi: 10.1089/dna.2013.2070.

Li, L., Han, M.X., Li, S., Xu, Y., and Wang, L. (2014). Hypoxia regulates the proliferation and osteogenic differentiation of human periodontal ligament cells under cyclic tensile stress via mitogen-activated protein kinase pathways. *J. Periodontol.* 85(3), 498-508. doi: 10.1902/jop.2013.130048.

Li, S., Zhang, H., Li, S., Yang, Y., Huo, B., and Zhang, D. (2015). Connexin 43 and ERK regulate tension-induced signal transduction in human periodontal ligament fibroblasts. *J. Orthop. Res.* 33(7), 1008-1014. doi: 10.1002/jor.22830.

Liao, C., and Hua, Y. (2013). Effect of hydrogen sulphide on the expression of osteoprotegerin and receptor activator of NF-kappaB ligand in human periodontal ligament cells induced by tension-force stimulation. *Arch. Oral Biol.* 58(12), 1784-1790. doi: 10.1016/j.archoralbio.2013.08.004.

Liu, J., Li, Q., Liu, S., Gao, J., Qin, W., Song, Y., et al. (2017). Periodontal Ligament Stem Cells in the Periodontitis Microenvironment Are Sensitive to Static Mechanical Strain. *Stem Cells Int.* 2017, 1380851. doi: 10.1155/2017/1380851.

Liu, M., Dai, J., Lin, Y., Yang, L., Dong, H., Li, Y., et al. (2012). Effect of the cyclic stretch on the expression of osteogenesis genes in human periodontal ligament cells. *Gene* 491(2), 187-193. doi: 10.1016/j.gene.2011.09.031.

Long, P., Hu, J., Piesco, N., Buckley, M., and Agarwal, S. (2001). Low magnitude of tensile strain inhibits IL-1beta-dependent induction of pro-inflammatory cytokines and induces synthesis of IL-10 in human periodontal ligament cells in vitro. *J. Dent. Res.* 80(5), 1416-1420. doi: 10.1177/00220345010800050601.

Long, P., Liu, F., Piesco, N.P., Kapur, R., and Agarwal, S. (2002). Signaling by mechanical strain involves transcriptional regulation of proinflammatory genes in human periodontal ligament cells in vitro. *Bone* 30(4), 547-552. doi: 10.1016/s8756-3282(02)00673-7.

Ma, J., Zhao, D., Wu, Y., Xu, C., and Zhang, F. (2015). Cyclic stretch induced gene expression of extracellular matrix and adhesion molecules in human periodontal ligament cells. *Arch. Oral Biol.* 60(3), 447-455. doi: 10.1016/j.archoralbio.2014.11.019.

Matsuda, N., Morita, N., Matsuda, K., and Watanabe, M. (1998a). Proliferation and differentiation of human osteoblastic cells associated with differential activation of MAP kinases in response to epidermal growth factor, hypoxia, and mechanical stress in vitro. *Biochem. Biophys. Res. Commun.* 249(2), 350-354. doi: 10.1006/bbrc.1998.9151.

Matsuda, N., Yokoyama, K., Takeshita, S., and Watanabe, M. (1998b). Role of epidermal growth factor and its receptor in mechanical stress-induced differentiation of human periodontal ligament cells in vitro. *Arch. Oral Biol.* 43(12), 987-997. doi: 10.1016/s0003-9969(98)00079-x.

Memmert, S., Damanaki, A., Weykopf, B., Rath-Deschner, B., Nokhbehsaim, M., Gotz, W., et al. (2019). Autophagy in periodontal ligament fibroblasts under biomechanical loading. *Cell Tissue Res.* doi: 10.1007/s00441-019-03063-1.

Memmert, S., Nogueira, A.V.B., Damanaki, A., Nokhbehsaim, M., Rath-Deschner, B., Götz, W., et al. (2020). Regulation of the autophagy-marker Sequestosome 1 in periodontal cells and tissues by biomechanical loading. *J. Orofac. Orthop.* 81(1), 10-21. doi: 10.1007/s00056-019-00197-3.

Meng, Y., Han, X., Huang, L., Bai, D., Yu, H., He, Y., et al. (2010). Orthodontic mechanical tension effects on the myofibroblast expression of alpha-smooth muscle actin. *Angle Orthod.* 80(5), 912-918. doi: 10.2319/101609-578.1.

Miura, S., Yamaguchi, M., Shimizu, N., and Abiko, Y. (2000). Mechanical stress enhances expression and production of plasminogen activator in aging human periodontal ligament cells. *Mech. Ageing Dev.* 112(3), 217-231. doi: 10.1016/s0047-6374(99)00095-0.

Molina, T., Kabsch, K., Alonso, A., Kohl, A., Komposch, G., and Tomakidi, P. (2001). Topographic changes of focal adhesion components and modulation of p125FAK

activation in stretched human periodontal ligament fibroblasts. *J. Dent. Res.* 80(11), 1984-1989. doi: 10.1177/00220345010800110701.

Monnouchi, S., Maeda, H., Fujii, S., Tomokiyo, A., Kono, K., and Akamine, A. (2011). The roles of angiotensin II in stretched periodontal ligament cells. *J. Dent. Res.* 90(2), 181-185. doi: 10.1177/0022034510382118.

Monnouchi, S., Maeda, H., Yuda, A., Hamano, S., Wada, N., Tomokiyo, A., et al. (2015). Mechanical induction of interleukin-11 regulates osteoblastic/cementoblastic differentiation of human periodontal ligament stem/progenitor cells. *J. Periodontal Res.* 50(2), 231-239. doi: 10.1111/jre.12200.

Nakashima, K., Tsuruga, E., Hisanaga, Y., Ishikawa, H., and Sawa, Y. (2009). Stretching stimulates fibulin-5 expression and controls microfibril bundles in human periodontal ligament cells. *J. Periodontal Res.* 44(5), 622-627. doi: 10.1111/j.1600-0765.2008.01170.x.

Narimiya, T., Wada, S., Kanzaki, H., Ishikawa, M., Tsuge, A., Yamaguchi, Y., et al. (2017). Orthodontic tensile strain induces angiogenesis via type IV collagen degradation by matrix metalloproteinase-12. *J. Periodontal Res.* 52(5), 842-852. doi: 10.1111/jre.12453.

Nazet, U., Schröder, A., Spanier, G., Wolf, M., Proff, P., and Kirschneck, C. (2020). Simplified method for applying static isotropic tensile strain in cell culture experiments with identification of valid RT-qPCR reference genes for PDL fibroblasts. *Eur. J. Orthod.* 42(4), 359-370. doi: 10.1093/ejo/cjz052.

Nemoto, T., Kajiya, H., Tsuzuki, T., Takahashi, Y., and Okabe, K. (2010). Differential induction of collagens by mechanical stress in human periodontal ligament cells. *Arch. Oral Biol.* 55(12), 981-987. doi: 10.1016/j.archoralbio.2010.08.004.

Ngan, P., Saito, S., Saito, M., Lanese, R., Shanfeld, J., and Davidovitch, Z. (1990). The interactive effects of mechanical stress and interleukin-1 beta on prostaglandin E and cyclic AMP production in human periodontal ligament fibroblasts in vitro: comparison with cloned osteoblastic cells of mouse (MC3T3-E1). *Arch. Oral Biol.* 35(9), 717-725. doi: 10.1016/0003-9969(90)90094-Q.

Nogueira, A.V., Nokhbehsaim, M., Eick, S., Bourauel, C., Jäger, A., Jepsen, S., et al. (2014a). Regulation of visfatin by microbial and biomechanical signals in PDL cells. *Clin. Oral Investig.* 18(1), 171-178. doi: 10.1007/s00784-013-0935-1.

Nogueira, A.V., Nokhbehsaim, M., Eick, S., Bourauel, C., Jäger, A., Jepsen, S., et al. (2014b). Biomechanical loading modulates proinflammatory and bone resorptive mediators in bacterial-stimulated PDL cells. *Mediators Inflamm.* 2014, 425421. doi: 10.1155/2014/425421.

Nokhbehsaim, M., Deschner, B., Bourauel, C., Reimann, S., Winter, J., Rath, B., et al. (2011a). Interactions of enamel matrix derivative and biomechanical loading in periodontal regenerative healing. *J. Periodontol.* 82(12), 1725-1734. doi: 10.1902/jop.2011.100678.

Nokhbehsaim, M., Deschner, B., Winter, J., Bourauel, C., Jäger, A., Jepsen, S., et al. (2012). Anti-inflammatory effects of EMD in the presence of biomechanical loading and interleukin-1β in vitro. *Clin. Oral Investig.* 16(1), 275-283. doi: 10.1007/s00784-010-0505-8.

Nokhbehsaim, M., Deschner, B., Winter, J., Bourauel, C., Rath, B., Jager, A., et al. (2011b). Interactions of regenerative, inflammatory and biomechanical signals on bone morphogenetic protein-2 in periodontal ligament cells. *J. Periodontal Res.* 46(3), 374-381. doi: 10.1111/j.1600-0765.2011.01357.x.

Nokhbehsaim, M., Deschner, B., Winter, J., Reimann, S., Bourauel, C., Jepsen, S., et al. (2010). Contribution of orthodontic load to inflammation-mediated periodontal destruction. *J. Orofac. Orthop.* 71(6), 390-402. doi: 10.1007/s00056-010-1031-7.

Ohzeki, K., Yamaguchi, M., Shimizu, N., and Abiko, Y. (1999). Effect of cellular aging on the induction of cyclooxygenase-2 by mechanical stress in human periodontal ligament cells. *Mech. Ageing Dev.* 108(2), 151-163. doi: 10.1016/s0047-6374(99)00006-8.

Ozawa, Y., Shimizu, N., and Abiko, Y. (1997). Low-energy diode laser irradiation reduced plasminogen activator activity in human periodontal ligament cells. *Lasers Surg. Med.* 21(5), 456-463. doi: 10.1002/(sici)1096-9101(1997)21:5<456::aid-lsm7>3.0.co;2-p.

Padial-Molina, M., Volk, S.L., Rodriguez, J.C., Marchesan, J.T., Galindo-Moreno, P., and Rios, H.F. (2013). Tumor necrosis factor-alpha and Porphyromonas gingivalis lipopolysaccharides decrease periostin in human periodontal ligament fibroblasts. *J. Periodontol.* 84(5), 694-703. doi: 10.1902/jop.2012.120078.

Pan, J., Wang, T., Wang, L., Chen, W., and Song, M. (2014). Cyclic strain-induced cytoskeletal rearrangement of human periodontal ligament cells via the Rho signaling pathway. *PloS One* 9(3), e91580. doi: 10.1371/journal.pone.0091580.

Papadopoulou, A., Iliadi, A., Eliades, T., and Kletsas, D. (2017). Early responses of human periodontal ligament fibroblasts to cyclic and static mechanical stretching. *Eur. J. Orthod.* 39(3), 258-263. doi: 10.1093/ejo/cjw075.

Papadopoulou, A., Todaro, A., Eliades, T., and Kletsas, D. (2019). Effect of hyperglycaemic conditions on the response of human periodontal ligament fibroblasts to mechanical stretching. *Eur. J. Orthod.* doi: 10.1093/ejo/cjz051.

Pelaez, D., Acosta Torres, Z., Ng, T.K., Choy, K.W., Pang, C.P., and Cheung, H.S. (2017). Cardiomyogenesis of periodontal ligament-derived stem cells by dynamic tensile strain. *Cell Tissue Res.* 367(2), 229-241. doi: 10.1007/s00441-016-2503-x.

Peverali, F.A., Basdra, E.K., and Papavassiliou, A.G. (2001). Stretch-mediated activation of selective MAPK subtypes and potentiation of AP-1 binding in human osteoblastic cells. *Mol. Med.* 7(1), 68-78.

Pinkerton, M.N., Wescott, D.C., Gaffey, B.J., Beggs, K.T., Milne, T.J., and Meikle, M.C. (2008). Cultured human periodontal ligament cells constitutively express multiple osteotropic cytokines and growth factors, several of which are responsive to mechanical deformation. *J. Periodontal Res.* 43(3), 343-351. doi: 10.1111/j.1600-0765.2007.01040.x.

Qin, J., and Hua, Y. (2016). Effects of hydrogen sulfide on the expression of alkaline phosphatase, osteocalcin and collagen type I in human periodontal ligament cells induced by tension force stimulation. *Mol. Med. Rep.* 14(4), 3871-3877. doi: 10.3892/mmr.2016.5680.

Rath-Deschner, B., Deschner, J., Reimann, S., Jager, A., and Gotz, W. (2009). Regulatory effects of biomechanical strain on the insulin-like growth factor system in human periodontal cells. *J. Biomech.* 42(15), 2584-2589. doi: 10.1016/j.jbiomech.2009.07.013.

Ren, D., Wei, F., Hu, L., Yang, S., Wang, C., and Yuan, X. (2015). Phosphorylation of Runx2, induced by cyclic mechanical tension via ERK1/2 pathway, contributes to osteodifferentiation of human periodontal ligament fibroblasts. *J. Cell. Physiol.* 230(10), 2426-2436. doi: 10.1002/jcp.24972.

Ritter, N., Mussig, E., Steinberg, T., Kohl, A., Komposch, G., and Tomakidi, P. (2007). Elevated expression of genes assigned to NF-kappaB and apoptotic pathways in human periodontal ligament fibroblasts following mechanical stretch. *Cell Tissue Res.* 328(3), 537-548. doi: 10.1007/s00441-007-0382-x.

Supplement 4.1 Risk of bias assessment for the methodological quality of the included *in vitro* studies

Saminathan, A., Vinoth, K.J., Wescott, D.C., Pinkerton, M.N., Milne, T.J., Cao, T., et al. (2012). The effect of cyclic mechanical strain on the expression of adhesion-related genes by periodontal ligament cells in two-dimensional culture. *J. Periodontal Res.* 47(2), 212-221. doi: 10.1111/j.1600-0765.2011.01423.x.

Shen, T., Qiu, L., Chang, H., Yang, Y., Jian, C., Xiong, J., et al. (2014). Cyclic tension promotes osteogenic differentiation in human periodontal ligament stem cells. *Int. J. Clin. Exp. Pathol.* 7(11), 7872-7880.

Shimizu, N., Goseki, T., Yamaguchi, M., Iwasawa, T., Takiguchi, H., and Abiko, Y. (1997). In vitro cellular aging stimulates interleukin-1 beta production in stretched human periodontal-ligament-derived cells. *J. Dent. Res.* 76(7), 1367-1375. doi: 10.1177/00220345970760070601.

Shimizu, N., Ozawa, Y., Yamaguchi, M., Goseki, T., Ohzeki, K., and Abiko, Y. (1998). Induction of COX-2 expression by mechanical tension force in human periodontal ligament cells. *J. Periodontol.* 69(6), 670-677. doi: 10.1902/jop.1998.69.6.670.

Shimizu, N., Yamaguchi, M., Goseki, T., Ozawa, Y., Saito, K., Takiguchi, H., et al. (1994). Cyclic-tension force stimulates interleukin-1 beta production by human periodontal ligament cells. *J. Periodontal Res.* 29(5), 328-333. doi: 10.1111/j.1600-0765.1994.tb01230.x.

Shimizu, N., Yamaguchi, M., Goseki, T., Shibata, Y., Takiguchi, H., Iwasawa, T., et al. (1995). Inhibition of prostaglandin E2 and interleukin 1-beta production by low-power laser irradiation in stretched human periodontal ligament cells. *J. Dent. Res.* 74(7), 1382-1388. doi: 10.1177/00220345950740071001.

Spencer, A.Y., and Lallier, T.E. (2009). Mechanical tension alters semaphorin expression in the periodontium. *J. Periodontol.* 80(10), 1665-1673. doi: 10.1902/jop.2009.090212.

Steinberg, T., Ziegler, N., Alonso, A., Kohl, A., Mussig, E., Proksch, S., et al. (2011). Strain response in fibroblasts indicates a possible role of the Ca(2+)-dependent nuclear transcription factor NM1 in RNA synthesis. *Cell Calcium* 49(4), 259-271. doi: 10.1016/j.ceca.2011.03.001.

Sun, C., Chen, L., Shi, X., Cao, Z., Hu, B., Yu, W., et al. (2016). Combined effects of proinflammatory cytokines and intermittent cyclic mechanical strain in inhibiting osteogenicity in human periodontal ligament cells. *Cell Biol. Int.* 40(9), 999-1007. doi: 10.1002/cbin.10641.

Sun, C., Liu, F., Cen, S., Chen, L., Wang, Y., Sun, H., et al. (2017). Tensile strength suppresses the osteogenesis of periodontal ligament cells in inflammatory microenvironments. *Mol. Med. Rep.* 16(1), 666-672. doi: 10.3892/mmr.2017.6644.

Suzuki, R., Nemoto, E., and Shimauchi, H. (2014). Cyclic tensile force up-regulates BMP-2 expression through MAP kinase and COX-2/PGE2 signaling pathways in human periodontal ligament cells. *Exp. Cell Res.* 323(1), 232-241. doi: 10.1016/j.yexcr.2014.02.013.

Symmank, J., Zimmermann, S., Goldschmitt, J., Schiegnitz, E., Wolf, M., Wehrbein, H., et al. (2019). Mechanically-induced GDF15 Secretion by Periodontal Ligament Fibroblasts Regulates Osteogenic Transcription. *Sci. Rep.* 9(1), 11516. doi: 10.1038/s41598-019-47639-x.

Takano, M., Yamaguchi, M., Nakajima, R., Fujita, S., Kojima, T., and Kasai, K. (2009). Effects of relaxin on collagen type I released by stretched human periodontal ligament cells. *Orthod. Craniofac. Res.* 12(4), 282-288. doi: 10.1111/j.1601-6343.2009.01463.x.

Tang, N., Zhao, Z., Zhang, L., Yu, Q., Li, J., Xu, Z., et al. (2012). Up-regulated osteogenic transcription factors during early response of human periodontal ligament stem cells to cyclic tensile strain. *Arch. Med. Sci.* 8(3), 422-430. doi: 10.5114/aoms.2012.28810.

Tantilertanant, Y., Niyompanich, J., Everts, V., Supaphol, P., Pavasant, P., and Sanchavanakit, N. (2019a). Cyclic tensile force stimulates BMP9 synthesis and in vitro mineralization by human periodontal ligament cells. *J. Cell. Physiol.* 234(4), 4528-4539. doi: 10.1002/jcp.27257.

Tantilertanant, Y., Niyompanich, J., Everts, V., Supaphol, P., Pavasant, P., and Sanchavanakit, N. (2019b). Cyclic tensile force-upregulated IL6 increases MMP3 expression by human periodontal ligament cells. *Arch. Oral Biol.* 107, 104495. doi: 10.1016/j.archoralbio.2019.104495.

Tsuji, K., Uno, K., Zhang, G.X., and Tamura, M. (2004). Periodontal ligament cells under intermittent tensile stress regulate mRNA expression of osteoprotegerin and tissue inhibitor of matrix metalloprotease-1 and -2. *J. Bone Miner. Metab.* 22(2), 94-103. doi: 10.1007/s00774-003-0456-0.

Tsuruga, E., Nakashima, K., Ishikawa, H., Yajima, T., and Sawa, Y. (2009). Stretching modulates oxytalan fibers in human periodontal ligament cells. *J. Periodontal Res.* 44(2), 170-174. doi: 10.1111/j.1600-0765.2008.01099.x.

Tsuruga, E., Oka, K., Hatakeyama, Y., Isokawa, K., and Sawa, Y. (2012). Latent transforming growth factor-beta binding protein 2 negatively regulates coalescence of oxytalan fibers induced by stretching stress. *Connect Tissue Res.* 53(6), 521-527. doi: 10.3109/03008207.2012.702816.

Wada, S., Kanzaki, H., Narimiya, T., and Nakamura, Y. (2017). Novel device for application of continuous mechanical tensile strain to mammalian cells. *Biol. Open* 6(4), 518-524. doi: 10.1242/bio.023671.

Wang, H., Feng, C., Jin, Y., Tan, W., and Wei, F. (2019a). Identification and characterization of circular RNAs involved in mechanical force-induced periodontal ligament stem cells. *J. Cell. Physiol.* 234(7), 10166-10177. doi: 10.1002/jcp.27686.

Wang, L., Pan, J., Wang, T., Song, M., and Chen, W. (2013). Pathological cyclic strain-induced apoptosis in human periodontal ligament cells through the RhoGDIalpha/caspase-3/PARP pathway. *PloS One* 8(10), e75973. doi: 10.1371/journal.pone.0075973.

Wang, Y., Hu, B., Hu, R., Tong, X., Zhang, M., Xu, C., et al. (2019b). TAZ contributes to osteogenic differentiation of periodontal ligament cells under tensile stress. *J. Periodontal Res.* doi: 10.1111/jre.12698.

Wang, Y., Li, Y., Fan, X., Zhang, Y., Wu, J., and Zhao, Z. (2011). Early proliferation alteration and differential gene expression in human periodontal ligament cells subjected to cyclic tensile stress. *Arch. Oral Biol.* 56(2), 177-186. doi: 10.1016/j.archoralbio.2010.09.009.

Wang, Y.F., Zuo, Z.H., Luo, P., Pang, F.S., and Hu, J.T. (2018). The effect of cyclic tensile force on the actin cytoskeleton organization and morphology of human periodontal ligament cells. *Biochem. Biophys. Res. Commun.* 506(4), 950-955. doi: 10.1016/j.bbrc.2018.10.163.

Wei, F., Liu, D., Feng, C., Zhang, F., Yang, S., Hu, Y., et al. (2015). microRNA-21 mediates stretch-induced osteogenic differentiation in human periodontal ligament stem cells. *Stem Cells Dev.* 24(3), 312-319. doi: 10.1089/scd.2014.0191.

Wei, F.L., Wang, J.H., Ding, G., Yang, S.Y., Li, Y., Hu, Y.J., et al. (2014). Mechanical force-induced specific MicroRNA expression in human periodontal ligament stem cells. *Cells Tissues Organs* 199(5-6), 353-363. doi: 10.1159/000369613.

Wescott, D.C., Pinkerton, M.N., Gaffey, B.J., Beggs, K.T., Milne, T.J., and Meikle, M.C. (2007). Osteogenic gene expression by human periodontal ligament cells under cyclic tension. *J. Dent. Res.* 86(12), 1212-1216. doi: 10.1177/154405910708601214.

Supplement 4.1 Risk of bias assessment for the methodological quality of the included *in vitro* studies

Wolf, M., Lossdorfer, S., Kupper, K., and Jager, A. (2014). Regulation of high mobility group box protein 1 expression following mechanical loading by orthodontic forces in vitro and in vivo. *Eur. J. Orthod.* 36(6), 624-631. doi: 10.1093/ejo/cjt037.

Wu, J., Song, M., Li, T., Zhu, Z., and Pan, J. (2015). The Rho-mDia1 signaling pathway is required for cyclic strain-induced cytoskeletal rearrangement of human periodontal ligament cells. *Exp. Cell Res.* 337(1), 28-36. doi: 10.1016/j.yexcr.2015.07.016.

Wu, Y., Ou, Y., Liao, C., Liang, S., and Wang, Y. (2019a). High-throughput sequencing analysis of the expression profile of microRNAs and target genes in mechanical force-induced osteoblastic/cementoblastic differentiation of human periodontal ligament cells. *Am. J. Transl. Res.* 11(6), 3398-3411.

Wu, Y., Zhao, D., Zhuang, J., Zhang, F., and Xu, C. (2016). Caspase-8 and Caspase-9 Functioned Differently at Different Stages of the Cyclic Stretch-Induced Apoptosis in Human Periodontal Ligament Cells. *PloS One* 11(12), e0168268. doi: 10.1371/journal.pone.0168268.

Wu, Y., Zhuang, J., Zhao, D., and Xu, C. (2019b). Interaction between caspase-3 and caspase-5 in the stretch-induced programmed cell death in the human periodontal ligament cells. *J. Cell. Physiol.* 234(8), 13571-13581. doi: 10.1002/jcp.28035.

Wu, Y., Zhuang, J., Zhao, D., Zhang, F., Ma, J., and Xu, C. (2017). Cyclic stretch-induced the cytoskeleton rearrangement and gene expression of cytoskeletal regulators in human periodontal ligament cells. *Acta Odontol. Scand.* 75(7), 507-516. doi: 10.1080/00016357.2017.1347823.

Xu, C., Fan, Z., Shan, W., Hao, Y., Ma, J., Huang, Q., et al. (2012). Cyclic stretch influenced expression of membrane connexin 43 in human periodontal ligament cell. *Arch. Oral Biol.* 57(12), 1602-1608. doi: 10.1016/j.archoralbio.2012.07.002.

Xu, C., Hao, Y., Wei, B., Ma, J., Li, J., Huang, Q., et al. (2011). Apoptotic gene expression by human periodontal ligament cells following cyclic stretch. *J. Periodontal Res.* 46(6), 742-748. doi: 10.1111/j.1600-0765.2011.01397.x.

Xu, H., Bai, D., Ruest, L.B., Feng, J.Q., Guo, Y.W., Tian, Y., et al. (2015). Expression analysis of alpha-smooth muscle actin and tenascin-C in the periodontal ligament under orthodontic loading or in vitro culture. *Int. J. Oral Sci.* 7(4), 232-241. doi: 10.1038/ijos.2015.26.

Xu, H.Y., Nie, E.M., Deng, G., Lai, L.Z., Sun, F.Y., Tian, H., et al. (2017). Periostin is essential for periodontal ligament remodeling during orthodontic treatment. *Mol. Med. Rep.* 15(4), 1800-1806. doi: 10.3892/mmr.2017.6200.

Yamaguchi, M., Ozawa, Y., Nogimura, A., Aihara, N., Kojima, T., Hirayama, Y., et al. (2004). Cathepsins B and L increased during response of periodontal ligament cells to mechanical stress in vitro. *Connect Tissue Res.* 45(3), 181-189. doi: 10.1080/03008200490514149.

Yamaguchi, M., and Shimizu, N. (1994). Identification of factors mediating the decrease of alkaline phosphatase activity caused by tension-force in periodontal ligament cells. *Gen. Pharmacol.* 25(6), 1229-1235. doi: 10.1016/0306-3623(94)90142-2.

Yamaguchi, M., Shimizu, N., Goseki, T., Shibata, Y., Takiguchi, H., Iwasawa, T., et al. (1994). Effect of different magnitudes of tension force on prostaglandin E2 production by human periodontal ligament cells. *Arch. Oral Biol.* 39(10), 877-884. doi: 10.1016/0003-9969(94)90019-1.

Yamaguchi, M., Shimizu, N., Ozawa, Y., Saito, K., Miura, S., Takiguchi, H., et al. (1997). Effect of tension-force on plasminogen activator activity from human periodontal ligament cells. *J. Periodontal Res.* 32(3), 308-314. doi: 10.1111/j.1600-0765.1997.tb00539.x.

Yamaguchi, M., Shimizu, N., Shibata, Y., and Abiko, Y. (1996). Effects of different magnitudes of tension-force on alkaline phosphatase activity in periodontal ligament cells. *J. Dent. Res.* 75(3), 889-894. doi: 10.1177/00220345960750030501.

Yamaguchi, N., Chiba, M., and Mitani, H. (2002). The induction of c-fos mRNA expression by mechanical stress in human periodontal ligament cells. *Arch. Oral Biol.* 47(6), 465-471. doi: 10.1016/s0003-9969(02)00022-5.

Yamashiro, K., Myokai, F., Hiratsuka, K., Yamamoto, T., Senoo, K., Arai, H., et al. (2007). Oligonucleotide array analysis of cyclic tension-responsive genes in human periodontal ligament fibroblasts. *Int. J. Biochem. Cell Biol.* 39(5), 910-921. doi: 10.1016/j.biocel.2007.01.015.

Yang, S.Y., Kim, J.W., Lee, S.Y., Kang, J.H., Ulziisaikhan, U., Yoo, H.I., et al. (2015). Upregulation of relaxin receptors in the PDL by biophysical force. *Clin. Oral Investig.* 19(3), 657-665. doi: 10.1007/s00784-014-1276-4.

Yang, S.Y., Wei, F.L., Hu, L.H., and Wang, C.L. (2016). PERK-eIF2alpha-ATF4 pathway mediated by endoplasmic reticulum stress response is involved in osteodifferentiation of human periodontal ligament cells under cyclic mechanical force. *Cell. Signal.* 28(8), 880-886. doi: 10.1016/j.cellsig.2016.04.003.

Yang, Y., Wang, B.K., Chang, M.L., Wan, Z.Q., and Han, G.L. (2018). Cyclic Stretch Enhances Osteogenic Differentiation of Human Periodontal Ligament Cells via YAP Activation. *Biomed Res. Int.* 2018, 2174824. doi: 10.1155/2018/2174824.

Yang, Y., Yang, Y., Li, X., Cui, L., Fu, M., Rabie, A.B., et al. (2010). Functional analysis of core binding factor a1 and its relationship with related genes expressed by human periodontal ligament cells exposed to mechanical stress. *Eur. J. Orthod.* 32(6), 698-705. doi: 10.1093/ejo/cjq010.

Yang, Y.Q., Li, X.T., Rabie, A.B., Fu, M.K., and Zhang, D. (2006). Human periodontal ligament cells express osteoblastic phenotypes under intermittent force loading in vitro. *Front. Biosci.* 11, 776-781. doi: 10.2741/1835.

Yoshino, H., Morita, I., Murota, S.I., and Ishikawa, I. (2003). Mechanical stress induces production of angiogenic regulators in cultured human gingival and periodontal ligament fibroblasts. *J. Periodontal Res.* 38(4), 405-410. doi: 10.1034/j.1600-0765.2003.00660.x.

Yu, W., Hu, B., Shi, X., Cao, Z., Ren, M., He, Z., et al. (2018). Nicotine inhibits osteogenic differentiation of human periodontal ligament cells under cyclic tensile stress through canonical Wnt pathway and alpha7 nicotinic acetylcholine receptor. *J. Periodontal Res.* 53(4), 555-564. doi: 10.1111/jre.12545.

Yuda, A., Maeda, H., Fujii, S., Monnouchi, S., Yamamoto, N., Wada, N., et al. (2015). Effect of CTGF/CCN2 on osteo/cementoblastic and fibroblastic differentiation of a human periodontal ligament stem/progenitor cell line. *J. Cell. Physiol.* 230(1), 150-159. doi: 10.1002/jcp.24693.

Zhao, D., Wu, Y., Xu, C., and Zhang, F. (2017). Cyclic-stretch induces apoptosis in human periodontal ligament cells by activation of caspase-5. *Arch. Oral Biol.* 73, 129-135. doi: 10.1016/j.archoralbio.2016.10.009.

Zhao, D., Wu, Y., Zhuang, J., Xu, C., and Zhang, F. (2016). Activation of NLRP1 and NLRP3 inflammasomes contributed to cyclic stretch-induced pyroptosis and release of IL-1beta in human periodontal ligament cells. *Oncotarget* 7(42), 68292-68302. doi: 10.18632/oncotarget.11944.

Zhuang, J., Wang, Y., Qu, F., Wu, Y., Zhao, D., and Xu, C. (2019). Gasdermin-d Played a Critical Role in the Cyclic Stretch-Induced Inflammatory Reaction in Human

Supplement 4.1 Risk of bias assessment for the methodological quality of the included *in vitro* studies

Periodontal Ligament Cells. *Inflammation* 42(2), 548-558. doi: 10.1007/s10753-018-0912-6.

Ziegler, N., Alonso, A., Steinberg, T., Woodnutt, D., Kohl, A., Mussig, E., et al. (2010). Mechano-transduction in periodontal ligament cells identifies activated states of MAP-kinases p42/44 and p38-stress kinase as a mechanism for MMP-13 expression. *BMC Cell Biol.* 11, 10. doi: 10.1186/1471-2121-11-10.

Supplement 4.2 Risk of bias assessment for the reporting quality of the included *in vitro* studies

Reference	Description of scientific background	Description objective	Justification for model	Study design description	Defined experimental outcomes	Ethical statement	Cell maintenance condition	Description of measurement precision and variability	Statistical analysis	Results description
Abiko et al. (1998)	+	+	?	+	+	-	+	+	+	+
Agarwal et al. (2003)	+	+	?	+	+	+	+	-	-	+
Arima et al. (2019)	+	+	?	+	+	+	+	+	+	+
Basdra et al. (1995)	+	+	?	+	+	-	+	-	-	+
Basdra et al. (1996)	+	+	?	+	+	-	+	-	-	+
Bolcato-Bellemin et al. (2000)	+	+	?	+	+	+	+	+	+	+
Chang et al. (2015)	+	+	?	+	+	+	+	+	+	+
Chang et al. (2017)	+	+	?	+	+	+	+	+	+	+
Chen et al. (2014)	+	?	?	+	-	+	+	?	+	+
Chen et al. (2015)	+	+	?	+	+	+	+	+	+	+
Chiba and Mitani (2004)	+	+	?	+	+	+	+	+	+	+
Cho et al. (2010)	+	+	?	?	?	+	+	?	+	+
Deschner et al. (2012)	+	+	?	+	+	+	+	-	-	+
Diercke et al. (2011)	+	+	?	+	?	+	+	+	+	+
Doi et al. (2003)	+	+	?	+	+	+	+	?	+	+
Fujihara et al. (2010)	+	+	?	+	+	-	?	+	+	+
Goto et al. (2011)	+	?	?	?	?	+	?	+	+	?
Hao et al. (2009)	+	+	?	+	+	+	+	+	+	+
He et al. (2004)	+	+	?	+	+	+	+	?	+	+
He et al. (2019)	+	+	?	+	+	+	+	+	+	+
Howard et al. (1998)	+	+	?	+	+	+	?	-	-	+
Huelter-Hassler et al. (2017)	+	+	+	+	+	+	+	+	+	+
Hülter-Hassler et al. (2017)	+	+	+	+	+	+	?	+	+	+
Jacobs et al. (2013)	+	+	?	+	+	n. a.	+	?	+	+
Jacobs et al. (2014)	+	+	?	+	+	n. a.	+	+	+	+
Jacobs et al. (2015)	+	+	?	+	+	n. a.	+	?	+	+
Jacobs et al. (2018)	+	+	?	+	+	n. a.	+	+	+	+
Jiang and Hua (2016)	+	+	?	+	+	+	?	+	+	+
Kaku et al. (2019)	+	+	?	+	+	+	?	+	+	+
Kanzaki et al. (2006)	+	+	?	+	?	+	?	+	+	+
Kanzaki et al. (2019)	+	+	?	+	?	-	?	+	+	+
Kikuiri et al. (2000)	+	+	?	+	+	-	+	+	+	+
Kim et al. (2007)	+	+	?	+	?	+	+	?	-	+
Kletsas et al. (2002)	+	+	?	+	?	-	+	+	+	+

Supplement 4.2 Risk of bias assessment for the reporting quality of the included *in vitro* studies

Reference	Description of scientific background	Description objective	Justification for model	Study design description	Defined experimental outcomes	Ethical statement	Cell maintenance condition	Description of measurement precision and variability	Statistical analysis	Results description
Konstantonis et al. (2014)	+	+	?	?	?	+	+	?	?	+
Kook and Lee (2012)	+	-	?	?	+	+	+	+	+	+
Lee et al. (2012)	+	+	?	+	?	+	?	?	+	+
Lee et al. (2015)	+	-	?	+	?	-	?	+	+	+
Li et al. (2013)	+	-	?	+	+	+	+	+	+	?
Li et al. (2014)	+	+	+	+	+	+	+	+	+	+
Li et al. (2015)	+	+	?	+	+	-	+	+	+	+
Liao and Hua (2013)	+	+	?	+	+	+	+	+	+	+
Liu et al. (2012)	+	+	?	+	+	+	+	+	+	+
Liu et al. (2017)	+	+	?	+	+	+	+	+	+	+
Long et al. (2001)	+	+	?	+	+	+	+	-	-	+
Long et al. (2002)	+	+	?	+	+	+	+	?	+	+
Ma et al. (2015)	+	+	?	+	+	+	+	+	+	+
Matsuda et al. (1998a)	+	+	?	+	+	-	?	-	-	+
Matsuda et al. (1998b)	+	+	?	+	+	+	?	-	-	+
Memmert et al. (2019)	+	+	?	+	+	+	+	+	+	+
Memmert et al. (2020)	+	+	+	?	+	+	+	+	+	+
Meng et al. (2010)	+	+	?	+	+	-	+	-	+	+
Miura et al. (2000)	+	+	?	+	?	-	+	+	+	?
Molina et al. (2001)	+	+	?	+	+	+	?	-	+	+
Monnouchi et al. (2011)	+	+	?	+	+	+	?	+	+	+
Monnouchi et al. (2015)	+	+	?	+	+	+	+	+	+	+
Nakashima et al. (2009)	+	+	?	+	?	+	+	-	-	?
Narimiya et al. (2017)	+	+	?	+	?	+	+	+	+	+
Nazet et al. (2020)	+	?	?	+	+	+	+	+	+	?
Nemoto et al. (2010)	+	+	?	+	?	+	+	+	+	+
Ngan et al. (1990)	+	+	?	+	?	-	?	?	-	+
Nogueira et al. (2014a)	+	+	?	+	?	+	?	+	+	+
Nogueira et al. (2014b)	+	+	?	+	?	+	?	+	+	+
Nokhbehsaim et al. (2010)	+	+	?	+	?	+	?	+	+	+
Nokhbehsaim et al. (2011a)	+	+	?	+	?	+	?	+	+	+
Nokhbehsaim et al. (2011b)	+	+	?	+	?	+	?	+	+	+
Nokhbehsaim et al. (2012)	+	+	?	+	+	+	?	+	+	+
Ohzeki et al. (1999)	+	+	?	?	?	-	+	+	+	+

Supplement 4.2 Risk of bias assessment for the reporting quality of the included *in vitro* studies

Reference	Description of scientific background	Description objective	Justification for model	Study design description	Defined experimental outcomes	Ethical statement	Cell maintenance condition	Description of measurement precision and variability	Statistical analysis	Results description
Ozawa et al. (1997)	+	+	+	+	?	-	?	+	+	+
Padial-Molina et al. (2013)	+	+	+	+	+	-	?	+	+	+
Pan et al. (2014)	+	+	?	+	+	+	+	+	+	+
Papadopoulou et al. (2017)	+	+	?	?	?	+	?	?	+	+
Papadopoulou et al. (2019)	+	+	?	+	?	+	?	+	+	+
Pelaez et al. (2017)	+	+	?	+	-	+	-	+	+	+
Peverali et al. (2001)	+	+	?	+	+	-	+	-	-	+
Pinkerton et al. (2008)	+	+	?	+	+	+	+	?	+	+
Qin and Hua (2016)	+	+	?	?	?	+	?	+	+	+
Rath-Deschner et al. (2009)	+	+	?	+	+	+	+	+	+	+
Ren et al. (2015)	+	+	?	+	+	-	+	+	+	+
Ritter et al. (2007)	+	+	?	+	+	+	+	?	+	+
Saminathan et al. (2012)	+	+	?	+	?	+	?	+	+	+
Shen et al. (2014)	+	+	?	+	+	+	+	+	+	+
Shimizu et al. (1994)	+	+	?	+	?	-	?	+	+	+
Shimizu et al. (1995)	+	?	+	+	?	-	+	+	+	+
Shimizu et al. (1997)	+	+	?	+	?	-	?	+	+	?
Shimizu et al. (1998)	+	+	+	+	?	-	?	+	+	+
Spencer and Lallier (2009)	+	+	?	+	?	+	?	-	-	-
Steinberg et al. (2011)	+	+	+	+	+	+	+	+	+	+
Sun et al. (2016)	+	+	?	+	+	+	+	+	+	+
Sun et al. (2017)	+	+	?	+	+	+	?	+	+	+
Suzuki et al. (2014)	+	+	?	+	+	+	+	+	+	+
Symmank et al. (2019)	+	+	?	+	+	-	?	?	?	+
Takano et al. (2009)	+	+	?	+	?	+	+	+	+	+
Tang et al. (2012)	+	+	?	+	+	+	+	+	+	+
Tantilertanant et al. (2019a)	+	+	?	+	+	+	+	+	+	+
Tantilertanant et al. (2019b)	+	+	?	+	+	+	+	+	+	+
Tsuji et al. (2004)	+	+	?	+	?	+	?	+	+	+
Tsuruga et al. (2009)	+	+	?	+	?	+	+	-	-	+
Tsuruga et al. (2012)	+	+	?	+	?	+	?	-	-	+
Wada et al. (2017)	+	+	?	+	?	+	?	+	+	+
Wang et al. (2011)	+	+	?	+	+	+	+	?	+	+
Wang et al. (2013)	+	+	?	+	+	+	+	+	+	+

Supplement 4.2 Risk of bias assessment for the reporting quality of the included *in vitro* studies

Reference	Description of scientific background	Description objective	Justification for model	Study design description	Defined experimental outcomes	Ethical statement	Cell maintenance condition	Description of measurement precision and variability	Statistical analysis	Results description
Wang et al. (2018)	+	+	?	?	?	-	?	+	+	?
Wang et al. (2019a)	+	+	?	+	+	+	+	+	+	+
Wang et al. (2019b)	+	+	?	+	+	+	+	+	+	+
Wei et al. (2014)	+	+	?	+	+	+	+	+	+	+
Wei et al. (2015)	+	+	?	+	+	+	+	?	+	+
Wescott et al. (2007)	+	+	?	+	+	+	+	-	-	+
Wolf et al. (2014)	+	+	?	+	?	+	?	+	+	+
Wu et al. (2015)	+	+	?	+	+	+	?	+	+	+
Wu et al. (2016)	+	+	?	+	+	+	+	+	+	+
Wu et al. (2017)	+	+	?	+	+	+	+	+	+	+
Wu et al. (2019a)	+	+	?	+	+	+	+	+	+	+
Wu et al. (2019b)	+	+	+	+	+	+	+	+	+	+
Xu et al. (2011)	+	+	?	+	+	+	+	?	+	+
Xu et al. (2012)	+	+	?	+	+	+	+	+	+	+
Xu et al. (2015)	+	+	?	+	?	+	?	+	+	+
Xu et al. (2017)	+	+	?	+	+	+	+	+	+	+
Yamaguchi and Shimizu (1994)	+	+	?	+	?	-	?	+	+	+
Yamaguchi et al. (1994)	+	+	+	+	?	-	+	+	+	+
Yamaguchi et al. (1996)	+	+	?	+	?	-	?	+	+	+
Yamaguchi et al. (1997)	+	+	?	?	?	-	?	+	+	+
Yamaguchi et al. (2002)	+	+	?	+	+	-	?	-	-	+
Yamaguchi et al. (2004)	+	+	?	+	?	+	?	+	+	?
Yamashiro et al. (2007)	+	+	?	?	+	+	?	?	+	+
Yang et al. (2006)	+	+	?	+	?	-	?	+	+	+
Yang et al. (2010)	+	+	?	+	+	-	+	+	+	+
Yang et al. (2015)	+	+	?	+	+	+	?	+	+	+
Yang et al. (2016)	+	+	?	+	?	-	+	+	+	+
Yang et al. (2018)	+	+	?	+	+	+	+	+	+	+
Yoshino et al. (2003)	+	+	?	+	?	-	+	?	+	+
Yu et al. (2018)	+	+	?	?	?	+	+	+	+	+
Yuda et al. (2015)	+	+	?	+	?	+	?	+	+	+
Zhao et al. (2016)	+	+	?	+	+	+	+	+	+	+
Zhao et al. (2017)	+	+	+	+	+	+	+	+	+	+
Zhuang et al. (2019)	+	+	+	+	?	+	+	+	+	+

Supplement 4.2 Risk of bias assessment for the reporting quality of the included *in vitro* studies

Reference	Description of scientific background	Description objective	Justification for model	Study design description	Defined experimental outcomes	Ethical statement	Cell maintenance condition	Description of measurement precision and variability	Statistical analysis	Results description
Ziegler et al. (2010)	+	?	+	+	+	+	+	-	-	?

Summary	Description of scientific background	Description objective	Justification for model	Study design description	Defined experimental outcomes	Ethical statement	Cell maintenance condition	Description of measurement precision and variability	Statistical analysis	Results description
Low risk of bias ("+")	137 (100%)	129 (94%)	14 (10%)	126 (92%)	85 (62%)	100 (73%)	87 (64%)	99 (72%)	117 (85%)	127 (93%)
Unknown/Incomplete ("?")	0 (0%)	5 (4%)	123 (90%)	11 (8%)	50 (36%)	0 (0%)	49 (36%)	20 (15%)	2 (1%)	9 (7%)
High risk of bias ("-")	0 (0%)	3 (2%)	0 (0%)	0 (0%)	2 (1%)	33(24%)	1 (1%)	18 (13%)	18 (13%)	1 (1%)
Not applicable ("n.a.")	0 (0%)	0 (0%)	0 (0%)	0 (0%)	0 (0%)	4 (3%)	0 (0%)	0 (0%)	0 (0%)	0 (0%)
Sum	**137**	**137**	**137**	**137**	**137**	**137**	**137**	**137**	**137**	**137**

References

Abiko, Y., Shimizu, N., Yamaguchi, M., Suzuki, H., and Takiguchi, H. (1998). Effect of aging on functional changes of periodontal tissue cells. *Ann. Periodontol.* 3(1), 350-369. doi: 10.1902/annals.1998.3.1.350.

Agarwal, S., Long, P., Seyedain, A., Piesco, N., Shree, A., and Gassner, R. (2003). A central role for the nuclear factor-κB pathway in anti-inflammatory and proinflammatory actions of mechanical strain. *FASEB J.* 17(8), 899-901. doi: 10.1096/fj.02-0901fje.

Arima, M., Hasegawa, D., Yoshida, S., Mitarai, H., Tomokiyo, A., Hamano, S., et al. (2019). R-spondin 2 promotes osteoblastic differentiation of immature human periodontal ligament cells through the Wnt/beta-catenin signaling pathway. *J. Periodontal Res.* 54(2), 143-153. doi: 10.1111/jre.12611.

Basdra, E.K., Kohl, A., and Komposch, G. (1996). Mechanical stretching of periodontal ligament fibroblasts--a study on cytoskeletal involvement. *J. Orofac. Orthop.* 57(1), 24-30. doi: 10.1007/BF02189045.

Basdra, E.K., Papavassiliou, A.G., and Huber, L.A. (1995). Rab and rho GTPases are involved in specific response of periodontal ligament fibroblasts to mechanical stretching. *Biochim. Biophys. Acta* 1268(2), 209-213. doi: 10.1016/0167-4889(95)00090-f.

Bolcato-Bellemin, A.L., Elkaim, R., Abehsera, A., Fausser, J.L., Haikel, Y., and Tenenbaum, H. (2000). Expression of mRNAs encoding for alpha and beta integrin subunits, MMPs, and TIMPs in stretched human periodontal ligament and gingival fibroblasts. *J. Dent. Res.* 79(9), 1712-1716. doi: 10.1177/00220345000790091201.

Chang, M., Lin, H., Fu, H., Wang, B., Han, G., and Fan, M. (2017). MicroRNA-195-5p regulates osteogenic differentiation of periodontal ligament cells under mechanical loading. *J. Cell. Physiol.* 232(12), 3762-3774. doi: 10.1002/jcp.25856.

Chang, M., Lin, H., Luo, M., Wang, J., and Han, G. (2015). Integrated miRNA and mRNA expression profiling of tension force-induced bone formation in periodontal ligament cells. *In Vitro Cell. Dev. Biol. Anim.* 51(8), 797-807. doi: 10.1007/s11626-015-9892-0.

Chen, Y., Mohammed, A., Oubaidin, M., Evans, C.A., Zhou, X., Luan, X., et al. (2015). Cyclic stretch and compression forces alter microRNA-29 expression of human periodontal ligament cells. *Gene* 566(1), 13-17. doi: 10.1016/j.gene.2015.03.055.

Chen, Y.J., Shie, M.Y., Hung, C.J., Wu, B.C., Liu, S.L., Huang, T.H., et al. (2014). Activation of focal adhesion kinase induces extracellular signal-regulated kinase-mediated osteogenesis in tensile force-subjected periodontal ligament fibroblasts but not in osteoblasts. *J. Bone Miner. Metab.* 32(6), 671-682. doi: 10.1007/s00774-013-0549-3.

Chiba, M., and Mitani, H. (2004). Cytoskeletal changes and the system of regulation of alkaline phosphatase activity in human periodontal ligament cells induced by mechanical stress. *Cell Biochem. Funct.* 22(4), 249-256. doi: 10.1002/cbf.1097.

Cho, J.H., Lee, S.K., Lee, J.W., and Kim, E.C. (2010). The role of heme oxygenase-1 in mechanical stress- and lipopolysaccharide-induced osteogenic differentiation in human periodontal ligament cells. *Angle Orthod.* 80(4), 552-559. doi: 10.2319/091509-520.1.

Deschner, B., Rath, B., Jager, A., Deschner, J., Denecke, B., Memmert, S., et al. (2012). Gene analysis of signal transduction factors and transcription factors in periodontal ligament cells following application of dynamic strain. *J. Orofac. Orthop.* 73(6), 486-495, 497. doi: 10.1007/s00056-012-0104-1.

Diercke, K., Kohl, A., Lux, C.J., and Erber, R. (2011). Strain-dependent up-regulation of ephrin-B2 protein in periodontal ligament fibroblasts contributes to osteogenesis during tooth movement. *J. Biol. Chem.* 286(43), 37651-37664. doi: 10.1074/jbc.M110.166900.

Doi, T., Ohno, S., Tanimoto, K., Honda, K., Tanaka, N., Ohno-Nakahara, M., et al. (2003). Mechanical stimuli enhances the expression of RGD-CAP/betaig-h3 in the periodontal ligament. *Arch. Oral Biol.* 48(8), 573-579. doi: 10.1016/s0003-9969(03)00103-1.

Supplement 4.2 Risk of bias assessment for the reporting quality of the included *in vitro* studies

Fujihara, C., Yamada, S., Ozaki, N., Takeshita, N., Kawaki, H., Takano-Yamamoto, T., et al. (2010). Role of mechanical stress-induced glutamate signaling-associated molecules in cytodifferentiation of periodontal ligament cells. *J. Biol. Chem.* 285(36), 28286-28297. doi: 10.1074/jbc.M109.097303.

Goto, K.T., Kajiya, H., Nemoto, T., Tsutsumi, T., Tsuzuki, T., Sato, H., et al. (2011). Hyperocclusion stimulates osteoclastogenesis via CCL2 expression. *J. Dent. Res.* 90(6), 793-798. doi: 10.1177/0022034511400742.

Hao, Y., Xu, C., Sun, S.Y., and Zhang, F.Q. (2009). Cyclic stretching force induces apoptosis in human periodontal ligament cells via caspase-9. *Arch. Oral Biol.* 54(9), 864-870. doi: 10.1016/j.archoralbio.2009.05.012.

He, Y., Macarak, E.J., Korostoff, J.M., and Howard, P.S. (2004). Compression and tension: differential effects on matrix accumulation by periodontal ligament fibroblasts in vitro. *Connect Tissue Res.* 45(1), 28-39. doi: 10.1080/03008200490278124.

He, Y., Xu, H., Xiang, Z., Yu, H., Xu, L., Guo, Y., et al. (2019). YAP regulates periodontal ligament cell differentiation into myofibroblast interacted with RhoA/ROCK pathway. *J. Cell. Physiol.* 234(4), 5086-5096. doi: 10.1002/jcp.27312.

Howard, P.S., Kucich, U., Taliwal, R., and Korostoff, J.M. (1998). Mechanical forces alter extracellular matrix synthesis by human periodontal ligament fibroblasts. *J. Periodontal Res.* 33(8), 500-508. doi: 10.1111/j.1600-0765.1998.tb02350.x.

Huelter-Hassler, D., Tomakidi, P., Steinberg, T., and Jung, B.A. (2017). Orthodontic strain affects the Hippo-pathway effector YAP concomitant with proliferation in human periodontal ligament fibroblasts. *Eur. J. Orthod.* 39(3), 251-257. doi: 10.1093/ejo/cjx012.

Hülter-Hassler, D., Wein, M., Schulz, S.D., Proksch, S., Steinberg, T., Jung, B.A., et al. (2017). Biomechanical strain-induced modulation of proliferation coincides with an ERK1/2-independent nuclear YAP localization. *Exp. Cell Res.* 361(1), 93-100. doi: 10.1016/j.yexcr.2017.10.006.

Jacobs, C., Grimm, S., Ziebart, T., Walter, C., and Wehrbein, H. (2013). Osteogenic differentiation of periodontal fibroblasts is dependent on the strength of mechanical strain. *Arch. Oral Biol.* 58(7), 896-904. doi: 10.1016/j.archoralbio.2013.01.009.

Jacobs, C., Schramm, S., Dirks, I., Walter, C., Pabst, A., Meila, D., et al. (2018). Mechanical loading increases pro-inflammatory effects of nitrogen-containing bisphosphonate in human periodontal fibroblasts. *Clin. Oral Investig.* 22(2), 901-907. doi: 10.1007/s00784-017-2168-1.

Jacobs, C., Walter, C., Ziebart, T., Dirks, I., Schramm, S., Grimm, S., et al. (2015). Mechanical loading influences the effects of bisphosphonates on human periodontal ligament fibroblasts. *Clin. Oral Investig.* 19(3), 699-708. doi: 10.1007/s00784-014-1284-4.

Jacobs, C., Walter, C., Ziebart, T., Grimm, S., Meila, D., Krieger, E., et al. (2014). Induction of IL-6 and MMP-8 in human periodontal fibroblasts by static tensile strain. *Clin. Oral Investig.* 18(3), 901-908. doi: 10.1007/s00784-013-1032-1.

Jiang, Z., and Hua, Y. (2016). Hydrogen sulfide promotes osteogenic differentiation of human periodontal ligament cells via p38-MAPK signaling pathway under proper tension stimulation. *Arch. Oral Biol.* 72, 8-13. doi: 10.1016/j.archoralbio.2016.08.008.

Kaku, M., Yamamoto, T., Yashima, Y., Izumino, J., Kagawa, H., Ikeda, K., et al. (2019). Acetaminophen reduces apical root resorption during orthodontic tooth movement in rats. *Arch. Oral Biol.* 102, 83-92. doi: 10.1016/j.archoralbio.2019.04.002.

Kanzaki, H., Chiba, M., Sato, A., Miyagawa, A., Arai, K., Nukatsuka, S., et al. (2006). Cyclical tensile force on periodontal ligament cells inhibits osteoclastogenesis through OPG induction. *J. Dent. Res.* 85(5), 457-462. doi: 10.1177/154405910608500512.

Kanzaki, H., Wada, S., Yamaguchi, Y., Katsumata, Y., Itohiya, K., Fukaya, S., et al. (2019). Compression and tension variably alter Osteoprotegerin expression via miR-3198 in periodontal ligament cells. *BMC Mol. Cell Biol.* 20(1), 6. doi: 10.1186/s12860-019-0187-2.

Kikuiri, T., Hasegawa, T., Yoshimura, Y., Shirakawa, T., and Oguchi, H. (2000). Cyclic tension force activates nitric oxide production in cultured human periodontal ligament cells. *J. Periodontol.* 71(4), 533-539. doi: 10.1902/jop.2000.71.4.533.

Kim, H.J., Choi, Y.S., Jeong, M.J., Kim, B.O., Lim, S.H., Kim, D.K., et al. (2007). Expression of UNCL during development of periodontal tissue and response of periodontal ligament fibroblasts to mechanical stress in vivo and in vitro. *Cell Tissue Res.* 327(1), 25-31. doi: 10.1007/s00441-006-0304-3.

Kletsas, D., Basdra, E.K., and Papavassiliou, A.G. (2002). Effect of protein kinase inhibitors on the stretch-elicited c-Fos and c-Jun up-regulation in human PDL osteoblast-like cells. *J. Cell. Physiol.* 190(3), 313-321. doi: 10.1002/jcp.10052.

Konstantonis, D., Papadopoulou, A., Makou, M., Eliades, T., Basdra, E., and Kletsas, D. (2014). The role of cellular senescence on the cyclic stretching-mediated activation of MAPK and ALP expression and activity in human periodontal ligament fibroblasts. *Exp. Gerontol.* 57, 175-180. doi: 10.1016/j.exger.2014.05.010.

Kook, S.H., and Lee, J.C. (2012). Tensile force inhibits the proliferation of human periodontal ligament fibroblasts through Ras-p38 MAPK up-regulation. *J. Cell. Physiol.* 227(3), 1098-1106. doi: 10.1002/jcp.22829.

Lee, S.I., Park, K.H., Kim, S.J., Kang, Y.G., Lee, Y.M., and Kim, E.C. (2012). Mechanical stress-activated immune response genes via Sirtuin 1 expression in human periodontal ligament cells. *Clin. Exp. Immunol.* 168(1), 113-124. doi: 10.1111/j.1365-2249.2011.04549.x.

Lee, S.Y., Yoo, H.I., and Kim, S.H. (2015). CCR5-CCL Axis in PDL during Orthodontic Biophysical Force Application. *J. Dent. Res.* 94(12), 1715-1723. doi: 10.1177/0022034515603926.

Li, L., Han, M., Li, S., Wang, L., and Xu, Y. (2013). Cyclic tensile stress during physiological occlusal force enhances osteogenic differentiation of human periodontal ligament cells via ERK1/2-Elk1 MAPK pathway. *DNA Cell Biol.* 32(9), 488-497. doi: 10.1089/dna.2013.2070.

Li, L., Han, M.X., Li, S., Xu, Y., and Wang, L. (2014). Hypoxia regulates the proliferation and osteogenic differentiation of human periodontal ligament cells under cyclic tensile stress via mitogen-activated protein kinase pathways. *J. Periodontol.* 85(3), 498-508. doi: 10.1902/jop.2013.130048.

Li, S., Zhang, H., Li, S., Yang, Y., Huo, B., and Zhang, D. (2015). Connexin 43 and ERK regulate tension-induced signal transduction in human periodontal ligament fibroblasts. *J. Orthop. Res.* 33(7), 1008-1014. doi: 10.1002/jor.22830.

Liao, C., and Hua, Y. (2013). Effect of hydrogen sulphide on the expression of osteoprotegerin and receptor activator of NF-kappaB ligand in human periodontal ligament cells induced by tension-force stimulation. *Arch. Oral Biol.* 58(12), 1784-1790. doi: 10.1016/j.archoralbio.2013.08.004.

Liu, J., Li, Q., Liu, S., Gao, J., Qin, W., Song, Y., et al. (2017). Periodontal Ligament Stem Cells in the Periodontitis Microenvironment Are Sensitive to Static Mechanical Strain. *Stem Cells Int.* 2017, 1380851. doi: 10.1155/2017/1380851.

Liu, M., Dai, J., Lin, Y., Yang, L., Dong, H., Li, Y., et al. (2012). Effect of the cyclic stretch on the expression of osteogenesis genes in human periodontal ligament cells. *Gene* 491(2), 187-193. doi: 10.1016/j.gene.2011.09.031.

Supplement 4.2 Risk of bias assessment for the reporting quality of the included *in vitro* studies

Long, P., Hu, J., Piesco, N., Buckley, M., and Agarwal, S. (2001). Low magnitude of tensile strain inhibits IL-1beta-dependent induction of pro-inflammatory cytokines and induces synthesis of IL-10 in human periodontal ligament cells in vitro. *J. Dent. Res.* 80(5), 1416-1420. doi: 10.1177/00220345010800050601.

Long, P., Liu, F., Piesco, N.P., Kapur, R., and Agarwal, S. (2002). Signaling by mechanical strain involves transcriptional regulation of proinflammatory genes in human periodontal ligament cells in vitro. *Bone* 30(4), 547-552. doi: 10.1016/s8756-3282(02)00673-7.

Ma, J., Zhao, D., Wu, Y., Xu, C., and Zhang, F. (2015). Cyclic stretch induced gene expression of extracellular matrix and adhesion molecules in human periodontal ligament cells. *Arch. Oral Biol.* 60(3), 447-455. doi: 10.1016/j.archoralbio.2014.11.019.

Matsuda, N., Morita, N., Matsuda, K., and Watanabe, M. (1998a). Proliferation and differentiation of human osteoblastic cells associated with differential activation of MAP kinases in response to epidermal growth factor, hypoxia, and mechanical stress in vitro. *Biochem. Biophys. Res. Commun.* 249(2), 350-354. doi: 10.1006/bbrc.1998.9151.

Matsuda, N., Yokoyama, K., Takeshita, S., and Watanabe, M. (1998b). Role of epidermal growth factor and its receptor in mechanical stress-induced differentiation of human periodontal ligament cells in vitro. *Arch. Oral Biol.* 43(12), 987-997. doi: 10.1016/s0003-9969(98)00079-x.

Memmert, S., Damanaki, A., Weykopf, B., Rath-Deschner, B., Nokhbehsaim, M., Gotz, W., et al. (2019). Autophagy in periodontal ligament fibroblasts under biomechanical loading. *Cell Tissue Res.* doi: 10.1007/s00441-019-03063-1.

Memmert, S., Nogueira, A.V.B., Damanaki, A., Nokhbehsaim, M., Rath-Deschner, B., Götz, W., et al. (2020). Regulation of the autophagy-marker Sequestosome 1 in periodontal cells and tissues by biomechanical loading. *J. Orofac. Orthop.* 81(1), 10-21. doi: 10.1007/s00056-019-00197-3.

Meng, Y., Han, X., Huang, L., Bai, D., Yu, H., He, Y., et al. (2010). Orthodontic mechanical tension effects on the myofibroblast expression of alpha-smooth muscle actin. *Angle Orthod.* 80(5), 912-918. doi: 10.2319/101609-578.1.

Miura, S., Yamaguchi, M., Shimizu, N., and Abiko, Y. (2000). Mechanical stress enhances expression and production of plasminogen activator in aging human periodontal ligament cells. *Mech. Ageing Dev.* 112(3), 217-231. doi: 10.1016/s0047-6374(99)00095-0.

Molina, T., Kabsch, K., Alonso, A., Kohl, A., Komposch, G., and Tomakidi, P. (2001). Topographic changes of focal adhesion components and modulation of p125FAK activation in stretched human periodontal ligament fibroblasts. *J. Dent. Res.* 80(11), 1984-1989. doi: 10.1177/00220345010800110701.

Monnouchi, S., Maeda, H., Fujii, S., Tomokiyo, A., Kono, K., and Akamine, A. (2011). The roles of angiotensin II in stretched periodontal ligament cells. *J. Dent. Res.* 90(2), 181-185. doi: 10.1177/0022034510382118.

Monnouchi, S., Maeda, H., Yuda, A., Hamano, S., Wada, N., Tomokiyo, A., et al. (2015). Mechanical induction of interleukin-11 regulates osteoblastic/cementoblastic differentiation of human periodontal ligament stem/progenitor cells. *J. Periodontal Res.* 50(2), 231-239. doi: 10.1111/jre.12200.

Nakashima, K., Tsuruga, E., Hisanaga, Y., Ishikawa, H., and Sawa, Y. (2009). Stretching stimulates fibulin-5 expression and controls microfibril bundles in human periodontal ligament cells. *J. Periodontal Res.* 44(5), 622-627. doi: 10.1111/j.1600-0765.2008.01170.x.

Narimiya, T., Wada, S., Kanzaki, H., Ishikawa, M., Tsuge, A., Yamaguchi, Y., et al. (2017). Orthodontic tensile strain induces angiogenesis via type IV collagen degradation by matrix metalloproteinase-12. *J. Periodontal Res.* 52(5), 842-852. doi: 10.1111/jre.12453.

Nazet, U., Schröder, A., Spanier, G., Wolf, M., Proff, P., and Kirschneck, C. (2020). Simplified method for applying static isotropic tensile strain in cell culture experiments with identification of valid RT-qPCR reference genes for PDL fibroblasts. *Eur. J. Orthod.* 42(4), 359-370. doi: 10.1093/ejo/cjz052.

Nemoto, T., Kajiya, H., Tsuzuki, T., Takahashi, Y., and Okabe, K. (2010). Differential induction of collagens by mechanical stress in human periodontal ligament cells. *Arch. Oral Biol.* 55(12), 981-987. doi: 10.1016/j.archoralbio.2010.08.004.

Ngan, P., Saito, S., Saito, M., Lanese, R., Shanfeld, J., and Davidovitch, Z. (1990). The interactive effects of mechanical stress and interleukin-1 beta on prostaglandin E and cyclic AMP production in human periodontal ligament fibroblasts in vitro: comparison with cloned osteoblastic cells of mouse (MC3T3-E1). *Arch. Oral Biol.* 35(9), 717-725. doi: 10.1016/0003-9969(90)90094-Q.

Nogueira, A.V., Nokhbehsaim, M., Eick, S., Bourauel, C., Jäger, A., Jepsen, S., et al. (2014a). Regulation of visfatin by microbial and biomechanical signals in PDL cells. *Clin. Oral Investig.* 18(1), 171-178. doi: 10.1007/s00784-013-0935-1.

Nogueira, A.V., Nokhbehsaim, M., Eick, S., Bourauel, C., Jäger, A., Jepsen, S., et al. (2014b). Biomechanical loading modulates proinflammatory and bone resorptive mediators in bacterial-stimulated PDL cells. *Mediators Inflamm.* 2014, 425421. doi: 10.1155/2014/425421.

Nokhbehsaim, M., Deschner, B., Bourauel, C., Reimann, S., Winter, J., Rath, B., et al. (2011a). Interactions of enamel matrix derivative and biomechanical loading in periodontal regenerative healing. *J. Periodontol.* 82(12), 1725-1734. doi: 10.1902/jop.2011.100678.

Nokhbehsaim, M., Deschner, B., Winter, J., Bourauel, C., Jäger, A., Jepsen, S., et al. (2012). Anti-inflammatory effects of EMD in the presence of biomechanical loading and interleukin-1β in vitro. *Clin. Oral Investig.* 16(1), 275-283. doi: 10.1007/s00784-010-0505-8.

Nokhbehsaim, M., Deschner, B., Winter, J., Bourauel, C., Rath, B., Jager, A., et al. (2011b). Interactions of regenerative, inflammatory and biomechanical signals on bone morphogenetic protein-2 in periodontal ligament cells. *J. Periodontal Res.* 46(3), 374-381. doi: 10.1111/j.1600-0765.2011.01357.x.

Nokhbehsaim, M., Deschner, B., Winter, J., Reimann, S., Bourauel, C., Jepsen, S., et al. (2010). Contribution of orthodontic load to inflammation-mediated periodontal destruction. *J. Orofac. Orthop.* 71(6), 390-402. doi: 10.1007/s00056-010-1031-7.

Ohzeki, K., Yamaguchi, M., Shimizu, N., and Abiko, Y. (1999). Effect of cellular aging on the induction of cyclooxygenase-2 by mechanical stress in human periodontal ligament cells. *Mech. Ageing Dev.* 108(2), 151-163. doi: 10.1016/s0047-6374(99)00006-8.

Ozawa, Y., Shimizu, N., and Abiko, Y. (1997). Low-energy diode laser irradiation reduced plasminogen activator activity in human periodontal ligament cells. *Lasers Surg. Med.* 21(5), 456-463. doi: 10.1002/(sici)1096-9101(1997)21:5<456::aid-lsm7>3.0.co;2-p.

Padial-Molina, M., Volk, S.L., Rodriguez, J.C., Marchesan, J.T., Galindo-Moreno, P., and Rios, H.F. (2013). Tumor necrosis factor-alpha and Porphyromonas gingivalis lipopolysaccharides decrease periostin in human periodontal ligament fibroblasts. *J. Periodontol.* 84(5), 694-703. doi: 10.1902/jop.2012.120078.

Supplement 4.2 Risk of bias assessment for the reporting quality of the included *in vitro* studies

Pan, J., Wang, T., Wang, L., Chen, W., and Song, M. (2014). Cyclic strain-induced cytoskeletal rearrangement of human periodontal ligament cells via the Rho signaling pathway. *PloS One* 9(3), e91580. doi: 10.1371/journal.pone.0091580.

Papadopoulou, A., Iliadi, A., Eliades, T., and Kletsas, D. (2017). Early responses of human periodontal ligament fibroblasts to cyclic and static mechanical stretching. *Eur. J. Orthod.* 39(3), 258-263. doi: 10.1093/ejo/cjw075.

Papadopoulou, A., Todaro, A., Eliades, T., and Kletsas, D. (2019). Effect of hyperglycaemic conditions on the response of human periodontal ligament fibroblasts to mechanical stretching. *Eur. J. Orthod.* doi: 10.1093/ejo/cjz051.

Pelaez, D., Acosta Torres, Z., Ng, T.K., Choy, K.W., Pang, C.P., and Cheung, H.S. (2017). Cardiomyogenesis of periodontal ligament-derived stem cells by dynamic tensile strain. *Cell Tissue Res.* 367(2), 229-241. doi: 10.1007/s00441-016-2503-x.

Peverali, F.A., Basdra, E.K., and Papavassiliou, A.G. (2001). Stretch-mediated activation of selective MAPK subtypes and potentiation of AP-1 binding in human osteoblastic cells. *Mol. Med.* 7(1), 68-78.

Pinkerton, M.N., Wescott, D.C., Gaffey, B.J., Beggs, K.T., Milne, T.J., and Meikle, M.C. (2008). Cultured human periodontal ligament cells constitutively express multiple osteotropic cytokines and growth factors, several of which are responsive to mechanical deformation. *J. Periodontal Res.* 43(3), 343-351. doi: 10.1111/j.1600-0765.2007.01040.x.

Qin, J., and Hua, Y. (2016). Effects of hydrogen sulfide on the expression of alkaline phosphatase, osteocalcin and collagen type I in human periodontal ligament cells induced by tension force stimulation. *Mol. Med. Rep.* 14(4), 3871-3877. doi: 10.3892/mmr.2016.5680.

Rath-Deschner, B., Deschner, J., Reimann, S., Jager, A., and Gotz, W. (2009). Regulatory effects of biomechanical strain on the insulin-like growth factor system in human periodontal cells. *J. Biomech.* 42(15), 2584-2589. doi: 10.1016/j.jbiomech.2009.07.013.

Ren, D., Wei, F., Hu, L., Yang, S., Wang, C., and Yuan, X. (2015). Phosphorylation of Runx2, induced by cyclic mechanical tension via ERK1/2 pathway, contributes to osteodifferentiation of human periodontal ligament fibroblasts. *J. Cell. Physiol.* 230(10), 2426-2436. doi: 10.1002/jcp.24972.

Ritter, N., Mussig, E., Steinberg, T., Kohl, A., Komposch, G., and Tomakidi, P. (2007). Elevated expression of genes assigned to NF-kappaB and apoptotic pathways in human periodontal ligament fibroblasts following mechanical stretch. *Cell Tissue Res.* 328(3), 537-548. doi: 10.1007/s00441-007-0382-x.

Saminathan, A., Vinoth, K.J., Wescott, D.C., Pinkerton, M.N., Milne, T.J., Cao, T., et al. (2012). The effect of cyclic mechanical strain on the expression of adhesion-related genes by periodontal ligament cells in two-dimensional culture. *J. Periodontal Res.* 47(2), 212-221. doi: 10.1111/j.1600-0765.2011.01423.x.

Shen, T., Qiu, L., Chang, H., Yang, Y., Jian, C., Xiong, J., et al. (2014). Cyclic tension promotes osteogenic differentiation in human periodontal ligament stem cells. *Int. J. Clin. Exp. Pathol.* 7(11), 7872-7880.

Shimizu, N., Goseki, T., Yamaguchi, M., Iwasawa, T., Takiguchi, H., and Abiko, Y. (1997). In vitro cellular aging stimulates interleukin-1 beta production in stretched human periodontal-ligament-derived cells. *J. Dent. Res.* 76(7), 1367-1375. doi: 10.1177/00220345970760070601.

Shimizu, N., Ozawa, Y., Yamaguchi, M., Goseki, T., Ohzeki, K., and Abiko, Y. (1998). Induction of COX-2 expression by mechanical tension force in human periodontal ligament cells. *J. Periodontol.* 69(6), 670-677. doi: 10.1902/jop.1998.69.6.670.

Shimizu, N., Yamaguchi, M., Goseki, T., Ozawa, Y., Saito, K., Takiguchi, H., et al. (1994). Cyclic-tension force stimulates interleukin-1 beta production by human periodontal ligament cells. *J. Periodontal Res.* 29(5), 328-333. doi: 10.1111/j.1600-0765.1994.tb01230.x.

Shimizu, N., Yamaguchi, M., Goseki, T., Shibata, Y., Takiguchi, H., Iwasawa, T., et al. (1995). Inhibition of prostaglandin E2 and interleukin 1-beta production by low-power laser irradiation in stretched human periodontal ligament cells. *J. Dent. Res.* 74(7), 1382-1388. doi: 10.1177/00220345950740071001.

Spencer, A.Y., and Lallier, T.E. (2009). Mechanical tension alters semaphorin expression in the periodontium. *J. Periodontol.* 80(10), 1665-1673. doi: 10.1902/jop.2009.090212.

Steinberg, T., Ziegler, N., Alonso, A., Kohl, A., Mussig, E., Proksch, S., et al. (2011). Strain response in fibroblasts indicates a possible role of the Ca(2+)-dependent nuclear transcription factor NM1 in RNA synthesis. *Cell Calcium* 49(4), 259-271. doi: 10.1016/j.ceca.2011.03.001.

Sun, C., Chen, L., Shi, X., Cao, Z., Hu, B., Yu, W., et al. (2016). Combined effects of proinflammatory cytokines and intermittent cyclic mechanical strain in inhibiting osteogenicity in human periodontal ligament cells. *Cell Biol. Int.* 40(9), 999-1007. doi: 10.1002/cbin.10641.

Sun, C., Liu, F., Cen, S., Chen, L., Wang, Y., Sun, H., et al. (2017). Tensile strength suppresses the osteogenesis of periodontal ligament cells in inflammatory microenvironments. *Mol. Med. Rep.* 16(1), 666-672. doi: 10.3892/mmr.2017.6644.

Suzuki, R., Nemoto, E., and Shimauchi, H. (2014). Cyclic tensile force up-regulates BMP-2 expression through MAP kinase and COX-2/PGE2 signaling pathways in human periodontal ligament cells. *Exp. Cell Res.* 323(1), 232-241. doi: 10.1016/j.yexcr.2014.02.013.

Symmank, J., Zimmermann, S., Goldschmitt, J., Schiegnitz, E., Wolf, M., Wehrbein, H., et al. (2019). Mechanically-induced GDF15 Secretion by Periodontal Ligament Fibroblasts Regulates Osteogenic Transcription. *Sci. Rep.* 9(1), 11516. doi: 10.1038/s41598-019-47639-x.

Takano, M., Yamaguchi, M., Nakajima, R., Fujita, S., Kojima, T., and Kasai, K. (2009). Effects of relaxin on collagen type I released by stretched human periodontal ligament cells. *Orthod. Craniofac. Res.* 12(4), 282-288. doi: 10.1111/j.1601-6343.2009.01463.x.

Tang, N., Zhao, Z., Zhang, L., Yu, Q., Li, J., Xu, Z., et al. (2012). Up-regulated osteogenic transcription factors during early response of human periodontal ligament stem cells to cyclic tensile strain. *Arch. Med. Sci.* 8(3), 422-430. doi: 10.5114/aoms.2012.28810.

Tantilertanant, Y., Niyompanich, J., Everts, V., Supaphol, P., Pavasant, P., and Sanchavanakit, N. (2019a). Cyclic tensile force stimulates BMP9 synthesis and in vitro mineralization by human periodontal ligament cells. *J. Cell. Physiol.* 234(4), 4528-4539. doi: 10.1002/jcp.27257.

Tantilertanant, Y., Niyompanich, J., Everts, V., Supaphol, P., Pavasant, P., and Sanchavanakit, N. (2019b). Cyclic tensile force-upregulated IL6 increases MMP3 expression by human periodontal ligament cells. *Arch. Oral Biol.* 107, 104495. doi: 10.1016/j.archoralbio.2019.104495.

Tsuji, K., Uno, K., Zhang, G.X., and Tamura, M. (2004). Periodontal ligament cells under intermittent tensile stress regulate mRNA expression of osteoprotegerin and tissue

Supplement 4.2 Risk of bias assessment for the reporting quality of the included *in vitro* studies

inhibitor of matrix metalloprotease-1 and -2. *J. Bone Miner. Metab.* 22(2), 94-103. doi: 10.1007/s00774-003-0456-0.

Tsuruga, E., Nakashima, K., Ishikawa, H., Yajima, T., and Sawa, Y. (2009). Stretching modulates oxytalan fibers in human periodontal ligament cells. *J. Periodontal Res.* 44(2), 170-174. doi: 10.1111/j.1600-0765.2008.01099.x.

Tsuruga, E., Oka, K., Hatakeyama, Y., Isokawa, K., and Sawa, Y. (2012). Latent transforming growth factor-beta binding protein 2 negatively regulates coalescence of oxytalan fibers induced by stretching stress. *Connect Tissue Res.* 53(6), 521-527. doi: 10.3109/03008207.2012.702816.

Wada, S., Kanzaki, H., Narimiya, T., and Nakamura, Y. (2017). Novel device for application of continuous mechanical tensile strain to mammalian cells. *Biol. Open* 6(4), 518-524. doi: 10.1242/bio.023671.

Wang, H., Feng, C., Jin, Y., Tan, W., and Wei, F. (2019a). Identification and characterization of circular RNAs involved in mechanical force-induced periodontal ligament stem cells. *J. Cell. Physiol.* 234(7), 10166-10177. doi: 10.1002/jcp.27686.

Wang, L., Pan, J., Wang, T., Song, M., and Chen, W. (2013). Pathological cyclic strain-induced apoptosis in human periodontal ligament cells through the RhoGDIalpha/caspase-3/PARP pathway. *PloS One* 8(10), e75973. doi: 10.1371/journal.pone.0075973.

Wang, Y., Hu, B., Hu, R., Tong, X., Zhang, M., Xu, C., et al. (2019b). TAZ contributes to osteogenic differentiation of periodontal ligament cells under tensile stress. *J. Periodontal Res.* doi: 10.1111/jre.12698.

Wang, Y., Li, Y., Fan, X., Zhang, Y., Wu, J., and Zhao, Z. (2011). Early proliferation alteration and differential gene expression in human periodontal ligament cells subjected to cyclic tensile stress. *Arch. Oral Biol.* 56(2), 177-186. doi: 10.1016/j.archoralbio.2010.09.009.

Wang, Y.F., Zuo, Z.H., Luo, P., Pang, F.S., and Hu, J.T. (2018). The effect of cyclic tensile force on the actin cytoskeleton organization and morphology of human periodontal ligament cells. *Biochem. Biophys. Res. Commun.* 506(4), 950-955. doi: 10.1016/j.bbrc.2018.10.163.

Wei, F., Liu, D., Feng, C., Zhang, F., Yang, S., Hu, Y., et al. (2015). microRNA-21 mediates stretch-induced osteogenic differentiation in human periodontal ligament stem cells. *Stem Cells Dev.* 24(3), 312-319. doi: 10.1089/scd.2014.0191.

Wei, F.L., Wang, J.H., Ding, G., Yang, S.Y., Li, Y., Hu, Y.J., et al. (2014). Mechanical force-induced specific MicroRNA expression in human periodontal ligament stem cells. *Cells Tissues Organs* 199(5-6), 353-363. doi: 10.1159/000369613.

Wescott, D.C., Pinkerton, M.N., Gaffey, B.J., Beggs, K.T., Milne, T.J., and Meikle, M.C. (2007). Osteogenic gene expression by human periodontal ligament cells under cyclic tension. *J. Dent. Res.* 86(12), 1212-1216. doi: 10.1177/154405910708601214.

Wolf, M., Lossdorfer, S., Kupper, K., and Jager, A. (2014). Regulation of high mobility group box protein 1 expression following mechanical loading by orthodontic forces in vitro and in vivo. *Eur. J. Orthod.* 36(6), 624-631. doi: 10.1093/ejo/cjt037.

Wu, J., Song, M., Li, T., Zhu, Z., and Pan, J. (2015). The Rho-mDia1 signaling pathway is required for cyclic strain-induced cytoskeletal rearrangement of human periodontal ligament cells. *Exp. Cell Res.* 337(1), 28-36. doi: 10.1016/j.yexcr.2015.07.016.

Wu, Y., Ou, Y., Liao, C., Liang, S., and Wang, Y. (2019a). High-throughput sequencing analysis of the expression profile of microRNAs and target genes in mechanical force-induced osteoblastic/cementoblastic differentiation of human periodontal ligament cells. *Am. J. Transl. Res.* 11(6), 3398-3411.

Wu, Y., Zhao, D., Zhuang, J., Zhang, F., and Xu, C. (2016). Caspase-8 and Caspase-9 Functioned Differently at Different Stages of the Cyclic Stretch-Induced Apoptosis in Human Periodontal Ligament Cells. *PloS One* 11(12), e0168268. doi: 10.1371/journal.pone.0168268.

Wu, Y., Zhuang, J., Zhao, D., and Xu, C. (2019b). Interaction between caspase-3 and caspase-5 in the stretch-induced programmed cell death in the human periodontal ligament cells. *J. Cell. Physiol.* 234(8), 13571-13581. doi: 10.1002/jcp.28035.

Wu, Y., Zhuang, J., Zhao, D., Zhang, F., Ma, J., and Xu, C. (2017). Cyclic stretch-induced the cytoskeleton rearrangement and gene expression of cytoskeletal regulators in human periodontal ligament cells. *Acta Odontol. Scand.* 75(7), 507-516. doi: 10.1080/00016357.2017.1347823.

Xu, C., Fan, Z., Shan, W., Hao, Y., Ma, J., Huang, Q., et al. (2012). Cyclic stretch influenced expression of membrane connexin 43 in human periodontal ligament cell. *Arch. Oral Biol.* 57(12), 1602-1608. doi: 10.1016/j.archoralbio.2012.07.002.

Xu, C., Hao, Y., Wei, B., Ma, J., Li, J., Huang, Q., et al. (2011). Apoptotic gene expression by human periodontal ligament cells following cyclic stretch. *J. Periodontal Res.* 46(6), 742-748. doi: 10.1111/j.1600-0765.2011.01397.x.

Xu, H., Bai, D., Ruest, L.B., Feng, J.Q., Guo, Y.W., Tian, Y., et al. (2015). Expression analysis of alpha-smooth muscle actin and tenascin-C in the periodontal ligament under orthodontic loading or in vitro culture. *Int. J. Oral Sci.* 7(4), 232-241. doi: 10.1038/ijos.2015.26.

Xu, H.Y., Nie, E.M., Deng, G., Lai, L.Z., Sun, F.Y., Tian, H., et al. (2017). Periostin is essential for periodontal ligament remodeling during orthodontic treatment. *Mol. Med. Rep.* 15(4), 1800-1806. doi: 10.3892/mmr.2017.6200.

Yamaguchi, M., Ozawa, Y., Nogimura, A., Aihara, N., Kojima, T., Hirayama, Y., et al. (2004). Cathepsins B and L increased during response of periodontal ligament cells to mechanical stress in vitro. *Connect Tissue Res.* 45(3), 181-189. doi: 10.1080/03008200490514149.

Yamaguchi, M., and Shimizu, N. (1994). Identification of factors mediating the decrease of alkaline phosphatase activity caused by tension-force in periodontal ligament cells. *Gen. Pharmacol.* 25(6), 1229-1235. doi: 10.1016/0306-3623(94)90142-2.

Yamaguchi, M., Shimizu, N., Goseki, T., Shibata, Y., Takiguchi, H., Iwasawa, T., et al. (1994). Effect of different magnitudes of tension force on prostaglandin E2 production by human periodontal ligament cells. *Arch. Oral Biol.* 39(10), 877-884. doi: 10.1016/0003-9969(94)90019-1.

Yamaguchi, M., Shimizu, N., Ozawa, Y., Saito, K., Miura, S., Takiguchi, H., et al. (1997). Effect of tension-force on plasminogen activator activity from human periodontal ligament cells. *J. Periodontal Res.* 32(3), 308-314. doi: 10.1111/j.1600-0765.1997.tb00539.x.

Yamaguchi, M., Shimizu, N., Shibata, Y., and Abiko, Y. (1996). Effects of different magnitudes of tension-force on alkaline phosphatase activity in periodontal ligament cells. *J. Dent. Res.* 75(3), 889-894. doi: 10.1177/00220345960750030501.

Yamaguchi, N., Chiba, M., and Mitani, H. (2002). The induction of c-fos mRNA expression by mechanical stress in human periodontal ligament cells. *Arch. Oral Biol.* 47(6), 465-471. doi: 10.1016/s0003-9969(02)00022-5.

Yamashiro, K., Myokai, F., Hiratsuka, K., Yamamoto, T., Senoo, K., Arai, H., et al. (2007). Oligonucleotide array analysis of cyclic tension-responsive genes in human periodontal ligament fibroblasts. *Int. J. Biochem. Cell Biol.* 39(5), 910-921. doi: 10.1016/j.biocel.2007.01.015.

Supplement 4.2 Risk of bias assessment for the reporting quality of the included *in vitro* studies

Yang, S.Y., Kim, J.W., Lee, S.Y., Kang, J.H., Ulziisaikhan, U., Yoo, H.I., et al. (2015). Upregulation of relaxin receptors in the PDL by biophysical force. *Clin. Oral Investig.* 19(3), 657-665. doi: 10.1007/s00784-014-1276-4.

Yang, S.Y., Wei, F.L., Hu, L.H., and Wang, C.L. (2016). PERK-eIF2alpha-ATF4 pathway mediated by endoplasmic reticulum stress response is involved in osteodifferentiation of human periodontal ligament cells under cyclic mechanical force. *Cell. Signal.* 28(8), 880-886. doi: 10.1016/j.cellsig.2016.04.003.

Yang, Y., Wang, B.K., Chang, M.L., Wan, Z.Q., and Han, G.L. (2018). Cyclic Stretch Enhances Osteogenic Differentiation of Human Periodontal Ligament Cells via YAP Activation. *Biomed Res. Int.* 2018, 2174824. doi: 10.1155/2018/2174824.

Yang, Y., Yang, Y., Li, X., Cui, L., Fu, M., Rabie, A.B., et al. (2010). Functional analysis of core binding factor a1 and its relationship with related genes expressed by human periodontal ligament cells exposed to mechanical stress. *Eur. J. Orthod.* 32(6), 698-705. doi: 10.1093/ejo/cjq010.

Yang, Y.Q., Li, X.T., Rabie, A.B., Fu, M.K., and Zhang, D. (2006). Human periodontal ligament cells express osteoblastic phenotypes under intermittent force loading in vitro. *Front. Biosci.* 11, 776-781. doi: 10.2741/1835.

Yoshino, H., Morita, I., Murota, S.I., and Ishikawa, I. (2003). Mechanical stress induces production of angiogenic regulators in cultured human gingival and periodontal ligament fibroblasts. *J. Periodontal Res.* 38(4), 405-410. doi: 10.1034/j.1600-0765.2003.00660.x.

Yu, W., Hu, B., Shi, X., Cao, Z., Ren, M., He, Z., et al. (2018). Nicotine inhibits osteogenic differentiation of human periodontal ligament cells under cyclic tensile stress through canonical Wnt pathway and alpha7 nicotinic acetylcholine receptor. *J. Periodontal Res.* 53(4), 555-564. doi: 10.1111/jre.12545.

Yuda, A., Maeda, H., Fujii, S., Monnouchi, S., Yamamoto, N., Wada, N., et al. (2015). Effect of CTGF/CCN2 on osteo/cementoblastic and fibroblastic differentiation of a human periodontal ligament stem/progenitor cell line. *J. Cell. Physiol.* 230(1), 150-159. doi: 10.1002/jcp.24693.

Zhao, D., Wu, Y., Xu, C., and Zhang, F. (2017). Cyclic-stretch induces apoptosis in human periodontal ligament cells by activation of caspase-5. *Arch. Oral Biol.* 73, 129-135. doi: 10.1016/j.archoralbio.2016.10.009.

Zhao, D., Wu, Y., Zhuang, J., Xu, C., and Zhang, F. (2016). Activation of NLRP1 and NLRP3 inflammasomes contributed to cyclic stretch-induced pyroptosis and release of IL-1beta in human periodontal ligament cells. *Oncotarget* 7(42), 68292-68302. doi: 10.18632/oncotarget.11944.

Zhuang, J., Wang, Y., Qu, F., Wu, Y., Zhao, D., and Xu, C. (2019). Gasdermin-d Played a Critical Role in the Cyclic Stretch-Induced Inflammatory Reaction in Human Periodontal Ligament Cells. *Inflammation* 42(2), 548-558. doi: 10.1007/s10753-018-0912-6.

Ziegler, N., Alonso, A., Steinberg, T., Woodnutt, D., Kohl, A., Mussig, E., et al. (2010). Mechano-transduction in periodontal ligament cells identifies activated states of MAP-kinases p42/44 and p38-stress kinase as a mechanism for MMP-13 expression. *BMC Cell Biol.* 11, 10. doi: 10.1186/1471-2121-11-10.

Supplement 5:

Summary on force application.

Herein, the studies included were summarized in terms of force apparatus used, force duration and force magnitude for both dynamic/static and equibiaxial/uniaxial tension.

Contents

Table S5.1 Force apparatuses used to apply dynamic equibiaxial tension

Type of apparatus	Publications	Number	Subtotal
Flexcell FX-5000 Tension Unit Flexcell Tension Plus System FX-5000T Flexercell FX-4000 Strain Unit Flexcell FX-4000T Flexcell FX 3000	Chang et al. (2015), Jiang and Hua (2016), Lee et al. (2015), Li et al. (2013), Li et al. (2014), Liu et al. (2012), Liu et al. (2017), Padial-Molina et al. (2013), Pan et al. (2014), Ren et al. (2015), Shen et al. (2014), Wang et al. (2013), Wang et al. (2019a), Wang et al. (2019b), Wei et al. (2014), Wei et al. (2015), Wu et al. (2015), Wu et al. (2019a), Xu et al. (2017), Yang et al. (2015), Yang et al. (2016), Yang et al. (2018), Yu et al. (2018), Zhao et al. (2016), Zhuang et al. (2019)	25	53
Flexercell Strain Unit	Abiko et al. (1998), Agarwal et al. (2003), Chang et al. (2017), Chiba and Mitani (2004), Doi et al. (2003), Kanzaki et al. (2006), Kikuiri et al. (2000), Long et al. (2002), Long et al. (2001), Miura et al. (2000), Ohzeki et al. (1999), Ozawa et al. (1997), Shimizu et al. (1998), Shimizu et al. (1997), Shimizu et al. (1995), Shimizu et al. (1994), Tsuji et al. (2004), Yamaguchi et al. (1996), Yamaguchi and Shimizu (1994), Yamaguchi et al. (1994), Yamaguchi et al. (2002), Yamashiro et al. (2007), Yoshino et al. (2003), Kanzaki et al. (2019)	24	
Flexercell Strain Unit Model FX-2000	Kim et al. (2007), Matsuda et al. (1998b), Matsuda et al. (1998a), Kaku et al. (2019)	4	
"*Cell Strain Unit*" (CSU) (silicone rubber membrane in disk)	Hao et al. (2009), Ma et al. (2015), Wu et al. (2017), Wu et al. (2016), Xu et al. (2012), Xu et al. (2011), Zhao et al. (2017), Wu et al. (2019b)	8	10
Circularly clamped compliant membrane with spherical cap and vacuum (Tecoflex membrane)	Howard et al. (1998)	1	
Plastic culture cylinder with elastic silicone membrane and movable plate	He et al. (2004)	1	
CESTRA cell strain device (based on Bioflex® plates)	Deschner et al. (2012), Nogueira et al. (2014a), Nogueira et al. (2014b), Nokhbehsaim et al. (2012), Nokhbehsaim et al. (2011b), Nokhbehsaim et al. (2011a), Nokhbehsaim et al. (2010), Memmert et al. (2020)	8	9
"*Cell Extender*" (Bioflex-based)	Wada et al. (2017)	1	
	Total number		**72**

Table S5.2 Force apparatuses used to apply dynamic uniaxial tension

Type of apparatus	Publications	Number	Subtotal
STREX STB-140	Arima et al. (2019), Goto et al. (2011), Nemoto et al. (2010), Monnouchi et al. (2015), Monnouchi et al. (2011), Nakashima et al. (2009), Suzuki et al. (2014), Tsuruga et al. (2012), Tsuruga et al. (2009), Yuda et al. (2015)	10	10
Six station stretching apparatus (silicone dishes and moving clamp)	Konstantonis et al. (2014), Papadopoulou et al. (2017), Papadopoulou et al. (2019)	3	10
Uniaxial stretch apparatus (Chulalongkorn University, silicone membrane)	Tantilertanant et al. (2019a), Tantilertanant et al. (2019b)	2	
"*A new model*" (silicone membrane and motor)	Yang et al. (2010), Yang et al. (2006)	2	
Scholertec NS-350 (Scholertec, silicone membrane)	Fujihara et al. (2010)	1	
"*Custom-made tensile device*" poly dimethyl siloxane (PDMS) gel and motor	Li et al. (2015)	1	
"*custom-built bioreactor system and linear actuator*"	Pelaez et al. (2017)	1	
Flexcell FX-4000 strain unit FX-5000T Flexcell Tension Plus unit	Chen et al. (2015), Cho et al. (2010), Lee et al. (2012), Pinkerton et al. (2008), Saminathan et al. (2012), Sun et al. (2016), Sun et al. (2017), Wescott et al. (2007)	8	8
Four-point bending system	He et al. (2019), Meng et al. (2010), Tang et al. (2012), Wang et al. (2011), Wang et al. (2018), Xu et al. (2015)	6	6
	Total number		**34**

Table S5.3 Force apparatuses used to apply static equibiaxial tension

Type of apparatus	Publications	Number	Subtotal
Flexercell Strain Unit	Bolcato-Bellemin et al. (2000), Yamaguchi et al. (1997)	2	11
Flexcell FX-5000 Tension System Flexercell Strain Unit FX5000-T FX-4000 Tension Plus System Flexercell Strain Unit FX 3000	Huelter-Hassler et al. (2017), Hülter-Hassler et al. (2017), Jacobs et al. (2013), Jacobs et al. (2014), Jacobs et al. (2015), Jacobs et al. (2018), Kook and Lee (2012), Liao and Hua (2013), Symmank et al. (2019)	9	
Petriperm dish and template	Basdra et al. (1996), Basdra et al. (1995), Diercke et al. (2011), Kletsas et al. (2002), Molina et al. (2001), Ngan et al. (1990), Peverali et al. (2001), Ritter et al. (2007), Spencer and Lallier (2009), Yamaguchi et al. (2004)	10	10
"*Cell Extender*" (Bioflex-based)	Narimiya et al. (2017), Wada et al. (2017)	2	7
CESTRA cell strain device (Bioflex-based)	Memmert et al. (2019), Memmert et al. (2020)	2	
"*loading platform with cylindrical posts*" (University of Bonn, Bioflex-based)	Rath-Deschner et al. (2009), Wolf et al. (2014)	2	
custom-made spherical cap silicone stamps Bioflex-based)	Nazet et al. (2020)	1	
Lumox culture dishes	Steinberg et al. (2011), Ziegler et al. (2010)	2	2
"*a tension incubator*"	Chen et al. (2014)	1	1
	Total number		**31**

Table S5.4 Force apparatuses used to apply static uniaxial tension

Type of apparatus	Publications	Number
"*in-house designed device*" (silicone dishes and moving clamp)	Papadopoulou et al. (2017)	1
STREX system	Takano et al. (2009)	1
	Total number	**2**

Table S5.5 Maximal force magnitude and force duration applied using dynamic equibiaxial tension depending on the frequency of force application

Frequency	Publications	Number
0.005 Hz	Agarwal et al. (2003) (48h; 3%, 6%, 8%, 15%), Long et al. (2002) (48h; 6%), Long et al. (2001) (48h; 6%)	3
0.05 Hz	Deschner et al. (2012) (24h; 3%), Nogueira et al. (2014a) (3d; 3%, 20%), Nogueira et al. (2014b) (3d; 3%, 20%), Nokhbehsaim et al. (2010) (6d; 3%, 20%), Nokhbehsaim et al. (2011a) (6d; 3%), Nokhbehsaim et al. (2011b) (6d; 3%, 20%), Nokhbehsaim et al. (2012) (6d; 3%, 20%)	7
0.1 Hz	Abiko et al. (1998) (5d; 18%), Chang et al. (2015) (72h; 12%), Chang et al. (2017) (72h; 12%), Hao et al. (2009) (48h; 1%, 10%, 20%), Jiang and Hua (2016) (48h; 5%), Kikuiri et al. (2000) (12h; 18%), Kim et al. (2007) (6d; 9%), Lee et al. (2015) (48h; 12%), Liu et al. (2012) (24h; 12%), Liu et al. (2017) (12h; 6%, 8%, 10%, 12%, 14%), Ma et al. (2015) (24h; 10%), Matsuda et al. (1998a) (1h; 9%), Matsuda et al. (1998b) (6d; 9%,18%), Memmert et al. (2020) (24h; 3%), Miura et al. (2000) (5d; 9%, 18%), Ohzeki et al. (1999) (5d; 9%, 18%), Ozawa et al. (1997) (5d; 18%), Padial-Molina et al. (2013) (7d; 14%), Pan et al. (2014) (24h; 10%), Shen et al. (2014) (24h; 12%), Shimizu et al. (1994) (5d: 9%, 18%), Shimizu et al. (1995) (5d; 18%), Shimizu et al. (1997) (5d; 9%, 18%), Shimizu et al. (1998) (5d; 18%), Wang et al. (2013) (24h; 20%), Wang et al. (2019b) (48h; 12%), Wu et al. (2015) (24h; 10%), Wu et al. (2016) (24h; 20%), Wu et al. (2017) (24h; 1%, 10%, 20%), Wu et al. (2019a) (24h; 10%), Wu et al. (2019b) (24h; 20%), Xu et al. (2011) (24h; 20%), Xu et al. (2012) (24h; 1%, 10%, 20%), Yamaguchi and Shimizu (1994) (3d; 24%), Yamaguchi et al. (1994) (5d; 18%), Yamaguchi et al. (1996) (5d; 24%), Yamashiro et al. (2007) (16h; 18%), Yang et al. (2015) (48h; 12%), Yang et al. (2018) (72h;10%), Zhao et al. (2016) (24h; 20%), Zhao et al. (2017) (24h; 10%, 20%), Zhuang et al. (2019) (24h; 20%)	42
0.17 Hz (1/6Hz)	Tsuji et al. (2004) (48h; 20%)	1
0.2 Hz	Yoshino et al. (2003) (48h; 7%, 14%, 21%)	1
0.5 Hz	Chiba and Mitani (2004) (5d; 15%), Doi et al. (2003) (48h; 7.2 kPa, 15.4 kPa), He et al. (2004) (24h; 10%), Howard et al. (1998) (24h; 5%, 10%), Kaku et al. (2019) (48h; 12%), Kanzaki et al. (2006) (72h; 15%), Kanzaki et al. (2019) (24h; 15%), Li et al. (2013) (48h; 10%), Li et al. (2014) (48h; 10%), Ren et al. (2015) (24h; 10%), Wada et al. (2017) (n.g; 15%), Xu et al. (2017) (48h; 10%), Yamaguchi et al. (2002) (6h; 15%), Yang et al. (2016) (24h; 10%), Yu et al. (2018) (72h; 12%)	15
1 Hz	Wang et al. (2019a) (12h; 10%), Wei et al. (2014) (12h; 10%), Wei et al. (2015) (48h; 10%)	3
	Total number	**72**

Table S5.6 Maximal force magnitude and force duration applied using dynamic uniaxial tension depending on the frequency of force application

Frequency	Publications	Number
0.005 Hz	Li et al. (2015) (24h; 5%), Yang et al. (2010) (24h; 12%)	2
0.01 Hz	Nakashima et al. (2009) (7d; 5%), Pinkerton et al. (2008) (24h; 12%), Saminathan et al. (2012) (24h; 12%), Wescott et al. (2007) (24h; 12%)	4
1/60 Hz (0.017 Hz)	Goto et al. (2011) (7d; 5%), Nemoto et al. (2010) (7d; 5%), Suzuki et al. (2014) (24h; 3%, 5%, 10%), Tsuruga et al. (2009) (7d; 5%), Tsuruga et al. (2012) (7d; 5%)	5
0.05 Hz	Yang et al. (2006) (24h; 310-320 grams force)	1
0.1 Hz	Chen et al. (2015) (24h; 12%)	1
0.2 Hz	Cho et al. (2010) (48h; 3%, 6%, 12%, 15%), Lee et al. (2012) (48h; 33%, 6%, 12%,15%)	2
0.5 Hz	Arima et al. (2019) (24h; 10%), Fujihara et al. (2010) (48h; 10%), He et al. (2019) (3h; 0.2%), Meng et al. (2010) (12h; 0.4%), Pelaez et al. (2017) (2h; 5%), Sun et al. (2016) (5d; 12%), Sun et al. (2017) (48h; 12%), Tang et al. (2012) (24h; 0.3%), Wang et al. (2011) (2h; 0.5%), Wang et al. (2018) (6h; 0.4%), Xu et al. (2015) (12h; 0.2%, 0.4%)	11
1 Hz	Konstantonis et al. (2014) (12h; 8%), Monnouchi et al. (2011) (1h; 8%, 12%), Monnouchi et al. (2015) (1h; 8%), Papadopoulou et al. (2017) (3h; 8%), Papadopoulou et al. (2019) (18h; 8%), Tantilertanant et al. (2019a) (48h; 10%), Tantilertanant et al. (2019b) (6h; 10%), Yuda et al. (2015) (3h; 8%)	8
	Total number	**34**

Table S5.7 Maximal force magnitude and force duration applied using static equibiaxial tension

Magnitude	Publications	Number
0.28 %	Ngan et al. (1990) (1h), Yamaguchi et al. (2004) (12h)	2
0.95 %	Ngan et al. (1990) (1h), Yamaguchi et al. (2004) (12h)	2
1 %	Jacobs et al. (2013) (12h), Jacobs et al. (2014) (12h)	2
1.09 %	Ngan et al. (1990) (1h), Yamaguchi et al. (2004) (12h)	2
1.5 %	Kook and Lee (2012) (1h), Liao and Hua (2013) (2h)	2
1.72 %	Ngan et al. (1990) (1h), Yamaguchi et al. (2004) (12h)	2
-100 kPa	Chen et al. (2014) (15d)	1
20 kPa	Bolcato-Bellemin et al. (2000) (12h)	1
2.5 %	Basdra et al. (1995) (1h), Basdra et al. (1996) (12h), Diercke et al. (2011) (72h), Huelter-Hassler et al. (2017) (24h), Kletsas et al. (2002) (24h), Molina et al. (2001) (72h), Peverali et al. (2001) (0.5h), Ritter et al. (2007) (6h), Steinberg et al. (2011) (24h), Yamaguchi et al. (2004) (24h), Ziegler et al. (2010) (6h)	11
3 %	Jacobs et al. (2018) (12h), Kook and Lee (2012) (1h), Rath-Deschner et al. (2009) (24h), Memmert et al. (2019) (24h), Memmert et al. (2020) (24h)	5
5 %	Jacobs et al. (2015) (12h), Jacobs et al. (2014) (12h), Jacobs et al. (2013) (12h), Kook and Lee (2012) (1h), Symmank et al. (2019) (12h)	5
7 %	Nazet et al. (2020) (48h)	1
9 %	Yamaguchi et al. (1997) (5d)	1
10 %	Jacobs et al. (2013) (12h), Jacobs et al. (2014) (12h), Jacobs et al. (2015) (12h), Kook and Lee (2012) (1h), Nazet et al. (2020) (48h), Spencer and Lallier (2009) (12h)	6
15 %	Narimiya et al. (2017) (24h), Wada et al. (2017) (24h)	2
16 %	Nazet et al. (2020) (48h)	1
18 %	Yamaguchi et al. (1997) (5d)	1
20 %	Memmert et al. (2019) (24h), Memmert et al. (2020) (24h), Rath-Deschner et al. (2009) (24h), Wolf et al. (2014) (8h)	4
35 %	Nazet et al. (2020) (72h)	1
	Total number	**52**

Table S5.8 Maximal force magnitude and force duration applied using static uniaxial tension

Magnitude	Publications	Number
5 %	Takano et al. (2009) (12h)	1
8 %	Papadopoulou et al. (2017) (3h)	1
10 %	Takano et al. (2009) (12h)	1
	Total number	**3**

Dynamic equibiaxial tension (72): longest duration and mainly used magnitude

Dynamic uniaxial tension (34): longest duration and mainly used magnitude

Static equibiaxial tension (52): Magnitude and corresponding longest duration

Static uniaxial tension (3): Magnitude and corresponding longest duration

References

Abiko, Y., Shimizu, N., Yamaguchi, M., Suzuki, H., and Takiguchi, H. (1998). Effect of aging on functional changes of periodontal tissue cells. *Ann. Periodontol.* 3(1), 350-369. doi: 10.1902/annals.1998.3.1.350.

Agarwal, S., Long, P., Seyedain, A., Piesco, N., Shree, A., and Gassner, R. (2003). A central role for the nuclear factor-κB pathway in anti-inflammatory and proinflammatory actions of mechanical strain. *FASEB J.* 17(8), 899-901. doi: 10.1096/fj.02-0901fje.

Arima, M., Hasegawa, D., Yoshida, S., Mitarai, H., Tomokiyo, A., Hamano, S., et al. (2019). R-spondin 2 promotes osteoblastic differentiation of immature human periodontal ligament cells through the Wnt/beta-catenin signaling pathway. *J. Periodontal Res.* 54(2), 143-153. doi: 10.1111/jre.12611.

Basdra, E.K., Kohl, A., and Komposch, G. (1996). Mechanical stretching of periodontal ligament fibroblasts--a study on cytoskeletal involvement. *J. Orofac. Orthop.* 57(1), 24-30. doi: 10.1007/BF02189045.

Basdra, E.K., Papavassiliou, A.G., and Huber, L.A. (1995). Rab and rho GTPases are involved in specific response of periodontal ligament fibroblasts to mechanical stretching. *Biochim. Biophys. Acta* 1268(2), 209-213. doi: 10.1016/0167-4889(95)00090-f.

Bolcato-Bellemin, A.L., Elkaim, R., Abehsera, A., Fausser, J.L., Haikel, Y., and Tenenbaum, H. (2000). Expression of mRNAs encoding for alpha and beta integrin subunits, MMPs, and TIMPs in stretched human periodontal ligament and gingival fibroblasts. *J. Dent. Res.* 79(9), 1712-1716. doi: 10.1177/00220345000790091201.

Chang, M., Lin, H., Fu, H., Wang, B., Han, G., and Fan, M. (2017). MicroRNA-195-5p regulates osteogenic differentiation of periodontal ligament cells under mechanical loading. *J. Cell. Physiol.* 232(12), 3762-3774. doi: 10.1002/jcp.25856.

Chang, M., Lin, H., Luo, M., Wang, J., and Han, G. (2015). Integrated miRNA and mRNA expression profiling of tension force-induced bone formation in periodontal ligament cells. *In Vitro Cell. Dev. Biol. Anim.* 51(8), 797-807. doi: 10.1007/s11626-015-9892-0.

Chen, Y., Mohammed, A., Oubaidin, M., Evans, C.A., Zhou, X., Luan, X., et al. (2015). Cyclic stretch and compression forces alter microRNA-29 expression of human periodontal ligament cells. *Gene* 566(1), 13-17. doi: 10.1016/j.gene.2015.03.055.

Chen, Y.J., Shie, M.Y., Hung, C.J., Wu, B.C., Liu, S.L., Huang, T.H., et al. (2014). Activation of focal adhesion kinase induces extracellular signal-regulated kinase-mediated osteogenesis in tensile force-subjected periodontal ligament fibroblasts but not in osteoblasts. *J. Bone Miner. Metab.* 32(6), 671-682. doi: 10.1007/s00774-013-0549-3.

Chiba, M., and Mitani, H. (2004). Cytoskeletal changes and the system of regulation of alkaline phosphatase activity in human periodontal ligament cells induced by mechanical stress. *Cell Biochem. Funct.* 22(4), 249-256. doi: 10.1002/cbf.1097.

Cho, J.H., Lee, S.K., Lee, J.W., and Kim, E.C. (2010). The role of heme oxygenase-1 in mechanical stress- and lipopolysaccharide-induced osteogenic differentiation in human periodontal ligament cells. *Angle Orthod.* 80(4), 552-559. doi: 10.2319/091509-520.1.

Deschner, B., Rath, B., Jager, A., Deschner, J., Denecke, B., Memmert, S., et al. (2012). Gene analysis of signal transduction factors and transcription factors in periodontal ligament cells following application of dynamic strain. *J. Orofac. Orthop.* 73(6), 486-495, 497. doi: 10.1007/s00056-012-0104-1.

Diercke, K., Kohl, A., Lux, C.J., and Erber, R. (2011). Strain-dependent up-regulation of ephrin-B2 protein in periodontal ligament fibroblasts contributes to osteogenesis during tooth movement. *J. Biol. Chem.* 286(43), 37651-37664. doi: 10.1074/jbc.M110.166900.

Doi, T., Ohno, S., Tanimoto, K., Honda, K., Tanaka, N., Ohno-Nakahara, M., et al. (2003). Mechanical stimuli enhances the expression of RGD-CAP/betaig-h3 in the periodontal ligament. *Arch. Oral Biol.* 48(8), 573-579. doi: 10.1016/s0003-9969(03)00103-1.

Fujihara, C., Yamada, S., Ozaki, N., Takeshita, N., Kawaki, H., Takano-Yamamoto, T., et al. (2010). Role of mechanical stress-induced glutamate signaling-associated molecules in cytodifferentiation of periodontal ligament cells. *J. Biol. Chem.* 285(36), 28286-28297. doi: 10.1074/jbc.M109.097303.

Goto, K.T., Kajiya, H., Nemoto, T., Tsutsumi, T., Tsuzuki, T., Sato, H., et al. (2011). Hyperocclusion stimulates osteoclastogenesis via CCL2 expression. *J. Dent. Res.* 90(6), 793-798. doi: 10.1177/0022034511400742.

Hao, Y., Xu, C., Sun, S.Y., and Zhang, F.Q. (2009). Cyclic stretching force induces apoptosis in human periodontal ligament cells via caspase-9. *Arch. Oral Biol.* 54(9), 864-870. doi: 10.1016/j.archoralbio.2009.05.012.

He, Y., Macarak, E.J., Korostoff, J.M., and Howard, P.S. (2004). Compression and tension: differential effects on matrix accumulation by periodontal ligament fibroblasts in vitro. *Connect Tissue Res.* 45(1), 28-39. doi: 10.1080/03008200490278124.

He, Y., Xu, H., Xiang, Z., Yu, H., Xu, L., Guo, Y., et al. (2019). YAP regulates periodontal ligament cell differentiation into myofibroblast interacted with RhoA/ROCK pathway. *J. Cell. Physiol.* 234(4), 5086-5096. doi: 10.1002/jcp.27312.

Howard, P.S., Kucich, U., Taliwal, R., and Korostoff, J.M. (1998). Mechanical forces alter extracellular matrix synthesis by human periodontal ligament fibroblasts. *J. Periodontal Res.* 33(8), 500-508. doi: 10.1111/j.1600-0765.1998.tb02350.x.

Huelter-Hassler, D., Tomakidi, P., Steinberg, T., and Jung, B.A. (2017). Orthodontic strain affects the Hippo-pathway effector YAP concomitant with proliferation in human periodontal ligament fibroblasts. *Eur. J. Orthod.* 39(3), 251-257. doi: 10.1093/ejo/cjx012.

Hülter-Hassler, D., Wein, M., Schulz, S.D., Proksch, S., Steinberg, T., Jung, B.A., et al. (2017). Biomechanical strain-induced modulation of proliferation coincides with an ERK1/2-independent nuclear YAP localization. *Exp. Cell Res.* 361(1), 93-100. doi: 10.1016/j.yexcr.2017.10.006.

Jacobs, C., Grimm, S., Ziebart, T., Walter, C., and Wehrbein, H. (2013). Osteogenic differentiation of periodontal fibroblasts is dependent on the strength of mechanical strain. *Arch. Oral Biol.* 58(7), 896-904. doi: 10.1016/j.archoralbio.2013.01.009.

Jacobs, C., Schramm, S., Dirks, I., Walter, C., Pabst, A., Meila, D., et al. (2018). Mechanical loading increases pro-inflammatory effects of nitrogen-containing bisphosphonate in human periodontal fibroblasts. *Clin. Oral Investig.* 22(2), 901-907. doi: 10.1007/s00784-017-2168-1.

Jacobs, C., Walter, C., Ziebart, T., Dirks, I., Schramm, S., Grimm, S., et al. (2015). Mechanical loading influences the effects of bisphosphonates on human periodontal ligament fibroblasts. *Clin. Oral Investig.* 19(3), 699-708. doi: 10.1007/s00784-014-1284-4.

Jacobs, C., Walter, C., Ziebart, T., Grimm, S., Meila, D., Krieger, E., et al. (2014). Induction of IL-6 and MMP-8 in human periodontal fibroblasts by static tensile strain. *Clin. Oral Investig.* 18(3), 901-908. doi: 10.1007/s00784-013-1032-1.

Jiang, Z., and Hua, Y. (2016). Hydrogen sulfide promotes osteogenic differentiation of human periodontal ligament cells via p38-MAPK signaling pathway under proper tension stimulation. *Arch. Oral Biol.* 72, 8-13. doi: 10.1016/j.archoralbio.2016.08.008.

Kaku, M., Yamamoto, T., Yashima, Y., Izumino, J., Kagawa, H., Ikeda, K., et al. (2019). Acetaminophen reduces apical root resorption during orthodontic tooth movement in rats. *Arch. Oral Biol.* 102, 83-92. doi: 10.1016/j.archoralbio.2019.04.002.

Kanzaki, H., Chiba, M., Sato, A., Miyagawa, A., Arai, K., Nukatsuka, S., et al. (2006). Cyclical tensile force on periodontal ligament cells inhibits osteoclastogenesis through OPG induction. *J. Dent. Res.* 85(5), 457-462. doi: 10.1177/154405910608500512.

Kanzaki, H., Wada, S., Yamaguchi, Y., Katsumata, Y., Itohiya, K., Fukaya, S., et al. (2019). Compression and tension variably alter Osteoprotegerin expression via miR-3198 in periodontal ligament cells. *BMC Mol. Cell Biol.* 20(1), 6. doi: 10.1186/s12860-019-0187-2.

Kikuiri, T., Hasegawa, T., Yoshimura, Y., Shirakawa, T., and Oguchi, H. (2000). Cyclic tension force activates nitric oxide production in

cultured human periodontal ligament cells. *J. Periodontol.* 71(4), 533-539. doi: 10.1902/jop.2000.71.4.533.
Kim, H.J., Choi, Y.S., Jeong, M.J., Kim, B.O., Lim, S.H., Kim, D.K., et al. (2007). Expression of UNCL during development of periodontal tissue and response of periodontal ligament fibroblasts to mechanical stress in vivo and in vitro. *Cell Tissue Res.* 327(1), 25-31. doi: 10.1007/s00441-006-0304-3.
Kletsas, D., Basdra, E.K., and Papavassiliou, A.G. (2002). Effect of protein kinase inhibitors on the stretch-elicited c-Fos and c-Jun up-regulation in human PDL osteoblast-like cells. *J. Cell. Physiol.* 190(3), 313-321. doi: 10.1002/jcp.10052.
Konstantonis, D., Papadopoulou, A., Makou, M., Eliades, T., Basdra, E., and Kletsas, D. (2014). The role of cellular senescence on the cyclic stretching-mediated activation of MAPK and ALP expression and activity in human periodontal ligament fibroblasts. *Exp. Gerontol.* 57, 175-180. doi: 10.1016/j.exger.2014.05.010.
Kook, S.H., and Lee, J.C. (2012). Tensile force inhibits the proliferation of human periodontal ligament fibroblasts through Ras-p38 MAPK up-regulation. *J. Cell. Physiol.* 227(3), 1098-1106. doi: 10.1002/jcp.22829.
Lee, S.I., Park, K.H., Kim, S.J., Kang, Y.G., Lee, Y.M., and Kim, E.C. (2012). Mechanical stress-activated immune response genes via Sirtuin 1 expression in human periodontal ligament cells. *Clin. Exp. Immunol.* 168(1), 113-124. doi: 10.1111/j.1365-2249.2011.04549.x.
Lee, S.Y., Yoo, H.I., and Kim, S.H. (2015). CCR5-CCL Axis in PDL during Orthodontic Biophysical Force Application. *J. Dent. Res.* 94(12), 1715-1723. doi: 10.1177/0022034515603926.
Li, L., Han, M., Li, S., Wang, L., and Xu, Y. (2013). Cyclic tensile stress during physiological occlusal force enhances osteogenic differentiation of human periodontal ligament cells via ERK1/2-Elk1 MAPK pathway. *DNA Cell Biol.* 32(9), 488-497. doi: 10.1089/dna.2013.2070.
Li, L., Han, M.X., Li, S., Xu, Y., and Wang, L. (2014). Hypoxia regulates the proliferation and osteogenic differentiation of human periodontal ligament cells under cyclic tensile stress via mitogen-activated protein kinase pathways. *J. Periodontol.* 85(3), 498-508. doi: 10.1902/jop.2013.130048.
Li, S., Zhang, H., Li, S., Yang, Y., Huo, B., and Zhang, D. (2015). Connexin 43 and ERK regulate tension-induced signal transduction in human periodontal ligament fibroblasts. *J. Orthop. Res.* 33(7), 1008-1014. doi: 10.1002/jor.22830.
Liao, C., and Hua, Y. (2013). Effect of hydrogen sulphide on the expression of osteoprotegerin and receptor activator of NF-kappaB ligand in human periodontal ligament cells induced by tension-force stimulation. *Arch. Oral Biol.* 58(12), 1784-1790. doi: 10.1016/j.archoralbio.2013.08.004.
Liu, J., Li, Q., Liu, S., Gao, J., Qin, W., Song, Y., et al. (2017). Periodontal Ligament Stem Cells in the Periodontitis Microenvironment Are Sensitive to Static Mechanical Strain. *Stem Cells Int.* 2017, 1380851. doi: 10.1155/2017/1380851.
Liu, M., Dai, J., Lin, Y., Yang, L., Dong, H., Li, Y., et al. (2012). Effect of the cyclic stretch on the expression of osteogenesis genes in human periodontal ligament cells. *Gene* 491(2), 187-193. doi: 10.1016/j.gene.2011.09.031.
Long, P., Hu, J., Piesco, N., Buckley, M., and Agarwal, S. (2001). Low magnitude of tensile strain inhibits IL-1beta-dependent induction of pro-inflammatory cytokines and induces synthesis of IL-10 in human periodontal ligament cells in vitro. *J. Dent. Res.* 80(5), 1416-1420. doi: 10.1177/00220345010800050601.
Long, P., Liu, F., Piesco, N.P., Kapur, R., and Agarwal, S. (2002). Signaling by mechanical strain involves transcriptional regulation of proinflammatory genes in human periodontal ligament cells in vitro. *Bone* 30(4), 547-552. doi: 10.1016/s8756-3282(02)00673-7.
Ma, J., Zhao, D., Wu, Y., Xu, C., and Zhang, F. (2015). Cyclic stretch induced gene expression of extracellular matrix and adhesion molecules in human periodontal ligament cells. *Arch. Oral Biol.* 60(3), 447-455. doi: 10.1016/j.archoralbio.2014.11.019.
Matsuda, N., Morita, N., Matsuda, K., and Watanabe, M. (1998a). Proliferation and differentiation of human osteoblastic cells associated with differential activation of MAP kinases in response to epidermal growth factor, hypoxia, and mechanical stress in vitro. *Biochem. Biophys. Res. Commun.* 249(2), 350-354. doi: 10.1006/bbrc.1998.9151.
Matsuda, N., Yokoyama, K., Takeshita, S., and Watanabe, M. (1998b). Role of epidermal growth factor and its receptor in mechanical stress-induced differentiation of human periodontal ligament cells in vitro. *Arch. Oral Biol.* 43(12), 987-997. doi: 10.1016/s0003-9969(98)00079-x.
Memmert, S., Damanaki, A., Weykopf, B., Rath-Deschner, B., Nokhbehsaim, M., Gotz, W., et al. (2019). Autophagy in periodontal ligament fibroblasts under biomechanical loading. *Cell Tissue Res.* doi: 10.1007/s00441-019-03063-1.
Memmert, S., Nogueira, A.V.B., Damanaki, A., Nokhbehsaim, M., Rath-Deschner, B., Götz, W., et al. (2020). Regulation of the autophagy-marker Sequestosome 1 in periodontal cells and tissues by biomechanical loading. *J. Orofac. Orthop.* 81(1), 10-21. doi: 10.1007/s00056-019-00197-3.
Meng, Y., Han, X., Huang, L., Bai, D., Yu, H., He, Y., et al. (2010). Orthodontic mechanical tension effects on the myofibroblast expression of alpha-smooth muscle actin. *Angle Orthod.* 80(5), 912-918. doi: 10.2319/101609-578.1.
Miura, S., Yamaguchi, M., Shimizu, N., and Abiko, Y. (2000). Mechanical stress enhances expression and production of plasminogen activator in aging human periodontal ligament cells. *Mech. Ageing Dev.* 112(3), 217-231. doi: 10.1016/s0047-6374(99)00095-0.
Molina, T., Kabsch, K., Alonso, A., Kohl, A., Komposch, G., and Tomakidi, P. (2001). Topographic changes of focal adhesion components and modulation of p125FAK activation in stretched human periodontal ligament fibroblasts. *J. Dent. Res.* 80(11), 1984-1989. doi: 10.1177/00220345010800110701.
Monnouchi, S., Maeda, H., Fujii, S., Tomokiyo, A., Kono, K., and Akamine, A. (2011). The roles of angiotensin II in stretched periodontal ligament cells. *J. Dent. Res.* 90(2), 181-185. doi: 10.1177/0022034510382118.
Monnouchi, S., Maeda, H., Yuda, A., Hamano, S., Wada, N., Tomokiyo, A., et al. (2015). Mechanical induction of interleukin-11 regulates osteoblastic/cementoblastic differentiation of human periodontal ligament stem/progenitor cells. *J. Periodontal Res.* 50(2), 231-239. doi: 10.1111/jre.12200.
Nakashima, K., Tsuruga, E., Hisanaga, Y., Ishikawa, H., and Sawa, Y. (2009). Stretching stimulates fibulin-5 expression and controls microfibril bundles in human periodontal ligament cells. *J. Periodontal Res.* 44(5), 622-627. doi: 10.1111/j.1600-0765.2008.01170.x.
Narimiya, T., Wada, S., Kanzaki, H., Ishikawa, M., Tsuge, A., Yamaguchi, Y., et al. (2017). Orthodontic tensile strain induces angiogenesis via type IV collagen degradation by matrix metalloproteinase-12. *J. Periodontal Res.* 52(5), 842-852. doi: 10.1111/jre.12453.
Nazet, U., Schröder, A., Spanier, G., Wolf, M., Proff, P., and Kirschneck, C. (2020). Simplified method for applying static isotropic tensile strain in cell culture experiments with identification of valid RT-qPCR reference genes for PDL fibroblasts. *Eur. J. Orthod.* 42(4), 359-370. doi: 10.1093/ejo/cjz052.
Nemoto, T., Kajiya, H., Tsuzuki, T., Takahashi, Y., and Okabe, K. (2010). Differential induction of collagens by mechanical stress in human periodontal ligament cells. *Arch. Oral Biol.* 55(12), 981-987. doi: 10.1016/j.archoralbio.2010.08.004.
Ngan, P., Saito, S., Saito, M., Lanese, R., Shanfeld, J., and Davidovitch, Z. (1990). The interactive effects of mechanical stress and interleukin-1 beta on prostaglandin E and cyclic AMP production in human periodontal ligament fibroblasts in vitro: comparison with cloned osteoblastic cells of mouse (MC3T3-E1). *Arch. Oral Biol.* 35(9), 717-725. doi: 10.1016/0003-9969(90)90094-Q.

Nogueira, A.V., Nokhbehsaim, M., Eick, S., Bourauel, C., Jäger, A., Jepsen, S., et al. (2014a). Regulation of visfatin by microbial and biomechanical signals in PDL cells. *Clin. Oral Investig.* 18(1), 171-178. doi: 10.1007/s00784-013-0935-1.
Nogueira, A.V., Nokhbehsaim, M., Eick, S., Bourauel, C., Jäger, A., Jepsen, S., et al. (2014b). Biomechanical loading modulates proinflammatory and bone resorptive mediators in bacterial-stimulated PDL cells. *Mediators Inflamm.* 2014, 425421. doi: 10.1155/2014/425421.
Nokhbehsaim, M., Deschner, B., Bourauel, C., Reimann, S., Winter, J., Rath, B., et al. (2011a). Interactions of enamel matrix derivative and biomechanical loading in periodontal regenerative healing. *J. Periodontol.* 82(12), 1725-1734. doi: 10.1902/jop.2011.100678.
Nokhbehsaim, M., Deschner, B., Winter, J., Bourauel, C., Jäger, A., Jepsen, S., et al. (2012). Anti-inflammatory effects of EMD in the presence of biomechanical loading and interleukin-1β in vitro. *Clin. Oral Investig.* 16(1), 275-283. doi: 10.1007/s00784-010-0505-8.
Nokhbehsaim, M., Deschner, B., Winter, J., Bourauel, C., Rath, B., Jager, A., et al. (2011b). Interactions of regenerative, inflammatory and biomechanical signals on bone morphogenetic protein-2 in periodontal ligament cells. *J. Periodontal Res.* 46(3), 374-381. doi: 10.1111/j.1600-0765.2011.01357.x.
Nokhbehsaim, M., Deschner, B., Winter, J., Reimann, S., Bourauel, C., Jepsen, S., et al. (2010). Contribution of orthodontic load to inflammation-mediated periodontal destruction. *J. Orofac. Orthop.* 71(6), 390-402. doi: 10.1007/s00056-010-1031-7.
Ohzeki, K., Yamaguchi, M., Shimizu, N., and Abiko, Y. (1999). Effect of cellular aging on the induction of cyclooxygenase-2 by mechanical stress in human periodontal ligament cells. *Mech. Ageing Dev.* 108(2), 151-163. doi: 10.1016/s0047-6374(99)00006-8.
Ozawa, Y., Shimizu, N., and Abiko, Y. (1997). Low-energy diode laser irradiation reduced plasminogen activator activity in human periodontal ligament cells. *Lasers Surg. Med.* 21(5), 456-463. doi: 10.1002/(sici)1096-9101(1997)21:5<456::aid-lsm7>3.0.co;2-p.
Padial-Molina, M., Volk, S.L., Rodriguez, J.C., Marchesan, J.T., Galindo-Moreno, P., and Rios, H.F. (2013). Tumor necrosis factor-alpha and Porphyromonas gingivalis lipopolysaccharides decrease periostin in human periodontal ligament fibroblasts. *J. Periodontol.* 84(5), 694-703. doi: 10.1902/jop.2012.120078.
Pan, J., Wang, T., Wang, L., Chen, W., and Song, M. (2014). Cyclic strain-induced cytoskeletal rearrangement of human periodontal ligament cells via the Rho signaling pathway. *PloS One* 9(3), e91580. doi: 10.1371/journal.pone.0091580.
Papadopoulou, A., Iliadi, A., Eliades, T., and Kletsas, D. (2017). Early responses of human periodontal ligament fibroblasts to cyclic and static mechanical stretching. *Eur. J. Orthod.* 39(3), 258-263. doi: 10.1093/ejo/cjw075.
Papadopoulou, A., Todaro, A., Eliades, T., and Kletsas, D. (2019). Effect of hyperglycaemic conditions on the response of human periodontal ligament fibroblasts to mechanical stretching. *Eur. J. Orthod.* doi: 10.1093/ejo/cjz051.
Pelaez, D., Acosta Torres, Z., Ng, T.K., Choy, K.W., Pang, C.P., and Cheung, H.S. (2017). Cardiomyogenesis of periodontal ligament-derived stem cells by dynamic tensile strain. *Cell Tissue Res.* 367(2), 229-241. doi: 10.1007/s00441-016-2503-x.
Peverali, F.A., Basdra, E.K., and Papavassiliou, A.G. (2001). Stretch-mediated activation of selective MAPK subtypes and potentiation of AP-1 binding in human osteoblastic cells. *Mol. Med.* 7(1), 68-78.
Pinkerton, M.N., Wescott, D.C., Gaffey, B.J., Beggs, K.T., Milne, T.J., and Meikle, M.C. (2008). Cultured human periodontal ligament cells constitutively express multiple osteotropic cytokines and growth factors, several of which are responsive to mechanical deformation. *J. Periodontal Res.* 43(3), 343-351. doi: 10.1111/j.1600-0765.2007.01040.x.
Rath-Deschner, B., Deschner, J., Reimann, S., Jager, A., and Gotz, W. (2009). Regulatory effects of biomechanical strain on the insulin-like growth factor system in human periodontal cells. *J. Biomech.* 42(15), 2584-2589. doi: 10.1016/j.jbiomech.2009.07.013.
Ren, D., Wei, F., Hu, L., Yang, S., Wang, C., and Yuan, X. (2015). Phosphorylation of Runx2, induced by cyclic mechanical tension via ERK1/2 pathway, contributes to osteodifferentiation of human periodontal ligament fibroblasts. *J. Cell. Physiol.* 230(10), 2426-2436. doi: 10.1002/jcp.24972.
Ritter, N., Mussig, E., Steinberg, T., Kohl, A., Komposch, G., and Tomakidi, P. (2007). Elevated expression of genes assigned to NF-kappaB and apoptotic pathways in human periodontal ligament fibroblasts following mechanical stretch. *Cell Tissue Res.* 328(3), 537-548. doi: 10.1007/s00441-007-0382-x.
Saminathan, A., Vinoth, K.J., Wescott, D.C., Pinkerton, M.N., Milne, T.J., Cao, T., et al. (2012). The effect of cyclic mechanical strain on the expression of adhesion-related genes by periodontal ligament cells in two-dimensional culture. *J. Periodontal Res.* 47(2), 212-221. doi: 10.1111/j.1600-0765.2011.01423.x.
Shen, T., Qiu, L., Chang, H., Yang, Y., Jian, C., Xiong, J., et al. (2014). Cyclic tension promotes osteogenic differentiation in human periodontal ligament stem cells. *Int. J. Clin. Exp. Pathol.* 7(11), 7872-7880.
Shimizu, N., Goseki, T., Yamaguchi, M., Iwasawa, T., Takiguchi, H., and Abiko, Y. (1997). In vitro cellular aging stimulates interleukin-1 beta production in stretched human periodontal-ligament-derived cells. *J. Dent. Res.* 76(7), 1367-1375. doi: 10.1177/00220345970760070601.
Shimizu, N., Ozawa, Y., Yamaguchi, M., Goseki, T., Ohzeki, K., and Abiko, Y. (1998). Induction of COX-2 expression by mechanical tension force in human periodontal ligament cells. *J. Periodontol.* 69(6), 670-677. doi: 10.1902/jop.1998.69.6.670.
Shimizu, N., Yamaguchi, M., Goseki, T., Ozawa, Y., Saito, K., Takiguchi, H., et al. (1994). Cyclic-tension force stimulates interleukin-1 beta production by human periodontal ligament cells. *J. Periodontal Res.* 29(5), 328-333. doi: 10.1111/j.1600-0765.1994.tb01230.x.
Shimizu, N., Yamaguchi, M., Goseki, T., Shibata, Y., Takiguchi, H., Iwasawa, T., et al. (1995). Inhibition of prostaglandin E2 and interleukin 1-beta production by low-power laser irradiation in stretched human periodontal ligament cells. *J. Dent. Res.* 74(7), 1382-1388. doi: 10.1177/00220345950740071001.
Spencer, A.Y., and Lallier, T.E. (2009). Mechanical tension alters semaphorin expression in the periodontium. *J. Periodontol.* 80(10), 1665-1673. doi: 10.1902/jop.2009.090212.
Steinberg, T., Ziegler, N., Alonso, A., Kohl, A., Mussig, E., Proksch, S., et al. (2011). Strain response in fibroblasts indicates a possible role of the Ca(2+)-dependent nuclear transcription factor NM1 in RNA synthesis. *Cell Calcium* 49(4), 259-271. doi: 10.1016/j.ceca.2011.03.001.
Sun, C., Chen, L., Shi, X., Cao, Z., Hu, B., Yu, W., et al. (2016). Combined effects of proinflammatory cytokines and intermittent cyclic mechanical strain in inhibiting osteogenicity in human periodontal ligament cells. *Cell Biol. Int.* 40(9), 999-1007. doi: 10.1002/cbin.10641.
Sun, C., Liu, F., Cen, S., Chen, L., Wang, Y., Sun, H., et al. (2017). Tensile strength suppresses the osteogenesis of periodontal ligament cells in inflammatory microenvironments. *Mol. Med. Rep.* 16(1), 666-672. doi: 10.3892/mmr.2017.6644.
Suzuki, R., Nemoto, E., and Shimauchi, H. (2014). Cyclic tensile force up-regulates BMP-2 expression through MAP kinase and COX-2/PGE2 signaling pathways in human periodontal ligament cells. *Exp. Cell Res.* 323(1), 232-241. doi: 10.1016/j.yexcr.2014.02.013.
Symmank, J., Zimmermann, S., Goldschmitt, J., Schiegnitz, E., Wolf, M., Wehrbein, H., et al. (2019). Mechanically-induced GDF15 Secretion by Periodontal Ligament Fibroblasts Regulates Osteogenic Transcription. *Sci. Rep.* 9(1), 11516. doi:

10.1038/s41598-019-47639-x.
Takano, M., Yamaguchi, M., Nakajima, R., Fujita, S., Kojima, T., and Kasai, K. (2009). Effects of relaxin on collagen type I released by stretched human periodontal ligament cells. *Orthod. Craniofac. Res.* 12(4), 282-288. doi: 10.1111/j.1601-6343.2009.01463.x.
Tang, N., Zhao, Z., Zhang, L., Yu, Q., Li, J., Xu, Z., et al. (2012). Up-regulated osteogenic transcription factors during early response of human periodontal ligament stem cells to cyclic tensile strain. *Arch. Med. Sci.* 8(3), 422-430. doi: 10.5114/aoms.2012.28810.
Tantilertanant, Y., Niyompanich, J., Everts, V., Supaphol, P., Pavasant, P., and Sanchavanakit, N. (2019a). Cyclic tensile force stimulates BMP9 synthesis and in vitro mineralization by human periodontal ligament cells. *J. Cell. Physiol.* 234(4), 4528-4539. doi: 10.1002/jcp.27257.
Tantilertanant, Y., Niyompanich, J., Everts, V., Supaphol, P., Pavasant, P., and Sanchavanakit, N. (2019b). Cyclic tensile force-upregulated IL6 increases MMP3 expression by human periodontal ligament cells. *Arch. Oral Biol.* 107, 104495. doi: 10.1016/j.archoralbio.2019.104495.
Tsuji, K., Uno, K., Zhang, G.X., and Tamura, M. (2004). Periodontal ligament cells under intermittent tensile stress regulate mRNA expression of osteoprotegerin and tissue inhibitor of matrix metalloprotease-1 and -2. *J. Bone Miner. Metab.* 22(2), 94-103. doi: 10.1007/s00774-003-0456-0.
Tsuruga, E., Nakashima, K., Ishikawa, H., Yajima, T., and Sawa, Y. (2009). Stretching modulates oxytalan fibers in human periodontal ligament cells. *J. Periodontal Res.* 44(2), 170-174. doi: 10.1111/j.1600-0765.2008.01099.x.
Tsuruga, E., Oka, K., Hatakeyama, Y., Isokawa, K., and Sawa, Y. (2012). Latent transforming growth factor-beta binding protein 2 negatively regulates coalescence of oxytalan fibers induced by stretching stress. *Connect Tissue Res.* 53(6), 521-527. doi: 10.3109/03008207.2012.702816.
Wada, S., Kanzaki, H., Narimiya, T., and Nakamura, Y. (2017). Novel device for application of continuous mechanical tensile strain to mammalian cells. *Biol. Open* 6(4), 518-524. doi: 10.1242/bio.023671.
Wang, H., Feng, C., Jin, Y., Tan, W., and Wei, F. (2019a). Identification and characterization of circular RNAs involved in mechanical force-induced periodontal ligament stem cells. *J. Cell. Physiol.* 234(7), 10166-10177. doi: 10.1002/jcp.27686.
Wang, L., Pan, J., Wang, T., Song, M., and Chen, W. (2013). Pathological cyclic strain-induced apoptosis in human periodontal ligament cells through the RhoGDIalpha/caspase-3/PARP pathway. *PloS One* 8(10), e75973. doi: 10.1371/journal.pone.0075973.
Wang, Y., Hu, B., Hu, R., Tong, X., Zhang, M., Xu, C., et al. (2019b). TAZ contributes to osteogenic differentiation of periodontal ligament cells under tensile stress. *J. Periodontal Res.* doi: 10.1111/jre.12698.
Wang, Y., Li, Y., Fan, X., Zhang, Y., Wu, J., and Zhao, Z. (2011). Early proliferation alteration and differential gene expression in human periodontal ligament cells subjected to cyclic tensile stress. *Arch. Oral Biol.* 56(2), 177-186. doi: 10.1016/j.archoralbio.2010.09.009.
Wang, Y.F., Zuo, Z.H., Luo, P., Pang, F.S., and Hu, J.T. (2018). The effect of cyclic tensile force on the actin cytoskeleton organization and morphology of human periodontal ligament cells. *Biochem. Biophys. Res. Commun.* 506(4), 950-955. doi: 10.1016/j.bbrc.2018.10.163.
Wei, F., Liu, D., Feng, C., Zhang, F., Yang, S., Hu, Y., et al. (2015). microRNA-21 mediates stretch-induced osteogenic differentiation in human periodontal ligament stem cells. *Stem Cells Dev.* 24(3), 312-319. doi: 10.1089/scd.2014.0191.
Wei, F.L., Wang, J.H., Ding, G., Yang, S.Y., Li, Y., Hu, Y.J., et al. (2014). Mechanical force-induced specific MicroRNA expression in human periodontal ligament stem cells. *Cells Tissues Organs* 199(5-6), 353-363. doi: 10.1159/000369613.
Wescott, D.C., Pinkerton, M.N., Gaffey, B.J., Beggs, K.T., Milne, T.J., and Meikle, M.C. (2007). Osteogenic gene expression by human periodontal ligament cells under cyclic tension. *J. Dent. Res.* 86(12), 1212-1216. doi: 10.1177/154405910708601214.
Wolf, M., Lossdorfer, S., Kupper, K., and Jager, A. (2014). Regulation of high mobility group box protein 1 expression following mechanical loading by orthodontic forces in vitro and in vivo. *Eur. J. Orthod.* 36(6), 624-631. doi: 10.1093/ejo/cjt037.
Wu, J., Song, M., Li, T., Zhu, Z., and Pan, J. (2015). The Rho-mDia1 signaling pathway is required for cyclic strain-induced cytoskeletal rearrangement of human periodontal ligament cells. *Exp. Cell Res.* 337(1), 28-36. doi: 10.1016/j.yexcr.2015.07.016.
Wu, Y., Ou, Y., Liao, C., Liang, S., and Wang, Y. (2019a). High-throughput sequencing analysis of the expression profile of microRNAs and target genes in mechanical force-induced osteoblastic/cementoblastic differentiation of human periodontal ligament cells. *Am. J. Transl. Res.* 11(6), 3398-3411.
Wu, Y., Zhao, D., Zhuang, J., Zhang, F., and Xu, C. (2016). Caspase-8 and Caspase-9 Functioned Differently at Different Stages of the Cyclic Stretch-Induced Apoptosis in Human Periodontal Ligament Cells. *PloS One* 11(12), e0168268. doi: 10.1371/journal.pone.0168268.
Wu, Y., Zhuang, J., Zhao, D., and Xu, C. (2019b). Interaction between caspase-3 and caspase-5 in the stretch-induced programmed cell death in the human periodontal ligament cells. *J. Cell. Physiol.* 234(8), 13571-13581. doi: 10.1002/jcp.28035.
Wu, Y., Zhuang, J., Zhao, D., Zhang, F., Ma, J., and Xu, C. (2017). Cyclic stretch-induced the cytoskeleton rearrangement and gene expression of cytoskeletal regulators in human periodontal ligament cells. *Acta Odontol. Scand.* 75(7), 507-516. doi: 10.1080/00016357.2017.1347823.
Xu, C., Fan, Z., Shan, W., Hao, Y., Ma, J., Huang, Q., et al. (2012). Cyclic stretch influenced expression of membrane connexin 43 in human periodontal ligament cell. *Arch. Oral Biol.* 57(12), 1602-1608. doi: 10.1016/j.archoralbio.2012.07.002.
Xu, C., Hao, Y., Wei, B., Ma, J., Li, J., Huang, Q., et al. (2011). Apoptotic gene expression by human periodontal ligament cells following cyclic stretch. *J. Periodontal Res.* 46(6), 742-748. doi: 10.1111/j.1600-0765.2011.01397.x.
Xu, H., Bai, D., Ruest, L.B., Feng, J.Q., Guo, Y.W., Tian, Y., et al. (2015). Expression analysis of alpha-smooth muscle actin and tenascin-C in the periodontal ligament under orthodontic loading or in vitro culture. *Int. J. Oral Sci.* 7(4), 232-241. doi: 10.1038/ijos.2015.26.
Xu, H.Y., Nie, E.M., Deng, G., Lai, L.Z., Sun, F.Y., Tian, H., et al. (2017). Periostin is essential for periodontal ligament remodeling during orthodontic treatment. *Mol. Med. Rep.* 15(4), 1800-1806. doi: 10.3892/mmr.2017.6200.
Yamaguchi, M., Ozawa, Y., Nogimura, A., Aihara, N., Kojima, T., Hirayama, Y., et al. (2004). Cathepsins B and L increased during response of periodontal ligament cells to mechanical stress in vitro. *Connect Tissue Res.* 45(3), 181-189. doi: 10.1080/03008200490514149.
Yamaguchi, M., and Shimizu, N. (1994). Identification of factors mediating the decrease of alkaline phosphatase activity caused by tension-force in periodontal ligament cells. *Gen. Pharmacol.* 25(6), 1229-1235. doi: 10.1016/0306-3623(94)90142-2.
Yamaguchi, M., Shimizu, N., Goseki, T., Shibata, Y., Takiguchi, H., Iwasawa, T., et al. (1994). Effect of different magnitudes of tension force on prostaglandin E2 production by human periodontal ligament cells. *Arch. Oral Biol.* 39(10), 877-884. doi: 10.1016/0003-9969(94)90019-1.
Yamaguchi, M., Shimizu, N., Ozawa, Y., Saito, K., Miura, S., Takiguchi, H., et al. (1997). Effect of tension-force on plasminogen activator activity from human periodontal ligament cells. *J. Periodontal Res.* 32(3), 308-314. doi: 10.1111/j.1600-0765.1997.tb00539.x.

Yamaguchi, M., Shimizu, N., Shibata, Y., and Abiko, Y. (1996). Effects of different magnitudes of tension-force on alkaline phosphatase activity in periodontal ligament cells. *J. Dent. Res.* 75(3)**,** 889-894. doi: 10.1177/00220345960750030501.
Yamaguchi, N., Chiba, M., and Mitani, H. (2002). The induction of c-fos mRNA expression by mechanical stress in human periodontal ligament cells. *Arch. Oral Biol.* 47(6)**,** 465-471. doi: 10.1016/s0003-9969(02)00022-5.
Yamashiro, K., Myokai, F., Hiratsuka, K., Yamamoto, T., Senoo, K., Arai, H., et al. (2007). Oligonucleotide array analysis of cyclic tension-responsive genes in human periodontal ligament fibroblasts. *Int. J. Biochem. Cell Biol.* 39(5)**,** 910-921. doi: 10.1016/j.biocel.2007.01.015.
Yang, S.Y., Kim, J.W., Lee, S.Y., Kang, J.H., Ulziisaikhan, U., Yoo, H.I., et al. (2015). Upregulation of relaxin receptors in the PDL by biophysical force. *Clin. Oral Investig.* 19(3)**,** 657-665. doi: 10.1007/s00784-014-1276-4.
Yang, S.Y., Wei, F.L., Hu, L.H., and Wang, C.L. (2016). PERK-eIF2alpha-ATF4 pathway mediated by endoplasmic reticulum stress response is involved in osteodifferentiation of human periodontal ligament cells under cyclic mechanical force. *Cell. Signal.* 28(8)**,** 880-886. doi: 10.1016/j.cellsig.2016.04.003.
Yang, Y., Wang, B.K., Chang, M.L., Wan, Z.Q., and Han, G.L. (2018). Cyclic Stretch Enhances Osteogenic Differentiation of Human Periodontal Ligament Cells via YAP Activation. *Biomed Res. Int.* 2018**,** 2174824. doi: 10.1155/2018/2174824.
Yang, Y., Yang, Y., Li, X., Cui, L., Fu, M., Rabie, A.B., et al. (2010). Functional analysis of core binding factor a1 and its relationship with related genes expressed by human periodontal ligament cells exposed to mechanical stress. *Eur. J. Orthod.* 32(6)**,** 698-705. doi: 10.1093/ejo/cjq010.
Yang, Y.Q., Li, X.T., Rabie, A.B., Fu, M.K., and Zhang, D. (2006). Human periodontal ligament cells express osteoblastic phenotypes under intermittent force loading in vitro. *Front. Biosci.* 11**,** 776-781. doi: 10.2741/1835.
Yoshino, H., Morita, I., Murota, S.I., and Ishikawa, I. (2003). Mechanical stress induces production of angiogenic regulators in cultured human gingival and periodontal ligament fibroblasts. *J. Periodontal Res.* 38(4)**,** 405-410. doi: 10.1034/j.1600-0765.2003.00660.x.
Yu, W., Hu, B., Shi, X., Cao, Z., Ren, M., He, Z., et al. (2018). Nicotine inhibits osteogenic differentiation of human periodontal ligament cells under cyclic tensile stress through canonical Wnt pathway and alpha7 nicotinic acetylcholine receptor. *J. Periodontal Res.* 53(4)**,** 555-564. doi: 10.1111/jre.12545.
Yuda, A., Maeda, H., Fujii, S., Monnouchi, S., Yamamoto, N., Wada, N., et al. (2015). Effect of CTGF/CCN2 on osteo/cementoblastic and fibroblastic differentiation of a human periodontal ligament stem/progenitor cell line. *J. Cell. Physiol.* 230(1)**,** 150-159. doi: 10.1002/jcp.24693.
Zhao, D., Wu, Y., Xu, C., and Zhang, F. (2017). Cyclic-stretch induces apoptosis in human periodontal ligament cells by activation of caspase-5. *Arch. Oral Biol.* 73**,** 129-135. doi: 10.1016/j.archoralbio.2016.10.009.
Zhao, D., Wu, Y., Zhuang, J., Xu, C., and Zhang, F. (2016). Activation of NLRP1 and NLRP3 inflammasomes contributed to cyclic stretch-induced pyroptosis and release of IL-1beta in human periodontal ligament cells. *Oncotarget* 7(42)**,** 68292-68302. doi: 10.18632/oncotarget.11944.
Zhuang, J., Wang, Y., Qu, F., Wu, Y., Zhao, D., and Xu, C. (2019). Gasdermin-d Played a Critical Role in the Cyclic Stretch-Induced Inflammatory Reaction in Human Periodontal Ligament Cells. *Inflammation* 42(2)**,** 548-558. doi: 10.1007/s10753-018-0912-6.
Ziegler, N., Alonso, A., Steinberg, T., Woodnutt, D., Kohl, A., Mussig, E., et al. (2010). Mechano-transduction in periodontal ligament cells identifies activated states of MAP-kinases p42/44 and p38-stress kinase as a mechanism for MMP-13 expression. *BMC Cell Biol.* 11**,** 10. doi: 10.1186/1471-2121-11-10.

Supplement 6 Selected publications reporting data on the top 10 most frequently investigated genes, proteins and metabolites

The publications are tabulated according to the direction of regulation reported ("increase of expression", "decrease of expression", "no effect of tension force on expression", and "other changes in expression").

Designations used in publications	Gene symbol	Articles reporting an increase of expression[1]		Articles reporting a decrease of expression[1]		Articles reporting no effect of tension force on expression[1]		Articles reporting other changes in expression	Total number of citations
		Gene	Protein/Metabolite	Gene	Protein/Metabolite	Gene	Protein/Metabolite		
Runx2 RUNX2 / p-RUNX2 CBFA1	*RUNX2*	Chang et al. (2017), Fujihara et al. (2010), He et al. (2019), Jiang and Hua (2016), Lee et al. (2015), Li et al. (2014), Li et al. (2015), Liu et al. (2017), Ren et al. (2015), Shen et al. (2014), Tang et al. (2012), Wada et al. (2017), Wang et al. (2019a), Wang et al. (2019b), Wei et al. (2014), Wei et al. (2015), Wu et al. (2019), Yang et al. (2018), Yu et al. (2018)	Jiang and Hua (2016), Li et al. (2014), Li et al. (2015), Shen et al. (2014), Tang et al. (2012), Wang et al. (2019b), Wei et al. (2014), Wu et al. (2019), Yu et al. (2018)	Nokhbehsaim et al. (2010), Nokhbehsaim et al. (2011)				Cho et al. (2010), Li et al. (2013), Sun et al. (2017), Sun et al. (2016), Yang et al. (2010)	**26**
ALP	*ALPP*	Chang et al. (2015), Chen et al. (2014), Fujihara et al. (2010), Jacobs et al. (2013), Jiang and Hua (2016), Konstantonis et al. (2014), Lee et al. (2015), Liu et al. (2017), Monnouchi et al. (2011), Papadopoulou et al. (2019), Shen et al. (2014), Yang et al. (2018)	Chang et al. (2017), Chen et al. (2014), Jiang and Hua (2016), Konstantonis et al. (2014), Matsuda et al. (1998), Nazet et al. (2020), Shen et al. (2014), Wei et al. (2015), Yang et al. (2006)	Yamaguchi et al. (1996)	Chiba and Mitani (2004), Yamaguchi and Shimizu (1994), Yamaguchi et al. (1996)			Nokhbehsaim et al. (2010), Qin and Hua (2016), Yamaguchi et al. (2002), Yang et al. (2010)	***24***
OCN OC Osteocalcin	*BGLAP*	Chang et al. (2015), Chen et al. (2014), Jiang and Hua (2016), Kim et al. (2007), Lee et al. (2015), Ren et al. (2015), Shen et al. (2014), Wang et al. (2019a), Wang et al. (2019b), Wei et al. (2014), Wei et al. (2015), Wu et al. (2019), Yang et al. (2016), Yang et al. (2018)	Chang et al. (2017), Chen et al. (2014), Jiang and Hua (2016), Shen et al. (2014), Wang et al. (2019b), Wei et al. (2014), Yang et al. (2006), Yang et al. (2018)					Jacobs et al. (2013), Qin and Hua (2016)	**18**
IL-1β IL1β	*IL1B*	Lee et al. (2012), Nokhbehsaim et al. (2010), Ritter et al. (2007), Shimizu et al. (1997), Wada et al. (2017)	Abiko et al. (1998), Kaku et al. (2019), Liu et al. (2017), Shimizu et al. (1994), Shimizu et al. (1995), Shimizu et al. (1997), Sun et al. (2016), Sun et al. (2017)	Nokhbehsaim et al. (2012)				Long et al. (2001), Zhao et al. (2016), Zhuang et al. (2019)	***16***

1. Increase = "Increase" or "Increase with Plateau"; Decrease = "Decrease" or "Decrease with Plateau"…
2. The citations in red font appeared more than once. - **(each citation is counted only once)**

Designations used in publications	Gene symbol	Articles reporting an increase of expression[1]		Articles reporting a decrease of expression[1]		Articles reporting no effect of tension force on expression[1]		Articles reporting other changes in expression	Total number of citations
		Gene	Protein/Metabolite	Gene	Protein/Metabolite	Gene	Protein/Metabolite		
COX2	*PTGS2*	Abiko et al. (1998), Agarwal et al. (2003), Jacobs et al. (2014), Jacobs et al. (2018), Nazet et al. (2020), Nokhbehsaim et al. (2010) (20%) , Nokhbehsaim et al. (2012) (20%) , Ohzeki et al. (1999), Shimizu et al. (1998), Suzuki et al. (2014), Wada et al. (2017), Wang et al. (2011)	Long et al. (2002), Nogueira et al. (2014)			Nokhbehsaim et al. (2012) (3%)		Nokhbehsaim et al. (2010) (3%)	**14**
OPG (Cytokine)	*TNFRSF11B*	Jacobs et al. (2013), Jacobs et al. (2015), Kanzaki et al. (2006), Kanzaki et al. (2019), Lee et al. (2015), Li et al. (2015), Liao and Hua (2013), Liu et al. (2017), Monnouchi et al. (2011), Spencer and Lallier (2009), Tsuji et al. (2004)	Jacobs et al. (2013), Jacobs et al. (2015), Kanzaki et al. (2006), Kanzaki et al. (2019), Li et al. (2015), Liao and Hua (2013), Tsuji et al. (2004)	Nogueira et al. (2014), Yang et al. (2006)	Nogueira et al. (2014), Yang et al. (2006)			Yang et al. (2010)	**14**
RANKL (Cytokine)	*TNFSF11*	Kanzaki et al. (2006), Kanzaki et al. (2019), Lee et al. (2015), Li et al. (2015), Liao and Hua (2013), Liu et al. (2017), Yang et al. (2010)	Li et al. (2015), Kaku et al. (2019)	Nogueira et al. (2014), Spencer and Lallier (2009)	Liao and Hua (2013), Nogueira et al. (2014)	Tsuji et al. (2004)		Jacobs et al. (2013), Jacobs et al. (2015), Monnouchi et al. (2011)	**14**
COL1A1 COLIα1 Collagen type-I (COL-1) Colα1 (collagen α1) COL1 COL-I	*COL1A1*	Chen et al. (2015), He et al. (2004), Lee et al. (2015), Takano et al. (2009), Wang et al. (2019b), Yang et al. (2018), Yu et al. (2018)	He et al. (2004), Qin and Hua (2016), Takano et al. (2009), Wang et al. (2019b), Yu et al. (2018)	Nemoto et al. (2010), Sun et al. (2017)	Sun et al. (2016), Sun et al. (2017)			Jacobs et al. (2013) Yamaguchi et al. (2002)	**13**
PGE_2	PGE_2		Abiko et al. (1998), Agarwal et al. (2003), Jacobs et al. (2014), Long et al. (2002), Ngan et al. (1990), Nogueira et al. (2014), Ohzeki et al. (1999), Shimizu et al. (1995), Shimizu et al. (1998), Suzuki et al. (2014), Yamaguchi et al. (1994)				Jacobs et al. (2018)		**12**
OSX SP7 Osx	*SP7*	Li et al. (2014), Li et al. (2015) Ren et al. (2015), Tang et al. (2012), Wang et al. (2019a), Wang et al. (2019b), Yang et al. (2018), Yu et al. (2018)	Chang et al. (2017), Li et al. (2014), Li et al. (2015), Tang et al. (2012), Wang et al. (2019b), Yu et al. (2018)	Li et al. (2013)				Li et al. (2013) (protein)	**10**

1. Increase = “Increase” or “Increase with Plateau”; Decrease = “Decrease” or “Decrease with Plateau”…
2. The citations in red font appeared more than once. - **(each citation is counted only once)**

References

Abiko, Y., Shimizu, N., Yamaguchi, M., Suzuki, H., and Takiguchi, H. (1998). Effect of aging on functional changes of periodontal tissue cells. *Ann. Periodontol.* 3(1), 350-369. doi: 10.1902/annals.1998.3.1.350.

Agarwal, S., Long, P., Seyedain, A., Piesco, N., Shree, A., and Gassner, R. (2003). A central role for the nuclear factor-κB pathway in anti-inflammatory and proinflammatory actions of mechanical strain. *FASEB J.* 17(8), 899-901. doi: 10.1096/fj.02-0901fje.

Chang, M., Lin, H., Fu, H., Wang, B., Han, G., and Fan, M. (2017). MicroRNA-195-5p regulates osteogenic differentiation of periodontal ligament cells under mechanical loading. *J. Cell. Physiol.* 232(12), 3762-3774. doi: 10.1002/jcp.25856.

Chang, M., Lin, H., Luo, M., Wang, J., and Han, G. (2015). Integrated miRNA and mRNA expression profiling of tension force-induced bone formation in periodontal ligament cells. *In Vitro Cell. Dev. Biol. Anim.* 51(8), 797-807. doi: 10.1007/s11626-015-9892-0.

Chen, Y., Mohammed, A., Oubaidin, M., Evans, C.A., Zhou, X., Luan, X., et al. (2015). Cyclic stretch and compression forces alter microRNA-29 expression of human periodontal ligament cells. *Gene* 566(1), 13-17. doi: 10.1016/j.gene.2015.03.055.

Chen, Y.J., Shie, M.Y., Hung, C.J., Wu, B.C., Liu, S.L., Huang, T.H., et al. (2014). Activation of focal adhesion kinase induces extracellular signal-regulated kinase-mediated osteogenesis in tensile force-subjected periodontal ligament fibroblasts but not in osteoblasts. *J. Bone Miner. Metab.* 32(6), 671-682. doi: 10.1007/s00774-013-0549-3.

Chiba, M., and Mitani, H. (2004). Cytoskeletal changes and the system of regulation of alkaline phosphatase activity in human periodontal ligament cells induced by mechanical stress. *Cell Biochem. Funct.* 22(4), 249-256. doi: 10.1002/cbf.1097.

Cho, J.H., Lee, S.K., Lee, J.W., and Kim, E.C. (2010). The role of heme oxygenase-1 in mechanical stress- and lipopolysaccharide-induced osteogenic differentiation in human periodontal ligament cells. *Angle Orthod.* 80(4), 552-559. doi: 10.2319/091509-520.1.

Fujihara, C., Yamada, S., Ozaki, N., Takeshita, N., Kawaki, H., Takano-Yamamoto, T., et al. (2010). Role of mechanical stress-induced glutamate signaling-associated molecules in cytodifferentiation of periodontal ligament cells. *J. Biol. Chem.* 285(36), 28286-28297. doi: 10.1074/jbc.M109.097303.

He, Y., Macarak, E.J., Korostoff, J.M., and Howard, P.S. (2004). Compression and tension: differential effects on matrix accumulation by periodontal ligament fibroblasts in vitro. *Connect Tissue Res.* 45(1), 28-39. doi: 10.1080/03008200490278124.

He, Y., Xu, H., Xiang, Z., Yu, H., Xu, L., Guo, Y., et al. (2019). YAP regulates periodontal ligament cell differentiation into myofibroblast interacted with RhoA/ROCK pathway. *J. Cell. Physiol.* 234(4), 5086-5096. doi: 10.1002/jcp.27312.

Jacobs, C., Grimm, S., Ziebart, T., Walter, C., and Wehrbein, H. (2013). Osteogenic differentiation of periodontal fibroblasts is dependent on the strength of mechanical strain. *Arch. Oral Biol.* 58(7), 896-904. doi: 10.1016/j.archoralbio.2013.01.009.

Jacobs, C., Schramm, S., Dirks, I., Walter, C., Pabst, A., Meila, D., et al. (2018). Mechanical loading increases pro-inflammatory effects of nitrogen-containing bisphosphonate in human periodontal fibroblasts. *Clin. Oral Investig.* 22(2), 901-907. doi: 10.1007/s00784-017-2168-1.

Jacobs, C., Walter, C., Ziebart, T., Dirks, I., Schramm, S., Grimm, S., et al. (2015). Mechanical loading influences the effects of bisphosphonates on human periodontal ligament fibroblasts. *Clin. Oral Investig.* 19(3), 699-708. doi: 10.1007/s00784-014-1284-4.

Jacobs, C., Walter, C., Ziebart, T., Grimm, S., Meila, D., Krieger, E., et al. (2014). Induction of IL-6 and MMP-8 in human periodontal fibroblasts by static tensile strain. *Clin. Oral Investig.* 18(3), 901-908. doi: 10.1007/s00784-013-1032-1.

Jiang, Z., and Hua, Y. (2016). Hydrogen sulfide promotes osteogenic differentiation of human periodontal ligament cells via p38-MAPK signaling pathway under proper tension stimulation. *Arch. Oral Biol.* 72, 8-13. doi: 10.1016/j.archoralbio.2016.08.008.

Kaku, M., Yamamoto, T., Yashima, Y., Izumino, J., Kagawa, H., Ikeda, K., et al. (2019). Acetaminophen reduces apical root resorption during orthodontic tooth movement in rats. *Arch. Oral Biol.* 102, 83-92. doi: 10.1016/j.archoralbio.2019.04.002.

Kanzaki, H., Chiba, M., Sato, A., Miyagawa, A., Arai, K., Nukatsuka, S., et al. (2006). Cyclical tensile force on periodontal ligament cells inhibits osteoclastogenesis through OPG induction. *J. Dent. Res.* 85(5), 457-462. doi: 10.1177/154405910608500512.

Kanzaki, H., Wada, S., Yamaguchi, Y., Katsumata, Y., Itohiya, K., Fukaya, S., et al. (2019). Compression and tension variably alter Osteoprotegerin expression via miR-3198 in periodontal ligament cells. *BMC Mol. Cell Biol.* 20(1), 6. doi: 10.1186/s12860-019-0187-2.

Kim, H.J., Choi, Y.S., Jeong, M.J., Kim, B.O., Lim, S.H., Kim, D.K., et al. (2007). Expression of UNCL during development of periodontal tissue and response of periodontal ligament fibroblasts to mechanical stress in vivo and in vitro. *Cell Tissue Res.* 327(1), 25-31. doi: 10.1007/s00441-006-0304-3.

Konstantonis, D., Papadopoulou, A., Makou, M., Eliades, T., Basdra, E., and Kletsas, D. (2014). The role of cellular senescence on the cyclic stretching-mediated activation of MAPK and ALP expression and activity in human periodontal ligament fibroblasts. *Exp. Gerontol.* 57, 175-180. doi: 10.1016/j.exger.2014.05.010.

Lee, S.I., Park, K.H., Kim, S.J., Kang, Y.G., Lee, Y.M., and Kim, E.C. (2012). Mechanical stress-activated immune response genes via Sirtuin 1 expression in human periodontal ligament cells. *Clin. Exp. Immunol.* 168(1), 113-124. doi: 10.1111/j.1365-2249.2011.04549.x.

Lee, S.Y., Yoo, H.I., and Kim, S.H. (2015). CCR5-CCL Axis in PDL during Orthodontic Biophysical Force Application. *J. Dent. Res.* 94(12), 1715-1723. doi: 10.1177/0022034515603926.

Li, L., Han, M., Li, S., Wang, L., and Xu, Y. (2013). Cyclic tensile stress during physiological occlusal force enhances osteogenic differentiation of human periodontal ligament cells via ERK1/2-Elk1 MAPK pathway. *DNA Cell Biol.* 32(9), 488-497. doi: 10.1089/dna.2013.2070.

Li, L., Han, M.X., Li, S., Xu, Y., and Wang, L. (2014). Hypoxia regulates the proliferation and osteogenic differentiation of human periodontal ligament cells under cyclic tensile stress via mitogen-activated protein kinase pathways. *J. Periodontol.* 85(3), 498-508. doi: 10.1902/jop.2013.130048.

Li, S., Zhang, H., Li, S., Yang, Y., Huo, B., and Zhang, D. (2015). Connexin 43 and ERK regulate tension-induced signal transduction in human periodontal ligament fibroblasts. *J. Orthop. Res.* 33(7), 1008-1014. doi: 10.1002/jor.22830.

Liao, C., and Hua, Y. (2013). Effect of hydrogen sulphide on the expression of osteoprotegerin and receptor activator of NF-kappaB ligand in human periodontal ligament cells induced by tension-force stimulation. *Arch. Oral Biol.* 58(12), 1784-1790. doi: 10.1016/j.archoralbio.2013.08.004.

Liu, J., Li, Q., Liu, S., Gao, J., Qin, W., Song, Y., et al. (2017). Periodontal Ligament Stem Cells in the Periodontitis Microenvironment Are Sensitive to Static Mechanical Strain. *Stem Cells Int.* 2017, 1380851. doi: 10.1155/2017/1380851.

Long, P., Hu, J., Piesco, N., Buckley, M., and Agarwal, S. (2001). Low magnitude of tensile strain inhibits IL-1beta-dependent induction of pro-inflammatory cytokines and induces synthesis of IL-10 in human periodontal ligament cells in vitro. *J. Dent. Res.* 80(5), 1416-1420. doi: 10.1177/00220345010800050601.

Long, P., Liu, F., Piesco, N.P., Kapur, R., and Agarwal, S. (2002). Signaling by mechanical strain involves transcriptional regulation of proinflammatory genes in human periodontal ligament cells in vitro. *Bone* 30(4), 547-552. doi: 10.1016/s8756-3282(02)00673-7.

Matsuda, N., Yokoyama, K., Takeshita, S., and Watanabe, M. (1998). Role of epidermal growth factor and its receptor in mechanical stress-induced differentiation of human periodontal ligament cells in vitro. *Arch. Oral Biol.* 43(12), 987-997. doi: 10.1016/s0003-9969(98)00079-x.

Monnouchi, S., Maeda, H., Fujii, S., Tomokiyo, A., Kono, K., and Akamine, A. (2011). The roles of angiotensin II in stretched periodontal ligament cells. *J. Dent. Res.* 90(2), 181-185. doi: 10.1177/0022034510382118.

Nazet, U., Schröder, A., Spanier, G., Wolf, M., Proff, P., and Kirschneck, C. (2020). Simplified method for applying static isotropic tensile strain in cell culture experiments with identification of valid RT-qPCR reference genes for PDL fibroblasts. *Eur. J. Orthod.* 42(4), 359-370. doi: 10.1093/ejo/cjz052.

Nemoto, T., Kajiya, H., Tsuzuki, T., Takahashi, Y., and Okabe, K. (2010). Differential induction of collagens by mechanical stress in human periodontal ligament cells. *Arch. Oral Biol.* 55(12), 981-987. doi: 10.1016/j.archoralbio.2010.08.004.

Ngan, P., Saito, S., Saito, M., Lanese, R., Shanfeld, J., and Davidovitch, Z. (1990). The interactive effects of mechanical stress and interleukin-1 beta on prostaglandin E and cyclic AMP production in human periodontal ligament fibroblasts in vitro: comparison with cloned osteoblastic cells of mouse (MC3T3-E1). *Arch. Oral Biol.* 35(9), 717-725. doi: 10.1016/0003-9969(90)90094-Q.

Nogueira, A.V., Nokhbehsaim, M., Eick, S., Bourauel, C., Jäger, A., Jepsen, S., et al. (2014). Biomechanical loading modulates proinflammatory and bone resorptive mediators in bacterial-stimulated PDL cells. *Mediators Inflamm.* 2014, 425421. doi: 10.1155/2014/425421.

Nokhbehsaim, M., Deschner, B., Bourauel, C., Reimann, S., Winter, J., Rath, B., et al. (2011). Interactions of enamel matrix derivative and biomechanical loading in periodontal regenerative healing. *J. Periodontol.* 82(12), 1725-1734. doi: 10.1902/jop.2011.100678.

Nokhbehsaim, M., Deschner, B., Winter, J., Bourauel, C., Jäger, A., Jepsen, S., et al. (2012). Anti-inflammatory effects of EMD in the presence of biomechanical loading and interleukin-1β in vitro. *Clin. Oral Investig.* 16(1), 275-283. doi: 10.1007/s00784-010-0505-8.

Nokhbehsaim, M., Deschner, B., Winter, J., Reimann, S., Bourauel, C., Jepsen, S., et al. (2010). Contribution of orthodontic load to inflammation-mediated periodontal destruction. *J. Orofac. Orthop.* 71(6), 390-402. doi: 10.1007/s00056-010-1031-7.

Ohzeki, K., Yamaguchi, M., Shimizu, N., and Abiko, Y. (1999). Effect of cellular aging on the induction of cyclooxygenase-2 by mechanical stress in human periodontal ligament cells. *Mech. Ageing Dev.* 108(2), 151-163. doi: 10.1016/s0047-6374(99)00006-8.

Papadopoulou, A., Todaro, A., Eliades, T., and Kletsas, D. (2019). Effect of hyperglycaemic conditions on the response of human periodontal ligament fibroblasts to mechanical stretching. *Eur. J. Orthod.* doi: 10.1093/ejo/cjz051.

Qin, J., and Hua, Y. (2016). Effects of hydrogen sulfide on the expression of alkaline phosphatase, osteocalcin and collagen type I in human periodontal ligament cells induced by tension force stimulation. *Mol. Med. Rep.* 14(4), 3871-3877. doi: 10.3892/mmr.2016.5680.

Ren, D., Wei, F., Hu, L., Yang, S., Wang, C., and Yuan, X. (2015). Phosphorylation of Runx2, induced by cyclic mechanical tension via ERK1/2 pathway, contributes to osteodifferentiation of human periodontal ligament fibroblasts. *J. Cell. Physiol.* 230(10), 2426-2436. doi: 10.1002/jcp.24972.

Ritter, N., Mussig, E., Steinberg, T., Kohl, A., Komposch, G., and Tomakidi, P. (2007). Elevated expression of genes assigned to NF-kappaB and apoptotic pathways in human periodontal ligament fibroblasts following mechanical stretch. *Cell Tissue Res.* 328(3), 537-548. doi: 10.1007/s00441-007-0382-x.

Shen, T., Qiu, L., Chang, H., Yang, Y., Jian, C., Xiong, J., et al. (2014). Cyclic tension promotes osteogenic differentiation in human periodontal ligament stem cells. *Int. J. Clin. Exp. Pathol.* 7(11), 7872-7880.

Shimizu, N., Goseki, T., Yamaguchi, M., Iwasawa, T., Takiguchi, H., and Abiko, Y. (1997). In vitro cellular aging stimulates interleukin-1 beta production in stretched human periodontal-ligament-derived cells. *J. Dent. Res.* 76(7), 1367-1375. doi: 10.1177/00220345970760070601.

Shimizu, N., Ozawa, Y., Yamaguchi, M., Goseki, T., Ohzeki, K., and Abiko, Y. (1998). Induction of COX-2 expression by mechanical tension force in human periodontal ligament cells. *J. Periodontol.* 69(6), 670-677. doi: 10.1902/jop.1998.69.6.670.

Shimizu, N., Yamaguchi, M., Goseki, T., Ozawa, Y., Saito, K., Takiguchi, H., et al. (1994). Cyclic-tension force stimulates interleukin-1 beta production by human periodontal ligament cells. *J. Periodontal Res.* 29(5), 328-333. doi: 10.1111/j.1600-0765.1994.tb01230.x.

Shimizu, N., Yamaguchi, M., Goseki, T., Shibata, Y., Takiguchi, H., Iwasawa, T., et al. (1995). Inhibition of prostaglandin E2 and interleukin 1-beta production by low-power laser irradiation in stretched human periodontal ligament cells. *J. Dent. Res.* 74(7), 1382-1388. doi: 10.1177/00220345950740071001.

Spencer, A.Y., and Lallier, T.E. (2009). Mechanical tension alters semaphorin expression in the periodontium. *J. Periodontol.* 80(10), 1665-1673. doi: 10.1902/jop.2009.090212.

Sun, C., Chen, L., Shi, X., Cao, Z., Hu, B., Yu, W., et al. (2016). Combined effects of proinflammatory cytokines and intermittent cyclic mechanical strain in inhibiting osteogenicity in human periodontal ligament cells. *Cell Biol. Int.* 40(9), 999-1007. doi: 10.1002/cbin.10641.

Sun, C., Liu, F., Cen, S., Chen, L., Wang, Y., Sun, H., et al. (2017). Tensile strength suppresses the osteogenesis of periodontal ligament cells in inflammatory microenvironments. *Mol. Med. Rep.* 16(1), 666-672. doi: 10.3892/mmr.2017.6644.

Suzuki, R., Nemoto, E., and Shimauchi, H. (2014). Cyclic tensile force up-regulates BMP-2 expression through MAP kinase and COX-2/PGE2 signaling pathways in human periodontal ligament cells. *Exp. Cell Res.* 323(1), 232-241. doi: 10.1016/j.yexcr.2014.02.013.

Takano, M., Yamaguchi, M., Nakajima, R., Fujita, S., Kojima, T., and Kasai, K. (2009). Effects of relaxin on collagen type I released by stretched human periodontal ligament cells. *Orthod. Craniofac. Res.* 12(4), 282-288. doi: 10.1111/j.1601-6343.2009.01463.x.

Tang, N., Zhao, Z., Zhang, L., Yu, Q., Li, J., Xu, Z., et al. (2012). Up-regulated osteogenic transcription factors during early response of human periodontal ligament stem cells to cyclic tensile strain. *Arch. Med. Sci.* 8(3), 422-430. doi: 10.5114/aoms.2012.28810.

Tsuji, K., Uno, K., Zhang, G.X., and Tamura, M. (2004). Periodontal ligament cells under intermittent tensile stress regulate mRNA expression of osteoprotegerin and tissue inhibitor of matrix metalloprotease-1 and -2. *J. Bone Miner. Metab.* 22(2), 94-103. doi: 10.1007/s00774-003-0456-0.

Wada, S., Kanzaki, H., Narimiya, T., and Nakamura, Y. (2017). Novel device for application of continuous mechanical tensile strain to mammalian cells. *Biol. Open* 6(4), 518-524. doi: 10.1242/bio.023671.

Wang, H., Feng, C., Jin, Y., Tan, W., and Wei, F. (2019a). Identification and characterization of circular RNAs involved in mechanical force-induced periodontal ligament stem cells. *J. Cell. Physiol.* 234(7), 10166-10177. doi: 10.1002/jcp.27686.

Wang, Y., Hu, B., Hu, R., Tong, X., Zhang, M., Xu, C., et al. (2019b). TAZ contributes to osteogenic differentiation of periodontal ligament cells under tensile stress. *J. Periodontal Res.* doi: 10.1111/jre.12698.

Wang, Y., Li, Y., Fan, X., Zhang, Y., Wu, J., and Zhao, Z. (2011). Early proliferation alteration and differential gene expression in human periodontal ligament cells subjected to cyclic tensile stress. *Arch. Oral Biol.* 56(2), 177-186. doi: 10.1016/j.archoralbio.2010.09.009.

Wei, F., Liu, D., Feng, C., Zhang, F., Yang, S., Hu, Y., et al. (2015). microRNA-21 mediates stretch-induced osteogenic differentiation in human periodontal ligament stem cells. *Stem Cells Dev.* 24(3), 312-319. doi: 10.1089/scd.2014.0191.

Wei, F.L., Wang, J.H., Ding, G., Yang, S.Y., Li, Y., Hu, Y.J., et al. (2014). Mechanical force-induced specific MicroRNA expression in human periodontal ligament stem cells. *Cells Tissues Organs* 199(5-6), 353-363. doi: 10.1159/000369613.

Wu, Y., Ou, Y., Liao, C., Liang, S., and Wang, Y. (2019). High-throughput sequencing analysis of the expression profile of microRNAs and target genes in mechanical force-induced osteoblastic/cementoblastic differentiation of human periodontal ligament cells. *Am. J. Transl. Res.* 11(6), 3398-3411.

Yamaguchi, M., and Shimizu, N. (1994). Identification of factors mediating the decrease of alkaline phosphatase activity caused by tension-force in periodontal ligament cells. *Gen. Pharmacol.* 25(6), 1229-1235. doi: 10.1016/0306-3623(94)90142-2.

Yamaguchi, M., Shimizu, N., Goseki, T., Shibata, Y., Takiguchi, H., Iwasawa, T., et al. (1994). Effect of different magnitudes of tension force on prostaglandin E2 production by human periodontal ligament cells. *Arch. Oral Biol.* 39(10), 877-884. doi: 10.1016/0003-9969(94)90019-1.

Yamaguchi, M., Shimizu, N., Shibata, Y., and Abiko, Y. (1996). Effects of different magnitudes of tension-force on alkaline phosphatase activity in periodontal ligament cells. *J. Dent. Res.* 75(3), 889-894. doi: 10.1177/00220345960750030501.

Yamaguchi, N., Chiba, M., and Mitani, H. (2002). The induction of c-fos mRNA expression by mechanical stress in human periodontal ligament cells. *Arch. Oral Biol.* 47(6), 465-471. doi: 10.1016/s0003-9969(02)00022-5.

Yang, S.Y., Wei, F.L., Hu, L.H., and Wang, C.L. (2016). PERK-eIF2alpha-ATF4 pathway mediated by endoplasmic reticulum stress response is involved in osteodifferentiation of human periodontal ligament cells under cyclic mechanical force. *Cell. Signal.* 28(8), 880-886. doi: 10.1016/j.cellsig.2016.04.003.

Yang, Y., Wang, B.K., Chang, M.L., Wan, Z.Q., and Han, G.L. (2018). Cyclic Stretch Enhances Osteogenic Differentiation of Human Periodontal Ligament Cells via YAP Activation. *Biomed Res. Int.* 2018, 2174824. doi: 10.1155/2018/2174824.

Yang, Y., Yang, Y., Li, X., Cui, L., Fu, M., Rabie, A.B., et al. (2010). Functional analysis of core binding factor a1 and its relationship with related genes expressed by human periodontal ligament cells exposed to mechanical stress. *Eur. J. Orthod.* 32(6), 698-705. doi: 10.1093/ejo/cjq010.

Yang, Y.Q., Li, X.T., Rabie, A.B., Fu, M.K., and Zhang, D. (2006). Human periodontal ligament cells express osteoblastic phenotypes under intermittent force loading in vitro. *Front. Biosci.* 11, 776-781. doi: 10.2741/1835.

Yu, W., Hu, B., Shi, X., Cao, Z., Ren, M., He, Z., et al. (2018). Nicotine inhibits osteogenic differentiation of human periodontal ligament cells under cyclic tensile stress through canonical Wnt pathway and alpha7 nicotinic acetylcholine receptor. *J. Periodontal Res.* 53(4), 555-564. doi: 10.1111/jre.12545.

Zhao, D., Wu, Y., Zhuang, J., Xu, C., and Zhang, F. (2016). Activation of NLRP1 and NLRP3 inflammasomes contributed to cyclic stretch-induced pyroptosis and release of IL-1beta in human periodontal ligament cells. *Oncotarget* 7(42), 68292-68302. doi: 10.18632/oncotarget.11944.

Zhuang, J., Wang, Y., Qu, F., Wu, Y., Zhao, D., and Xu, C. (2019). Gasdermin-d Played a Critical Role in the Cyclic Stretch-Induced Inflammatory Reaction in Human Periodontal Ligament Cells. *Inflammation* 42(2), 548-558. doi: 10.1007/s10753-018-0912-6.

Supplement 6 Selected publications reporting data on the top 10 most frequently investigated genes, proteins and metabolites

The publications are tabulated according to the direction of regulation reported ("increase of expression", "decrease of expression", "no effect of tension force on expression", and "other changes in expression").

Designations used in publications	Gene symbol	Articles reporting an increase of expression[1]		Articles reporting a decrease of expression[1]		Articles reporting no effect of tension force on expression[1]		Articles reporting other changes in expression	Total number of citations
		Gene	Protein/Metabolite	Gene	Protein/Metabolite	Gene	Protein/Metabolite		
Runx2 RUNX2 / p-RUNX2 CBFA1	*RUNX2*	Chang et al. (2017), Fujihara et al. (2010), He et al. (2019), Jiang and Hua (2016), Lee et al. (2015), Li et al. (2014), Li et al. (2015), Liu et al. (2017), Ren et al. (2015), Shen et al. (2014), Tang et al. (2012), Wada et al. (2017), Wang et al. (2019a), Wang et al. (2019b), Wei et al. (2014), Wei et al. (2015), Wu et al. (2019), Yang et al. (2018), Yu et al. (2018)	Jiang and Hua (2016), Li et al. (2014), Li et al. (2015), Shen et al. (2014), Tang et al. (2012), Wang et al. (2019b), Wei et al. (2014), Wu et al. (2019), Yu et al. (2018)	Nokhbehsaim et al. (2010), Nokhbehsaim et al. (2011)				Cho et al. (2010), Li et al. (2013), Sun et al. (2017), Sun et al. (2016), Yang et al. (2010)	**26**
ALP	*ALPP*	Chang et al. (2015), Chen et al. (2014), Fujihara et al. (2010), Jacobs et al. (2013), Jiang and Hua (2016), Konstantonis et al. (2014), Lee et al. (2015), Liu et al. (2017), Monnouchi et al. (2011), Papadopoulou et al. (2019), Shen et al. (2014), Yang et al. (2018)	Chang et al. (2017), Chen et al. (2014), Jiang and Hua (2016), Konstantonis et al. (2014), Matsuda et al. (1998), Nazet et al. (2020), Shen et al. (2014), Wei et al. (2015), Yang et al. (2006)	Yamaguchi et al. (1996)	Chiba and Mitani (2004), Yamaguchi and Shimizu (1994), Yamaguchi et al. (1996)			Nokhbehsaim et al. (2010), Qin and Hua (2016), Yamaguchi et al. (2002), Yang et al. (2010)	***24***
OCN OC Osteocalcin	*BGLAP*	Chang et al. (2015), Chen et al. (2014), Jiang and Hua (2016), Kim et al. (2007), Lee et al. (2015), Ren et al. (2015), Shen et al. (2014), Wang et al. (2019a), Wang et al. (2019b), Wei et al. (2014), Wei et al. (2015), Wu et al. (2019), Yang et al. (2016), Yang et al. (2018)	Chang et al. (2017), Chen et al. (2014), Jiang and Hua (2016), Shen et al. (2014), Wang et al. (2019b), Wei et al. (2014), Yang et al. (2006), Yang et al. (2018)					Jacobs et al. (2013), Qin and Hua (2016)	**18**
IL-1β IL1β	*IL1B*	Lee et al. (2012), Nokhbehsaim et al. (2010), Ritter et al. (2007), Shimizu et al. (1997), Wada et al. (2017)	Abiko et al. (1998), Kaku et al. (2019), Liu et al. (2017), Shimizu et al. (1994), Shimizu et al. (1995), Shimizu et al. (1997), Sun et al. (2016), Sun et al. (2017)	Nokhbehsaim et al. (2012)				Long et al. (2001), Zhao et al. (2016), Zhuang et al. (2019)	***16***

1. Increase = "Increase" or "Increase with Plateau"; Decrease = "Decrease" or "Decrease with Plateau"…
2. The citations in red font appeared more than once. - **(each citation is counted only once)**

Designations used in publications	Gene symbol	Articles reporting an increase of expression[1]		Articles reporting a decrease of expression[1]		Articles reporting no effect of tension force on expression[1]		Articles reporting other changes in expression	Total number of citations
		Gene	Protein/Metabolite	Gene	Protein/Metabolite	Gene	Protein/Metabolite		
COX2	*PTGS2*	Abiko et al. (1998), Agarwal et al. (2003), Jacobs et al. (2014), Jacobs et al. (2018), Nazet et al. (2020), Nokhbehsaim et al. (2010) (20%) , Nokhbehsaim et al. (2012) (20%) , Ohzeki et al. (1999), Shimizu et al. (1998), Suzuki et al. (2014), Wada et al. (2017), Wang et al. (2011)	Long et al. (2002), Nogueira et al. (2014)			Nokhbehsaim et al. (2012) (3%)		Nokhbehsaim et al. (2010) (3%)	**14**
OPG (Cytokine)	*TNFRSF11B*	Jacobs et al. (2013), Jacobs et al. (2015), Kanzaki et al. (2006), Kanzaki et al. (2019), Lee et al. (2015), Li et al. (2015), Liao and Hua (2013), Liu et al. (2017), Monnouchi et al. (2011), Spencer and Lallier (2009), Tsuji et al. (2004)	Jacobs et al. (2013), Jacobs et al. (2015), Kanzaki et al. (2006), Kanzaki et al. (2019), Li et al. (2015), Liao and Hua (2013), Tsuji et al. (2004)	Nogueira et al. (2014), Yang et al. (2006)	Nogueira et al. (2014), Yang et al. (2006)			Yang et al. (2010)	**14**
RANKL (Cytokine)	*TNFSF11*	Kanzaki et al. (2006), Kanzaki et al. (2019), Lee et al. (2015), Li et al. (2015), Liao and Hua (2013), Liu et al. (2017), Yang et al. (2010)	Li et al. (2015), Kaku et al. (2019)	Nogueira et al. (2014), Spencer and Lallier (2009)	Liao and Hua (2013), Nogueira et al. (2014)	Tsuji et al. (2004)		Jacobs et al. (2013), Jacobs et al. (2015), Monnouchi et al. (2011)	**14**
COL1A1 COLIα1 Collagen type-I (COL-1) Colα1 (collagen α1) COL1 COL-I	*COL1A1*	Chen et al. (2015), He et al. (2004), Lee et al. (2015), Takano et al. (2009), Wang et al. (2019b), Yang et al. (2018), Yu et al. (2018)	He et al. (2004), Qin and Hua (2016), Takano et al. (2009), Wang et al. (2019b), Yu et al. (2018)	Nemoto et al. (2010), Sun et al. (2017)	Sun et al. (2016), Sun et al. (2017)			Jacobs et al. (2013) Yamaguchi et al. (2002)	**13**
PGE_2	PGE_2		Abiko et al. (1998), Agarwal et al. (2003), Jacobs et al. (2014), Long et al. (2002), Ngan et al. (1990), Nogueira et al. (2014), Ohzeki et al. (1999), Shimizu et al. (1995), Shimizu et al. (1998), Suzuki et al. (2014), Yamaguchi et al. (1994)				Jacobs et al. (2018)		**12**
OSX SP7 Osx	*SP7*	Li et al. (2014), Li et al. (2015) Ren et al. (2015), Tang et al. (2012), Wang et al. (2019a), Wang et al. (2019b), Yang et al. (2018), Yu et al. (2018)	Chang et al. (2017), Li et al. (2014), Li et al. (2015), Tang et al. (2012), Wang et al. (2019b), Yu et al. (2018)	Li et al. (2013)				Li et al. (2013) (protein)	**10**

1. Increase = “Increase” or “Increase with Plateau”; Decrease = “Decrease” or “Decrease with Plateau”…
2. The citations in red font appeared more than once. - **(each citation is counted only once)**

References

Abiko, Y., Shimizu, N., Yamaguchi, M., Suzuki, H., and Takiguchi, H. (1998). Effect of aging on functional changes of periodontal tissue cells. *Ann. Periodontol.* 3(1), 350-369. doi: 10.1902/annals.1998.3.1.350.

Agarwal, S., Long, P., Seyedain, A., Piesco, N., Shree, A., and Gassner, R. (2003). A central role for the nuclear factor-κB pathway in anti-inflammatory and proinflammatory actions of mechanical strain. *FASEB J.* 17(8), 899-901. doi: 10.1096/fj.02-0901fje.

Chang, M., Lin, H., Fu, H., Wang, B., Han, G., and Fan, M. (2017). MicroRNA-195-5p regulates osteogenic differentiation of periodontal ligament cells under mechanical loading. *J. Cell. Physiol.* 232(12), 3762-3774. doi: 10.1002/jcp.25856.

Chang, M., Lin, H., Luo, M., Wang, J., and Han, G. (2015). Integrated miRNA and mRNA expression profiling of tension force-induced bone formation in periodontal ligament cells. *In Vitro Cell. Dev. Biol. Anim.* 51(8), 797-807. doi: 10.1007/s11626-015-9892-0.

Chen, Y., Mohammed, A., Oubaidin, M., Evans, C.A., Zhou, X., Luan, X., et al. (2015). Cyclic stretch and compression forces alter microRNA-29 expression of human periodontal ligament cells. *Gene* 566(1), 13-17. doi: 10.1016/j.gene.2015.03.055.

Chen, Y.J., Shie, M.Y., Hung, C.J., Wu, B.C., Liu, S.L., Huang, T.H., et al. (2014). Activation of focal adhesion kinase induces extracellular signal-regulated kinase-mediated osteogenesis in tensile force-subjected periodontal ligament fibroblasts but not in osteoblasts. *J. Bone Miner. Metab.* 32(6), 671-682. doi: 10.1007/s00774-013-0549-3.

Chiba, M., and Mitani, H. (2004). Cytoskeletal changes and the system of regulation of alkaline phosphatase activity in human periodontal ligament cells induced by mechanical stress. *Cell Biochem. Funct.* 22(4), 249-256. doi: 10.1002/cbf.1097.

Cho, J.H., Lee, S.K., Lee, J.W., and Kim, E.C. (2010). The role of heme oxygenase-1 in mechanical stress- and lipopolysaccharide-induced osteogenic differentiation in human periodontal ligament cells. *Angle Orthod.* 80(4), 552-559. doi: 10.2319/091509-520.1.

Fujihara, C., Yamada, S., Ozaki, N., Takeshita, N., Kawaki, H., Takano-Yamamoto, T., et al. (2010). Role of mechanical stress-induced glutamate signaling-associated molecules in cytodifferentiation of periodontal ligament cells. *J. Biol. Chem.* 285(36), 28286-28297. doi: 10.1074/jbc.M109.097303.

He, Y., Macarak, E.J., Korostoff, J.M., and Howard, P.S. (2004). Compression and tension: differential effects on matrix accumulation by periodontal ligament fibroblasts in vitro. *Connect Tissue Res.* 45(1), 28-39. doi: 10.1080/03008200490278124.

He, Y., Xu, H., Xiang, Z., Yu, H., Xu, L., Guo, Y., et al. (2019). YAP regulates periodontal ligament cell differentiation into myofibroblast interacted with RhoA/ROCK pathway. *J. Cell. Physiol.* 234(4), 5086-5096. doi: 10.1002/jcp.27312.

Jacobs, C., Grimm, S., Ziebart, T., Walter, C., and Wehrbein, H. (2013). Osteogenic differentiation of periodontal fibroblasts is dependent on the strength of mechanical strain. *Arch. Oral Biol.* 58(7), 896-904. doi: 10.1016/j.archoralbio.2013.01.009.

Jacobs, C., Schramm, S., Dirks, I., Walter, C., Pabst, A., Meila, D., et al. (2018). Mechanical loading increases pro-inflammatory effects of nitrogen-containing bisphosphonate in human periodontal fibroblasts. *Clin. Oral Investig.* 22(2), 901-907. doi: 10.1007/s00784-017-2168-1.

Jacobs, C., Walter, C., Ziebart, T., Dirks, I., Schramm, S., Grimm, S., et al. (2015). Mechanical loading influences the effects of bisphosphonates on human periodontal ligament fibroblasts. *Clin. Oral Investig.* 19(3), 699-708. doi: 10.1007/s00784-014-1284-4.

Jacobs, C., Walter, C., Ziebart, T., Grimm, S., Meila, D., Krieger, E., et al. (2014). Induction of IL-6 and MMP-8 in human periodontal fibroblasts by static tensile strain. *Clin. Oral Investig.* 18(3), 901-908. doi: 10.1007/s00784-013-1032-1.

Jiang, Z., and Hua, Y. (2016). Hydrogen sulfide promotes osteogenic differentiation of human periodontal ligament cells via p38-MAPK signaling pathway under proper tension stimulation. *Arch. Oral Biol.* 72, 8-13. doi: 10.1016/j.archoralbio.2016.08.008.

Kaku, M., Yamamoto, T., Yashima, Y., Izumino, J., Kagawa, H., Ikeda, K., et al. (2019). Acetaminophen reduces apical root resorption during orthodontic tooth movement in rats. *Arch. Oral Biol.* 102, 83-92. doi: 10.1016/j.archoralbio.2019.04.002.

Kanzaki, H., Chiba, M., Sato, A., Miyagawa, A., Arai, K., Nukatsuka, S., et al. (2006). Cyclical tensile force on periodontal ligament cells inhibits osteoclastogenesis through OPG induction. *J. Dent. Res.* 85(5), 457-462. doi: 10.1177/154405910608500512.

Kanzaki, H., Wada, S., Yamaguchi, Y., Katsumata, Y., Itohiya, K., Fukaya, S., et al. (2019). Compression and tension variably alter Osteoprotegerin expression via miR-3198 in periodontal ligament cells. *BMC Mol. Cell Biol.* 20(1), 6. doi: 10.1186/s12860-019-0187-2.

Kim, H.J., Choi, Y.S., Jeong, M.J., Kim, B.O., Lim, S.H., Kim, D.K., et al. (2007). Expression of UNCL during development of periodontal tissue and response of periodontal ligament fibroblasts to mechanical stress in vivo and in vitro. *Cell Tissue Res.* 327(1), 25-31. doi: 10.1007/s00441-006-0304-3.

Konstantonis, D., Papadopoulou, A., Makou, M., Eliades, T., Basdra, E., and Kletsas, D. (2014). The role of cellular senescence on the cyclic stretching-mediated activation of MAPK and ALP expression and activity in human periodontal ligament fibroblasts. *Exp. Gerontol.* 57, 175-180. doi: 10.1016/j.exger.2014.05.010.

Lee, S.I., Park, K.H., Kim, S.J., Kang, Y.G., Lee, Y.M., and Kim, E.C. (2012). Mechanical stress-activated immune response genes via Sirtuin 1 expression in human periodontal ligament cells. *Clin. Exp. Immunol.* 168(1), 113-124. doi: 10.1111/j.1365-2249.2011.04549.x.

Lee, S.Y., Yoo, H.I., and Kim, S.H. (2015). CCR5-CCL Axis in PDL during Orthodontic Biophysical Force Application. *J. Dent. Res.* 94(12), 1715-1723. doi: 10.1177/0022034515603926.

Li, L., Han, M., Li, S., Wang, L., and Xu, Y. (2013). Cyclic tensile stress during physiological occlusal force enhances osteogenic differentiation of human periodontal ligament cells via ERK1/2-Elk1 MAPK pathway. *DNA Cell Biol.* 32(9), 488-497. doi: 10.1089/dna.2013.2070.

Li, L., Han, M.X., Li, S., Xu, Y., and Wang, L. (2014). Hypoxia regulates the proliferation and osteogenic differentiation of human periodontal ligament cells under cyclic tensile stress via mitogen-activated protein kinase pathways. *J. Periodontol.* 85(3), 498-508. doi: 10.1902/jop.2013.130048.

Li, S., Zhang, H., Li, S., Yang, Y., Huo, B., and Zhang, D. (2015). Connexin 43 and ERK regulate tension-induced signal transduction in human periodontal ligament fibroblasts. *J. Orthop. Res.* 33(7), 1008-1014. doi: 10.1002/jor.22830.

Liao, C., and Hua, Y. (2013). Effect of hydrogen sulphide on the expression of osteoprotegerin and receptor activator of NF-kappaB ligand in human periodontal ligament cells induced by tension-force stimulation. *Arch. Oral Biol.* 58(12), 1784-1790. doi: 10.1016/j.archoralbio.2013.08.004.

Liu, J., Li, Q., Liu, S., Gao, J., Qin, W., Song, Y., et al. (2017). Periodontal Ligament Stem Cells in the Periodontitis Microenvironment Are Sensitive to Static Mechanical Strain. *Stem Cells Int.* 2017, 1380851. doi: 10.1155/2017/1380851.

Long, P., Hu, J., Piesco, N., Buckley, M., and Agarwal, S. (2001). Low magnitude of tensile strain inhibits IL-1beta-dependent induction of pro-inflammatory cytokines and induces synthesis of IL-10 in human periodontal ligament cells in vitro. *J. Dent. Res.* 80(5), 1416-1420. doi: 10.1177/00220345010800050601.

Long, P., Liu, F., Piesco, N.P., Kapur, R., and Agarwal, S. (2002). Signaling by mechanical strain involves transcriptional regulation of proinflammatory genes in human periodontal ligament cells in vitro. *Bone* 30(4), 547-552. doi: 10.1016/s8756-3282(02)00673-7.

Matsuda, N., Yokoyama, K., Takeshita, S., and Watanabe, M. (1998). Role of epidermal growth factor and its receptor in mechanical stress-induced differentiation of human periodontal ligament cells in vitro. *Arch. Oral Biol.* 43(12), 987-997. doi: 10.1016/s0003-9969(98)00079-x.

Monnouchi, S., Maeda, H., Fujii, S., Tomokiyo, A., Kono, K., and Akamine, A. (2011). The roles of angiotensin II in stretched periodontal ligament cells. *J. Dent. Res.* 90(2), 181-185. doi: 10.1177/0022034510382118.

Nazet, U., Schröder, A., Spanier, G., Wolf, M., Proff, P., and Kirschneck, C. (2020). Simplified method for applying static isotropic tensile strain in cell culture experiments with identification of valid RT-qPCR reference genes for PDL fibroblasts. *Eur. J. Orthod.* 42(4), 359-370. doi: 10.1093/ejo/cjz052.

Nemoto, T., Kajiya, H., Tsuzuki, T., Takahashi, Y., and Okabe, K. (2010). Differential induction of collagens by mechanical stress in human periodontal ligament cells. *Arch. Oral Biol.* 55(12), 981-987. doi: 10.1016/j.archoralbio.2010.08.004.

Ngan, P., Saito, S., Saito, M., Lanese, R., Shanfeld, J., and Davidovitch, Z. (1990). The interactive effects of mechanical stress and interleukin-1 beta on prostaglandin E and cyclic AMP production in human periodontal ligament fibroblasts in vitro: comparison with cloned osteoblastic cells of mouse (MC3T3-E1). *Arch. Oral Biol.* 35(9), 717-725. doi: 10.1016/0003-9969(90)90094-Q.

Nogueira, A.V., Nokhbehsaim, M., Eick, S., Bourauel, C., Jäger, A., Jepsen, S., et al. (2014). Biomechanical loading modulates proinflammatory and bone resorptive mediators in bacterial-stimulated PDL cells. *Mediators Inflamm.* 2014, 425421. doi: 10.1155/2014/425421.

Nokhbehsaim, M., Deschner, B., Bourauel, C., Reimann, S., Winter, J., Rath, B., et al. (2011). Interactions of enamel matrix derivative and biomechanical loading in periodontal regenerative healing. *J. Periodontol.* 82(12), 1725-1734. doi: 10.1902/jop.2011.100678.

Nokhbehsaim, M., Deschner, B., Winter, J., Bourauel, C., Jäger, A., Jepsen, S., et al. (2012). Anti-inflammatory effects of EMD in the presence of biomechanical loading and interleukin-1β in vitro. *Clin. Oral Investig.* 16(1), 275-283. doi: 10.1007/s00784-010-0505-8.

Nokhbehsaim, M., Deschner, B., Winter, J., Reimann, S., Bourauel, C., Jepsen, S., et al. (2010). Contribution of orthodontic load to inflammation-mediated periodontal destruction. *J. Orofac. Orthop.* 71(6), 390-402. doi: 10.1007/s00056-010-1031-7.

Ohzeki, K., Yamaguchi, M., Shimizu, N., and Abiko, Y. (1999). Effect of cellular aging on the induction of cyclooxygenase-2 by mechanical stress in human periodontal ligament cells. *Mech. Ageing Dev.* 108(2), 151-163. doi: 10.1016/s0047-6374(99)00006-8.

Papadopoulou, A., Todaro, A., Eliades, T., and Kletsas, D. (2019). Effect of hyperglycaemic conditions on the response of human periodontal ligament fibroblasts to mechanical stretching. *Eur. J. Orthod.* doi: 10.1093/ejo/cjz051.

Qin, J., and Hua, Y. (2016). Effects of hydrogen sulfide on the expression of alkaline phosphatase, osteocalcin and collagen type I in human periodontal ligament cells induced by tension force stimulation. *Mol. Med. Rep.* 14(4), 3871-3877. doi: 10.3892/mmr.2016.5680.

Ren, D., Wei, F., Hu, L., Yang, S., Wang, C., and Yuan, X. (2015). Phosphorylation of Runx2, induced by cyclic mechanical tension via ERK1/2 pathway, contributes to osteodifferentiation of human periodontal ligament fibroblasts. *J. Cell. Physiol.* 230(10), 2426-2436. doi: 10.1002/jcp.24972.

Ritter, N., Mussig, E., Steinberg, T., Kohl, A., Komposch, G., and Tomakidi, P. (2007). Elevated expression of genes assigned to NF-kappaB and apoptotic pathways in human periodontal ligament fibroblasts following mechanical stretch. *Cell Tissue Res.* 328(3), 537-548. doi: 10.1007/s00441-007-0382-x.

Shen, T., Qiu, L., Chang, H., Yang, Y., Jian, C., Xiong, J., et al. (2014). Cyclic tension promotes osteogenic differentiation in human periodontal ligament stem cells. *Int. J. Clin. Exp. Pathol.* 7(11), 7872-7880.

Shimizu, N., Goseki, T., Yamaguchi, M., Iwasawa, T., Takiguchi, H., and Abiko, Y. (1997). In vitro cellular aging stimulates interleukin-1 beta production in stretched human periodontal-ligament-derived cells. *J. Dent. Res.* 76(7), 1367-1375. doi: 10.1177/00220345970760070601.

Shimizu, N., Ozawa, Y., Yamaguchi, M., Goseki, T., Ohzeki, K., and Abiko, Y. (1998). Induction of COX-2 expression by mechanical tension force in human periodontal ligament cells. *J. Periodontol.* 69(6), 670-677. doi: 10.1902/jop.1998.69.6.670.

Shimizu, N., Yamaguchi, M., Goseki, T., Ozawa, Y., Saito, K., Takiguchi, H., et al. (1994). Cyclic-tension force stimulates interleukin-1 beta production by human periodontal ligament cells. *J. Periodontal Res.* 29(5), 328-333. doi: 10.1111/j.1600-0765.1994.tb01230.x.

Shimizu, N., Yamaguchi, M., Goseki, T., Shibata, Y., Takiguchi, H., Iwasawa, T., et al. (1995). Inhibition of prostaglandin E2 and interleukin 1-beta production by low-power laser irradiation in stretched human periodontal ligament cells. *J. Dent. Res.* 74(7), 1382-1388. doi: 10.1177/00220345950740071001.

Spencer, A.Y., and Lallier, T.E. (2009). Mechanical tension alters semaphorin expression in the periodontium. *J. Periodontol.* 80(10), 1665-1673. doi: 10.1902/jop.2009.090212.

Sun, C., Chen, L., Shi, X., Cao, Z., Hu, B., Yu, W., et al. (2016). Combined effects of proinflammatory cytokines and intermittent cyclic mechanical strain in inhibiting osteogenicity in human periodontal ligament cells. *Cell Biol. Int.* 40(9), 999-1007. doi: 10.1002/cbin.10641.

Sun, C., Liu, F., Cen, S., Chen, L., Wang, Y., Sun, H., et al. (2017). Tensile strength suppresses the osteogenesis of periodontal ligament cells in inflammatory microenvironments. *Mol. Med. Rep.* 16(1), 666-672. doi: 10.3892/mmr.2017.6644.

Suzuki, R., Nemoto, E., and Shimauchi, H. (2014). Cyclic tensile force up-regulates BMP-2 expression through MAP kinase and COX-2/PGE2 signaling pathways in human periodontal ligament cells. *Exp. Cell Res.* 323(1), 232-241. doi: 10.1016/j.yexcr.2014.02.013.

Takano, M., Yamaguchi, M., Nakajima, R., Fujita, S., Kojima, T., and Kasai, K. (2009). Effects of relaxin on collagen type I released by stretched human periodontal ligament cells. *Orthod. Craniofac. Res.* 12(4), 282-288. doi: 10.1111/j.1601-6343.2009.01463.x.

Tang, N., Zhao, Z., Zhang, L., Yu, Q., Li, J., Xu, Z., et al. (2012). Up-regulated osteogenic transcription factors during early response of human periodontal ligament stem cells to cyclic tensile strain. *Arch. Med. Sci.* 8(3), 422-430. doi: 10.5114/aoms.2012.28810.

Tsuji, K., Uno, K., Zhang, G.X., and Tamura, M. (2004). Periodontal ligament cells under intermittent tensile stress regulate mRNA expression of osteoprotegerin and tissue inhibitor of matrix metalloprotease-1 and -2. *J. Bone Miner. Metab.* 22(2), 94-103. doi: 10.1007/s00774-003-0456-0.

Wada, S., Kanzaki, H., Narimiya, T., and Nakamura, Y. (2017). Novel device for application of continuous mechanical tensile strain to mammalian cells. *Biol. Open* 6(4), 518-524. doi: 10.1242/bio.023671.

Wang, H., Feng, C., Jin, Y., Tan, W., and Wei, F. (2019a). Identification and characterization of circular RNAs involved in mechanical force-induced periodontal ligament stem cells. *J. Cell. Physiol.* 234(7), 10166-10177. doi: 10.1002/jcp.27686.

Wang, Y., Hu, B., Hu, R., Tong, X., Zhang, M., Xu, C., et al. (2019b). TAZ contributes to osteogenic differentiation of periodontal ligament cells under tensile stress. *J. Periodontal Res.* doi: 10.1111/jre.12698.

Wang, Y., Li, Y., Fan, X., Zhang, Y., Wu, J., and Zhao, Z. (2011). Early proliferation alteration and differential gene expression in human periodontal ligament cells subjected to cyclic tensile stress. *Arch. Oral Biol.* 56(2), 177-186. doi: 10.1016/j.archoralbio.2010.09.009.

Wei, F., Liu, D., Feng, C., Zhang, F., Yang, S., Hu, Y., et al. (2015). microRNA-21 mediates stretch-induced osteogenic differentiation in human periodontal ligament stem cells. *Stem Cells Dev.* 24(3), 312-319. doi: 10.1089/scd.2014.0191.

Wei, F.L., Wang, J.H., Ding, G., Yang, S.Y., Li, Y., Hu, Y.J., et al. (2014). Mechanical force-induced specific MicroRNA expression in human periodontal ligament stem cells. *Cells Tissues Organs* 199(5-6), 353-363. doi: 10.1159/000369613.

Wu, Y., Ou, Y., Liao, C., Liang, S., and Wang, Y. (2019). High-throughput sequencing analysis of the expression profile of microRNAs and target genes in mechanical force-induced osteoblastic/cementoblastic differentiation of human periodontal ligament cells. *Am. J. Transl. Res.* 11(6), 3398-3411.

Yamaguchi, M., and Shimizu, N. (1994). Identification of factors mediating the decrease of alkaline phosphatase activity caused by tension-force in periodontal ligament cells. *Gen. Pharmacol.* 25(6), 1229-1235. doi: 10.1016/0306-3623(94)90142-2.

Yamaguchi, M., Shimizu, N., Goseki, T., Shibata, Y., Takiguchi, H., Iwasawa, T., et al. (1994). Effect of different magnitudes of tension force on prostaglandin E2 production by human periodontal ligament cells. *Arch. Oral Biol.* 39(10), 877-884. doi: 10.1016/0003-9969(94)90019-1.

Yamaguchi, M., Shimizu, N., Shibata, Y., and Abiko, Y. (1996). Effects of different magnitudes of tension-force on alkaline phosphatase activity in periodontal ligament cells. *J. Dent. Res.* 75(3), 889-894. doi: 10.1177/00220345960750030501.

Yamaguchi, N., Chiba, M., and Mitani, H. (2002). The induction of c-fos mRNA expression by mechanical stress in human periodontal ligament cells. *Arch. Oral Biol.* 47(6), 465-471. doi: 10.1016/s0003-9969(02)00022-5.

Yang, S.Y., Wei, F.L., Hu, L.H., and Wang, C.L. (2016). PERK-eIF2alpha-ATF4 pathway mediated by endoplasmic reticulum stress response is involved in osteodifferentiation of human periodontal ligament cells under cyclic mechanical force. *Cell. Signal.* 28(8), 880-886. doi: 10.1016/j.cellsig.2016.04.003.

Yang, Y., Wang, B.K., Chang, M.L., Wan, Z.Q., and Han, G.L. (2018). Cyclic Stretch Enhances Osteogenic Differentiation of Human Periodontal Ligament Cells via YAP Activation. *Biomed Res. Int.* 2018, 2174824. doi: 10.1155/2018/2174824.

Yang, Y., Yang, Y., Li, X., Cui, L., Fu, M., Rabie, A.B., et al. (2010). Functional analysis of core binding factor a1 and its relationship with related genes expressed by human periodontal ligament cells exposed to mechanical stress. *Eur. J. Orthod.* 32(6), 698-705. doi: 10.1093/ejo/cjq010.

Yang, Y.Q., Li, X.T., Rabie, A.B., Fu, M.K., and Zhang, D. (2006). Human periodontal ligament cells express osteoblastic phenotypes under intermittent force loading in vitro. *Front. Biosci.* 11, 776-781. doi: 10.2741/1835.

Yu, W., Hu, B., Shi, X., Cao, Z., Ren, M., He, Z., et al. (2018). Nicotine inhibits osteogenic differentiation of human periodontal ligament cells under cyclic tensile stress through canonical Wnt pathway and alpha7 nicotinic acetylcholine receptor. *J. Periodontal Res.* 53(4), 555-564. doi: 10.1111/jre.12545.

Zhao, D., Wu, Y., Zhuang, J., Xu, C., and Zhang, F. (2016). Activation of NLRP1 and NLRP3 inflammasomes contributed to cyclic stretch-induced pyroptosis and release of IL-1beta in human periodontal ligament cells. *Oncotarget* 7(42), 68292-68302. doi: 10.18632/oncotarget.11944.

Zhuang, J., Wang, Y., Qu, F., Wu, Y., Zhao, D., and Xu, C. (2019). Gasdermin-d Played a Critical Role in the Cyclic Stretch-Induced Inflammatory Reaction in Human Periodontal Ligament Cells. *Inflammation* 42(2), 548-558. doi: 10.1007/s10753-018-0912-6.

Supplement 8: Gene List Analysis

Summary of the pathway analysis applied using “dynamic” and “static” differential expressed gene (DEG) lists (Figures 3 and 5, Table 4). Pathway analysis was done quering the “GeneOntology/Biological Process” and GeneAnalytics’ “SuperPath” databases using the complete DEG lists (Table 4, Figures 5A and 5B) and the nodes included in the individual subnetworks (Figures 5C and 5D). To increase specificity, results from both databases were filtered according to the proportion of query genes in relation to the number of background genes of the specific database entry and a cut-off of ≥0.05 (i.e. 5 %) was applied.

Contents

Gene list – Dynamic tension DEGs

Table S8.1 Enriched GeneOntology/Biological Process terms

Ratio: Number of genes in gene set divided by the total number of background genes in the specific GeneOntology/Biological Process term. A ratio cut-off ≥ 0.05 was applied. The top 10 most significant enriched terms (i.e. those with the highest -$\log_{10}$(FDR) values) were selected.

Gene list	GO Term	Ratio	-$\log_{10}$(FDR)
Complete	GO.0009719: response to endogenous stimulus	0.05	36.16
	GO.0071495: cellular response to endogenous stimulus	0.05	30.14
	GO.0070848: response to growth factor	0.09	30.14
	GO.0001503: ossification	0.15	29.10
	GO.0071363: cellular response to growth factor stimulus	0.09	28.91
	GO.0051270: regulation of cellular component movement	0.06	27.80
	GO.0030334: regulation of cell migration	0.06	27.77
	GO.0072359: circulatory system development	0.06	27.54
	GO.2000145: regulation of cell motility	0.06	27.54
	GO.0045597: positive regulation of cell differentiation	0.06	27.36
Cluster #1	GO.0048661: positive regulation of smooth muscle cell proliferation	0.09	8.97
	GO.0007196: adenylate cyclase-inhibiting G protein-coupled glutamate receptor signaling pathway	0.56	8.97
	GO.1904705: regulation of vascular smooth muscle cell proliferation	0.12	8.38
	GO.0050729: positive regulation of inflammatory response	0.06	8.13
	GO.0032642: regulation of chemokine production	0.08	7.64
	GO.1904707: positive regulation of vascular smooth muscle cell proliferation	0.16	7.52
	GO.0007193: adenylate cyclase-inhibiting G protein-coupled receptor signaling pathway	0.07	7.44
	GO.0032722: positive regulation of chemokine production	0.09	6.61
	GO.0051966: regulation of synaptic transmission, glutamatergic	0.08	6.47
	GO.0031663: lipopolysaccharide-mediated signaling pathway	0.13	5.81
Cluster #2	GO.0070848: response to growth factor	0.05	23.23
	GO.0071363: cellular response to growth factor stimulus	0.05	22.47
	GO.0051216: cartilage development	0.12	19.23
	GO.0061448: connective tissue development	0.09	18.94
	GO.0003007: heart morphogenesis	0.08	17.64
	GO.0050678: regulation of epithelial cell proliferation	0.06	17.06
	GO.0048514: blood vessel morphogenesis	0.05	16.87
	GO.0055024: regulation of cardiac muscle tissue development	0.18	16.68
	GO.0060393: regulation of pathway-restricted SMAD protein phosphorylation	0.19	15.67
	GO.0003206: cardiac chamber morphogenesis	0.11	15.47
Cluster #3	GO.0060079: excitatory postsynaptic potential	0.09	14.10
	GO.0035235: ionotropic glutamate receptor signaling pathway	0.24	14.10
	GO.0098976: excitatory chemical synaptic transmission	0.38	6.97
	GO.0001964: startle response	0.11	5.79
	GO.0097553: calcium ion transmembrane import into cytosol	0.05	4.87
	GO.0060134: prepulse inhibition	0.14	3.82
	GO.1903539: protein localization to postsynaptic membrane	0.13	3.77
	GO.0035249: synaptic transmission, glutamatergic	0.09	3.51
	GO.0007616: long-term memory	0.06	3.20
Cluster #4	GO.0001649: osteoblast differentiation	0.10	12.50
	GO.0002076: osteoblast development	0.22	6.80
	GO.0031214: biomineral tissue development	0.06	6.56
	GO.0045124: regulation of bone resorption	0.08	4.09
	GO.0045669: positive regulation of osteoblast differentiation	0.05	3.60
	GO.0060346: bone trabecula formation	0.25	3.37
	GO.0060389: pathway-restricted SMAD protein phosphorylation	0.15	3.11
	GO.0034505: tooth mineralization	0.14	3.08
	GO.0042487: regulation of odontogenesis of dentin-containing tooth	0.14	3.08
	GO.0002063: chondrocyte development	0.09	2.77
Cluster #5	GO.0050718: positive regulation of interleukin-1 beta secretion	0.16	7.23

Gene list	GO Term	Ratio	-log10(FDR)
	GO.0051402: neuron apoptotic process	0.05	2.96
Cluster 6	GO.0030199: collagen fibril organization	0.08	3.68
	GO.0044319: wound healing, spreading of cells	0.08	2.57
	GO.0042310: vasoconstriction	0.06	2.46
	GO.0045777: positive regulation of blood pressure	0.05	2.33

Table S8.2 Enriched GeneAnalytics' SuperPathways

Ratio: Number of genes in gene set divided by the total number of background genes in the specific SuperPath. The top 10 most significant enriched terms (i.e. those with the highest Score) were selected.

Gene list	SuperPath Name	Ratio	Score
Complete	ERK Signaling	0.05	115.97
	Akt Signaling	0.06	96.02
	PAK Pathway	0.06	95.94
	PEDF Induced Signaling	0.06	91.03
	TGF-Beta Pathway	0.06	84.03
	Interleukin-4 and 13 Signaling	0.18	70.16
	Lung Fibrosis	0.27	70.05
	Integrin Pathway	0.06	66.46
	Hippo Signaling Pathway	0.14	66.29
	Pathways in Cancer	0.06	65.92
Cluster #1	Rheumatoid Arthritis	0.08	37.32
	GPCRs, Class C Metabotropic Glutamate, Pheromone	0.31	37.04
	Th1 Differentiation Pathway	0.08	32.22
	IL-10 Pathway	0.14	31.41
	Taste Transduction	0.07	30.90
	T Cell Receptor Signaling Pathway	0.04	30.56
	Phospholipase D Signaling Pathway	0.04	30.40
	Transcription_Role of VDR in Regulation of Genes Involved in Osteoporosis	0.11	29.60
	Interleukin-10 Signaling	0.10	28.99
	Malaria	0.10	28.85
Cluster #2	ERK Signaling	0.03	81.42
	PAK Pathway	0.04	77.43
	PEDF Induced Signaling	0.04	74.29
	Akt Signaling	0.04	72.97
	TGF-Beta Pathway	0.04	70.06
	Interleukin-4 and 13 Signaling	0.13	66.96
	Pathways in Cancer	0.04	63.44
	Cardiomyocyte Differentiation Through BMP Receptors	0.45	62.49
	Human Embryonic Stem Cell Pluripotency	0.09	61.85
	TGF-beta Signaling Pathway (KEGG)	0.14	58.94
Cluster #3	Nicotine Addiction	0.18	63.13
	Amyotrophic Lateral Sclerosis (ALS)	0.10	47.79
	Amphetamine Addiction	0.07	44.99
	Circadian Entrainment	0.03	44.11
	CAMP Signaling Pathway	0.03	36.72
	Dopamine-DARPP32 Feedback Onto CAMP Pathway	0.03	36.29
	SALM Protein Interactions at The Synapses	0.19	34.67
	Post NMDA Receptor Activation Events	0.10	30.81
	Neurophysiological Process Glutamate Regulation of Dopamine D1A Receptor Signaling	0.06	27.81
	Protein-protein Interactions at Synapses	0.06	27.57
Cluster #4	Development_Hedgehog and PTH Signaling Pathways in Bone and Cartilage Development	0.13	34.33
	Transcription_Role of VDR in Regulation of Genes Involved in Osteoporosis	0.11	33.30
	Osteoblast Signaling	0.29	32.17
	Interleukin-11 Signaling Pathway	0.07	18.16
	FGF Signaling Pathway	0.06	17.88
	Regulation of Retinoblastoma Protein	0.05	17.12

Gene list	SuperPath Name	Ratio	Score
	TGF-beta Receptor Signaling (WikiPathways)	0.05	16.97
	Endochondral Ossification	0.05	16.49
	TGF-beta Signaling Pathways	0.03	14.82
	Parathyroid Hormone Synthesis, Secretion and Action	0.03	14.39
Cluster #5	NOD-like Receptor Signaling Pathway	0.03	41.05
	Nucleotide-binding Oligomerization Domain (NOD) Pathway	0.10	32.03
	Nucleotide-binding Domain, Leucine Rich Repeat Containing Receptor (NLR) Signaling Pathways	0.08	31.12
	Toll-like Receptor Signaling Pathway	0.01	26.29
	Apoptosis and Autophagy	0.02	23.41
	Necroptosis	0.02	16.71
	Shigellosis	0.01	15.09
	Innate Immune System	0.00	13.99
	Measles	0.01	13.68
Cluster #6	Integrin Pathway	0.02	39.05
	Phospholipase-C Pathway	0.02	34.17
	Focal Adhesion	0.02	33.83
	Degradation of The Extracellular Matrix	0.02	33.35
	Cytoskeleton Remodeling Regulation of Actin Cytoskeleton By Rho GTPases	0.03	30.98
	ERK Signaling	0.01	29.68
	Smooth Muscle Contraction	0.11	27.75
	MiRNA Targets in ECM and Membrane Receptors	0.09	26.73
	Actin Nucleation By ARP-WASP Complex	0.01	20.13
	Cell Adhesion_Endothelial Cell Contacts By Non-junctional Mechanisms	0.08	19.29

Gene list – Static tension DEGs

Table S8.3 Enriched GeneOntology Biological Process terms

Ratio: Number of genes in gene set divided by the total number of background genes in the specific GeneOntology/Biological Process term. A ratio cut-off ≥ 0.05 was applied. The top 10 most significant enriched terms (i.e. those with the highest -$\log_{10}$(FDR) values) were selected.

Network	GO Term	Ratio	-$\log_{10}$(FDR)
Complete	GO.0001503: ossification	0.06	10.08
	GO.0009612: response to mechanical stimulus	0.05	8.97
	GO.0031960: response to corticosteroid	0.06	8.91
	GO.0071260: cellular response to mechanical stimulus	0.10	8.40
	GO.0007565: female pregnancy	0.06	8.32
	GO.0062013: positive regulation of small molecule metabolic process	0.07	8.21
	GO.0051384: response to glucocorticoid	0.07	7.99
	GO.0097191: extrinsic apoptotic signaling pathway	0.09	7.88
	GO.0008625: extrinsic apoptotic signaling pathway via death domain receptors	0.19	7.54
	GO.0048660: regulation of smooth muscle cell proliferation	0.06	6.99
Cluster #1	GO.0008625: extrinsic apoptotic signaling pathway via death domain receptors	0.16	7.78
	GO.0097191: extrinsic apoptotic signaling pathway	0.06	7.66
	GO.2000134: negative regulation of G1/S transition of mitotic cell cycle	0.05	6.14
	GO.0031571: mitotic G1 DNA damage checkpoint	0.06	5.08
	GO.2000811: negative regulation of anoikis	0.17	4.91
	GO.0048661: positive regulation of smooth muscle cell proliferation	0.05	4.89
	GO.0001836: release of cytochrome c from mitochondria	0.14	4.74
	GO.0043567: regulation of insulin-like growth factor receptor signaling pathway	0.13	4.69
	GO.1900740: positive regulation of protein insertion into mitochondrial membrane involved in apoptotic signaling pathway	0.12	4.60
	GO.1902895: positive regulation of pri-miRNA transcription by RNA polymerase II	0.12	4.60
Cluster #2	GO.0022617: extracellular matrix disassembly	0.09	6.26
	GO.0051043: regulation of membrane protein ectodomain proteolysis	0.13	4.23
	GO.0002675: positive regulation of acute inflammatory response	0.12	4.18
	GO.0030574: collagen catabolic process	0.08	3.92
	GO.0070498: interleukin-1-mediated signaling pathway	0.06	3.68
	GO.0032963: collagen metabolic process	0.06	3.64
	GO.0051155: positive regulation of striated muscle cell differentiation	0.05	3.59
	GO.1905049: negative regulation of metallopeptidase activity	0.33	3.54
	GO.0031622: positive regulation of fever generation	0.29	3.47
	GO.0060558: regulation of calcidiol 1-monooxygenase activity	0.29	3.47
Cluster #3	GO.0042487: regulation of odontogenesis of dentin-containing tooth	0.14	3.48
	GO.0002076: osteoblast development	0.11	3.44
	GO.0071295: cellular response to vitamin	0.09	3.35
	GO.0001958: endochondral ossification	0.08	3.29
	GO.0045124: regulation of bone resorption	0.05	3.09
Cluster #4	GO.0006501: C-terminal protein lipidation	0.18	3.92
	GO.0044804: autophagy of nucleus	0.12	3.64
Cluster #5	GO.0045725: positive regulation of glycogen biosynthetic process	0.12	3.68
	GO.0046628: positive regulation of insulin receptor signaling pathway	0.13	3.68
	GO.0048009: insulin-like growth factor receptor signaling pathway	0.14	3.68
	GO.0014065: phosphatidylinositol 3-kinase signaling	0.06	3.54
Cluster #6	GO.0050919: negative chemotaxis	0.09	4.83
	GO.1990138: neuron projection extension	0.05	4.46
	GO.0071526: semaphorin-plexin signaling pathway	0.08	3.38
	GO.0048675: axon extension	0.06	3.19

Table S8.4 Enriched GeneAnalytics' SuperPathways

Ratio: Number of genes in gene set divided by the total number of background genes in specific SuperPath. The top 10 most significant enriched terms (i.e. those with the highest Score) were selected.

Gene list	SuperPath Name	Ratio	Score
Complete	Senescence and Autophagy in Cancer	0.15	76.37
	Transcription_Role of VDR in Regulation of Genes Involved in Osteoporosis	0.27	66.96
	ERK Signaling	0.02	64.47
	Apoptosis Modulation and Signaling	0.07	62.14
	Cell Adhesion_ECM Remodeling	0.20	61.73
	Pathways in Cancer	0.04	61.42
	Photodynamic Therapy-induced NF-kB Survival Signaling	0.23	59.03
	Akt Signaling	0.03	58.38
	Interleukin-4 and 13 Signaling	0.11	56.77
	Apoptotic Pathways in Synovial Fibroblasts	0.03	53.00
Cluster #2	Photodynamic Therapy-induced AP-1 Survival Signaling.	0.16	53.00
	TNFR1 Pathway	0.04	44.37
	DREAM Repression and Dynorphin Expression	0.04	43.47
	Direct P53 Effectors	0.06	43.04
	Toll-like Receptor Signaling Pathway	0.03	42.49
	Apoptosis Modulation and Signaling	0.04	42.00
	Pathways in Cancer	0.02	37.74
	Interleukin-4 and 13 Signaling	0.06	37.67
	Human Cytomegalovirus Infection	0.03	37.28
	Endometrial Cancer	0.03	36.40
Cluster #2	Photodynamic Therapy-induced NF-kB Survival Signaling	0.13	39.60
	Cell Adhesion_ECM Remodeling	0.10	37.53
	GPCR Pathway	0.01	36.02
	HIF-1 Signaling Pathway	0.06	32.53
	Interleukin-4 and 13 Signaling	0.05	32.15
	NF-KappaB Family Pathway	0.03	31.61
	Akt Signaling	0.01	31.17
	PAK Pathway	0.01	31.15
	Matrix Metalloproteinases	0.09	30.74
	Cytokine Signaling in Immune System	0.01	29.80
Cluster #3	Transcription_Role of VDR in Regulation of Genes Involved in Osteoporosis	0.09	35.40
	Osteoblast Signaling	0.21	29.60
	Development_Hedgehog and PTH Signaling Pathways in Bone and Cartilage Development	0.08	25.17
	Interleukin-11 Signaling Pathway	0.05	15.18
	FGF Signaling Pathway	0.04	14.99
	Notch-mediated HES/HEY Network	0.04	14.93
	Regulation of Retinoblastoma Protein	0.04	14.49
Cluster #4	Autophagy Pathway	0.05	31.79
	Autophagy - Animal	0.03	28.97
	Cellular Senescence (REACTOME)	0.01	22.08
	Senescence and Autophagy in Cancer	0.03	20.84
Cluster #5	Immune Response Function of MEF2 in T Lymphocytes	0.03	22.92
	Development IGF-1 Receptor Signaling	0.02	21.82
	EGFR Transactivation By Gastrin	0.12	18.92
	NFAT and Cardiac Hypertrophy	0.01	17.98
	IL-2 Pathway	0.01	17.95
	IGF1 Pathway	0.07	17.48
	Factors and Pathways Affecting Insulin-like Growth Factor (IGF1)-Akt Signaling	0.06	17.19
	P70S6K Signaling	0.01	17.18
	Integrins in Angiogenesis	0.04	16.05
	PI3K-Akt Signaling Pathway	0.01	15.92
Cluster #6	Axon Guidance	0.03	34.21
	Semaphorin Interactions	0.04	20.53

4. Publication II

Effect of Different Parameters of In Vitro Static Tensile Strain on Human Periodontal Ligament Cells Simulating the Tension Side of Orthodontic Tooth Movement

Changyun Sun, Mila Janjic Rankovic, Matthias Folwaczny, Thomas Stocker, Sven Otto, Andrea Wichelhaus, and Uwe Baumert

Int. J. Mol. Sci. 2022, 23(3), 1525

PubMed: https://www.ncbi.nlm.nih.gov/pubmed/35163446

PubMedCentral: https://www.ncbi.nlm.nih.gov/pmc/articles/PMC8835937/

DOI: https://doi.org/10.3390/ijms23031525

International Journal of
Molecular Sciences

MDPI

Article

Effect of Different Parameters of In Vitro Static Tensile Strain on Human Periodontal Ligament Cells Simulating the Tension Side of Orthodontic Tooth Movement

Changyun Sun [1], Mila Janjic Rankovic [1], Matthias Folwaczny [2], Thomas Stocker [1], Sven Otto [3], Andrea Wichelhaus [1] and Uwe Baumert [1,*]

[1] Department of Orthodontics and Dentofacial Orthopedics, University Hospital, LMU Munich, 80336 Munich, Germany; cysun.stomatology@gmail.com (C.S.); mila_janjic@yahoo.com (M.J.R.); th.stocker@med.uni-muenchen.de (T.S.); kfo.sekretariat@med.uni-muenchen.de (A.W.)
[2] Department of Conservative Dentistry and Periodontology, University Hospital, LMU Munich, 80336 Munich, Germany; mfolwa@dent.med.uni-muenchen.de
[3] Department of Oral and Maxillofacial Surgery and Facial Plastic Surgery, University Hospital, LMU Munich, 80336 Munich, Germany; sven.otto@med.uni-muenchen.de
* Correspondence: uwe.baumert@med.uni-muenchen.de

Abstract: This study aimed to investigate the effects of different magnitudes and durations of static tensile strain on human periodontal ligament cells (hPDLCs), focusing on osteogenesis, mechanosensing and inflammation. Static tensile strain magnitudes of 0%, 3%, 6%, 10%, 15% and 20% were applied to hPDLCs for 1, 2 and 3 days. Cell viability was confirmed via live/dead cell staining. Reference genes were tested by reverse transcription quantitative real-time polymerase chain reaction (RT-qPCR) and assessed. The expressions of *TNFRSF11B*, *ALPL*, *RUNX2*, *BGLAP*, *SP7*, *FOS*, *IL6*, *PTGS2*, *TNF*, IL1B, IL8, IL10 and PGE2 were analyzed by RT-qPCR and/or enzyme-linked immunosorbent assay (ELISA). *ALPL* and *RUNX2* both peaked after 1 day, reaching their maximum at 3%, whereas *BGLAP* peaked after 3 days with its maximum at 10%. *SP7* peaked after 1 day at 6%, 10% and 15%. *FOS* peaked after 3 days with its maximum at 3%, 6% and 15%. The expressions of *IL6* and *PTGS2* both peaked after 1 day, with their minimum at 10%. PGE2 peaked after 1 day (maximum at 20%). The ELISA of IL6 peaked after 3 days, with the minimum at 10%. In summary, the lower magnitudes promoted osteogenesis and caused less inflammation, while the higher magnitudes inhibited osteogenesis and enhanced inflammation. Among all magnitudes, 10% generally caused a lower level of inflammation with a higher level of osteogenesis.

Keywords: periodontal ligament cells; tensile strain; bone remodeling; stretching; orthodontic tooth movement

Citation: Sun, C.; Janjic Rankovic, M.; Folwaczny, M.; Stocker, T.; Otto, S.; Wichelhaus, A.; Baumert, U. Effect of Different Parameters of In Vitro Static Tensile Strain on Human Periodontal Ligament Cells Simulating the Tension Side of Orthodontic Tooth Movement. *Int. J. Mol. Sci.* **2022**, *23*, 1525. https://doi.org/10.3390/ijms23031525

Academic Editor: Orfeo Sbaizero

Received: 16 December 2021
Accepted: 26 January 2022
Published: 28 January 2022

1. Introduction

The aim of orthodontic tooth movement (OTM) is to align malpositioned teeth by applying external forces ("orthodontic forces") to the teeth and thus stimulating bone remodeling [1]. Located between the teeth and the alveolar bone, the human periodontal ligament (hPDL) and the cells it contains play an essential role in withstanding mechanical forces in physiological, pathological and therapeutical conditions, e.g., orthodontic treatment [2].

During OTM, mechanical stimulation triggers complex aseptic inflammatory cellular and molecular processes causing the remodeling of the surrounding tissues, ultimately leading to bone resorption on the compression side and bone formation on the tension side. Inflammation is regulated by a large array of mediator molecules [3], including pro-inflammatory molecules such as interleukin 1B (IL1B), tumor necrosis factor (TNF), interleukin 6 (IL6) and interleukin 8 (IL8), as well as prostaglandin-endoperoxide synthase 2 (*PTGS2*; also known as *COX2*), prostaglandin E2 (PGE2) and anti-inflammatory

molecules such as interleukin 10 (IL10) [4]. Various molecules mediating osteoclasto-/osteoblastogenesis are upregulated at different stages of bone remodeling during this aseptic inflammatory process [5], including transcription factors (e.g., *Runt*-related transcription factor 2 (*RUNX2*) and *SP7*, also known as osterix) [6–8] and early or late osteoblastic marker genes such as alkaline phosphatase (*ALPL*), bone-matrix protein-bone gamma-carboxyglutamate protein (*BGLAP*, also known as osteocalcin) [9], as well as receptor activator of nuclear factor kappa ligand (*RANKL*) and osteoprotegerin (*OPG*) [10]. The proto-oncogene FOS is an immediate/early gene essential for mechanical stimulation. Its dimerization with JUN forms the heterodimeric activator protein 1 (AP1), which then binds to different promoters of osteoblast-specific genes, activating the proliferation and differentiation of osteoblasts in periodontal tissue [2,11].

Appropriate mechanical loading is essential for the homeostasis and thus the controlled and coordinated remodeling of both the PDL and the alveolar bone. A lack of mechanical stimuli will lead to the atrophy of PDL and/or bone. In contrast, excessive force affects PDL and bone in a similar manner resulting in periodontal attachment loss and/or loss of alveolar bone, respectively, finally leading to uncontrolled tooth movement and/or root resorption [1,12]. Taken together, optimal therapeutical forces are crucial for well-regulated tissue remodeling. Clinically, therapeutic tooth movement is centrally based on careful mechanical stimulation as low and as short as possible, sufficient to achieve the desired biological responses [1,12]. Therefore, parameters of mechanical stimulation eligible to induce therapeutic tissue remodeling within the periodontal and osseous tissues need to be further defined [1,12].

To gain improved insight into the effects of therapeutic forces on the expression and regulation of relevant genes involved in tooth movement and bone remodeling, different in vitro force application models have been suggested specifically in terms of compressive forces [7,13–15]. Regarding tension, different in vitro models have been applied addressing distinct issues [16–18], i.e., apoptosis [19,20], pyroptosis [21], angiogenesis [22], osteogenesis [23] and inflammation [24], but most of these studies focused on specific tension magnitudes only. Even in those studies considering different magnitudes, tension was only applied for a single period of time [25–28].

Therefore, aim of this study was to investigate the effects of different tensile strain magnitudes and durations on human periodontal ligament cells (hPDLCs), with special emphasis on gene expression related to bone remodeling, mechanosensing and inflammation.

2. Results

A custom-made apparatus was constructed (Figure 1) to apply different magnitudes of static equibiaxial tensile strain to adherent cells growing on a flexible membrane. Static cell stretching was achieved by spherical caps placed below the membrane (Figure 1) leading to an increase in membrane area. Herein, static cell stretching of hPDLCs of different magnitudes (0% = control, 3%, 6%, 10%, 15 % and 20%) was applied to hPDLCs with the respective, matching spherical caps for 1, 2 and 3 days. In the remaining parts of this manuscript, the magnitude of static tensile strain was represented by the percentage of stretch applied. Cell viability was assessed by live/dead cell staining, and the expression of target genes related to bone remodeling, mechanosensation and inflammation was quantified using reverse transcription quantitative real-time polymerase chain reaction (RT-qPCR) and/or enzyme-linked immunosorbent assay (ELISA).

2.1. Cell Viability

Since the maximum equibiaxial tensile strain is induced in the central part of the membrane [29], cells growing in this area of each membrane were used for viability testing with live/dead cell staining (Figure 2). The viability of hPDLCs remained unaffected as compared to the untreated control samples independent of tension magnitude and duration.

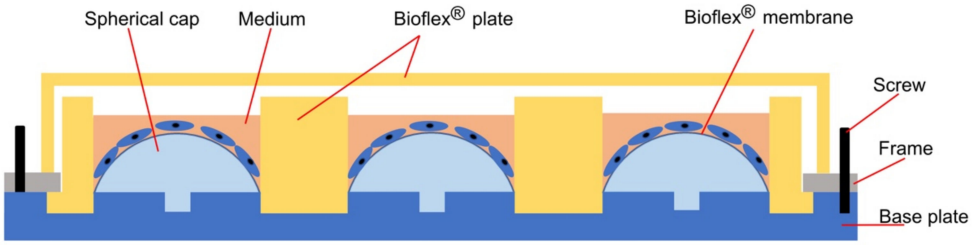

Figure 1. Experimental setup used to apply tensile strain: cells were seeded on the elastic silicone membrane of a BioFlex® plate and incubated overnight. Afterward, spherical caps with defined shapes were inserted into the base plate to statically apply a 3%, 6%, 10%, 15% or 20% increase of the membrane area. No tensile strain was applied to the control wells. After placing the BioFlex® plate onto the base plate, the outer frame was fixed with screws, thus applying tensile strain of predefined magnitudes to the cells growing on the membrane (more details can be found in Section 4.2).

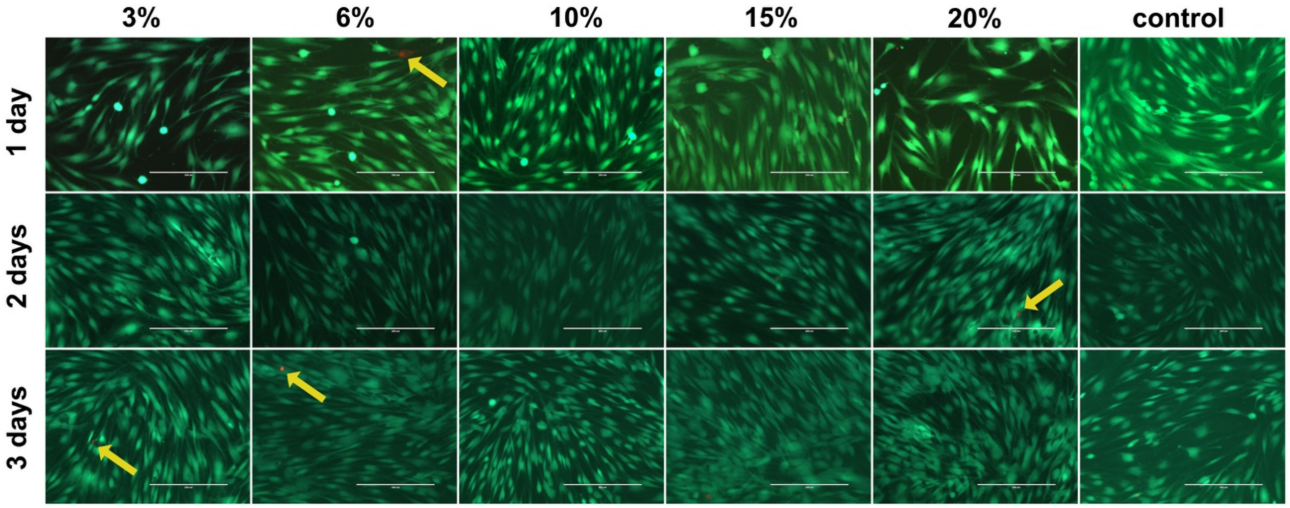

Figure 2. Cell viability of human periodontal ligament cells (hPDLCs) as assessed by live/dead cell staining. Microscopic images (bar: 200 µm) of cells growing in the center of each well were used herein, representing different tensile strain magnitudes and durations. Live cells are indicated by green staining, and dead cells are indicated by red staining (yellow arrows).

2.2. Reference Gene Selection

For validation of reference genes, the expression of a panel of eight pre-selected genes was assessed with RT-qPCR using samples exposed to 0%, 10% and 20% cell stretching for 1 and 3 days. Considering the C_q values, the most abundant reference gene was *RNA18S5* with mean C_q values ranging from 8.03 ± 0.53 to 8.55 ± 0.32 (Figure 3a; Supplementary Table S1.1).

The RefFinder program was used to identify the most stable reference gene within the panel, which calculated comprehensive gene stability values for each gene based on four different algorithms (Figure 3b; Supplementary Tables S1.2 and S1.3). Accordingly, *RPL22* (RefFinder gene stability: 2.115), *GAPDH* and *POLR2A* (both 2.449) were the most stable reference genes tested (Figure 3b and Supplement 1). The "Minimum Information for Publication of Quantitative Real-Time PCR Experiment" (MIQE) guidelines recommend using more than one reference gene for normalization to improve the quality of data [30]. Albeit RefFinder calculated the same gene stability values for both *GAPDH* and *POLR2A*, the latter was selected together with *RPL22* as reference genes for normalization, due to a comparable level of expression as for most of the target genes analyzed in this study.

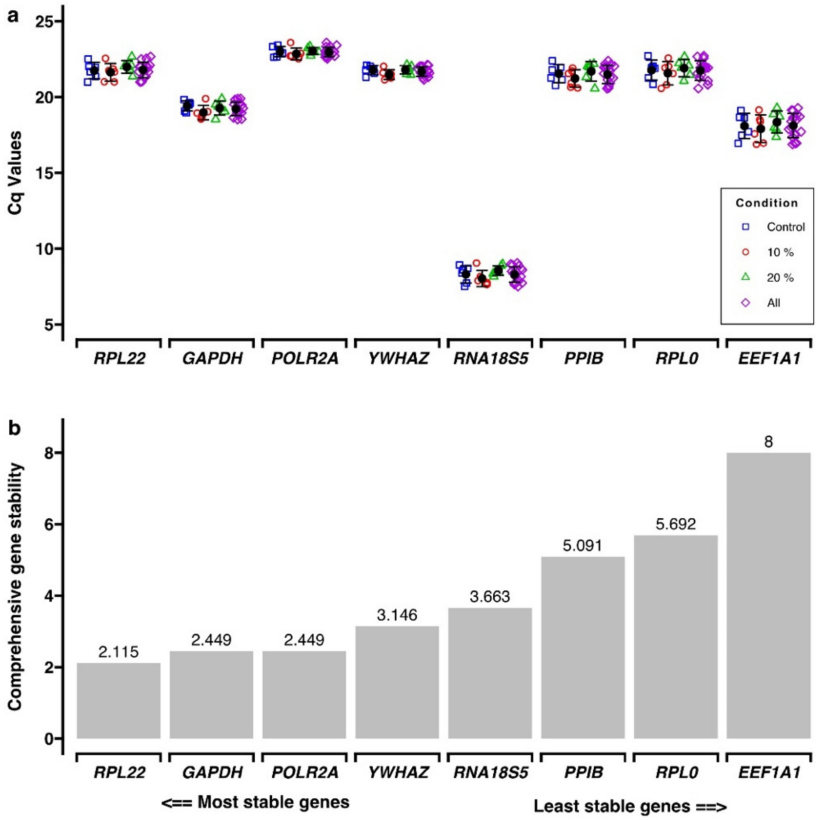

Figure 3. Reference gene primer stability was obtained with RefFinder. (**a**). C_q values for the panel of reference genes, using samples exposed to different tensile strain magnitudes for 1 and 3 days. Average expression (all) for the three magnitudes was also calculated. Six quantitative real-time polymerase chain reaction (qPCR) runs were analyzed representing three biological replicates with two technical replicates each (Supplement 1). (**b**). Comprehensive gene stability analysis for the panel of reference genes. Lower values indicate higher gene stability (Supplement 1).

2.3. Expression of Target Genes

Cell stretching was applied to hPDLCs for up to three days using six different magnitudes (0%, 3%, 6%, 10%, 15% and 20%). Afterward, expression of target genes was analyzed with RT-qPCR (reference genes: *RPL22* and *POLR2A*) and/or ELISA. A total of thirteen different loci were included, representing three different functional groups: bone-remodeling-related genes, including *ALPL*, *RUNX2*, *BGLAP*, *SP7*, TNF and *TNFRSF11B*, the mechanosensation-related locus *FOS* and the inflammation-related loci, including IL6, PTGS2, PGE2, IL1B, IL8 and IL10. The differences in gene expression between the test groups and the corresponding controls were analyzed. Tensile strain duration dependency was determined for each magnitude separately, and magnitude dependency was assessed for each duration. If not otherwise stated, mean fold changes (FC) and adjusted P ($P_{adj.}$) values after Bonferroni correction for multiple testing are reported. Descriptive statistics for each analyte and tension/duration combination are summarized in Table 1.

The protein concentrations of TNF, IL1B, IL8 and IL10 in the supernatants were all below the detection limit and were therefore not further analyzed. The gene expression of tumor necrosis factor-alpha receptor superfamily member 11B (*TNFRSF11B*, also known as *OPG*) was below the detection limit (C_q values > 35) and therefore not further analyzed.

Table 1. Summary statistics and comparison of the effects of static tensile strain on target gene expression (*ALPL*, *BGLAP*, *PTGS2*, *FOS*, *IL6*, *RUNX2* and *SP7*) reported as fold change, PGE2 and IL6 in hPDLCs. Results are shown as mean (±SD) and 95% confidence interval [95% CI]. *P*-values were obtained with Kruskal–Wallis test (KW) and adjusted by the Bonferroni correction for multiple tests (adjusted P, $P_{adj.}$).

Analyte	Magnitude	Duration of Tensile Strain Application (Days)							KW of Duration (Magnitude Fixed)
		1 Day		2 Days		3 Days			
		Mean (SD)	[95% CI]	Mean (SD)	[95% CI]	Mean (SD)	[95% CI]	$P_{adj.}$	Sign.
ALPL (FC)	3	2.94 (0.35)	[3.35;3.37]	0.57 (0.03)	[0.57;0.63]	0.65 (0.09)	[0.70;0.80]	0.002	**
	6	2.45 (0.21)	[2.61;2.68]	0.56 (0.11)	[0.56;0.79]	0.84 (0.12)	[0.91;1.02]	0.001	**
	10	1.66 (0.84)	[2.45;2.52]	0.72 (0.07)	[0.75;0.82]	0.97 (0.14)	[1.08;1.20]	0.051	n.s.
	15	2.37 (0.28)	[2.58;2.76]	0.57 (0.05)	[0.58;0.62]	0.73 (0.03)	[0.76;0.76]	0.001	**
	20	1.76 (0.17)	[1.90;1.97]	0.84 (0.14)	[0.99;1.05]	0.68 (0.18)	[0.83;0.92]	0.002	**
KW of magnitude (duration fixed)		<0.001 ***		<0.001 ***		0.001 **			
BGLAP (FC)	3	1.11 (0.48)	[1.05;2.04]	0.19 (0.08)	[0.28;0.30]	0.80 (0.15)	[0.96;1.01]	0.001	**
	6	1.40 (0.23)	[1.62;1.70]	0.25 (0.07)	[0.32;0.35]	1.73 (0.27)	[2.05;2.08]	0.002	**
	10	1.06 (0.21)	[1.21;1.34]	0.73 (0.12)	[0.81;0.85]	3.35 (0.84)	[3.74;4.70]	0.001	**
	15	1.67 (0.73)	[2.25;2.85]	0.21 (0.03)	[0.22;0.24]	2.68 (0.66)	[3.04;3.40]	0.001	**
	20	1.00 (0.21)	[1.13;1.34]	0.42 (0.17)	[0.59;0.65]	2.14 (0.40)	[2.51;2.65]	0.001	**
KW of magnitude (duration fixed)		0.077 n.s.		<0.001 ***		<0.001 ***			
PTGS2 (FC)	3	3.12 (0.75)	[3.47;4.07]	0.81 (0.07)	[0.83;0.93]	1.35 (0.12)	[1.45;1.48]	0.001	**
	6	3.30 (0.54)	[3.93;4.01]	0.79 (0.11)	[0.86;0.91]	1.58 (0.28)	[1.77;1.97]	0.001	**
	10	2.08 (0.81)	[2.63;2.72]	0.96 (0.09)	[1.02;1.05]	1.45 (0.35)	[1.82;1.95]	0.004	**
	15	3.64 (0.24)	[3.78;3.94]	0.83 (0.07)	[0.85;0.94]	1.61 (0.16)	[1.75;1.80]	0.001	**
	20	2.21 (0.61)	[2.74;2.76]	1.30 (0.49)	[1.65;1.65]	0.91 (0.27)	[1.22;1.26]	0.014	*
KW of magnitude (duration fixed)		<0.001 ***		0.017 *		0.001 **			
FOS (FC)	3	0.79 (0.09)	[0.83;0.91]	1.02 (0.11)	[1.08;1.19]	1.85 (0.15)	[2.01;2.07]	0.001	**
	6	0.81 (0.09)	[0.84;0.98]	0.82 (0.19)	[0.85;1.14]	1.87 (0.46)	[2.23;2.30]	0.003	**
	10	0.80 (0.05)	[0.84;0.85]	0.82 (0.09)	[0.90;0.91]	1.52 (0.17)	[1.73;1.73]	0.003	**
	15	0.86 (0.35)	[0.75;1.58]	0.77 (0.10)	[0.87;0.91]	2.05 (0.25)	[2.17;2.43]	0.003	**
	20	0.78 (0.18)	[0.93;1.02]	1.16 (0.45)	[1.65;1.65]	1.48 (0.24)	[1.66;1.79]	0.012	*
KW of magnitude (duration fixed)		0.041 *		0.024 *		0.001 **			
IL6 (FC)	3	1.76 (0.24)	[1.92;2.08]	0.46 (0.05)	[0.51;0.52]	0.92 (0.15)	[1.06;1.15]	0.001	**
	6	1.67 (0.14)	[1.78;1.83]	0.41 (0.03)	[0.43;0.46]	1.11 (0.17)	[1.17;1.39]	0.001	**
	10	1.01 (0.41)	[1.33;1.53]	0.57 (0.02)	[0.57;0.59]	1.21 (0.14)	[1.32;1.37]	0.018	*
	15	2.01 (0.80)	[2.96;3.11]	0.38 (0.03)	[0.39;0.42]	1.03 (0.14)	[1.14;1.21]	0.001	**
	20	1.19 (0.14)	[1.30;1.38]	0.50 (0.10)	[0.56;0.67]	0.92 (0.14)	[1.00;1.06]	0.001	**
KW of magnitude (duration fixed)		<0.001 ***		<0.001 ***		0.036 *			

Table 1. *Cont.*

Analyte	Magnitude	Duration of Tensile Strain Application (Days)						KW of Duration (Magnitude Fixed)	
		1 Day		2 Days		3 Days			
		Mean (SD)	[95% CI]	Mean (SD)	[95% CI]	Mean (SD)	[95% CI]	$P_{adj.}$	Sign.
RUNX2 (FC)	3	2.49 (0.20)	[2.65;2.78]	0.77 (0.07)	[0.83;0.83]	0.70 (0.12)	[0.84;0.87]	0.003	**
	6	2.15 (0.26)	[2.38;2.48]	0.80 (0.03)	[0.82;0.85]	0.89 (0.16)	[1.08;1.10]	0.003	**
	10	1.60 (0.84)	[2.37;2.44]	0.63 (0.04)	[0.67;0.69]	1.04 (0.18)	[1.25;1.27]	0.064	n.s.
	15	2.08 (0.15)	[2.22;2.30]	0.85 (0.04)	[0.86;0.92]	0.82 (0.07)	[0.86;0.92]	0.003	**
	20	1.32 (0.16)	[1.44;1.54]	0.81 (0.17)	[0.98;1.03]	0.62 (0.21)	[0.85;0.90]	0.002	**
KW of magnitude (duration fixed)		<0.001 ***		<0.001 ***		0.002 **			
SP7 (FC)	3	2.18 (0.64)	[2.76;2.97]	2.75 (1.61)	[4.17;4.29]	0.50 (0.08)	[0.54;0.60]	0.003	**
	6	4.84 (2.33)	[6.56;6.94]	2.96 (1.24)	[3.94;4.17]	1.20 (1.32)	[2.07;3.53]	0.018	*
	10	4.22 (3.01)	[7.70;8.07]	1.56 (0.74)	[2.42;2.51]	1.84 (0.70)	[2.22;2.92]	0.140	n.s.
	15	4.34 (1.38)	[4.18;7.11]	3.20 (2.12)	[5.36;5.51]	2.37 (0.61)	[2.42;3.48]	0.059	n.s.
	20	0.65 (0.13)	[0.67;0.88]	0.84 (0.35)	[1.25;1.27]	0.81 (0.46)	[0.92;1.54]	0.519	n.s.
KW of magnitude (duration fixed)		<0.001 ***		0.022 *		0.002 **			
PGE2 (pg/well)	0	938.7 (80.1)	[1002.1;1002.6]	603.7 (16.6)	[615.3;629.6]	498.3 (32.3)	[526.3;542.6]	0.001	**
	3	1318.5 (166.3)	[1437.6;1477.3]	1165.5 (38.0)	[1197.8;1198.7]	1075.0 (67.1)	[1130.2;1131.5]	0.034	*
	6	1246.0 (83.8)	[1331.5;1348.9]	1080.2 (56.9)	[1110.2;1171.1]	934.5 (135.6)	[963.4;1195.3]	0.005	**
	10	1466.3 (143.4)	[1590.9;1591.6]	1096.7 (30.4)	[1130.2;1134.0]	972.2 (103.3)	[1093.4;1099.7]	0.002	**
	15	1625.5 (86.0)	[1642.1;1769.5]	1451.6 (190.9)	[1678.3;1709.5]	1240.2 (81.0)	[1321.7;1358.0]	0.006	**
	20	1962.5 (270.1)	[2140.6;2236.1]	1779.1 (96.5)	[1856.2;1885.7]	1456.2 (73.6)	[1505.3;1556.1]	0.003	**
KW of magnitude (duration fixed)		<0.001 ***		<0.001 ***		<0.001 ***			
IL6 (pg/well)	0	133.5 (20.6)	[157.1;159.8]	143.1 (13.4)	[147.2;166.8]	277.7 (35.1)	[305.1;312.5]	0.002	**
	3	308.6 (60.4)	[381.1;387.4]	300.5 (21.7)	[325.2;327.9]	512.4 (28.6)	[532.1;559.9]	0.003	**
	6	179.0 (12.1)	[184.6;198.8]	192.0 (24.5)	[211.7;216.8]	488.1 (71.1)	[549.0;563.2]	0.003	**
	10	203.4 (34.7)	[241.5;250.6]	186.3 (16.0)	[200.0;201.7]	335.0 (18.5)	[350.6;357.6]	0.003	**
	15	176.3 (4.5)	[179.5;180.0]	208.1 (8.4)	[215.1;220.0]	502.5 (46.2)	[541.5;574.6]	0.001	**
	20	316.1 (53.9)	[375.1;387.3]	291.3 (22.0)	[303.4;324.9]	506.0 (30.3)	[532.7;539.2]	0.003	**
KW of magnitude (duration fixed)		<0.001 ***		<0.001 ***		<0.001 ***			

* $P_{adj.} < 0.05$; ** $P_{adj.} < 0.01$; *** $P_{adj.} < 0.001$; n.s., not significant.

2.3.1. Bone-Remodeling-Related Target Genes

Expression of bone-remodeling-related genes *ALPL*, *RUNX2*, *BGLAP* and *SP7* was evaluated using RT-qPCR (reference genes: *RPL22* and *POLR2A*). The results are shown in Figure 4 and summarized in Table 1.

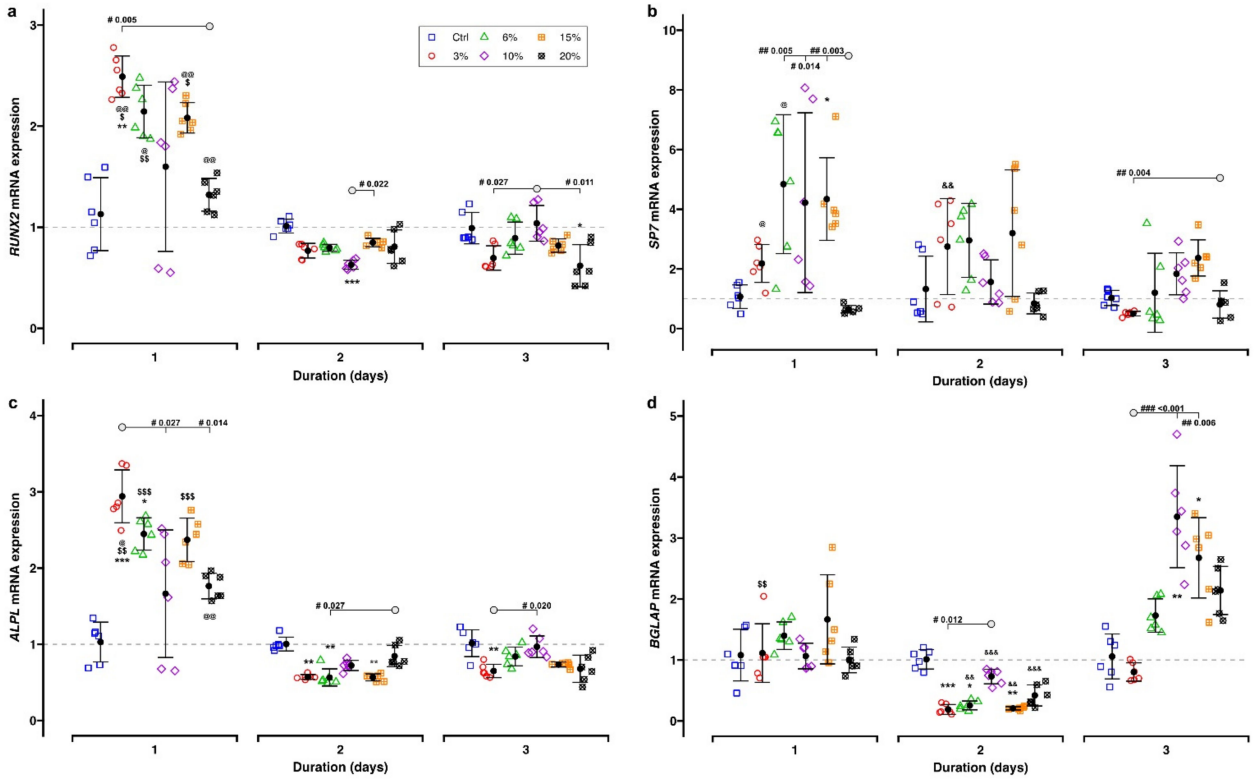

Figure 4. Reverse transcription quantitative real-time polymerase chain reaction (RT-qPCR) results for genes related to bone remodeling after 1 to 3 days of static tensile strain application: (**a**) *RUNX2*, (**b**) *SP7*, (**c**) *ALPL* and (**d**) *BGLAP*. Each experimental unit is summarized by mean (●) and error bars representing SD. The ΔΔCq method was applied, and *RPL22* and *POLR2A* were used as reference genes. Gene expression of controls is indicated by the gray dashed line. Analysis of differences between the test and control groups was carried out with the Kruskal–Wallis test followed by Bonferroni correction for multiple testing. Significant differences between groups are indicated as follows: *, test group vs. corresponding control; effects of duration: $, 1 day vs. 2 days; @, 1 day vs. 3 days; &, 2 days vs. 3 days; effects of magnitudes ("#") are indicated by $P_{adj.}$ values; "○" defines the counterpart of comparisons. Levels of significance: $P_{adj.} < 0.05$: *, $, @, #; $P_{adj.} < 0.01$: **, $$, @@, &&, ##; $P_{adj.} < 0.001$: ***, $$$, &&&, ###.

Generally, the gene expression of *RUNX2* and *ALPL* showed similar dependency on the duration and magnitude of cell stretching. The transcription of both genes showed a significant increase after 1 day of cell stretching (*RUNX2* mean range: 1.32–2.49; *ALPL* mean range: 1.66–2.94), which declined at Days 2 and 3 and ultimately reached control levels (*RUNX2*: 0.62–1.04; *ALPL*: 0.56–0.97) (Figure 4a,c). For both genes, the highest gene expression was found after 3% cell stretching at Day 1 (*RUNX2*: 2.49 ± 0.20, $P_{adj.} = 0.001$; *ALPL*: 2.94 ± 0.35, $P_{adj.} < 0.001$), showing significant differences in comparison to further test groups (*RUNX2*: 3% vs. 20%, $P_{adj.} = 0.005$; *ALPL*: 3% vs. 10%, $P_{adj.} = 0.027$, 3% vs. 20%, $P_{adj.} = 0.014$). The transcriptional activity of both genes increased less after exposure to higher stretching levels (*RUNX2*: 20%, 1.32 ± 0.16; *ALPL:* 10%, 1.66 ± 0.84 and 20%, 1.76 ± 0.17), and differences compared to the controls did not reach statistical significance ($P_{adj.} > 0.05$). Independent of the stretching level, the expression of both target genes either returned to the control levels or was even lower at Days 2 and 3.

Identical to *RUNX2* and *ALPL*, *SP7* expression was also inversely related to the duration of the mechanical stimulation (Figure 4b). The specific amount of stretching applied to the cells caused inconsistent effects on *SP7* gene expression. While lower tensile strain levels (6%, 10% and 15%) led to significant upregulation, maximum cell stretching (20%) induced a downregulation of *SP7* expression which did not reach significance.

Except for 3% magnitude, the *BGLAP* gene was also differentially expressed, mostly depending on the duration of the mechanical stimulation (Figure 4d, Table 1). After 1 day, its gene expression was initially not statistically different from the corresponding controls (mean FC range: 1.00–1.67). A statistically significant downregulation was found for the remaining tensile strain magnitudes (mean FC range: 0.21–0.42) except 10% (mean FC: 0.73) after 2 days. After 3 days of 10% and 15% tensile strain application, a statistically significant upregulation of *BGLAP* was found (FC; 10%: 3.35 ± 0.84; 15%: 2.68 ± 0.66). Cell stretching of 3% led to a significant temporary downregulation (0.19 ± 0.08, $P_{adj.} < 0.001$) at Day 2 only. Maximum *BGLAP* gene expression was identified with 10% cell stretching at Day 3 (FC: 3.35 ± 0.84, $P_{adj.} = 0.001$).

2.3.2. Mechanosensation-Related Target Genes

Generally, *FOS* gene expression remained unchanged at Days 1 and 2, independent of the tensile strain magnitude (mean FC range: 0.77–1.16; Figure 5, Table 1). After three days of cell stretching, upregulation was induced (mean FC range: 1.48–2.05) showing no differences between the various force magnitudes.

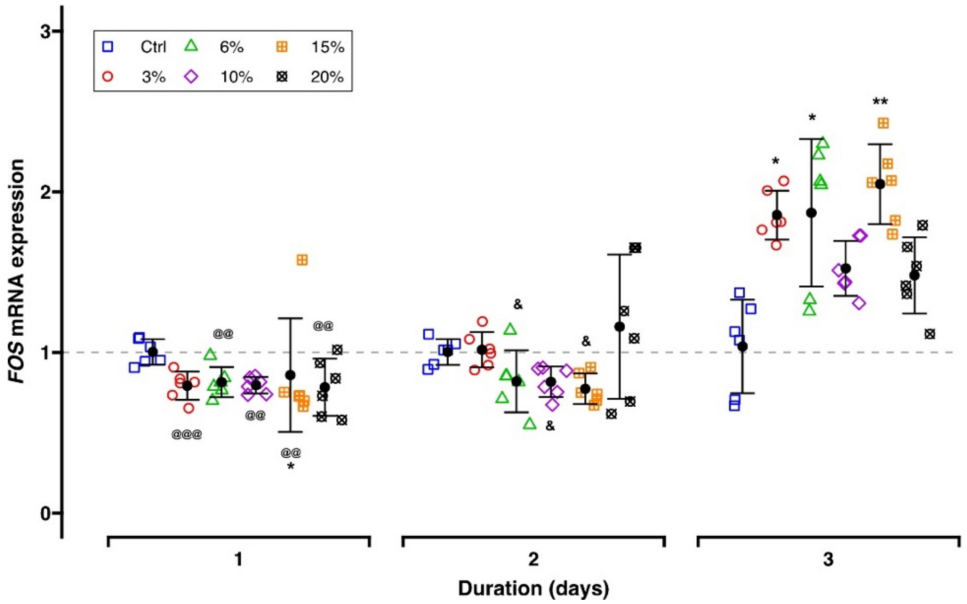

Figure 5. RT-qPCR results of the mechanosensation-related gene *FOS*. Each experimental unit is summarized by mean (●) and error bars representing SD. The ΔΔCq method was applied, and *RPL22* and *POLR2A* were used as reference genes. Gene expression of controls is indicated by the gray dashed line. Analysis of differences between the test and control groups was carried out with the Kruskal–Wallis test followed by Bonferroni correction for multiple testing. Significant differences between groups are indicated as follows: *, test group vs. corresponding control; effects of duration: @, Day 1 vs. Day 3; &, Day 2 vs. Day 3. Levels of significance: $P_{adj.} < 0.05$: *, &; $P_{adj.} < 0.01$: **, @@, $P_{adj.} < 0.001$: @@@.

2.3.3. Inflammation-Related Target Genes

The gene expressions of *IL6* and *PTGS2* on the transcriptional level, as well as the corresponding ELISA results, are given in Figure 6 and Table 1.

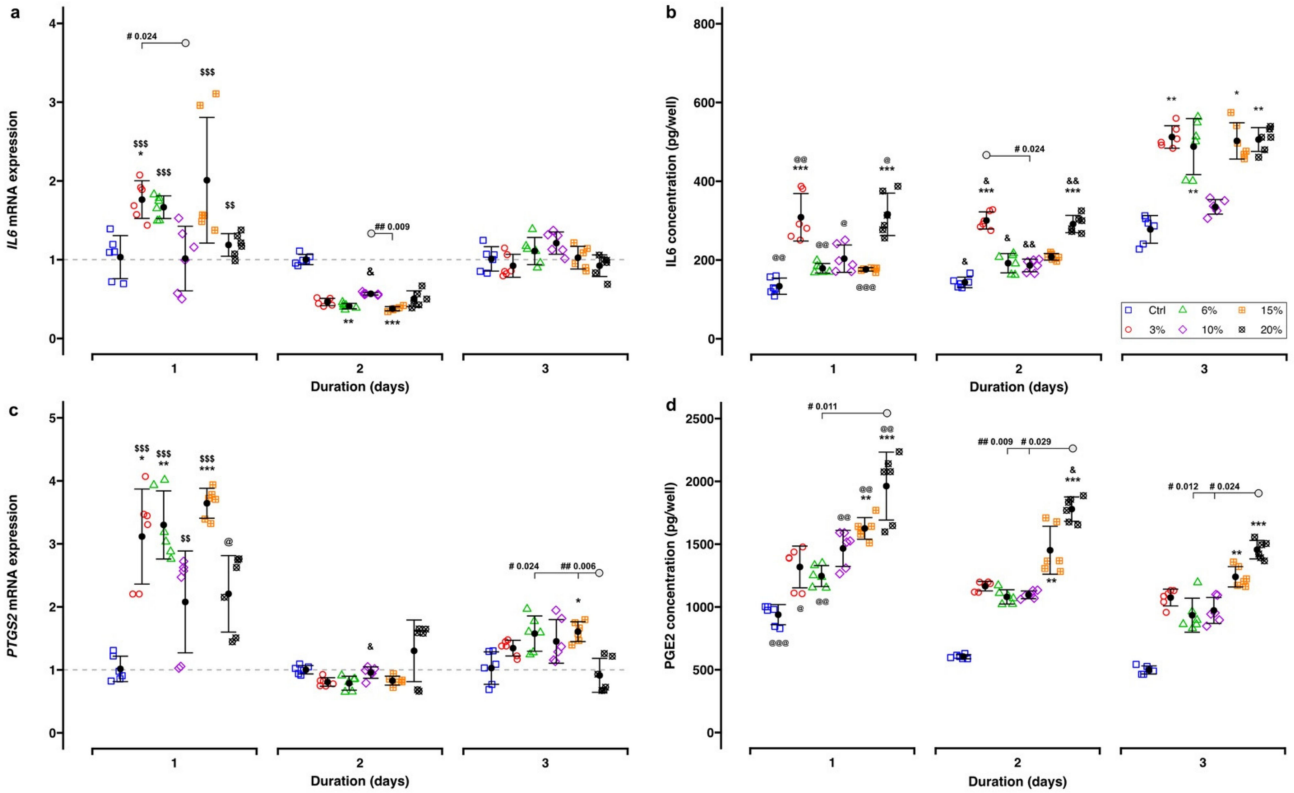

Figure 6. Expression of inflammation-related genes and metabolites: (**a**) *IL6* gene, (**b**) IL6 in the supernatant, (**c**) *PTGS2* gene, (**d**) PGE2 in the supernatant. Each experimental unit is summarized by mean (●) and error bars representing SD. The ΔΔCq method was applied, and *RPL22* and *POLR2A* were used as reference genes. Gene expression of controls is indicated by the gray dashed line. Analysis of differences between the test and control groups was carried out with the Kruskal–Wallis test followed by Bonferroni correction for multiple testing. Significant differences between groups are indicated as follows: *, test groups vs. corresponding control; effect of tensile strain duration: $, Day 1 vs. Day 2; @, Day 1 vs. Day 3; &, Day 2 vs. Day 3; effect of tensile strain magnitude ("#") are reported with $P_{adj.}$ values and "○" defines the counterpart of comparisons. Levels of significance: $P_{adj.} < 0.05$: *, @, &, #; $P_{adj.} < 0.01$: **, $$, @@, &&, ##; $P_{adj.} < 0.001$: ***, $$$, @@@.

Generally, *IL6* gene expression was increased in cells exposed to tensile strain as compared to the controls at Day 1 (mean FC range: 1.01–2.01), but it was significantly attenuated at Day 2 (mean FC range: 0.38–0.57), finally returning to control levels at Day 3 (mean FC range: 0.92–1.21) (Table 1, Figure 6a). The maximum *IL6* gene expression was observed at Day 1 following the application of 15% cell stretching (FC: 2.01 ± 0.80), whereas the lower magnitudes of 3% and 6% induced a less pronounced upregulation (mean FC range: 1.67–1.76). *IL6* gene expression remained unaffected for both the 10% and 20% tensile strain. Two days of cell stretching led to a downregulation of *IL6* gene expression (mean FC range: 0.38–0.57), which was statistically significant for the 6% (FC: 0.41 ± 0.03, $P_{adj.} = 0.002$) and 15% tensile strain (FC: 0.38 ± 0.03, $P_{adj.} < 0.001$) compared to the corresponding controls only. After 3 days of tensile strain application, *IL6* gene expression reached the level of the corresponding control.

Regarding the translational level, IL6 concentration in the cell culture supernatant was dependent on the duration of cell stretching (Table 1, Figure 6b). It was elevated during the first two days in comparison to untreated controls (176.3–316.1 pg/well, which corresponded to a ratio of 1.32–2.37) followed by a further increase after 3 days of cell stretching independent of its magnitude (335.0–512.4 pg/well; ratio: 1.21–1.85). The highest IL6 concentrations were identified with 3% (1 day: ratio = 2.31, $P_{adj.} < 0.001$; 2 days: 2.10, $P_{adj.} < 0.001$; 3 days: 1.85, $P_{adj.} = 0.006$) and 20% tensile strain independent of the duration

(1 day: 2.37, $P_{adj.} < 0.001$; 2 days: 2.04, $P_{adj.} < 0.001$; 3 days: 1.82, $P_{adj.} = 0.008$). Generally, the lowest IL6 concentrations were found after 10% cell stretching at all time points.

PTGS2 gene expression was initially upregulated (Day 1) (mean FC range: 2.08–3.64) (Table 1, Figure 6c), showing the strongest increase for the 15% tensile strain (FC: 3.64 ± 0.24, $P_{adj.} < 0.001$). At Day 2 (mean FC range: 0.79–1.30) *PTGS2* gene expression remained unchanged, whereas at Day 3 almost no effect on gene expression was observed (mean FC range: 0.91–1.61).

Exposure of hPDLCs to tensile strain caused a significant upregulation of PGE2 during the entire observation period, reaching the maximum amount at Day 1 (1246.0–1962.5 pg/well, which corresponded to a ratio of 1.33–2.09 relative to the control) (Table 1, Figure 6d). With lower levels of tensile strain (3%, 6% and 10%), no differences were found compared to the unexposed control in terms of PGE2 expression. Only magnitudes of 15% (1 day: 1.73, $P_{adj.} = 0.001$; 2 days: 2.40, $P_{adj.} = 0.001$; 3 days: 2.49, $P_{adj.} = 0.001$) and 20% (1 day: 2.09, $P_{adj.} < 0.001$; 2 days: 2.95, $P_{adj.} < 0.001$; 3 days: 2.92, $P_{adj.} < 0.001$) significantly amplified PGE2 concentrations.

3. Discussion

Physical loading induces both compression and tensile forces in tissues and cells, influencing and modulating their physiology. It is well established that tension triggers cellular mechanisms, including those leading to bone remodeling at the whole-body level. As such, physiological activities in the orofacial region such as mastication and various non-physiological impacts, i.e., therapeutical stimulation during orthodontic tooth movement induce tensile forces in the periodontal ligament (PDL), promoting tissue and especially bone remodeling therein.

Therefore, the effect of tension on hPDLCs has been widely addressed in numerous in vitro studies, which have been recently reviewed [16,31]. In most of these in vitro studies, the effects of exclusively one specific tensile strain magnitude were analyzed, commonly for a maximum of 48 h using tension devices based on cells growing on a flexible membrane, similar to the one proposed in this study [16]. However, the combined effects of different magnitudes together with various durations on hPDLCs have rarely been compared. Herein, we applied different levels of cell stretching (i.e., 3%, 6%, 10%, 15% and 20%) for various periods of time (i.e., 1, 2 and 3 days), to cover a broad range of tensile strain parameters, and analyzed their impact on the regulation of bone remodeling, mechanosensing and inflammation processes in hPDLCs.

3.1. Selection of Tensile Strain Parameters

In a recently published systematic review [16], different sources were identified to deduce clinical relevant tensile strain magnitudes for in vitro studies: (1) tensile strain derived from mastication or OTM [32–35], (2) finite element simulation including biomechanical confirmation [36,37], (3) the specific anatomy of the periodontium including the PDL width [38], or (4) previously published studies [39–41]. Based on finite element simulations and biomechanical testing, it was shown that bodily movement of a premolar tooth with 1 N pressure induced 1% strain in the PDL on the tension side [36], whereas strains of 6–7% for intrusive and 8–25% for horizontal tooth movement in the PDL were reported after application of 3 N intrusive loading [37]. Similar results were obtained considering the specific anatomy of the PDL in vivo: application of 1 N and 3 N forces to incisors led to an increase in PDL width of ~12% [38]. A recent systematic review reported 10% tensile strain as the most frequently applied magnitude [16]. Herein, 10% tensile strain was selected as being equivalent to a physiological force exposure, whereas 20% cell stretching is commonly used to investigate the influence of pathogenic stimuli on cellular mechanotransduction in hPDLCs [39–41] and therefore was considered the upper limit of tensile strain in this study. Magnitudes of 3% and 6% were applied to determine the lower limit of the mechanical stimulus affecting gene expression [39,41].

In line with most of the previous studies, the total observation period in the current study did not exceed 3 days, avoiding the repetition of cell feeding, which might have unpredictably affected cellular physiology. Based on these considerations, tensile strain magnitudes of 0%, 3%, 6%, 10%, 15% and 20% were applied for 1, 2 and 3 days in this study.

3.2. Effect of Different Parameters of Tensile Strain on Bone Remodeling

The osteogenic differentiation of hPDLCs plays an essential role in the bone remodeling of the periodontium [9,42]. Different genetic loci are involved in its regulation, including but not limited to *RUNX2*, *SP7*, *ALPL*, *BGLAP* and *TNFRSF11B*. Among them, *RUNX2* is considered as one of the key regulators of bone remodeling that is upregulated in both preosteoblasts and immature osteoblasts but downregulated in mature osteoblasts [43]. Expression of *RUNX2* is stimulated by mechanical compression in osteoblasts [13] and mechanical tension in hPDLCs [44]. *RUNX2* is essential for the regulation of several downstream loci involved in osteoblast differentiation and bone-matrix synthesis, including alkaline phosphatase (*ALPL*) and osterix (*SP7*) [45,46]. Being an essential transcription factor for osteogenic differentiation the latter acts downstream of *RUNX2* [6,47]. Belonging to the zinc finger-containing transcription factors of the SP family, *SP7* is expressed in osteoblasts. Its expression is essential for the differentiation of preosteoblasts into mature osteoblasts [6,45]. ALPL expression has been commonly accepted as an early marker for new bone formation [48], which in turn is activated by *RUNX2*, and thus is essential for osteoblast maturation [9,48]. It plays a central role in osteogenic mineralization, bone calcification and mineralization [49–51]. *BGLAP* is the most abundant non-collagenous bone-matrix protein produced by mature osteoblasts [49]. Its expression is regulated among others by *RUNX2* and *SP7* [9,45], and it is highly expressed in the late stage of osteoblast differentiation and mineralization [49].

In this study, expression of *RUNX2*, *SP7*, *ALPL* and *BGLAP* roughly followed a time dependent pattern, showing similarity with the timeline of events occurring during osteogenesis [9]. *RUNX2*, as one of the key regulators of bone remodeling, was upregulated after 1 day of cell stretching only. This finding is consistent with a previous study, showing a considerably amplified *RUNX2* expression within the first 24 h of cell stretching, increasing 6 h after the start of the mechanical stimulation [52]. *RUNX2* upregulation has also been observed in several studies applying dynamic tensile strain [23,42,48,53].

Comparable with the *RUNX2* gene, the *ALPL* gene was also differentially expressed depending on the observation period. The maximum upregulation of *ALPL* gene expression was identified after 1 day of tensile strain application, followed by a slight downregulation afterward, with lower levels (3% and 6%) resulting in stronger gene expression. Similar findings have been reported for 1% and 5% tensile strain [54], whereas other studies report no correlation between *ALPL* gene expression and tensile strain magnitude [49,55]. These contradicting results might be due to differences in the experimental conditions.

SP7, another gene acting downstream of *RUNX2* in the osteoblast differentiation pathway, showed a sustained upregulation, which was most evident for 6% to 15% tensile strain, while 20% caused an adverse effect independent of its duration. The maximum upregulation of *SP7* gene expression was identified at Day 1 for most magnitudes. These results were consistent with other studies, which reported upregulation of *SP7* in hPDLCs after 1 day of tensile strain application [23,45,47]. Similar to *RUNX2*, downregulation was found herein for 20% magnitude at all time points, indicating an inhibitory effect of high magnitude cell stretching for osteogenic differentiation.

BGLAP expression tended to increase with the length of cell stretching applied, revealing the highest expression after 3 days at 6% to 20%. A similar late regulation pattern of *BGLAP* has been reported in other studies [49,54]. The decreasing expression of *BGLAP* after 2 days of cell stretching observed herein might be explained by the cell proliferation of young osteoblasts, considering the heterogeneous characteristics of hPDLCs [56] and the specific characteristic of *BGLAP*, which is mainly upregulated in mature osteoblasts [9].

Similarly, downregulation of *BGLAP* was also identified in stretched osteoblasts, which was attributed to the presence of osteoblasts in different stages of development [54].

Interestingly, *TNFRSF11B* gene expression was below the detection limit in all experimental conditions in this study. In contrast, upregulation of *TNFRSF11B* has been reported previously in hPDLCs after exposure to static tensile strain for 12 h but not for longer periods of time [16,54,57]. Thus, one might assume that the *TNFRSF11B* gene is already upregulated by tensile strain in shorter time periods than covered in the present study.

3.3. Effect of Different Parameters of Tensile Strain on Mechanosensing

FOS is an immediate/early response gene which is essential for the perception of mechanical stimulation. Dimerization of FOS with JUN creates the active heterodimeric transcription factor AP1, which plays a central role in osteoblast proliferation and differentiation [11,34]. Regardless of tension magnitudes, upregulation of *FOS* in hPDLCs was only observed after 3 days of tension in this study. Other studies have reported upregulation of *FOS* in stretched hPDLCs as early as after 15 min [58,59] and 3 h [60] of tensile strain application. Shorter force application intervals should be added in further studies, considering the early response characteristics of *FOS*.

3.4. Effect of Different Parameters of Tensile Strain on Inflammation

It has been demonstrated that inflammation is induced by mechanical stimuli during OTM [3] and regulated by several cytokines and chemokines [61]. Among others, IL6, PGE2, *PTGS2*, TNF, IL8 and IL1B play key roles in inflammation and bone resorption, while IL10 is regarded as an anti-inflammatory mediator. As an inflammatory cytokine, IL6 is involved in osteoclastogenesis [4,52] and its regulation by tensile strain has been reported in several previous in vitro studies [52,55,62,63].

In this study, *IL6* gene expression was upregulated after 1 day of cell stretching depending on the magnitude, but no effect was found after 3 days. In contrast, on the translational level the total amount of IL6 increased with the length of cell stretching for all magnitudes in the current study. In a study of Jacobs et al. [62] no significant time dependency was found for *IL6* gene expression, but it tended to correlate with the strength of tensile strain application. It was suggested that lower strain magnitudes induce anti-inflammatory effects whereas higher magnitudes lead to pro-inflammatory effects [62]. A similar conclusion was proposed by Wada et al. [52], who reported an upregulated *IL6* gene expression after 15% strain application within the first 24 h. On the other hand, Nazet et al. [55] reported a decreased *IL6* gene expression after 16% and 35% tensile strain applied for 48 h. The inconsistent results observed in these studies might be due to the pro- and anti-inflammatory properties of IL6, together with the complex regulation pathway [63].

PTGS2 is a key enzyme involved in PGE2 biosynthesis and both play essential roles in inflammation and bone resorption in response to mechanical stimuli [64,65]. Generally, increasing *PTGS2* expression and PGE2 synthesis is reported after exposure of hPDLCs to increasing magnitudes of static tensile strain [55,62]. Concerning the effects of tensile strain duration on *PTGS2* gene expression, partially contradicting results have been reported [52,55]. Interestingly, no significant difference in the transcription of the *PTGS2* gene for different magnitudes was found herein in general, whereas PGE2 expression was significantly amplified after tensile strain application with higher magnitudes (15% and 20%). Taken together, it seems reasonable to assume that higher magnitudes of tensile strain lead to increased inflammation and should thus be avoided in clinical situations.

IL1B, TNF, IL8 and IL10 were below the detection limits of the ELISA systems applied in this study. So far, expression of IL8 and IL10 after tensile strain application has been reported for cells exposed to dynamic tensile strain only [4,66]. Though upregulation of IL1B and TNF has been previously reported for static tensile strain [49,52], the different molecular response might be due to individual difference among cells from different donors.

A growing portion of orthodontic patients presents with periodontal disease [1,67,68]. Periodontitis has been associated not only with numerous chronic systemic inflammatory

and autoimmune conditions, such as atherosclerosis, diabetes mellitus and rheumatoid arthritis [69], but also with macular degeneration [70] and colorectal cancer [71]. It has been hypothesized that pro-inflammatory mediators (e.g., IL6 and IL1B), which are highly expressed locally within inflamed periodontal tissue, will be spread systematically, ultimately amplifying different pre-existing non-oral inflammation [71]. It has been proposed that OTM and periodontitis share some molecular pathways, particularly in terms of inflammation and osteogenesis/osteclastogenesis. Yet, the interrelation between both conditions as well as the association between periodontitis and several distinct systemic diseases remain to be elucidated. Herein, the expression of several genes coding for pro-inflammatory mediators was positively correlated with the exposure of PDL cells against tensile strain. In order to avoid an exaggerated expression of pro-inflammatory stimuli during orthodontic tooth movement that might additionally enhance periodontitis-associated inflammation and tissue destruction, lower therapeutic forces might be appropriate for the orthodontic treatment of patients with a history of periodontitis as compared to periodontally healthy patients.

3.5. Clinical Relevance

In this study the effects of different tension parameters applied to hPDLCs were analyzed with reference to bone remodeling, mechanosensing and inflammation. The expression of genes regulating bone remodeling was clearly dependent on the duration of tensile strain application. Generally, lower magnitudes ($\leq$15%) enhanced bone remodeling, whereas 20% tensile strain attenuated bone remodeling. Upregulation of inflammation-related genes was correlated with higher tensile strain (15% and 20%). Though it is difficult to transfer in vitro results to the in vivo situation, it seems to be reasonable to assume that excessive forces might lead to adverse effects in clinical situations, especially in patients with a high susceptibility of periodontitis or associated diseases. Light orthodontic forces seem to be beneficial for coordinated bone remodeling and the maintenance of periodontal tissue homeostasis, ultimately enabling efficient tooth movement.

3.6. Strengths and Limitations of the Study

In this study, an apparatus was designed and manufactured to apply different levels of tensile strain simultaneously. This was achieved by using 3D designed and printed caps, which allowed the parameterized variation of tensile strain magnitudes.

Different tensile strain magnitudes and durations were applied to hPDLCs derived from the same donor and treated the same way throughout all experimental procedures. Regulation of genetic loci related to bone remodeling, mechanosensation and inflammation were investigated in this study, which was followed by a comprehensive analysis of their strain magnitude and duration-related expression.

Additionally, the stability of a panel of reference genes was evaluated using samples from the experimental condition and the corresponding controls and analyzed by four different algorithms calculating reference gene stability. Based on the computational analysis, the two most stable reference genes were selected to reduce variations in RT-qPCR experiments [30].

Though a comprehensive range of tensile strain magnitudes and durations was selected in this study, the first sampling took place after 1 day of strain application. Thus, early response genes, such as *FOS*, might have been undetectable. Taking this into account, additional earlier sampling points with regard to the initiation of the force application might have been appropriate.

Sample collection was performed after unloading of the experimental setup. Its disassembly and the time needed for sample preparation comprised a relevant delay between unloading and sample collection (i.e., cell lysates for gene expression studies, or collection of cell culture supernatants), leading to a possible change of cellular activity and/or physiology.

The PDL is considered as the main target of mechanical stimulation within the periodontium [12,72]. The effects of in vitro mechanical stimulation on PDL cells have been summarized in several recent reviews [16–18,73,74]. Independent of the specific isolation technique applied, it is commonly accepted that isolated PDL cells in fact represent a heterogeneous cell phenotype, which is primarily determined by the anatomical origin (middle third of the root) and the fibroblastic growth characteristics [56,75]. Long-term cultivation of hPDLCs typically leads to changes in cell morphology, growth rate, gene expression and response to mechanical stimulation [16,56,76–78]. To address this problem and to increase phenotypic homogeneity, hPDLCs are normally used in in vitro studies only with low passage numbers (passage ≤ 7) [56]. Nevertheless, it should be mentioned that clonal selection has been observed in hPDLCs as early as Passage 2, whereas *RUNX2*, *COL1A1* and *ALPL* expressions were not shown to be affected by passage number [79]. Yet, the particular phenotype of PDL cells as used herein has not been additionally confirmed based on molecular markers. Only a comparably small number of primary PDL cells can be harvested from one healthy donor. Hence, a balance between absolute cell amount and passage number must be achieved to conduct cell culture experiments, if pooling of cells from different individuals or the usage of immortalized primary cell lines should be avoided [56,80]. Since many different parameters have been tested herein to thoroughly delineate the effects of tensile strain on hPDLCs, a considerably large number of donor-specific cells was required. Thus, hPDLCs isolated according to standard protocols originating from one donor were used at Passages 5–6 [56].

Nevertheless, to gain insight into the biological variability of gene regulation during tensile strain application, cells derived from different donors should be included in future studies [60,81].

4. Materials and Methods

4.1. Primary Cell Culture

HPDLCs were obtained from the healthy first premolars of a 15-year-old female, which were removed due to orthodontic reasons with informed consent from the patient and her legal custodian. This study was conducted in accordance with the Declaration of Helsinki (https://www.wma.net/what-we-do/medical-ethics/declaration-of-helsinki/; accessed on 27 January 2022). Approval for the collection and use of hPDLCs was obtained from the ethics committee of the Ludwig-Maximilians-Universität München (project number 045-09).

Cells were derived from tissue samples obtained from the middle third of the roots using the explant technique as described by Somerman, et al. [75]. HPDLCs were cultivated with low glucose DMEM (21885025, Gibco, Life Technologies, Carlsbad, CA, USA) supplemented with 10% FBS (F7524; Sigma-Aldrich, St. Louis, MO, USA), 2% MEM vitamins (M6895; Biochrom, Berlin, Germany) and 1% of antibiotic/antimycotic (15240-062; Life Technologies, Carlsbad, CA, USA). Cells were grown in a humidified atmosphere with 5% CO_2 at 37 °C and passaged in regular intervals of 3 to 4 days using 0.05% trypsin-EDTA solution (59417C; Sigma-Aldrich, St. Louis, MO, USA). Cells from Passages 5–6 were used in all experiments.

4.2. Tensile Strain Application Using a Custom-Made Tension Apparatus

Based on previous publications [55,82], an apparatus (Figures 1 and 7) was constructed: (1) to apply different magnitudes of static equibiaxial tensile strain to adherent cells and (2) to feed cells without the relaxation of the flexible substrate delivering tensile strain to these cells. The apparatus consisted of five parts: a "base plate", 3D-printed pinned spherical caps, a BioFlex® Collagen-I coated Culture Plate (BF-3001C, Flexcell Intl. Corp., Hillsborough, NC, USA), a "frame" and screws (Figure 7).

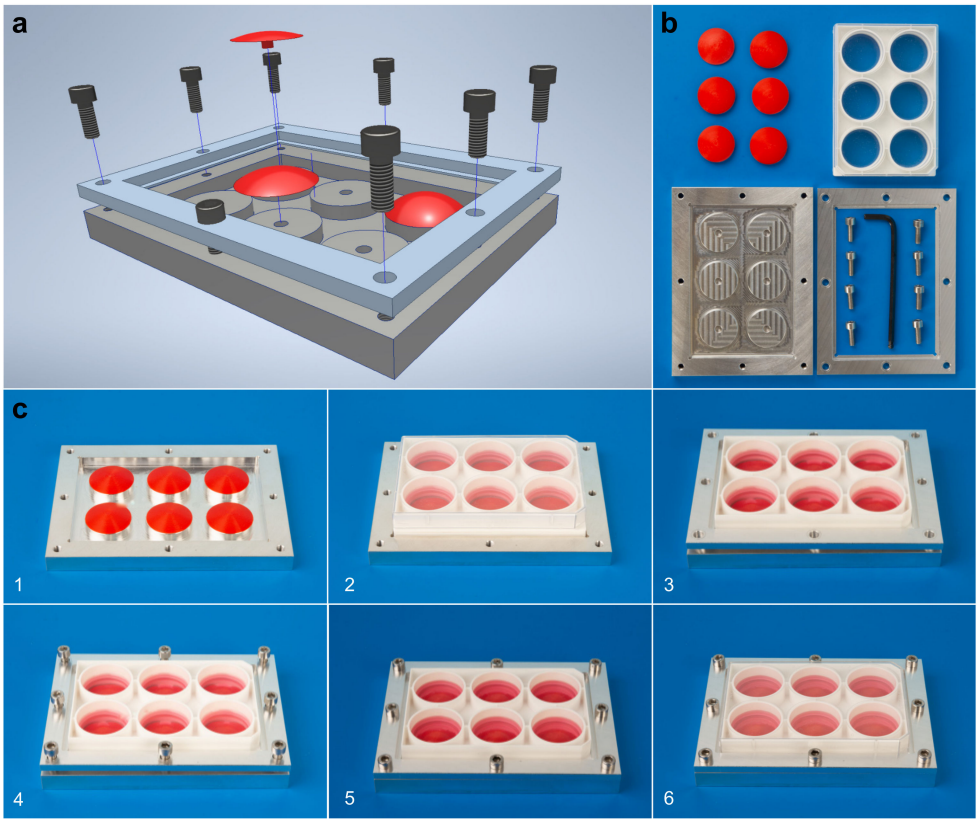

Figure 7. Experimental setup used to apply tensile strain. The apparatus consisted of 5 parts: the base plate, the pinned spherical cap, the BioFlex® plate, the frame and the screws. After assembly, the cell-attached membrane was fitted onto the pinned spherical cap and stretched, producing predefined magnitudes of tensile strain. (**a**) 3D representation of the apparatus; (**b**) parts of the apparatus; (**c**) step-by-step (1–6) assembly of the apparatus.

The base plate, frame and spherical caps were constructed using a CAD program (Autodesk® Inventor® Professional 2019, Autodesk Inc., San Rafael, CA, USA) according to data published elsewhere [55,82]. Prototypes of the base plate, the frame and spherical caps representing different tensile strain levels [55] (Table 2) were printed with a 3D printer (Ultimaker 3, Ultimaker, Geldermalsen, The Netherlands) using a polylactic acid filament (Ultimaker PLA filament 2.85 mm, part no. 1618, Ultimaker); a polyvinyl alcohol filament was used to print the support structures (Ultimaker PVA filament 2.85 mm, Ultimaker). The final base plates and frames were made from aluminum by the workshop of the Department of Physics, LMU München. The 3D-printed spherical caps were used in the experiments.

Table 2. Cap parameters and media volume.

Parameter	Membrane Area Increase					
	0% (Control)	3%	6%	10%	15%	20%
Radius r (mm) [1]	n.a.	50.62	36.82	29.54	25.25	22.82
Height h (mm) [1]	n.a.	2.94	4.16	5.38	6.58	7.60
Volume of medium (mL)	2.89	4.37	4.96	5.54	6.08	6.52

[1] Nazet et al. [55], Figure 1 with b = 17.0 mm.

HPDLCs were seeded at a cell density of 1.2×10^5 cells/well on 6-well collagen-I coated BioFlex® Culture Plates (Flexcell Intl. Corp., Hillsborough, NC, USA) and incubated overnight. Immediately prior to the assembly of the apparatus, the culture medium was changed. Then, the tensile strain application apparatus was assembled in a sterile environ-

ment as follows (Figure 7b,c): (1) 3D-printed spherical pinned caps were symmetrically inserted into the aluminum base plate; (2) the cover of the BioFlex® plate was removed, and the plate was vertically placed onto the caps; (3) the frame was placed on the edges of the plate and screws were crosswise tightened symmetrically to fix the frame, plate and base plate and thus applying tensile strain to the adherent cells. The plate was covered and placed back into the CO_2 incubator.

The elastic membranes including the attached cells were stretched by caps of different parameters (Table 2), resulting in an increase of membrane area of 0% (i.e., control), 3%, 6%, 10%, 15% and 20% and thus applying tensile strain to the cells [55]. Controls (0% tensile strain) were defined as wells without caps. All strain magnitudes were applied for 1, 2 and 3 days in two identical sets of apparatuses: one set for cell viability testing and the other for gene expression measurement and ELISA. For each tensile strain magnitude, three biological replicates were allocated for each duration. All assembled apparatuses were incubated and treated under the same conditions.

4.3. Cell Viability

The cell viability of hPDLCs for all magnitude/duration combinations was assessed using a live/dead cell staining kit (PK-CA707-30002, PromoKine, Heidelberg, Germany) according to the manufacturer's instructions. Following strain release and removal of the supernatants, all wells were washed twice with PBS. Afterward, the BioFlex® plates' silicone membranes were cut out and placed in pre-labeled cell culture dishes (628160, CELLSTAR®, Greiner Bio-One GmbH, Frickenhausen, Germany). The membranes were then covered with fresh staining solution and incubated for 40 min in complete darkness at room temperature. Fluorescence microphotographs were taken of the centers of each membrane with a fluorescence microscope (EVOS® *FL*, Invitrogen, Carlsbad, CA, USA) using 10× and 20× objectives.

4.4. Sample Preparation

After 1, 2 and 3 days of tensile strain application, the plate covers of the specific setup were removed. Cell culture supernatants from all wells were collected individually for ELISA (see below). The volume of each sample was recorded, and the samples were stored at −20 °C for further ELISA analysis. Next, the adherent cells were washed twice with sterile PBS, and cell lysates were prepared from each well using 750 µL RNA lysis buffer (R0160-1-50; Zymo, Irvine, CA, USA) according to the manufacturer's instructions. Cell lysates were stored at −80 °C until all samples were collected.

4.5. Gene Expression Analysis

Analysis of *PTGS2*, *IL6*, *FOS*, *RUNX2*, *SP7*, *ALPL*, *BGLAP*, *TNFRSF11B* and *TNF* gene expressions following tensile strain application was carried out for all experimental magnitude/duration combinations according to previously described protocols [14]. A synopsis of the sample preparation and quantitative RT-PCR (RT-qPCR) is given below. A checklist according to the "Minimum Information for Publication of Quantitative Real-Time PCR Experiment" (MIQE) guidelines [30,83] is provided in Supplementary Table S2.1.

Total RNA preparation: Total RNA preparation was carried out using the Quick-RNA™ MicroPrep Kit (R1051; Zymo, Ivine, CA, USA) according to the manufacturer's instructions. The following two steps were included in the procedure to reduce possible genomic DNA contamination: (I) defrosted cell lysates were centrifuged through QIAshredder™ columns (Qiagen, Hilden, Germany) before column purification; (II) during column purification, Dnase I digestion (Zymo) was applied. Finally, total RNA was eluted with 15 µL of Dnase/Rnase-free water (Zymo). Rnase inhibitor (Rnasin®, N2515; Promega, Madison, WI, USA) was added to each eluate at a final concentration of 1 U/µL. The total RNA preparations were stored at −80 °C until further use.

PCR primer selection: Generally, primer sequences were selected from public sources for both genes of interest and potential reference genes (Table 3). All primer pairs used

were tested in silico according to the MIQE guidelines [30] as previously published [14] (Supplementary Tables S2.1 and S2.2). If not otherwise mentioned, unmodified primers were synthesized by Metabion GmbH (Planegg/Steinkirchen, Germany; Oligonucleotide Purification Cartridge OPC® purification). Optimal annealing temperatures were determined with gradient PCR using the qPCR cycling program as specified in the MIQE checklist (Supplementary Table S2.1). Primer specificity was confirmed by agarose gel electrophoresis. Primer efficiencies were evaluated using standard curves prepared from serial dilutions of cDNA as specified in Supplementary Table S2.3 and quantified in the LightCycler® 480 using the primer pairs detailed in Table 3.

Reference gene selection: A panel of reference genes (*EEF1A1*, *GAPDH*, *POLR2A*, *PPIB*, *RNA18SN5*, *RPL0*, *RPL22* and *YWHAZ*) was selected from public sources [55,84]. Evaluation of these reference genes was carried out using cDNA sampled from control, 10% and 20% after 1 and 3 days of static tensile strain application. RT-qPCR was performed as described below using gene-specific primers (Supplementary Table S2.3). The raw C_q values (Supplementary Table S1.1) were analyzed using RefFinder [85] (URL: https://www.heartcure.com.au/reffinder/ (accessed on 30 March 2021)), and the most stable genes were used as reference genes in RT-qPCR (Table 3).

RT-qPCR: Total RNA samples were thawed, and RNA concentration was determined photometrically (NanoDrop ND-1000, Peqlab, Erlangen, Germany). All RNA samples (600 ng each) were reverse transcribed to cDNA in a total reaction volume of 20 µL using the SuperScript™ IV First-Strand Synthesis System (18091050, Thermo Fisher Scientific, Waltham, MA, USA) and random primers as described by the manufacturer. Quantitative PCR was performed with the Luminaris Color HiGreen qPCR Master Mix Kit (K0392; Thermo Fisher Scientific, Waltham, MA, USA) following the instructions of the manufacturer using 2 µL cDNA (1:5 prediluted) in each PCR reaction. Each qPCR reaction included an initial Uracil-DNA glycosylase pre-treatment step to prevent carry-over contamination. Further details of the RT-qPCR reaction conditions are summarized in the MIQE checklist (Supplementary Table S2.1).

Gene expression calculation: Expression of target genes was quantified using the ΔΔCq method [86] with the selected reference genes *POLR2A* and *RPL22*. For each tension/duration combination, six qPCR reactions were analyzed representing three biological replicates with two technical replicates each.

4.6. Enzyme-Linked Immunosorbent Assay

Complete cell culture supernatant from all wells was collected for ELISA. The protein concentration of IL6, IL1B, IL8, TNF and IL10 was determined using the following DuoSet human ELISA kits (all from R&D Systems, Minneapolis, MN, USA): IL6 (DY206-05), IL1B (DY201-05), IL8/CXCL8 (DY208-05), TNF (DY210-5) and IL10 (DY217B-05). The PGE2 concentration in the cell culture supernatant was determined using the "PGE2 High Sensitivity ELISA kit" (ADI-931-001; Enzo Life Sciences (ELS) AG, Lausen, CH). All measurements were conducted using a microplate reader (Varioscan, Thermo Electron Corporation, Vantaa, Finland). For each magnitude/duration combination three biological replicates were measured twice. The measurements were reported as "concentration per well" (ng/well) using the well-specific volumes of each supernatant.

4.7. Statistics

Descriptive statistics of the gene expression and ELISA results are reported as mean ± standard deviation (SD) and 95% confidence intervals. All calculations were based on three biological replicates with two technical replicates for each gene/magnitude/duration combination. For each gene locus and marker molecule, differences between the different tensile strain magnitudes and durations were evaluated using the Kruskal–Wallis test followed by Bonferroni correction for multiple comparisons ($P_{adj.}$). All statistical procedures were carried out using IBM SPSS Statistics 27 (IBM Corp., Armonk, NY, USA). All test procedures were two-tailed considering $P_{adj.}$ values < 0.05 significant.

Table 3. Specification of the PCR primers used for gene quantification.

Gene	GenBank Accession Number	Primer Sequence (f: 5′-Forward Primer-3′; r: 5′-Reverse Primer-3′)	Annealing Temp. (°C)	Data Acquisition Temp. (°C)	Amplicon Size (bp)	Primer Efficiency	Source
PTGS2	NM_000963.4	f: AAGCCTTCTCTAACCTCTCC r: GCCCTCGCTTATGATCTGTC	58	77	234	1.995	Janjic Rankovic et al. [14], Shi et al. [87]
IL6	NM_000600.5	f: TGGCAGAAAACAACCTGAACC r: TGGCTTGTTCCTCACTACTCTC	58	76	168	1.955	Janjic Rankovic et al. [14], Shi et al. [87]
FOS	NM_005252.4	f: GCTTTGCAGACCGAGATTGC r: TTGAGGAGAGGCAGGGTGAA	58	83	203	1.860	Janjic Rankovic et al. [14]
RUNX2	NM_001015051.4	f: GCGCATTCCTCATCCCAGTA r: GGCTCAGGTAGGAGGGGTAA	58	81	176	1.954	Shi et al. [7], Janjic Rankovic et al. [14]
SP7	NM_001173467.3	f: GGCACAAAGAAGCCGTACTC r: CACTGGGCAGACAGTCAGAA	61	81	247	1.935	Gronthos et al. [88]
ALPL	NM_001127501.4	f: GGACCATTCCCACGTCTTCAC r: CCTTGTAGCCAGGCCCATTG	64	80	137	1.968	Liu et al. [26]
BGLAP	NM_199173.6	f: AGCGAGGTAGTGAAGAGAC r: GAAAGCCGATGTGGTCAG	64	82	142	2.076	Gartland et al. [89]
TNFRSF11B	NM_001066	f: TCAAGCAGGAGTGCAATCG r: AGAATGCCTCCTCACACAGG	64	81	342	1.941	Yang et al. [46]
TNF	NM_000594.4	Commercial primer pair from realtimeprimers.com (Order information: VHPS-9415 †)	58	79	173	1.967	Janjic Rankovic et al. [14], Shi et al. [87]
POLR2A	NM_000937.5	f: TCGCTTACTGTCTTCCTGTTGG r: TGTGTTGGCAGTCACCTTCC	58	79	108	1.886	Nazet et al. [55]
RPL22	NM_000983.4	f: TGATTGCACCCACCCTGTAG r: GGTTCCCAGCTTTTCCGTTC	61	75	98	1.939	Nazet et al. [55]

† Real Time Primers, LLC, Elkins Park, PA, USA (primer sequences are disclosed upon purchase).

5. Conclusions

This study covered a broad range of tensile strain magnitudes and durations, with focus on bone remodeling, mechanosensing and inflammation. Generally, lower magnitudes were in favor of osteogenesis and resulted in less or even inhibited inflammation. Higher magnitudes led to an inhibition of osteogenesis and induced a higher level of inflammation. Among all magnitudes applied, 10% was optimal with higher levels of osteogenesis without evoking significant inflammation at the same time. The results showed an improved insight into the biological regulations of hPDLCs after exposure to different levels of tensile strain for a maximum period of 3 days. The current data might be useful in defining appropriate forces for OTM in clinical situations. Light orthodontic forces seem to be beneficial for coordinated bone remodeling and the maintenance of periodontal tissue homeostasis, ultimately enabling efficient tooth movement. The current results suggest that different force magnitudes might affect the expression of inflammatory- and bone-remodeling-related factors differently. These observations might be of relevance for future clinical studies, especially on interdisciplinary topics such as the application of orthodontic force as a regenerative stimulus to enhance periodontal defect healing.

Supplementary Materials: The following are available online at https://www.mdpi.com/article/10.3390/ijms23031525/s1.

Author Contributions: Conceptualization, U.B., A.W. and C.S.; Methodology, U.B., C.S., M.J.R. and T.S.; Software, U.B. and T.S.; Validation, U.B., C.S. and T.S.; Formal Analysis, U.B., C.S. and M.J.R.; Investigation, U.B., C.S. and M.J.R.; Resources, U.B. and A.W.; Data Curation, U.B., C.S. and M.J.R.;

Writing—Original Draft Preparation, U.B. and C.S.; Writing—Review and Editing, U.B., C.S., M.J.R., M.F., T.S. and S.O.; Supervision, U.B., A.W. and M.F. All authors have read and agreed to the published version of the manuscript.

Funding: Changyun Sun was supported by a grant from the China Scholarship Council (CSC File No 201809370043).

Institutional Review Board Statement: The study was conducted according to the guidelines of the Declaration of Helsinki. Approval for the collection and use of hPDLCs was obtained from the ethics committee of the Ludwig-Maximilians-Universität München (project number 045-09; primal date of approval 24 March 2009; latest amendment approved on 23 July 2019).

Informed Consent Statement: Informed consent was obtained from all subjects involved in the study.

Data Availability Statement: All authors confirm that all related data supporting the findings of this study are given in the article and its Supplementary Materials.

Acknowledgments: The authors would like to give great thanks to Christine Schreindorfer and Laure Djaleu (both from the Department of Orthodontics, University Hospital, LMU Munich) for their assistance regarding the lab work. The aid of Jürgen Aust in the final manufacturing of the tension apparatus is gratefully acknowledged.

Conflicts of Interest: The authors declare that there is no conflict of interest regarding this manuscript.

Abbreviations

ALPL	Alkaline phosphatase, biomineralization associated
BGLAP	Bone gamma-carboxyglutamate protein
ELISA	Enzyme-linked immunosorbent assay
FC	Fold change
IL10	Interleukin 10
IL1B	Interleukin 1B
IL6	Interleukin 6
IL8	Interleukin 8
KW	Kruskal-Wallis test
MIQE	Minimum Information for Publication of Quantitative Real-Time PCR Experiment
OPG	Osteoprotegerin
OTM	Orthodontic teeth movement
$P_{adj.}$	Adjusted *P*
PDL	Periodontal ligament
PDLCs	Periodontal ligament cells
PGE2	Prostaglandin E2
PTGS2	Prostaglandin-endoperoxide synthase 2
qPCR	Quantitative real-time polymerase chain reaction
RANKL	Receptor activator of the nuclear factor kappa ligand
RT-qPCR	Reverse transcription qPCR
RUNX2	*Runt*-related transcription factor 2
SD	Standard deviation
TNF	Tumor necrosis factor α
TNFRSF11B	Tumor necrosis factor-alpha receptor superfamily member 11B

References

1. Wichelhaus, A. *Orthodontic Therapy—Fundamental Treatment Concepts*; Georg Thieme: New York, NY, USA, 2017.
2. Pavasant, P.; Yongchaitrakul, T. Role of mechanical stress on the function of periodontal ligament cells. *Periodontology 2000* **2011**, *56*, 154–165. [CrossRef]
3. Yamaguchi, M.; Kasai, K. Inflammation in periodontal tissues in response to mechanical forces. *Arch. Immunol. Ther. Exp.* **2005**, *53*, 388–398.
4. Long, P.; Hu, J.; Piesco, N.; Buckley, M.; Agarwal, S. Low magnitude of tensile strain inhibits IL-1beta-dependent induction of pro-inflammatory cytokines and induces synthesis of IL-10 in human periodontal ligament cells in vitro. *J. Dent. Res.* **2001**, *80*, 1416–1420. [CrossRef]

5. Zeichner-David, M. Genetic influences on orthodontic tooth movement. In *Biological Mechanisms of Tooth Movement*, 2nd ed.; Krishnan, V., Davidovitch, Z., Eds.; Wiley: Chichester, UK, 2015; pp. 145–163.
6. Li, L.; Han, M.; Li, S.; Wang, L.; Xu, Y. Cyclic tensile stress during physiological occlusal force enhances osteogenic differentiation of human periodontal ligament cells via ERK1/2-Elk1 MAPK pathway. *DNA Cell Biol.* **2013**, *32*, 488–497. [CrossRef] [PubMed]
7. Shi, J.; Folwaczny, M.; Wichelhaus, A.; Baumert, U. Differences in RUNX2 and P2RX7 gene expression between mono- and coculture of human periodontal ligament cells and human osteoblasts under compressive force application. *Orthod. Craniofacial Res.* **2019**, *22*, 168–176. [CrossRef] [PubMed]
8. Nakashima, K.; Zhou, X.; Kunkel, G.; Zhang, Z.; Deng, J.M.; Behringer, R.R.; de Crombrugghe, B. The novel zinc finger-containing transcription factor osterix is required for osteoblast differentiation and bone formation. *Cell* **2002**, *108*, 17–29. [CrossRef]
9. Rutkovskiy, A.; Stensløkken, K.O.; Vaage, I.J. Osteoblast Differentiation at a Glance. *Med. Sci. Monit. Basic Res.* **2016**, *22*, 95–106. [CrossRef]
10. Boyce, B.F.; Xing, L. Biology of RANK, RANKL, and osteoprotegerin. *Arthritis Res. Ther.* **2007**, *9* (Suppl. S1), S1. [CrossRef]
11. Yamaguchi, N.; Chiba, M.; Mitani, H. The induction of c-fos mRNA expression by mechanical stress in human periodontal ligament cells. *Arch. Oral Biol.* **2002**, *47*, 465–471. [CrossRef]
12. Krishnan, V.; Davidovitch, Z. Biology of orthodontic tooth movement. In *Biological Mechanisms of Tooth Movement*, 2nd ed.; Krishnan, V., Davidovitch, Z., Eds.; Wiley: Chichester, UK, 2015; pp. 15–29.
13. Baumert, U.; Golan, I.; Becker, B.; Hrala, B.P.; Redlich, M.; Roos, H.A.; Palmon, A.; Reichenberg, E.; Müßig, D. Pressure simulation of orthodontic force in osteoblasts: A pilot study. *Orthod. Craniofacial Res.* **2004**, *7*, 3–9. [CrossRef] [PubMed]
14. Janjic Rankovic, M.; Docheva, D.; Wichelhaus, A.; Baumert, U. Effect of static compressive force on in vitro cultured PDL fibroblasts: Monitoring of viability and gene expression over 6 days. *Clin. Oral Investig.* **2020**, *24*, 2497–2511. [CrossRef] [PubMed]
15. Benjakul, S.; Jitpukdeebodintra, S.; Leethanakul, C. Effects of low magnitude high frequency mechanical vibration combined with compressive force on human periodontal ligament cells in vitro. *Eur. J. Orthod.* **2018**, *40*, 356–363. [CrossRef]
16. Sun, C.; Janjic Rankovic, M.; Folwaczny, M.; Otto, S.; Wichelhaus, A.; Baumert, U. Effect of Tension on Human Periodontal Ligament Cells: Systematic Review and Network Analysis. *Front. Bioeng. Biotechnol.* **2021**, *9*, 695053. [CrossRef] [PubMed]
17. Li, M.; Zhang, C.; Yang, Y. Effects of mechanical forces on osteogenesis and osteoclastogenesis in human periodontal ligament fibroblasts: A systematic review of in vitro studies. *Bone Jt. Res.* **2019**, *8*, 19–31. [CrossRef] [PubMed]
18. Spitz, A.; Christovam, I.O.; Maranon-Vasquez, G.A.; Masterson, D.F.; Adesse, D.; Maia, L.C.; Bolognese, A.M. Global gene expression profile of periodontal ligament cells submitted to mechanical loading: A systematic review. *Arch. Oral Biol.* **2020**, *118*, 104884. [CrossRef] [PubMed]
19. Zhao, D.; Wu, Y.; Xu, C.; Zhang, F. Cyclic-stretch induces apoptosis in human periodontal ligament cells by activation of caspase-5. *Arch. Oral Biol.* **2017**, *73*, 129–135. [CrossRef]
20. Wang, L.; Yang, X.; Wan, L.; Wang, S.; Pan, J.; Liu, Y. ARHGAP17 inhibits pathological cyclic strain-induced apoptosis in human periodontal ligament fibroblasts via Rac1/Cdc42. *Clin. Exp. Pharmacol. Physiol.* **2020**, *47*, 1591–1599. [CrossRef] [PubMed]
21. Zhao, D.; Wu, Y.; Zhuang, J.; Xu, C.; Zhang, F. Activation of NLRP1 and NLRP3 inflammasomes contributed to cyclic stretch-induced pyroptosis and release of IL-1beta in human periodontal ligament cells. *Oncotarget* **2016**, *7*, 68292–68302. [CrossRef]
22. Yoshino, H.; Morita, I.; Murota, S.I.; Ishikawa, I. Mechanical stress induces production of angiogenic regulators in cultured human gingival and periodontal ligament fibroblasts. *J. Periodontal Res.* **2003**, *38*, 405–410. [CrossRef]
23. Yang, Y.; Wang, B.K.; Chang, M.L.; Wan, Z.Q.; Han, G.L. Cyclic Stretch Enhances Osteogenic Differentiation of Human Periodontal Ligament Cells via YAP Activation. *Biomed Res. Int.* **2018**, *2018*, 2174824. [CrossRef]
24. Zhuang, J.; Wang, Y.; Qu, F.; Wu, Y.; Zhao, D.; Xu, C. Gasdermin-d Played a Critical Role in the Cyclic Stretch-Induced Inflammatory Reaction in Human Periodontal Ligament Cells. *Inflammation* **2019**, *42*, 548–558. [CrossRef] [PubMed]
25. Cho, J.H.; Lee, S.K.; Lee, J.W.; Kim, E.C. The role of heme oxygenase-1 in mechanical stress- and lipopolysaccharide-induced osteogenic differentiation in human periodontal ligament cells. *Angle Orthod.* **2010**, *80*, 552–559. [CrossRef] [PubMed]
26. Liu, J.; Li, Q.; Liu, S.; Gao, J.; Qin, W.; Song, Y.; Jin, Z. Periodontal Ligament Stem Cells in the Periodontitis Microenvironment Are Sensitive to Static Mechanical Strain. *Stem Cells Int.* **2017**, *2017*, 1380851. [CrossRef]
27. Long, P.; Liu, F.; Piesco, N.P.; Kapur, R.; Agarwal, S. Signaling by mechanical strain involves transcriptional regulation of proinflammatory genes in human periodontal ligament cells in vitro. *Bone* **2002**, *30*, 547–552. [CrossRef]
28. Agarwal, S.; Long, P.; Seyedain, A.; Piesco, N.; Shree, A.; Gassner, R. A central role for the nuclear factor-κB pathway in anti-inflammatory and proinflammatory actions of mechanical strain. *FASEB J.* **2003**, *17*, 899–901. [CrossRef] [PubMed]
29. Gilbert, J.A.; Weinhold, P.S.; Banes, A.J.; Link, G.W.; Jones, G.L. Strain profiles for circular cell culture plates containing flexible surfaces employed to mechanically deform cells in vitro. *J. Biomech.* **1994**, *27*, 1169–1177. [CrossRef]
30. Bustin, S.A.; Benes, V.; Garson, J.A.; Hellemans, J.; Huggett, J.; Kubista, M.; Mueller, R.; Nolan, T.; Pfaffl, M.W.; Shipley, G.L.; et al. The MIQE guidelines: *M*inimum *I*nformation for publication of *Q*uantitative real-time PCR *E*xperiments. *Clin. Chem.* **2009**, *55*, 611–622. [CrossRef]
31. Yang, L.; Yang, Y.; Wang, S.; Li, Y.; Zhao, Z. In vitro mechanical loading models for periodontal ligament cells: From two-dimensional to three-dimensional models. *Arch. Oral Biol.* **2015**, *60*, 416–424. [CrossRef]
32. Li, L.; Han, M.X.; Li, S.; Xu, Y.; Wang, L. Hypoxia regulates the proliferation and osteogenic differentiation of human periodontal ligament cells under cyclic tensile stress via mitogen-activated protein kinase pathways. *J. Periodontol.* **2014**, *85*, 498–508. [CrossRef]

33. Ren, D.; Wei, F.; Hu, L.; Yang, S.; Wang, C.; Yuan, X. Phosphorylation of Runx2, induced by cyclic mechanical tension via ERK1/2 pathway, contributes to osteodifferentiation of human periodontal ligament fibroblasts. *J. Cell. Physiol.* **2015**, *230*, 2426–2436. [CrossRef]
34. Konstantonis, D.; Papadopoulou, A.; Makou, M.; Eliades, T.; Basdra, E.; Kletsas, D. The role of cellular senescence on the cyclic stretching-mediated activation of MAPK and ALP expression and activity in human periodontal ligament fibroblasts. *Exp. Gerontol.* **2014**, *57*, 175–180. [CrossRef] [PubMed]
35. Chen, Y.; Mohammed, A.; Oubaidin, M.; Evans, C.A.; Zhou, X.; Luan, X.; Diekwisch, T.G.; Atsawasuwan, P. Cyclic stretch and compression forces alter microRNA-29 expression of human periodontal ligament cells. *Gene* **2015**, *566*, 13–17. [CrossRef]
36. Andersen, K.L.; Norton, L.A. A device for the application of known simulated orthodontic forces to human cells in vitro. *J. Biomech.* **1991**, *24*, 649–654. [CrossRef]
37. Natali, A.N.; Pavan, P.G.; Scarpa, C. Numerical analysis of tooth mobility: Formulation of a non-linear constitutive law for the periodontal ligament. *Dent. Mater.* **2004**, *20*, 623–629. [CrossRef] [PubMed]
38. Mühlemann, H.R.; Zander, H.A. Tooth mobility (III): The mechanism of tooth mobility. *J. Periodontol.* **1954**, *25*, 128–153. [CrossRef]
39. Hao, Y.; Xu, C.; Sun, S.Y.; Zhang, F.Q. Cyclic stretching force induces apoptosis in human periodontal ligament cells via caspase-9. *Arch. Oral Biol.* **2009**, *54*, 864–870. [CrossRef]
40. Memmert, S.; Damanaki, A.; Weykopf, B.; Rath-Deschner, B.; Nokhbehsaim, M.; Gotz, W.; Golz, L.; Till, A.; Deschner, J.; Jager, A. Autophagy in periodontal ligament fibroblasts under biomechanical loading. *Cell Tissue Res.* **2019**, *378*, 499–511. [CrossRef]
41. Nogueira, A.V.; Nokhbehsaim, M.; Eick, S.; Bourauel, C.; Jäger, A.; Jepsen, S.; Rossa, C., Jr.; Deschner, J.; Cirelli, J.A. Biomechanical loading modulates proinflammatory and bone resorptive mediators in bacterial-stimulated PDL cells. *Mediat. Inflamm.* **2014**, *2014*, 425421. [CrossRef]
42. Chang, M.; Lin, H.; Fu, H.; Wang, B.; Han, G.; Fan, M. MicroRNA-195-5p regulates osteogenic differentiation of periodontal ligament cells under mechanical loading. *J. Cell. Physiol.* **2017**, *232*, 3762–3774. [CrossRef]
43. Komori, T. Regulation of Proliferation, Differentiation and Functions of Osteoblasts by Runx2. *Int. J. Mol. Sci.* **2019**, *20*, 1694. [CrossRef]
44. Ziros, P.G.; Gil, A.P.; Georgakopoulos, T.; Habeos, I.; Kletsas, D.; Basdra, E.K.; Papavassiliou, A.G. The bone-specific transcriptional regulator Cbfa1 is a target of mechanical signals in osteoblastic cells. *J. Biol. Chem.* **2002**, *277*, 23934–23941. [CrossRef]
45. Li, S.; Zhang, H.; Li, S.; Yang, Y.; Huo, B.; Zhang, D. Connexin 43 and ERK regulate tension-induced signal transduction in human periodontal ligament fibroblasts. *J. Orthop. Res.* **2015**, *33*, 1008–1014. [CrossRef]
46. Yang, Y.; Yang, Y.; Li, X.; Cui, L.; Fu, M.; Rabie, A.B.; Zhang, D. Functional analysis of core binding factor a1 and its relationship with related genes expressed by human periodontal ligament cells exposed to mechanical stress. *Eur. J. Orthod.* **2010**, *32*, 698–705. [CrossRef]
47. Tang, N.; Zhao, Z.; Zhang, L.; Yu, Q.; Li, J.; Xu, Z.; Li, X. Up-regulated osteogenic transcription factors during early response of human periodontal ligament stem cells to cyclic tensile strain. *Arch. Med. Sci.* **2012**, *8*, 422–430. [CrossRef]
48. Jiang, Z.; Hua, Y. Hydrogen sulfide promotes osteogenic differentiation of human periodontal ligament cells via p38-MAPK signaling pathway under proper tension stimulation. *Arch. Oral Biol.* **2016**, *72*, 8–13. [CrossRef] [PubMed]
49. Chen, Y.J.; Shie, M.Y.; Hung, C.J.; Wu, B.C.; Liu, S.L.; Huang, T.H.; Kao, C.T. Activation of focal adhesion kinase induces extracellular signal-regulated kinase-mediated osteogenesis in tensile force-subjected periodontal ligament fibroblasts but not in osteoblasts. *J. Bone Miner. Metab.* **2014**, *32*, 671–682. [CrossRef] [PubMed]
50. Chiba, M.; Mitani, H. Cytoskeletal changes and the system of regulation of alkaline phosphatase activity in human periodontal ligament cells induced by mechanical stress. *Cell Biochem. Funct.* **2004**, *22*, 249–256. [CrossRef] [PubMed]
51. Yamaguchi, M.; Shimizu, N. Identification of factors mediating the decrease of alkaline phosphatase activity caused by tension-force in periodontal ligament cells. *Gen. Pharmacol.* **1994**, *25*, 1229–1235. [CrossRef]
52. Wada, S.; Kanzaki, H.; Narimiya, T.; Nakamura, Y. Novel device for application of continuous mechanical tensile strain to mammalian cells. *Biol. Open* **2017**, *6*, 518–524. [CrossRef] [PubMed]
53. Wu, Y.; Ou, Y.; Liao, C.; Liang, S.; Wang, Y. High-throughput sequencing analysis of the expression profile of microRNAs and target genes in mechanical force-induced osteoblastic/cementoblastic differentiation of human periodontal ligament cells. *Am. J. Transl. Res.* **2019**, *11*, 3398–3411. [PubMed]
54. Jacobs, C.; Grimm, S.; Ziebart, T.; Walter, C.; Wehrbein, H. Osteogenic differentiation of periodontal fibroblasts is dependent on the strength of mechanical strain. *Arch. Oral Biol.* **2013**, *58*, 896–904. [CrossRef] [PubMed]
55. Nazet, U.; Schröder, A.; Spanier, G.; Wolf, M.; Proff, P.; Kirschneck, C. Simplified method for applying static isotropic tensile strain in cell culture experiments with identification of valid RT-qPCR reference genes for PDL fibroblasts. *Eur. J. Orthod.* **2020**, *42*, 359–370. [CrossRef] [PubMed]
56. Marchesan, J.T.; Scanlon, C.S.; Soehren, S.; Matsuo, M.; Kapila, Y.L. Implications of cultured periodontal ligament cells for the clinical and experimental setting: A review. *Arch. Oral Biol.* **2011**, *56*, 933–943. [CrossRef] [PubMed]
57. Jacobs, C.; Walter, C.; Ziebart, T.; Dirks, I.; Schramm, S.; Grimm, S.; Krieger, E.; Wehrbein, H. Mechanical loading influences the effects of bisphosphonates on human periodontal ligament fibroblasts. *Clin. Oral Investig.* **2015**, *19*, 699–708. [CrossRef] [PubMed]
58. Kletsas, D.; Basdra, E.K.; Papavassiliou, A.G. Effect of protein kinase inhibitors on the stretch-elicited c-Fos and c-Jun up-regulation in human PDL osteoblast-like cells. *J. Cell. Physiol.* **2002**, *190*, 313–321. [CrossRef]

59. Peverali, F.A.; Basdra, E.K.; Papavassiliou, A.G. Stretch-mediated activation of selective MAPK subtypes and potentiation of AP-1 binding in human osteoblastic cells. *Mol. Med.* **2001**, *7*, 68–78. [CrossRef] [PubMed]
60. Papadopoulou, A.; Iliadi, A.; Eliades, T.; Kletsas, D. Early responses of human periodontal ligament fibroblasts to cyclic and static mechanical stretching. *Eur. J. Orthod.* **2017**, *39*, 258–263. [CrossRef]
61. Lee, S.I.; Park, K.H.; Kim, S.J.; Kang, Y.G.; Lee, Y.M.; Kim, E.C. Mechanical stress-activated immune response genes via Sirtuin 1 expression in human periodontal ligament cells. *Clin. Exp. Immunol.* **2012**, *168*, 113–124. [CrossRef]
62. Jacobs, C.; Walter, C.; Ziebart, T.; Grimm, S.; Meila, D.; Krieger, E.; Wehrbein, H. Induction of IL-6 and MMP-8 in human periodontal fibroblasts by static tensile strain. *Clin. Oral Investig.* **2014**, *18*, 901–908. [CrossRef]
63. Scheller, J.; Chalaris, A.; Schmidt-Arras, D.; Rose-John, S. The pro- and anti-inflammatory properties of the cytokine interleukin-6. *Biochim. Biophys. Acta* **2011**, *1813*, 878–888. [CrossRef] [PubMed]
64. Ohzeki, K.; Yamaguchi, M.; Shimizu, N.; Abiko, Y. Effect of cellular aging on the induction of cyclooxygenase-2 by mechanical stress in human periodontal ligament cells. *Mech. Ageing Dev.* **1999**, *108*, 151–163. [CrossRef]
65. Suzuki, R.; Nemoto, E.; Shimauchi, H. Cyclic tensile force up-regulates BMP-2 expression through MAP kinase and COX-2/PGE2 signaling pathways in human periodontal ligament cells. *Exp. Cell Res.* **2014**, *323*, 232–241. [CrossRef] [PubMed]
66. Nokhbehsaim, M.; Deschner, B.; Winter, J.; Bourauel, C.; Jäger, A.; Jepsen, S.; Deschner, J. Anti-inflammatory effects of EMD in the presence of biomechanical loading and interleukin-1β in vitro. *Clin. Oral Investig.* **2012**, *16*, 275–283. [CrossRef]
67. Gkantidis, N.; Christou, P.; Topouzelis, N. The orthodontic-periodontic interrelationship in integrated treatment challenges: A systematic review. *J. Oral Rehabil.* **2010**, *37*, 377–390. [CrossRef] [PubMed]
68. Vanarsdall, R.L., Jr.; Blasi, I., Jr.; Secchi, A.G. Periodontal-orthodontic interrelationships. In *Orthodontics—Current Principles and Techniques*, 6th ed.; Graber, L.W., Vanarsdall, R.L., Jr., Vig, K.W.L., Huang, G.J., Eds.; Elsevier: St. Louis, MO, USA, 2017; pp. 623–658.
69. Monsarrat, P.; Blaizot, A.; Kemoun, P.; Ravaud, P.; Nabet, C.; Sixou, M.; Vergnes, J.N. Clinical research activity in periodontal medicine: A systematic mapping of trial registers. *J. Clin. Periodontol.* **2016**, *43*, 390–400. [CrossRef]
70. Di Spirito, F.; La Rocca, M.; De Bernardo, M.; Rosa, N.; Sbordone, C.; Sbordone, L. Possible Association of Periodontal Disease and Macular Degeneration: A Case-Control Study. *Dent. J.* **2020**, *9*, 1. [CrossRef]
71. Di Spirito, F.; Toti, P.; Pilone, V.; Carinci, F.; Lauritano, D.; Sbordone, L. The Association between Periodontitis and Human Colorectal Cancer: Genetic and Pathogenic Linkage. *Life* **2020**, *10*, 211. [CrossRef]
72. Krishnan, V.; Viecilli, R.F.; Davidovitch, Z. Cellular and molecular biology behind orthodontic tooth movement. In *Biological Mechanisms of Tooth Movement*, 2nd ed.; Krishnan, V., Davidovitch, Z., Eds.; Wiley: Chichester, UK, 2015; pp. 30–50.
73. Janjic, M.; Docheva, D.; Trickovic Janjic, O.; Wichelhaus, A.; Baumert, U. In Vitro Weight-Loaded Cell Models for Understanding Mechanodependent Molecular Pathways Involved in Orthodontic Tooth Movement: A Systematic Review. *Stem Cells Int.* **2018**, *2018*, 3208285. [CrossRef]
74. Vansant, L.; Cadenas De Llano-Perula, M.; Verdonck, A.; Willems, G. Expression of biological mediators during orthodontic tooth movement: A systematic review. *Arch. Oral Biol.* **2018**, *95*, 170–186. [CrossRef]
75. Somerman, M.J.; Archer, S.Y.; Imm, G.R.; Foster, R.A. A comparative study of human periodontal ligament cells and gingival fibroblasts in vitro. *J. Dent. Res.* **1988**, *67*, 66–70. [CrossRef]
76. Goseki, T.; Shimizu, N.; Iwasawa, T.; Takiguchi, H.; Abiko, Y. Effects of in vitro cellular aging on alkaline phosphatase, cathepsin activities and collagen secretion of human periodontal ligament derived cells. *Mech. Ageing Dev.* **1996**, *91*, 171–183. [CrossRef]
77. Sawa, Y.; Phillips, A.; Hollard, J.; Yoshida, S.; Braithwaite, M.W. Impairment of osteocalcin production in senescent periodontal ligament fibroblasts. *Tissue Cell* **2000**, *32*, 198–204. [CrossRef] [PubMed]
78. Abiko, Y.; Shimizu, N.; Yamaguchi, M.; Suzuki, H.; Takiguchi, H. Effect of aging on functional changes of periodontal tissue cells. *Ann. Periodontol.* **1998**, *3*, 350–369. [CrossRef]
79. Itaya, T.; Kagami, H.; Okada, K.; Yamawaki, A.; Narita, Y.; Inoue, M.; Sumita, Y.; Ueda, M. Characteristic changes of periodontal ligament-derived cells during passage. *J. Periodontal Res.* **2009**, *44*, 425–433. [CrossRef] [PubMed]
80. Stoddart, M.J.; Richards, R.G.; Alini, M. In vitro experiments with primary mammalian cells: To pool or not to pool? *Eur. Cell. Mater.* **2012**, *24*, i–ii. [CrossRef] [PubMed]
81. Mayahara, K.; Kobayashi, Y.; Takimoto, K.; Suzuki, N.; Mitsui, N.; Shimizu, N. Aging stimulates cyclooxygenase-2 expression and prostaglandin E2 production in human periodontal ligament cells after the application of compressive force. *J. Periodontal Res.* **2007**, *42*, 8–14. [CrossRef] [PubMed]
82. Toume, S.; Gefen, A.; Weihs, D. Printable low-cost, sustained and dynamic cell stretching apparatus. *J. Biomech.* **2016**, *49*, 1336–1339. [CrossRef] [PubMed]
83. Bustin, S.A.; Beaulieu, J.F.; Huggett, J.; Jaggi, R.; Kibenge, F.S.; Olsvik, P.A.; Penning, L.C.; Toegel, S. MIQE précis: Practical implementation of minimum standard guidelines for fluorescence-based quantitative real-time PCR experiments. *BMC Mol. Biol.* **2010**, *11*, 74. [CrossRef]
84. Chirieleison, S.M.; Marsh, R.A.; Kumar, P.; Rathkey, J.K.; Dubyak, G.R.; Abbott, D.W. Nucleotide-binding oligomerization domain (NOD) signaling defects and cell death susceptibility cannot be uncoupled in X-linked inhibitor of apoptosis (XIAP)-driven inflammatory disease. *J. Biol. Chem.* **2017**, *292*, 9666–9679. [CrossRef]
85. Xie, F.; Xiao, P.; Chen, D.; Xu, L.; Zhang, B. miRDeepFinder: A miRNA analysis tool for deep sequencing of plant small RNAs. *Plant Mol. Biol.* **2012**, *80*, 75–84. [CrossRef]

86. Livak, K.J.; Schmittgen, T.D. Analysis of relative gene expression data using real-time quantitative PCR and the $2^{-\Delta\Delta C}$T Method. *Methods* **2001**, *25*, 402–408. [CrossRef] [PubMed]
87. Shi, J.; Baumert, U.; Folwaczny, M.; Wichelhaus, A. Influence of static forces on the expression of selected parameters of inflammation in periodontal ligament cells and alveolar bone cells in a co-culture in vitro model. *Clin. Oral Investig.* **2019**, *23*, 2617–2628. [CrossRef] [PubMed]
88. Gronthos, S.; Zannettino, A.C.; Hay, S.J.; Shi, S.; Graves, S.E.; Kortesidis, A.; Simmons, P.J. Molecular and cellular characterisation of highly purified stromal stem cells derived from human bone marrow. *J. Cell Sci.* **2003**, *116*, 1827–1835. [CrossRef] [PubMed]
89. Gartland, A.; Buckley, K.A.; Dillon, J.P.; Curran, J.M.; Hunt, J.A.; Gallagher, J.A. Isolation and Culture of Human Osteobalsts. In *Human Cell Culture Protocols*, 2nd ed.; Picot, J., Ed.; Methods in Molecular Medicine; Humana Press: Totowa, NJ, USA, 2005; pp. 29–54.

Supplement 1

To manuscript

"Effect of different parameters of in vitro static tensile strain on human periodontal ligament cells simulating the tension side of orthodontic tooth movement"

Reference gene selection with RefFinder

URL: https://www.heartcure.com.au/reffinder/ (30-03-2021)

References

1. **BestKeeper**: Pfaffl MW, Tichopad A, Prgomet C, Neuvians TP. 2004. Determination of stable housekeeping genes, differentially regulated target genes and sample integrity: BestKeeper--Excel-based tool using pair-wise correlations. Biotechnology Letters 26:509-515.
2. **NormFinder**: Andersen CL, Jensen JL, Orntoft TF. 2004. Normalization of real-time quantitative reverse transcription-PCR data: a model-based variance estimation approach to identify genes suited for normalization, applied to bladder and colon cancer data sets. Cancer Research 64:5245-5250.
3. **Genorm**: Vandesompele J, De Preter K, Pattyn F, Poppe B, Van Roy N, De Paepe A, Speleman F. 2002. Accurate normalization of real-time quantitative RT-PCR data by geometric averaging of multiple internal control genes. Genome Biology 3:RESEARCH0034.
4. **The comparative delta-Ct method**: Silver N, Best S, Jiang J, Thein SL. 2006. Selection of housekeeping genes for gene expression studies in human reticulocytes using real-time PCR. BMC Molecular Biology 7:33.

Contents

Supplementary Table S1.1: Raw data (Cq)

#	Sample type	Day	GAPDH	YWHAZ	PPIB	RPL0	RPL22	EEF1A1	POLR2A	RNA18S5
1	10%	1	18.94	21.14	21.55	22.02	21.85	18.39	22.71	7.89
2	10%	1	19.89	22.03	21.92	22.57	22.55	19.14	23.59	9.05
3	10%	1	19.03	21.26	21.72	21.93	21.74	18.51	22.53	8.16
4	20%	1	19.90	22.04	22.19	22.67	22.67	19.28	23.35	8.98
5	20%	1	19.51	21.72	21.96	22.23	22.10	18.86	22.96	8.50
6	20%	1	19.36	21.47	22.14	22.07	21.97	18.71	22.99	8.41
7	control	1	19.57	21.88	21.96	21.90	22.01	18.63	23.02	8.70
8	control	1	19.83	22.02	22.39	22.72	22.51	19.11	23.32	8.92
9	control	1	19.47	21.58	21.79	22.03	21.96	18.67	22.90	8.39
10	10%	3	18.55	21.51	20.65	20.81	21.01	16.96	22.66	7.69
11	10%	3	18.64	21.37	20.60	20.57	21.00	16.88	22.71	7.63
12	10%	3	18.80	21.60	20.92	21.55	21.66	17.57	22.88	7.76
13	20%	3	19.05	21.89	21.30	21.93	22.02	17.98	22.93	8.36
14	20%	3	19.26	22.13	22.04	21.46	21.81	17.88	23.23	8.87
15	20%	3	18.53	21.52	20.56	21.07	21.36	17.36	22.73	8.16
16	control	3	18.96	21.31	20.76	20.83	20.99	16.94	22.63	7.50
17	control	3	19.07	21.78	21.26	21.93	21.67	17.71	22.65	7.74
18	control	3	19.63	22.10	21.14	21.26	21.35	17.48	23.42	8.60

	Cq Values			
	Control (N=6)	10 % (N=6)	20 % (N=6)	All (N=18)
EEF1A1				
Mean (SD)	18.1 (0.838)	17.9 (0.915)	18.3 (0.720)	18.1 (0.799)
Median [Min; Max]	18.2 [16.9; 19.1]	18.0 [16.9; 19.1]	18.3 [17.4; 19.3]	18.2 [16.9; 19.3]
GAPDH				
Mean (SD)	19.4 (0.338)	19.0 (0.483)	19.3 (0.460)	19.2 (0.448)
Median [Min; Max]	19.5 [19.0; 19.8]	18.9 [18.6; 19.9]	19.3 [18.5; 19.9]	19.2 [18.5; 19.9]
POLR2A				
Mean (SD)	23.0 (0.331)	22.8 (0.381)	23.0 (0.223)	23.0 (0.310)
Median [Min; Max]	23.0 [22.6; 23.4]	22.7 [22.5; 23.6]	23.0 [22.7; 23.4]	22.9 [22.5; 23.6]
PPIB				
Mean (SD)	21.6 (0.601)	21.2 (0.574)	21.7 (0.644)	21.5 (0.605)
Median [Min; Max]	21.5 [20.8; 22.4]	21.2 [20.6; 21.9]	22.0 [20.6; 22.2]	21.6 [20.6; 22.4]
RNA18S5				
Mean (SD)	8.31 (0.565)	8.03 (0.534)	8.55 (0.315)	8.30 (0.504)
Median [Min; Max]	8.50 [7.50; 8.92]	7.83 [7.63; 9.05]	8.46 [8.16; 8.98]	8.38 [7.50; 9.05]
RPL0				
Mean (SD)	21.8 (0.657)	21.6 (0.763)	21.9 (0.568)	21.8 (0.642)
Median [Min; Max]	21.9 [20.8; 22.7]	21.7 [20.6; 22.6]	22.0 [21.1; 22.7]	21.9 [20.6; 22.7]
RPL22				
Mean (SD)	21.7 (0.535)	21.6 (0.581)	22.0 (0.425)	21.8 (0.510)
Median [Min; Max]	21.8 [21.0; 22.5]	21.7 [21.0; 22.6]	22.0 [21.4; 22.7]	21.8 [21.0; 22.7]
YWHAZ				
Mean (SD)	21.8 (0.294)	21.5 (0.314)	21.8 (0.271)	21.7 (0.312)
Median [Min; Max]	21.8 [21.3; 22.1]	21.4 [21.1; 22.0]	21.8 [21.5; 22.1]	21.7 [21.1; 22.1]

Supplementary Table S1.2: Summary table of RefFinder results

Method	Ranking Order (Better--Good--Average)							
	1	**2**	**3**	**4**	**5**	**6**	**7**	**8**
Delta CT	*RPL22*	*GAPDH*	*RNA18S5*	*PPIB*	*RPL0*	*POLR2A*	*YWHAZ*	*EEF1A1*
BestKeeper	*POLR2A*	*YWHAZ*	*GAPDH*	*RPL22*	*RNA18S5*	*RPL0*	*PPIB*	*EEF1A1*
Normfinder	*RPL22*	*GAPDH*	*RNA18S5*	*PPIB*	*RPL0*	*POLR2A*	*YWHAZ*	*EEF1A1*
Genorm	*YWHAZ | POLR2A*		*GAPDH*	*RNA18S5*	*RPL22*	*PPIB*	*RPL0*	*EEF1A1*
Recommended comprehensive ranking	RPL22	GAPDH	*POLR2A*	*YWHAZ*	*RNA18S5*	*PPIB*	*RPL0*	*EEF1A1*

Supplementary Table S1.3: Comprehensive gene stability

Genes	Geomean of ranking values
RPL22	2.11
GAPDH	2.45
POLR2A	2.45
YWHAZ	3.15
RNA18S5	3.66
PPIB	5.09
RPL0	5.69
EEF1A1	8.00

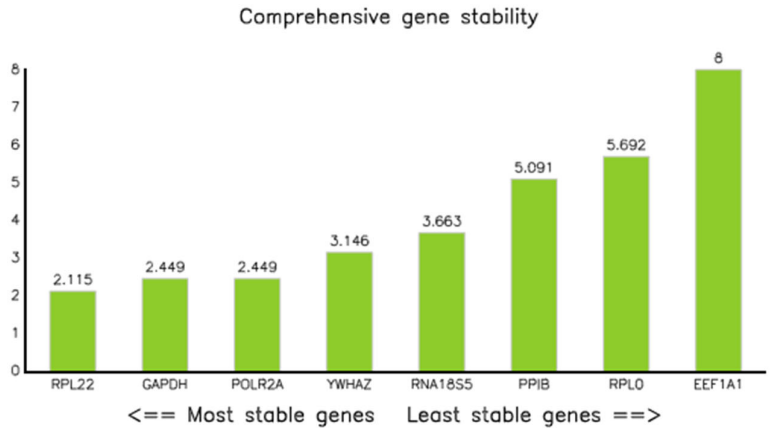

Supplementary Table S1.4: Gene stability by Delta CT method

Genes	Average of STDEV
RPL22	0.33
GAPDH	0.35
RNA18S5	0.36
PPIB	0.39
RPL0	0.40
POLR2A	0.41
YWHAZ	0.45
EEF1A1	0.49

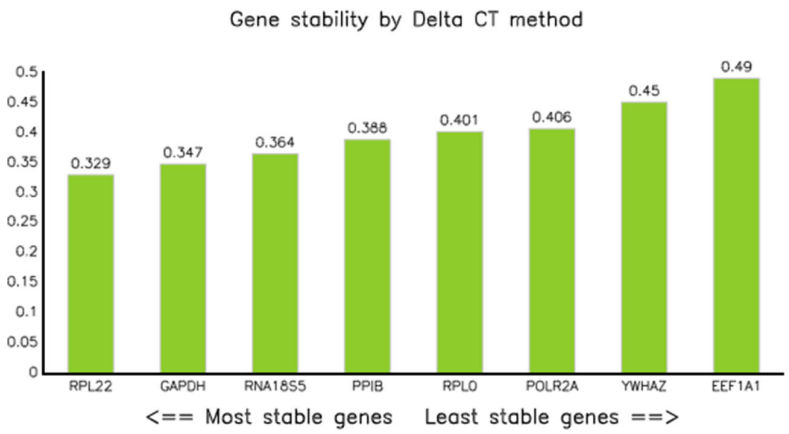

Supplementary Table S1.5: Gene stability by BestKeeper

CP data of housekeeping Genes by BEST KEEPER								
	GAPDH	***YWHAZ***	***PPIB***	***RPL0***	***RPL22***	***EEF1A1***	***POLR2A***	***RNA18S5***
n	18	18	18	18	18	18	18	18
geo Mean [CP]	19.22	21.68	21.48	21.74	21.78	18.10	22.95	8.28
AR Mean [CP]	19.22	21.69	21.49	21.75	21.79	18.11	22.96	8.30
min [CP]	18.53	21.14	20.56	20.57	20.99	16.88	22.53	7.50
max [CP]	19.90	22.13	22.39	22.72	22.67	19.28	23.59	9.05
std dev [+/- CP]	0.38	0.27	0.53	0.52	0.39	0.70	0.25	0.43
CV [% CP]	1.98	1.24	2.45	2.41	1.81	3.85	1.08	5.13
min [x-fold]	-1.61	-1.46	-1.90	-2.26	-1.73	-2.33	-1.34	-1.72
max [x-fold]	1.61	1.36	1.87	1.97	1.85	2.27	1.55	1.70
std dev [+/- x-fold]	1.30	1.20	1.44	1.44	1.31	1.62	1.19	1.34

Pearson correlation coefficient (r) by BEST KEEPER								
	GAPDH	***YWHAZ***	***PPIB***	***RPL0***	***RPL22***	***EEF1A1***	***POLR2A***	***RNA18S5***
YWHAZ	0.680	-	-	-	-	-	-	-
p-value	0.002	-	-	-	-	-	-	-
PPIB	0.827	0.450	-	-	-	-	-	-
p-value	0.001	0.061	-	-	-	-	-	-
RPL0	0.777	0.408	0.864	-	-	-	-	-
p-value	0.001	0.093	0.001	-	-	-	-	-
RPL22	0.802	0.529	0.870	0.966	-	-	-	-
p-value	0.001	0.024	0.001	0.001	-	-	-	-
EEF1A1	0.807	0.352	0.919	0.955	0.948	-	-	-
p-value	0.001	0.153	0.001	0.001	0.001	-	-	-
POLR2A	0.823	0.839	0.571	0.523	0.645	0.538	-	-
p-value	0.001	0.001	0.013	0.026	0.004	0.021	-	-
RNA18S5	0.851	0.772	0.797	0.695	0.805	0.766	0.865	-
p-value	0.001	0.001	0.001	0.001	0.001	0.001	0.001	-

Pearson correlation coefficient (r)								
BestKeeper vs.	***GAPDH***	***YWHAZ***	***PPIB***	***RPL0***	***RPL22***	***EEF1A1***	***POLR2A***	***RNA18S5***
coeff. of corr. [r]	0.919	0.660	0.920	0.898	0.947	0.928	0.784	0.931
p-value	0.001	0.003	0.001	0.001	0.001	0.001	0.001	0.001

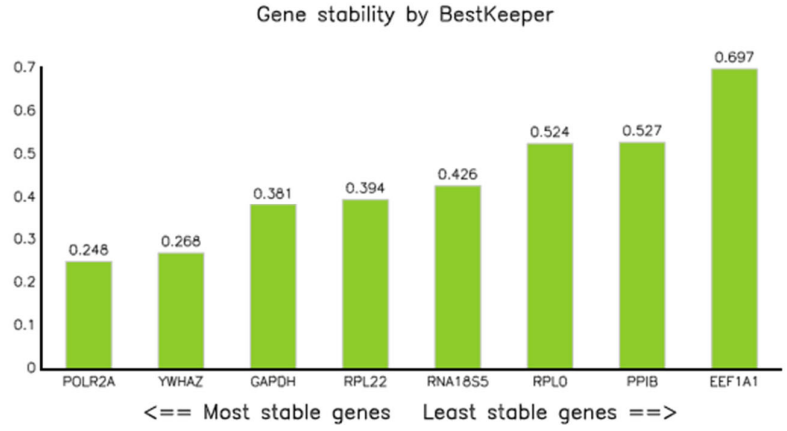

Supplementary Table S1.6: Gene stability by normFinder

Gene name	Stability value
RPL22	0.119
GAPDH	0.174
RNA18S5	0.216
PPIB	0.259
RPL0	0.301
POLR2A	0.327
YWHAZ	0.394
EEF1A1	0.442

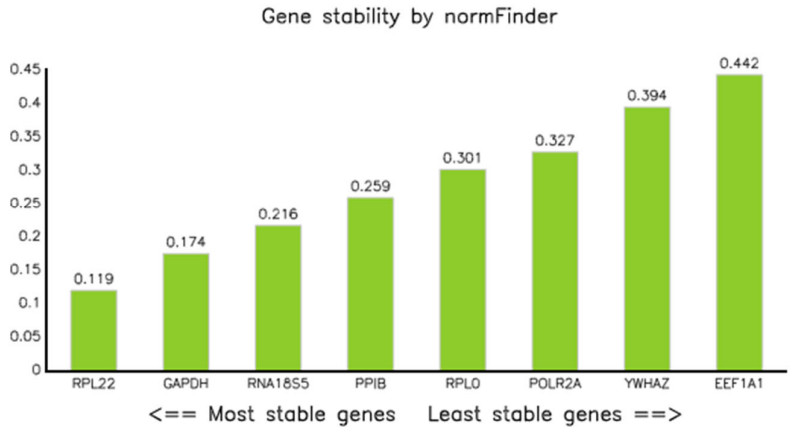

Supplementary Table S1.7: Gene stability by Genorm

Gene name	Stability value
YWHAZ | POLR2A	0.176
GAPDH	0.255
RNA18S5	0.274
RPL22	0.309
PPIB	0.343
RPL0	0.366
EEF1A1	0.397

Supplement 2

To the manuscript

"Effect of different parameters of in vitro static tensile strain on human periodontal ligament cells simulating the tension side of orthodontic tooth movement"

Contents

Supplementary Table S2.1: MIQE checklist for the RT-qPCR workflow

Reference: Bustin et al. (2010). BMC Mol Biol; 11:74.

	Details	Checklist
Sample/Template		
Source	If cancer, was biopsy screened for adjacent normal tissue?	Human periodontal ligament cells were isolated from health teeth using the explant technique described by Somerman et al. (1988) as previously published (Janjic Rankovic et al. 2020; Shi et al. 2019a; Shi et al. 2019b)
Method of preservation	Liquid N2/RNAlater/formalin	Preserved in liquid nitrogen
Storage time (if appropriate)	If using samples >6 months old	12 months
Handling	Fresh/frozen/formalin	Cell lysates were prepared using RNA lysis buffer from Quick-RNA™ MicroPrep kit (R1051; Zymo). After directly frozen in liquid nitrogen, cell lysates were stored at -80°C until further use for RNA extraction.
Extraction method	TriZol/columns	Defrosted cells lysates were passed through QIAshredder™ columns (Qiagen) to shear genomic DNA. The Quick-RNA™ Miniprep Kit (Zymo) was used for further RNA purification. After primary column purification, DNase I digestion was applied to reduce genomic DNA contamination as described by the manufacturer (Zymo). Finally, DNase/RNase-free water was used to elute the RNA from the columns. Before storage in the -80°C, RNase inhibitor RNasin® (Promega) was added to each preparation.
RNA:DNA-free	Intron-spanning primers/no RT control	Most primers were intron-spanning (Supplementary Table 2.2). Treatment with QIAshredder™ columns (Qiagen) and DNase I (Zymo) digestion were applied to reduce genomic DNA contamination. RT- (no RT) controls were tested and showed no contamination of genomic DNA.
Concentration	Nanodrop/ribogreen/microfluidics	Purity and concentration of extracted RNA were detected photometrically (Nanodrop ND-1000; PeqLab). Ratio of $A_{260/280}$>1.8 was found, indicating free of protein contamination during RNA preparations.
RNA: integrity	Microfluidics/3':5' assay	No.
Inhibition-free	Method of testing	Serial dilution of cDNA; as shown in “Primer efficiency” in Table 3 of the manuscript.
Assay optimisation/validation		
Accession number	RefSeq XX_1234567	Table 3 of the manuscript; Supplementary Table S2.2
Amplicon details	Exon location, amplicon size	Supplementary Table S2.2
Primer sequence	Even if previously published	Table 3 of the manuscript; Supplementary Tables S2.2 and S2.3. The sequence of the purchased primers from Realtimeprimers.com was disclosed upon purchase.

	Details	Checklist
*Probe sequence**	Identify LNA or other substitutions	No probes were used.
In silico	BLAST/Primer-BLAST/m-fold	Primer-BLAST, UCSC In-Silico PCR, Beacon Designer Free Edition, Primer-Check, uMELT, UNAfold and ENSEMBL were used for *in silico* test.
empirical	Primer concentration/annealing temperature	The optimal annealing temperatures were first identified by gradient PCR (Biometra TProfessional Gradient; Biometra, Goettingen, Germany) and then were finalized by qPCR on Roche LightCycler® 480 (LC480). Optimal annealing temperatures are recorded in Table 3 of the manuscript.
Priming conditions	Oligo-dT/random/combination/target-specific	The SuperScript® IV First Strand Synthesis System (Invitrogen) was used for cDNA synthesis with random hexamers provided. For each cDNA synthesis reaction, 600 ng total RNA was used. Target-specific primers for qPCR were used after assessment, as shown in Table 3 of the manuscript.
PCR efficiency	Dilution curve	Information on serial dilutions and primer efficiency was summarized in Supplementary Table S2.3. For each gene, two technical replicates were used for each dilution for qPCR. For analysis of qPCR including the standard curves, LC480 software version 1.5.0.39 was used.
Linear dynamic range	Spanning unknown targets	The analysing software for qPCR appointed the linear dynamic range automatically.
Limits of detection	LOD detection/accurate quantification	The analysing software for qPCR appointed the LOD automatically.
Intra-assay variation	Copy numbers not Cq	Each gene was detected on one individual plate.
RT/PCR		
Protocols	Detailed description, concentrations, volumes	For real-time PCR, the Luminaris Color HiGreen qPCR Master Mix Kit (K0392; Thermo Fisher Scientific, Vilnius, Lithuania) was used to detect gene expression of *PTGS2*, *IL6*, *TNF*, *RANKL*, *RUNX2*, *SP7*, *ALPL*, and *BGLAP* using the LightCycler® 480 with LC480 software version 1.5.0.39 (both from Roche Molecular Diagnostics, Basel, Switzerland). According to the manufacturer' protocol, 2 µl diluted cDNA (1:5 with double distilled, sterile water), 0.6 µl gene-specific forward primer, 0.6 µl gene-specific reverse primers, 6.8 µl PCR water and 10 µl qPCR Mastermix were added for reaction. PCR reactions proceeded as follows: 2 min of pretreatment of Uracil-DNA glycosylase (UDG) at 50 °C, 10 min of initial denaturation at 95 °C and 45 cycles of amplifications. Each amplification was consisted of four steps: 15 s of denaturation at 95 °C, 30 s of specific annealing temperature for each primer pair, 30 s of elongation at 72 °C and 5 s of data acquisition at the given temperature. For each plate, both no template controls (NTC) and no RT (reverse transcriptase) controls were added. NTCs were included for detection of primer dimers, while no RT controls were assessed for genomic DNA contamination.

	Details	Checklist
Reagents	Supplier, Lot number	Primers for genes were either acquired commercially or synthesized using sequences from related literatures. Primers from related literatures were verified by *in silico* tests using related bioinformatic tools given in Supplementary Table S2.2. All primers were synthesized by Metabion GmbH (Planegg/Steinkirchen, Germany; Oligonucleotide Purification Cartridge OPC® purification) or purchased from realtimeprimers.com. Information on the kits used (Quick-RNA™ MicroPrep kit; SuperScript® IV First Strand Synthesis kit, Invitrogen; Luminaris Color HiGreen qPCR Master Mix Kit) were all given in the manuscript.
Duplicate RT	ΔCq	No, but two technical replicates were repeated for each biological replicate at minimum.
NTC	Cq & melt curves	Yes
NAC	ΔCq beginning:end of qPCR	No, as no probes were used.
Positive control	Inter-run calibrators	No, each gene was tested on one plate with all samples included.
Data analysis		
Specialist software	e.g., QBAsePlus	IBM SPSS Statistics 26 (IBM Corp., Armonk, NY, USA)
Statistical justification	e.g., biological replicates	For each force magnitude for every force duration, three biological replicates were used. Each biological replicate was repeated with two technical replicates, giving a total of 6 amplifications of qPCR.
Transparent, validated normalisation	e.g., GeNorm summary	After testing with RT-qPCR using cDNA from some samples and assessment with Reffinder, *RPL22* and *POLR2A* were proved to be most stable in this experiment among the panel of reference genes. Therefore, *RPL22* and *POLR2A* were used as reference genes for following analysis.

Supplementary Table S2.2: *In-silico* analysis of the RT-qPCR primer

Official gene symbol	**Reference sequence** (NCBI GenBank)	**5'-forward primer-3'** (length / T_m / %GC / max. ΔG hairpin & self-dimer / Self-comp./Self-3'-comp.)	**5'-reverse primer-3'** (length / T_m / %GC / max. ΔG hairpin & self-dimer / Self-comp./Self-3'-comp.)	**Primer location** (max. ΔG cross-dimer)	**Amplicon** (length, %GC, T_m, SSAT)	**Amplicon location** (bp of Start/Stop)	**Intron-spanning** (length, bp)	**In silico qPCR specificity**	**Variants targeted** (Transcript/ Splice)	**Primer sequence source**
Genes of interest										
ALPL	NM_001127501.4	GGACCATTCCCACGTCTTCAC (21 / 58.2°C / 57% / -1.3 & -3.3 / 4/0)	CCTTGTAGCCAGGCCCATTG (20 / 57.9°C / 60% / -1.3 & -4.4 / 5/3)	Exon 1 (0)	137bp, 55%, 90.5°C, No	1330 / 1466	Yes (597)	Yes (BLAST, UCSC)	Yes	(Liu et al. 2017)
BGLAP	NM_199173.6	AGCGAGGTAGTGAAGAGAC (19 / 52.6°C / 53% / n.f. & n.f. / 2/1)	GAAAGCCGATGTGGTCAG (18 / 52.3°C / 56% / n.f. & n.f. / 2/1)	Exon 3/4 (-1.1)	142bp, 61%, 93.5°C, No	175 / 316	Yes (201)	Yes (BLAST, UCSC)	Yes	(Gartland et al. 2005)
PTGS2	NM_000963.4	AAGCCTTCTCTAACCTCTCC (20 / 52.9°C / 50% / n.f. & -0.5 / 5/0)	GCCCTCGCTTATGATCTGTC (20 / 55.2°C / 55% / n.f. & -2.0 / 4/1)	Exon 4/5 (-2.9)	234bp, 45%, 88°C, No	510 / 743	Yes (430)	Yes (BLAST, UCSC)	Yes	(Janjic Rankovic et al. 2020; Shi et al. 2019a)
FOS	NM_005252.4	GCTTTGCAGACCGAGATTGC (20 / 57.2°C / 55% / -2.0 & -3.4 / 4/2)	TTGAGGAGAGGCAGGGTGAA (20 / 57.3°C / 55% / n.f. & n.f. / 2/0)	Exon 4 (-2.0)	203bp, 57%, 93.5°C, No	687 / 889	No	Yes (BLAST, UCSC)	Yes	(Janjic Rankovic et al. 2020)
IL6	NM_000600.5	TGGCAGAAAACAACCTGAACC (21 / 56.5°C / 48% / -1.1 & -1.1 / 3/0)	TGGCTTGTTCCTCACTACTCTC (22 / 56.9% / 50% / n.f. & n.f. / 2/0)	Exon 2/3 (-3.3)	168bp, 43%, 85.5°C, No	317 / 484	Yes (707)	Yes (BLAST, UCSC)	Yes	(Janjic Rankovic et al. 2020; Shi et al. 2019a)
RUNX2	NM_001015051.4	GCGCATTCCTCATCCCAGTA (20 / 56.9°C / 55% / n.f. & -5.2 / 4/2)	GGCTCAGGTAGGAGGGGTAA (20 / 56.9°C / 60% / -1.0 & -1.0 / 3/1)	Exon 6/7 (-2.9)	176bp, 57%, 92.0°C, No	947 / 1122	Yes (20131)	Yes (BLAST, UCSC)	Yes	(Janjic Rankovic et al. 2020; Shi et al. 2019b)
SP7	NM_001173467.3	GGCACAAAGAAGCCGTACTC (20 / 56.2°C / 55% / -2.4 & -2.4 / 4/0)	CACTGGGCAGACAGTCAGAA (20 / 56.6°C / 55% / -2.5 & -2.5 / 5/1)	Exon 3 (-2.4)	247bp, 57%, 93°C, No	383 / 629	No	Yes (BLAST, UCSC)	Yes	(Gronthos et al. 2003)
TNFRSF11B	NM_002546.4	TCAAGCAGGAGTGCAATCG (19 / 54.9°C / 53% / -2.0 & -3.4 / 6/4)	AGAATGCCTCCTCACACAGG (20 / 56.3°C / 55% / -1.3 & -1.3 / 4/1)	Exon 2/4 (-4.1)	342bp, 46%, 88.5°C/91°C, Yes	342 / 683	Yes (6020)	Yes (BLAST, UCSC)	Yes	(Yang et al. 2010)
TNF	NM_000594.4	Commercial primer (20 / 55.9°C / 55% / n.f. & n.f. / 3/0)	Commercial primer (20 / 54.2°C / 45% / n.f. & -4.4 / 6/2)	Exon 4 (-2.0)	173bp, 50%, 85.5°C, Yes	Commercial primer from realtimeprimers.com (Order information: VHPS-9415)	No	Yes (BLAST, UCSC)	Yes	Realtimeprimers.com; (Janjic Rankovic et al. 2020; Shi et al. 2019a)
Reference genes										
EEF1A1	NM_001402.6	CCTGCCTCTCCAGGATGTCTAC (22 / 59.0°C / 59% / -3.0 & -3.0 / 5/2)	GGAGCAAAGGTGACCACCATAC (22 / 58.7°C / 55% / -1.5. & -3.2 / 6/2)	Exon 5/6 (–2.9)	105bp, 52%, 88°C, No	804 / 908	Yes (87)	Yes (BLAST/UCSC)	Yes	(Nazet et al. 2020)
GAPDH	NM_002046.7	CTCCTGTTCGACAGTCAGCC (20 / 57.4°C / 60% / -2.5 & -3.1 / 6/1)	CGACCAAATCCGTTGACTCC (20 / 55.9°C/ 55%/ -0.7 & -0.7 / 3/1)	Exon 1 / 2-3 (–3.8)	103bp, 58%, 91°C, No	12 / 114	Yes, rev. primer on exon junction	Yes (BLAST/UCSC)	Yes	(Chirieleison et al. 2017)
POLR2A	NM_000937.5	TCGCTTACTGTCTTCCTGTTGG (22 / 57.8°C / 50% / n.f. & n.f. / 3/0)	TGTGTTGGCAGTCACCTTCC (20 / 57.4°C / 55% / -1.3 & -1.3 / 3/3)	Exon 21/22 (–2.5)	108bp, 53%, 89.5°C, No	3811 / 3918	Yes (468)	Yes (BLAST/UCSC)	Yes	(Nazet et al. 2020)
PPIB	NM_000942.5	TTCCATCGTGTAATCAAGGACTTC (24 / 56.7°C / 42% / -1.3 & -1.3 / 4/2)	GCTCACCGTAGATGCTCTTTC (21 / 56.1°C / 52% / -0.7 & -0.7 / 4/0)	Exon 3/4 (–2.1)	88bp, 53%, 87°C, No	313 / 400	Yes (3194)	Yes (BLAST/UCSC)	Yes	(Nazet et al. 2020)
RNA18SN5	NR_003286.4	AACTGCGAATGGCTCATTAAATC (23 / 55.8°C / 39% / -1.7 & -1.7 / 6/3)	GCCCGTCGGCATGTATTAG (19 / 55.2°C / 58% / -2.4 & -2.4 / 5/1)	n.a. (–2.4)	103bp, 46%, 85.5°C, No	84 / 186	No (rRNA)	No (RNA45S5 also targeted)	—	(Nazet et al. 2020)

Official gene symbol	**Reference sequence** (NCBI GenBank)	**5'-forward primer-3'** (length / T_m / %GC / max. ΔG hairpin & self-dimer / Self-comp./Self-3'-comp.)	**5'-reverse primer-3'** (length / T_m / %GC / max. ΔG hairpin & self-dimer / Self-comp./Self-3'-comp.)	**Primer location** (max. ΔG cross-dimer)	**Amplicon** (length, %GC, T_m, SSAT)	**Amplicon location** (bp of Start/Stop)	**Intron-spanning** (length, bp)	**In silico qPCR specificity**	**Variants targeted** (Transcript/ Splice)	**Primer sequence source**
RPL0	NM_001002.4	GAAACTCTGCATTCTCGCTTCC (22 / 57.4°C / 50% / -0.6 & -3.4 / 4/0)	GACTCGTTTGTACCCGTTGATG (22 / 57.1°C / 50% / n.f. & -2.0 / 4/0)	Exon 6/7 (–1.8)	120bp, 50%, 89°C, No	702 / 821	Yes (1091)	Yes (BLAST/UCSC)	Yes	(Nazet et al. 2020)
RPL22	NM_000983.4	TGATTGCACCCACCCTGTAG (20 / 56.6°C / 55% / n.f. & -3.4 / 4/2)	GGTTCCCAGCTTTTCCGTTC (20 / 56.4°C / 55% / n.f. & -3.0 / 4/0)	Exon 2/3 (–1.5)	98bp, 44%, 84°C, No	91 / 188	Yes (4597)	Yes (BLAST/UCSC)	Yes	(Nazet et al. 2020)
YWHAZ	NM_003406.4	AGGAGATTACTACCGTTACTTGGC (24 / 57.8°C / 46% / n.f. & n.f. / 4/2)	AGCTTCTTGGTATGCTTGTTGTG (23 / 57.4°C / 43% / -1.8 & -3.0 / 4/0)	Exon 8/9 (–2.2)	91bp, 47%, 86°C, No	491 / 581	Yes (617)	Yes (BLAST/UCSC)	Yes	(Nazet et al. 2020)

T_m, melting temperature of primer or qPCR product (amplicon); %GC, percent of guanin/cytosine content; bp, base pairs; max. ΔG hairpin, maximal ΔG of hairpin; max. ΔG self-dimer, maximal ΔG of self-dimer; Self-comp., self complementary; Self-3'-comp., self 3' complementary; max. ΔG Cross-dimer, maximal ΔG of cross-dimer; SSAT, secondary structures at annealing temperature (at primer binding sites); n.f., not found.

To perform silico analysis of RT-qPCR primers, their targets and corresponding amplification products, the following programs and online resources were used. All URLs were valid on 02-12-2020.

a. Primer-BLAST (URL: https://www.ncbi.nlm.nih.gov/tools/primer-blast/) was used to check the "length" of primer, "In silico qPCR specificity", possible co-amplification of genomic DNA, "Self-comp." and "Self-3'-comp".
b. UCSC In-Silico PCR (URL: https://genome.ucsc.edu/cgi-bin/hgPcr) was used to check "In silico qPCR specificity" and RT-qPCR in genomic context.
c. "Amplicon (length)", "Amplicon location (bp of Start/Stop)", "Intron-spanning (length)" was identified or calculated by either Primer-BLAST or UCSC In-Silico PCR
d. Beacon Designer™ Free Edition (Premier BioSoft International, Palo Alto, CA, USA, URL: http://www.premierbiosoft.com/qOligo/Oligo.jsp?PID=1) was used to identify primers' specifications (T_m, %GC, max. ΔG hairpin & max. ΔG self-dimer, max. ΔG cross-dimer).
e. Primer-Check (URL: http://projects.insilico.us/SpliceCenter/PrimerCheck.jsp) was used to check for "Primer location", which means the exon/intron binding sites.
f. uMelt (URL: https://dna-utah.org/umelt/quartz/) was used to check "Amplicon (%GC, Tm)", which means GC content and melting temperature of the amplicon.
g. UNAFold@IDT-DNA (URL: http://eu.idtdna.com/UNAFold?, maximum sequence length 255 bases) was used to check "Amplicon (SSAT)", to identify occurrence of secondary structures in the RT-qPCR product during the annealing step. mFold @ http://www.unafold.org/mfold/applications/dna-folding-form.php :
h. ENSEMBL (URL: https://www.ensembl.org) was used to check "Variants targeted (Transcript/Splice)".

Supplementary Table S2.3: Primer validation by RT-qPCR

Gene symbol	Primer sequence (f: 5'-forward primer-3'; r: 5'-reverse primer-3')	Primer sequence source	Prediluted cDNA (1:5) used?	Specificity by melting curve / T_m (°C)	Specificity by agarose gel / amplicon size (bp)	Annealing temp. (°C)/ data acquisition temp. (°C)	Dilution series used for efficiency testing	Primer efficiency			
								Effici-ency	Error	Slope	Y inter-cept
Genes of interest											
ALPL	f: GGACCATTCCCACGTCTTCAC r: CCTTGTAGCCAGGCCCATTG	(Liu et al. 2017)	Undiluted	Yes / 82.3	Yes / 137	64 / 80	Undil., 1:4, 1:16, 1:64, 1:256, 1:1024	1.968	0.0291	-3.401	37.70
BGLAP	f: AGCGAGGTAGTGAAGAGAC r: GAAAGCCGATGTGGTCAG	(Gartland et al. 2005)	Prediluted	Yes / 84.6	Yes / 142	64 / 82	Predil., 1:4, 1:16, 1:64, 1:256, 1:1024	2.076	0.00897	-3.152	35.71
PTGS2	f: AAGCCTTCTCTAACCTCTCC r: GCCCTCGCTTATGATCTGTC	(Janjic Rankovic et al. 2020; Shi et al. 2019a)	Prediluted	Yes / 79.4	Yes / 234	58 / 77	Predil., 1:4, 1:16, 1:64, 1:256	1.995	0.0356	-3.335	35.95
FOS	f: GCTTTGCAGACCGAGATTGC r: TTGAGGAGAGGCAGGGTGAA	(Janjic Rankovic et al. 2020)	Prediluted	Yes / 84.7	Yes / 203	58 / 83	Predil., 1:4, 1:16, 1:64, 1:256	1.860	0.0327	3.711	37.74
IL6	f: TGGCAGAAAACAACCTGAACC r: TGGCTTGTTCCTCACTACTCTC	(Janjic Rankovic et al. 2020; Shi et al. 2019a)	Prediluted	Yes / 78.1	Yes / 168	58 / 76	Predil., 1:4, 1:16, 1:64, 1:256	1.955	0.0231	-3.434	39.18
RUNX2	f: GCGCATTCCTCATCCCAGTA r: GGCTCAGGTAGGAGGGGTAA	(Janjic Rankovic et al. 2020; Shi et al. 2019b)	Prediluted	Yes / 83.1	Yes / 176	58 / 81	Predil., 1:4, 1:16, 1:64, 1:256, 1:1024	1.954	0.0129	-3.437	34.96
SP7	f: GGCACAAAGAAGCCGTACTC r: CACTGGGCAGACAGTCAGAA	(Gronthos et al. 2003)	Undiluted	Yes / 84	Yes / 247	61 / 81	Undil., 1:4, 1:16, 1:32, 1:64, 1:128	1.935	0.0367	-3.489	36.28
TNFRSF11B	f: TCAAGCAGGAGTGCAATCG r: AGAATGCCTCCTCACACAGG	(Yang et al. 2010)	Prediluted	Yes / 83	Yes / 342	64 / 81	Predil., 1:5, 1:25, 1:125, 1:625	1.941	0.0211	-3.473	32.63
TNF	Commercial primer pair from realtimeprimers.com (Order information: VHPS-9415)	(Janjic Rankovic et al. 2020; Shi et al. 2019a)	Undiluted	Yes / 81	Yes / 173	58 / 79	Undil., 1:4, 1:16, 1:32, 1:64, 1:128	1.967	0.0421	-3.404	37.27
Reference genes											
EEF1A1	f: CCTGCCTCTCCAGGATGTCTAC r: GGAGCAAAGGTGACCACCATAC	(Nazet et al. 2020)	Prediluted	Yes / 79.9	Yes / 105	61 / 77	Predil., 1:10, 1:100, 1:1000, 1;10,000	1.981	0.00773	-3.367	30.06
GAPDH	f: CTCCTGTTCGACAGTCAGCC r: CGACCAAATCCGTTGACTCC	(Chirieleison et al. 2017)	Prediluted	Yes / 82.4	Yes / 103	52 / 79	Predil., 1:10, 1:100, 1:1000, 1;10,000	1.970	0.00209	-3.396	31.55
POLR2A	f: TCGCTTACTGTCTTCCTGTTGG r: TGTGTTGGCAGTCACCTTCC	(Nazet et al. 2020)	Prediluted	Yes / 81.9	Yes / 108	58 / 79	Predil., 1:10, 1:100, 1:1000, 1;10,000	1.886	0.0150	-3.630	37.25

Gene symbol	Primer sequence (f: 5'-forward primer-3'; r: 5'-reverse primer-3')	Primer sequence source	Prediluted cDNA (1:5) used?	Specificity by melting curve / T_m (°C)	Specificity by agarose gel / amplicon size (bp)	Annealing temp. (°C)/ data acquisition temp. (°C)	Dilution series used for efficiency testing	Primer efficiency			
								Effici-ency	Error	Slope	Y inter-cept
PPIB	f: TTCCATCGTGTAATCAAGGACTTC r: GCTCACCGTAGATGCTCTTTC	(Nazet et al. 2020)	Prediluted	Yes / 80.1	Yes / 88	55 / 77	Predil., 1:10, 1:100, 1:1000, 1;10,000	1.909	0.00896	-3.560	35.93
RNA18S5	f: AACTGCGAATGGCTCATTAAATC r: GCCCGTCGGCATGTATTAG	(Nazet et al. 2020)	Prediluted	Yes / 77.8	Yes / 103	55 / 55	Predil., 1:10, 1:100, 1:1000, 1;10,000	1.869	0.00242	-3.682	21.57
RPL0	f: GAAACTCTGCATTCTCGCTTCC r: GACTCGTTTGTACCCGTTGATG	(Nazet et al. 2020)	Prediluted	Yes / 81.3	Yes / 120	64 / 79	Predil., 1:10, 1:100, 1:1000, 1;10,000	2.010	0.0430	-3.299	33.73
RPL22	f: TGATTGCACCCACCCTGTAG r: GGTTCCCAGCTTTTCCGTTC	(Nazet et al. 2020)	Prediluted	Yes / 77.6	Yes / 98	61 / 75	Predil., 1:10, 1:100, 1:1000, 1;10,000	1.939	0.0160	-3.478	34.41
YWHAZ	f: AGGAGATTACTACCGTTACTTGGC r: AGCTTCTTGGTATGCTTGTTGTG	(Nazet et al. 2020)	Prediluted	Yes / 78.9	Yes / 91	55 / 76	Predil., 1:10, 1:100, 1:1000, 1;10,000	1.945	0.0216	-3.462	34.89

References

Chirieleison SM, Marsh RA, Kumar P, Rathkey JK, Dubyak GR, Abbott DW (2017). Nucleotide-binding oligomerization domain (NOD) signaling defects and cell death susceptibility cannot be uncoupled in X-linked inhibitor of apoptosis (XIAP)-driven inflammatory disease. J Biol Chem; 292(23):9666-9679.

Gartland A, Buckley KA, Dillon JP, Curran JM, Hunt JA, Gallagher JA (2005). Isolation and Culture of Human Osteobalsts. In: Picot J (Ed.). Human Cell Culture Protocols. [Methods in Molecular Medicine; 107] 2nd Ed. Totowa, NJ: Humana Press; pp. 29-54.

Gronthos S, Zannettino AC, Hay SJ, Shi S, Graves SE, Kortesidis A, Simmons PJ (2003). Molecular and cellular characterisation of highly purified stromal stem cells derived from human bone marrow. J Cell Sci; 116(Pt 9):1827-35.

Janjic Rankovic M, Docheva D, Wichelhaus A, Baumert U (2020). Effect of static compressive force on in vitro cultured PDL fibroblasts: monitoring of viability and gene expression over 6 days. Clin Oral Investig; 24(7):2497-2511.

Liu J, Li Q, Liu S, Gao J, Qin W, Song Y, Jin Z (2017). Periodontal Ligament Stem Cells in the Periodontitis Microenvironment Are Sensitive to Static Mechanical Strain. Stem Cells Int; 2017:1380851.

Nazet U, Schröder A, Spanier G, Wolf M, Proff P, Kirschneck C (2020). Simplified method for applying static isotropic tensile strain in cell culture experiments with identification of valid RT-qPCR reference genes for PDL fibroblasts. Eur J Orthod; 42(4):359-370.

Shi J, Baumert U, Folwaczny M, Wichelhaus A (2019a). Influence of static forces on the expression of selected parameters of inflammation in periodontal ligament cells and alveolar bone cells in a co-culture in vitro model. Clin Oral Investig; 23(6):2617-2628.

Shi J, Folwaczny M, Wichelhaus A, Baumert U (2019b). Differences in RUNX2 and P2RX7 gene expression between mono- and coculture of human periodontal ligament cells and human osteoblasts under compressive force application. Orthod Craniofac Res; 22(3):168-176.

Somerman MJ, Archer SY, Imm GR, Foster RA (1988). A comparative study of human periodontal ligament cells and gingival fibroblasts *in vitro*. J Dent Res; 67(1):66-70.

Yang Y, Yang Y, Li X, Cui L, Fu M, Rabie AB, Zhang D (2010). Functional analysis of core binding factor a1 and its relationship with related genes expressed by human periodontal ligament cells exposed to mechanical stress. Eur J Orthod; 32(6):698-705.

References

Baumert U, Golan I, Becker B, Hrala BP, Redlich M, Roos HA, Palmon A, Reichenberg E, Müßig D (2004). Pressure simulation of orthodontic force in osteoblasts: a pilot study. Orthod Craniofac Res; 7(1):3-9.

Bustin SA, Benes V, Garson JA, Hellemans J, Huggett J, Kubista M, Mueller R, Nolan T, Pfaffl MW, Shipley GL, Vandesompele J, Wittwer CT (2009). The MIQE guidelines: *M*inimum *I*nformation for publication of *Q*uantitative real-time PCR *E*xperiments. Clin Chem; 55(4):611-22.

Bustin SA, Beaulieu JF, Huggett J, Jaggi R, Kibenge FS, Olsvik PA, Penning LC, Toegel S (2010). MIQE précis: Practical implementation of minimum standard guidelines for fluorescence-based quantitative real-time PCR experiments. BMC Mol Biol; 11:74.

Dong-Xu L, Hong-Ning W, Chun-Ling W, Hong L, Ping S, Xiao Y (2011). Modulus of elasticity of human periodontal ligament by optical measurement and numerical simulation. Angle Orthod; 81(2):229-36.

Hao Y, Xu C, Sun SY, Zhang FQ (2009). Cyclic stretching force induces apoptosis in human periodontal ligament cells via caspase-9. Arch Oral Biol; 54(9):864-70.

He Y, Macarak EJ, Korostoff JM, Howard PS (2004). Compression and tension: differential effects on matrix accumulation by periodontal ligament fibroblasts in vitro. Connect Tissue Res; 45(1):28-39.

Janjic M, Docheva D, Trickovic Janjic O, Wichelhaus A, Baumert U (2018). In Vitro Weight-Loaded Cell Models for Understanding Mechanodependent Molecular Pathways Involved in Orthodontic Tooth Movement: A Systematic Review. Stem Cells Int; 2018:3208285.

Janjic Rankovic M, Docheva D, Wichelhaus A, Baumert U (2020). Effect of static compressive force on in vitro cultured PDL fibroblasts: monitoring of viability and gene expression over 6 days. Clin Oral Investig; 24(7):2497-2511.

Kletsas D, Basdra EK, Papavassiliou AG (2002). Effect of protein kinase inhibitors on the stretch-elicited c-Fos and c-Jun up-regulation in human PDL osteoblast-like cells. J Cell Physiol; 190(3):313-21.

Krishnan V, Davidovitch Z (2006). Cellular, molecular, and tissue-level reactions to orthodontic force. Am J Orthod Dentofacial Orthop; 129(4):469.e1-32.

Krishnan V, Davidovitch Z (2015). Biology of orthodontic tooth movement. In: Krishnan V, Davidovitch Z (Eds.). Biological Mechanisms of Tooth Movement.] 2nd. Chichester, UK: Wiley; pp. 15-29.

Marchesan JT, Scanlon CS, Soehren S, Matsuo M, Kapila YL (2011). Implications of cultured periodontal ligament cells for the clinical and experimental setting: a review. Arch Oral Biol; 56(10):933-43.

Memmert S, Damanaki A, Weykopf B, Rath-Deschner B, Nokhbehsaim M, Gotz W, Golz L, Till A, Deschner J, Jager A (2019). Autophagy in periodontal ligament fibroblasts under biomechanical loading. Cell Tissue Res; 378(3):499-511.

Mühlemann HR (1954). Tooth mobility (V): tooth mobility changes through artificial trauma. J Periodontol; 25(3):202-208.

Mühlemann HR, Zander HA (1954). Tooth mobility (III): the mechanism of tooth mobility. J Periodontol; 25(2):128-153.

Natali AN, Pavan PG, Scarpa C (2004). Numerical analysis of tooth mobility: formulation of a non-linear constitutive law for the periodontal ligament. Dent Mater; 20(7):623-9.

Nazet U, Schröder A, Spanier G, Wolf M, Proff P, Kirschneck C (2020). Simplified method for applying static isotropic tensile strain in cell culture experiments with identification of valid RT-qPCR reference genes for PDL fibroblasts. Eur J Orthod; 42(4):359-370.

Nogueira AV, Nokhbehsaim M, Eick S, Bourauel C, Jäger A, Jepsen S, Rossa C, Jr., Deschner J, Cirelli JA (2014). Biomechanical loading modulates proinflammatory and bone resorptive mediators in bacterial-stimulated PDL cells. Mediators Inflamm; 2014:425421.

Papadopoulou A, Iliadi A, Eliades T, Kletsas D (2017). Early responses of human periodontal ligament fibroblasts to cyclic and static mechanical stretching. Eur J Orthod; 39(3):258-263.

Pavasant P, Yongchaitrakul T (2011). Role of mechanical stress on the function of periodontal ligament cells. Periodontol 2000; 56(1):154-65.

Peverali FA, Basdra EK, Papavassiliou AG (2001). Stretch-mediated activation of selective MAPK subtypes and potentiation of AP-1 binding in human osteoblastic cells. Mol Med; 7(1):68-78.

Rutkovskiy A, Stensløkken KO, Vaage IJ (2016). Osteoblast Differentiation at a Glance. Med Sci Monit Basic Res; 22:95-106.

Shi J, Baumert U, Folwaczny M, Wichelhaus A (2019). Influence of static forces on the expression of selected parameters of inflammation in periodontal ligament cells and alveolar bone cells in a co-culture in vitro model. Clin Oral Investig; 23(6):2617-2628.

Sun C, Janjic Rankovic M, Folwaczny M, Otto S, Wichelhaus A, Baumert U (2021). Effect of Tension on Human Periodontal Ligament Cells: Systematic Review and Network Analysis. Front Bioeng Biotechnol; 9:695053.

Sun C, Janjic Rankovic M, Folwaczny M, Stocker T, Otto S, Wichelhaus A, Baumert U (2022). Effect of Different Parameters of In Vitro Static Tensile Strain on Human Periodontal Ligament Cells Simulating the Tension Side of Orthodontic Tooth Movement. Int J Mol Sci; 23(3):1525.

Tantilertanant Y, Niyompanich J, Everts V, Supaphol P, Pavasant P, Sanchavanakit N (2019). Cyclic tensile force stimulates BMP9 synthesis and in vitro mineralization by human periodontal ligament cells. J Cell Physiol; 234(4):4528-4539.

Toume S, Gefen A, Weihs D (2016). Printable low-cost, sustained and dynamic cell stretching apparatus. J Biomech; 49(8):1336-1339.

Wichelhaus A (2017). Orthodontic Therapy - Fundamental Treatment Concepts. New York, USA: Georg Thieme.

Xie F, Xiao P, Chen D, Xu L, Zhang B (2012). miRDeepFinder: a miRNA analysis tool for deep sequencing of plant small RNAs. Plant Mol Biol; 80:75-84.

Yang L, Yang Y, Wang S, Li Y, Zhao Z (2015). In vitro mechanical loading models for periodontal ligament cells: from two-dimensional to three-dimensional models. Arch Oral Biol; 60(3):416-24.

Acknowledgements

I would like to give my most sincere gratitude to all supporting me all the time during my PhD study:

I would like to give my deep gratitude to Prof. Dr. med. dent. Andrea Wichelhaus, who has provided me the valuable opportunity of PhD study in the Department of Orthodontics. She has given me great help during my PhD study with the construction of the apparatus, as well as her kindly supervision.

Heartful gratitude to PD Dr. rer. nat. Uwe Baumert, who led me into the world of biology. He has given me great help for every step of my PhD study, from the selection of my PhD project, design of the experiment, experimental techniques, data analysis to manuscript writing and revision. I am extremely thankful for all the timely help he gave, which supported me to continue with each step of my PhD study.

I want to give my sincere thanks to Prof. Dr. Dr. Matthias Folwaczny, who has given great help during all my PhD study, including but not limited to the supervision of my PhD study, valuable suggestions for my PhD projects and wonderful revisions of the manuscripts.

Heartful gratitude to Mila Janjic Rankovic, PhD, who has given me grateful support and help. Her encouragement and warm-hearted help strongly supported me during my whole PhD study.

Great thanks to Dipl.-Ing. Thomas Stocker, who has given timely huge help for the construction of the apparatus and valuable suggestions for both the experiment and the manuscripts.

I am grateful for the help of Prof. Dr. Dr. Sven Otto, who has given great suggestions for my study.

I also want to give thanks to my colleagues in our lab, Christine Schreindorfer, Lisa Reuther and Laure Djaleu, who have offered great help for the experimental techniques and regarded me as a member of the big family.

Many thanks to Dr. Julia Diegelmann and Mrs. Brigitte Hackl from the Department of Conservative Dentistry and Parodontology Research Laboratory for their help during my experiments.

I would give thanks for my beloved parents, my husband, my sister and brother, my nephew and niece. They are always the tough background for me, giving me the courage to chasing my dreams.